

MODEL INFORMED DRUG DEVELOPMENT AND PRECISION  
DOSING FOR DRUG-DRUG-GENE-INTERACTIONS

APPLICATION OF PHYSIOLOGICALLY-BASED PHARMACOKINETIC MODELING

DISSERTATION

zur Erlangung des Grades des Doktors der Naturwissenschaften  
der Naturwissenschaftlich-Technischen Fakultät  
der Universität des Saarlandes

von

Jan-Georg Wojtyniak  
Diplom Pharmazeut / Apotheker

Saarbrücken

2021

Tag des Kolloquiums:

Dekan:

Berichterstatter:

Vorsitz:

Akad. Mitarbeiter:

22. Juni 2021

Prof. Dr. Jörn Walter

Prof. Dr. Thorsten Lehr

Prof. Dr. Markus R. Meyer

Prof. Dr. Christian Ducho

Dr. Charlotte Dahlem

Die vorliegende Arbeit wurde von Mai 2016 bis Dezember 2020 unter Anleitung von Herrn Professor Dr. Thorsten Lehr in der Fachrichtung Klinische Pharmazie der Naturwissenschaftlich-Technischen Fakultät der Universität des Saarlandes angefertigt.



## INCLUDED PUBLICATIONS

---

PUBLICATION I - DATA DIGITIZING: **Jan-Georg Wojtyniak**, Hannah Britz, Dominik Selzer, Matthias Schwab, and Thorsten Lehr. "Data digitizing: accurate and precise data extraction for quantitative systems pharmacology and physiologically-based pharmacokinetic modeling." In: *CPT: Pharmacometrics & Systems Pharmacology* 9.6 (June 2020), pp. 322–331. DOI: 10.1002/psp4.12511

PUBLICATION II - ZOPTARELIN DOXORUBICIN: Nina Hanke, Michael Teifel, Daniel Moj, **Jan-Georg Wojtyniak**, Hannah Britz, Babette Aicher, Herbert Sindermann, Nicola Ammer, and Thorsten Lehr. "A physiologically based pharmacokinetic (PBPK) parent-metabolite model of the chemotherapeutic zoptarelin doxorubicin — integration of in vitro results, Phase I and Phase II data and model application for drug-drug interaction potential analysis." In: *Cancer Chemotherapy and Pharmacology* 81.2 (Feb. 2018), pp. 291–304. DOI: 10.1007/s00280-017-3495-2

PUBLICATION III - SIMVASTATIN: **Jan-Georg Wojtyniak**, Dominik Selzer, Matthias Schwab, and Thorsten Lehr. "Physiologically based precision dosing approach for drug-drug-gene interactions: a simvastatin network analysis." In: *Clinical Pharmacology & Therapeutics* (Dec. 2020). DOI: 10.1002/cpt.2111

## CONTRIBUTION REPORT

---

Following the contributor roles taxonomy (CRediT) [4, 5], the author would like to declare his contributions to the publications included in this thesis.<sup>1</sup>

**PUBLICATION I - DATA DIGITIZING:** Conceptualization, Methodology, Software, Validation, Formal Analysis, Investigation, Data Curation, Writing - Original Draft, Writing - Review & Editing, Visualization, Project Administration

**PUBLICATION II - ZOPTARELIN DOXORUBICIN:** Methodology, Software, Validation, Formal Analysis, Data Curation, Writing - Original Draft, Writing - Review & Editing, Visualization

**PUBLICATION III - SIMVASTATIN:** Conceptualization, Methodology, Software, Validation, Formal Analysis, Investigation, Data Curation, Writing - Original Draft, Writing - Review & Editing, Visualization, Project Administration

---

<sup>1</sup> For a description of the different taxonomy categories see appendix Chapter B

## ABSTRACT

---

The global demand for pharmaceuticals is continuously growing. As a result, one can observe an increase in adverse drug reactions, which pose a critical risk to patients. The primary triggers for adverse drug reactions are drug-drug- and drug-gene-interactions. Model-informed drug discovery and development as well as model-informed precision dosing can help to mitigate the risks of drug-drug and drug-gene interactions.

Thus, this work aimed to improve and to apply physiologically-based pharmacokinetic modeling strategies in the context of model-informed drug discovery and development as well as model-informed precision dosing.

For this purpose, best practices for data digitization as an essential step in the development process of most physiologically-based pharmacokinetic models have been established. Moreover, models for zoptyarelin doxorubicin and simvastatin were developed and evaluated. The zoptyarelin doxorubicin model was used to guide the development process of this drug. In contrast, the simvastatin model was utilized in a drug-drug-gene interaction network to generate 10 368 dose recommendations for different interaction scenarios, which were made available in a digital decision support system.

In conclusion, the work can be seen as a beacon project to illustrate how physiologically-based pharmacokinetic modeling of drug-drug and drug-gene interactions can be applied in model-informed drug discovery and development as well as in model-informed precision dosing.

## ZUSAMMENFASSUNG

---

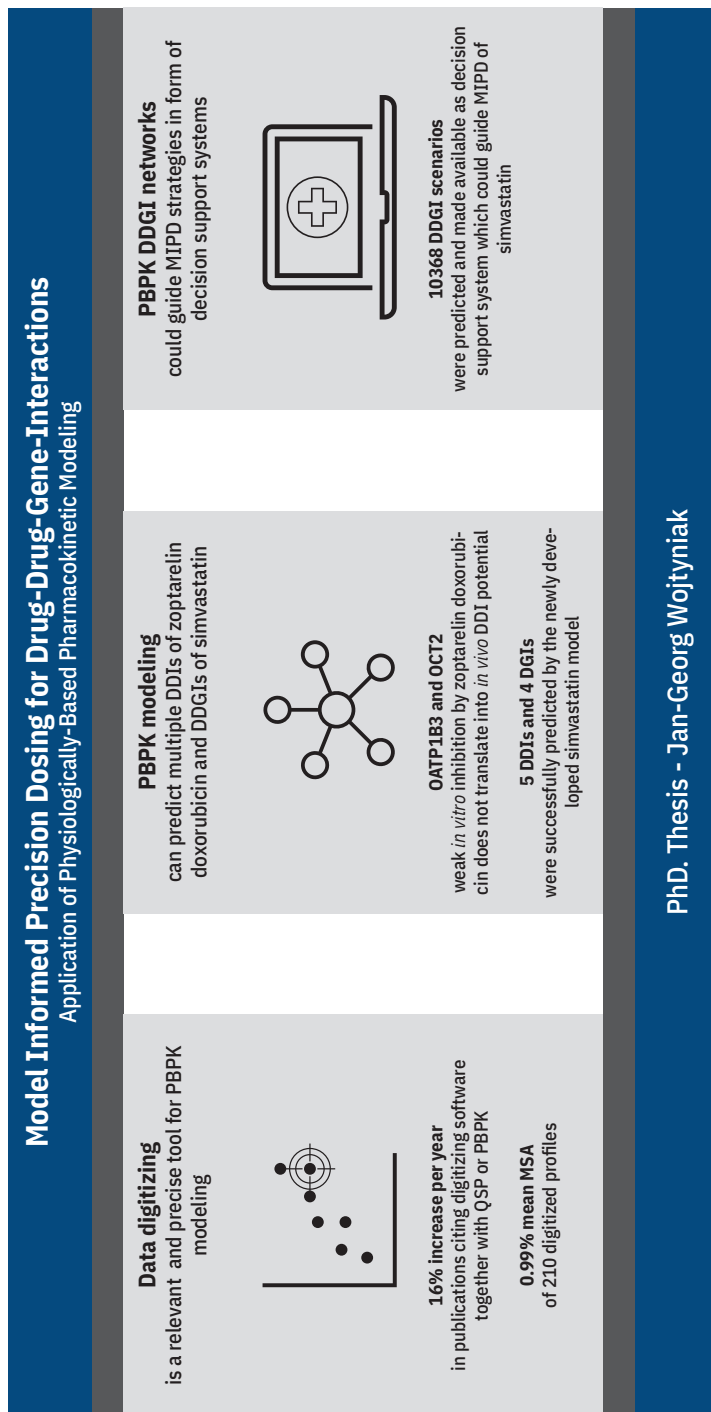
Der globale Arzneimittelbedarf steigt kontinuierlich an. Infolgedessen kommt es vermehrt zu unerwünschten Arzneimittelwirkungen, die eine Gefahr für Patienten darstellen. Eine wichtige Rolle beim Auftreten unerwünschter Arzneimittelwirkungen spielen Arzneimittel-Arzneimittel- und Arzneimittel-Gen-Wechselwirkungen. Um das Risiko solcher Wechselwirkungen zu minimieren, kann die modellgestützte Arzneimittelentwicklung und Präzisionsdosierung angewendet werden.

Das Ziel dieser Arbeit war es, physiologie-basierte pharmakokinetische Modelle zum Zweck der modellgestützten Arzneimittelentwicklung und Präzisionsdosierung einzusetzen.

Dafür wurde die Datendigitalisierung als wesentlicher Bestandteil der Entwicklung neuer physiologie-basierter pharmakokinetischer Modelle untersucht. Außerdem wurden Modelle für Zoptarelin Doxorubicin und Simvastatin entwickelt. Das Zoptarelin Doxorubicin Modell wurde verwendet, um die Entwicklung dieses Medikaments zu unterstützen. Mittels des Simvastatin Modells wurden in einem Interaktionsnetzwerk 10 368 Dosisempfehlungen für verschiedene Szenarien generiert und in einem digitalen Entscheidungsunterstützungssystem verfügbar gemacht.

Zusammenfassend kann die Arbeit als Leuchtturmprojekt gesehen werden, das zeigt, wie die physiologie-basierte pharmakokinetische Modellierung von Arzneimittel-Arzneimittel- und Arzneimittel-Gen-Wechselwirkungen in der modellgestützte Arzneimittelentwicklung und Präzisionsdosierung angewendet werden kann.





Graphical abstract. PBPK: Physiologically-Based Pharmacokinetic Modeling; QSP: Quantitative Systems Pharmacology; MSA: Median Symmetric Accuracy; DDI: Drug-Drug Interaction; DDDI: Drug-Drug-Gene Interaction; OATP1B3: Organic Anion-Transporting Polypeptide 1B3; OCT2: Organic Cation Transporter 2; MIPD: Model Informed Precision Dosing



*Ein Mensch, gestellt auf harte Probe,  
Besteht sie, und mit höchstem Lobe.  
Doch sieh da: es versagt der gleiche,  
Wird er gestellt auf eine weiche!*

— Eugen Roth - Ernst und heiter [6]

## DANKSAGUNG

---

An dieser Stelle danke ich all jenen, die mir bei der Realisierung meiner Promotion mit Rat und Tat geholfen haben. Allen voran danke ich meinem betreuenden Professor Thorsten Lehr für sein jederzeit offenes Ohr und die vielen guten Ratschläge und Ideen mit denen er unsere gemeinsamen Projekte vorangetrieben hat. Weiterhin danke ich ganz besonders Herrn Professor Matthias Schwab und dem Team des Dr. Margarete Fischer-Bosch-Institut für klinische Pharmakologie sowie Siv Jönsson und der Universität Uppsala ohne deren Unterstützung meine Arbeit wahrscheinlich nicht hätte realisiert werden können. Ebenfalls besonderer Dank geht an Professor Markus R. Meyer, für seine Unterstützung als wissenschaftlicher Begleiter und Zweitgutachter dieser Arbeit.

Vielen Dank auch an meinen Arbeitskreis, mit dem ich jederzeit bei einem Kaffee und einem Stück Kuchen die aktuellen Probleme besprechen konnte. Dabei besonderen Dank an Fatima Marok und Simeon Rüdesheim für ihre Arbeit am U-PGx Projekt sowie Anna Roh und den vielen Studenten und wissenschaftlichen Mitarbeitern die bei der Erstellung und Evaluierung des One-Page-Summary-Sheets geholfen haben. Ebenfalls geht ein großes Dankeschön an Nina Hanke und Dominik Selzer für Ihre unermüdliche Unterstützung bei der Umsetzung und Fertigstellung dieser Arbeit.

Weiterhin danke ich meinen Freunden aus Schul-, Studium- und Arbeitsleben deren einzelne Auflistung leider den Rahmen dieser Danksagung sprengen würde, ohne die diese Arbeit aber sicherlich nicht möglich gewesen wäre. Ganz besonderer Dank geht an meiner Familie und insbesondere an meine Mutter Brigitte, meinen Vater Volker und meinen Bruder Daniel, die mir mit viel gutem Essen und moralischer Unterstützung die Jahre über zur Seite gestanden sind. Abschließend danke ich noch einmal von ganzem Herzen meiner Frau Melissa, die durch ein ausgewogenes Abwechslungsprogramm und mit viel Fürsorge sichergestellt hat, dass ich die Promotion psychisch und physisch gut überstanden habe.



# CONTENTS

---

## I INTRODUCTION AND AIMS

1	INTRODUCTION	3
1.1	Adverse Drug Reactions . . . . .	3
1.2	Drug-Drug-Gene Interactions . . . . .	4
1.3	Examples: Zoptarelin Doxorubicin and Simvastatin . .	5
1.4	Model Informed Drug Development and Precision Dosing	7
1.5	Modeling Strategies for Drug-Drug-Gene Interactions .	9
2	AIMS	13

## II INCLUDED MANUSCRIPTS

3	RESULTS	17
3.1	Publication I - Data Digitizing . . . . .	17
3.1.1	Reference . . . . .	17
3.1.2	Author Contributions . . . . .	17
3.1.3	Copyright . . . . .	17
3.2	Publication II - Zoptarelin Doxorubicin . . . . .	29
3.2.1	Reference . . . . .	29
3.2.2	Author Contributions . . . . .	29
3.2.3	Copyright . . . . .	30
3.3	Publication III - Simvastatin . . . . .	45
3.3.1	Reference . . . . .	45
3.3.2	Author Contributions . . . . .	45
3.3.3	Copyright . . . . .	45

## III DISCUSSION AND CONCLUSIONS

4	DISCUSSION	59
4.1	Data Digitizing for Model Development . . . . .	59
4.2	Zoptarelin Doxorubicin Drug-Drug Interaction Potential	60
4.3	Simvastatin Drug-Drug-Gene Interaction Network . . .	61
5	CONCLUSIONS	65

	BIBLIOGRAPHY	67
--	--------------	----

## IV APPENDIX

A	SUPPORTING INFORMATION	81
A.1	Publication I - Data Digitizing . . . . .	81
A.2	Publication II - Zoptarelin Doxorubicin . . . . .	111
A.3	Publication III - Simvastatin . . . . .	133
B	CREDIT CATEGORIES	317
C	PUBLICATIONS	319
C.1	Original Articles . . . . .	319

c.2	Conference Abstracts . . . . .	320
c.3	Oral Presentations . . . . .	321
c.4	Book Chapters . . . . .	322
c.5	Others . . . . .	322
D	CURRICULUM VITAE	323

## LIST OF FIGURES

---

Figure 1.1	Total Nominal Spending on Medicines . . . . .	3
Figure 1.2	Zoptarelin Doxorubicin Molecular Structure . . . . .	5
Figure 1.3	Simvastatin Molecular Structure . . . . .	6
Figure 1.4	Pharmacometrics in Drug Development . . . . .	8
Figure 1.5	PBPK Model Development Process . . . . .	9
Figure 1.6	PBPK Model Building Blocks . . . . .	10
Figure 1.7	PBPK Modeling for DDGI Predictions . . . . .	11
Figure 4.1	Relevance of CYP Isoforms . . . . .	62

## LIST OF TABLES

---

Table 3.1	Author Contributions - Data Digitizing . . . . .	17
Table 3.2	Author Contributions - Zoptarelin Doxorubicin . . . . .	29
Table 3.3	Author contributions - Simvastatin . . . . .	45

## ABBREVIATIONS

---

---

<b>Notation</b>	<b>Description</b>
$K_M$	Michaelis-Menten Constant
ADE	Adverse Drug Event
ADR	Adverse Drug Reaction
AUC	Area Under the Plasma-Concentration Time Curve
$C_{max}$	Peak Plasma Concentration
CRediT	Contributor Roles Taxonomy
CYP	Cytochrome P450
CYP3A4	Cytochrome P450 3A4
DDGI	Drug-Drug-Gene-Interaction
DDI	Drug-Drug-Interaction
DGI	Drug-Gene-Interaction

---

<b>Notation</b>	<b>Description</b>
DNA	Deoxyribonucleic Acid
DSS	Decision Support System
EMA	European Medicine Agency
FDA	Food and Drug Administration
GC-MS	Gas Chromatography–Mass Spectrometry
HMG-CoA	$\beta$ -Hydroxy $\beta$ -Methylglutaryl-Coenzyme A
HPLC	High-Performance Liquid Chromatography
LADME	Liberation, Absorption, Distribution, Metabolization, Excretion
LDL-C	Low-Density Lipoprotein Cholesterol
LHRHR	Luteinizing Hormone-Releasing Hormone Receptor
LLOD	Lower Limit of Detection
MID3	Model-Informed Drug Discovery and Development
MIPD	Model-Informed Precision Dosing
MSA	Median Symmetric Accuracy
NCA	Non-Compartmental Analysis
NCB	Net Clinical Benefit
NTE	New Therapeutic Entity
NVSS	National Vital Statistics System
OATP1B1	Solute Carrier Organic Anion Transporter Family Member 1B1
OATP1B3	Solute Carrier Organic Anion Transporter Family Member 1B3
OCT2	Organic Cation Transporter 2
PBPK	Physiologically-Based Pharmacokinetic
PD	Pharmacodynamic
PGx	Pharmacogenomic
PK	Pharmacokinetic
PMx	Pharmacometrics
QC	Quality Control
QSP	Quantitative Systems Pharmacology
SA	Simvastatin Acid
SL	Simvastatin Lactone
USA	United States of America



## Part I

### INTRODUCTION AND AIMS

The chapter provides an overview of why drug-drug-gene interactions (DDGIs) place a heavy burden on our health care system. It also explains how DDGIs can be overcome with the help of model-informed drug discovery and development (MIDD), model-informed precision dosing (MIPD) and in particular with physiologically-based pharmacokinetic (PBPK) modeling. Finally, it specifies the aims of the presented work.



## INTRODUCTION

---

### 1.1 ADVERSE DRUG REACTIONS AND ADVERSE DRUG EVENTS

Adverse drug reactions (ADRs) and adverse drug events (ADEs) are an essential and increasing burden for our healthcare and economic system [7, 8]. An ADR is “a response to a medicinal product which is noxious and unintended” while an ADE is “an injury resulting from medical intervention related to a drug” [8]. They are assumed to be a leading cause of morbidity and death worldwide as shown for instance by a meta-analysis of 39 prospective studies, which found that ADRs are responsible for 1.0% to 16.8% of admissions to hospitals in the United States of America (USA) [7].

Significantly related to the frequency of ADRs is the sharp increase in pharmaceuticals use as observed over the last decades. For instance, the number of prescriptions dispensed in the USA rose from 5.308 billion in 2014 up to 5.770 billion in 2018 [9]. Even more striking: when looking at the total nominal spending on medicines, they reached a volume of 482 billion \$ in 2018, as shown in Figure 1.1 [10].

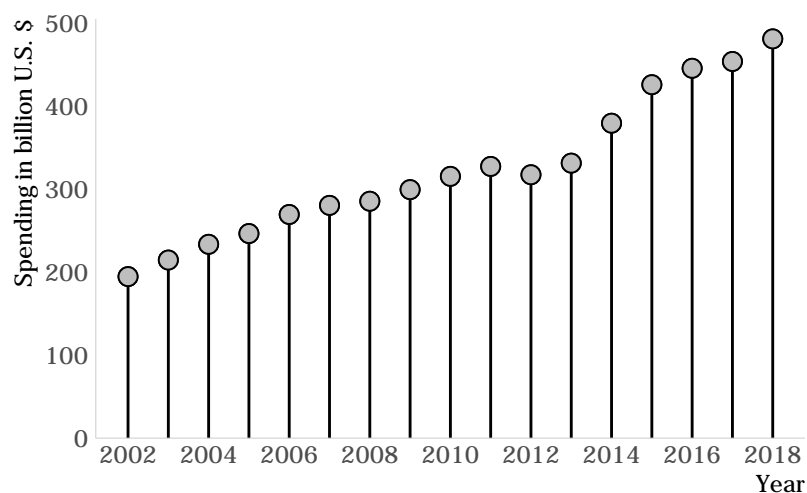


Figure 1.1: Total nominal spending on medicines in the USA from 2002 to 2018 [10].

As a result, it is estimated that 60% of the elderly take at least one prescription medicine per week [11]. In parallel, the incidence of ADRs is increasing too, as shown by an analysis from the USA National Vital Statistics System (NVSS) that showed an increase in ADR-related deaths from 8 to 12 per 1000 persons per year, during the timespan from 1999 to 2006 [8]. In contrast, it is estimated that 70% of ADRs, which lead

to an emergency department visit are preventable [8]. Reasons for ADRs are manifold and can be traced back to medication errors, drug interactions, diseases, or patient characteristics [8, 12]. Nevertheless, the impact of ADRs on our social and economic system remains vast and has even led to the development of a specialized branch of research called pharmacovigilance [12, 13].

## 1.2 DRUG-DRUG-, DRUG-GENE- AND DRUG-DRUG-GENE INTERACTIONS

To tackle ADRs, a drug therapy tailored to the patient's needs, characteristics, and circumstances is required [12, 14–16]. This therapy individualization is summarized under the term “precision dosing” [14–16]. Precision dosing is defined as “dose selection by a prescriber for an individual patient at a given time” [14]. Furthermore, it “focuses on the individualization of drug treatment regimens based on patient factors known to alter drug disposition and/or response” [16]. Very well known factors which are capable of altering drug disposition are drug-drug-interactions (DDIs), drug-gene-interactions (DGIs) and the combination of both, DDGIs [17–23].

DDI means that one drug, commonly called the perpetrator, alters the pharmacokinetic (PK) or pharmacodynamic (PD) profile of another drug, which is then called the victim compound [20]. DDIs do often happen in polypharmaceutical settings like in cancer treatments [24, 25]. A DGI, on the other hand, occurs “when an individual carrying one or more variant forms of a gene that codes for a drug-metabolizing enzyme or drug transporter with altered function receives a drug that is a substrate for the given enzyme or transporter” [17].

Unfortunately, although investigation of DDIs during drug development is mandatory and the knowledge about DGIs on pharmacotherapy is continuously growing, the development of precision dosing recommendations is lagging [16, 26, 27]. One reason for this is that DDI effects in certain situations cannot be investigated in a clinical trial [2]. For example, DDI studies of new therapeutic entities (NTEs) in oncology require special ethical considerations that may prevent a study from being conducted [2]. Thus, in such scenarios, advanced translational strategies are necessary to interpolate preclinical investigations to predict clinical effects [2].

Another reason is that clinical studies alone are often not sufficient to reflect the complicated situation of a post-approval setting. For instance, since the majority of polymorphisms are quite rare, most clinical trials compare DGIs individually rather than in combination to recruit a sufficient number of patients [3, 16]. The same applies to DDIs studies where mostly dedicated index drugs are used for effect quantification [27]. Moreover, commonly only homogeneous study populations are selected for clinical DDI studies, consisting of young and healthy individuals

without comorbidities or comedications. This is done to reduce the potential impact of covariates on study outcome and to ensure significant results [16, 28]. However, in a real-life polymedication environment, where people regularly take more than five drugs [29], DDIs and DGIs occur not purely as individual cases but rather in combination and as DDGIs [3, 21]. Therefore, novel approaches are needed to integrate the information on DDIs and DGIs obtained in clinical studies to apply them to more complex DDGI scenarios. This way precision dosing recommendations could be generated, and ADRs prevented [3, 20–23].

### 1.3 CASE EXAMPLES: ZOPTARELIN DOXORUBICIN AND SIMVASTATIN

Zoptarelin doxorubicin was an investigational chemotherapeutic agent designed for drug targeting of luteinizing hormone-releasing hormone receptor (LHRHR) positive tumors [2, 30]. It is a fusion molecule of the chemotherapeutic doxorubicin and a small peptide agonist to LHRHR [31]. The structure of zoptarelin doxorubicin is shown in Figure 1.2.

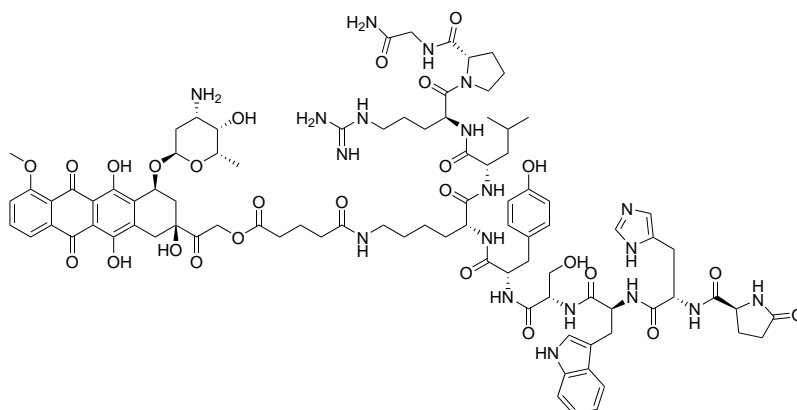


Figure 1.2: Molecular structure of zoptarelin doxorubicin [31].

It was hypothesized that by adding the LHRHR agonistic moiety, improved internalization of zoptarelin doxorubicin in LHRHR positive tumor cells and a reduced cardiotoxicity compared to unconjugated doxorubicin could be achieved [2, 30]. Zoptarelin doxorubicin is mainly metabolized by spontaneous and carboxylesterase-mediated hydrolysis [2]. In *in vitro* experiments, zoptarelin doxorubicin shows inhibitory effects on solute carrier organic anion transporter family member 1B3 (OATP1B3) and organic cation transporter 2 (OCT2) with  $IC_{50}$  values of  $16.5 \mu\text{mol l}^{-1}$  and  $3.26 \mu\text{mol l}^{-1}$ , respectively [2]. As a consequence, *in vivo* interactions with prominent substrates of those transporters like simvastatin (OATP1B3) and metformin (OCT2) were likely and had to be further investigated during the development process [2]. However, clinical DDI studies with deoxyribonucleic acid (DNA) intercalating agents are hardly feasible due to ethical aspects [2]. In the case of zoptarelin doxorubicin this could have led to a knowledge gap and

potential patient safety risks [2].

As already indicated, another good example compound which is prone to be influenced by DDGIs is simvastatin. Simvastatin is an oral  $\beta$ -hydroxy  $\beta$ -methylglutaryl-coenzyme A (HMG-CoA) reductase inhibitor and counts to the most prescribed drugs in industrial nations [9]. Although simvastatin shows excellent cost-effectiveness and an optimal benefit-risk ratio [32, 33], over-dosage can lead to rhabdomyolysis which is a feared and potentially life-threatening ADR [34]. Multiple single DGIs and DDIs have been identified to change simvastatin PK and subsequently raise the risk of over-dosages [35–39]. This is because simvastatin has a complex PK with high inter-individual variability, which involves many different drug transporters and metabolic enzymes [39–41]. A simplified overview of processes relevant to simvastatin's PK is given in Figure 1.3.

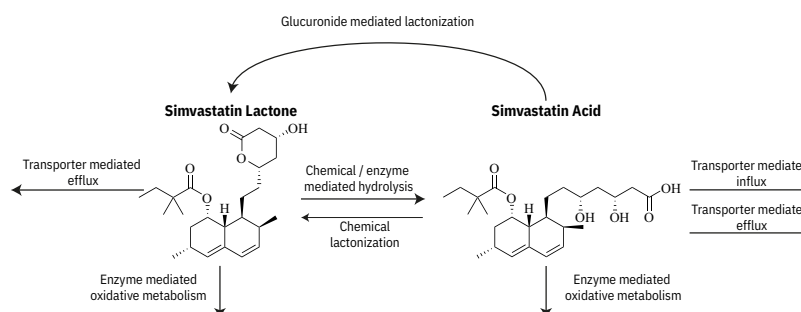


Figure 1.3: Simvastatin lactone and simvastatin acid molecular structure. Simvastatin is given as a prodrug (simvastatin lactone), which is hydrolysed by chemical and enzymatic processes to the more active form simvastatin acid [42]. Both are substrates for different transporters [43–45] and undergo further oxidative metabolism [42]. In addition, simvastatin acid can lactonize back to simvastatin lactone by chemical lactonization or via a glucuronide intermediate metabolite [42].

Hence, if a DGI or DDI alter transporter or enzyme activity, simvastatin's PK can change dramatically, as observed in several clinical trials [35–39]. To compare the effects more or less independent of the given dose it is helpful to look at the relative change of non-compartmental analysis (NCA) parameters like area under the plasma-concentration time curve (AUC) under DGI or DDI conditions compared to placebo as calculated in Equation 1.1.

By doing so, a relative change of  $-94\%$  (simvastatin acid (SA), AUC) under rifampicin co-treatment [46] and a relative change of  $+1117\%$  (SA, AUC) under clarithromycin co-treatment [47] is observed. Unfortunately, despite these already very strong observed effects for single DDIs, no recommendations for combined effects of DGIs and DDIs in the form of DDGIs for simvastatin were available [26]. That is because

investigation and evaluation of all possible combination scenarios, as outlined in Section 1.2, is of course not feasible with clinical trials alone [3, 16].

$$\%NCA_{change} = \frac{NCA_{obs,DDI/DGI} - NCA_{obs,placebo}}{NCA_{obs,placebo}} * 100 \quad (1.1)$$

where:

$\%NCA_{change}$	Relative change of the NCA estimate under DDI or DGI compared to placebo
$NCA_{obs,DDI/DGI}$	Observed NCA estimate under DDI or DGI conditions
$NCA_{obs,placebo}$	Observed NCA estimate under placebo conditions

#### 1.4 MODEL INFORMED DRUG DEVELOPMENT AND PRECISION DOSING - THE USE OF PHARMACOMETRICS

To overcome the knowledge gaps mentioned above MID3 and MIPD strategies can be applied [14–16, 48–52]. MID3 is a “quantitative framework for prediction and extrapolation, centered on knowledge and inference generated from integrated models of compound, mechanism and disease level data and aimed at improving the quality, efficiency and cost effectiveness of decision making” [52]. MIPD on the other hand is the targeted use of pharmacometrics (PMx) modeling techniques together with the individually measured patient and disease characteristics to find the optimal dose for a patient [53]. Thereby, PMx is a science that aims to quantify drug, disease, and clinical trial characteristics using mathematics and statistics [54]. Since its debut in the 1950s PMx has evolved into an essential cornerstone of pharmacotherapy, which, as shown in Figure 1.4, can be found in each phase of a drug’s life-cycle [51, 52, 54–57].

While PMx initially focused on empirical or semi-mechanistic models, the recently available computing power made it possible to develop physiologically more accurate models [58–67]. Subsequently, they are called physiologically-based pharmacokinetic (PBPK) models, and they are seen as one of the main pillars of the modeling and simulation revolution in pharmaceutical sciences [59, 60, 67]. PBPK models are multiple compartment systems and try to depict the physiological situation as detailed as necessary [59, 66]. Thus, their parameters and equations are based on real tissue characteristics like volume, surface area, or protein expression [59, 66]. Compartments are mathematically connected to represent the blood flow and to simulate the liberation, absorption, distribution, metabolization and excretion (LADME) behavior of drugs [59, 66]. PBPK models vary in complexity and can be

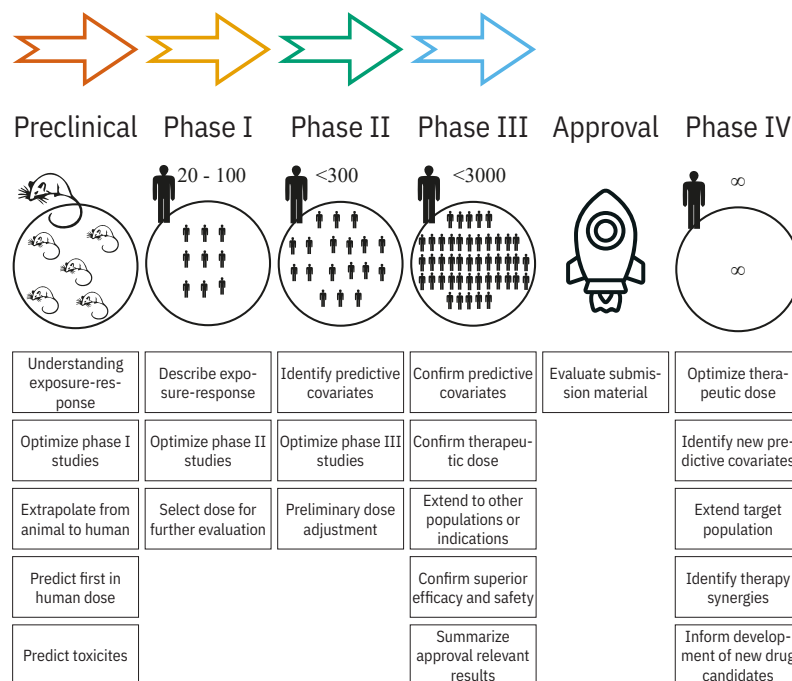


Figure 1.4: Different phases of drug development and tasks that can be informed by PMx techniques. Adapted from Mould and Upton [55].

established as minimal or whole-body PBPK models [61, 62, 64, 68]. Moreover, they can be integrated into systems biology networks [63, 69]. To establish a PBPK model, system and drug dependent parameters are required [59, 66]. System dependent parameters describe the physiological environment and include the aforementioned parameters like tissue characteristics [59, 66]. Drug dependent parameters are compound-specific parameters such as lipophilicity, acidity, or molecular weight [59, 66]. Figure 1.5 visualizes the step-by-step process for the development of a PBPK model, while Figure 1.6 summarizes the structure of a whole-body PBPK model and the different building blocks [1, 66, 67].

Since its conceptualization in 1937 [70], PBPK modeling has proven its usefulness in many different application areas [66, 70–72]. Issues that can be addressed with PBPK modeling are, for example, cross-species extrapolations or scaling to special populations like pediatric or organ impaired patients [66]. Due to these versatile application possibilities, especially for questions which for ethical reasons, or due to their feasibility can hardly be answered by clinical studies, PBPK modeling is recognized by regulatory agencies like the Food and Drug Administration (FDA) and the European Medicine Agency (EMA) as valuable method [51, 66, 70–72]. They emphasize, for example, the use of PBPK modeling to explore and quantitatively predict the PK of drugs for DDIs and to support dose selection and labeling [27]. Although



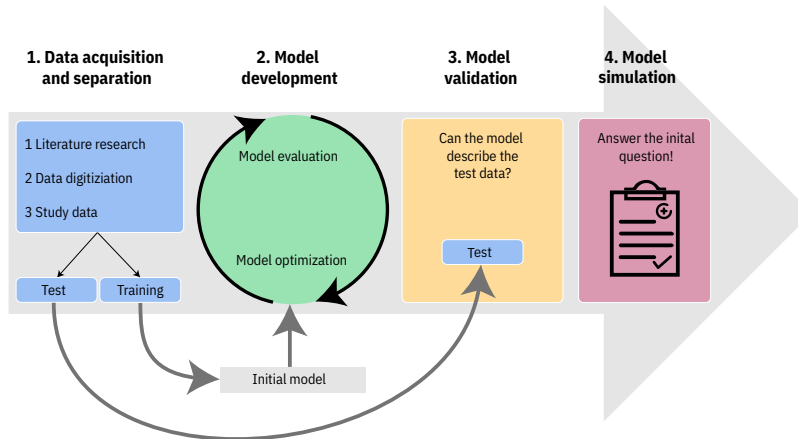


Figure 1.5: Stepwise PBPK model development workflow. In a first step, data are acquired. The data are then split into training and test dataset. Following, an initial model is set up and continuously refined. In step three, the model has to be validated and can lastly be used to answer the initial questions.

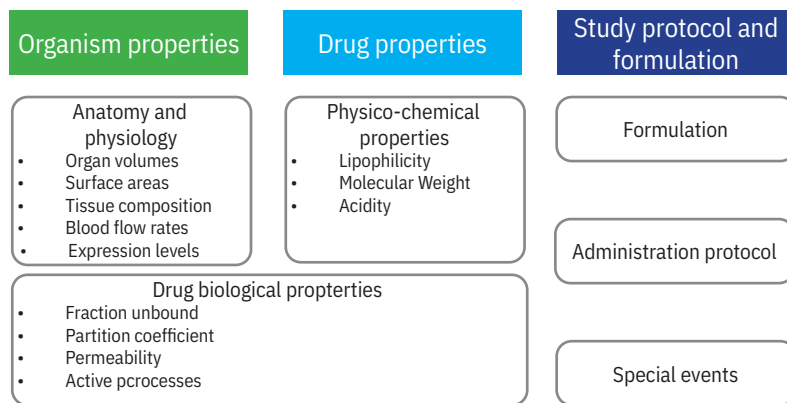
the potential of PBPK modeling is acknowledged, the technique is, as already mentioned, relatively new compared to other MID3 and MIPD strategies [3, 48, 65]. Thus, best practices for PBPK modeling are currently under development, and many work steps important for PBPK model building require a detailed evaluation [1].

#### 1.5 PHYSIOLOGICALLY BASED PHARMACOKINETIC MODELING STRATEGIES FOR DRUG-DRUG-, DRUG-GENE- AND DRUG-DRUG-GENE INTERACTIONS

As mentioned, PBPK modeling is regularly used and emphasized for DDI assessment and predictions, for instance, during the drug development process [2, 51, 66, 70–72]. The convenient aspect of the PBPK approach is that the models can be developed individually for each substance [3, 74–79]. Subsequently, they can be connected as required to investigate the DDI of interest [2, 3, 74–79]. Thus, theoretically, networks of any size can be created even for very complicated DDIs [2, 3, 76–78]. The first examples of such DDI networks can already be found in the literature [3, 76–78]. Besides, PBPK modeling can also be used to predict DGIs [3, 76]. By combining the two approaches for DGIs and DDIs, complex interactions can be predicted similarly for DDGIs [3, 80]. Figure 1.7 illustrates the process with a puzzle in which the individual building blocks are developed separately and then put together for therapy optimization.

Thus, PBPK driven MIPD is a useful technique to derive therapy recommendations and this way to come as close as possible to the ultimate goal of a pharmacotherapy tailored to the patient [3, 15, 16, 50]. This

### Building blocks of a PBPK model



### Structure of a PBPK model

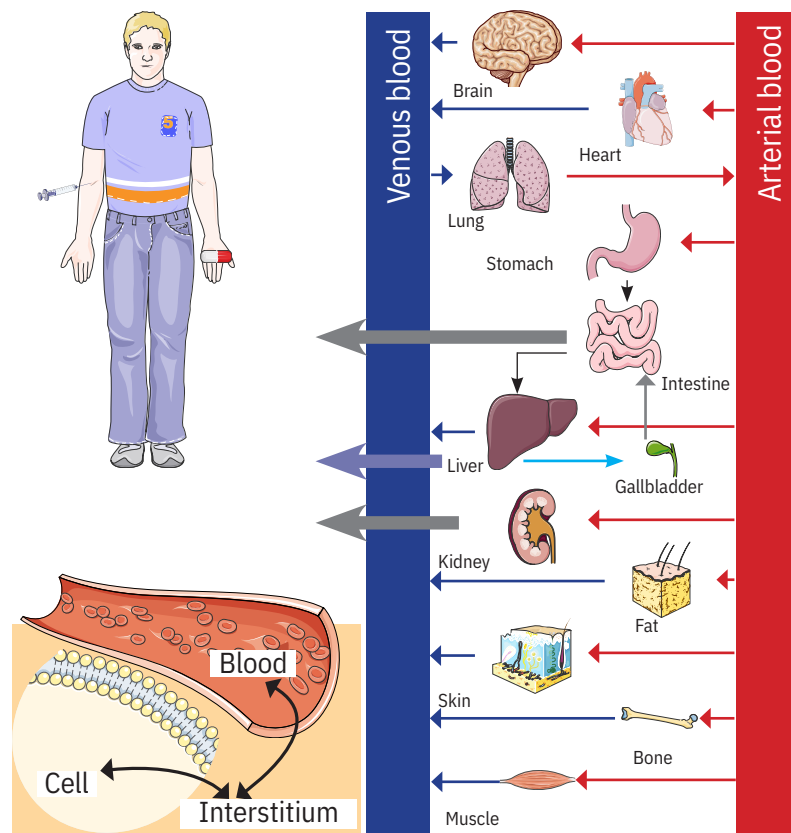


Figure 1.6: PBPK model building blocks and model structure. The upper part lists different sources of information necessary for the development of a PBPK model. The lower part of the figure visualizes the different compartments in a PBPK model, which represent the organ tissues. Each compartment is further subdivided into vascular, interstitial, and intracellular space. Adapted from Kuepfer et al. [66]. Illustrations of organs were taken from CC BY 3.0 Servier Medical Art by Servier [73].

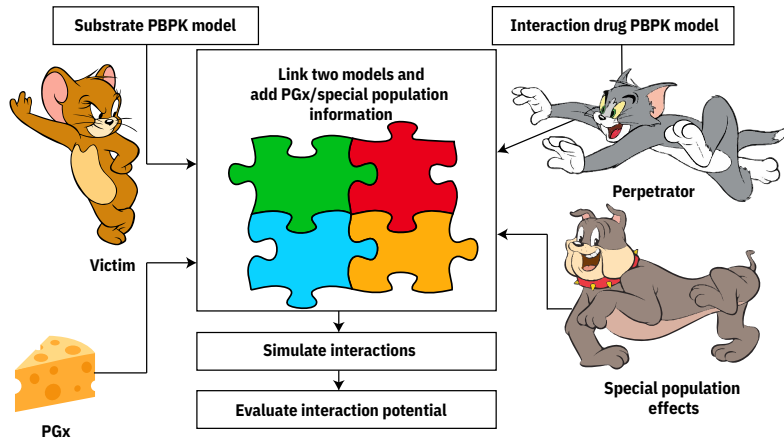


Figure 1.7: PBPK modeling approach for the prediction of DDGIs. Substrate and interaction PBPK models are developed individually and afterward connected. In addition, pharmacogenomic (PGx) and special population effects can be included. Tom and Jerry illustrations were taken from CC BY-NC 4.0 by pngimg.com [81].

way, ADRs could be prevented, lives saved and the healthcare system's burden reduced [15]. However, the pure distribution of PBPK models is not sufficient [16]. Rather, the recommendations derived from them must be made available in a way that they can be easily implemented in a clinical setting [16]. Thereby, decision support systems (DSSs) have been proven to be important tools to integrate the derived knowledge [16, 50]. Such systems allow clinicians to enter their patient characteristics, genotype information, and comedication data [3]. Subsequently, the system evaluates the input information, compares them with the MIPD analyses results, and generates an individual therapy recommendation [3].



One aim of this thesis was to improve current PBPK modeling strategies. Further, PBPK modeling of DDIs, DGIs, and DDGIs should be applied in the context of MID3 and MIPD for the example compounds zoptarelin doxorubicin and simvastatin, respectively. The thesis' aims were realized within the scope of the following projects:

**PROJECT I - DATA DIGITIZING:** The project aimed to assess the relevance of data digitizing for PBPK modeling and to establish recommendations for the digitization workflow. For this purpose, the general usage of data digitizing software in quantitative systems pharmacology (QSP) and PBPK modeling should be analyzed. Subsequently, the accuracy and precision of relevant digitizing software packages should be evaluated. Moreover, investigation of discrepancies between reported and graphically presented data as well as identification of covariates which might influence the digitizing process was aspired. Finally, recommendations regarding the creation of digitizable plots and the digitization process itself should be proposed.

**PROJECT II - ZOPTARELIN DOXORUBICIN:** Purpose of the second project was to support the drug development process of the anticancer drug zoptarelin doxorubicin. In detail, a whole-body PBPK model of zoptarelin doxorubicin and its active metabolite doxorubicin should be established. Further, the model should be used to assess the DDI potential for OATP1B3 and OCT2 substrates.

**PROJECT III - SIMVASTATIN:** The third project's objective was to establish dose recommendations for different DDGIs of simvastatin. In order to achieve this, the following specific goals have been defined. The first part aimed to develop a PBPK simvastatin DDGI network, including DDIs of five clinically relevant perpetrator drugs and the DGIs of four PGx relevant polymorphisms. The second objective was to use the developed network and to derive new dose recommendations in the context of MIPD. Finally, the results should be made publicly available as a web-based DSS for easy and quick access, especially for health care professionals.



## Part II

### INCLUDED MANUSCRIPTS

This chapter presents the scientific publications used for the presented work.





## RESULTS

---

### 3.1 PUBLICATION I - DATA DIGITIZING: ACCURATE AND PRECISE DATA EXTRACTION FOR QUANTITATIVE SYSTEMS PHARMACOLOGY AND PHYSIOLOGICALLY-BASED PHARMACOKINETIC MODELING

#### 3.1.1 *Reference*

**Jan-Georg Wojtyniak**, Hannah Britz, Dominik Selzer, Matthias Schwab, and Thorsten Lehr. "Data digitizing: accurate and precise data extraction for quantitative systems pharmacology and physiologically-based pharmacokinetic modeling." In: *CPT: Pharmacometrics & Systems Pharmacology* 9.6 (June 2020), pp. 322–331. DOI: 10.1002/psp4.12511

#### 3.1.2 *Author Contributions*

Following CRediT [4, 5], the contributions of the individual authors are listed in Table 3.1.<sup>1</sup>

Table 3.1: Author contributions for Publication I - Data Digitizing

Jan-Georg Wojtyniak	See included publications and contribution report on page vi
Hannah Britz	Conceptualization, Investigation, Writing - Review & Editing, Visualization
Dominik Selzer	Conceptualization, Software, Formal Analysis, Writing - Review & Editing
Matthias Schwab	Conceptualization, Writing - Review & Editing
Thorsten Lehr	Conceptualization, Investigation, Project Administration, Writing - Original Draft, Writing - Review & Editing

#### 3.1.3 *Copyright*

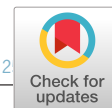
This is an open access article under the terms of the Creative Commons Attribution-NonCommercial License (CC BY-NC 4.0), which permits use, distribution and reproduction in any medium, provided the origi-

---

<sup>1</sup> For a description of the different taxonomy categories see appendix Chapter B

nal work is properly cited and is not used for commercial purposes.

©2020 The Authors Some Rights Reserved



Citation: CPT Pharmacometrics Syst. Pharmacol. (2020) XX, 1–10; doi:10.1002/psp4.12

## ARTICLE

# Data Digitizing: Accurate and Precise Data Extraction for Quantitative Systems Pharmacology and Physiologically-Based Pharmacokinetic Modeling

Jan-Georg Wojtyniak<sup>1,2</sup>, Hannah Britz<sup>1</sup>, Dominik Selzer<sup>1</sup>, Matthias Schwab<sup>2,3,4</sup> and Thorsten Lehr<sup>1,\*</sup>

In quantitative systems pharmacology (QSP) and physiologically-based pharmacokinetic (PBPK) modeling, data digitizing is a valuable tool to extract numerical information from published data presented as graphs. To quantify their relevance, a literature search revealed a remarkable mean increase of 16% per year in publications citing digitizing software together with QSP or PBPK. Accuracy, precision, confounder influence, and variability were investigated using scaled median symmetric accuracy ( $\zeta$ ), thus finding excellent accuracy (mean  $\zeta = 0.99\%$ ). Although significant, no relevant confounders were found (mean  $\zeta \pm SD$  circles =  $0.69\% \pm 0.68\%$  vs. triangles =  $1.3\% \pm 0.62\%$ ). Analysis of 181 literature peak plasma concentration values revealed a considerable discrepancy between reported and *post hoc* digitized data with 85% having  $\zeta > 5\%$ . Our findings suggest that data digitizing is precise and important. However, because the greatest pitfall comes from pre-existing errors, we recommend always making published data available as raw values.

### Study Highlights

#### WHAT IS THE CURRENT KNOWLEDGE ON THE TOPIC?

☑ In quantitative systems pharmacology (QSP) and physiologically-based pharmacokinetic (PBPK) modeling, data digitizer becomes a valuable tool to translate literature data from a graphical representation into numerical values.

#### WHAT QUESTION DID THIS STUDY ADDRESS?

☑ This study investigated the usage of digitizing software in QSP and PBPK modeling. Moreover, it evaluated the software accuracy, precision, confounder influence, and variability between software. In addition, the discrepancies between reported and graphically presented data were analyzed.

#### WHAT DOES THIS STUDY ADD TO OUR KNOWLEDGE?

☑ The results of this study contributed to an improved understanding of the precision and accuracy of digitizing software.

#### HOW MIGHT THIS CHANGE DRUG DISCOVERY, DEVELOPMENT, AND/OR THERAPEUTICS?

☑ The study findings could help improve the quality of the QSP and PBPK models, which were developed based on digitized literature data. Furthermore, they can protect the modeler from using biased data that could subsequently lead to false *in silico* predictions and hence hamper the drug discovery and development process or, even worse, harm patients as a result of erroneously derived therapy recommendations.

During the past few years, quantitative systems pharmacology (QSP) and especially physiologically-based pharmacokinetics modeling (PBPK) have proven to be an important cornerstone of model-informed drug discovery and development.<sup>1</sup> However, for model development, time-dependent data of pharmacological relevant processes are a crucial requirement. Unfortunately, published data are typically presented in aggregate form as plots or graphs without providing access to the underlying raw, uncondensed data. As a result, researchers must extract the information of interest from the graphical representation to use the data for their modeling approaches. Despite the potential to automatically data-mine population average

pharmacokinetic (PK) data for certain applications,<sup>2</sup> data extraction from graphical representations still requires manual efforts. To illustrate the scale of this issue, it should be noted that PBPK projects not uncommonly rely on extracted data gathered from up to 50 articles.<sup>3–9</sup> Fortunately, several off-the-shelf digitization software packages that allow the extraction of numerical information from their two-dimensional graphical representation are currently available.<sup>10–13</sup> These software solutions have been in active use for some time for the well-established population PK approaches.<sup>14</sup> However, neither for them nor for QSP or PBPK modeling is information available regarding the importance and use of digitizing software. Moreover, to the best of our knowledge,

<sup>1</sup>Clinical Pharmacy, Saarland University, Saarbrücken, Germany; <sup>2</sup>Dr. Margarete Fischer-Bosch-Institute of Clinical Pharmacology, Stuttgart, Germany; <sup>3</sup>Department of Clinical Pharmacology, Pharmacy and Biochemistry, University Tübingen, Tübingen, Germany; <sup>4</sup>Cluster of Excellence iFIT (EXC2180) "Image-guided and Functionally Instructed Tumor Therapies", University of Tübingen, Tübingen, Germany. \*Correspondence: Thorsten Lehr (thorsten.lehr@mx.uni-saarland.de)

Received: October 10, 2019; accepted: April 9, 2020. doi:10.1002/psp4.12511

there is no systematic evaluation of the accuracy and precision of these software solutions, nor have any interfering factors that could potentially bias the digitized output been identified. In addition, little is known about the extent of discrepancy between reported and graphically presented data that is typically only revealed after *post hoc* digitization and the nature of these errors and confounding factors when it comes to the digitization process. Consequently, these factors can potentially interfere with model development and evaluation processes and ultimately lead to false predictions and questionable model-based decisions.

Thus, the first objective of this analysis was to assess the general usage of the data digitizing software for QSP and PBPK modeling. Second, this analysis aimed to evaluate the accuracy and precision of a relevant digitizing software. Moreover, discrepancies between reported and graphically presented data were quantified, and the covariates influencing the digitizing process were identified. Finally, recommendations regarding the creation of digitizable plots and graphs and the digitization process itself were proposed.

## METHODS

### Literature search

In a first step, literature published between January 2005 and September 2019 were queried for terms regarding the most common digitizing software in combination with the two terminologies “systems pharmacology” and “physiologically based pharmacokinetic.” For this purpose, the software Publish or Perish<sup>15</sup> was used using the Google Scholar search engine for terminology queries. Google Scholar was used because the search engine allows a full-text analysis, which was a prerequisite because the use of digitizing software is, in most cases, only mentioned in the Methods sections of texts. For each digitizing software, the search query “systems pharmacology OR physiologically based pharmacokinetic AND software name” was used. The search was performed by one author (J.-G.W.) and reviewed by two other authors (H.B., D.S.). The search query results were not further edited or restricted by specific exclusion criteria. Moreover, no gray literature analysis was performed. Subsequently, the annual publications that contain the terms were used as a surrogate marker of importance. Furthermore, Poisson regression was applied to describe and predict the trends in software usage from 2005 to 2021. Moreover, a detailed search for publications from 2012 to 2019 in *CPT: Pharmacometrics & Systems Pharmacology (CPT:PSP)* was also performed. For this, the search query “systems pharmacology OR physiologically based pharmacokinetic AND software name” was used. To identify unreported uses of digitization, all publications from *CPT:PSP* containing only the terms “systems pharmacology OR physiologically based pharmacokinetic” without the name of a digitization software were selected. Following this, the cumulative publication frequency was calculated. Afterward, based on the assumption that data digitization is necessary for every project related to QSP or PBPK, the relative frequency of unreported digitizing software usage was estimated. Finally, to investigate the reporting rate of digitizing techniques in the methods, all published articles from *CPT:PSP* from 2018 were reviewed manually to identify articles related to PBPK that referenced a digitizing software and most likely had used literature data.

### Software evaluation

A study was performed to assess the accuracy and precision of the digitizing software GetData Graph Digitizer<sup>10</sup> and to identify the interfering factors that potentially have an influence on the digitized output. As study inclusion criteria, the subjects had to be at least 18 years old and be able to use the digitization software independently after a standardized software introduction. Furthermore, they had to give informed consent and, following this, were randomly split into two groups (group 1 and group 2). All subjects had to fill out a standardized questionnaire to collect demographics such as age and education. They were asked to digitize the same steady-state plasma concentration-time graph of a hypothetical drug (two-compartment model, absorption constant ( $K_a$ ) = 3 hour<sup>-1</sup>, plasma clearance (CL) = 4 L/hour, central volume of distribution ( $V_1$ ) = 20 L, intercompartmental clearance (Q) = 3 L/hour, peripheral volume of distribution ( $V_2$ ) = 70 L, oral bioavailability ( $F$ ) = 100%, dose = 1 mg simulated using Berkeley Madonna V 8.3.18 developed by Robert Macey and George Oster, University of California, Berkeley, CA) three times in a row. The two-compartment model was chosen as it can be easily parametrized and because the simulations can be easily reproduced. To minimize a possible bias attributed to learning effects, the plasma concentration-time profile in group 1 consists of 10 values marked as circles following 10 values marked as triangles (sample time points: 0, 1, 2, 3, 5, 7, 10, 13, 16, 20, 24, 25, 26, 27, 29, 31, 34, 37, 40, 44). The profile in group 2 was designed as triangles first and circles last. The random allocation sequence for the study subjects was generated with Excel 2016 (Microsoft, Redmond, WA) using a two-sized block randomization and implemented via consecutive questionnaire numbers. No blinding was performed. To validate that demographics are equally distributed within the groups, an analysis of variance (ANOVA) or chi-square goodness-of-fit tests were performed for continuous and categorical demographics, respectively. If the study data were missing, it was imputed with calculated median values for continuous variables and with calculated modal values for categorical variables. To evaluate a potential bias attributed to missing values, statistical analyses were performed with and without imputed values whenever necessary, and the results were compared afterward.

For comparing accuracy and precision, the scaled median symmetric accuracy ( $\zeta$ )<sup>16</sup> and  $\zeta$  standard deviation (SD) were calculated as shown in Eqs. 1–4. Scaling (minimum–maximum normalization<sup>17</sup>) as depicted in Eq. 1 was independently performed for time and concentration values.  $\zeta$  was calculated over the combined vector of scaled values for time and concentration values.

$$X_{\text{scaled}} = \frac{X - X_{\text{min}}}{X_{\text{max}} - X_{\text{min}}} + \varepsilon_{\text{machine}} \quad (1)$$

$$Q_i = \frac{X_{\text{scaled, digitized}}}{X_{\text{scaled, simulated}}} \quad (2)$$

$$\zeta = 100 * \left( \exp \left( \text{median} \left( \left| \log_e(Q_i) \right| \right) \right) - 1 \right) \quad (3)$$

$$SD = \sqrt{\frac{1}{n-1} \sum_{i=1}^n (x_i - \bar{x})^2} \quad (4)$$

With  $x_{\text{scaled}}$  = scaled value,  $x$  = original value,  $x_{\text{min}}$  = minimum of the original values,  $x_{\text{max}}$  = maximum of the original values,  $\epsilon_{\text{machine}}$  = machine epsilon,  $Q_i$  = accuracy ratio,  $x_{\text{scaled,digitized}}$  = scaled digitized value,  $x_{\text{scaled,simulated}}$  = scaled simulated value,  $n$  = number of  $\zeta$  values, and  $x_i = \zeta$ ,  $\bar{x}$  = mean  $\zeta$ .

Because  $\zeta$  for values equal zero is not defined, the machine epsilon (2.2E-16) was added to each value. Afterward, the impact of demographic variables (age, sex, education, average computer usage per day, experience with digitizing software, and right-handedness) and study-specific variables (digitizing time, symbol shape, type of computer used, and mouse usage) on  $\zeta$  were investigated using multiple linear regression. Moreover, to analyze if multiple digitization leads to better results, an ANOVA with different repetitions on  $\zeta$  was performed.

The required study sample size was calculated for comparing two sample means with an equal variance. Because no literature reference values were available, a mean  $\zeta$  of 5% and a variance of 2% for circle shapes were assumed. Furthermore, a 1.5% increase of  $\zeta$  in the triangle group was assumed compared with circles. From this, the necessity of at least 62 subjects was calculated to get a significant result with a statistical power of 80%, and a significance level of 5% and a dropout rate of 10% were assumed ( $28 \cdot 2 \cdot 1.1 = 61.6$ ).

Subsequently, to investigate the impact of the use of digitized data on parameter estimation, the PK parameters of the hypothetical drug were estimated for each of the digitized profiles via nonlinear optimization using the lbfgsb3 R package.<sup>18</sup> Afterward, the relative deviation compared

to the parameters used for simulation were calculated and visualized.

Consequently, a substudy with 14 subjects from the main study group was conducted to compare the accuracy and precision of the digitization software packages DataThief, Engauge Digitizer, and GetData Graph Digitizer. In this study, the subjects digitized the graph from group 1 with each digitization software. Afterward,  $\zeta$  and  $\zeta$  SD were calculated for the digitized profiles and subsequently analyzed via an ANOVA and pairwise  $t$ -test. The graphs of both groups and an overview of the whole study procedure are shown in **Figure 1**. The three digitization software packages DataThief, Engauge Digitizer, and GetData Graph Digitizer were selected based on the criteria of software availability, usability, included features, and the feedback from a small user survey (10 subjects from our group). A comprehensive list of the different digitization software features can be found in **Table S1**.

#### Analysis of published PK data

Finally, the extent of discrepancy between the reported and graphically presented data were investigated based on published sample time points and mean peak plasma concentration ( $C_{\text{max}}$ ) values. For this, digitized readouts as well as published raw values from single and multiple dose profiles that were previously digitized in-house with GetData Graph Digitizer were used. A complete list from all studies included can be found in the supplementary material in Tables S2 and S3. Unscaled  $\zeta$  was calculated individually for all available values. Following this, a stepwise multivariate linear regression analysis (forward inclusion  $P \leq 0.05$ , backward elimination  $P \leq 0.01$ ) was performed to investigate the relationship between the  $\zeta$  values and the portable

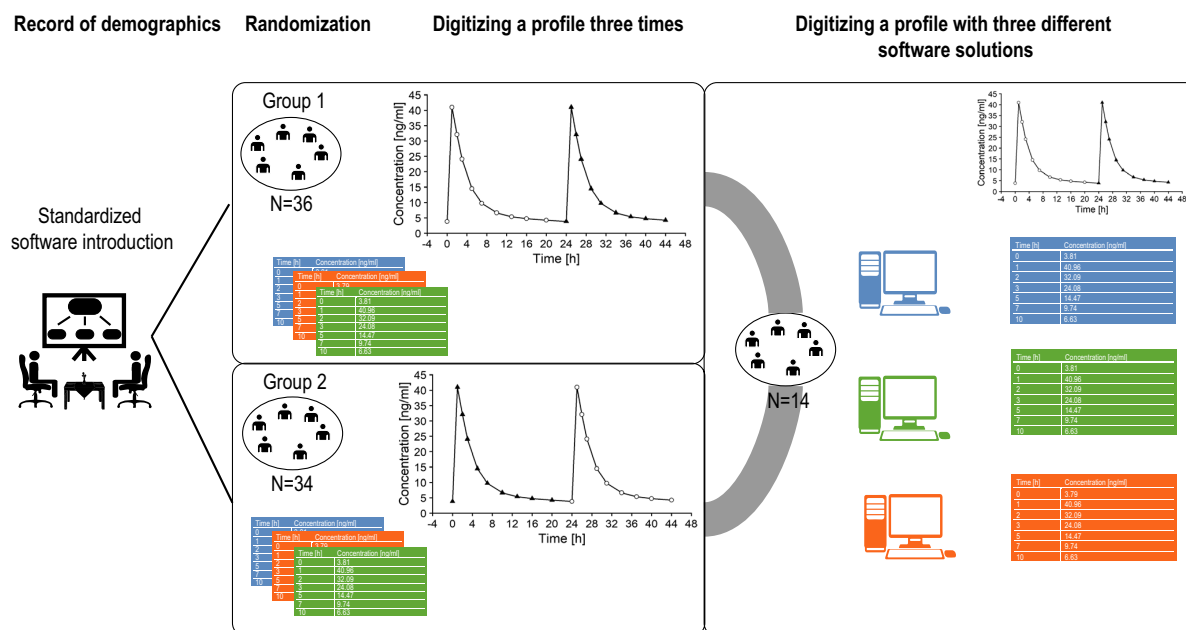


**Figure 1** Schematic overview of the study protocol as well as the concentration-time profiles digitized by study subjects.

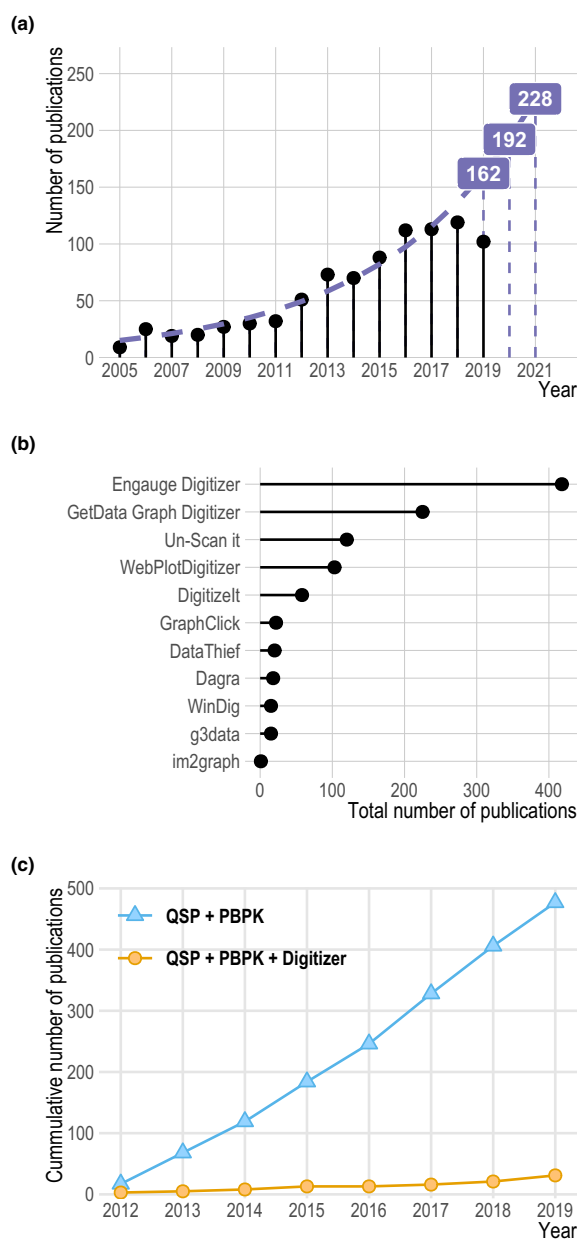


**Figure 2** Results from literature search. **(a)** Number of publications containing the terms “systems pharmacology” or “physiologically based pharmacokinetic” and the names of the digitization software packages investigated during the past few years. Labels and the dashed purple line shows model-estimated values. Solid lollipops represent the observed values. **(b)** Total number of publications containing the terms “systems pharmacology” or “physiologically based pharmacokinetic” and the name of the digitization software package for each package investigated. The names investigated were “Engauge Digitizer,” “GetData Graph Digitizer,” “Un-Scan it,” “WebPlotDigitizer,” “Digitizelt,” “GraphClick,” “DataThief,” “Dagra,” “WinDig,” “g3data,” and “im2graph.” **(c)** Analysis of the cumulative publication frequency in *CPT: Pharmacometrics & Systems Pharmacology* of the terms “systems pharmacology” or “physiologically based pharmacokinetic” (blue solid line, triangles) when compared with “systems pharmacology” or “physiologically based pharmacokinetic” (orange solid line, circles) investigated during the the past few years. QSP, quantitative systems pharmacology; PBPK, physiologically-based pharmacokinetics.

Engauge Digitizer was most frequently cited, followed by the GetData Graph Digitizer (see **Figure b2**). For most software, an increase in use during the analyzed time span was observed. Arithmetic mean increase per year was 16%, with the highest increase for WebPlotDigitizer (87%) and the highest decrease for DataThief (–8%) (see **Figure S1**).

The Publish or Perish search query for QSP or PBPK in the journal *CPT:PSP* from 2012 to 2019 revealed 477 publications. In contrast, for the search terms QSP or PBPK and the names of the most important digitization software packages, only 31 entries were found. Based on the assumption that every QSP or PBPK project requires the use of digitization software, these findings led to an underreporting rate of 94%. **Figure 2c** shows the cumulative number of publications for both search queries. In addition, after the manual review of articles published in *CPT:PSP* in 2018, 20 original research articles that presented PBPK modeling results were found. Among those, 16 used concentration-time or other PK data for model development or validation. Among the 16 studies, 12 used literature data that most likely had to be digitized, 3 had access to individual level data, and 1 study used data from a database for their model development. Among the 12 studies that used literature information, 17% ( $n = 2$ ) reported that they had used a digitization software, leading to an underreporting rate of 83%. A detailed overview of the manual review process is shown in **Figure S2** and **Table S4**.

#### Software evaluation

Overall, 70 subjects (51% male) were enrolled in our study. Their mean age was 30 years (range of 18–65 years), and they engaged in a mean computer usage of 4.1 ( $\pm 3.0$ ) hours per day. Only 4% of them had worked with a digitizing software before. All subjects had an educational degree, with the lowest being lower secondary school-leaving certificate and the highest being a doctorate. Demographic characteristics and the number of subjects were equally distributed in both groups as summarized in **Table 1**. The ANOVA and chi-square goodness-of-fit tests revealed no significant differences in study demographics between the groups, with

document format (PDF) (scanned vs. not scanned), the publishing year, and the investigated parameter ( $C_{max}$  or sample time points). In addition, for values that revealed a  $\zeta$  greater than 5%, a root cause analysis was performed.

All graphical and statistical analysis as well as the sample size calculations were performed using R and R-Studio.<sup>19,20</sup>

## RESULTS

### Literature search

Digitizing software is increasingly used in QSP and PBPK modeling as shown in **Figure 2a**. The free and open-source

Table 1 Study demographics

Parameter and descriptive measures	Group 1, N = 36	Group 2, N = 34	Total, N = 70
Age, y, mean (SD)	30 (13)	30 (12)	30 (13)
Average computer usage per day, hour, mean (SD)	4.5 (3.1)	3.7 (2.9)	4.1 (3.0)
Mouse usage, count (%)	31 (86)	30 (88)	61 (87)
No experience with digitization software, count (%)	33 (92)	34 (100)	67 (96)
Right-handedness, count (%)	30 (83)	32 (94)	62 (89)
Male, count (%)	20 (56)	16 (47)	36 (51)

SD, standard deviation.

*P* values always greater than 0.08. The demographic information for all study participants was complete. Thus, no data had to be imputed.

Mean  $\zeta$  was small for all digitized profiles (0.99%), indicating excellent accuracy. Furthermore,  $\zeta$  SD was low (0.72%), revealing a good precision of the software. The regression analysis revealed a significant ( $P < 0.001$ ) effect of symbol shape and digitizing time on  $\zeta$ . These effects are visualized in **Figure 3**. Triangles had a 1.9-fold increased mean  $\zeta$  when compared with circles (1.3% vs. 0.69%) and, hence, were less accurately digitized. Furthermore, subjects digitizing slowly were more accurate than subjects digitizing faster (**Figure 3b**). Besides that, no other covariates had a significant effect on  $\zeta$ .

From the first to the last repetition, the mean digitizing time declined moderately (first, 3.01 minutes; second, 2.24 minutes; third, 2.16 minutes). No statistical difference in accuracy or precision was observed between the three replicates as shown in **Figure S3**.

Furthermore, the estimated PK parameters based on the digitized profiles revealed only small deviations when compared with the parameters used for profile simulation with a mean modulus of the relative deviation of 0.5%. The deviation of all parameters is visualized in **Figure 3c**.

An ANOVA analysis of the performed substudy revealed statistically significant differences in accuracy and precision among the investigated software (**Figure 3d**). GetData Graph Digitizer and Engauge Digitizer had a similar mean  $\zeta$  value (0.2%), whereas DataThief had a markedly increased value (0.5%). The  $\zeta$  SD was 0.1%, 0.2%, and 0.4% for GetData Graph Digitizer, Engauge Digitizer, and DataThief, respectively.

#### Analysis of published PK data

For investigating the literature profile quality, 181 mean  $C_{\max}$  values and 3499 sample time points of concentration-time profiles obtained from 81 literature studies published between 1984 and 2017, which were presented as graphs and as numeric values, were analyzed. Digitization was carried out as part of two of our in-house model developments (simvastatin, ketoconazole). The digitized profiles were originally derived from graphs that had either linear or logarithmic scaled axes and were depicted either as single or panel plots. Therefore, 3% of the sample time points and 85% of the mean  $C_{\max}$  values had a  $\zeta$  greater than 5%. The linear regression analysis revealed that besides the parameter investigated (sample time points or  $C_{\max}$ ), neither the PDF format (scanned vs. not scanned) nor the publishing year had a significant effect on  $\zeta$ .

The subsequently performed root cause analysis found for all sample time points with  $\zeta$  greater 5% a justification, namely, either the x axis was not sufficiently resolved or the x axis in the graphic had an uneven resolution. In contrast, a reason for the discrepancy could be identified in only 40% of the mean  $C_{\max}$  values with  $\zeta$  greater than 5%. Specifically, they were caused either by poor graphic quality, incorrect labeling, or different types of central tendencies presented in the table and graphic. For the remaining digitized mean  $C_{\max}$  values, no justification could be found, leading to an assumption of either incorrectly stated mean  $C_{\max}$  values in the depicted concentration-time profile or in the presented table. An overview of the error frequencies and  $\zeta$  distribution is presented in **Figure 4**.

Finally, based on the most important study findings, a digitization algorithm as depicted in **Figure 5** was formulated that can help guide scientists through the digitization process.

## DISCUSSION

### Literature search

The reuse of data through digitization from published articles is an easy-to-use and attractive way for gathering necessary information, especially in QSP and PBPK modeling. This is also evident in the investigated publication frequencies of “systems pharmacology” or “physiologically based pharmacokinetic” in combination with the names of the investigated digitization software solutions. Thus, a remarkable, constant, and exponential increase in the number of literature references was observed. This was observed not only for the pooled number of publication frequencies but also for most of the software packages themselves. However, it should be mentioned that because of the large number of different software solutions, it is very unlikely that all digitizing software available was investigated. In addition, we assume that the actual number of unreported digitizing software usage is significantly higher and that the software is often not reported. This is supported by the cumulative number of publications from 2012 to 2019 in the journal *CPT:PSP*, where 477 publications citing “systems pharmacology” or “physiologically based pharmacokinetic” are published but only 31 publications additionally mention the name of a digitizer software. Subsequently, even if not every publication on the subject requires digitization software, this still suggests a massive underreporting. This assumption is further validated by the manual review of publications

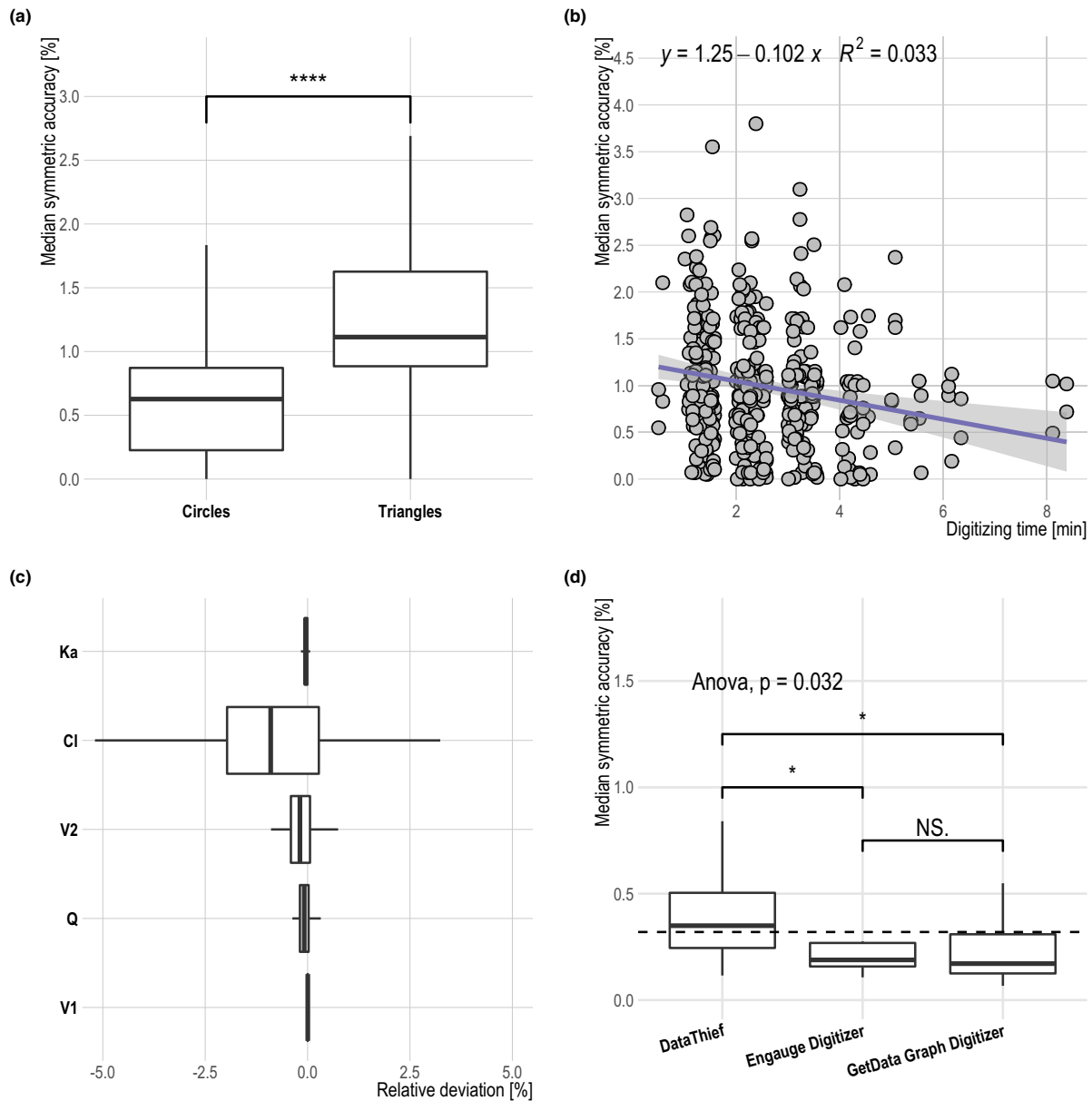


**Figure 3** Results from the multiple linear regression analysis. Influence of the symbol shape (a) on median symmetric accuracy is visualized as a boxplot with the Wilcoxon rank sum test. Effect of digitizing time (b) on median symmetric accuracy is depicted as a scatterplot with linear regression formula and coefficient of determination. (c) Relative pharmacokinetic parameter deviation of the estimated parameters when compared with the values used for profile simulation is shown as boxplots. Parameter estimation was performed for each digitization run. (d) Median symmetric accuracy for different digitization software shown as boxplots. ANOVA as well as pairwise Wilcoxon rank sum tests were performed. ANOVA  $P$  value is stated. For Wilcoxon rank sum test  $P$  values, the following annotation was used: \*\*\*\* $\leq 0.0001$ , \*\* $\leq 0.01$ ; \* $\leq 0.05$ ; NS  $> 0.05$ . In addition, in d arithmetic, the mean of all groups is shown as a dashed line. All boxplots visualize the following descriptive statistics: The median value, the interquartile range, and the 1.5-fold interquartile range. ANOVA, analysis of variance; NS, not significant.

from 2018 in *CPT:PSP* on PBPK modeling, revealing a reporting rate of 17%.

As a drawback of the performed literature search, one can state that the search query results were not further revised, and no gray literature analysis was carried out as

recommended for systematic reviews. However, the purpose of the literature search was not the development of a systematic and exhaustive review but, rather, the identification of general trends. For this reason, the methodology differs from that of a systematic review. For example, search



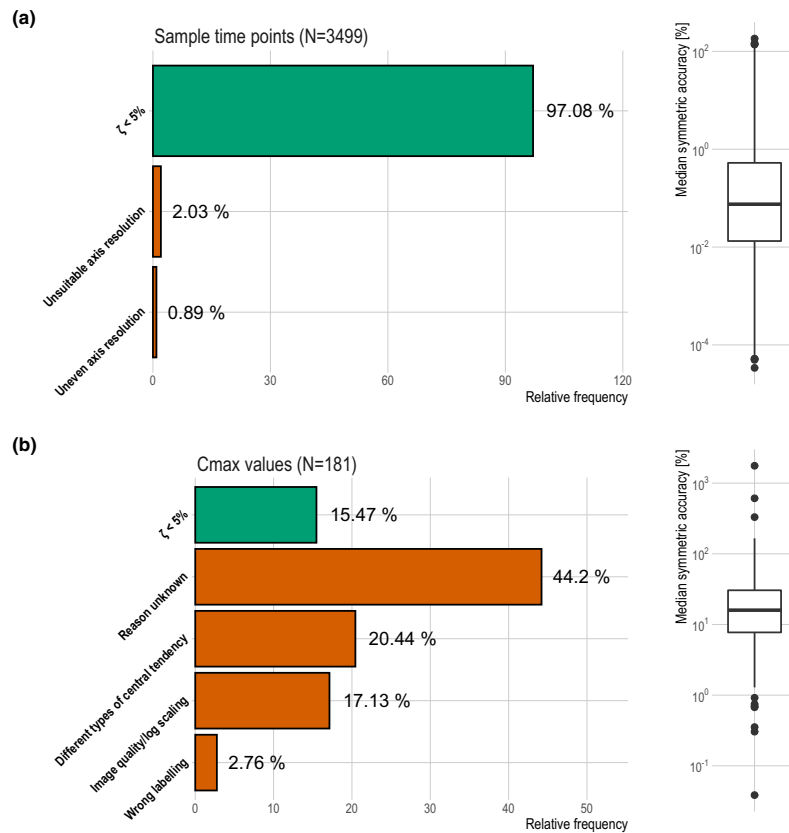


**Figure 4** Discrepancy between reported and graphically presented sample time points and mean  $C_{\max}$  values. Relative frequency of  $\zeta < 5\%$  and justifications for  $\zeta$  values  $\geq 5\%$  were presented as bar charts. Distribution of  $\zeta$  values were in addition shown as boxplots. **(a)** depicts the results for digitized sample time points while **(b)** displays the digitized mean  $C_{\max}$  values.  $C_{\max}$ , peak plasma concentration.

queries were not carried out in various databases such as PubMed or Embase as recommended for systematic reviews. Instead, the search engine Google Scholar was used, whose algorithm screens many different databases and sources; moreover, this is better suited to get an overview of the frequency of use in literature.

Nevertheless, it can be assumed that the usage of digitizing software in QSP and PBPK modeling will further increase in the next few years as shown in **Figure 2**.

### Software evaluation

For the study with 70 subjects,  $\zeta$  was chosen as an error metric because of its intuitive interpretation as a relative error.<sup>16</sup> With a mean  $\zeta$  of 0.99% and a mean  $\zeta$  SD of 0.725%, the digitized readouts were tremendously accurate and precise. This is also reflected in the accuracy of the PK parameters subsequently fitted to the digitized profiles showing a mean modulus of relative deviation of 0.5% when compared with the original values. This further suggests the assumption that the accuracy of individual digitized values is less important because they are not independently analyzed in the model but as time-dependent series of values. Apart from this, the symbol shape and digitizing time revealed a significant effect on the accuracy ( $\zeta$ ), leading, for example, to a 1.9-fold

lower mean  $\zeta$  value for circles when compared with triangles. Nevertheless, these effects are still negligible, considering the overall small  $\zeta$ . Although the average digitizing time declined with each repetition, no advantages in accuracy were observed if the same graph was digitized more than once. Based on these results, we recommend that one-time, slow-paced digitizing is sufficient for a proper readout.

The additionally performed substudy revealed significant differences in accuracy comparing DataThief and the two software products Engauge Digitizer and GetData Graph Digitizer. Here, DataThief showed a 1.5-fold decline in accuracy when compared with Engauge Digitizer and GetData Graph Digitizer. As mentioned previously, this effect is still negligible because the mean  $\zeta$  for all three software packages was still less than 0.6%. This led to the assumption that although significant differences between the software exist, accuracy is still excellent, and thus, other software features are more important. For example, the freely available and open-source software Engauge Digitizer is still under active development on GitHub, providing a wide range of functionalities and available in different languages for multiple operating systems. Although this might raise the question of whether, apart from the software, other factors such as the operating system also have an impact on

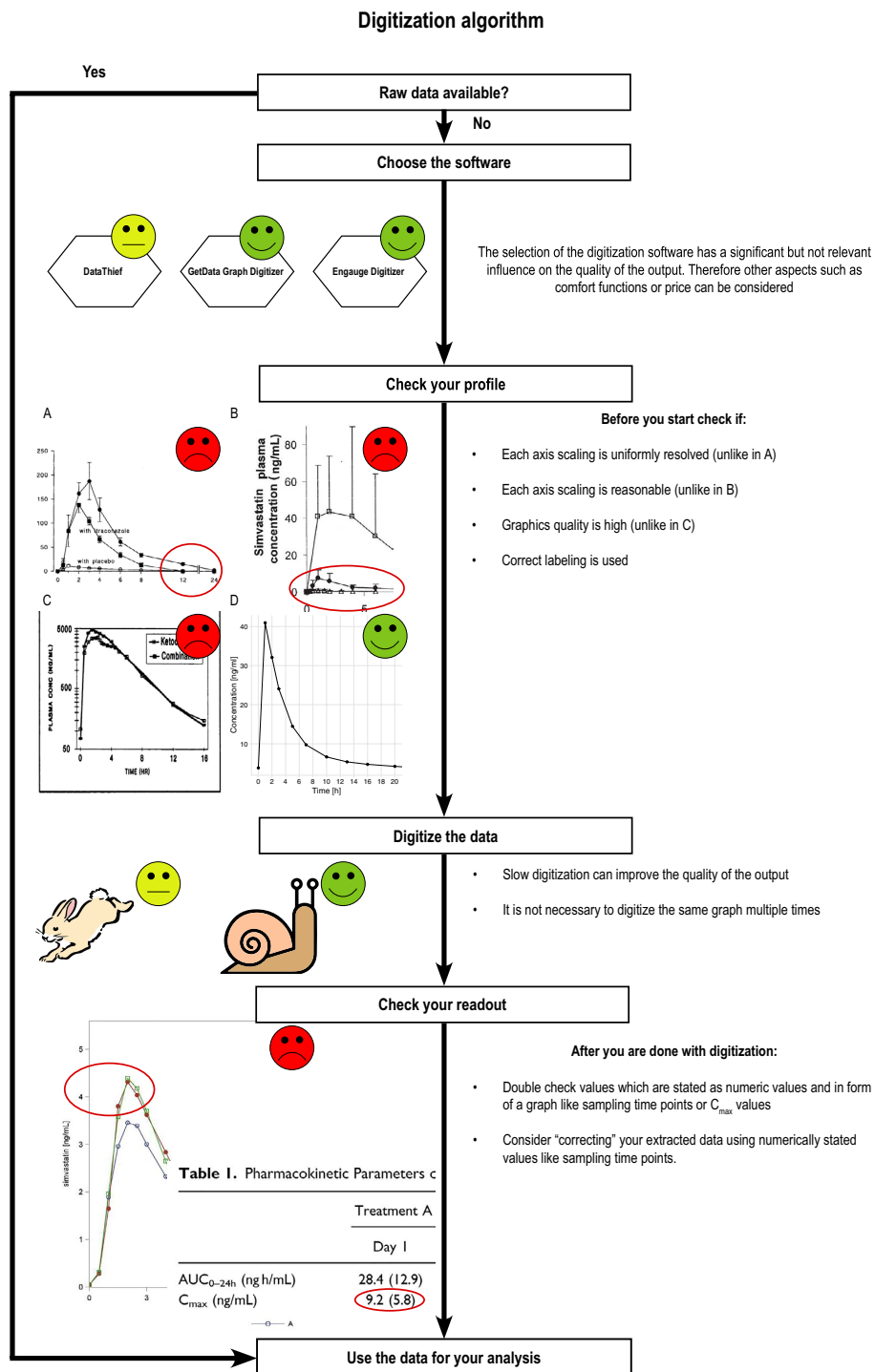


**Figure 5** Proposed digitization algorithm to improve the daily digitizing and graph creation practice in the fields of quantitative systems pharmacology and physiologically-based pharmacokinetics. Examples are taken from refs. 22 to 25. AUC<sub>0-24h</sub>, area under the plasma concentration-time curve calculated from 0 to 24 hours post dose; C<sub>max</sub>, peak plasma concentration.

accuracy, at least for Engauge, this is very unlikely because it is programmed in Qt, an operating system-independent programming language.<sup>12,21</sup>

#### Analysis of published PK data

Data that were redundantly presented as numeric values as well as in a graphs or plots were analyzed using  $\zeta$  as an error metric for the differences between reported values and the corresponding digitized graphical representation. If  $\zeta$  was  $> 5\%$ , the graphs and plots were further explored to determine the article properties that may impede researchers from retrieving correct readouts.  $\zeta$  of the digitized sample time points were in good agreement with the results derived from the previously conducted study. However, a few sources of errors could be identified. Specifically, the resolution of the axes seemed to have an important influence on the quality of the digitized readout. If one of the axis resolutions is uneven or the resolution does not allow cleanly distinguishing between individual measuring points, the result can be falsified. Surprisingly, with 80% of the 181 mean  $C_{\max}$  values having a  $\zeta > 5\%$  and a maximum  $\zeta$  of 1760%, alarmingly large differences between the published numerical values and the values in graphs were found. Even worse, as shown in **Figure 4**, after the performed root cause analysis for 40% of the  $C_{\max}$  values with  $\zeta$  greater 5%, no justification could still be identified. This leads to the assumption that either the wrong graph was plotted or a wrong  $C_{\max}$  was reported. Based on these findings, we strongly recommend that published data should additionally always be made available as raw data. Furthermore, if such access is available, digitizing reported and graphically presented data should be avoided; instead, raw data should be used. Moreover, if access to raw data is not available, researchers should check that each axis scaling is uniformly and optimally resolved, the graphics quality is high, and the correct labeling is used. In addition, they should try to double check their digitized values based on values that are additionally published in a numeric form. However, although following the last recommendation may prevent the use of corrupted data, there is no option to correct the readout if the errors that are already present before digitization get detected. Consequently, it is very likely that many profiles cannot be reused after all. For this reason, it is hoped that in the long run, all data published in condensed form as graphs will also be made available to scientists as raw values.

In summary, it was found that digitizing software has become more popular, especially in QSP and PBPK modeling. The presented results indicate that they are a great tool to gather data from graphical representations with excellent accuracy and precision. Moreover, neither user-dependent nor software-dependent relevant confounders could be identified. Although the digitizing time, symbol shape, and software used had a statistically significant influence on digitizing accuracy, the impact on the routine digitizing practice seems negligible. Digitizing a graph more than once did not improve the quality of the readout and thus is redundant. However, it was also found that the greatest danger of incorrectly derived analysis results based on digitized data does not come from the process of digitizing but from pre-existing errors in the published data. Overall, the results of this study

are the results of the first systematic investigation on the accuracy and precision of digitizing software. Hopefully, the derived recommendations as summarized in **Figure 5** may guide and improve the daily digitizing and graph creation practice in the field of QSP and PBPK modeling and eventually enhance the quality of models developed based on digitized readouts.

**Supporting Information.** Supplementary information accompanies this paper on the *CPT: Pharmacometrics & Systems Pharmacology* website ([www.psp-journal.com](http://www.psp-journal.com)).

**Acknowledgments.** The authors thank Ina Schneider and Melanie Titze who carried out the face-to-face interviews and helped design the study and analysis. In addition, the authors thank all the study subjects who diligently digitized our simulated profiles.

**Funding.** This work was funded by the Robert Bosch Stiftung (Stuttgart, Germany), the European Commission Horizon 2020 UPgX grant 668353, a grant from the German Federal Ministry of Education and Research (BMBF 031L0188D), the nanoCELL consortium grant 03XP0196C, the VISION consortium grant 031L0153A and the Deutsche Forschungsgemeinschaft (DFG, German Research Foundation) under Germany's Excellence Strategy—EXC 2180—390900677.

[Correction added on 19 June 2020 after first publication: Funding Information section was included.]

**Conflict of Interest.** The authors declared no competing interests for this work.

**Author Contributions.** J.-G.W., H.B., D.S., M.S., and T.L. wrote the manuscript. J.-G.W., H.B., D.S., M.S., and T.L. designed the research. J.-G.W., H.B., and T.L. performed the research. J.-G.W. and D.S. analyzed the data.

**Data Availability Statement.** The datasets generated and analyzed during the current study as well as the scripts for reproducing the analysis results are available on request from the corresponding author.

- Lippert, J. *et al.* Open systems pharmacology community—an open access, open source, open science approach to modeling and simulation in pharmaceutical sciences. *CPT Pharmacometrics Syst. Pharmacol.* **8**, 878–882 (2019).
- Wang, Z. *et al.* Literature mining on pharmacokinetics numerical data: a feasibility study. *J. Biomed. Inform.* **42**, 726–735 (2009).
- Türk, D. *et al.* Physiologically based pharmacokinetic models for prediction of complex CYP2C8 and OATP1B1 (SLCO1B1) drug-drug-gene interactions: a modeling network of gemfibrozil, repaglinide, pioglitazone, rifampicin, clarithromycin and itraconazole. *Clin. Pharmacokinet.* **58**, 1595–1607 (2019).
- Britz, H. *et al.* Physiologically-based pharmacokinetic models for CYP1A2 drug-drug interaction prediction: a modeling network of fluvoxamine, theophylline, caffeine, rifampicin, and midazolam. *CPT Pharm. Syst. Pharmacol.* **8**, 296–307 (2019).
- Hanke, N. *et al.* PBPK models for CYP3A4 and P-gp DDI prediction: a modeling network of rifampicin, itraconazole, clarithromycin, midazolam, alfentanil, and digoxin. *CPT Pharm. Syst. Pharmacol.* **7**, 647–659 (2018).
- Hanke, N. *et al.* A physiologically based pharmacokinetic (PBPK) parent-metabolite model of the chemotherapeutic zoletarelin doxorubicin-integration of in vitro results, Phase I and Phase II data and model application for drug-drug interaction potential analysis. *Cancer Chemother. Pharmacol.* **81**, 291–304 (2018).
- Moj, D. *et al.* A comprehensive whole-body physiologically based pharmacokinetic model of dabigatran etexilate, dabigatran and dabigatran glucuronide in healthy adults and renally impaired patients. *Clin. Pharmacokinet.* **58**, 1577–1593 (2019).
- Schaefer, N., Moj, D., Lehr, T., Schmidt, P.H. & Ramsthaler, F. The feasibility of physiologically based pharmacokinetic modeling in forensic medicine illustrated by the example of morphine. *Int. J. Legal Med.* **132**, 415–424 (2018).

Data Digitizing in QSP and PBPK Modeling  
Wojtyniak et al.

10

9. Moj, D. *et al.* Clarithromycin, midazolam, and digoxin: application of PBPK modeling to gain new insights into drug-drug interactions and co-medication regimens. *AAPS J.* **19**, 298–312 (2017).
10. GetData Graph Digitizer <<http://getdata-graph-digitizer.com/index.php>>.
11. Connected Researchers Graph digitizer comparison—16 ways to digitize your data <<http://connectedresearchers.com/graph-digitizer-comparison-16-ways-to-digitize-your-data/>>.
12. Engauge Digitizer <<http://markumitchell.github.io/engage-digitizer/>>.
13. DataThief III <<https://www.datathief.org/>>.
14. Ocampo-Pelland, A.S., Gastonguay, M.R., French, J.F. & Riggs, M.M. Model-based meta-analysis for development of a population-pharmacokinetic (PPK) model for Vitamin D3 and its 25OHD3 metabolite using both individual and arm-level data. *J. Pharmacokinet. Pharmacodyn.* **43**, 191–206 (2016).
15. Publish or Perish (version 7.12.2505.7183) <<https://harzing.com/resources/publish-or-perish>>.
16. Morley, S.K., Brito, T.V. & Welling, D.T. Measures of model performance based on the log accuracy ratio. *Sp. Weather* **16**, 69–88 (2018).
17. Patro, S.G.K. & Sahu, K.K. Normalization: a preprocessing stage. *IARJSET* **20–22** (2015).
18. Nash, J.C., Zhu, C., Byrd, R., Nocedal, J. & Morales, J.L. lbfgsb3: limited memory BFGS minimizer with bounds on parameters <<https://cran.r-project.org/package=lbfgsb3>> (2015).
19. R Development Core Team. R: A Language and Environment for Statistical Computing, Version 3.6.1 (R Foundation for Statistical Computing, Vienna, Austria, 2008) <<https://www.r-project.org>>.
20. RStudio Team. RStudio: Integrated Development Environment for R, Version 1.2.1114 (RStudio, Boston, MA, 2016) <<http://www.rstudio.com/>>.
21. Qt | Cross-platform software development for embedded & desktop <<https://www.qt.io/>>.
22. Winsemius, A. *et al.* Pharmacokinetic interaction between simvastatin and fenofibrate with staggered and simultaneous dosing: Does it matter? *J. Clin. Pharmacol.* **54**, 1038–1047 (2014).
23. Neuvonen, P.J., Kantola, T. & Kivistö, K.T. Simvastatin but not pravastatin is very susceptible to interaction with the CYP3A4 inhibitor itraconazole. *Clin. Pharmacol. Ther.* **63**, 332–341 (1998).
24. Chung, E., Nafziger, A.N., Kazierad, D.J. & Bertino, J.S. Comparison of midazolam and simvastatin as cytochrome P450 3A probes. *Clin. Pharmacol. Ther.* **79**, 350–361 (2006).
25. Knupp, C.A., Brater, D.C., Relue, J. & Barbhaiya, R.H. Pharmacokinetics of didanosine and ketoconazole after coadministration to patients seropositive for the human immunodeficiency virus. *J. Clin. Pharmacol.* **33**, 912–927 (1993).

© 2020 The Authors. *CPT: Pharmacometrics & Systems Pharmacology* published by Wiley Periodicals LLC on behalf of American Society for Clinical Pharmacology and Therapeutics. This is an open access article under the terms of the Creative Commons Attribution-NonCommercial License, which permits use, distribution and reproduction in any medium, provided the original work is properly cited and is not used for commercial purposes.

3.2 PUBLICATION II - A PHYSIOLOGICALLY BASED PHARMACOKINETIC (PBPk) PARENT-METABOLITE MODEL OF THE CHEMOTHERAPEUTIC ZOPTARELIN DOXORUBICIN — INTEGRATION OF IN VITRO RESULTS, PHASE I AND PHASE II DATA AND MODEL APPLICATION FOR DRUG-DRUG INTERACTION POTENTIAL ANALYSIS

3.2.1 *Reference*

Nina Hanke, Michael Teifel, Daniel Moj, **Jan-Georg Wojtyniak**, Hannah Britz, Babette Aicher, Herbert Sindermann, Nicola Ammer, and Thorsten Lehr. "A physiologically based pharmacokinetic (PBPk) parent-metabolite model of the chemotherapeutic zoptarelin doxorubicin — integration of in vitro results, Phase I and Phase II data and model application for drug-drug interaction potential analysis." In: *Cancer Chemotherapy and Pharmacology* 81.2 (Feb. 2018), pp. 291–304. DOI: 10.1007/s00280-017-3495-2

3.2.2 *Author Contributions*

Following CRediT [4, 5], the contributions of the individual authors are listed in Table 3.2.<sup>2</sup>

Table 3.2: Author contributions for Publication II - Zoptarelin Doxorubicin

Nina Hanke	Conceptualization, Data Curation, Formal Analysis, Investigation, Methodology, Software, Validation, Visualization, Writing - Original Draft, Writing - Review & Editing
Michael Teifel	Project Administration, Data Curation, Investigation, Validation, Writing - Review & Editing
Daniel Moj	Validation, Software, Visualization, Writing - Original Draft, Writing - Review & Editing
Jan-Georg Wojtyniak	See included publications and contribution report on page vi
Hannah Britz	Methodology, Software, Validation, Formal Analysis, Data Curation, Writing - Original Draft, Writing - Review & Editing, Visualization
Babette Aicher	Project Administration, Writing - Review & Editing
Herbert Sindermann	Data Curation, Investigation, Validation, Writing - Review & Editing

<sup>2</sup> For a description of the different taxonomy categories see also appendix Chapter B

Nicola Ammer	Project Administration, Writing - Review & Editing
Thorsten Lehr	Project Administration, Writing - Original Draft, Writing - Review & Editing

### 3.2.3 *Copyright*

Reprinted by permission from Springer Nature Customer Service Centre GmbH: Springer Nature, Cancer Chemotherapy and Pharmacology.

“A physiologically based pharmacokinetic (PBPK) parent-metabolite model of the chemotherapeutic zoptarelin doxorubicin — integration of in vitro results, Phase I and Phase II data and model application for drug-drug interaction potential analysis.” Hanke et al. ©2017, advance online publication, 04 December 2017 (doi: 10.1007/s00280-017-3495-2 Cancer Chemother. Pharmacol.)



# A physiologically based pharmacokinetic (PBPK) parent-metabolite model of the chemotherapeutic zoptarelin doxorubicin—integration of in vitro results, Phase I and Phase II data and model application for drug–drug interaction potential analysis

Nina Hanke<sup>1</sup> · Michael Teifel<sup>2</sup> · Daniel Moj<sup>1</sup> · Jan-Georg Wojtyniak<sup>1</sup> · Hannah Britz<sup>1</sup> · Babette Aicher<sup>2</sup> · Herbert Sindermann<sup>2</sup> · Nicola Ammer<sup>2</sup> · Thorsten Lehr<sup>1</sup>

Received: 1 September 2017 / Accepted: 28 November 2017 / Published online: 4 December 2017  
© Springer-Verlag GmbH Germany, part of Springer Nature 2017

## Abstract

**Purpose** Zoptarelin doxorubicin is a fusion molecule of the chemotherapeutic doxorubicin and a luteinizing hormone-releasing hormone receptor (LHRHR) agonist, designed for drug targeting to LHRHR positive tumors. The aim of this study was to establish a physiologically based pharmacokinetic (PBPK) parent-metabolite model of zoptarelin doxorubicin and to apply it for drug–drug interaction (DDI) potential analysis.

**Methods** The PBPK model was built in a two-step procedure. First, a model for doxorubicin was developed, using clinical data of a doxorubicin study arm. Second, a parent-metabolite model for zoptarelin doxorubicin was built, using clinical data of three different zoptarelin doxorubicin studies with a dosing range of 10–267 mg/m<sup>2</sup>, integrating the established doxorubicin model. DDI parameters determined in vitro were implemented to predict the impact of zoptarelin doxorubicin on possible victim drugs.

**Results** In vitro, zoptarelin doxorubicin inhibits the drug transporters organic anion-transporting polypeptide 1B3 (OATP1B3) and organic cation transporter 2 (OCT2). The model was applied to evaluate the in vivo inhibition of these transporters in a generic manner, predicting worst-case scenario decreases of 0.5% for OATP1B3 and of 2.5% for OCT2 transport rates. Specific DDI simulations using PBPK models of simvastatin (OATP1B3 substrate) and metformin (OCT2 substrate) predict no significant changes of the plasma concentrations of these two victim drugs during co-administration.

**Conclusions** The first whole-body PBPK model of zoptarelin doxorubicin and its active metabolite doxorubicin has been successfully established. Zoptarelin doxorubicin shows no potential for DDIs via OATP1B3 and OCT2.

**Keywords** AEZS-108 · AN-152 · Doxorubicin · PBPK modeling · Drug–drug interaction · Targeted chemotherapy

## Introduction

Zoptarelin doxorubicin (also known as AEZS-108, AN-152 and ZEN-008) is a fusion molecule of the chemotherapeutic doxorubicin and an LHRHR agonist [1]. The DNA intercalating agent doxorubicin is chemically linked to the carrier molecule D-Lys6-LHRH, which enables specific binding and selective uptake of zoptarelin doxorubicin by tumors expressing receptors for LHRH (“drug targeting”), followed by the intracellular release of the active component doxorubicin. The rationale for the synthesis and development of this hybrid molecule is to increase the cytotoxic specificity, while decreasing the general toxicity when compared to doxorubicin alone.

**Electronic supplementary material** The online version of this article (<https://doi.org/10.1007/s00280-017-3495-2>) contains supplementary material, which is available to authorized users.

✉ Thorsten Lehr  
thorsten.lehr@mx.uni-saarland.de

<sup>1</sup> Clinical Pharmacy, Saarland University, Campus C2 2, 66123 Saarbruecken, Germany

<sup>2</sup> Aeterna Zentaris GmbH, Weismuellerstr. 50, 60314 Frankfurt, Germany

In vitro, zoptarelin doxorubicin has shown stronger anti-proliferative effects in human LHRHR positive ovarian and endometrial cancer cells compared to doxorubicin [2], as well as higher cytotoxic potency in LHRHR expressing human oral and laryngeal carcinoma cells [3]. In nude mice bearing subcutaneous human LHRHR positive endometrial and ovarian tumors, equimolar doses of zoptarelin doxorubicin were significantly more effective in tumor growth inhibition compared to doxorubicin. Furthermore, in the high-dose study arm, seven of the ten mice treated with doxorubicin died, while all ten mice treated with zoptarelin doxorubicin survived [4]. Growth of subcutaneous human urinary bladder cell tumors in nude mice was more potently inhibited by zoptarelin doxorubicin compared to doxorubicin [5].

In clinical Phase I and Phase II studies, zoptarelin doxorubicin has shown therapeutic activity in patients with LHRHR positive ovarian and endometrial cancer [6, 7]. The PK properties of zoptarelin doxorubicin have been assessed in the first-in-human, dose escalation Phase I study in patients. Plasma half-life and clearance were calculated to be approximately 2 h and 1 L/(min\*m<sup>2</sup>), with the reservation that in this early study the measured plasma concentrations showed a high variability [8]. Due to the size and hydrophilicity of zoptarelin doxorubicin (decapeptide coupled via a glutaryl linker to doxorubicin), passive distribution into tissues is limited, but cellular entry is expected to be facilitated by target binding to LHRHR, followed by internalization of the drug–receptor complex and intracellular cleavage to release the doxorubicin moiety within the target cells. In aqueous solution and in blood plasma, zoptarelin doxorubicin is subject to spontaneous and carboxylesterase-mediated hydrolysis into doxorubicin and probably D-Lys6-LHRH-glutarate. Metabolite profiles in liver microsomal incubations suggest a minor role of oxidative metabolism compared to hydrolysis.

Doxorubicin PK studies in patients show that doxorubicin follows a multiphasic disposition after intravenous infusion. The initial distribution half-life of approximately 5 min indicates rapid tissue uptake, while a terminal half-life of 20–48 h reflects slow elimination from tissues. Steady-state distribution volumes exceed 20–30 L/kg revealing extensive drug uptake into tissues. Plasma clearance is in the range of 8–20 mL/min/kg and is governed by metabolism and biliary excretion [9–11].

To evaluate the zoptarelin doxorubicin DDI potential in vitro, a DDI screening on cytochrome P450 (CYP) enzymes and recommended drug transporters has been performed. In these assays, zoptarelin doxorubicin showed no inhibition or induction of CYP enzymes, but in the transporter studies, zoptarelin doxorubicin inhibited OATP1B3 and OCT2 with IC<sub>50</sub> values of 16.5 and 3.26 μmol/L, respectively. Doxorubicin itself and D-Lys6-LHRH-glutarate inhibited OATP1B3 with IC<sub>50</sub> values > 100 μmol/L

and OCT2 with IC<sub>50</sub> values > 200 μmol/L. Based on these results, in vivo interactions with drugs that are substrates of OATP1B3 (e.g. simvastatin) or OCT2 (e.g. metformin) could not be ruled out. As these victim drugs are widely used, their co-administration with zoptarelin doxorubicin would be very likely, creating a need to investigate the impact of these potential DDIs. However, clinical DDI studies involving DNA intercalating agents are, for ethical reasons, difficult to conduct. PBPK modeling offers an excellent alternative to dedicated clinical DDI studies and is recommended and supported by the FDA (US Food and Drug Administration) and EMA (European Medicines Agency) to predict the magnitude of in vivo DDIs from in vitro results [12, 13].

The objectives of this modeling investigation were (1) to establish the first whole-body PBPK model of zoptarelin doxorubicin and its active metabolite doxorubicin, (2) to apply the zoptarelin doxorubicin model for a general assessment of the DDI potential with OATP1B3 and OCT2 victim drugs and (3) to predict the magnitude of zoptarelin doxorubicin DDIs with simvastatin and metformin in worst-case scenarios.

## Materials and methods

### Clinical studies used

The results of three different clinical studies with PK blood sampling were available for model development (Table 1). Study 1 (ZEN-008-Z023) is a Phase I first-in-human sequential group dose escalation and PK study, performed in 17 female patients with LHRHR positive tumors. Zoptarelin doxorubicin was administered as a 2-h intravenous infusion, once every 21 days, in doses of 10, 20, 40, 80, 160 or 267 mg/m<sup>2</sup> [8]. Data of two patients were excluded due to bioanalytical issues. Study 2 (AEZS-108-046) is a combined Phase I/II study, with PK sampling performed in a sub-set of 14 male or female patients with locally advanced unresectable or metastatic LHRHR positive urothelial carcinoma who failed platinum-based chemotherapy. Zoptarelin doxorubicin was administered as a 2-h infusion every 21 days in doses of 160, 210 or 267 mg/m<sup>2</sup> (results not published, yet). Data of four patients were excluded because of sample hemolysis. Study 3 (AEZS-108-053) is a Phase I cardiac safety and PK study comparing zoptarelin doxorubicin and doxorubicin therapy in 21 and 11 female patients, respectively, with locally advanced recurrent or metastatic cancer. Zoptarelin doxorubicin was administered as a 2-h infusion of 267 mg/m<sup>2</sup>. Doxorubicin was administered as a 1-h infusion of 60 mg/m<sup>2</sup> (results not published, yet). Data of two patients were excluded due to sampling issues. Details on the patient demographics of these studies (age, weight, body surface area) are listed in Table 1.



**Table 1** Studies used for zoptarelin doxorubicin PBPK model development and evaluation

Dose (mg/m <sup>2</sup> )	Administration	n	Women (%)	Age (years)	Weight (kg)	BSA (m <sup>2</sup> )	Dataset	Study references
<b>Doxorubicin</b>								
36	iv (96 h), SD	7	50 <sup>a</sup>	30.0 <sup>a</sup>	64.0 <sup>a</sup>	1.73 <sup>a</sup>	Training	[15]
30	iv (bolus), QD	7	50 <sup>a</sup>	30.0 <sup>a</sup>	64.0 <sup>a</sup>	1.73 <sup>a</sup>	Training	[16]
60 <sup>a</sup>	iv (1 h), SD <sup>a</sup>	3 <sup>a</sup>	100 <sup>a</sup>	71.0 (67–74) <sup>a</sup>	67.0 (58–84) <sup>a</sup>	1.64 (1.57–1.77) <sup>a</sup>	Training	[18]
60	iv (1 h), SD	9	100	59.9 (44–74)	64.1 (41–84)	1.63 (1.28–1.81)	Training	Study 3 (AEZS-108-053)
<b>Zoptarelin doxorubicin</b>								
10	iv (2 h), SD	1	100	58.0	84.0	1.89	Training	Study 1 (ZEN-008-Z023)
20	iv (2 h), SD	1	100	48.0	65.0	1.70	Training	Study 1 (ZEN-008-Z023)
40	iv (2 h), SD	1	100	69.0	145.0	2.48	Training	Study 1 (ZEN-008-Z023)
80	iv (2 h), SD	1	100	44.0	55.0	1.63	Training	Study 1 (ZEN-008-Z023)
160	iv (2 h), SD	6	100	59.3 (55–69)	83.2 (58–107)	1.89 (1.60–2.12)	Test	Study 1 (ZEN-008-Z023)
267	iv (2 h), SD	5	100	48.8 (31–63)	66.9 (59–85)	1.73 (1.64–1.89)	Test	Study 1 (ZEN-008-Z023)
160	iv (2 h), SD	3	0	64.0 (63–65)	78.3 (69–90)	1.97 (1.84–2.07)	Test	Study 2 (AEZS-108-046)
210	iv (2 h), SD	3	29	66.0 (55–83)	89.6 (64–121)	2.02 (1.71–2.38)	Test	Study 2 (AEZS-108-046)
267	iv (2 h), SD	4	25	69.0 (62–87)	70.0 (52–86)	1.81 (1.51–1.98)	Test	Study 2 (AEZS-108-046)
267	iv (2 h), SD	21	100	61.6 (46–78)	71.4 (45–108)	1.73 (1.35–2.13)	Training	Study 3 (AEZS-108-053)

Values given for age, weight and BSA are arithmetic means, minima and maxima

<sup>a</sup>Assumed, BSA: body surface area, iv: intravenous, n: number of individuals studied, QD: once daily, SD: single dose, test: test dataset (model evaluation), training: training dataset (model development and parameter optimization)

To supplement the measurements of the doxorubicin arm of Study 3, published human in vivo data of doxorubicin in plasma, white blood cells, urine and feces were added, to build the “training dataset” for the development and parameter optimization of the doxorubicin model. As training data for zoptarelin doxorubicin model development and parameter optimization, the four lowest dose applications of Study 1 (10, 20, 40, 80 mg/m<sup>2</sup>) plus the measurements of Study 3 (267 mg/m<sup>2</sup>, highest clinical dose) were chosen. Evaluation of the zoptarelin doxorubicin model was carried out with the clinical data of the remaining dosing groups of Study 1 as well as the complete clinical Study 2 as the “test dataset”.

## Software

PBPK modeling was performed with PK-Sim® and MoBi® (Open Systems Pharmacology Suite, Version 7.0.0, Bayer AG, Leverkusen, Germany). Parameter optimization was accomplished using the Monte Carlo algorithm of the “Parameter Identification Toolbox” in MATLAB® (Version R2013b, The MathWorks, Inc., Natick, MA, USA). Sensitivity analysis was performed within PK-Sim®. Graphics and PK parameter analyses were compiled with MATLAB® R2013b.

## Doxorubicin model development

Model development was started with the establishment of a model of the active metabolite doxorubicin. To limit the

parameters to be optimized during model development, the minimal number of processes necessary was implemented into the model. For the doxorubicin model these are (1) doxorubicin binding to DNA, (2) an unspecific metabolic hepatic clearance and (3) an unspecific elimination to bile. Glomerular filtration and enterohepatic cycling were enabled, as they are active under physiological conditions. A diagram of the PBPK model structure is given in Zoptarelin Doxorubicin Supplementary Fig. 1.

To model the binding of doxorubicin to DNA as the cause of the extensive distribution into and slow elimination from body tissues, a binding partner was implemented into the DNA-rich organs, with published values for  $K_d$  and  $k_{off}$  [14]. In the literature, there are reports of doxorubicin concentration measurements in plasma and white blood cells [15, 16] that were utilized to inform the distribution (cellular permeability, see below) and DNA binding processes. As there is no white blood cell (WBC) compartment in PK-Sim, the red blood cell (RBC) compartment was used as a substitute to represent the nucleated white blood cells. The volume of this red blood cell compartment is larger than the physiological volume of the white blood cells; therefore, a relative concentration of DNA binding sites (that are absent in the anucleate RBCs) was implemented into the RBC compartment and estimated. The DNA binding site reference concentration (concentration in the tissue with the highest concentration of binding sites) was also optimized.

To account for hepatic metabolism to doxorubicinol and other metabolites, an unspecific metabolic first-order clearance was implemented into the liver and optimized.

To model biliary excretion, an unspecific first-order transport from liver to bile was implemented and estimated. As the lipophilicity of doxorubicin is very low ( $\log P = 1.27$ ), calculated passive cellular permeability is low. However, doxorubicin has been reported to be a substrate of diverse transporters, including the human isoforms of OATP1A and OATP1B [17]. To accurately describe the available clinical data, passive cellular permeability was increased, to compensate for active transport processes that have not been implemented into the model.

To obtain values for the parameters that could not be adequately informed from literature or in-house preclinical studies, optimization was performed by simultaneously fitting the model to the data of the doxorubicin arm of Study 3 (9 patients), measured doxorubicin plasma and white blood cell intracellular concentration–time profiles of Speth et al. [15, 16] (two studies with mean values of 7 patients each) and published fraction of doxorubicin dose administered excreted unchanged to urine and feces information [18].

### Zoptarelin doxorubicin model development

The final doxorubicin model was then used in the establishment of the zoptarelin doxorubicin model, together with clinically observed plasma concentration–time profiles of zoptarelin doxorubicin and doxorubicin following intravenous administration of zoptarelin doxorubicin. The following processes were implemented into the zoptarelin doxorubicin model: (1) zoptarelin doxorubicin binding to the LHRHR target, (2) internalization of zoptarelin doxorubicin by LHRHR and (3) hydrolysis of zoptarelin doxorubicin to release the active doxorubicin moiety within blood plasma as well as intracellularly. A diagram of the PBPK model structure is given in Zoptarelin Doxorubicin Supplementary Fig. 1.

To model the binding of zoptarelin doxorubicin to its target LHRHR, this receptor was implemented and values for  $K_d$ ,  $k_{off}$  as well as the LHRHR reference concentration were estimated. Expression of LHRHR is described in the literature to occur in non-malignant pituitary, ovary, testis, prostate and breast cells, as well as in cancer cells of diverse origin [19, 20]. In the model, LHRHR was implemented into the gonadal compartment (approximate organ volume of 0.013 L). To compensate for the missing pituitary, prostate, breast and, most notably, cancer cell expression, as these tissues are not represented in standard PK-Sim individuals, LHRHR expression was further added at a 50% expression level to the lung compartment (approximate organ volume of 1 L). The lung was chosen as a well perfused organ with no special pharmacokinetic function in this analysis (as would

have been the case with liver or kidney). Implementation of zoptarelin doxorubicin binding to LHRHR into the model clearly improved the shape of the simulated zoptarelin doxorubicin plasma concentration–time curves.

Internalization of zoptarelin doxorubicin was implemented as a cellular uptake facilitated by LHRHR (into gonads and lung), followed by intracellular hydrolysis to release the doxorubicin moiety. As  $K_M$  value of this uptake process an  $IC_{50}$  value of 7.45 nmol/L was used, measured in a radio ligand displacement assay with very low concentrations of the radiolabeled ligand [21]. Therefore, it was assumed that  $IC_{50} = K_i$  and this value was used as  $K_M$  value for the internalization process. A very similar  $IC_{50}$  value of 10 nmol/L has been described in the literature for the binding of the endogenous agonist LHRH to LHRHR [22]. The internalization turnover number was estimated.

To model the hydrolysis of zoptarelin doxorubicin to D-Lys6-LHRH-glutarate and doxorubicin, a hydrolytic clearance was implemented into blood plasma, gonads and lung. The hydrolysis rate in plasma was optimized, informed by the measured concentrations of zoptarelin doxorubicin being hydrolyzed and of doxorubicin resulting from this hydrolysis. The hydrolysis rate in gonads and lung was assumed to be the same as in plasma.

Parameter optimization was performed by simultaneously fitting the model to measured zoptarelin doxorubicin and doxorubicin plasma concentration–time profiles after administration of zoptarelin doxorubicin obtained in Study 1 (10, 20, 40, 80 mg/m<sup>2</sup>) and Study 3 (267 mg/m<sup>2</sup>).

### Virtual population characteristics

To predict the variability of the simulated plasma concentration–time profiles, virtual populations of 100 individuals were generated according to the population demographics of each respective dosing group of the Studies 1, 2 and 3. The ICRP (International Commission on Radiological Protection) database in PK-Sim [23] was used for generation of virtual Caucasian populations. In the generated virtual populations, age, height, weight, corresponding organ volumes, tissue compositions, blood flow rates, etc. are varied by an implemented algorithm within the limits of the ICRP database. In addition, the zoptarelin doxorubicin hydrolysis rate, the reference concentrations of the binding partners LHRHR and DNA, as well as the doxorubicin hepatic and biliary clearance rates were set to be log-normally distributed with variabilities of 25%CV (relative standard deviation). To create a virtual population for the DDI predictions, reflecting an even larger demographic variability and representing the target cancer patient population, preliminary demographics of a large clinical Phase III study (Study 4, AEZS-108-050 [24]) were used.

### Model evaluation

Model performance was evaluated by comparison of the predicted concentration–time profiles of the virtual populations to the plasma concentrations observed in the clinical studies, which had not been used during parameter optimization (test dataset). All population predictions compared to observed plasma concentration–time profiles are documented in the “Results” section or in the supplementary material, together with predicted compared to observed  $AUC_{last}$  and  $C_{max}$  values of all studies. Furthermore, the biological plausibility of optimized parameters was checked and sensitivity analyses were conducted for the doxorubicin and zoptarelin doxorubicin models.

Sensitivity of the final models to single parameters (local sensitivity analysis) was investigated, measured as changes of the AUC extrapolated to infinity ( $AUC_{inf}$ ) of a simulation of the highest applied dose. All parameters relevant to the respective model were included into the analysis, optimized parameters as well as parameters fixed to literature values. Parameters were defined as relevant if they have been optimized (see Zoptarelin Doxorubicin Supplementary Tables 4 and 5), if they might have a strong influence due to calculation methods used in the model (lipophilicity, fraction unbound), if they are related to optimized parameters (doxorubicin-DNA  $K_d$ , doxorubicin-DNA  $k_{off}$ , doxorubicin blood/plasma ratio) or if they had significant impact in former models (solubility, intestinal permeability, EHC continuous fraction, cellular permeability, blood/plasma ratio, GFR fraction). A sensitivity value of  $-1.0$  signifies that a 10% increase of the examined parameter causes a 10% decrease of the simulated  $AUC_{inf}$ .

### General assessment of the zoptarelin doxorubicin DDI potential

To obtain a general statement on the DDI potential of zoptarelin doxorubicin, the final model was applied to predict the in vivo inhibition of OATP1B3 and OCT2 in a generic manner (independent of the victim drug affected by this inhibition), by calculating the relative change of these transporters’  $K_M$  values due to inhibition by zoptarelin doxorubicin.

Assuming a competitive inhibition and Michaelis–Menten kinetics, we expect a change in the  $K_M$  value of the transport of the affected victim drugs, but not of the maximal transport rate, as competitive inhibition can be overcome by high victim drug concentrations. Therefore, the inhibition is characterized by the relative change of  $K_M$  according to Eq. 2:

$$K_M \text{ apparent, victim drug } (\mu\text{mol/L}) = K_M \text{ victim drug} * \left( 1 + \frac{\text{inhibitor concentration}}{\text{inhibitor } K_i} \right) \quad (1)$$

$$K_M \text{ apparent, victim drug } (\%) = 100\% * \left( 1 + \frac{\text{inhibitor concentration}}{\text{inhibitor } K_i} \right) \quad (2)$$

Simulations to assess the DDI potential of zoptarelin doxorubicin were performed for the highest clinical dose of 267 mg/m<sup>2</sup> zoptarelin doxorubicin as intravenous infusion over 2 h. OATP1B3 is predominantly expressed at the basolateral membranes of hepatocytes located around the central vein, facilitating the uptake of organic anions for hepatic clearance [25]. To estimate the effect of zoptarelin doxorubicin on OATP1B3, predicted population interstitial unbound concentrations of zoptarelin doxorubicin in the liver were used as input for Eq. 2. OCT2 is mainly expressed at the basolateral membrane of renal tubule cells, facilitating the uptake of organic cations from the blood for subsequent renal secretion [26]. To estimate the impact of zoptarelin doxorubicin on OCT2, predicted population interstitial unbound concentrations of zoptarelin doxorubicin in the kidney were employed.

The zoptarelin doxorubicin  $K_i$  values for inhibition of OATP1B3 and OCT2 were calculated from  $IC_{50}$  values determined in vitro (16.5 and 3.26  $\mu\text{mol/L}$ ), the substrate concentrations applied in these assays (0.05  $\mu\text{mol/L}$  estradiol-17beta-glucuronide and 10.0  $\mu\text{mol/L}$  metformin) and the OATP1B3 and OCT2 transport  $K_M$  values for these substrates (15.8 [27] and 990.0  $\mu\text{mol/L}$  [28]), according to the Cheng-Prusoff equation for competitive inhibition [29]:

$$K_i = \frac{IC_{50}}{1 + \text{substrate concentration} / K_M} \quad (3)$$

$K_i$  values for pure competitive inhibition are independent of the affected victim substrate, the substrate concentration and the assay conditions [30]. Therefore, the relative changes of  $K_M$  calculated from Eq. 2 are in theory applicable to all putative zoptarelin doxorubicin victim drugs transported by OATP1B3 and OCT2.

### Specific assessment of the zoptarelin doxorubicin DDI potential

To evaluate the in vivo interaction potential of zoptarelin doxorubicin with actual OATP1B3 and OCT2 victim drugs, the model was coupled to PBPK models of simvastatin and metformin (for details on the simvastatin and metformin PBPK models see the Simvastatin and Metformin Supplementaries). Simvastatin acid, the pharmacologically active metabolite of the prodrug simvastatin, is recommended by the FDA as a victim drug for the clinical investigation of OATP1B1/1B3 DDIs [31]. Metformin is recommended by the FDA as well-established substrate of the cationic

transport system for the use in clinical studies of DDIs involving OCT2/MATE [31].

Simvastatin is administered in the form of the inactive lactone that is hydrolyzed after ingestion to the active simvastatin acid. Only the acid form is transported by OATP1B1 and OATP1B3 from blood plasma into hepatocytes. The model applied for DDI prediction is a whole-body parent-metabolite PBPK model of simvastatin lactone and simvastatin acid. Because of the overlapping substrate specificities of OATP1B1 and OATP1B3, it is difficult to pinpoint the exact contribution of each isoform to simvastatin acid transport [32]. As the goal of this analysis was to assess worst-case scenarios, a combined OATP1B1/3 transport was modeled and this whole transport was inhibited with the zoptarelin doxorubicin  $K_i$  determined for OATP1B3, even though OATP1B1 was not affected *in vitro*. This approach results in an overprediction of the impact of OATP1B3 inhibition, but avoids underprediction of the DDI potential due to misspecification of the OATP1B3 contribution.

As worst-case co-administration scenarios, simultaneous administrations of 267 mg/m<sup>2</sup> zoptarelin doxorubicin with 80 mg simvastatin (once daily, day 5) or 1000 mg metformin (three times daily, day 5) were simulated, and victim drug plasma concentrations with and without co-administration of zoptarelin doxorubicin were assessed in population predictions. Different time intervals between the start of zoptarelin doxorubicin infusion and the day 5 morning dose of the victim drugs were simulated, to find the administration schemes resulting in highest drug–drug interaction impact for worst-case scenario assessment.

## Results

A comprehensive parent-metabolite PBPK model for the prediction of zoptarelin doxorubicin and doxorubicin concentrations following different intravenous doses of zoptarelin doxorubicin has been successfully developed.

A schematic representation of the parent-metabolite model structure is shown in Zoptarelin Doxorubicin Supplementary Fig. 1. All drug-dependent parameters of the final model, taken from literature or preclinical studies as well as all optimized parameter values, are given in Zoptarelin Doxorubicin Supplementary Table 4. All system-dependent parameters of the final model, particularly expression levels of the implemented binding partners in the different tissues with their geometric standard deviations of lognormal distribution in virtual populations, are given in Zoptarelin Doxorubicin Supplementary Table 5. No other system-dependent parameters were changed or adjusted.

## PBPK model development and performance

The established doxorubicin and zoptarelin doxorubicin PBPK models show excellent descriptive and predictive performance.

The data used for doxorubicin model development consisted of individual plasma concentration–time profiles following application of 60 mg/m<sup>2</sup> of doxorubicin to a total of nine patients. These measurements were supplemented by literature data of white blood cell concentrations and excretion to urine and feces information (Table 1). Predicted and observed doxorubicin plasma concentrations of Study 3 as well as fractions excreted to urine and feces following administration of doxorubicin are presented in Zoptarelin Doxorubicin Supplementary Fig. 2 (training dataset). Predicted and observed doxorubicin plasma and white blood cell concentrations following administration of doxorubicin as published by Speth et al. are shown in Zoptarelin Doxorubicin Supplementary Fig. 3 (training dataset). These concentrations were fitted with lower weight compared to the measurements of Study 3, given the age of the data and the assumption underlying the blood cell concentrations that 10<sup>9</sup> cells equal a volume of 1 mL, knowing that white blood cells are very diverse in size and shape. Prediction of the doxorubicin concentrations resulting from administration of zoptarelin doxorubicin is presented in Figs. 1 and 2 as well as in Zoptarelin Doxorubicin Supplementary Figs. 4 and 5.

The data used for zoptarelin doxorubicin model establishment included individual plasma concentration–time profiles collected in three clinical trials, following application of seven different doses of zoptarelin doxorubicin in a range of 10–267 mg/m<sup>2</sup>. Plasma concentrations of zoptarelin doxorubicin and doxorubicin were collected in a total of 46 patients (Table 1). Model performance of the final zoptarelin doxorubicin model is demonstrated in Fig. 1 and Zoptarelin Doxorubicin Supplementary Fig. 4 for the studies used during parameter optimization (training dataset) and in Fig. 2 and Zoptarelin Doxorubicin Supplementary Fig. 5 for the independent clinical data (test dataset).

As can be seen in Fig. 1, the inter-individual variability of the measured concentrations is wider for zoptarelin doxorubicin than for doxorubicin. This is unexpected, as the variability of its main ADME mechanism, namely the hydrolysis of zoptarelin doxorubicin to doxorubicin, affects both analytes. The more pronounced variability of the parent compound concentrations in blood plasma, where zoptarelin doxorubicin and doxorubicin are sampled, might result from its very low permeability compared to doxorubicin, which extensively distributes into body tissues [11]. The predicted variability in the population simulations is also wider for zoptarelin doxorubicin.

Furthermore, the variance of the measured concentrations in the very first clinical Study 1 is higher than in the

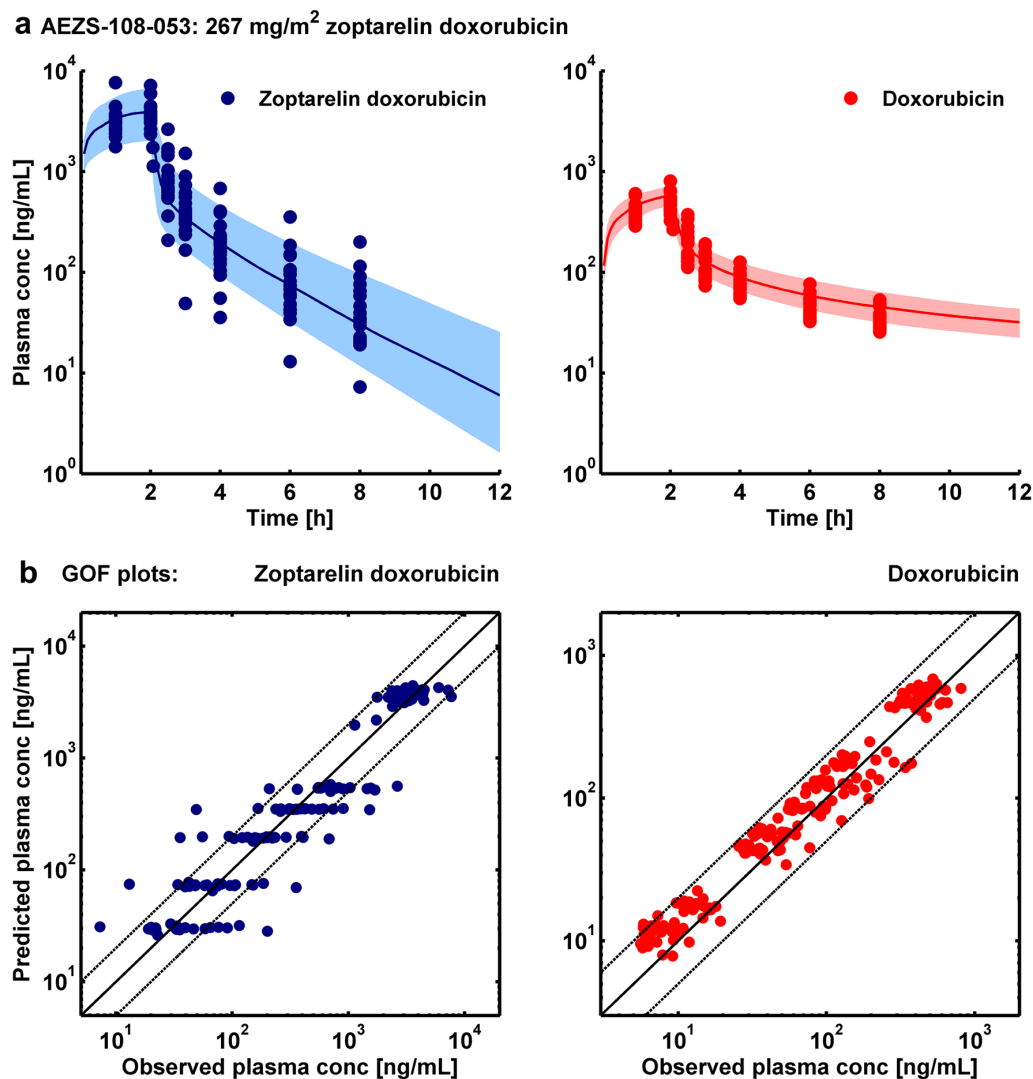


**Fig. 1** Training dataset: **a** Population simulations (semilog scale) compared to observed data of zoptarelin doxorubicin (blue) and doxorubicin plasma concentrations (red) following intravenous administration of 267 mg/m<sup>2</sup> zoptarelin doxorubicin. Clinical data (Study 3,  $n=21$ ) are shown as dots. Population simulation medians are shown as lines; the shaded areas depict the 5th–95th percentile popula-

tion prediction intervals. **b** Goodness of fit (GOF) plots (log scale) demonstrating the correlation of individual predicted with observed zoptarelin doxorubicin (blue) and doxorubicin plasma concentrations (red) of the study shown above. The solid lines represent the line of unity; the dashed lines indicate twofold deviation

following trials (see Zoptarelin Doxorubicin Supplementary Fig. 5, test dataset). This high variability might be the result of errors in sampling time or of hydrolytic cleavage of zoptarelin doxorubicin prior to freezing of some of the blood samples [8]. These issues could be resolved and, therefore, did not affect later measurements.

Precision of model parameter estimates is shown in the tables listing the drug-dependent and system-dependent

zoptarelin doxorubicin PBPK model parameters (Zoptarelin Doxorubicin Supplementary Tables 4 and 5).

Using the final model, pharmacokinetic parameters ( $AUC_{last}$  and  $C_{max}$ ) of all dosing groups have been calculated from population simulations as mean values with standard deviation and compared to observed values (see Zoptarelin Doxorubicin Supplementary Tables 1 and 2). Prediction errors for  $AUC_{last}$  and  $C_{max}$  values are also

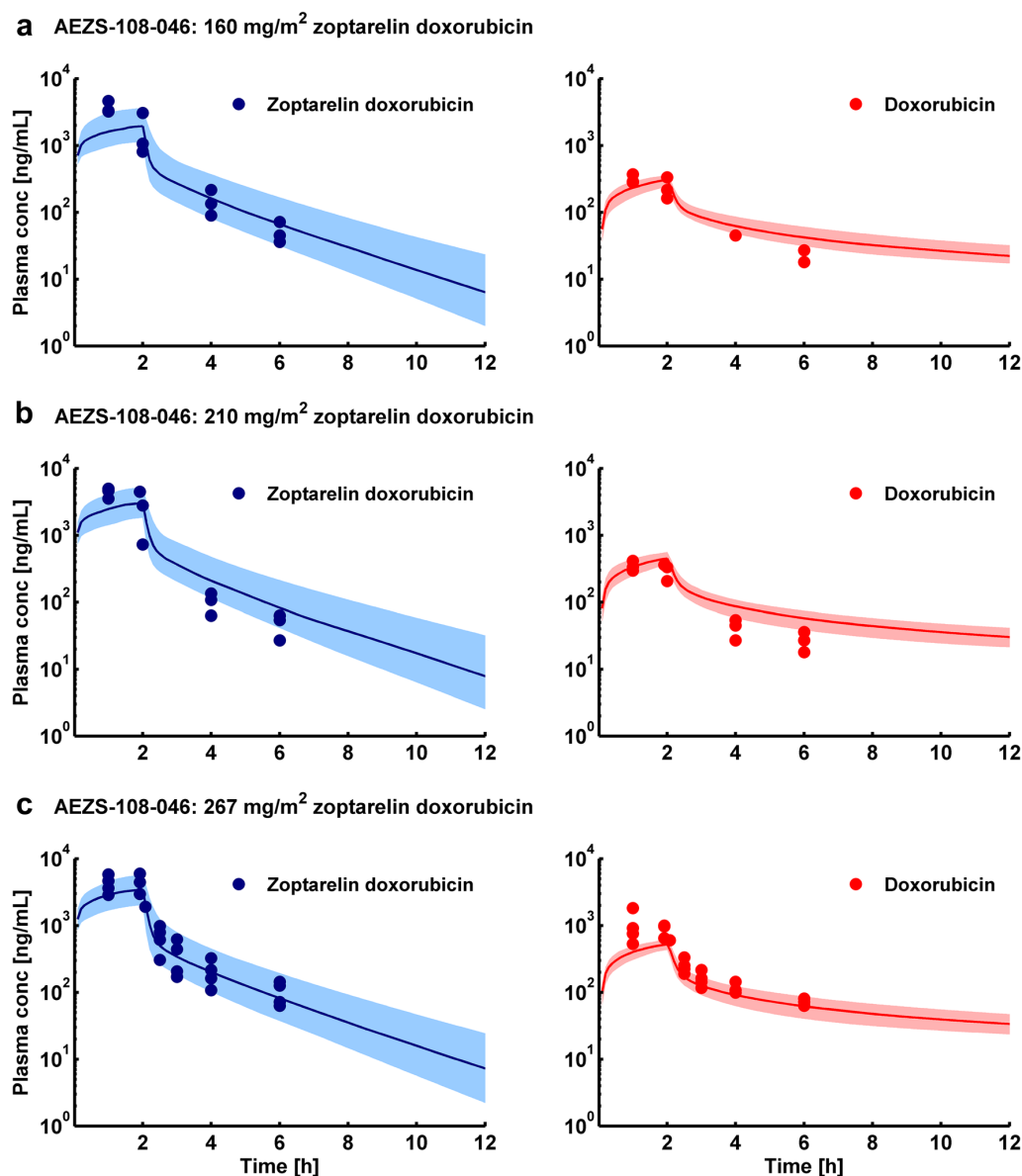


**Fig. 2** Test dataset: Population simulations (semilog scale) compared to observed data of zoptarelin doxorubicin (blue) and doxorubicin plasma concentrations (red) following intravenous administration of 160, 210 or 267 mg/m<sup>2</sup> zoptarelin doxorubicin. Clinical data (Study

2,  $n=3$ ,  $n=3$  and  $n=4$ ) are shown as dots. Population simulation medians are shown as lines; the shaded areas depict the 5th–95th percentile population prediction intervals

given in Zoptarelin Doxorubicin Supplementary Tables 1 and 2. Plots of predicted versus observed  $AUC_{last}$  and  $C_{max}$  values with twofold prediction success limits are shown in Zoptarelin Doxorubicin Supplementary Fig. 6.

### PBPK model sensitivity analysis

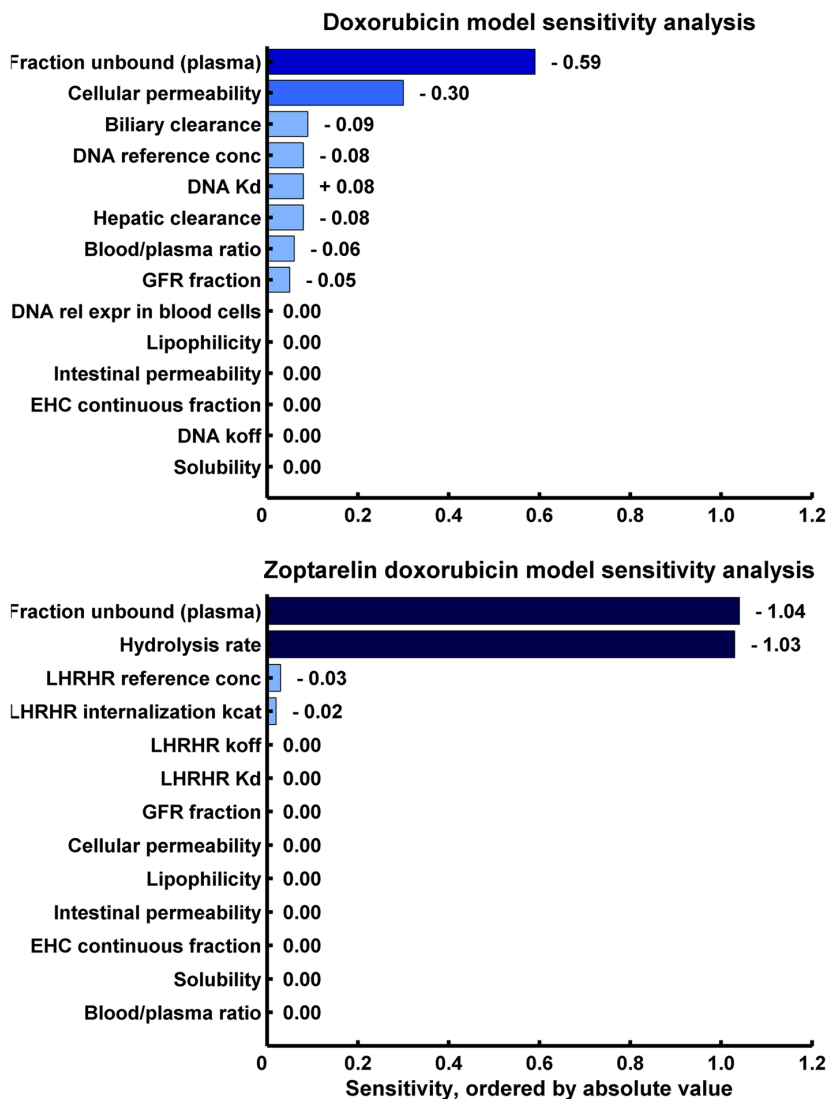
Sensitivity analyses were conducted for the doxorubicin and the zoptarelin doxorubicin model, with simulations of

single intravenous administrations of 60 mg/m<sup>2</sup> doxorubicin (1-h infusion) and of 267 mg/m<sup>2</sup> zoptarelin doxorubicin (2-h infusion), respectively. The investigated model parameters and results are listed in Fig. 3. The doxorubicin model is sensitive to the values of fraction unbound in plasma (sensitivity value of  $-0.6$ ) and cellular permeability (sensitivity value of  $-0.3$ ). The zoptarelin doxorubicin model is sensitive to the values of fraction unbound in plasma (sensitivity value of  $-1.0$ ) and zoptarelin doxorubicin hydrolysis rate (sensitivity value of  $-1.0$ ).

### General assessment of the zoptarelin doxorubicin DDI potential

To obtain a general assessment of the in vivo DDI potential of zoptarelin doxorubicin via OATP1B3 and OCT2, independently of the substrate affected by this inhibition, the relative changes of the apparent  $K_M$  values for these two transporters were calculated according to Eq. 2. As input inhibitor concentrations, predicted population interstitial unbound concentrations of zoptarelin doxorubicin in the liver and the kidney, respectively, were used (267 mg/m<sup>2</sup> zoptarelin doxorubicin, 2-h infusion). Zoptarelin doxorubicin  $K_i$  values were calculated to be 16.45  $\mu\text{mol/L}$  for

**Fig. 3** Doxorubicin and zoptarelin doxorubicin model sensitivity analysis results. Conc: concentration, EHC: enterohepatic circulation, GFR: glomerular filtration rate,  $k_{\text{cat}}$ : catalytic rate constant,  $K_d$ : dissociation constant,  $k_{\text{off}}$ : dissociation rate constant, LHRHR: luteinizing hormone-releasing hormone receptor, rel expr: relative expression, normalized to tissue with highest expression



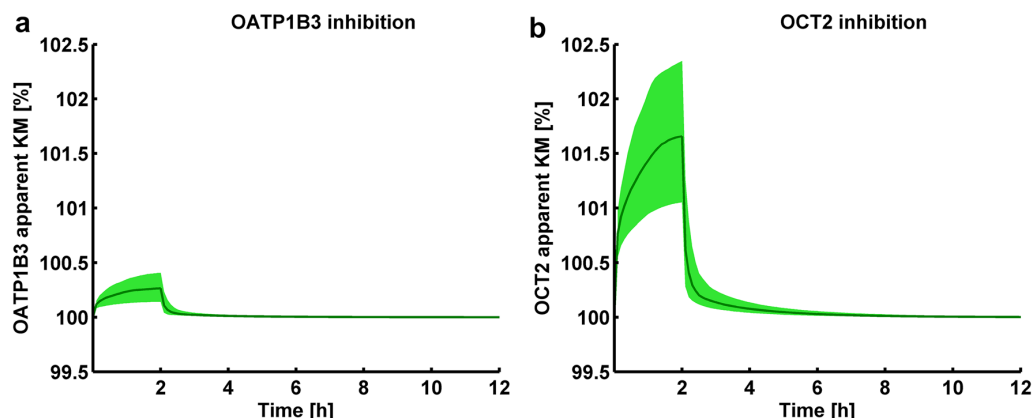


**Fig. 4** Zoptarelin doxorubicin DDI potential: Maximum impact of zoptarelin doxorubicin on OATP1B3 and OCT2. **a** Relative change of OATP1B3 apparent  $K_M$  during inhibition by 267 mg/m<sup>2</sup> zoptarelin doxorubicin. **b** Relative change of OCT2 apparent  $K_M$  during inhibition

by 267 mg/m<sup>2</sup> zoptarelin doxorubicin. Population simulation medians are shown as lines; the shaded areas depict the 5th–95th percentile population prediction intervals

OATP1B3 and 3.23  $\mu$ mol/L for OCT2 (see “Materials and methods”). The resulting relative changes of apparent  $K_M$  values amount to less than 0.5% for OATP1B3 and to less than 2.5% for OCT2, as illustrated in Fig. 4.

To rate the impact of a 2.5% change in  $K_M$ , the relation of initial reaction velocity  $v_0$  and  $K_M$  can be applied:

$$v_0 = \frac{V_{\max} * \text{substrate concentration}}{K_M + \text{substrate concentration}} \quad (4)$$

For substrate concentrations significantly below  $K_M$  and unchanged maximal reaction velocity  $V_{\max}$  (competitive inhibition assumed), a 2.5% increase of  $K_M$  results in a 2.5% decrease of initial reaction velocity. For higher substrate concentrations, the influence of increased  $K_M$  will be even smaller.

### DDI potential of zoptarelin doxorubicin with simvastatin and metformin

For specific DDI predictions with simvastatin and metformin, victim drug steady-state plasma concentrations after administration of the highest common doses of 80 mg simvastatin (once daily, day 5) or 1000 mg metformin (three times daily, day 5) with and without co-administration of 267 mg/m<sup>2</sup> zoptarelin doxorubicin were simulated.

Testing of different time intervals between the start of zoptarelin doxorubicin infusion and administration of the victim drugs showed highest DDI impact on simvastatin acid, when the zoptarelin doxorubicin infusion is started 2 h after the administration of simvastatin (zoptarelin doxorubicin  $C_{\max}$  at the time of simvastatin acid  $C_{\max}$ ); and highest DDI impact on metformin, when the zoptarelin doxorubicin

infusion is started 1 h before the administration of metformin (zoptarelin doxorubicin  $C_{\max}$  at the time of metformin  $C_{\max}$ ).

The identified administration regimens for maximum DDI impact and the resulting plasma concentrations of zoptarelin doxorubicin, simvastatin acid and metformin are illustrated in Fig. 5a, b. Victim drug plasma concentrations of simvastatin acid and metformin, with and without co-administration of zoptarelin doxorubicin are presented in Fig. 5c, d. DDI impact on victim drug AUC and  $C_{\max}$  values, simulated with the different tested dosing regimens is shown in Zoptarelin Doxorubicin Supplementary Table 3. The identified worst-case co-administration scenarios result in a 0.114% increase of the plasma AUC<sub>96–120</sub> of simvastatin acid and a 0.096% increase of the AUC<sub>96–104</sub> of metformin, due to liver and kidney uptake inhibition.

## Discussion

### Doxorubicin model

The presented doxorubicin model is the first whole-body PBPK model developed with clinical data from humans and a mechanistic implementation of the binding of doxorubicin to DNA. This binding is essential to describe the pharmacokinetics of doxorubicin, as it is the driving force behind the unusual distribution behavior of this drug [33]. The developed model accurately describes doxorubicin plasma concentrations following direct administration of doxorubicin and also very successfully predicts the concentrations of doxorubicin released following administration of a variety of different doses of zoptarelin doxorubicin.



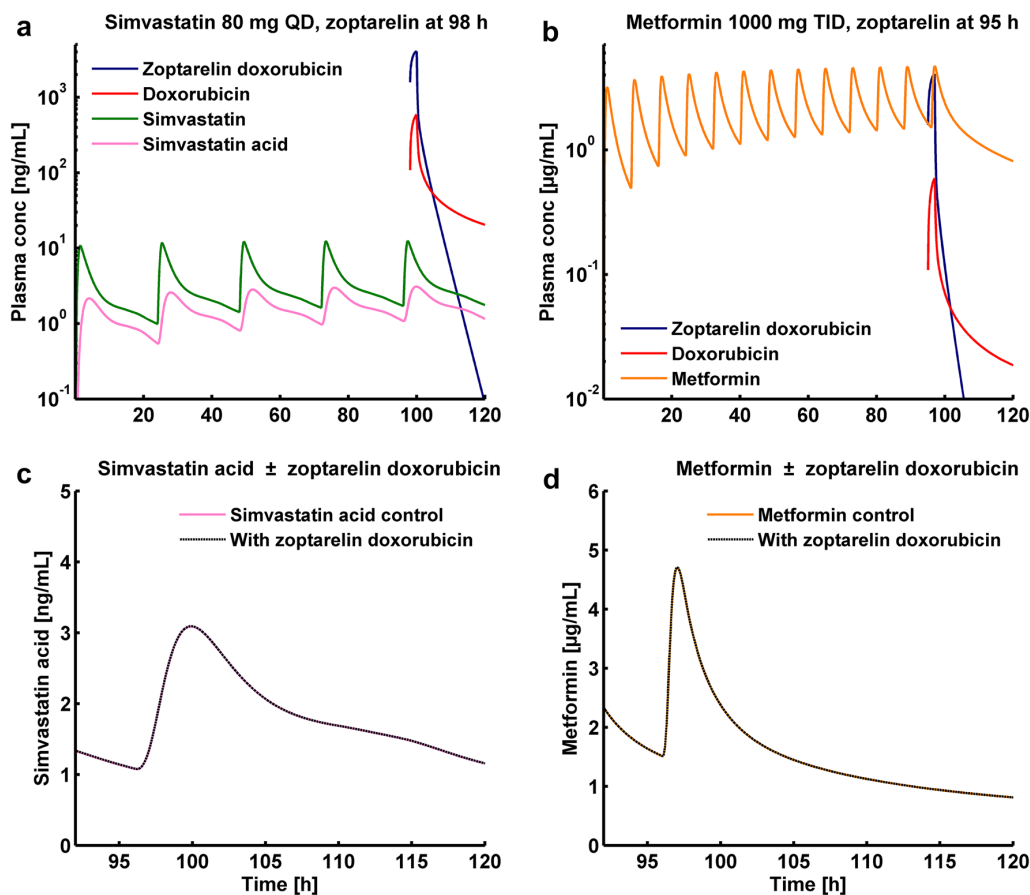


**Fig. 5** Zoptarelin doxorubicin DDI potential: Specific DDI worst-case scenario predictions with simvastatin acid and metformin as OATP1B3 and OCT2 victim drugs. **a** Predicted zoptarelin doxorubicin (blue), doxorubicin (red), simvastatin (green) and simvastatin acid (pink) plasma concentrations (semilog scale) of a typical individual during administration of 80 mg simvastatin every 24 h, plus 267 mg/m<sup>2</sup> zoptarelin doxorubicin once, on the morning of day 5. The last administration of simvastatin is at 96 h; zoptarelin doxorubicin infusion (2 h) is started 2 h later at 98 h, resulting in simultaneous peak plasma concentrations of zoptarelin doxorubicin and simvastatin acid at 100 h. **b** Predicted zoptarelin doxorubicin (blue), doxorubicin (red) and metformin (dark yellow) plasma concentra-

tions (semilog scale) of a typical individual during administration of 1000 mg metformin every 8 h, plus 267 mg/m<sup>2</sup> zoptarelin doxorubicin once, on the morning of day 5. The last administration of metformin is at 96 h; zoptarelin doxorubicin infusion (2 h) is started 1 h earlier, at 95 h, resulting in simultaneous peak plasma concentrations of zoptarelin doxorubicin and metformin at 97 h. **c** Overlay of predicted simvastatin acid plasma concentrations using the administration protocol shown in **a**, without (pink) and during co-administration of zoptarelin doxorubicin (dashed black line). **d** Overlay of predicted metformin plasma concentrations using the administration protocol shown in **b**, without (dark yellow) and during co-administration of zoptarelin doxorubicin (dashed black line)

The sensitivity of the doxorubicin model to the value of fraction unbound is to be expected, as this parameter determines the doxorubicin concentration available for all pharmacokinetic processes. The value used in the model has been carefully determined in vitro at Aeterna Zentaris and has not been optimized. The doxorubicin fraction unbound measured in-house (26.3%) is in very good accordance with the literature (25%, [34]). The moderate sensitivity of the model to the cellular permeability value underlines the influence of this parameter. Adjustment of this value greatly improved

the model performance and, therefore, it has been included into the set of optimized parameters.

Several other PBPK models of doxorubicin have been developed so far, mostly established from animal data with the benefit of measured doxorubicin concentrations in different tissues [35–38]. Among those is a very nice model of doxorubicin in mice, that has been extrapolated to humans including evaluation of the predicted serum concentrations with actual clinical data, as well as mechanistic modeling of DNA binding to describe the tissue distribution of doxorubicin [35]. The only other model directly developed from

human data lacks a mechanistic implementation of the tissue binding, but features a physiologically based description of the effects of aging on the distribution clearance of doxorubicin [36].

In the presented doxorubicin model, DNA binding sites have so far only been implemented into 8 of the 22 model compartments, resulting in an overestimation of the doxorubicin accumulation in these tissues and an underestimation of the doxorubicin concentration in the tissues without binding partner (not counting the blood cell compartment, as the DNA concentration within this volume has been separately adjusted to match literature data). Although the DNA binding site reference concentration of the virtual patients has been optimized ( $K_d$  and  $k_{off}$  have been fixed to literature values), the obtained value is biologically plausible. A rough estimate of the number of DNA base pairs per human is  $6.0 \times 10^{22}$  ( $6.0 \times 10^9$  base pairs per cell,  $1.0 \times 10^{13}$  cells per human). This equals 0.1 mol of base pairs per human. As the doxorubicin binding partner was implemented only into the 8 most important tissues of the model patient, these DNA binding sites are distributed into 4 L of tissue with equal expression of this binding partner, resulting in a reference concentration of 0.025 mol/L. The optimized value of 0.046 mol/L is in the same order of magnitude. Furthermore, there are reports of binding of doxorubicin not only to DNA, but (with a lower affinity) also to cardiolipin and DNA-associated enzymes, which have not been implemented into the model [9, 39]. To predict the doxorubicin concentrations and pharmacodynamics within a distinct organ, the distribution of the DNA binding sites will have to be implemented in an anatomically correct way, as has been proposed by Gustafson et al. [35].

Despite minor limitations, this model is a suitable basis for further refinement and subsequent extrapolation to vulnerable populations receiving doxorubicin treatment such as children, elderly and patients with organ impairment.

### Zoptarelin doxorubicin model

The presented zoptarelin doxorubicin model is the first PBPK model of zoptarelin doxorubicin and accurately describes and predicts plasma concentrations of zoptarelin doxorubicin and its active metabolite doxorubicin following infusion of different doses of zoptarelin doxorubicin. This is remarkable, as the model has been developed with data collected in three clinical trials investigating patients with different types of cancer.

As for the doxorubicin model, the sensitivity of the zoptarelin doxorubicin model to the value of fraction unbound was to be expected and the value used in the model has also been carefully measured in-house. The relatively high sensitivity of the model to the zoptarelin doxorubicin hydrolysis rate value emphasizes the impact of this parameter on the

elimination of zoptarelin doxorubicin and on the predicted AUC.

The primary aim of this PBPK analysis was to assess the DDI potential of zoptarelin doxorubicin with OATP1B3 and OCT2 victim drugs. Future applications of the presented model could include the implementation of a tumor compartment to enable the prediction of zoptarelin doxorubicin and doxorubicin concentrations in the target tissue and to answer questions regarding efficacy and pharmacodynamics of zoptarelin doxorubicin. For a first estimate, the model can be employed to simulate the internalization and intracellular concentrations of zoptarelin doxorubicin as well as the resulting concentrations of doxorubicin in the gonads. The lack of a tumor compartment (compensated by a low expression of LHRHR in the lung) does not impact the results and interpretation of the presented PBPK analysis of the interaction with OATP1B3 and OCT2, as these DDIs are determined by the concentrations in liver and kidney.

### Zoptarelin doxorubicin DDI potential

Zoptarelin doxorubicin shows no inhibition or induction of cytochrome P450 enzymes in vitro, as well as no inhibition of investigated transporters other than OATP1B3 ( $IC_{50} = 16.5 \mu\text{mol/L}$ ) and OCT2 ( $IC_{50} = 3.26 \mu\text{mol/L}$ ). P-glycoprotein (P-gp), breast cancer resistance protein (BCRP), organic anion transporter 1 (OAT1), OAT3 and OATP1B1 are not inhibited in vitro ( $IC_{50}$  values  $> 200 \mu\text{mol/L}$ ). The predicted maximum relative changes of transport rate during treatment with the highest clinical dose of zoptarelin doxorubicin are 0.5% for OATP1B3 and 2.5% for OCT2 at the end of the infusion. In line with this general interaction potential assessment, no impact of zoptarelin doxorubicin on plasma concentrations of the OATP1B3 and OCT2 victim drugs simvastatin acid and metformin was found in worst-case scenario simulations. These results are in accordance with the expectations due to low interstitial concentrations of zoptarelin doxorubicin in relation to the zoptarelin doxorubicin  $K_i$  values for inhibition of OATP1B3 and OCT2. As zoptarelin doxorubicin (MW = 1893.06 g/mol) is a 10-amino acid polypeptide linked to doxorubicin and positively charged at two amino groups at physiological pH, its passive permeability is low, leading to low interstitial concentrations.

This example demonstrates that PBPK modeling is a valuable technique to analyze the risk of investigational drugs suspected to cause drug–drug interactions in vivo. In vitro results and pharmacokinetic data from early clinical studies are used to establish mechanistic and physiologically based models that allow the in vivo prediction of drug–drug interactions. This approach is supported by drug approval agencies [12, 13] and can help to minimize patient risk, costs

and time needed for drug development. Furthermore, PBPK modeling has the capability to generate information whenever the conduct of clinical trials is not ethical, as is the case in all frail populations such as children, elderly and patients.

## Conclusion

This is the first report of a whole-body PBPK model of zoptarelin doxorubicin and its active metabolite doxorubicin. The model was applied for the evaluation of the zoptarelin doxorubicin drug–drug interaction potential (1) by a general assessment of the OATP1B3 and OCT2 inhibition potential of zoptarelin doxorubicin in vivo and (2) by specific DDI simulations of the impact of zoptarelin doxorubicin on simvastatin acid and metformin exposure in worst-case scenarios. No DDI potential of zoptarelin doxorubicin was detected in these analyses.

**Acknowledgements** The authors gratefully acknowledge the patients that participated in the clinical studies and the medical staff involved in patient care and study execution.

## Compliance with ethical standards

**Funding** This study was funded by Aeterna Zentaris.

**Conflict of interest** Nina Hanke, Daniel Moj, Jan-Georg Wojtyniak and Hannah Britz declare that they have no conflict of interest. Michael Teifel, Babette Aicher, Herbert Sindermann and Nicola Ammer are employees of Aeterna Zentaris. Thorsten Lehr has received research grants from Aeterna Zentaris.

**Ethical approval** All procedures performed in studies involving human participants were in accordance with the ethical standards of the institutional and/or national research committee and with the 1964 Helsinki declaration and its later amendments or comparable ethical standards. This article does not contain any studies with animals performed by any of the authors.

**Informed consent** Informed consent was obtained from all individual participants included in the study.

## References

- Nagy A, Schally A, Armatis P, Szepeshazi K, Halmos G, Kovacs M, Zarandi M, Groot K, Miyazaki M, Jungwirth A, Horvath J (1996) Cytotoxic analogs of luteinizing hormone-releasing hormone containing doxorubicin or 2-pyrrolinodoxorubicin, a derivative 500–1000 times more potent. *Proc Natl Acad Sci USA* 93:7269–7273
- Westphalen S, Kotulla G, Kaiser F, Krauss W, Werning G, Elsasser HP, Nagy A, Schulz KD, Gründker C, Schally A, Emons G (2000) Receptor mediated antiproliferative effects of the cytotoxic LHRH agonist AN-152 in human ovarian and endometrial cancer cell lines. *Int J Oncol* 17:1063–1069
- Krebs LJ, Wang X, Nagy A, Schally A, Rasad PN, Liebowa C (2002) A conjugate of doxorubicin and an analog of Luteinizing hormone-releasing hormone shows increased efficacy against oral and laryngeal cancers. *Oral Oncol* 38:657–663
- Gründker C, Völker P, Griesinger F, Ramaswamy A, Nagy A, Schally A, Emons G (2002) Antitumor effects of the cytotoxic luteinizing hormone-releasing hormone analog AN-152 on human endometrial and ovarian cancers xenografted into nude mice. *Am J Obstet Gynecol* 187:528–537
- Szepeshazi K, Schally A, Keller G, Block NL, Bente D, Halmos G, Szalontay L, Vidaurre I, Rick FG (2012) Receptor-targeted therapy of human experimental urinary bladder cancers with cytotoxic LH-RH analog AN-152 (AEZS-108). *Oncotarget* 3:686–699
- Emons G, Gorchev G, Harter P, Wimberger P, Stähle A, Hanker L, Hilpert F, Beckmann MW, Dall P, Gründker C, Sindermann H, Sehoul J (2014) Efficacy and safety of AEZS-108 (LHRH agonist linked to doxorubicin) in women with advanced or recurrent endometrial cancer expressing LHRH receptors: a multicenter phase 2 trial (AGO-GYN5). *Int J Gynecol Cancer* 24:260–265
- Emons G, Gorchev G, Sehoul J, Wimberger P, Stähle A, Hanker L, Hilpert F, Sindermann H, Gründker C, Harter P (2014) Efficacy and safety of AEZS-108 (INN: zoptarelin doxorubicin acetate) an LHRH agonist linked to doxorubicin in women with platinum refractory or resistant ovarian cancer expressing LHRH receptors: a multicenter phase II trial of the ago-study group. *Gynecol Oncol* 133:427–432
- Emons G, Kaufmann M, Gorchev G, Tsekova V, Gründker C, Günthert AR, Hanker LC, Velikova M, Sindermann H, Engel J, Schally A (2010) Dose escalation and pharmacokinetic study of AEZS-108 (AN-152), an LHRH agonist linked to doxorubicin, in women with LHRH receptor-positive tumors. *Gynecol Oncol* 119:457–461
- Tacar O, Sriamornsak P, Dass CR (2013) Doxorubicin: An update on anticancer molecular action, toxicity and novel drug delivery systems. *J Pharm Pharmacol* 65:157–170
- Pfizer Inc (2011) Doxorubicin prescribing information. Pfizer Inc, New York
- Speth PAJ, Van Hoesel Q, Haanen C (1988) Clinical pharmacokinetics of doxorubicin. *Clin Pharmacokinet* 15:15–31
- Food US and Drug Administration—Center for Drug Evaluation and Research (2016) Physiologically based pharmacokinetic analyses—format and content. Draft Guidance for Industry
- European Medicines Agency (2016) Guideline on the qualification and reporting of physiologically based pharmacokinetic (PBPK) modelling and simulation
- Yao F, Duan J, Wang Y, Zhang Y, Guo Y, Guo H, Kang X (2015) Nanopore single-molecule analysis of DNA-doxorubicin interactions. *Anal Chem* 87:338–342
- Speth PA, Linssen PC, Holdrinet RS, Haanen C (1987) Plasma and cellular adriamycin concentrations in patients with myeloma treated with ninety-six-hour continuous infusion. *Clin Pharmacol Ther* 41:661–665
- Speth PA, Linssen PC, Boezeman JB, Wessels HM, Haanen C (1987) Cellular and plasma adriamycin concentrations in long-term infusion therapy of leukemia patients. *Cancer Chemother Pharmacol* 20:305–310
- Durmus S, Naik J, Buil L, Wagenaar E, Van Tellingen O, Schinkel AH (2014) In vivo disposition of doxorubicin is affected by mouse Oatp1a/1b and human OATP1A/1B transporters. *Int J Cancer* 135:1700–1710
- American Society of Health-System Pharmacists (2009) AHFS drug information. American Society of Health-System Pharmacists, Bethesda

19. Schang AL, Quérat B, Simon V, Garrel G, Bleux C, Counis R, Cohen-Tannoudji J, Laverrière JN (2012) Mechanisms underlying the tissue-specific and regulated activity of the *Gnrhr* promoter in mammals. *Front Endocrinol (Lausanne)* 3:162
20. Aguilar-Rojas A, Huerta-Reyes M (2009) Human gonadotropin-releasing hormone receptor-activated cellular functions and signaling pathways in extra-pituitary tissues and cancer cells. *Oncol Rep* 22:981–990
21. Halmos G, Nagy A, Lamharzi N, Schally A (1999) Cytotoxic analogs of luteinizing hormone-releasing hormone bind with high affinity to human breast cancers. *Cancer Lett* 136:129–136
22. Cho N, Harada M, Imaeda T, Imada T, Matsumoto H, Hayase Y, Sasaki S, Furuya S, Suzuki N, Okubo S, Ogi K, Endo S, Onda H, Fujino M (1998) Discovery of a novel, potent, and orally active nonpeptide antagonist of the human luteinizing hormone-releasing hormone (LHRH) receptor. *J Med Chem* 41:4190–4195
23. Valentin J (2002) Basic anatomical and physiological data for use in radiological protection: reference values. *Ann ICRP* 32:1–277
24. Miller DS, Gabra H, Emons G, McMeekin DS, Oza AM, Temkin SM, Vergote I (2014) ZoptEC: Phase III study of zoptarelin doxorubicin (AEZS-108) in platinum-taxane pretreated endometrial cancer (Study AEZS-108–050). *J Clin Oncol* 32:15 (suppl)
25. König J, Cui Y, Nies AT, Keppler D (2000) Localization and genomic organization of a new hepatocellular organic anion transporting polypeptide. *J Biol Chem* 275:23161–23168
26. Koepsell H, Endou H (2004) The SLC22 drug transporter family. *Pflugers Arch Eur J Physiol* 447:666–676
27. Gui C, Miao Y, Thompson L, Wahlgren B, Mock M, Stieger B, Hagenbuch B (2008) Effect of pregnane X receptor ligands on transport mediated by human OATP1B1 and OATP1B3. *Eur J Pharmacol* 584:57–65
28. Kimura N, Masuda S, Tanihara Y, Ueo H, Okuda M, Katsura T, Inui K (2005) Metformin is a superior substrate for renal organic cation transporter OCT2 rather than hepatic OCT1. *Drug Metab Pharmacokinet* 20:379–386
29. Yung-Chi C, Prusoff WH (1973) Relationship between the inhibition constant (KI) and the concentration of inhibitor which causes 50 per cent inhibition (I50) of an enzymatic reaction. *Biochem Pharmacol* 22:3099–3108
30. Rodrigues AD (2008) Drug-drug interactions, 2nd edn. CRC Press, Taylor and Francis, Boca Raton
31. Food US and Drug Administration (2012) Drug interaction studies—Study design, data analysis, implications for dosing, and labeling recommendations. Draft Guidance for Industry
32. Kunze A, Huwlyer J, Camenisch G, Poller B (2014) Prediction of organic anion-transporting polypeptide 1B1- and 1B3-mediated hepatic uptake of statins based on transporter protein expression and activity data. *Drug Metab Dispos* 42:1514–1521
33. Terasaki T, Iga T, Sugiyama Y, Hanano M (1982) Experimental evidence of characteristic tissue distribution of adriamycin. Tissue DNA concentration as a determinant. *J Pharm Pharmacol* 34:597–600
34. Pfizer Inc (2013) Doxorubicin prescribing information. Pfizer Inc, New York
35. Gustafson DL, Rastatter JC, Colombo T, Long ME (2002) Doxorubicin pharmacokinetics: macromolecule binding, metabolism, and excretion in the context of a physiologic model. *J Pharm Sci* 91:1488–1501
36. Li J, Gwilt PR (2003) The effect of age on the early disposition of doxorubicin. *Cancer Chemother Pharmacol* 51:395–402
37. Hu L, Au JLS, Wientjes MG (2007) Computational modeling to predict effect of treatment schedule on drug delivery to prostate in humans. *Clin Cancer Res* 13:1278–1287
38. Dubbelboer IR, Lilienberg E, Sjögren E, Lennernäs H (2017) A model-based approach to assessing the importance of intracellular binding sites in doxorubicin disposition. *Mol Pharm* 14:686–698
39. Goormaghtigh E, Chatelain P, Caspers J, Ruyschaert JM (1980) Evidence of a complex between adriamycin derivatives and cardiolipin: possible role in cardiotoxicity. *Biochem Pharmacol* 29:3003–3010

### 3.3 PUBLICATION III - PHYSIOLOGICALLY BASED PRECISION DOSING APPROACH FOR DRUG-DRUG-GENE INTERACTIONS: A SIMVASTATIN NETWORK ANALYSIS

#### 3.3.1 *Reference*

**Jan-Georg Wojtyniak**, Dominik Selzer, Matthias Schwab, and Thorsten Lehr. "Physiologically based precision dosing approach for drug-drug-gene interactions: a simvastatin network analysis." In: *Clinical Pharmacology & Therapeutics* (Dec. 2020). DOI: 10.1002/cpt.2111

#### 3.3.2 *Author Contributions*

Following CRediT [4, 5], the contributions of the individual authors are listed in Table 3.3.<sup>3</sup>

Table 3.3: Author contributions for Publication III - Simvastatin

Jan-Georg Wojtyniak	See included publications and contribution report on page vi
Dominik Selzer	Formal Analysis, Methodology, Writing - Review & Editing
Matthias Schwab	Conceptualization, Writing - Review & Editing
Thorsten Lehr	Conceptualization, Project Administration, Formal Analysis, Methodology, Writing - Review & Editing

#### 3.3.3 *Copyright*

This is an open access article under the terms of the Creative Commons Attribution-NonCommercial License (CC BY-NC 4.0), which permits use, distribution and reproduction in any medium, provided the original work is properly cited and is not used for commercial purposes.

©2020 The Authors Some Rights Reserved

<sup>3</sup> For a description of the different taxonomy categories see also appendix Chapter B



# Physiologically Based Precision Dosing Approach for Drug-Drug-Gene Interactions: A Simvastatin Network Analysis

Jan-Georg Wojtyniak<sup>1,2</sup> , Dominik Selzer<sup>1</sup>, Matthias Schwab<sup>2,3,4</sup> and Thorsten Lehr<sup>1,\*</sup>

Drug-drug interactions (DDIs) and drug-gene interactions (DGIs) are well known mediators for adverse drug reactions (ADRs), which are among the leading causes of death in many countries. Because physiologically based pharmacokinetic (PBPK) modeling has demonstrated to be a valuable tool to improve pharmacotherapy affected by DDIs or DGIs, it might also be useful for precision dosing in extensive interaction network scenarios. The presented work proposes a novel approach to extend the prediction capabilities of PBPK modeling to complex drug-drug-gene interaction (DDGI) scenarios. Here, a whole-body PBPK network of simvastatin was established, including three polymorphisms (*SLCO1B1* (rs4149056), *ABCG2* (rs2231142), and *CYP3A5* (rs776746)) and four perpetrator drugs (clarithromycin, gemfibrozil, itraconazole, and rifampicin). Exhaustive network simulations were performed and ranked to optimize 10,368 DDGI scenarios based on an exposure marker cost function. The derived dose recommendations were translated in a digital decision support system, which is available at [simvastatin.precisiondosing.de](http://simvastatin.precisiondosing.de). Although the network covers only a fraction of possible simvastatin DDGIs, it provides guidance on how PBPK modeling could be used to individualize pharmacotherapy in the future. Furthermore, the network model is easily extendable to cover additional DDGIs. Overall, the presented work is a first step toward a vision on comprehensive precision dosing based on PBPK models in daily clinical practice, where it could drastically reduce the risk of ADRs.

## Study Highlights

### WHAT IS THE CURRENT KNOWLEDGE ON THE TOPIC?

☑ Drug-drug interactions (DDIs), drug-gene interactions, and drug-drug-gene interactions (DDGIs) are well known triggers of adverse drug reactions that might be preventable by precision dosing. One example compound prone to DDGIs is simvastatin.

### WHAT QUESTION DID THIS STUDY ADDRESS?

☑ How physiologically based pharmacokinetic (PBPK) modeling can be utilized for model-informed precision dosing (MIPD) of complex DDGIs.

### WHAT DOES THIS STUDY ADD TO OUR KNOWLEDGE?

☑ This study presents whole-body PBPK models for simvastatin lactone and simvastatin acid, including variation of four

pharmacogenes and was tested against four DDI perpetrator drugs and one DDI victim. In addition, the model was used to develop a digital decision support system based on dose recommendations for 10,368 simulated interaction scenarios.

### HOW MIGHT THIS CHANGE CLINICAL PHARMACOLOGY OR TRANSLATIONAL SCIENCE?

☑ The presented dose recommendations might help to better assess risks of simvastatin therapy in pharmacogenomic and polypharmacy context. Furthermore, the study highlights and guides how PBPK can help to bring MIPD into daily clinical practice.

Adverse drug reactions (ADRs) are a burden to our health care and economic systems. The US Food and Drug Administration (FDA) assumes that annually > 2,216,000 serious ADRs in hospitalized patients lead to over 106,000 deaths in the United

States—ranking them as the fourth leading cause of death.<sup>1,2</sup> The associated costs are tremendous and are estimated to add up to US \$200 billion per year.<sup>1</sup> This situation is likely to become more acute as a result of ever-growing prescription use. According to

<sup>1</sup>Clinical Pharmacy, Saarland University, Saarbrücken, Germany; <sup>2</sup>Dr. Margarete Fischer-Bosch-Institute of Clinical Pharmacology, Stuttgart, Germany; <sup>3</sup>Departments of Clinical Pharmacology and Pharmacy and Biochemistry, University of Tübingen, Tübingen, Germany; <sup>4</sup>Cluster of Excellence iFIT (EXC2180) "Image-guided and Functionally Instructed Tumor Therapies", University of Tübingen, Tübingen, Germany. \*Correspondence: Thorsten Lehr ([thorsten.lehr@mx.uni-saarland.de](mailto:thorsten.lehr@mx.uni-saarland.de))

Received August 4, 2020; accepted November 7, 2020. doi:10.1002/cpt.2111

## ARTICLE

the Centers for Disease Control and Prevention, the proportion of Americans taking > 5 prescription drugs on a regular basis has almost tripled in the past 20 years.<sup>3</sup>

Drug-drug interactions (DDIs) and drug-gene interactions (DGIs) are the most common reasons for ADRs.<sup>2,4,5</sup> Unfortunately, in current clinical practice DDIs and DGIs are considered separate entities that are typically handled in a nonholistic fashion.<sup>4</sup> However, as shown recently, 19% of potentially clinically significant interactions occur as a combination of DDIs and DGIs (drug-drug-gene interaction (DDGIs)).<sup>4,5</sup> Tackling DDIs, DGIs, or DDGIs using guidelines on dose adaptation could reduce the number of ADRs substantially, because it is assumed that 80% of ADRs

are dose-related and, hence, could be prevented.<sup>6,7</sup> This concept can be summarized as precision dosing for DDIs and DGIs.<sup>8</sup>

The current approach of developing such guidelines would be the investigation of DDGIs in clinical trials analogous to presently conducted trials on DDIs and DGIs.<sup>8,9</sup> Those studies are typically performed in healthy volunteers, in a homogenous study population and with a controlled treatment plan (Figure 1a).<sup>8</sup> Consequently, they do not reflect the situation in multimorbid patients, affected by polypharmacy and genetic polymorphisms, which is the patient group most susceptible to ADRs (Figure 1b).<sup>1,8</sup> Moreover, due to the combinatorial explosion of all possible DDGIs, exhaustive studies might not be feasible at all (Figure 1c).

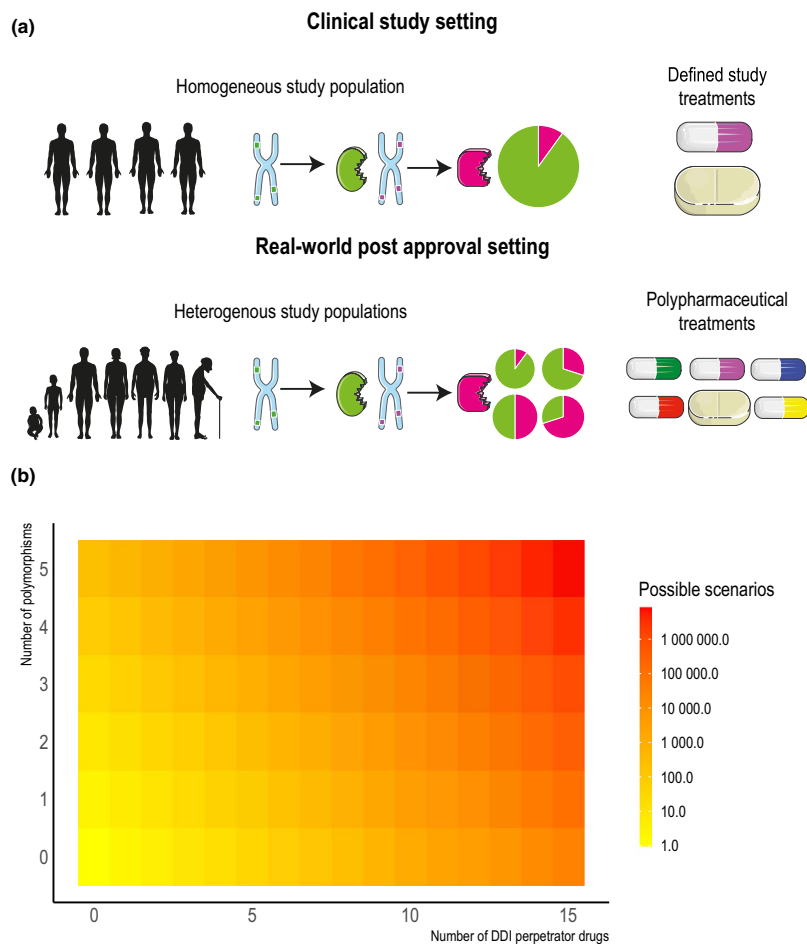


**Figure 1** Difference between a clinical study setting and a real-world post-approval setting. (a) The upper part shows the research situation in a clinical setting. A homogenous study population receives a defined treatment regimen in a standardized procedure. The subsequently obtained results are used for the development of therapy recommendations for the post-approval setting. The lower part depicts the real-world postapproval setting with a higher variability in demographics, variant distribution, and a higher degree in polypharmacy compared with the clinical study population. As a result, as shown in (b) various possible DDGI scenarios are conceivable depending on the amount of concomitantly used perpetrator drugs and occurring polymorphisms. For the calculation it was assumed that each perpetrator has two DDI states (preparator is given or perpetrator is not given) and each clinically relevant polymorphism could have three independent phenotypes. Following the number of possible scenarios was calculated with  $n_{\text{scenarios}} = 2^x \text{perpetrator} * 3^y \text{polymorphism}$ . The increase of possible DDGI scenarios is shown as a heatmap. The number of possible DDGI scenarios is shown on a log-scale. Some figure elements are taken from smart.servi.com (CC BY 3.0). DDGI, drug-drug-gene interaction; DDI, drug-drug interaction.

To overcome this problem, a promising approach would be the application of whole-body physiologically based pharmacokinetic (PBPK) modeling.<sup>4</sup> PBPK models hold the capability to predict the DDGI potential of drugs *in silico* and to develop alternative precision dosing regimens for patients.<sup>4</sup> The reliability of this technique has already been demonstrated in several DDI and DGI studies and is acknowledged by regulatory agencies.<sup>10–12</sup> However, although PBPK modeling has been accepted as a useful option to predict the extent of DDGIs, examples on how PBPK modeling can be used for model informed precision dosing (MIPD) are still scarce.<sup>12</sup>

Thus, the aim of this work was to illustrate the complexity of DDIs, DGIs, and DDGIs based on the example of simvastatin. Simvastatin was selected as it is among the most prescribed drugs in industrial nations and is highly susceptible to potentially life-threatening ADRs due to its complex pharmacokinetics (PKs).<sup>13–18</sup> Moreover, this work should provide guidance for the development of an PBPK-based MIPD approach. Therefore, a comprehensive simvastatin DDGI PBPK network model was implemented to serve a web-based decision support system that offers quick and easy access to optimized dose recommendations for individual patients.

## METHODS

### Software

PBPK model development was performed with PK-Sim and MoBi (version 8 – Build 21) as part of the Open Systems Pharmacology Suite.<sup>19</sup> Model parameter identification was accomplished using Monte-Carlo optimization. Local sensitivity analysis was also performed within PK-Sim. Published plasma concentration-time profiles were digitized using GetData Graph Digitizer (version 2.26.0.20, S. Fedorov).<sup>20</sup> Graphics and statistical analysis were produced and implemented using R (version 3.6.3).<sup>21</sup>

### Simvastatin PBPK model building

The simvastatin model was developed in a stepwise procedure. In a first step, physicochemical parameters of simvastatin lactone (SL) and simvastatin acid (SA) as well as information on absorption, distribution, metabolism, and excretion processes were extracted from literature. Subsequently, mean plasma concentration-time profiles of SL and SA after oral single dose and multiple dose administration were digitized from published studies and separated into training and test datasets for model development and evaluation, respectively. Model input parameters, which were not available as PK-Sim reference values or that could not be informed from published literature values were optimized by fitting the model to measured plasma concentration-time profiles from the training dataset. PBPK study simulations were built based on healthy individuals with the reported mean values for age, weight, height, and genetic background, as stated in the corresponding study protocol, respectively. If parameter information was lacking, a PK-Sim mean individual (healthy male European, 30 years of age, body weight of 73 kg, a height of 176 cm, and based on the International Commission on Radiological Protection database) with wild type genotype was substituted. For all simulated individuals, glomerular filtration and enterohepatic cycling was implemented. A detailed description of the model development process, including information about digitized studies and model parameters can be found in the **Supplementary Material, chapter 2**.

### DGI implementation and DDI network development

DGI effects were implemented assuming a changed enzyme turnover number ( $k_{cat}$ ) compared with wild type. Here, the homozygous wild type  $k_{cat}$  as well as  $k_{cat}$  for homozygous polymorphic individuals were

estimated during model training (see **Supplementary Material, chapter 1.1.2** and **chapter 2.4**).

A DDI network was built to further evaluate the performance of the developed model. Thus, previously developed models of clarithromycin, gemfibrozil, itraconazole, rifampicin, and midazolam were coupled with the simvastatin model.<sup>12,22,23</sup> Population mean profiles as well as area under the curve (AUC) and peak plasma concentration ( $C_{max}$ ) values were predicted and compared against observed study data to evaluate the network quality.<sup>20</sup>

A detailed overview on the implementation of the DDI network, including relevant interaction parameters from *in vitro* experiments as well as the mathematical implementation of the drug interaction processes, is provided in the **Supplementary Material in chapter 1** and **chapter 3**.

### PBPK network evaluation and sensitivity analysis

PBPK model evaluation was performed using different statistical and graphical evaluation techniques. Predicted plasma concentration-time profiles were compared with observed profiles. Moreover, goodness-of-fit plots for predicted vs. observed plasma concentrations were examined. Mean relative deviation<sup>24</sup> and median symmetric accuracy<sup>25</sup> were calculated for all differences between observed and predicted plasma concentrations. In addition, the performance was evaluated by comparison of the noncompartmental analysis parameters AUC from last dose to last observation and  $C_{max}$ . AUC was computed using a linear-up log-down method. Geometric mean fold errors (GMFEs) were derived for differences between observed and predicted AUC and  $C_{max}$  values. For DGI and DDI predictions, AUC effect ratios were compared, in which a deviation of the observed from the predicted effect ratio less than two times was considered sufficient. Finally, local sensitivity analysis of the final model to single parameter changes was calculated as relative changes of the AUC of one dosing interval in steady-state conditions. A detailed overview of performance measurements and the local sensitivity analysis can be found in the **Supplementary Material, chapter 1.4**.

### Dose optimization

Simvastatin dose optimization for several DDGI scenarios, including individual DDIs and DGIs was performed. As reference, plasma concentration-time profiles for SL and SA in a mean individual after administration of 5 mg up to 80 mg (5 mg steps) SL once daily for 7 days were simulated and SL and SA AUCs from the time of the last dose up to 24 hours postdose derived. In a second step, a DDGI matrix was set up covering every possible combination of the three polymorphisms *SLCO1B1* (rs4149056), *ABCG2* (rs2231142), and *CYP3A5* (rs776746) and comedication with the four perpetrator drugs clarithromycin, itraconazole, gemfibrozil, and rifampicin. DDGI scenarios were simulated with administered SL doses according to the reference (7 days + 24 hours postdose) and reasonable perpetrator dosing regimens (see **Table 1**). For each simulation, SL and

**Table 1** Investigated perpetrator regimens

Perpetrator	Half-life, monotherapy	Regimen
Clarithromycin	3.3–4.9 hours	500 mg b.i.d.
Itraconazole	~ 24 hours	200 mg daily
Rifampicin	2.5 hours	600 mg daily concomitant with simvastatin
Rifampicin	2.5 hours	600 mg daily 17 hours after simvastatin dosing
Gemfibrozil	7.6 hours	600 mg b.i.d.



## ARTICLE

SA AUCs were calculated. Following, relative AUC deviations of SL and SA from the reference values were computed for each DDGI scenario with an exposure marker cost function as shown in Eq. 1:

$$\text{Exposure Marker} = \frac{|AUC_{SL-DDGI} - AUC_{SL-ref}|}{AUC_{SL-ref}} + \frac{|AUC_{SA-DDGI} - AUC_{SA-ref}|}{AUC_{SA-ref}} \quad (1)$$

With Exposure Marker = Relative differences of SL and SA exposure per simvastatin dose as a cost function for dose optimization (the smaller the better),  $AUC_{SL-DDGI}$  = AUC for SL under DDGI condition,  $AUC_{SL-ref}$  = reference AUC for SL,  $AUC_{SA-DDGI}$  = AUC for SA under DDGI condition,  $AUC_{SA-ref}$  = reference AUC for SA.

For each DDGI scenario, the exposure marker cost function was minimized to identify the simvastatin dose with the smallest exposure deviation (matching exposure). For different therapeutic dose levels of simvastatin (20 mg, 40 mg, and 60 mg) relative frequency of recommended doses and the relationship between the number of DDGIs and the optimal dose level were analyzed. Moreover, a hierarchical Euclidian distance cluster analysis stratified against the DDIs and DGI was performed to identify patterns for generalized dose recommendations. Clustering was computed with complete linkage using the *hclust* function in R.

Results from the dose optimization were transferred into a DDS web application implemented with the R package “shiny,” allowing users to easily filter simulation analysis tailored to DDGIs and simvastatin doses of interest.

## RESULTS

## Simvastatin PBPK model building and evaluation

We successfully developed a whole-body PBPK model of SL and SA. For placebo and DGI model development and evaluation mean data from 57 studies were extracted including 59 SL and 57 SA plasma-concentration time profiles, which represent information from 1,271 study participants. For DGI implementation, plasma-concentration time profiles or AUC and  $C_{max}$  values for *SLCO1B1* (rs4149056) c.521C/C, c.521T/C, c.521T/T, *ABCB1* (rs1128503 rs2032582 and rs1045642) c.1236T-c.2677T-c.3435T, c.1236C-c.2677G-c.3435C, *ABCG2* (rs2231142) c.421A/A, c.421C/A, c.421C/C, and *CYP3A5* (rs776746) *CYP3A5\*3\*3*, *CYP3A5\*3\*1*, *CYP3A5\*1\*1* were used for model development and optimization. System-dependent parameters like reference concentrations and enzyme expression profiles were taken from the PK-Sim database or extracted from literature as described in **Supplementary Material, chapter 1.3**. Doses available for model development and evaluation ranged from 10 mg to 80 mg simvastatin after single and multiple doses.

Extensive model evaluations, as described in the **Supplementary Material, chapter 2.3**, revealed good model performance for placebo PK profiles. Mean ratios predicted vs. observed AUCs were 1 for SL and 0.9 for SA. Mean predicted vs. observed  $C_{max}$  ratios were 0.9 and 0.8 for SL and SA, respectively. GMFE values were 1.3 for SL AUC, 1.5 for SL  $C_{max}$ , 1.5 for SA AUC, and 1.7 for SA  $C_{max}$ , respectively.

## DGI model evaluation

The model was capable to precisely describe and predict the DGI profiles in the training and test datasets. The average AUC ratio was 1.0 for SL and 0.7 for SA, whereas the mean  $C_{max}$  ratio was

0.8 for SL and 0.6 for SA. For DGI the GMFE values were 1.3 for SL AUC and 1.4 for SL  $C_{max}$ , 1.8 for SA AUC, and 2.2 for SA  $C_{max}$ , respectively (see **Supplementary Material, chapter 2.4.6**). **Figure 2a** shows an example prediction of SA for *SLCO1B1* (rs4149056) c.521C/C and c.521T/T genotype.

## DDI network development

A DDI network was built by coupling models for clarithromycin, gemfibrozil, itraconazole, rifampicin, and midazolam with the newly derived simvastatin model (see **Supplementary Material, chapter 3**). **Figure 2b** shows an example prediction of SL under clarithromycin cotreatment. Mean predicted vs. observed AUC ratios for SL, SA, and midazolam were 1.2, 1.5, and 0.9, respectively. Average predicted vs. observed  $C_{max}$  ratios for SL, SA, and midazolam were 0.9, 1.1, and 1, respectively. GMFE values were 1.3 for both SL AUC and  $C_{max}$ , 1.7 and 1.8 for SA AUC and  $C_{max}$ , as well as 1.1 for both midazolam AUC and  $C_{max}$ .

Moreover, predicted DDI and DGI effect ratios were in good agreement with observed effect ratios, as shown in **Figure 2c**. Overall, only 1 of 18 AUC effect ratios for SL and 1 of 14 AUC effect ratios for SA showed a deviation from the observed effect ratio greater than twofold. **Figure 3** summarizes the metabolic and transportation processes involved in the DDI network and visualizes the relationships between the included compounds and processes.

## Dose optimization

For each simvastatin therapeutic dose (5 to 80 mg in 5 mg steps) 648 DDGIs were optimized, which led to a total of 10,368 DDGI dose recommendations derived from the exposure marker cost function as described in Eq. 1. Cluster analysis revealed that cluster groups differ vastly with several subclusters and no observable pattern (**Figure 4a**). Thus, no generally applicable rule could be established on how to dose simvastatin.

Descriptive statistics revealed that for 13% (60 mg simvastatin therapeutic dose) to 25% (20 mg simvastatin therapeutic dose) of the investigated DDGI scenarios no alternative simvastatin dose could be found. Median optimal dose levels over all investigated DDGIs were 5 mg, 10 mg, and 20 mg for simvastatin therapeutic doses of 20 mg, 40 mg, and 60 mg, respectively. Analyses of the number of DDGIs against the optimal doses revealed a trend for all therapeutic dose levels: a greater number of DDGIs leads toward a lower optimal dose. For a therapeutic dose level of 40 mg, results are visualized in **Figure 4a** (cluster analysis), **Figure 4b** (relative frequency of optimal doses), and **Figure 4c** (number of DDGIs against optimal dose values).

DDGI network simulations were processed and transferred into a web-based interactive decision support system, which can be accessed at [simvastatin.precisiondosing.de](http://simvastatin.precisiondosing.de). The system allows users to investigate simvastatin DDGI situations of interest and explore different scenarios. Here, the user can select a given simvastatin dose, the active comedication, and the *SLCO1B1*, *ABCG2*, and *CYP3A5* genotype. Then, the application presents the optimization results, including recommended dose compared with therapeutic dose and allows the further investigation

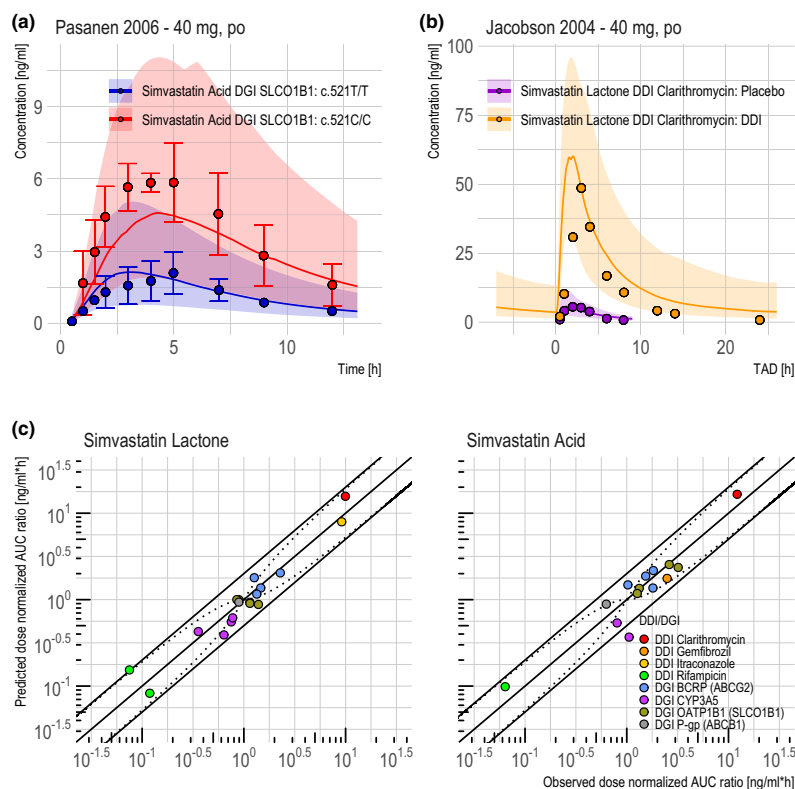


**Figure 2** Example profiles and model evaluation plots for the developed simvastatin PBPK DDGI network. **(a)** Example profiles of the observed vs. predicted simvastatin acid plasma concentration-time profiles for SLC01B1 (rs4149056) c.521C/C, and c.521T/T genotypes.<sup>54</sup> **(b)** Example profiles of the predicted vs. observed simvastatin lactone plasma concentration-time profiles with and without clarithromycin co-treatment.<sup>55</sup> In **a** and **b** dots are observed mean values extracted from literature. Error bars display the observed SDs. Solid lines show the predicted median profile of 100 simulated individuals. Shaded area depicts the predicted 90% confidence interval. **(c)** Depicts the observed vs. predicted dose normalized AUC effect ratios (dose normalized AUC under DDI/DDGI conditions divided by dose normalized AUC under placebo conditions). Solid lines show the line of identity as well as the twofold deviations. Dotted lines are the quality limits as proposed by Guest *et al.*<sup>56</sup> AUC, area under the curve; DDGI, drug-drug-gene interaction; DDI, drug-drug interaction; PBPK, physiologicallybased pharmacokinetic.

of SL and SA exposures for the placebo situation, the investigated DDGI situation, and the situation after dose optimization. **Figure 5** depicts case examples analyzed with the support system.

## DISCUSSION

PBPK modeling is increasingly applied during preclinical and clinical development allowing prospective prediction of drug exposure for various scenarios. Investigation of DDIs for regulatory labeling recommendations and problems regarding organ impairment, drug absorption, and pediatric starting dose selection demonstrated the usefulness of this class of mechanistical models in the past.<sup>26</sup> Because DDIs and DGIs can be considered as major drivers of ADRs<sup>2,4,5</sup> the application of PBPK-based MIPD to reduce the incidence of ADRs seems sensible. However, efforts toward the application of physiologically based models for MIPD are still scarce.<sup>12</sup> In this work, we investigated the adaption of PBPK modeling approaches for precision dosing regarding DDGI-sensible compounds in

complex interaction networks and the integration of finding into a decision support system.

Current techniques to address MIPD typically include Bayesian adaptive control methods.<sup>8,27</sup> However, these approaches are limited to interactions, which are already studied and implemented in the model.<sup>8</sup> An extension with other, clinically untested perpetrator or victim drugs or further genetic polymorphisms, is challenging or even impossible. In contrast, PBPK models are well-suited to tackle this limitation and are emphasized by regulatory agencies to investigate new, untested scenarios.<sup>4,8,10–12</sup> At the moment, most whole-body PBPK models purely account for interindividual variability by adapting the physiology of the underlying virtual patient. Hence, the estimation of individual parameters, as it is accomplished in Bayesian methods, is hardly feasible. Consequently, future developments should focus on connecting approaches like maximum *a posteriori* estimation to the realm of PBPK modeling in order to allow PBPK Bayesian techniques to come within reach, combining the best from both worlds. As an application example, such models could use the interindividual variability of a metabolic enzyme

ARTICLE

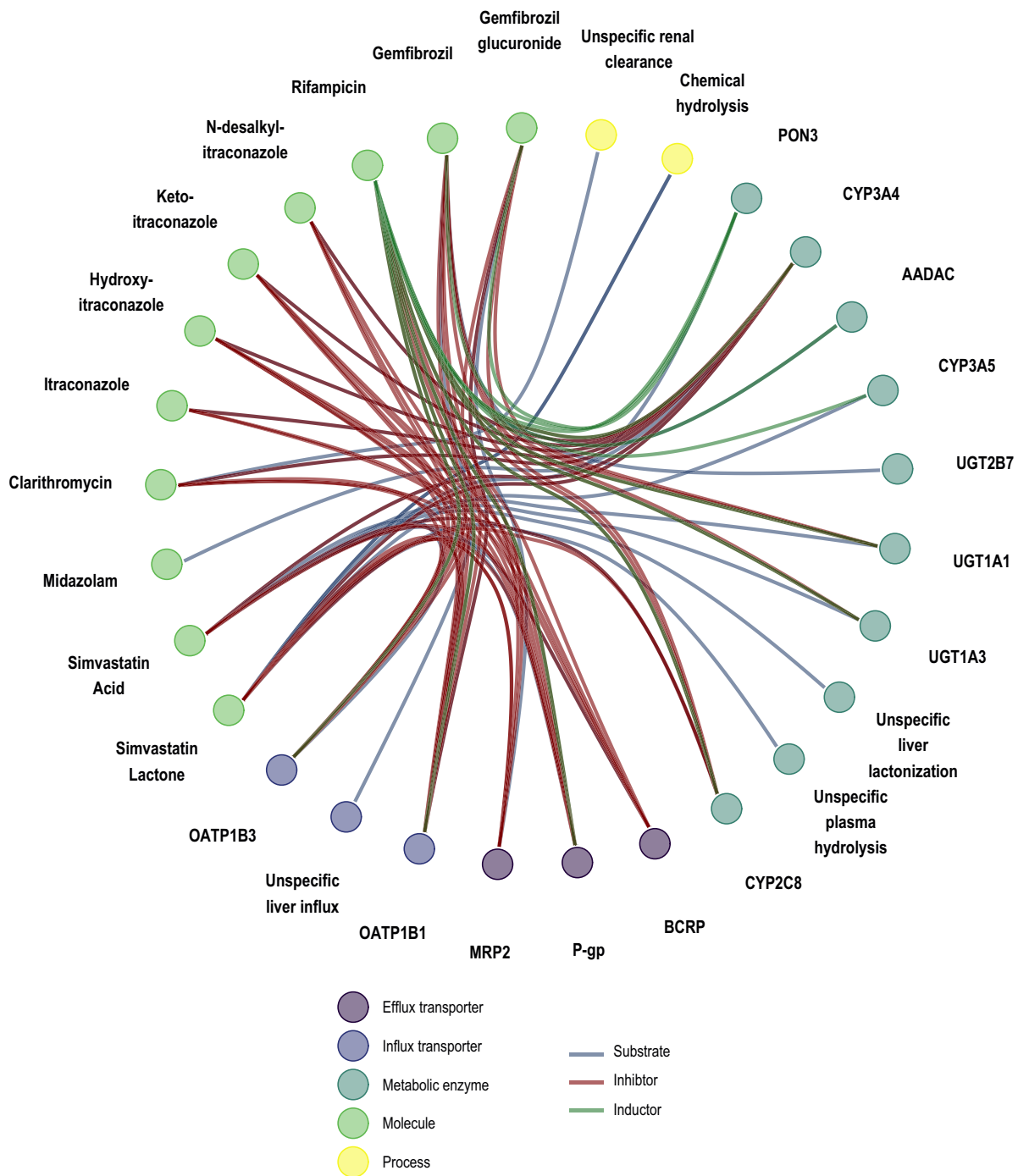


**Figure 3** Relationships between the PK pathways of the compounds included in the presented DDGI network. For the six different drugs simvastatin, itraconazole, rifampicin, gemfibrozil, clarithromycin, and midazolam metabolic, inhibitory and inductive effects are shown as lines. DDGI, drug-drug-gene interaction; PK, pharmacokinetic.

and, based on the measured individual plasma concentration of a harmless reference substance, predict the optimal treatment regime for another compound that is metabolized by this very enzyme. This will require further technical development, the availability of

sufficient individual data, and additional physiological knowledge, but could consequently improve the precision of the PBPK-based MIPD approach. Fortunately, the continuous research efforts, as for example, shown by the open systems pharmacology community,

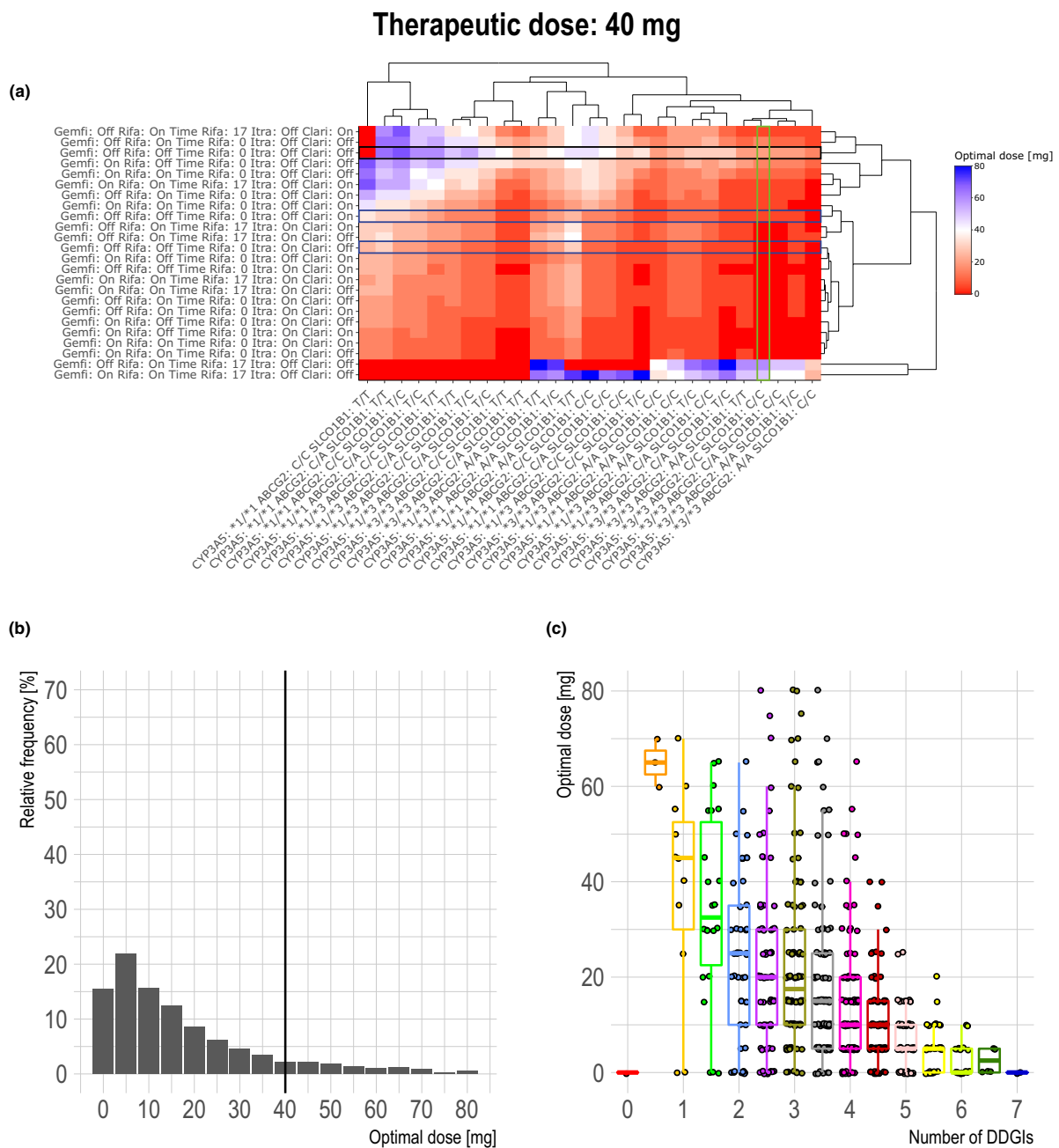


**Figure 4** Results from the dose optimization analysis. **(a)** Heatmap of the performed cluster analysis. Investigated DGIs are shown on the x-axis, whereas DDIs are listed on the y-axis. A color-coding as described on the right side of the plot depicts the optimal doses for each DDGI combination. Cluster analysis results are shown as dendrograms on the right and top site of the heatmap. Furthermore, simvastatin treatment without additional DDI-partner, single cotreatment with itraconazole or clarithromycin and the DGI situation for SLC01B1 (rs4149056) c.521C/C are highlighted with rectangles. **(b)** Shows the relative distribution of optimal doses for simvastatin. Solid lines depict the therapeutic dose. **(c)** Boxplots visualizing the number of DDGIs against the optimal simvastatin doses. All boxplots show the following descriptive statistics: The median value, the interquartile range, and the 1.5-fold interquartile range. All analyzes are shown for a therapeutic dose level of 40 mg simvastatin. DDGI, drug-drug-gene interaction; DDI, drug-drug interaction; DGI, drug-gene interaction.

constantly extend the library of available PBPK models and model features.<sup>28</sup> This progressive trend is encouraging that current knowledge and technical gaps can steadily be narrowed.

We demonstrated the applicability of physiologically based precision dosing using the example of simvastatin. Because it is among the drugs most frequently involved in major interactions,

## ARTICLE

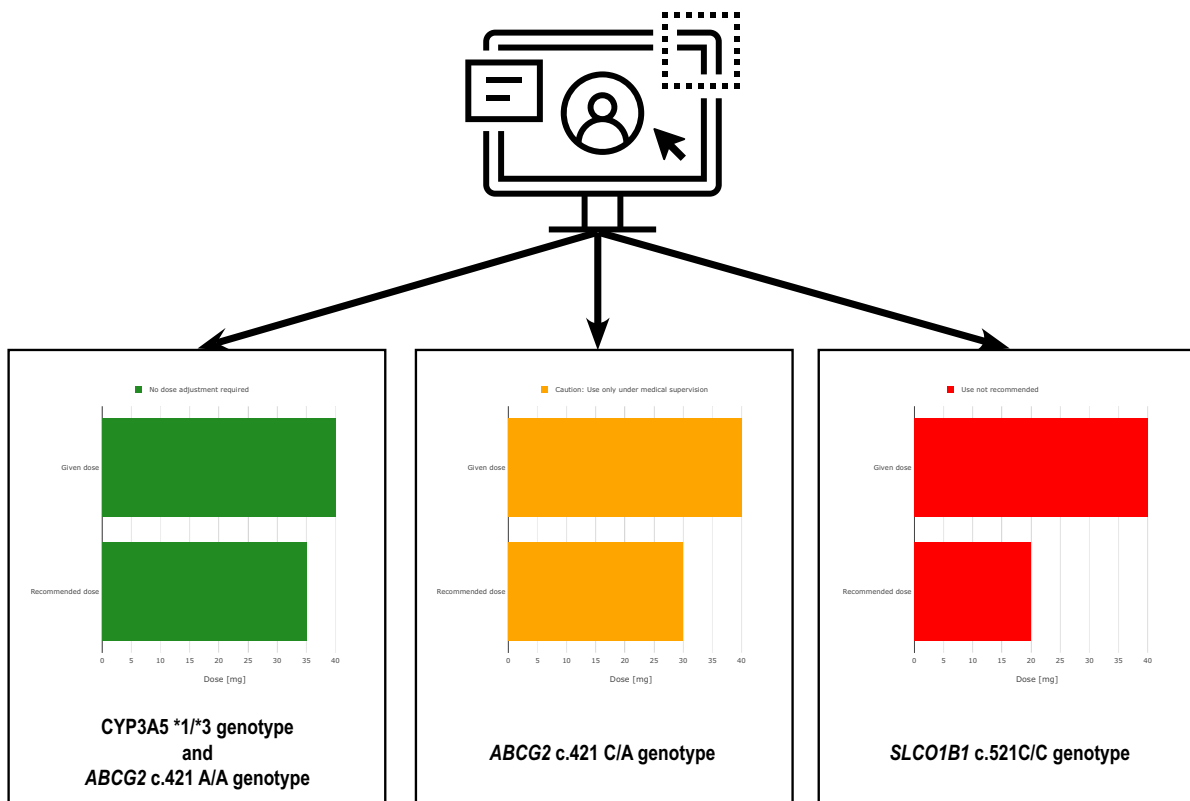


**Figure 5** Case examples analyzed with the developed decision support system. Therapeutic simvastatin dose was 40 mg and SL and SA exposure deviation were equally weighted. From left to right, different recommendations for action are given depending on the deviation between the optimal dose under DDGI condition compared with the therapeutic dose. DDGI, drug-drug-gene interaction; SA, simvastatin acid; SL, simvastatin lactone.

simvastatin is a perfect candidate to showcase the feasibility of physiologically based dose recommendations for known DGIs and comedication with frequently used DDI partners.<sup>5</sup> For simvastatin, only two whole-body or semimechanistic PBPK models are described in the literature yet.<sup>29,30</sup> Despite good predictive performance for the area of application, they typically focused on a single polymorphism (e.g., *SLCO1B1* (rs4149056)) and one DDI CYP3A4 inhibition effect. In contrast, our work vastly broadens the area of application by the successful development of a newly built whole-body simvastatin PBPK model covering multiple crucial PK processes. Subsequently, the model was connected to a comprehensive DDGI network to extensively study and simulate complex DDGI scenarios. The final model covered four important polymorphisms in the *ABCB1*, *SLCO1B1*, *ABCG2*, and *CYP3A5* genes<sup>20,31–35</sup> relevant for simvastatin's PK and was tested using previously developed and evaluated models for the perpetrators itraconazole, rifampicin, clarithromycin, gemfibrozil, and the victim midazolam.<sup>10–12,23</sup> The simvastatin network showed overall good descriptive and predictive performance and was hence used for further dose optimization analysis. Despite good performance, the model has some limitations, which are primarily caused by insufficient or lacking model input data. For example, for all studies where no information about the genotype was provided,

homozygous wild type genotypes were assumed. Fortunately, the prediction of included placebo profiles with unknown genotype showed that this assumption is sufficient to achieve good model accuracy. Information about the known polymorphism in *ABCB1* was rare and could only be included in the model training dataset and not for testing. Moreover, for some simvastatin PK pathways no data regarding their significance or activity could be gathered (see **Supplementary Material, chapter 2**). Those pathways and associated processes could either not be included in the model or their affinity ( $K_m$ ) or activity ( $k_{cat}$ ) values had to be estimated. Here, additional *in vitro* studies could help to fill this knowledge gaps in the future and, subsequently, further improve the model quality.<sup>36</sup>

Although precision dosing is considered a public health need, the amount and availability of recommendations for adjustments in case of DDGIs, including DDIs and DGIs, are lagging behind. For simvastatin, 5 pharmacogenes are listed on pharngkb.org as level 2 variants, which equals at least moderate evidence for a significant influence on the pharmacotherapy.<sup>15</sup> Yet, only for one polymorphism in *SLCO1B1* (rs4149056) recommendations on how to adapt the dose are on hand.<sup>15,37,38</sup> For the poor function *SLCO1B1* genotype (c.521C/C) low dosing, prescription of an alternative statin or routine creatine kinase surveillance is typically

recommended.<sup>37,38</sup> Our developed model-based dose recommendations agree on the Clinical Pharmacogenetics Implementation Consortium (CPIC) guideline by also recommending an alternative drug for the *SLCO1B1* c.521C/C polymorphism (see **Figure 5**).<sup>37,38</sup> The FDA drug label of simvastatin (Zocor) contraindicates the concomitant use of strong CYP3A4 inhibitors like itraconazole or clarithromycin.<sup>39</sup> This is also reflected by the presented PBPK DDGI network as shown in **Figure 4a** (red highlighting rectangles) for single clarithromycin or itraconazole cotreatment. Except for DDGIs with some CYP3A5 activity (\*1/\*1 or \*1/\*3), the model always predicts that no optimal simvastatin dose could be found (optimal dose = 0 mg). This is not surprising, because the originally published clarithromycin and itraconazole models did not include CYP3A5 inhibition (see **Supplementary Material, chapter 3**).<sup>10,23</sup> Although there are hints of CYP3A5 inhibition by itraconazole or clarithromycin in past studies, information available were too sparse to include this process in the models.<sup>40,41</sup> This lack of information is most likely due to the fact that the *CYP3A5*\*3/\*3 nonexpressor genotype is the major genotype in many populations without recent African ancestry. Although only 10–25% of Europeans have detectable levels of hepatic CYP3A5, this rate increases to 55–95% in African Americans.<sup>42–44</sup> For scenarios where CYP3A5 shows activity, it partly replaces the metabolic clearance of CYP3A4 in the network. Whether this holds true and a DDGI with clarithromycin or itraconazole and CYP3A5 only leads to a slightly increased SL exposure should be further investigated.

Apart from individual DDIs or DGIs, there is currently no recommendation for simvastatin DDGIs available.<sup>39</sup> Unfortunately, this is not only the case for simvastatin but reflects the situation for the majority of available drugs.<sup>4</sup> The standard to overcome this deficiency are clinical trials. However, due to the combinatorial explosion of possibilities for complex DDGIs exhaustive investigation via clinical studies is not feasible.<sup>4,9</sup> As shown in the performed cluster analysis (**Figure 4a**) for complicated DDGIs, no generally valid rule or therapy recommendation can be given, making it indeed necessary to investigate DDGIs on an individual level. With the rapid increase in efficiency and availability of computational resources (e.g., via cloud computing) the application of rich PBPK DDGI networks for MIPD, as shown in the presented study, seems feasible. Yet, clinical studies evaluating more complex situations like DDGIs are urgently needed to challenge, refine, and validate MIPD predictions.<sup>12</sup>

Even though the presented work exceeds the number of currently available dose recommendations by far, it still only applies to a small fraction of possible simvastatin DDGIs. Furthermore, it should be noted that dose optimization was only performed for matching exposure and not linked with a pharmacodynamic (PD) model connecting SL and SA exposure with drug efficacy like change in LDL levels or drug toxicity.<sup>43,45,46</sup> Such a PBPK/PD MIPD decision support system could enable clinicians to individually balance therapy risks and chances.<sup>47,48</sup> However, as recent investigations have shown, those models should also regard the exposure of SL, which had not been recognized for a long time.<sup>49</sup> Results from Tahaa *et al.* indicate that SL could be more relevant for drug's toxicity, whereas SA could be more important

for efficacy.<sup>49</sup> For this reason, the exposure marker cost function used for dose optimization was derived from both exposure deviations in order to account for SL exposure deviations as well. By further implementing a weighting factor, the clinician is still free to set the influence for both species individually. Nevertheless, this highlights that further models and model extensions are required to enlarge the current network. Fortunately, the established PBPK network shows enough flexibility to be extended as soon as more models for PD effects, perpetrator, or victim compounds are available.<sup>10–12,23</sup> Such models can then easily be linked with the current network and subsequently be used for further optimizations.<sup>10–12,23</sup>

The simulation analyses for DDGI scenarios were simulated for 7 days + 24 hours postdose. Although, for single drug treatment, this simulation time should be sufficient to reach PK steady-state conditions for all compounds investigated,<sup>50–53</sup> this assumption might not hold true for complex DDGI scenarios. However, as *a priori* effect estimations of complex DDGI scenarios on drug half-lives is not feasible, this should be considered for any follow-up simulation analysis.

As stated by Gonzalez and coworkers, a precision dosing strategy for clinical practice does not only rely on the development of predictive dosing models, but also on the integration into a decision support system accessible by the physician.<sup>8</sup> Thus, we provide an exemplary implementation of such a system for simvastatin to demonstrate ease of use for modeling nonexperts via a web-based solution.

In conclusion, a novel physiologically based precision dosing approach was successfully developed to study complex DDGI network scenarios for the model drug simvastatin. Findings from extensive cluster analysis of various DDGIs showed no generalized pattern for dose adjustments suggesting the need for individualized MIPD approaches to ensure effectiveness of therapy and prevention of severe ADRs. It could be demonstrated that adaption of whole-body PBPK modeling for MIPD allows the flexible extension and requalification of already established interaction networks more easily and with greater confidence for unknown scenarios than already established tooling for MIPD. Future developments should focus on enhancing the capabilities of PBPK modeling by integration of Bayesian adaptive control mechanisms like maximum *a posteriori* estimation allowing more fine-grained personalized readjustment for DDI-sensible and DGI-sensible drugs. Efforts for open access model deployment should be promoted for more widespread utilization. Besides open access to models, the integration with easy to use decision support systems is crucial to allow the adaption into clinical practice. Thus, for further use, all simvastatin DDGI network model files are publicly available (<https://github.com/Clinical-Pharmacy-Saarland-University>) and the physiologically based precision dosing decision support system is deployed for open access at [simvastatin.precisiondosing.de](http://simvastatin.precisiondosing.de).

#### SUPPORTING INFORMATION

Supplementary information accompanies this paper on the *Clinical Pharmacology & Therapeutics* website ([www.cpt-journal.com](http://www.cpt-journal.com)).

#### FUNDING

This work was funded by the Robert Bosch Stiftung (Stuttgart, Germany), the European Commission Horizon 2020 UPGx grant 668353, a grant

## ARTICLE

from the German Federal Ministry of Education and Research (BMBF 031L0188D), and the Deutsche Forschungsgemeinschaft (DFG, German Research Foundation) under Germany's Excellence Strategy—EXC 2180—390900677.

## ACKNOWLEDGMENTS

Open access funding enabled and organized by Projekt DEAL.

## CONFLICT OF INTEREST

The authors declared no competing interests for this work.

## AUTHOR CONTRIBUTIONS

J.-G.W., D.S., M.S., and T.L. wrote the manuscript. J.-G.W., M.S., and T.L. designed the research. J.-G.W. performed the research. J.-G.W., D.S., and T.L. analyzed the data.

© 2020 The Authors. *Clinical Pharmacology & Therapeutics* published by Wiley Periodicals LLC on behalf of American Society for Clinical Pharmacology and Therapeutics.

This is an open access article under the terms of the Creative Commons Attribution-NonCommercial License, which permits use, distribution and reproduction in any medium, provided the original work is properly cited and is not used for commercial purposes.

- Elsevier. Elsevier joins forces with pharmaceutical industry leaders to build new drug-drug interaction risk calculator <<https://www.elsevier.com/about/press-releases/clinical-solutions/elsevier-joins-forces-with-pharmaceutical-industry-leaders-to-build-new-drug-drug-interaction-risk-calculator>> (2019). Accessed July 12, 2020.
- US Food and Drug Administration. Preventable adverse drug reactions: a focus on drug interactions <<https://www.fda.gov/drugs/drug-interactions-labeling/preventable-adverse-drug-reactions-focus-drug-interactions>> (2018). Accessed July 12, 2020.
- Carr, T. Too many meds? America's love affair with prescription medication <<https://www.consumerreports.org/prescription-on-drugs/too-many-meds-americas-love-affair-with-prescription-medication/>> (2017). Accessed July 12, 2020.
- Malki, M.A. & Pearson, E.R. Drug-drug-gene interactions and adverse drug reactions. *Pharmacogenomics J.* **20**, 355–366 (2020).
- Verbeurgt, P., Mamiya, T. & Oesterheld, J. How common are drug and gene interactions? Prevalence in a sample of 1143 patients with CYP2C9, CYP2C19 and CYP2D6 genotyping. *Pharmacogenomics* **15**, 655–665 (2014).
- Routledge, P.A., O'Mahony, M.S. & Woodhouse, K.W. Adverse drug reactions in elderly patients. *Br. J. Clin. Pharmacol.* **57**, 121–126 (2004).
- Alhawassi, T.M., Krass, I., Bajorek, B.V. & Pont, L.G. A systematic review of the prevalence and risk factors for adverse drug reactions in the elderly in the acute care setting. *Clin. Interv. Aging* **9**, 2079–2086 (2014).
- Gonzalez, D. *et al.* Precision dosing: public health need, proposed framework, and anticipated impact. *Clin. Transl. Sci.* **10**, 443–454 (2017).
- Tornio, A., Filppula, A.M., Niemi, M. & Backman, J.T. Clinical studies on drug-drug interactions involving metabolism and transport: methodology, pitfalls, and interpretation. *Clin. Pharmacol. Ther.* **105**, 1345–1361 (2019).
- Britz, H. *et al.* Physiologically-based pharmacokinetic models for CYP1A2 drug-drug interaction prediction: a modeling network of fluvoxamine, theophylline, caffeine, rifampicin, and midazolam. *CPT Pharmacometrics Syst. Pharmacol.* **8**, 296–307 (2019).
- Hanke, N. *et al.* PBPK models for CYP3A4 and P-gp DDI prediction: a modeling network of rifampicin, itraconazole, clarithromycin, midazolam, alfentanil, and digoxin. *CPT Pharmacometrics Syst. Pharmacol.* **7**, 647–659 (2018).
- Türk, D. *et al.* Physiologically based pharmacokinetic models for prediction of complex CYP2C8 and OATP1B1 (SLCO1B1) drug–drug–gene interactions: a modeling network of gemfibrozil, repaglinide, pioglitazone, rifampicin, clarithromycin and itraconazole. *Clin. Pharmacokinet.* **58**, 1595–1607 (2019).
- Mendes, P., Robles, P.G. & Mathur, S. Statin-induced rhabdomyolysis: a comprehensive review of case reports. *Physiother. Can.* **66**, 124–132 (2014).
- Drugs.com. Simvastatin drug interactions <<https://www.drugs.com/drug-interactions/simvastatin.html>> Accessed July 5, 2020.
- Whirl-Carrillo, M. *et al.* Pharmacogenomics knowledge for personalized medicine. *Clin. Pharmacol. Ther.* **92**, 414–417 (2012).
- Talreja, O., Kerndt, C.C. & Cassagnol, M.S. StatPearls <<http://www.ncbi.nlm.nih.gov/pubmed/30422514>> (2020). Accessed July 31, 2020.
- Moßhammer, D., Schaeffeler, E., Schwab, M. & Mörike, K. Mechanisms and assessment of statin-related muscular adverse effects. *Br. J. Clin. Pharmacol.* **78**, 454–466 (2014).
- IQVIA Institute for Human Data Science. Medicine use and spending in the U.S. <<https://www.iqvia.com/insights/the-iqvia-institute/reports/medicine-use-and-spending-in-the-us-a-review-of-2018-and-outlook-to-2023>> (2019).
- Open Systems Pharmacology Community. Open systems pharmacology suite <[www.open-systems-pharmacology.org](http://www.open-systems-pharmacology.org)> (2019). Accessed July 31, 2020.
- Wojtyniak, J., Britz, H., Selzer, D., Schwab, M. & Lehr, T. Data digitizing: accurate and precise data extraction for quantitative systems pharmacology and physiologically-based pharmacokinetic modeling. *CPT Pharmacometrics Syst. Pharmacol.* **9**, 322–331 (2020).
- R Core Team. *R: A Language and Environment for Statistical Computing* <<https://www.r-project.org/>> (2020).
- Hanke, N. *et al.* PBPK models for CYP3A4 and P-gp DDI prediction: a modeling network of rifampicin, itraconazole, clarithromycin, midazolam, alfentanil, and digoxin. *CPT Pharmacometrics Syst. Pharmacol.* **7**, 647–659 (2018).
- Moj, D. *et al.* Clarithromycin, midazolam, and digoxin: application of PBPK modeling to gain new insights into drug-drug interactions and co-medication regimens. *AAPS J.* **19**, 298–312 (2017).
- Edgington, A.N., Schmitt, W. & Willmann, S. Development and evaluation of a generic physiologically based pharmacokinetic model for children. *Clin. Pharmacokinet.* **45**, 1013–1034 (2006).
- Morley, S.K., Brito, T.V. & Welling, D.T. Measures of model performance based on the log accuracy ratio. *Space Weather* **16**, 69–88 (2018).
- Wagner, C. *et al.* Application of physiologically based pharmacokinetic (PBPK) modeling to support dose selection: report of an FDA public workshop on PBPK. *CPT Pharmacometrics Syst. Pharmacol.* **4**, 226–230 (2015).
- Mould, D.R., D'Haens, G. & Upton, R.N. Clinical decision support tools: the evolution of a revolution. *Clin. Pharmacol. Ther.* **99**, 405–418 (2016).
- Lippert, J. *et al.* Open systems pharmacology community—an open access, open source, open science approach to modeling and simulation in pharmaceutical sciences. *CPT Pharmacometrics Syst. Pharmacol.* **8**, 878–882 (2019).
- Lippert, J. *et al.* A mechanistic, model-based approach to safety assessment in clinical development. *CPT Pharmacometrics Syst. Pharmacol.* **1**, e13 (2012).
- Tsamandouras, N. *et al.* Development and application of a mechanistic pharmacokinetic model for simvastatin and its active metabolite simvastatin acid using an integrated population PBPK approach. *Pharm. Res.* **32**, 1864–1883 (2015).
- Kim, K.-A., Park, P.-W., Lee, O.-J., Kang, D.-K. & Park, J.-Y. Effect of polymorphic CYP3A5 genotype on the single-dose simvastatin pharmacokinetics in healthy subjects. *J. Clin. Pharmacol.* **47**, 87–93 (2007).

32. Choi, H.Y. *et al.* Impact of CYP2D6, CYP3A5, CYP2C19, CYP2A6, SLC01B1, ABCB1, and ABCG2 gene polymorphisms on the pharmacokinetics of simvastatin and simvastatin acid. *Pharmacogenet. Genomics* **25**, 595–608 (2015).
33. Pasanen, M.K., Neuvonen, M., Neuvonen, P.J. & Niemi, M. SLC01B1 polymorphism markedly affects the pharmacokinetics of simvastatin acid. *Pharmacogenet. Genomics* **16**, 873–879 (2006).
34. Keskitalo, J.E., Pasanen, M.K., Neuvonen, P.J. & Niemi, M. Different effects of the ABCG2 c.421C>A SNP on the pharmacokinetics of fluvastatin, pravastatin and simvastatin. *Pharmacogenomics* **10**, 1617–1624 (2009).
35. Keskitalo, J.E., Kurkinen, K.J., Neuvonen, P.J. & Niemi, M. ABCB1 haplotypes differentially affect the pharmacokinetics of the acid and lactone forms of simvastatin and atorvastatin. *Clin. Pharmacol. Ther.* **84**, 457–461 (2008).
36. Kuepfer, L. *et al.* Applied concepts in PBPK modeling: how to build a PBPK/PD model. *CPT Pharmacometrics Syst. Pharmacol.* **5**, 516–531 (2016).
37. Bank, P. *et al.* Comparison of the Guidelines of the Clinical Pharmacogenetics Implementation Consortium and the Dutch Pharmacogenetics Working Group. *Clin. Pharmacol. Ther.* **103**, 599–618 (2018).
38. Ramsey, L.B. *et al.* The clinical pharmacogenetics implementation consortium guideline for SLC01B1 and simvastatin-induced myopathy: 2014 update. *Clin. Pharmacol. Ther.* **96**, 423–428 (2014).
39. Merck & Co., Inc. Zocor (Simvastatin) [package insert]. U.S. Food and Drug Administration website <[https://www.accessdata.fda.gov/drugsatfda\\_docs/label/2019/019766s100lbl.pdf](https://www.accessdata.fda.gov/drugsatfda_docs/label/2019/019766s100lbl.pdf)> Accessed July 5, 2020.
40. Shirasaka, Y. *et al.* Effect of CYP3A5 expression on the inhibition of CYP3A-catalyzed drug metabolism: impact on modeling CYP3A-mediated drug-drug interactions. *Drug Metab. Dispos.* **41**, 1566–1574 (2013).
41. Michaud, V. & Turgeon, J. Assessment of competitive and mechanism-based inhibition by clarithromycin: use of domperidone as a CYP3A probe-drug substrate and various enzymatic sources including a new cell-based assay with freshly isolated human hepatocytes. *Drug Metab. Lett.* **4**, 69–76 (2010).
42. Bains, R.K. *et al.* Molecular diversity and population structure at the cytochrome P450 3A5 gene in Africa. *BMC Genet.* **14**, 34 (2013).
43. Scherer, N., Dings, C., Böhm, M., Laufs, U. & Lehr, T. Alternative treatment regimens with the PCSK9 inhibitors alirocumab and evolocumab: a pharmacokinetic and pharmacodynamic modeling approach. *J. Clin. Pharmacol.* **57**, 846–854 (2017).
44. Kuehl, P. *et al.* Sequence diversity in CYP3A promoters and characterization of the genetic basis of polymorphic CYP3A5 expression. *Nat. Genet.* **27**, 383–391 (2001).
45. Kim, J. *et al.* A population pharmacokinetic-pharmacodynamic model for simvastatin that predicts low-density lipoprotein-cholesterol reduction in patients with primary hyperlipidaemia. *Basic Clin. Pharmacol. Toxicol.* **109**, 156–163 (2011).
46. Tsamandouras, N. *et al.* Identification of the effect of multiple polymorphisms on the pharmacokinetics of simvastatin and simvastatin acid using a population-modeling approach. *Clin. Pharmacol. Ther.* **96**, 90–100 (2014).
47. Marshall, S. *et al.* Model-informed drug discovery and development: current industry good practice and regulatory expectations and future perspectives. *CPT Pharmacometrics Syst. Pharmacol.* **8**, 87–96 (2019).
48. EFPIA MID3 Workgroup, *et al.* Good practices in model-informed drug discovery and development: practice, application, and documentation. *CPT Pharmacometrics Syst. Pharmacol.* **5**, 93–122 (2016).
49. Taha, D.A. *et al.* The role of acid-base imbalance in statin-induced myotoxicity. *Transl. Res.* **174**, 140–160.e14 (2016).
50. Todd, P.A. & Ward, A.G. A review of its pharmacodynamic and pharmacokinetic properties, and therapeutic use in dyslipidaemia. *Drugs* **36**, 314–339 (1988).
51. Acocella, G. Clinical pharmacokinetics of rifampicin. *Clin. Pharmacokinet.* **3**, 108–127 (1978).
52. Heykants, J. *et al.* The clinical pharmacokinetics of itraconazole: an overview. *Mycoses* **32**(suppl. 1), 67–87 (1989).
53. Rodvold, K.A. Clinical pharmacokinetics of clarithromycin. *Clin. Pharmacokinet.* **37**, 385–398 (1999).
54. Pasanen, M.K., Fredrikson, H., Neuvonen, P.J. & Niemi, M. Different effects of SLC01B1 polymorphism on the pharmacokinetics of atorvastatin and rosuvastatin. *Clin. Pharmacol. Ther.* **82**, 726–733 (2007).
55. Jacobson, T.A. Comparative pharmacokinetic interaction profiles of pravastatin, simvastatin, and atorvastatin when coadministered with cytochrome P450 inhibitors. *Am. J. Cardiol.* **94**, 1140–1146 (2004).
56. Guest, E.J., Aarons, L., Houston, J.B., Rostami-Hodjegan, A. & Galetin, A. Critique of the two-fold measure of prediction success for ratios: application for the assessment of drug-drug interactions. *Drug Metab. Dispos.* **39**, 170–173 (2011).



## Part III

### DISCUSSION AND CONCLUSIONS

The chapter provides a comprehensive and concluding discussion of the results presented in this thesis.



## DISCUSSION

---

Our modern healthcare and economic system is heavily burdened by ADRs and ADEs [7, 8]. Significant drivers of ADRs and ADEs are DDIs, DGIs, and DDGIs [17, 19, 82]. A promising solution to overcome them, is to improve the drug development process by MID3 as well as to optimize post-marketing drug therapy regimen by MIPD techniques [3, 50, 51]. PBPK modeling, which belongs to the MID3 and MIPD portfolio, is particularly useful for this purpose as it can also reduce the number of expensive and complex clinical trials that would otherwise have had to be carried out to investigate the DDGIs [52, 83–85].

Thus, the presented work had three objectives. Namely, to improve the PBPK modeling workflow, to support the drug development process of the NTE zoptarelin doxorubicin and to propose therapy recommendations for simvastatin DDGIs including the development of a DSS.

### 4.1 DATA DIGITIZING FOR MODEL DEVELOPMENT

The first publication presented in this thesis focused on data digitizing as an important cornerstone of PBPK and QSP modeling (see Section 3.1). Commonly, PBPK models rely on *a priori* information for estimating unknown system and drug dependent parameters [1, 74–79]. Hence, the quality and accuracy of a PBPK model is correlated with the amount of data and information available for parameter estimation [86]. Moreover, like for other predictive models, training and test data are necessary to evaluate the predictive performance of PBPK models [1, 78, 87]. Unfortunately, if published, the necessary information and in particular, clinical time-dependent data like plasma-concentration time profiles are rarely available as tabulated numerical values as described in Section 3.1. They are often presented in a condensed way as mean profiles and in the form of graphs (see Section 3.1). This is where data digitizing is a useful and increasingly used technique to translate the graphical presentation into numerical values to overcome potential knowledge gaps [1]. As shown in Section 3.1, a 16 % increase per year in publications citing digitizing software together with PBPK or QSP was found. It was also observed that the investigated digitizing software showed an overwhelming precision with a mean median symmetric accuracy (MSA) of 0.99 % [1]. In contrast, it was noticed that digitized data errors are rather related to preexisting inconsistencies in the published manuscripts.

These findings are of high importance also for the established simvastatin PBPK DDGI network, as presented in Section 3.3 and Section A.3, because a PBPK model developed with biased data, could lead to false predictions [1, 52, 88]. Following, this can result in unsafe dose recommendations which pose potentially harm for patients [1, 52, 88]. For this reason, it is important to follow the workflow presented in Section 3.1, which includes some quality control (QC) approaches to verify data quality and integrity. If identified inconsistencies cannot be resolved, the digitized data should be used very carefully and only if they are critical for model development. To mitigate the risk of "outlier data" that subsequently bias the final PBPK model, one could follow the law of large numbers and increase the number of digitized studies [89]. For example, in the model presented in Section 3.3 and Section A.3, in total 132 simvastatin lactone (SL) and SA profiles were digitized to reduce the impact of single, potentially biased profiles.

Another approach for identifying model misspecifications is the aforementioned use of training and test datasets as shown in Figure 1.5. However, for PBPK modeling, currently, no best practices how to separate the available data in test and training datasets are established. In contrast, for other predictive modeling strategies, recommendations are on hand [87, 90]. For example, one regular approach is to follow the Pareto principle, which would mean a random distribution of all data available at a ratio of 80 to 20 in training and test dataset [87, 90–92]. Nevertheless, this would only make limited sense for developing a PBPK model, since, as shown in Section 3.3 and Section A.3, literature data are only sparsely available for many investigated effects. For example, for most of the investigated DDIs only one profile and sometimes only a single peak plasma concentration ( $C_{\max}$ ) or AUC value were on hand (see Section 3.3 and Section A.3).

Another problem is that many sampling points have a dependence on the study in which they were generated. However, especially time-dependent measurements differ in the number and distribution of sampling points per study (see Section A.3). Thus, not every profile is suitable for informing a model regarding, for instance, terminal elimination or  $C_{\max}$ . For the two reasons mentioned above, a purely random split could easily lead to uneven distribution, making either the implementation of an effect or its evaluation impossible [92]. Therefore, for most published PBPK models, a subjective, manual division of the data into test and training was performed [74–79]. The influence of this procedure on model quality, as well as rational, alternative best practices should be part of further investigations.

#### 4.2 ZOPTARELIN DOXORUBICIN DRUG-DRUG INTERACTION POTENTIAL

The second publication aimed to assess the DDI potential of zoptarelin doxorubicin concerning OATP1B3 and OCT2 (see Section 3.2 and

Section A.2). The detection and characterization of DDIs is an integral part of drug development, and detailed regulatory guidance on this topic is available [27, 93, 94]. Experiments for DDI characterization are commonly carried out in the preclinical development phase to identify drug interaction potentials [94]. Unfortunately, the translation of these preclinical results into clinical effects proves to be difficult [3, 94]. For this reason, extensive clinical studies have to be carried out regularly [27]. However, this is problematic in particular for oncological substances [24, 25]. As cancer patients receive many drugs at once that cannot be discontinued during a clinical study, they are very susceptible to DDIs [24, 25]. This circumstance also makes the interpretation of clinical study results difficult [24, 25]. In addition, the performance of such studies with NTEs whose efficacy and toxicity have not yet been conclusively investigated can be ethically challenging [2]. All in all, new techniques are needed to better translate the preclinical data and possibly avoid clinical studies altogether [2].

Two such approaches were presented in detail in Section 3.2. The first promising technique utilized PBPK modeling to predict unbound tissue concentration of zoletarelin doxorubicin in organs where OATP1B3 and OCT2 are expressed. Subsequently, a relative change of apparent Michaelis-Menten constant ( $K_M$ ) and transportation velocity of OATP1B3 and OCT2 could be calculated, indicating a limited risk for a clinical relevant DDI. Going even further; by developing additional PBPK models for the OATP1B3 and OCT2 substrates simvastatin and metformin, clinical worst-case scenarios were predicted further confirming this assumption (see Section 3.2). Besides, these precursor models of simvastatin and metformin laid the foundation for further DDGI networks as shown in Section 3.3 and by Hanke et al. [80].

#### 4.3 SIMVASTATIN DRUG-DRUG-GENE INTERACTION NETWORK

The third publication dealt with the development of a simvastatin PBPK DDGI network, the derivation of dose recommendations, and the establishment of a DSS (see Section 3.3).

Simvastatin shows a complex PK, which is influenced by several DDIs and DGIs (see Figure 1.3). Despite several available PK models for simvastatin, no recommendations for potential DDGIs are on hand so far [3, 39, 95–98]. This could be because previously developed models were only empirical or semi-mechanistical simvastatin PK models [3, 39, 95–98]. Although they are well suited to study single influencing factors, they are limited in their extensibility [59]. For instance, for each feature added to such a model, additional study data are required to quantify the observed effects [59]. In contrast, whole-body PBPK models are capable of also predicting unobserved DDIs by coupling individually developed models together as depicted in Figure 1.7 [74–79]. Thus, even if the presented simvastatin model (see Section 3.3)

does currently not cover every conceivable simvastatin DDGIs, it can be easily extended to do so. Fortunately, due to the active scientific community, likely, further perpetrator and victim models will soon be available, which then can be coupled with the established simvastatin model to derive further recommendations for DDGIs [99].

Besides, a particular focus was placed on the correct implementation of cytochrome P450 3A4 (CYP3A4). Cytochrome P450 (CYP) enzymes account for roundabout 75 % of the total drug metabolism [100] and CYP3A4 in particular, has a leading role within the CYP family [101], as shown in Figure 4.1. This also applies to simvastatin whereas CYP3A4 is the most influencing metabolic enzyme of simvastatin's PK and also responsible for many of simvastatin related DDIs (see Section 3.3 and Section A.3).

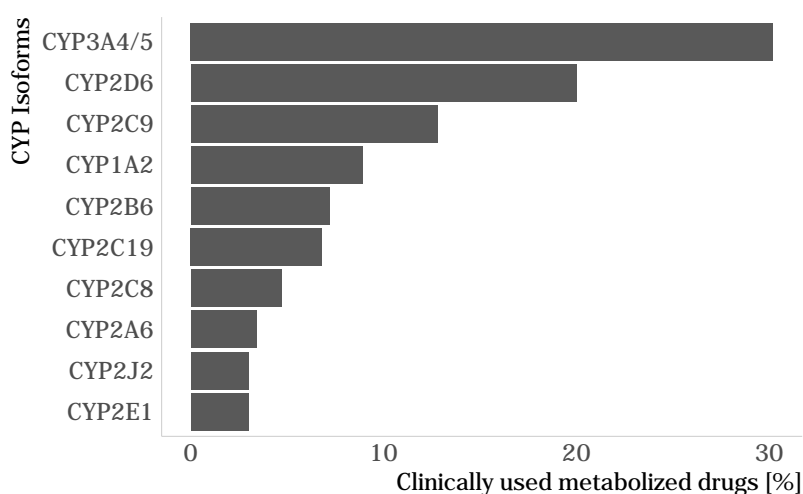


Figure 4.1: Fraction of clinically used drugs metabolized by various CYP isoforms [101].

To validate the correct implementation of CYP3A4 into the model, it was extensively evaluated as shown in Section A.3. This includes, as recommended by the recently released EMA guideline on how to report a PBPK model, sensitivity analyses [102]. Thereby, the final sensitivity analysis, as presented in Section A.3 nicely showed the importance of CYP3A4 on SL and SA exposure in the model.

Although several different DDIs and DGIs could be predicted accurately by the presented work, it has to be noted that some of the data available may only be of limited credibility for model evaluation. By performing QCs measures as described in Section 3.1, several studies revealed unexpected heterogeneity regarding their presented data. For example, Choi et al. [103] listed AUC and  $C_{max}$  values for many different DGIs. However, QCs revealed that presented dose-normalized values shown by Choi et al. [103] for SA were significant and consis-

tently larger than to most of the studies available (see Section A.3). A possible explanation could have been the ethnicity of the study populations. While most of the available studies recruited predominantly Caucasians, it can be assumed that Choi et al. [103], because their study was conducted in Korea, had mainly involved Koreans. The assumption of PK differences for simvastatin among various ethnic groups was partly confirmed by another recent study focusing on simvastatin PK changes between the three East Asian populations and Caucasian's [104].

Another problem concerning the NCA values' quality was encountered in the DDI study with itraconazole [105]. In this study for quantification of SL and SA exposure, different analysis techniques (high-performance liquid chromatography (HPLC) and gas chromatography–mass spectrometry (GC-MS)) were used. As a result the lower limit of detection (LLOD) for SL was high ( $10 \text{ ng ml}^{-1}$ ), which led to many SL samples below the LLOD in the placebo phase. Moreover, in the same study, SA was quantified as total SA after hydrolysis of SL and other SL metabolites in the probes. All in all, this meant that the plasma concentration-time profiles given by Neuvonen, Kantola, and Kivistö [105] could not directly be used for model evaluation. Similar conclusions were drawn by Tsamandouras et al. [95] in his attempt of reusing the data for model evaluation. Luckily, Neuvonen, Kantola, and Kivistö [105] stated that for SL an at least 10-fold increase in exposure under itraconazole co-treatment was observed compared to placebo. This value was subsequently used for model evaluation. In contrast, a published increase of SA exposure was not be used for evaluation since, due to assay limitations mentioned earlier, it could not be compared to any model output.

Both examples, the data from Choi et al. [103] and Neuvonen, Kantola, and Kivistö [105], highlight the necessity of additional DDI and DGI or even DDGI intervention studies to support further PBPK model development and evaluation. Also, the same conclusion as drawn in Section 3.1 applies. Instead of condensed information, the complete study protocol and observed raw values for such interaction studies should be available. This way, for example, the question of which ethnicity the participants in the study performed by Choi et al. [103] belong to could have been answered.

After model development and evaluation, the final model was used to optimize several DDGI scenarios using matching exposure. For this purpose, a combined exposure marker for SL and SA was derived as described in Section 3.3. An alternative approach would have been to couple the model with a suitable PD model extension. However, this was waived since neither an appropriate extension was available nor the necessary data were on hand. For example, in a study by Lippert et al. [96] a toxicodynamic marker for simvastatin acid was derived as a

function of solute carrier organic anion transporter family member 1B1 (OATP1B1) transporter activity. However, this toxicodynamic marker would not have been suitable for the presented work since the aim was to cover several DDGIs, some of them not focusing on OATP1B1. Moreover, as described by Taha et al. [106] there is evidence that the toxicokinetic of simvastatin is more dependent on exposure of SL compared to SA. Thus, a suitable PD model extension should differentiate between the effects of SL and SA exposure. Moreover, it should not only focus on simvastatin toxicokinetics but also cover therapy relevant efficacy biomarkers like low-density lipoprotein cholesterol (LDL-C) [107]. If both components, efficacy and toxicity of simvastatin, would be covered by a PD model extension, it could be coupled with the presented simvastatin PK model to calculate a therapy related net clinical benefit (NCB) [108]. The NCB could subsequently be used to compare different therapy regimens and optimize them under DDGIs conditions based on hard endpoints like probabilities for ADEs or therapy success rates. Similar approaches can already be found in the literature [109]. However, until then, matching exposure is a suitable alternative as this approach is, for instance, recommended for other applications like pediatric extrapolation [110].

The results from the dose optimization process were afterward transferred into an interactive DSS that allows deriving MIPD recommendations tailored to each DDGI of interest (see Section 3.3). However, it has to be noted that although PBPK modeling is emphasized for the prediction of DDIs and DGIs [51, 66, 70–72, 76] further evaluation whether also complicated DDGIs can be predicted using PBPK modeling, is still pending.

Apart from that, the developed DSS has yet to prove its acceptance and usefulness in clinical practice. For this purpose, further studies and user surveys should be conducted. Those could focus on the perceived usefulness and the perceived ease-of-use of the tool as parameters related to the probability that a technology will be accepted by potential users [111, 112]. Nevertheless, even if further evaluations of the presented DSS are needed, it shows exemplarily how MIPD can be truly brought from pure theory to the patient's bedside [48].



## CONCLUSIONS

---

The presented work added valuable knowledge on improving digitized data quality, necessary for PBPK model development and evaluation. This will most likely also affect the accuracy of the developed PBPK models and thus their quality for use in MID3 and MIPD. Further, it was shown how to assess the DDI potential of NTEs based on the example of zoptarelin doxorubicin using PBPK MID3 techniques instead of ethically challenging clinical DDI studies. Moreover, complex DDGIs scenarios for simvastatin were addressed with a PBPK MIPD approach. Finally, the derived simvastatin therapy recommendations were made available online in the form of a newly developed DSS. Since PBPK MIPD is a novel approach in the management of DDGIs, additional studies will be necessary to conclusively evaluate this technique, especially in the prevention of ADEs.



## BIBLIOGRAPHY

---

- [1] **Jan-Georg Wojtyniak** et al. "Data digitizing: accurate and precise data extraction for quantitative systems pharmacology and physiologically-based pharmacokinetic modeling." In: *CPT: Pharmacometrics & Systems Pharmacology* 9.6 (June 2020), pp. 322–331. DOI: 10.1002/psp4.12511.
- [2] Nina Hanke et al. "A physiologically based pharmacokinetic (PBPK) parent-metabolite model of the chemotherapeutic zoptarelin doxorubicin — integration of in vitro results, Phase I and Phase II data and model application for drug-drug interaction potential analysis." In: *Cancer Chemotherapy and Pharmacology* 81.2 (Feb. 2018), pp. 291–304. DOI: 10.1007/s00280-017-3495-2.
- [3] **Jan-Georg Wojtyniak** et al. "Physiologically based precision dosing approach for drug-drug-gene interactions: a simvastatin network analysis." In: *Clinical Pharmacology & Therapeutics* (Dec. 2020). DOI: 10.1002/cpt.2111.
- [4] Alex O. Holcombe. "Contributorship, not authorship: use CRediT to indicate who did what." In: *Publications* 7.3 (July 2019), p. 48. DOI: 10.3390/publications7030048.
- [5] Amy Brand et al. "Beyond authorship: attribution, contribution, collaboration, and credit." In: *Learned Publishing* 28.2 (Apr. 2015), pp. 151–155. DOI: 10.1087/20150211.
- [6] Eugen Roth. *Ernst und heiter*. München: Deutscher Taschenbuch Verlag, 1976. ISBN: 3423000104.
- [7] J. Lazarou, B. H. Pomeranz, and P. N. Corey. "Incidence of adverse drug reactions in hospitalized patients." In: *Journal of the American Medical Association* 279.15 (Apr. 1998), pp. 1200–1205. ISSN: 0098-7484. DOI: 10.1001/jama.279.15.1200.
- [8] D. Formica et al. "The economic burden of preventable adverse drug reactions: a systematic review of observational studies." In: *Expert Opinion on Drug Safety* 17.7 (July 2018), pp. 681–695. ISSN: 1744-764X. DOI: 10.1080/14740338.2018.1491547.
- [9] IQVIA Institute for Human Data Science. *Medicine Use and Spending in the U.S. A Review of 2018 and Outlook to 2023*. 2019. URL: <https://www.iqvia.com/insights/the-iqvia-institute/reports/medicine-use-and-spending-in-the-us-a-review-of-2018-and-outlook-to-2023> (visited on 10/31/2020).

- [10] IQVIA Institute for Human Data Science. *Total nominal spending on medicines in the U.S. from 2002 to 2018*. Ed. by Statista. 2020. URL: <https://www.statista.com/statistics/238689/us-total-expenditure-on-medicine/> (visited on 05/10/2020).
- [11] Patrick Vallance and Trevor G. Smart. "The future of pharmacology." In: *British Journal of Pharmacology* 147.S1 (Jan. 2006), pp. 304–307. ISSN: 0007-1188. DOI: 10.1038/sj.bjp.0706454.
- [12] Jamie J. Coleman and Sarah K. Pontefract. "Adverse drug reactions." In: *Clinical Medicine* 16.5 (Oct. 2016), pp. 481–485. ISSN: 1473-4893. DOI: 10.7861/clinmedicine.16-5-481.
- [13] J. E. Campbell, M. Gossell-Williams, and M. G. Lee. "A review of pharmacovigilance." In: *West Indian Medical Journal* 63.7 (Dec. 2014), pp. 771–774. ISSN: 0043-3144. DOI: 10.7727/wimj.2013.251.
- [14] Thomas M. Polasek, Sepehr Shakib, and Amin Rostami-Hodjegan. "Precision dosing in clinical medicine: present and future." In: *Expert Review of Clinical Pharmacology* 11.8 (Aug. 2018), pp. 743–746. ISSN: 1751-2441. DOI: 10.1080/17512433.2018.1501271.
- [15] Thomas M. Polasek, Carl M. J. Kirkpatrick, and Amin Rostami-Hodjegan. "Precision dosing to avoid adverse drug reactions." In: *Therapeutic Advances in Drug Safety* 10 (Dec. 2019). ISSN: 2042-0986. DOI: 10.1177/2042098619894147.
- [16] Daniel Gonzalez et al. "Precision dosing: public health need, proposed framework, and anticipated impact." In: *Clinical and Translational Science* 10.6 (Nov. 2017), pp. 443–454. ISSN: 1752-8062. DOI: 10.1111/cts.12490.
- [17] Paul Westervelt et al. "Drug-gene interactions: inherent variability in drug maintenance dose requirements." In: *P & T* 39.9 (Sept. 2014), pp. 630–637. ISSN: 1052-1372.
- [18] Dan M. Roden et al. "Pharmacogenomics." In: *The Lancet* 394.10197 (Aug. 2019), pp. 521–532. DOI: 10.1016/s0140-6736(19)31276-0.
- [19] K. A. Phillips et al. "Potential role of pharmacogenomics in reducing adverse drug reactions." In: *Journal of the American Medical Association* 286.18 (Nov. 2001), pp. 2270–2279. ISSN: 0098-7484. DOI: 10.1001/jama.286.18.2270.
- [20] Aleksi Tornio et al. "Clinical studies on drug–drug interactions involving metabolism and transport: methodology, pitfalls, and interpretation." In: *Clinical Pharmacology & Therapeutics* 105.6 (June 2019), pp. 1345–1361. ISSN: 1532-6535. DOI: 10.1002/cpt.1435.

- [21] Mustafa Adnan Malki and Ewan Robert Pearson. "Drug–drug–gene interactions and adverse drug reactions." In: *The Pharmacogenomics Journal* 20.3 (Dec. 2019), pp. 355–366. ISSN: 1473-1150. DOI: 10.1038/s41397-019-0122-0.
- [22] Camelia Bucşa et al. "How many potential drug–drug interactions cause adverse drug reactions in hospitalized patients?" In: *European Journal of Internal Medicine* 24.1 (Jan. 2013), pp. 27–33. ISSN: 1879-0828. DOI: 10.1016/j.ejim.2012.09.011.
- [23] Maria Cristina Soares Rodrigues and Cesar de Oliveira. "Drug–drug interactions and adverse drug reactions in polypharmacy among older adults: an integrative review." In: *Revista Latino-Americana de Enfermagem* 24 (Sept. 2016), e2800. ISSN: 1518-8345. DOI: 10.1590/1518-8345.1316.2800.
- [24] R. Riechelmann and D. Girardi. "Drug interactions in cancer patients: a hidden risk?" In: *Journal of Research in Pharmacy Practice* 5.2 (2016), pp. 77–78. DOI: 10.4103/2279-042X.179560.
- [25] Lauren A. Mar cath et al. "Prevalence of drug–drug interactions in oncology patients enrolled on National Clinical Trials Network oncology clinical trials." In: *BMC Cancer* 18.1 (Nov. 2018), p. 1155. DOI: 10.1186/s12885-018-5076-0.
- [26] M. Whirl-Carrillo et al. "Pharmacogenomics knowledge for personalized medicine." In: *Clinical Pharmacology and Therapeutics* 92.4 (Oct. 2012), pp. 414–417. ISSN: 1532-6535. DOI: 10.1038/clpt.2012.96.
- [27] Food and Drug Administration Center for Drug Evaluation Research. *Clinical Drug Interaction Studies — Cytochrome P450 Enzyme- and Transporter-Mediated Drug Interactions Guidance for Industry*. 2020. URL: <https://www.fda.gov/media/134581/download> (visited on 10/31/2020).
- [28] Curt D. Furberg. "To whom do the research findings apply?" In: *Heart* 87.6 (June 2002), pp. 570–574. ISSN: 1468-201X. DOI: 10.1136/heart.87.6.570.
- [29] Christina J. Charlesworth et al. "Polypharmacy among adults aged 65 years and older in the united states: 1988–2010." In: *The Journals of Gerontology Series A: Biological Sciences and Medical Sciences* 70.8 (Aug. 2015), pp. 989–995. ISSN: 1758-535X. DOI: 10.1093/gerona/glv013.
- [30] J. Engel et al. "AEZS-108: a targeted cytotoxic analog of LHRH for the treatment of cancers positive for LHRH receptors." In: *Expert Opinion on Investigational Drugs* 21.6 (June 2012), pp. 891–899. DOI: 10.1517/13543784.2012.685128.
- [31] PubChem. *Compound summary zoptarelin doxorubicin*. URL: <https://pubchem.ncbi.nlm.nih.gov/compound/16134409> (visited on 10/18/2020).

- [32] Christopher Stomberg et al. "A cost-effectiveness analysis of over-the-counter statins." In: *The American Journal of Managed Care* 22.5 (May 2016), e294–e303. ISSN: 1936-2692.
- [33] Huseyin Naci, Jasper Brugts, and Tony Ades. "Comparative tolerability and harms of individual statins." In: *Circulation: Cardiovascular Quality and Outcomes* 6.4 (July 2013), pp. 390–399. ISSN: 1941-7705. DOI: 10.1161/circoutcomes.111.000071.
- [34] Polyana Mendes, Priscila Games Robles, and Sunita Mathur. "Statin-induced rhabdomyolysis: a comprehensive review of case reports." In: *Physiotherapy Canada* 66.2 (Apr. 2014), pp. 124–132. ISSN: 0300-0508. DOI: 10.3138/ptc.2012-65.
- [35] Kenneth A. Kellick et al. "A clinician's guide to statin drug-drug interactions." In: *Journal of Clinical Lipidology* 8.3 (May 2014), pp. 30–46. ISSN: 1933-2874. DOI: 10.1016/j.jacl.2014.02.010.
- [36] Takeshi Hirota and Ichiro Ieiri. "Drug–drug interactions that interfere with statin metabolism." In: *Expert Opinion on Drug Metabolism & Toxicology* 11.9 (June 2015), pp. 1435–1447. ISSN: 1744-7607. DOI: 10.1517/17425255.2015.1056149.
- [37] Stefano Bellosta, Rodolfo Paoletti, and Alberto Corsini. Safety of Statins: Focus on Clinical Pharmacokinetics and Drug Interactions. In: *Circulation* vol. 109.S23 (June 2004), pp. 50–57. ISSN: 1524-4539. DOI: 10.1161/01.CIR.0000131519.15067.1f.
- [38] M. Niemi. "Transporter pharmacogenetics and statin toxicity." In: *Clinical Pharmacology & Therapeutics* 87.1 (Jan. 2010), pp. 130–133. ISSN: 1532-6535. DOI: 10.1038/clpt.2009.197.
- [39] N. Tsamandouras et al. "Identification of the effect of multiple polymorphisms on the pharmacokinetics of simvastatin and simvastatin acid using a population-modeling approach." In: *Clinical Pharmacology & Therapeutics* 96.1 (July 2014), pp. 90–100. ISSN: 0009-9236. DOI: 10.1038/clpt.2014.55.
- [40] AbZ-Pharma GmbH. *Fachinformation Simvastatin AbZ 10 mg / 20 mg / 40 mg / 80 mg Filmtabletten*. 2016. URL: <https://www.fachinfo.de/> (visited on 10/31/2020).
- [41] drugbank.com. *Simvastatin*. URL: <https://www.drugbank.ca/drugs/DB00641> (visited on 06/11/2020).
- [42] Terje R. Pedersen and Jonathan A. Tobert. "Simvastatin: a review." In: *Expert Opinion on Pharmacotherapy* 5.12 (Dec. 2004), pp. 2583–2596. ISSN: 1465-6566. DOI: 10.1517/14656566.5.12.2583.
- [43] Marja K. Pasanen et al. "SLCO1B1 polymorphism markedly affects the pharmacokinetics of simvastatin acid." In: *Pharmacogenetics and Genomics* 16.12 (Dec. 2006), pp. 873–879. ISSN: 1744-6872. DOI: 10.1097/01.fpc.0000230416.82349.90.

- [44] J. E. Keskkitalo et al. "ABCB1 haplotypes differentially affect the pharmacokinetics of the acid and lactone forms of simvastatin and atorvastatin." In: *Clinical Pharmacology & Therapeutics* 84.4 (Oct. 2008), pp. 457–61. ISSN: 0009-9236. DOI: 10.1038/clpt.2008.25.
- [45] Jenni E. Keskkitalo et al. "Different effects of the ABCG2 c.421c>a SNP on the pharmacokinetics of fluvastatin, pravastatin and simvastatin." In: *Pharmacogenomics* 10.10 (Oct. 2009), pp. 1617–1624. ISSN: 1744-8042. DOI: 10.2217/pgs.09.85.
- [46] Carl Kyrklund et al. "Rifampin greatly reduces plasma simvastatin and simvastatin acid concentrations." In: *Clinical pharmacology and therapeutics* 68.6 (Dec. 2000), pp. 592–597. ISSN: 0009-9236. DOI: 10.1067/mcp.2000.111414.
- [47] Terry A. Jacobson. "Comparative pharmacokinetic interaction profiles of pravastatin, simvastatin, and atorvastatin when coadministered with cytochrome P450 inhibitors." In: *The American journal of cardiology* 94.9 (Nov. 2004), pp. 1140–1146. ISSN: 0002-9149. DOI: 10.1016/j.amjcard.2004.07.080.
- [48] Ron J. Keizer et al. "Model-informed precision dosing at the bedside: scientific challenges and opportunities." In: *CPT: Pharmacometrics & Systems Pharmacology* 7.12 (Dec. 2018), pp. 785–787. ISSN: 2163-8306. DOI: 10.1002/psp4.12353.
- [49] Thomas M. Polasek et al. "What does it take to make model-informed precision dosing common practice? report from the 1st asian symposium on precision dosing." In: *The AAPS Journal* 21.2 (Jan. 2019), p. 17. ISSN: 1550-7416. DOI: 10.1208/s12248-018-0286-6.
- [50] Thomas M. Polasek, Sepehr Shakib, and Amin Rostami-Hodjegan. "Precision medicine technology reality not hype - the example of model-informed precision dosing." In: *F1000Research* 8 (Dec. 2019), p. 1709. DOI: 10.12688/f1000research.20489.2.
- [51] Scott Marshall et al. "Model-informed drug discovery and development: current industry good practice and regulatory expectations and future perspectives." In: *CPT: Pharmacometrics & Systems Pharmacology* 8.2 (Feb. 2019), pp. 87–96. ISSN: 2163-8306. DOI: 10.1002/psp4.12372.
- [52] EFPIA MID3 Workgroup et al. "Good practices in model-informed drug discovery and development: practice, application, and documentation." In: *CPT: Pharmacometrics & Systems Pharmacology* 5.3 (Mar. 2016), pp. 93–122. ISSN: 2163-8306. DOI: 10.1002/psp4.12049.

- [53] Frontiers. *Model-Informed Precision Dosing in the Clinic*. 2020. URL: <https://www.frontiersin.org/research-topics/10097/model-informed-precision-dosing-in-the-clinic> (visited on 05/03/2020).
- [54] Jeffrey S. Barrett et al. "Pharmacometrics: a multidisciplinary field to facilitate critical thinking in drug development and translational research settings." In: *Journal of Clinical Pharmacology* 48.5 (May 2008), pp. 632–649. ISSN: 0091-2700. DOI: 10.1177/0091270008315318.
- [55] D. R. Mould and R. N. Upton. "Basic concepts in population modeling, simulation, and model-based drug development." In: *CPT: Pharmacometrics & Systems Pharmacology* 1.9 (Sept. 2012), p. 6. ISSN: 2163-8306. DOI: 10.1038/psp.2012.4.
- [56] D. R. Mould and R. N. Upton. "Basic concepts in population modeling, simulation, and model-based drug development-part 2: introduction to pharmacokinetic modeling methods." In: *CPT: Pharmacometrics & Systems Pharmacology* 2.4 (Apr. 2013), p. 38. ISSN: 2163-8306. DOI: 10.1038/psp.2013.14.
- [57] R. N. Upton and D. R. Mould. "Basic concepts in population modeling, simulation, and model-based drug development: part 3-introduction to pharmacodynamic modeling methods." In: *CPT: Pharmacometrics & Systems Pharmacology* 3.1 (Jan. 2014), p. 88. ISSN: 2163-8306. DOI: 10.1038/psp.2013.71.
- [58] Jogarao V. S. Gobburu. Pharmacometrics 2020. In: *The Journal of Clinical Pharmacology* vol. 50.S9 (Sept. 2010), pp. 151–157. ISSN: 1552-4604. DOI: 10.1177/0091270010376977.
- [59] Hm Jones and K. Rowland-Yeo. "Basic concepts in physiologically based pharmacokinetic modeling in drug discovery and development." In: *CPT: Pharmacometrics & Systems Pharmacology* 2.8 (Aug. 2013), p. 63. ISSN: 2163-8306. DOI: 10.1038/psp.2013.41.
- [60] Malcolm Rowland, Carl Peck, and Geoffrey Tucker. "Physiologically-based pharmacokinetics in drug development and regulatory science." In: *Annual Review of Pharmacology and Toxicology* 51 (2011), pp. 45–73. ISSN: 1545-4304. DOI: 10.1146/annurev-pharmtox-010510-100540.
- [61] Andrea N. Edginton et al. "Whole body physiologically-based pharmacokinetic models: their use in clinical drug development." In: *Expert Opinion on Drug Metabolism & Toxicology* 4.9 (Aug. 2008), pp. 1143–1152. ISSN: 1742-5255. DOI: 10.1517/17425255.4.9.1143.
- [62] Ivan Nestorov. "Whole body pharmacokinetic models." In: *Clinical Pharmacokinetics* 42.10 (2003), pp. 883–908. ISSN: 0312-5963. DOI: 10.2165/00003088-200342100-00002.



- [63] V. R. Knight-Schrijver et al. "The promises of quantitative systems pharmacology modelling for drug development." In: *Computational and Structural Biotechnology Journal* 14 (Sept. 2016), pp. 363–370. ISSN: 2001-0370. DOI: 10.1016/j.csbj.2016.09.002.
- [64] Ivan Nestorov. "Whole-body physiologically based pharmacokinetic models." In: *Expert Opinion on Drug Metabolism & Toxicology* 3.2 (Apr. 2007), pp. 235–249. ISSN: 1742-5255. DOI: 10.1517/17425255.3.2.235.
- [65] J. G. Wagner. "History of pharmacokinetics." In: *Pharmacology & Therapeutics* 12.3 (1981), pp. 537–562. ISSN: 0163-7258. DOI: 10.1016/0163-7258(81)90097-8.
- [66] L. Kuepfer et al. "Applied concepts in PBPK modeling: how to build a PBPK/PD model." In: *CPT: Pharmacometrics & Systems Pharmacology* 5.10 (Oct. 2016), pp. 516–531. ISSN: 2163-8306. DOI: 10.1002/psp4.12134.
- [67] Sheila Annie Peters. *Physiologically-Based Pharmacokinetic (PBPK) Modeling and Simulations: Principles, Methods, and Applications in the Pharmaceutical Industry*. Hoboken, N.J: John Wiley & Sons, Inc., 2011. 430 pp. ISBN: 9780470484067. DOI: 10.1002/9781118140291.
- [68] Yanguang Cao and William J. Jusko. "Applications of minimal physiologically-based pharmacokinetic models." In: *Journal of Pharmacokinetics and Pharmacodynamics* 39.6 (Dec. 2012), pp. 711–723. ISSN: 1573-8744. DOI: 10.1007/s10928-012-9280-2.
- [69] Amin Rostami-Hodjegan. "Reverse translation in PBPK and QSP: going backwards in order to go forward with confidence." In: *Clinical Pharmacology & Therapeutics* 103.2 (Feb. 2018), pp. 224–232. ISSN: 1532-6535. DOI: 10.1002/cpt.904.
- [70] Masoud Jamei. "Recent advances in development and application of physiologically-based pharmacokinetic (PBPK) models: a transition from academic curiosity to regulatory acceptance." In: *Current Pharmacology Reports* 2.3 (2016), pp. 161–169. ISSN: 2198-641X. DOI: 10.1007/s40495-016-0059-9.
- [71] P. Zhao et al. "Applications of physiologically based pharmacokinetic (PBPK) modeling and simulation during regulatory review." In: *Clinical Pharmacology & Therapeutics* 89.2 (Feb. 2011), pp. 259–267. ISSN: 1532-6535. DOI: 10.1038/clpt.2010.298.
- [72] Jennifer E. Sager et al. "Physiologically based pharmacokinetic (PBPK) modeling and simulation approaches: a systematic review of published models, applications, and model verification." In: *Drug Metabolism and Disposition* 43.11 (Nov. 2015), pp. 1823–1837. ISSN: 1521-009X. DOI: 10.1124/dmd.115.065920.

- [73] CC BY 3.0 Servier Medical Art by Servier. *Smart Servier Medical Art*. 2020. URL: <https://smart.servier.com/> (visited on 11/11/2020).
- [74] Nadine Schaefer et al. "The feasibility of physiologically based pharmacokinetic modeling in forensic medicine illustrated by the example of morphine." In: *International journal of legal medicine* 132.2 (Mar. 2018), pp. 415–424. ISSN: 1437-1596. DOI: 10.1007/s00414-017-1754-8.
- [75] Daniel Moj et al. "Clarithromycin, midazolam, and digoxin: application of PBPK modeling to gain new insights into drug–drug interactions and co-medication regimens." In: *The AAPS journal* 19.1 (2016), pp. 298–312. ISSN: 1550-7416. DOI: 10.1208/s12248-016-0009-9.
- [76] Denise Türk et al. "Physiologically based pharmacokinetic models for prediction of complex CYP2C8 and OATP1B1 (SLCO1B1) drug–drug–gene interactions: a modeling network of gemfibrozil, repaglinide, pioglitazone, rifampicin, clarithromycin and itraconazole." In: *Clinical pharmacokinetics* 58.12 (Dec. 2019), pp. 1595–1607. ISSN: 1179-1926. DOI: 10.1007/s40262-019-00777-x.
- [77] Hannah Britz et al. "Physiologically-based pharmacokinetic models for CYP 1A2 drug–drug interaction prediction: a modeling network of fluvoxamine, theophylline, caffeine, rifampicin, and midazolam." In: *CPT: Pharmacometrics & Systems Pharmacology* 8.5 (May 2019), pp. 296–307. ISSN: 2163-8306. DOI: 10.1002/psp4.12397.
- [78] Nina Hanke et al. "PBPK models for CYP3A4 and P-gp DDI prediction: a modeling network of rifampicin, itraconazole, clarithromycin, midazolam, alfentanil, and digoxin." In: *CPT: Pharmacometrics & Systems Pharmacology* 7.10 (Oct. 2018), pp. 647–659. ISSN: 2163-8306. DOI: 10.1002/psp4.12343.
- [79] Daniel Moj et al. "A comprehensive whole-body physiologically based pharmacokinetic model of dabigatran etexilate, dabigatran and dabigatran glucuronide in healthy adults and renally impaired patients." In: *Clinical Pharmacokinetics* 58.12 (Dec. 2019), pp. 1577–1593. ISSN: 1179-1926. DOI: 10.1007/s40262-019-00776-y.
- [80] Nina Hanke et al. "A comprehensive whole-body physiologically based pharmacokinetic drug–drug–gene interaction model of metformin and cimetidine in healthy adults and renally impaired individuals." In: *Clinical Pharmacokinetics* 59.11 (May 2020), pp. 1419–1431. DOI: 10.1007/s40262-020-00896-w. URL: <https://dx.doi.org/10.1007/s40262-020-00896-w>.

- [81] CC BY-NC 4.0 by pngimg.com. *PNG images: Tom and Jerry*. 2020. URL: [http://pngimg.com/imgs/heroes/tom\\_and\\_jerry/](http://pngimg.com/imgs/heroes/tom_and_jerry/) (visited on 06/01/2020).
- [82] Jia Guo. "Pharmacogenomics review." en. Feb. 2019. DOI: 10.13140/RG.2.2.10839.93607. URL: [https://www.researchgate.net/publication/331703642\\_Pharmacogenomics\\_review](https://www.researchgate.net/publication/331703642_Pharmacogenomics_review) (visited on 10/31/2020).
- [83] Steven M. Paul et al. "How to improve R&D productivity: the pharmaceutical industry's grand challenge." In: *Nature Reviews Drug Discovery* 9.3 (Feb. 2010), pp. 203–214. DOI: 10.1038/nrd3078.
- [84] Joseph A. DiMasi, Henry G. Grabowski, and Ronald W. Hansen. "Innovation in the pharmaceutical industry: new estimates of R&D costs." In: *Journal of Health Economics* 47 (May 2016), pp. 20–33. DOI: 10.1016/j.jhealeco.2016.01.012.
- [85] Aylin Sertkaya et al. "Key cost drivers of pharmaceutical clinical trials in the United States." In: *Clinical Trials (London, England)* 13.2 (Apr. 2016), pp. 117–126. ISSN: 1740-7753. DOI: 10.1177/1740774515625964.
- [86] A. Guisasola et al. "The influence of experimental data quality and quantity on parameter estimation accuracy." In: *Education for Chemical Engineers* 1.1 (Jan. 2006), pp. 139–145. DOI: 10.1205/ece06016.
- [87] Garrett Grolemond Hadley Wickham. *R for Data Science*. O'Reilly UK Ltd., Jan. 1, 2017. ISBN: 1491910399. URL: [https://www.ebook.de/de/product/23900484/hadley\\_wickham\\_garrett\\_grolemond\\_r\\_for\\_data\\_science.html](https://www.ebook.de/de/product/23900484/hadley_wickham_garrett_grolemond_r_for_data_science.html).
- [88] T. H. T. Nguyen et al. "Model evaluation of continuous data pharmacometric models: metrics and graphics." In: *CPT: Pharmacometrics & Systems Pharmacology* 6.2 (Feb. 2017), pp. 87–109. ISSN: 2163-8306. DOI: 10.1002/psp4.12161.
- [89] F. M. Dekking et al. *A Modern Introduction to Probability and Statistics*. Springer London Ltd, May 6, 2005. 488 pp. ISBN: 1852338962. URL: [https://www.ebook.de/de/product/3054516/f\\_m\\_dekking\\_c\\_kraaikamp\\_h\\_p\\_lopuhaa\\_l\\_e\\_meester\\_a\\_modern\\_introduction\\_to\\_probability\\_and\\_statistics.html](https://www.ebook.de/de/product/3054516/f_m_dekking_c_kraaikamp_h_p_lopuhaa_l_e_meester_a_modern_introduction_to_probability_and_statistics.html).
- [90] GoogleDevelopers. *Training and Test Sets: Splitting Data*. Feb. 10, 2020. URL: <https://developers.google.com/machine-learning/crash-course/training-and-test-sets/splitting-data> (visited on 06/02/2020).
- [91] Nick Bunkley. *Joseph Juran, 103, Pioneer in Quality Control, Dies*. Mar. 3, 2008. URL: <https://www.nytimes.com/2008/03/03/business/03juran.html> (visited on 06/02/2020).

- [92] Mayukh Bhattacharyya. 3 *Things You Need To Know Before You Train-Test Split*. Dec. 4, 2019. URL: <https://towardsdatascience.com/3-things-you-need-to-know-before-you-train-test-split-869dfabb7e50> (visited on 06/02/2020).
- [93] European Medicines Agency. *Guideline on the investigation of drug interactions*. June 21, 2012. URL: [https://www.ema.europa.eu/en/documents/scientific-guideline/guideline-investigation-drug-interactions-revision-1\\_en.pdf](https://www.ema.europa.eu/en/documents/scientific-guideline/guideline-investigation-drug-interactions-revision-1_en.pdf) (visited on 10/31/2020).
- [94] Food and Drug Administration Center for Drug Evaluation Research. *In Vitro Drug Interaction Studies — Cytochrome P450 Enzyme- and Transporter-Mediated Drug Interactions Guidance for Industry*. 2020. URL: <https://www.fda.gov/media/134582/download> (visited on 10/31/2020).
- [95] Nikolaos Tsamandouras et al. "Development and application of a mechanistic pharmacokinetic model for simvastatin and its active metabolite simvastatin acid using an integrated population PBPK approach." In: *Pharmaceutical Research* 32.6 (June 2015), pp. 1864–1883. DOI: 10.1007/s11095-014-1581-2.
- [96] J. Lippert et al. "A mechanistic, model-based approach to safety assessment in clinical development." In: *CPT: Pharmacometrics & Systems Pharmacology* 1.1 (Nov. 2012), p. 13. ISSN: 2163-8306. DOI: 10.1038/psp.2012.14.
- [97] Jimyon Kim et al. "A population pharmacokinetic-pharmacodynamic model for simvastatin that predicts low-density lipoprotein-cholesterol reduction in patients with primary hyperlipidaemia." In: *Basic & Clinical Pharmacology & Toxicology* 109.3 (Sept. 2011), pp. 156–163. ISSN: 17427835. DOI: 10.1111/j.1742-7843.2011.00700.x.
- [98] Seok Joon Jin et al. "Population pharmacokinetic analysis of simvastatin and its active metabolite with the characterization of atypical complex absorption kinetics." In: *Pharmaceutical Research* 31.7 (July 2014), pp. 1801–1812. ISSN: 1573-904X. DOI: 10.1007/s11095-013-1284-0.
- [99] Jörg Lippert et al. "Open systems pharmacology community—an open access, open source, open science approach to modeling and simulation in pharmaceutical sciences." In: *CPT: Pharmacometrics & Systems Pharmacology* 8.12 (Nov. 2019), pp. 878–882. DOI: 10.1002/psp4.12473.
- [100] F. Peter Guengerich. "Cytochrome P450 and chemical toxicology." In: *Chemical Research in Toxicology* 21.1 (Jan. 2008), pp. 70–83. DOI: 10.1021/tx700079z.

- [101] Ulrich M. Zanger and Matthias Schwab. "Cytochrome p450 enzymes in drug metabolism: regulation of gene expression, enzyme activities, and impact of genetic variation." In: *Pharmacology & Therapeutics* 138.1 (Apr. 2013), pp. 103–141. DOI: 10.1016/j.pharmthera.2012.12.007.
- [102] European Medicines Agency. *Guideline on the reporting of physiologically based pharmacokinetic (PBPK) modelling and simulation*. Dec. 13, 2018. URL: [https://www.ema.europa.eu/en/documents/scientific-guideline/guideline-reporting-physiologically-based-pharmacokinetic-pbpbk-modelling-simulation\\_en.pdf](https://www.ema.europa.eu/en/documents/scientific-guideline/guideline-reporting-physiologically-based-pharmacokinetic-pbpbk-modelling-simulation_en.pdf) (visited on 10/31/2020).
- [103] Hee Youn Choi et al. "Impact of CYP2D6, CYP3A5, CYP2C19, CYP2A6, SLCO1B1, ABCB1, and ABCG2 gene polymorphisms on the pharmacokinetics of simvastatin and simvastatin acid." In: *Pharmacogenetics and Genomics* 25.12 (Dec. 2015), pp. 595–608. ISSN: 1744-6880. DOI: 10.1097/FPC.000000000000176.
- [104] Tomoko Hasunuma et al. "Absence of ethnic differences in the pharmacokinetics of moxifloxacin, simvastatin, and meloxicam among three East Asian populations and Caucasians." In: *British Journal of Clinical Pharmacology* 81.6 (Mar. 2016), pp. 1078–1090. ISSN: 1365-2125. DOI: 10.1111/bcp.12884.
- [105] Pertti J. Neuvonen, Teemu Kantola, and Kari T. Kivistö. "Simvastatin but not pravastatin is very susceptible to interaction with the CYP3A4 inhibitor itraconazole." In: *Clinical Pharmacology and Therapeutics* 63.3 (Mar. 1998), pp. 332–341. ISSN: 0009-9236. DOI: 10.1016/S0009-9236(98)90165-5.
- [106] Dhiaa A. Taha et al. "The role of acid-base imbalance in statin-induced myotoxicity." In: *Translational research : the journal of laboratory and clinical medicine* 174 (Aug. 2016), 140–160.e14. ISSN: 1878-1810. DOI: 10.1016/j.trsl.2016.03.015.
- [107] Christie M. Ballantyne et al. "Efficacy, safety and effect on biomarkers related to cholesterol and lipoprotein metabolism of rosuvastatin 10 or 20 mg plus ezetimibe 10 mg vs. simvastatin 40 or 80 mg plus ezetimibe 10 mg in high-risk patients: results of the GRAVITY randomized study." In: *Atherosclerosis* 232.1 (Jan. 2014), pp. 86–93. ISSN: 1879-1484. DOI: 10.1016/j.atherosclerosis.2013.10.022.
- [108] Adrian Towse. Net Clinical Benefit: The Art and Science of Jointly Estimating Benefits and Risks of Medical Treatment. In: *Value in Health* vol. 13 (June 2010), pp. 30–32. DOI: 10.1111/j.1524-4733.2010.00753.x.

- [109] Paul A. Reilly et al. "The effect of dabigatran plasma concentrations and patient characteristics on the frequency of ischemic stroke and major bleeding in atrial fibrillation patients." In: *Journal of the American College of Cardiology* 63.4 (Feb. 2014), pp. 321–328. ISSN: 0735-1097. DOI: 10.1016/j.jacc.2013.07.104.
- [110] Yeruk Mulugeta et al. "Exposure matching for extrapolation of efficacy in pediatric drug development." In: *The Journal of Clinical Pharmacology* 56.11 (Oct. 2016), pp. 1326–1334. DOI: 10.1002/jcph.744.
- [111] Younghwa Lee, Kenneth A. Kozar, and Kai R.T. Larsen. "The technology acceptance model: past, present, and future." In: *Communications of the Association for Information Systems* 12 (2003). DOI: 10.17705/1cais.01250.
- [112] Bahlol Rahimi et al. "A systematic review of the technology acceptance model in health informatics." In: *Applied Clinical Informatics* 9.3 (July 2018), pp. 604–634. ISSN: 1869-0327. DOI: 10.1055/s-0038-1668091.

Part IV

APPENDIX







## SUPPORTING INFORMATION

---

A.1 SUPPORTING INFORMATION PUBLICATION I - DATA DIGITIZING:  
ACCURATE AND PRECISE DATA EXTRACTION FOR QUANTITATIVE  
SYSTEMS PHARMACOLOGY AND PHYSIOLOGICALLY-BASED PHAR-  
MACOKINETIC MODELING

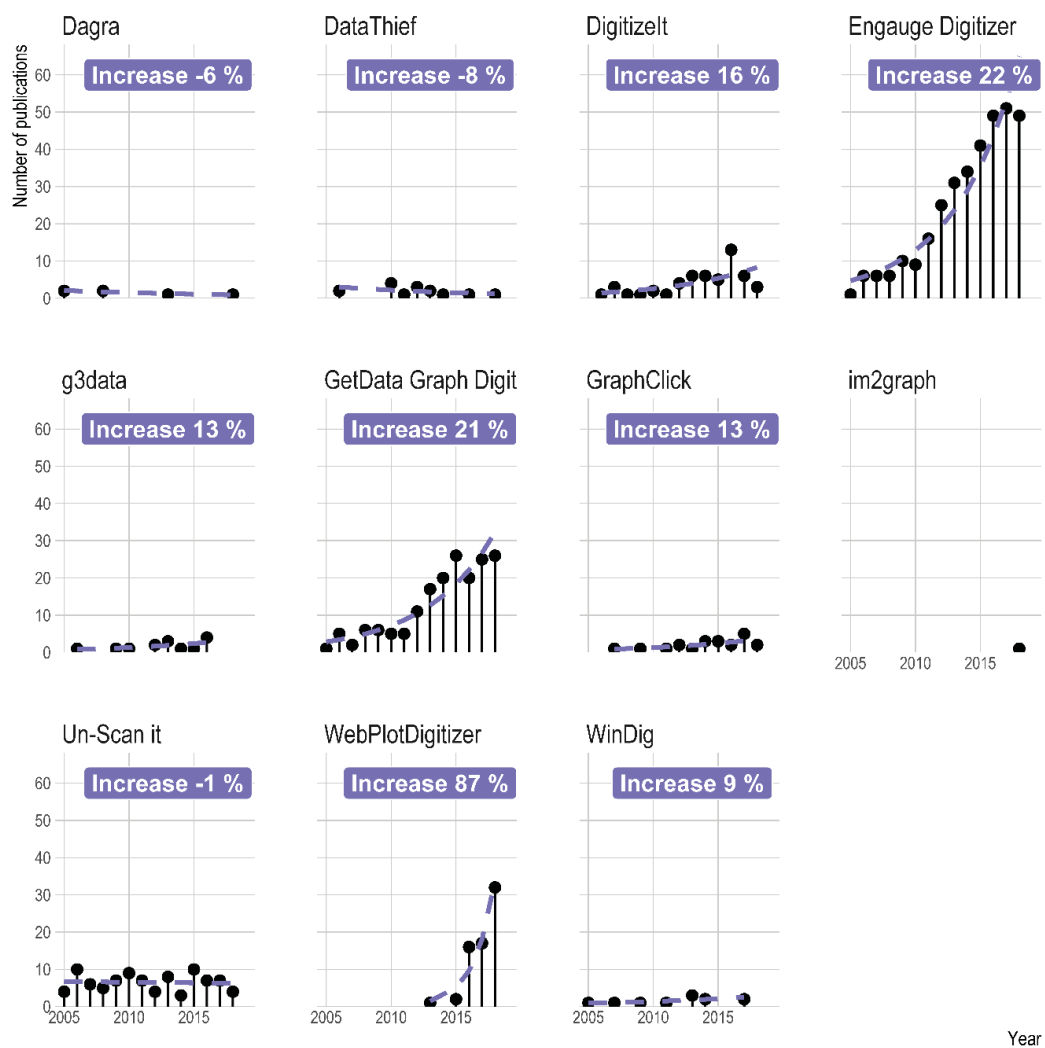


Figure S1 Number of publications containing the terms “systems pharmacology” or “physiologically based pharmacokinetic” and the names of the digitization software packages investigated over the last few years. Labels and dashed purple line show model estimated values and increase per year using Poisson regression. For all subplots, solid lollipops represent the observed values.

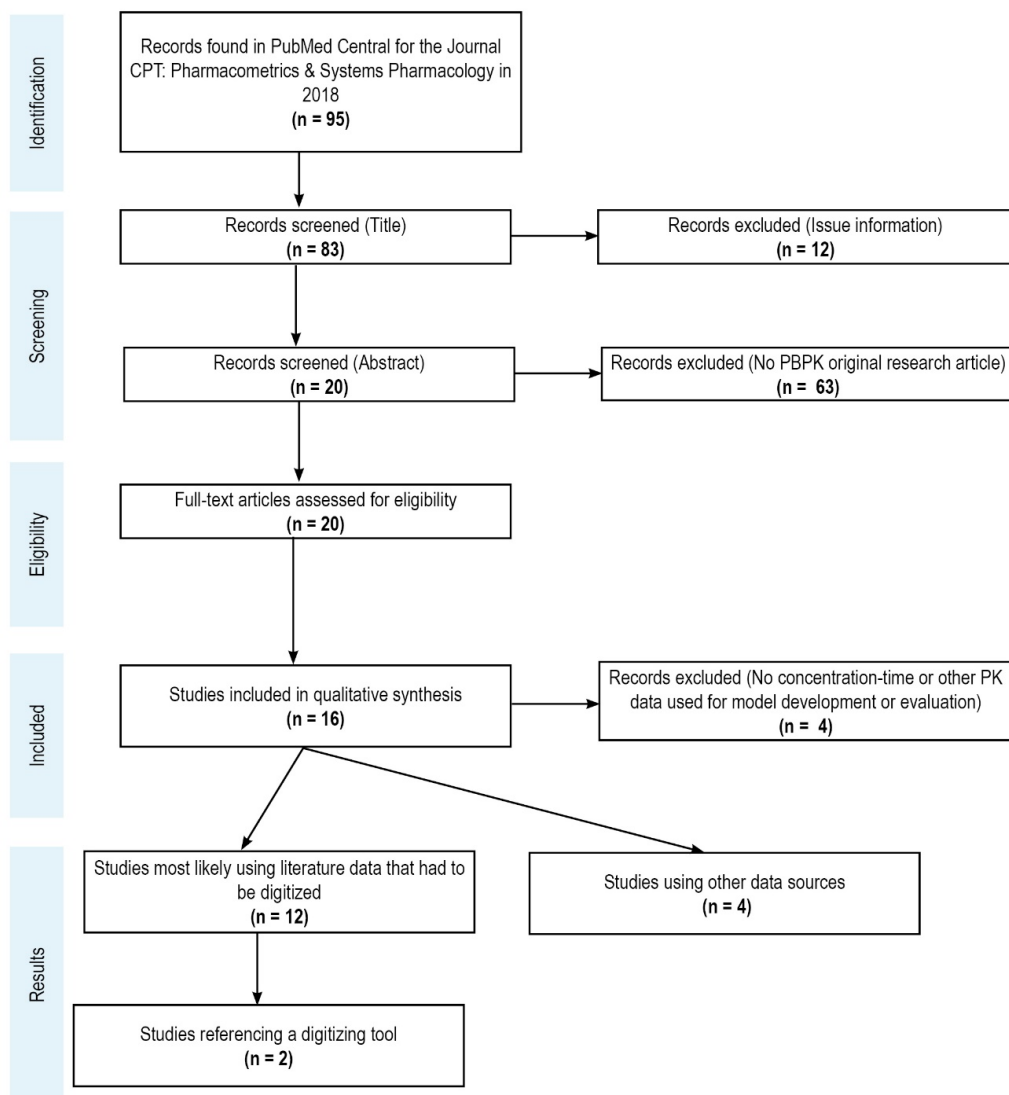


Figure S2 Flow-chart of the performed literature search in CPT CPT: PSP (Online ISSN: 2163-8306) from 2018. Records were reviewed manually in order to identify articles related to PBPK that referenced a digitizing software and most likely had used literature data.

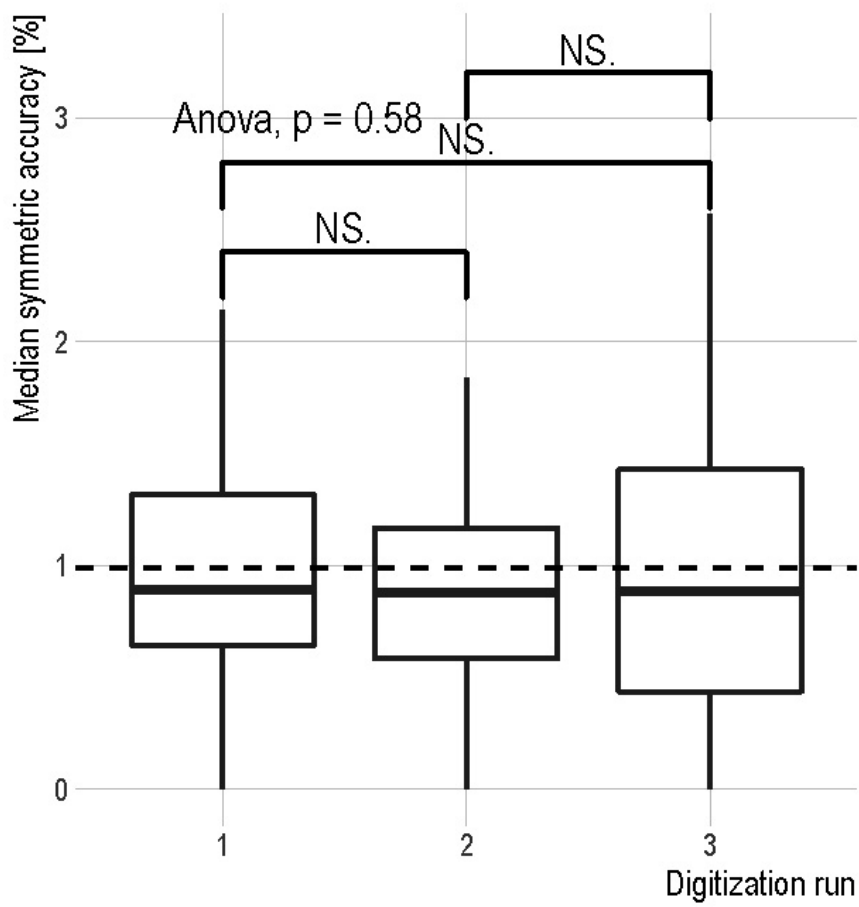


Figure S3 Boxplot of the median symmetric accuracy for each digitization run performed in the study. In addition, arithmetic mean of all groups is shown as dashed line.

Software Name	Platform	Cost [\$]	Total number of publication frequencies	Features
Dagra	Windows	49.95	18	<b>Import:</b> From clipboard, via built-in screen-shot tool. <b>Supported formats:</b> .bmp, .emf, .gif, .jpg, .jpeg, .png, .tif, .tiff, .wmf. <b>Digitizing features:</b> One graph at once, point digitization (1 point per click), curve digitization (curve tracing using Bezier curves), zoom panel, axis scaling: linear, log <sub>10</sub> or log <sub>e</sub> . <b>Export:</b> To clipboard, to text file, Dagra files can be opened in Matlab, Python or Excel. <b>Other:</b> Appearance rating from 0 (not appealing) to 10 (appealing): 3
DataThief	Windows, MacOS, Unix	25	20	<b>Supported formats:</b> .gif, .jpg, .jpeg, .png <b>Digitizing features:</b> One graph at once, point digitization (1 point per click), curve digitization (line tracing), can digitize polar coordinates, axis scaling: user defined <b>Export:</b> To text file <b>Other</b> Appearance rating from 0 (not appealing) to 10 (appealing): 6, written in Java (no installation required)
dcsDigitiser	Windows	423	0	Trial version could not be tested since the software interfere with windows defender.
DigitizeIt	Windows, MacOS, Unix	49	58	<b>Import:</b> From clipboard. <b>Supported formats:</b> .bmp, .jfif, .gif, .jpg, .jpeg, .png, .tif, .tiff, .ico <b>Digitizing features:</b> One graph at once, point digitization (1 point per click or automatic), curve digitization (line tracing), axis scaling: linear, logarithmic, 1/x. <b>Export:</b> To csv, to clipboard <b>Other</b> Appearance rating from 0 (not appealing) to 10 (appealing): 7, graphs can be zoomed, mirrored and rotated, can handle tilted or distorted graphs, axes do not need to be orthogonal
Engauge	Windows, MacOS, Unix	Free	418	<b>Supported formats:</b> .bmp, .cur, .gif, .icns, .ico, .jpeg, .jpg, .pbm, .pdf, .pgm, .ppm, .png, .pgm, .tga, .tif, .tiff, .wbmp, .webp, .xbm, .xpm <b>Digitizing features:</b> Multiple graphs at once, point digitization (1 point per click or automatic), curve digitization (line tracing cubic spline interpolation), axis scaling: linear, logarithmic, date and

				time values, or as degrees, minutes and seconds, can digitize polar coordinates, image processing, grid lines <b>Export:</b> To csv/tsv, to clipboard <b>Other</b> Appearance rating from 0 (not appealing) to 10 (appealing): 8, various wizards (interactive tutorials), axes checker, axes with only one known coordinate (floating axes) can be digitized, geometry window displays geometric information about the selected curve, curve Fitting Window fits a polynomial function to the selected curve, various customization options.
g3data	Windows	Free	15	Could not be tested because the software needs separate compilation.
GetData	Windows	30	225	<b>Import:</b> From clipboard. <b>Supported formats:</b> .bmp, .jpg, .tif, .pcx <b>Digitizing features:</b> One graph at once, point digitization (1 point per click), curve digitization (curve tracing), zoom panel, axis scaling: linear, log <sub>10</sub> <b>Export:</b> To clipboard, to text file, to csv <b>Other</b> Appearance rating from 0 (not appealing) to 10 (appealing): 8
GraphClick	MacOS	Free	22	No longer under development.
im2graph	Windows, Linux	Free	1	For installation of the freeware version a download-link is required. However, we did not receive a link and thus, could not test the software.
Un-Scan it	Windows, MacOS	345	120	<b>Import:</b> From clipboard <b>Supported formats:</b> .bmp, .gif, .jpeg, .jpg, .tiff, .png, .tga, .pcx <b>Digitizing features:</b> One graph at once, point digitization (1 point per click), curve digitization (curve tracing – also for intersecting lines and dashed/dotted lines), bar-chart digitization, contour plot digitization, shape/Drawing digitization, polar coordinate digitization, zoom panel, separate “graph-screen-mode”, axis scaling: linear, log <sub>10</sub> <b>Export:</b> To clipboard, to text file, to csv file <b>Other</b> Appearance rating from 0 (not appealing) to 10 (appealing): 7, grid line filters, automatic line follow mode, raster scan mode, corrects for tilted graphs and variable line thickness, various post-processing features (area integration between cursors / data smoothing etc.).

WebPlotDigitizer	Web based	Free	103	<p><b>Supported formats:</b> Not directly stated. Probably the most important formats. <b>Digitizing features:</b> One graph at once, point digitization (1 point per click or automatic), curve digitization (curve tracing), bar-chart digitization, ternary diagram digitization, map with scale bar digitization, polar coordinate digitization, image digitization, zoom panel, axis scaling: linear, log<sub>10</sub>, measurement calculations (distance, area, angle), dataset cleaning functions (sorting/renaming), can remove gridlines <b>Export:</b> To csv file, save project as .json file, to plotly, to clipboard</p> <p><b>Other</b> Appearance rating from 0 (not appealing) to 10 (appealing): 8, as software or as browser-plugin available, can run javascripts</p>
WinDig	Windows	Free	15	Could not be tested since it is only available as 16bit version
xyExtract	Windows	45	2	Could not be tested since no windows 10 version is available.

**Table S2: Studies used for comparing published numeric and digitized  $C_{\max}$  values**

<b>Author</b>	<b>Mean <math>\zeta</math> [%]</b>	<b>Smallest <math>\zeta</math> [%]</b>	<b>Largest <math>\zeta</math> [%]</b>	<b>N <math>\zeta</math></b>	<b>Reference</b>
Alakhali 2013	1.3	1.3	1.3	1	<sup>1</sup>
Ayalasomayajula 2007	2.8	0.75	4.1	4	<sup>2</sup>
Ayalasomayajula 2016	12	6.8	17	2	<sup>3</sup>
Backman 2000	15	2.5	41	4	<sup>4</sup>
Bergman 2009	13	8.4	20	4	<sup>5</sup>
Boulenc 2016	15	9.4	23	3	<sup>6</sup>
Cermak 2009	19	9	36	4	<sup>7</sup>
Chin 1995	3.4	3.4	3.4	1	<sup>8</sup>
Dai 2013	13	0.92	25	4	<sup>9</sup>
Daneshmend 1984	16	4.6	37	8	<sup>10</sup>
Devineni 2015	16	13	23	4	<sup>11</sup>
Dingemans 2014	15	5.8	35	8	<sup>12</sup>
Eap 2004	17	7.9	27	2	<sup>13</sup>
Huang 1986	19	8.2	29	3	<sup>14</sup>
Jacobson 2004	13	0.35	42	6	<sup>15</sup>
Kang 2004	0.038	0.038	0.038	1	<sup>16</sup>
Kantola 1998	17	6.8	35	6	<sup>17</sup>
Keskitalo 2008	24	11	35	4	<sup>18</sup>
Keskitalo 2009	20	4.9	64	6	<sup>19</sup>
Kim 2007	32	25	40	3	<sup>20</sup>



Knupp 1993	15	15	15	1	21
Kosoglou 2011	22	7.2	33	4	22
Krishna 2012	8.9	1.3	16	8	23
Kyrklund 2000	25	12	35	4	24
Lam 2003	18	14	23	2	25
Lilja 1998	21	11	34	4	26
Lilja 2000	31	31	31	1	27
Lilja 2004	13	3.7	27	4	28
McKenney 2006	21	20	22	2	29
Neuvonen 1998	89	19	160	2	30
Obrien 2003	34	23	49	4	31
Pasanen 2006	18	5	34	6	32
Polk 1999	12	12	12	1	33
Polli 2013	16	2.9	29	2	34
Sekar 2008	4.3	4.3	4.3	1	35
Shanmugam 2011	6.7	0.3	13	2	36
Stephen 1991	9.8	9.8	9.8	1	37
Stoch 2009	7.9	3.9	12	4	38
Sugimoto 2001	9.9	5.7	14	2	39
Teng 2013	16	4.5	31	4	40
Tham 2006	170	0.67	330	2	41
Tubic-Grozdanis 2008	18	7	50	6	42

Tuteja 2014	32	13	54	4	43
Ucar 2004	32	2.2	63	4	44
Winsemius 2014	94	52	170	12	45
Xu 2014	440	0.69	1800	6	46
Zhao 2015	24	3.7	54	10	47

a: Number of values extracted from the study for which  $\zeta$  was calculated

## References

- Alakhali, K., Hassan, Y., Mohamed, N. & Mordi, M. N. Pharmacokinetic of simvastatin study in Malaysian. *IOSR J. Pharm.* **3**, 46–51 (2013).
- Ayalasomayajula, S. P. *et al.* Evaluation of the potential for steady-state pharmacokinetic interaction between vildagliptin and simvastatin in healthy subjects. *Curr. Med. Res. Opin.* **23**, 2913–20 (2007).
- Ayalasomayajula, S. *et al.* In vitro and clinical evaluation of OATP-mediated drug interaction potential of sacubitril/valsartan (LCZ696). *J. Clin. Pharm. Ther.* **41**, 424–31 (2016).
- Backman, J. T., Kyrklund, C., Kivistö, K. T., Wang, J. S. & Neuvonen, P. J. Plasma concentrations of active simvastatin acid are increased by gemfibrozil. *Clin. Pharmacol. Ther.* **68**, 122–9 (2000).
- Bergman, A. J. *et al.* Effect of sitagliptin on the pharmacokinetics of simvastatin. *J. Clin. Pharmacol.* **49**, 483–8 (2009).
- Boulenc, X. *et al.* CYP3A4-based drug-drug interaction: CYP3A4 substrates' pharmacokinetic properties and ketoconazole dose regimen effect. *Eur. J. Drug Metab. Pharmacokinet.* **41**, 45–54 (2016).
- Cermak, R., Wein, S., Wolfram, S. & Langguth, P. Effects of the flavonol quercetin on the bioavailability of simvastatin in pigs. *Eur. J. Pharm. Sci.* **38**, 519–24 (2009).
- Chin, T. W. F., Loeb, M. & Fong, I. W. Effects of an acidic beverage (Coca-Cola) on absorption of ketoconazole. *Antimicrob. Agents Chemother.* **39**, 1671–5 (1995).
- Dai, L.-L. *et al.* Assessment of a pharmacokinetic and pharmacodynamic interaction between simvastatin and Ginkgo biloba extracts in healthy subjects. *Xenobiotica.* **43**, 862–7 (2013).
- Daneshmend, T. K. *et al.* Influence of food on the pharmacokinetics of ketoconazole. *Antimicrob. Agents Chemother.* **25**, 1–3 (1984).
- Devineni, D. *et al.* Effect of canagliflozin on the pharmacokinetics of glyburide, metformin, and simvastatin in healthy participants. *Clin. Pharmacol. drug Dev.* **4**, 226–36 (2015).
- Dingemans, J., Nicolas, L. B. & Bortel, L. Van Investigation of combined CYP3A4 inductive/inhibitory properties by studying statin interactions: A model study with the renin inhibitor ACT-178882. *Eur. J. Clin. Pharmacol.* **70**, 675–684 (2014).
- Eap, C. *et al.* Oral administration of a low dose of midazolam (75 microg) as an in vivo probe for CYP3A activity. *Eur. J. Clin. Pharmacol.* **60**, 237–246 (2004).
- Huang, Y. C., Colaizzi, J. L., Bierman, R. H., Woestenborghs, R. & Heykants, J. Pharmacokinetics and dose proportionality of ketoconazole in normal volunteers. *Antimicrob. Agents Chemother.* **30**, 206–10 (1986).

15. Jacobson, T. A. Comparative pharmacokinetic interaction profiles of pravastatin, simvastatin, and atorvastatin when coadministered with cytochrome P450 inhibitors. *Am. J. Cardiol.* **94**, 1140–6 (2004).
16. Kang, B. K. *et al.* Development of self-microemulsifying drug delivery systems (SMEDDS) for oral bioavailability enhancement of simvastatin in beagle dogs. *Int. J. Pharm.* **274**, 65–73 (2004).
17. Kantola, T., Kivistö, K. T. & Neuvonen, P. J. Erythromycin and verapamil considerably increase serum simvastatin and simvastatin acid concentrations. *Clin. Pharmacol. Ther.* **64**, 177–82 (1998).
18. Keskitalo, J. E., Kurkinen, K. J., Neuvonen, P. J. & Niemi, M. ABCB1 haplotypes differentially affect the pharmacokinetics of the acid and lactone forms of simvastatin and atorvastatin. *Clin. Pharmacol. Ther.* **84**, 457–61 (2008).
19. Keskitalo, J. E., Pasanen, M. K., Neuvonen, P. J. & Niemi, M. Different effects of the ABCG2 c.421C>A SNP on the pharmacokinetics of fluvastatin, pravastatin and simvastatin. *Pharmacogenomics* **10**, 1617–24 (2009).
20. Kim, K.-A., Park, P.-W., Lee, O.-J., Kang, D.-K. & Park, J.-Y. Effect of polymorphic CYP3A5 genotype on the single-dose simvastatin pharmacokinetics in healthy subjects. *J. Clin. Pharmacol.* **47**, 87–93 (2007).
21. Knupp, C. A., Brater, D. C., Relue, J. & Barbhuiya, R. H. Pharmacokinetics of didanosine and ketoconazole after coadministration to patients seropositive for the human immunodeficiency virus. *J. Clin. Pharmacol.* **33**, 912–7 (1993).
22. Kosoglou, T. *et al.* Assessment of potential pharmacokinetic interactions of ezetimibe/simvastatin and extended-release niacin tablets in healthy subjects. *Eur. J. Clin. Pharmacol.* **67**, 483–92 (2011).
23. Krishna, G. *et al.* Effect of posaconazole on the pharmacokinetics of simvastatin and midazolam in healthy volunteers. *Expert Opin. Drug Metab. Toxicol.* **8**, 1–10 (2012).
24. Kyrklund, C. *et al.* Rifampin greatly reduces plasma simvastatin and simvastatin acid concentrations. *Clin. Pharmacol. Ther.* **68**, 592–7 (2000).
25. Lam, Y. W. F., Alfaro, C. L., Ereshefsky, L. & Miller, M. Pharmacokinetic and pharmacodynamic interactions of oral midazolam with ketoconazole, fluoxetine, fluvoxamine, and nefazodone. *J. Clin. Pharmacol.* **43**, 1274–82 (2003).
26. Lilja, J. J., Kivistö, K. T. & Neuvonen, P. J. Grapefruit juice-simvastatin interaction: effect on serum concentrations of simvastatin, simvastatin acid, and HMG-CoA reductase inhibitors. *Clin. Pharmacol. Ther.* **64**, 477–83 (1998).
27. Lilja, J. J., Kivistö, K. T. & Neuvonen, P. J. Duration of effect of grapefruit juice on the pharmacokinetics of the CYP3A4 substrate simvastatin. *Clin. Pharmacol. Ther.* **68**, 384–90 (2000).
28. Lilja, J. J., Neuvonen, M. & Neuvonen, P. J. Effects of regular consumption of grapefruit juice on the pharmacokinetics of simvastatin. *Br. J. Clin. Pharmacol.* **58**, 56–60 (2004).
29. McKenney, J. M. *et al.* Study of the pharmacokinetic interaction between simvastatin and prescription omega-3-acid ethyl esters. *J. Clin. Pharmacol.* **46**, 785–91 (2006).
30. Neuvonen, P. J., Kantola, T. & Kivistö, K. T. Simvastatin but not pravastatin is very susceptible to interaction with the CYP3A4 inhibitor itraconazole. *Clin. Pharmacol. Ther.* **63**, 332–341 (1998).
31. O'Brien, S. G. *et al.* Effects of imatinib mesylate (STI571, Glivec) on the pharmacokinetics of simvastatin, a cytochrome p450 3A4 substrate, in patients with chronic myeloid leukaemia. *Br. J. Cancer* **89**, 1855–9 (2003).
32. Pasanen, M. K., Neuvonen, M., Neuvonen, P. J. & Niemi, M. SLCO1B1 polymorphism markedly affects the pharmacokinetics of simvastatin acid. *Pharmacogenet. Genomics* **16**, 873–9 (2006).
33. Polk, R. E. *et al.* Pharmacokinetic interaction between ketoconazole and amprenavir after single doses in healthy men. *Pharmacotherapy* **19**, 1378–84 (1999).
34. Polli, J. W. *et al.* Evaluation of drug interactions of GSK1292263 (a GPR119 agonist) with statins: From in vitro data to clinical study design. *Xenobiotica* **43**, 498–508 (2013).
35. Sekar, V. J., Lefebvre, E., Pauw, M. De, Vangeneugden, T. & Hoetelmans, R. M. Pharmacokinetics of darunavir/ritonavir and ketoconazole following co-administration in HIV-healthy volunteers. *Br. J. Clin.*

- Pharmacol.* **66**, 215–221 (2008).
36. Shanmugam, S., Ryu, J.-K., Yoo, S.-D., Choi, H.-G. & Woo, J.-S. Evaluation of Pharmacokinetics of Simvastatin and Its Pharmacologically Active Metabolite from Controlled-Release Tablets of Simvastatin in Rodent and Canine Animal Models. *Biomol. Ther.* **19**, 248–254 (2011).
  37. Piscitelli, S. C. *et al.* Effects of ranitidine and sucralfate on ketoconazole bioavailability. *Antimicrob. Agents Chemother.* **35**, 1765–1771 (1991).
  38. Stoch, S. A. *et al.* Effect of different durations of ketoconazole dosing on the single-dose pharmacokinetics of midazolam: Shortening the paradigm. *J. Clin. Pharmacol.* **49**, 398–406 (2009).
  39. Sugimoto, K. *et al.* Different effects of St John's Wort on the pharmacokinetics of simvastatin and pravastatin. *Clin. Pharmacol. Ther.* **70**, 518–524 (2001).
  40. Teng, R., Mitchell, P. D. & Butler, K. A. Pharmacokinetic interaction studies of co-administration of ticagrelor and atorvastatin or simvastatin in healthy volunteers. *Eur. J. Clin. Pharmacol.* **69**, 477–87 (2013).
  41. Tham, L. S. *et al.* Ketoconazole renders poor CYP3A phenotype status with midazolam as probe drug. *Ther. Drug Monit.* **28**, 255–261 (2006).
  42. Tubic-Grozdanis, M. *et al.* Pharmacokinetics of the CYP 3A substrate simvastatin following administration of delayed versus immediate release oral dosage forms. *Pharm. Res.* **25**, 1591–600 (2008).
  43. Tuteja, S. *et al.* Pharmacokinetic interactions of the microsomal triglyceride transfer protein inhibitor, lomitapide, with drugs commonly used in the management of hypercholesterolemia. *Pharmacotherapy* **34**, 227–39 (2014).
  44. Ucar, M. *et al.* Carbamazepine markedly reduces serum concentrations of simvastatin and simvastatin acid. *Eur. J. Clin. Pharmacol.* **59**, 879–82 (2004).
  45. Winsemius, A. *et al.* Pharmacokinetic interaction between simvastatin and fenofibrate with staggered and simultaneous dosing: Does it matter? *J. Clin. Pharmacol.* **54**, 1038–47 (2014).
  46. Xu, D. *et al.* Decreased exposure of simvastatin and simvastatin acid in a rat model of type 2 diabetes. *Acta Pharmacol. Sin.* **35**, 1215–25 (2014).
  47. Zhao, Q., Jiang, J. & Hu, P. Effects of four traditional Chinese medicines on the pharmacokinetics of simvastatin. *Xenobiotica* **8254**, 1–8 (2015).

**Table S3: Studies used for comparing published numeric and digitized sample time point values**

<b>Author</b>	<b>Mean <math>\zeta</math> [%]</b>	<b>Smallest <math>\zeta</math> [%]</b>	<b>Largest <math>\zeta</math> [%]</b>	<b>N <math>\zeta^a</math></b>	<b>Reference</b>
Alakhali 2013	0.64	0	2.2	10	<sup>1</sup>
Ayalasomayajula 2007	0.01	0	0.057	71	<sup>2</sup>
Ayalasomayajula 2016	5.8	0	47	24	<sup>3</sup>
Backman 2000	0.29	3.40E-05	2.3	40	<sup>4</sup>
Bergman 2004	0.0051	0	0.045	76	<sup>5</sup>
Bergman 2009	0.54	5.00E-04	4.2	44	<sup>6</sup>
Cermak 2009	1	0	4.5	56	<sup>7</sup>
Chung 2006	1	6.80E-04	9.5	24	<sup>8</sup>
Dai 2013	0.0027	0	0.028	98	<sup>9</sup>
DeGorter 2012	0.83	0.031	3	11	<sup>10</sup>
Derks 2010	0.0081	0	0.071	44	<sup>11</sup>
Devineni 2015	0.64	0	4.7	45	<sup>12</sup>
Falcao 2013	0.68	0	9.4	43	<sup>13</sup>
Geboers 2016	0.24	0	2.9	99	<sup>14</sup>
Gehin 2015	0.86	3.10E-04	18	49	<sup>15</sup>
Hasunuma 2016	0.68	0.032	4	22	<sup>16</sup>
Hoch 2013	0.1	0	2.5	118	<sup>17</sup>
Hoch 2013	0.017	0	0.07	48	<sup>18</sup>
Hsyu 2001	0.001	0	0.0053	49	<sup>19</sup>
Itkonen 2015	0.28	0	2.6	65	<sup>20</sup>
Jacobson 2004	0	0	0	34	<sup>21</sup>

Kang 2004	1.6	0.0029	13	11	22
Kantola 1998	0.29	0.0042	5.4	46	23
Kasichayanula 2012	1.6	0	13	43	24
Keskitalo 2009	0.42	0	2.7	59	25
Kim 2007	1.7	0.0083	9.3	33	26
Kosoglou 2011	0.014	0	0.056	56	27
Krishna 2007	0	0	0	8	28
Krishna 2009	0	0	0	78	29
Krishna 2012	1.4	0	11	63	30
Kyrklund 2000	0.071	0	1.2	40	31
Lee 2017	1.1	0.0021	9.3	20	32
Lilja 1998	0.23	0	3.3	35	33
Lilja 2000	0.069	0	1.3	80	34
Lilja 2004	0.33	0	4.1	38	35
Marino 2000	32	0.21	140	18	36
Martin 2016	0.62	0	8.3	22	37
McKenney 2006	0.0031	0	0.019	88	38
Mousa 2000	0.82	0.013	4.5	20	39
NDA 206679	4.1	6.20E-04	74	72	40
NDA 22425	0.0053	0	0.024	94	41
Neuvonen 1998	0.14	5.20E-05	0.72	22	42
O'Brien 2003	0.82	0	5.6	38	43

Offman 2017	0.023	0	0.075	60	44
Park 2016	0.046	0	0.18	52	45
Pasanen 2006	0.43	0	1.3	60	46
Patel 2011	0.0064	0	0.026	44	47
Polli 2013	1.5	0.019	17	18	48
Prueksaritanont 2005	1.6	2.90E-04	15	49	49
Schmitt 2011	0.43	0	7.6	46	50
Shanmugam 2011	2.7	0.082	19	23	51
Simard 2001	0.013	0	0.089	89	52
Sugimoto 2001	42	0.16	180	29	53
Sunkara 2007	0.014	0	0.077	66	54
Teng 2013	1.3	0	23	44	55
Teng 2013	0.03	0	0.087	91	56
Tubic-Grozdanis 2008	1.1	0.005	16	84	57
Tuteja 2014	0.2	0	3.2	44	58
Ucar 2004	0.45	0	4.8	40	59
Vree 2001	2.4	0.058	15	34	60
Winsemius 2014	0.21	0	6.4	204	61
Xu 2014	1	0	9.3	92	62
Yu 2009	1.6	0.002	22	46	63
Zhao 2015	1.6	0	19	92	64
Zhi 2003	2.2	0	25	35	65

Ziviani 2001	0.0092	0	0.044	47	66
--------------	--------	---	-------	----	----

a: Number of values extracted from the study for which  $\zeta$  was calculated

## References

- Alakhali, K., Hassan, Y., Mohamed, N. & Mordi, M. N. Pharmacokinetic of simvastatin study in Malaysian. *IOSR J. Pharm.* **3**, 46–51 (2013).
- Ayalasomayajula, S. P. *et al.* Evaluation of the potential for steady-state pharmacokinetic interaction between vildagliptin and simvastatin in healthy subjects. *Curr. Med. Res. Opin.* **23**, 2913–20 (2007).
- Ayalasomayajula, S. *et al.* In vitro and clinical evaluation of OATP-mediated drug interaction potential of sacubitril/valsartan (LCZ696). *J. Clin. Pharm. Ther.* **41**, 424–31 (2016).
- Backman, J. T., Kyrklund, C., Kivistö, K. T., Wang, J. S. & Neuvonen, P. J. Plasma concentrations of active simvastatin acid are increased by gemfibrozil. *Clin. Pharmacol. Ther.* **68**, 122–9 (2000).
- Bergman, A. J. *et al.* Simvastatin does not have a clinically significant pharmacokinetic interaction with fenofibrate in humans. *J. Clin. Pharmacol.* **44**, 1054–62 (2004).
- Bergman, A. J. *et al.* Effect of sitagliptin on the pharmacokinetics of simvastatin. *J. Clin. Pharmacol.* **49**, 483–8 (2009).
- Cermak, R., Wein, S., Wolfram, S. & Langguth, P. Effects of the flavonol quercetin on the bioavailability of simvastatin in pigs. *Eur. J. Pharm. Sci.* **38**, 519–24 (2009).
- Chung, E., Nafziger, A. N., Kazierad, D. J. & Bertino, J. S. Comparison of midazolam and simvastatin as cytochrome P450 3A probes. *Clin. Pharmacol. Ther.* **79**, 350–361 (2006).
- Dai, L.-L. *et al.* Assessment of a pharmacokinetic and pharmacodynamic interaction between simvastatin and Ginkgo biloba extracts in healthy subjects. *Xenobiotica*. **43**, 862–7 (2013).
- DeGorter, M. K., Urquhart, B. L., Gradhand, U., Tirona, R. G. & Kim, R. B. Disposition of atorvastatin, rosuvastatin, and simvastatin in *oatp1b2*<sup>-/-</sup> mice and intraindividual variability in human subjects. *J. Clin. Pharmacol.* **52**, 1689–97 (2012).
- Derks, M. *et al.* Coadministration of dalcetrapib with pravastatin, rosuvastatin, or simvastatin: no clinically relevant drug-drug interactions. *J. Clin. Pharmacol.* **50**, 1188–201 (2010).
- Devineni, D. *et al.* Effect of canagliflozin on the pharmacokinetics of glyburide, metformin, and simvastatin in healthy participants. *Clin. Pharmacol. drug Dev.* **4**, 226–36 (2015).
- Falcão, A., Pinto, R., Nunes, T. & Soares-da-Silva, P. Effect of repeated administration of eslicarbazepine acetate on the pharmacokinetics of simvastatin in healthy subjects. *Epilepsy Res.* **106**, 244–9 (2013).
- Geboers, S., Stappaerts, J., Tack, J., Annaert, P. & Augustijns, P. In vitro and in vivo investigation of the gastrointestinal behavior of simvastatin. *Int. J. Pharm.* **510**, 296–303 (2016).
- Gehin, M. *et al.* Pharmacokinetic interactions between simvastatin and setipiprant, a CRTH2 antagonist. *Eur. J. Clin. Pharmacol.* **71**, 15–23 (2015).
- Hasunuma, T. *et al.* Absence of ethnic differences in the pharmacokinetics of moxifloxacin, simvastatin, and meloxicam among three East Asian populations and Caucasians. *Br. J. Clin. Pharmacol.* **81**, 1078–1090 (2016).
- Hoch, M., Hoever, P., Alessi, F., Theodor, R. & Dingemans, J. Pharmacokinetic interactions of almorexant with midazolam and simvastatin, two CYP3A4 model substrates, in healthy male subjects. *Eur. J. Clin. Pharmacol.* **69**, 523–32 (2013).
- Hoch, M., Hoever, P., Theodor, R. & Dingemans, J. Almorexant effects on CYP3A4 activity studied by its simultaneous and time-separated administration with simvastatin and atorvastatin. *Eur. J. Clin.*



- Pharmacol.* **69**, 1235–45 (2013).
19. Hsyu, P. H., Schultz-Smith, M. D., Lillibridge, J. H., Lewis, R. H. & Kerr, B. M. Pharmacokinetic interactions between nelfinavir and 3-hydroxy-3-methylglutaryl coenzyme A reductase inhibitors atorvastatin and simvastatin. *Antimicrob. Agents Chemother.* **45**, 3445–50 (2001).
  20. Itkonen, M. K. *et al.* Clopidogrel Has No Clinically Meaningful Effect on the Pharmacokinetics of the Organic Anion Transporting Polypeptide 1B1 and Cytochrome P450 3A4 Substrate Simvastatin. *Drug Metab. Dispos.* **43**, 1655–60 (2015).
  21. Jacobson, T. A. Comparative pharmacokinetic interaction profiles of Pravastatin, Simvastatin, and Atorvastatin when coadministered with cytochrome P450 inhibitors. *Am. J. Cardiol.* **94**, 1140–1146 (2004).
  22. Kang, B. K. *et al.* Development of self-microemulsifying drug delivery systems (SMEDDS) for oral bioavailability enhancement of simvastatin in beagle dogs. *Int. J. Pharm.* **274**, 65–73 (2004).
  23. Kantola, T., Kivistö, K. T. & Neuvonen, P. J. Erythromycin and verapamil considerably increase serum simvastatin and simvastatin acid concentrations. *Clin. Pharmacol. Ther.* **64**, 177–82 (1998).
  24. Kasichayanula, S. *et al.* Lack of pharmacokinetic interactions between dapagliflozin and simvastatin, valsartan, warfarin, or digoxin. *Adv. Ther.* **29**, 163–77 (2012).
  25. Keskitalo, J. E., Pasanen, M. K., Neuvonen, P. J. & Niemi, M. Different effects of the ABCG2 c.421C>A SNP on the pharmacokinetics of fluvastatin, pravastatin and simvastatin. *Pharmacogenomics* **10**, 1617–24 (2009).
  26. Kim, K.-A., Park, P.-W., Lee, O.-J., Kang, D.-K. & Park, J.-Y. Effect of polymorphic CYP3A5 genotype on the single-dose simvastatin pharmacokinetics in healthy subjects. *J. Clin. Pharmacol.* **47**, 87–93 (2007).
  27. Kosoglou, T. *et al.* Assessment of potential pharmacokinetic interactions of ezetimibe/simvastatin and extended-release niacin tablets in healthy subjects. *Eur. J. Clin. Pharmacol.* **67**, 483–92 (2011).
  28. Krishna, G., Parsons, A., Kantesaria, B. & Mant, T. Evaluation of the pharmacokinetics of posaconazole and rifabutin following co-administration to healthy men. *Curr. Med Res. Opin.* **23**, 545–552 (2007).
  29. Krishna, G., Moton, A., Lei, M., Medlock, M. M. & McLeod, J. Pharmacokinetics and absorption of posaconazole oral suspension under various gastric conditions in healthy volunteers. *Antimicrob. Agents Chemother.* **53**, 958–966 (2009).
  30. Krishna, G. *et al.* Effect of posaconazole on the pharmacokinetics of simvastatin and midazolam in healthy volunteers. *Expert Opin. Drug Metab. Toxicol.* **8**, 1–10 (2012).
  31. Kyrklund, C. *et al.* Rifampin greatly reduces plasma simvastatin and simvastatin acid concentrations. *Clin. Pharmacol. Ther.* **68**, 592–7 (2000).
  32. Lee, E. B. *et al.* Disease–Drug Interaction of Sarilumab and Simvastatin in Patients with Rheumatoid Arthritis. *Clin. Pharmacokinet.* **56**, 607–615 (2017).
  33. Lilja, J. J., Kivistö, K. T. & Neuvonen, P. J. Grapefruit juice-simvastatin interaction: effect on serum concentrations of simvastatin, simvastatin acid, and HMG-CoA reductase inhibitors. *Clin. Pharmacol. Ther.* **64**, 477–83 (1998).
  34. Lilja, J. J., Kivistö, K. T. & Neuvonen, P. J. Duration of effect of grapefruit juice on the pharmacokinetics of the CYP3A4 substrate simvastatin. *Clin. Pharmacol. Ther.* **68**, 384–90 (2000).
  35. Lilja, J. J., Neuvonen, M. & Neuvonen, P. J. Effects of regular consumption of grapefruit juice on the pharmacokinetics of simvastatin. *Br. J. Clin. Pharmacol.* **58**, 56–60 (2004).
  36. Marino, M. R., Vachharajani, N. N. & Hadjilambri, O. W. Irbesartan does not affect the pharmacokinetics of simvastatin in healthy subjects. *J. Clin. Pharmacol.* **40**, 875–9 (2000).
  37. Martin, P. *et al.* Effects of Fostamatinib on the Pharmacokinetics of Oral Contraceptive, Warfarin, and the Statins Rosuvastatin and Simvastatin: Results From Phase I Clinical Studies. *Drugs R. D.* **16**, 93–107 (2016).
  38. McKenney, J. M. *et al.* Study of the pharmacokinetic interaction between simvastatin and prescription omega-3-acid ethyl esters. *J. Clin. Pharmacol.* **46**, 785–91 (2006).

39. Mousa, O., Brater, D. C., Sunblad, K. J. & Hall, S. D. The interaction of diltiazem with simvastatin. *Clin. Pharmacol. Ther.* **67**, 267–74 (2000).
40. Food and Drug Administration (FDA) NDA 206-679: Flolipid. 1–183 (2011).
41. Food and Drug Administration (FDA) NDA 22425: Dronedarone. *Cent. drug Eval. Res.* (2006).
42. Neuvonen, P. J., Kantola, T. & Kivistö, K. T. Simvastatin but not pravastatin is very susceptible to interaction with the CYP3A4 inhibitor itraconazole. *Clin. Pharmacol. Ther.* **63**, 332–341 (1998).
43. O'Brien, S. G. *et al.* Effects of imatinib mesylate (STI571, Glivec) on the pharmacokinetics of simvastatin, a cytochrome p450 3A4 substrate, in patients with chronic myeloid leukaemia. *Br. J. Cancer* **89**, 1855–9 (2003).
44. Offman, E., Davidson, M. & Nilsson, C. Assessment of pharmacokinetic interaction between omega-3 carboxylic acids and the statins rosuvastatin and simvastatin: Results of 2 phase I studies in healthy volunteers. *J. Clin. Lipidol.* **11**, 739–748 (2017).
45. Park, S. J. *et al.* Pomegranate juice does not affect the disposition of simvastatin in healthy subjects. *Eur. J. Drug Metab. Pharmacokinet.* **41**, 339–344 (2016).
46. Pasanen, M. K., Neuvonen, M., Neuvonen, P. J. & Niemi, M. SLCO1B1 polymorphism markedly affects the pharmacokinetics of simvastatin acid. *Pharmacogenet. Genomics* **16**, 873–9 (2006).
47. Patel, C. G. *et al.* Two-way pharmacokinetic interaction studies between saxagliptin and cytochrome P450 substrates or inhibitors: simvastatin, diltiazem extended-release, and ketoconazole. *Clin. Pharmacol.* **3**, 13–25 (2011).
48. Polli, J. W. *et al.* Evaluation of drug interactions of GSK1292263 (a GPR119 agonist) with statins: From in vitro data to clinical study design. *Xenobiotica* **43**, 498–508 (2013).
49. Prueksaritanont, T. *et al.* Interconversion pharmacokinetics of simvastatin and its hydroxy acid in dogs: Effects of gemfibrozil. *Pharm. Res.* **22**, 1101–1109 (2005).
50. Schmitt, C., Kuhn, B., Zhang, X., Kivitz, A. J. & Grange, S. Disease-drug-drug interaction involving tocilizumab and simvastatin in patients with rheumatoid arthritis. *Clin. Pharmacol. Ther.* **89**, 735–40 (2011).
51. Shanmugam, S., Ryu, J.-K., Yoo, S.-D., Choi, H.-G. & Woo, J.-S. Evaluation of Pharmacokinetics of Simvastatin and Its Pharmacologically Active Metabolite from Controlled-Release Tablets of Simvastatin in Rodent and Canine Animal Models. *Biomol. Ther.* **19**, 248–254 (2011).
52. Simard, C. *et al.* Study of the drug-drug interaction between simvastatin and cisapride in man. *Eur. J. Clin. Pharmacol.* **57**, 229–34 (2001).
53. Sugimoto, K. *et al.* Different effects of St John's Wort on the pharmacokinetics of simvastatin and pravastatin. *Clin. Pharmacol. Ther.* **70**, 518–524 (2001).
54. Sunkara, G. *et al.* Evaluation of a pharmacokinetic interaction between valsartan and simvastatin in healthy subjects. *Curr. Med. Res. Opin.* **23**, 631–40 (2007).
55. Teng, R., Mitchell, P. D. & Butler, K. A. Pharmacokinetic interaction studies of co-administration of ticagrelor and atorvastatin or simvastatin in healthy volunteers. *Eur. J. Clin. Pharmacol.* **69**, 477–87 (2013).
56. Teng, S. *et al.* Impact of Tesamorelin, a Growth Hormone-Releasing Factor (GRF) Analogue, on the Pharmacokinetics of Simvastatin and Ritonavir in Healthy Volunteers. *Clin. Pharmacol. Drug Dev.* **2**, 237–245 (2013).
57. Tubic-Grozdanic, M. *et al.* Pharmacokinetics of the CYP 3A substrate simvastatin following administration of delayed versus immediate release oral dosage forms. *Pharm. Res.* **25**, 1591–600 (2008).
58. Tuteja, S. *et al.* Pharmacokinetic interactions of the microsomal triglyceride transfer protein inhibitor, lomitapide, with drugs commonly used in the management of hypercholesterolemia. *Pharmacotherapy* **34**, 227–39 (2014).
59. Ucar, M. *et al.* Carbamazepine markedly reduces serum concentrations of simvastatin and simvastatin acid. *Eur. J. Clin. Pharmacol.* **59**, 879–82 (2004).

60. Vree, T. B. *et al.* Variable plasma/liver and tissue esterase hydrolysis of simvastatin in healthy volunteers after a single oral dose. *Clin. Drug Investig.* **21**, 643–652 (2001).
61. Winsemius, A. *et al.* Pharmacokinetic interaction between simvastatin and fenofibrate with staggered and simultaneous dosing: Does it matter? *J. Clin. Pharmacol.* **54**, 1038–47 (2014).
62. Xu, D. *et al.* Decreased exposure of simvastatin and simvastatin acid in a rat model of type 2 diabetes. *Acta Pharmacol. Sin.* **35**, 1215–25 (2014).
63. Yu, R. Z. *et al.* Lack of pharmacokinetic interaction of mipomersen sodium (ISIS 301012), a 2'-O-methoxyethyl modified antisense oligonucleotide targeting apolipoprotein B-100 messenger RNA, with simvastatin and ezetimibe. *Clin. Pharmacokinet.* **48**, 39–50 (2009).
64. Zhao, Q., Jiang, J. & Hu, P. Effects of four traditional Chinese medicines on the pharmacokinetics of simvastatin. *Xenobiotica* **8254**, 1–8 (2015).
65. Zhi, J., Moore, R., Kanitra, L. & Mulligan, T. E. Effects of orlistat, a lipase inhibitor, on the pharmacokinetics of three highly lipophilic drugs (amiodarone, fluoxetine, and simvastatin) in healthy volunteers. *J. Clin. Pharmacol.* **43**, 428–35 (2003).
66. Ziviani, L. *et al.* The effects of lacidipine on the steady/state plasma concentrations of simvastatin in healthy subjects. *Br. J. Clin. Pharmacol.* **51**, 147–52 (2001).

**Table S3: Studies used for comparing published numeric and digitized sample time point values**

<b>Author</b>	<b>Mean <math>\zeta</math> [%]</b>	<b>Smallest <math>\zeta</math> [%]</b>	<b>Largest <math>\zeta</math> [%]</b>	<b>N <math>\zeta^a</math></b>	<b>Reference</b>
Alakhali 2013	0.64	0	2.2	10	<sup>1</sup>
Ayalasomayajula 2007	0.01	0	0.057	71	<sup>2</sup>
Ayalasomayajula 2016	5.8	0	47	24	<sup>3</sup>
Backman 2000	0.29	3.40E-05	2.3	40	<sup>4</sup>
Bergman 2004	0.0051	0	0.045	76	<sup>5</sup>
Bergman 2009	0.54	5.00E-04	4.2	44	<sup>6</sup>
Cermak 2009	1	0	4.5	56	<sup>7</sup>
Chung 2006	1	6.80E-04	9.5	24	<sup>8</sup>
Dai 2013	0.0027	0	0.028	98	<sup>9</sup>
DeGorter 2012	0.83	0.031	3	11	<sup>10</sup>
Derks 2010	0.0081	0	0.071	44	<sup>11</sup>
Devineni 2015	0.64	0	4.7	45	<sup>12</sup>
Falcao 2013	0.68	0	9.4	43	<sup>13</sup>
Geboers 2016	0.24	0	2.9	99	<sup>14</sup>
Gehin 2015	0.86	3.10E-04	18	49	<sup>15</sup>
Hasunuma 2016	0.68	0.032	4	22	<sup>16</sup>
Hoch 2013	0.1	0	2.5	118	<sup>17</sup>
Hoch 2013	0.017	0	0.07	48	<sup>18</sup>
Hsyu 2001	0.001	0	0.0053	49	<sup>19</sup>
Itkonen 2015	0.28	0	2.6	65	<sup>20</sup>
Jacobson 2004	0	0	0	34	<sup>21</sup>

Kang 2004	1.6	0.0029	13	11	22
Kantola 1998	0.29	0.0042	5.4	46	23
Kasichayanula 2012	1.6	0	13	43	24
Keskitalo 2009	0.42	0	2.7	59	25
Kim 2007	1.7	0.0083	9.3	33	26
Kosoglou 2011	0.014	0	0.056	56	27
Krishna 2007	0	0	0	8	28
Krishna 2009	0	0	0	78	29
Krishna 2012	1.4	0	11	63	30
Kyrklund 2000	0.071	0	1.2	40	31
Lee 2017	1.1	0.0021	9.3	20	32
Lilja 1998	0.23	0	3.3	35	33
Lilja 2000	0.069	0	1.3	80	34
Lilja 2004	0.33	0	4.1	38	35
Marino 2000	32	0.21	140	18	36
Martin 2016	0.62	0	8.3	22	37
McKenney 2006	0.0031	0	0.019	88	38
Mousa 2000	0.82	0.013	4.5	20	39
NDA 206679	4.1	6.20E-04	74	72	40
NDA 22425	0.0053	0	0.024	94	41
Neuvonen 1998	0.14	5.20E-05	0.72	22	42
O'Brien 2003	0.82	0	5.6	38	43

Offman 2017	0.023	0	0.075	60	44
Park 2016	0.046	0	0.18	52	45
Pasanen 2006	0.43	0	1.3	60	46
Patel 2011	0.0064	0	0.026	44	47
Polli 2013	1.5	0.019	17	18	48
Prueksaritanont 2005	1.6	2.90E-04	15	49	49
Schmitt 2011	0.43	0	7.6	46	50
Shanmugam 2011	2.7	0.082	19	23	51
Simard 2001	0.013	0	0.089	89	52
Sugimoto 2001	42	0.16	180	29	53
Sunkara 2007	0.014	0	0.077	66	54
Teng 2013	1.3	0	23	44	55
Teng 2013	0.03	0	0.087	91	56
Tubic-Grozdanis 2008	1.1	0.005	16	84	57
Tuteja 2014	0.2	0	3.2	44	58
Ucar 2004	0.45	0	4.8	40	59
Vree 2001	2.4	0.058	15	34	60
Winsemius 2014	0.21	0	6.4	204	61
Xu 2014	1	0	9.3	92	62
Yu 2009	1.6	0.002	22	46	63
Zhao 2015	1.6	0	19	92	64
Zhi 2003	2.2	0	25	35	65

Ziviani 2001	0.0092	0	0.044	47	66
--------------	--------	---	-------	----	----

a: Number of values extracted from the study for which  $\zeta$  was calculated

## References

1. Alakhali, K., Hassan, Y., Mohamed, N. & Mordi, M. N. Pharmacokinetic of simvastatin study in Malaysian. *IOSR J. Pharm.* **3**, 46–51 (2013).
2. Ayalasomayajula, S. P. *et al.* Evaluation of the potential for steady-state pharmacokinetic interaction between vildagliptin and simvastatin in healthy subjects. *Curr. Med. Res. Opin.* **23**, 2913–20 (2007).
3. Ayalasomayajula, S. *et al.* In vitro and clinical evaluation of OATP-mediated drug interaction potential of sacubitril/valsartan (LCZ696). *J. Clin. Pharm. Ther.* **41**, 424–31 (2016).
4. Backman, J. T., Kyrklund, C., Kivistö, K. T., Wang, J. S. & Neuvonen, P. J. Plasma concentrations of active simvastatin acid are increased by gemfibrozil. *Clin. Pharmacol. Ther.* **68**, 122–9 (2000).
5. Bergman, A. J. *et al.* Simvastatin does not have a clinically significant pharmacokinetic interaction with fenofibrate in humans. *J. Clin. Pharmacol.* **44**, 1054–62 (2004).
6. Bergman, A. J. *et al.* Effect of sitagliptin on the pharmacokinetics of simvastatin. *J. Clin. Pharmacol.* **49**, 483–8 (2009).
7. Cermak, R., Wein, S., Wolfram, S. & Langguth, P. Effects of the flavonol quercetin on the bioavailability of simvastatin in pigs. *Eur. J. Pharm. Sci.* **38**, 519–24 (2009).
8. Chung, E., Nafziger, A. N., Kazierad, D. J. & Bertino, J. S. Comparison of midazolam and simvastatin as cytochrome P450 3A probes. *Clin. Pharmacol. Ther.* **79**, 350–361 (2006).
9. Dai, L.-L. *et al.* Assessment of a pharmacokinetic and pharmacodynamic interaction between simvastatin and Ginkgo biloba extracts in healthy subjects. *Xenobiotica*. **43**, 862–7 (2013).
10. DeGorter, M. K., Urquhart, B. L., Gradhand, U., Tirona, R. G. & Kim, R. B. Disposition of atorvastatin, rosuvastatin, and simvastatin in *oatp1b2*<sup>-/-</sup> mice and intraindividual variability in human subjects. *J. Clin. Pharmacol.* **52**, 1689–97 (2012).
11. Derks, M. *et al.* Coadministration of dalcetrapib with pravastatin, rosuvastatin, or simvastatin: no clinically relevant drug-drug interactions. *J. Clin. Pharmacol.* **50**, 1188–201 (2010).
12. Devineni, D. *et al.* Effect of canagliflozin on the pharmacokinetics of glyburide, metformin, and simvastatin in healthy participants. *Clin. Pharmacol. drug Dev.* **4**, 226–36 (2015).
13. Falcão, A., Pinto, R., Nunes, T. & Soares-da-Silva, P. Effect of repeated administration of eslicarbazepine acetate on the pharmacokinetics of simvastatin in healthy subjects. *Epilepsy Res.* **106**, 244–9 (2013).
14. Geboers, S., Stappaerts, J., Tack, J., Annaert, P. & Augustijns, P. In vitro and in vivo investigation of the gastrointestinal behavior of simvastatin. *Int. J. Pharm.* **510**, 296–303 (2016).
15. Gehin, M. *et al.* Pharmacokinetic interactions between simvastatin and setipiprant, a CRTH2 antagonist. *Eur. J. Clin. Pharmacol.* **71**, 15–23 (2015).
16. Hasunuma, T. *et al.* Absence of ethnic differences in the pharmacokinetics of moxifloxacin, simvastatin, and meloxicam among three East Asian populations and Caucasians. *Br. J. Clin. Pharmacol.* **81**, 1078–1090 (2016).
17. Hoch, M., Hoever, P., Alessi, F., Theodor, R. & Dingemans, J. Pharmacokinetic interactions of almorexant with midazolam and simvastatin, two CYP3A4 model substrates, in healthy male subjects. *Eur. J. Clin. Pharmacol.* **69**, 523–32 (2013).
18. Hoch, M., Hoever, P., Theodor, R. & Dingemans, J. Almorexant effects on CYP3A4 activity studied by its simultaneous and time-separated administration with simvastatin and atorvastatin. *Eur. J. Clin.*

- Pharmacol.* **69**, 1235–45 (2013).
19. Hsyu, P. H., Schultz-Smith, M. D., Lillibridge, J. H., Lewis, R. H. & Kerr, B. M. Pharmacokinetic interactions between nelfinavir and 3-hydroxy-3-methylglutaryl coenzyme A reductase inhibitors atorvastatin and simvastatin. *Antimicrob. Agents Chemother.* **45**, 3445–50 (2001).
  20. Itkonen, M. K. *et al.* Clopidogrel Has No Clinically Meaningful Effect on the Pharmacokinetics of the Organic Anion Transporting Polypeptide 1B1 and Cytochrome P450 3A4 Substrate Simvastatin. *Drug Metab. Dispos.* **43**, 1655–60 (2015).
  21. Jacobson, T. A. Comparative pharmacokinetic interaction profiles of Pravastatin, Simvastatin, and Atorvastatin when coadministered with cytochrome P450 inhibitors. *Am. J. Cardiol.* **94**, 1140–1146 (2004).
  22. Kang, B. K. *et al.* Development of self-microemulsifying drug delivery systems (SMEDDS) for oral bioavailability enhancement of simvastatin in beagle dogs. *Int. J. Pharm.* **274**, 65–73 (2004).
  23. Kantola, T., Kivistö, K. T. & Neuvonen, P. J. Erythromycin and verapamil considerably increase serum simvastatin and simvastatin acid concentrations. *Clin. Pharmacol. Ther.* **64**, 177–82 (1998).
  24. Kasichayanula, S. *et al.* Lack of pharmacokinetic interactions between dapagliflozin and simvastatin, valsartan, warfarin, or digoxin. *Adv. Ther.* **29**, 163–77 (2012).
  25. Keskitalo, J. E., Pasanen, M. K., Neuvonen, P. J. & Niemi, M. Different effects of the ABCG2 c.421C>A SNP on the pharmacokinetics of fluvastatin, pravastatin and simvastatin. *Pharmacogenomics* **10**, 1617–24 (2009).
  26. Kim, K.-A., Park, P.-W., Lee, O.-J., Kang, D.-K. & Park, J.-Y. Effect of polymorphic CYP3A5 genotype on the single-dose simvastatin pharmacokinetics in healthy subjects. *J. Clin. Pharmacol.* **47**, 87–93 (2007).
  27. Kosoglou, T. *et al.* Assessment of potential pharmacokinetic interactions of ezetimibe/simvastatin and extended-release niacin tablets in healthy subjects. *Eur. J. Clin. Pharmacol.* **67**, 483–92 (2011).
  28. Krishna, G., Parsons, A., Kantesaria, B. & Mant, T. Evaluation of the pharmacokinetics of posaconazole and rifabutin following co-administration to healthy men. *Curr. Med Res. Opin.* **23**, 545–552 (2007).
  29. Krishna, G., Moton, A., Lei, M., Medlock, M. M. & McLeod, J. Pharmacokinetics and absorption of posaconazole oral suspension under various gastric conditions in healthy volunteers. *Antimicrob. Agents Chemother.* **53**, 958–966 (2009).
  30. Krishna, G. *et al.* Effect of posaconazole on the pharmacokinetics of simvastatin and midazolam in healthy volunteers. *Expert Opin. Drug Metab. Toxicol.* **8**, 1–10 (2012).
  31. Kyrklund, C. *et al.* Rifampin greatly reduces plasma simvastatin and simvastatin acid concentrations. *Clin. Pharmacol. Ther.* **68**, 592–7 (2000).
  32. Lee, E. B. *et al.* Disease–Drug Interaction of Sarilumab and Simvastatin in Patients with Rheumatoid Arthritis. *Clin. Pharmacokinet.* **56**, 607–615 (2017).
  33. Lilja, J. J., Kivistö, K. T. & Neuvonen, P. J. Grapefruit juice-simvastatin interaction: effect on serum concentrations of simvastatin, simvastatin acid, and HMG-CoA reductase inhibitors. *Clin. Pharmacol. Ther.* **64**, 477–83 (1998).
  34. Lilja, J. J., Kivistö, K. T. & Neuvonen, P. J. Duration of effect of grapefruit juice on the pharmacokinetics of the CYP3A4 substrate simvastatin. *Clin. Pharmacol. Ther.* **68**, 384–90 (2000).
  35. Lilja, J. J., Neuvonen, M. & Neuvonen, P. J. Effects of regular consumption of grapefruit juice on the pharmacokinetics of simvastatin. *Br. J. Clin. Pharmacol.* **58**, 56–60 (2004).
  36. Marino, M. R., Vachharajani, N. N. & Hadjilambris, O. W. Irbesartan does not affect the pharmacokinetics of simvastatin in healthy subjects. *J. Clin. Pharmacol.* **40**, 875–9 (2000).
  37. Martin, P. *et al.* Effects of Fostamatinib on the Pharmacokinetics of Oral Contraceptive, Warfarin, and the Statins Rosuvastatin and Simvastatin: Results From Phase I Clinical Studies. *Drugs R. D.* **16**, 93–107 (2016).
  38. McKenney, J. M. *et al.* Study of the pharmacokinetic interaction between simvastatin and prescription omega-3-acid ethyl esters. *J. Clin. Pharmacol.* **46**, 785–91 (2006).



39. Mousa, O., Brater, D. C., Sunblad, K. J. & Hall, S. D. The interaction of diltiazem with simvastatin. *Clin. Pharmacol. Ther.* **67**, 267–74 (2000).
40. Food and Drug Administration (FDA) NDA 206-679: Flolipid. 1–183 (2011).
41. Food and Drug Administration (FDA) NDA 22425: Dronedarone. *Cent. drug Eval. Res.* (2006).
42. Neuvonen, P. J., Kantola, T. & Kivistö, K. T. Simvastatin but not pravastatin is very susceptible to interaction with the CYP3A4 inhibitor itraconazole. *Clin. Pharmacol. Ther.* **63**, 332–341 (1998).
43. O'Brien, S. G. *et al.* Effects of imatinib mesylate (STI571, Glivec) on the pharmacokinetics of simvastatin, a cytochrome p450 3A4 substrate, in patients with chronic myeloid leukaemia. *Br. J. Cancer* **89**, 1855–9 (2003).
44. Offman, E., Davidson, M. & Nilsson, C. Assessment of pharmacokinetic interaction between omega-3 carboxylic acids and the statins rosuvastatin and simvastatin: Results of 2 phase I studies in healthy volunteers. *J. Clin. Lipidol.* **11**, 739–748 (2017).
45. Park, S. J. *et al.* Pomegranate juice does not affect the disposition of simvastatin in healthy subjects. *Eur. J. Drug Metab. Pharmacokinet.* **41**, 339–344 (2016).
46. Pasanen, M. K., Neuvonen, M., Neuvonen, P. J. & Niemi, M. SLCO1B1 polymorphism markedly affects the pharmacokinetics of simvastatin acid. *Pharmacogenet. Genomics* **16**, 873–9 (2006).
47. Patel, C. G. *et al.* Two-way pharmacokinetic interaction studies between saxagliptin and cytochrome P450 substrates or inhibitors: simvastatin, diltiazem extended-release, and ketoconazole. *Clin. Pharmacol.* **3**, 13–25 (2011).
48. Polli, J. W. *et al.* Evaluation of drug interactions of GSK1292263 (a GPR119 agonist) with statins: From in vitro data to clinical study design. *Xenobiotica* **43**, 498–508 (2013).
49. Prueksaritanont, T. *et al.* Interconversion pharmacokinetics of simvastatin and its hydroxy acid in dogs: Effects of gemfibrozil. *Pharm. Res.* **22**, 1101–1109 (2005).
50. Schmitt, C., Kuhn, B., Zhang, X., Kivitz, A. J. & Grange, S. Disease-drug-drug interaction involving tocilizumab and simvastatin in patients with rheumatoid arthritis. *Clin. Pharmacol. Ther.* **89**, 735–40 (2011).
51. Shanmugam, S., Ryu, J.-K., Yoo, S.-D., Choi, H.-G. & Woo, J.-S. Evaluation of Pharmacokinetics of Simvastatin and Its Pharmacologically Active Metabolite from Controlled-Release Tablets of Simvastatin in Rodent and Canine Animal Models. *Biomol. Ther.* **19**, 248–254 (2011).
52. Simard, C. *et al.* Study of the drug-drug interaction between simvastatin and cisapride in man. *Eur. J. Clin. Pharmacol.* **57**, 229–34 (2001).
53. Sugimoto, K. *et al.* Different effects of St John's Wort on the pharmacokinetics of simvastatin and pravastatin. *Clin. Pharmacol. Ther.* **70**, 518–524 (2001).
54. Sunkara, G. *et al.* Evaluation of a pharmacokinetic interaction between valsartan and simvastatin in healthy subjects. *Curr. Med. Res. Opin.* **23**, 631–40 (2007).
55. Teng, R., Mitchell, P. D. & Butler, K. A. Pharmacokinetic interaction studies of co-administration of ticagrelor and atorvastatin or simvastatin in healthy volunteers. *Eur. J. Clin. Pharmacol.* **69**, 477–87 (2013).
56. Teng, S. *et al.* Impact of Tesamorelin, a Growth Hormone-Releasing Factor (GRF) Analogue, on the Pharmacokinetics of Simvastatin and Ritonavir in Healthy Volunteers. *Clin. Pharmacol. Drug Dev.* **2**, 237–245 (2013).
57. Tubic-Grozdanic, M. *et al.* Pharmacokinetics of the CYP 3A substrate simvastatin following administration of delayed versus immediate release oral dosage forms. *Pharm. Res.* **25**, 1591–600 (2008).
58. Tuteja, S. *et al.* Pharmacokinetic interactions of the microsomal triglyceride transfer protein inhibitor, lomitapide, with drugs commonly used in the management of hypercholesterolemia. *Pharmacotherapy* **34**, 227–39 (2014).
59. Ucar, M. *et al.* Carbamazepine markedly reduces serum concentrations of simvastatin and simvastatin acid. *Eur. J. Clin. Pharmacol.* **59**, 879–82 (2004).

60. Vree, T. B. *et al.* Variable plasma/liver and tissue esterase hydrolysis of simvastatin in healthy volunteers after a single oral dose. *Clin. Drug Investig.* **21**, 643–652 (2001).
61. Winsemius, A. *et al.* Pharmacokinetic interaction between simvastatin and fenofibrate with staggered and simultaneous dosing: Does it matter? *J. Clin. Pharmacol.* **54**, 1038–47 (2014).
62. Xu, D. *et al.* Decreased exposure of simvastatin and simvastatin acid in a rat model of type 2 diabetes. *Acta Pharmacol. Sin.* **35**, 1215–25 (2014).
63. Yu, R. Z. *et al.* Lack of pharmacokinetic interaction of mipomersen sodium (ISIS 301012), a 2'-O-methoxyethyl modified antisense oligonucleotide targeting apolipoprotein B-100 messenger RNA, with simvastatin and ezetimibe. *Clin. Pharmacokinet.* **48**, 39–50 (2009).
64. Zhao, Q., Jiang, J. & Hu, P. Effects of four traditional Chinese medicines on the pharmacokinetics of simvastatin. *Xenobiotica* **8254**, 1–8 (2015).
65. Zhi, J., Moore, R., Kanitra, L. & Mulligan, T. E. Effects of orlistat, a lipase inhibitor, on the pharmacokinetics of three highly lipophilic drugs (amiodarone, fluoxetine, and simvastatin) in healthy volunteers. *J. Clin. Pharmacol.* **43**, 428–35 (2003).
66. Ziviani, L. *et al.* The effects of lacidipine on the steady/state plasma concentrations of simvastatin in healthy subjects. *Br. J. Clin. Pharmacol.* **51**, 147–52 (2001).

**Table S4: Study records identified in “CPT: Pharmacometrics & Systems Pharmacology” in 2018 as original PBPK research articles**

Year	Title	PBPK original research article	Data digitized	Data digitization mentioned	Digitizing tool cited	Reference
2018	Applied Concepts in PBPK Modeling: How to Extend an Open Systems Pharmacology Model to the Special Population of Pregnant Women	Yes	Most likely	No	No	1
2018	Quantitative Systems Pharmacology Modeling of Acid Sphingomyelinase Deficiency and the Enzyme Replacement Therapy Olipudase Alfa Is an Innovative Tool for Linking Pathophysiology and Pharmacology	Yes	Unlikely (access to clinical study data)	No	No	2
2018	Drug Dosing in Pregnant Women: Challenges and Opportunities in Using Physiologically Based Pharmacokinetic Modeling and Simulations	Yes	Unlikely (no concentration-time or other PK data used)	No	No	3
2018	A Strategy to Refine the Phenotyping Approach and Its Implementation to Predict Drug Clearance: A Physiologically Based Pharmacokinetic Simulation Study	Yes	Most likely	No	No	4
2018	Physiologically Based Pharmacokinetic Approach to Determine Dosing on Extracorporeal Life Support: Fluconazole in Children on ECMO	Yes	Most likely	No	No	5
2018	PBPK Models for CYP3A4 and P-gp DDI Prediction: A Modeling Network of Rifampicin, Itraconazole, Clarithromycin, Midazolam, Alfentanil, and Digoxin	Yes	Yes	No	No	6
2018	Using a Vancomycin PBPK Model in Special Populations to Elucidate Case-Based Clinical PK Observations	Yes	Most likely	Yes	GetData Graph Digitizer	7
2018	A Partial Differential Equation Approach to Inhalation Physiologically Based Pharmacokinetic Modeling	Yes	Unlikely (no concentration-time or other PK data used)	No	No	8
2018	Quantitative Prediction of OATP-Mediated Drug-Drug Interactions With Model-Based Analysis of Endogenous Biomarker Kinetics	Yes	Most likely	No	No	9
2018	Drugs Being Eliminated via the Same Pathway Will Not Always Require Similar Pediatric Dose Adjustments	Yes	Unlikely (no concentration-time or other PK data used)	No	No	10
2018	Comprehensive PBPK Model of Rifampicin for Quantitative Prediction of Complex Drug-Drug Interactions: CYP3A/2C9 Induction and OATP Inhibition Effects	Yes	Most likely	No	No	11
2018	PBPK Modeling of Coproporphyrin I as an Endogenous Biomarker for Drug Interactions Involving Inhibition of Hepatic OATP1B1 and OATP1B3	Yes	Most likely	No	No	12
2018	PBPK Model of Morphine Incorporating Developmental Changes in Hepatic OCT1 and UGT2B7 Proteins to Explain the Variability in Clearances in Neonates and Small Infants	Yes	Most likely	Yes	GetData Graph Digitizer	13
2018	A Quantitative Systems Pharmacology Kidney Model of Diabetes Associated Renal Hyperfiltration and the Effects of SGLT Inhibitors	Yes	Yes	No	No	14

2018	Application of PBPK Modeling and Virtual Clinical Study Approaches to Predict the Outcomes of CYP2D6 Genotype-Guided Dosing of Tamoxifen	Yes	Most likely	No	No	15
2018	Prediction of the Pharmacokinetics of Pravastatin as an OATP Substrate Using Plateable Human Hepatocytes With Human Plasma Data and PBPK Modeling	Yes	Most likely	No	No	16
2018	Development, Verification, and Prediction of Osimertinib Drug-Drug Interactions Using PBPK Modeling Approach to Inform Drug Label	Yes	Unlikely (access to clinical study data)	No	No	17
2018	Pediatric Dosing of Ganciclovir and Valganciclovir: How Model-Based Simulations Can Prevent Underexposure and Potential Treatment Failure	Yes	Unlikely (access to database)	No	No	18
2018	A Novel PBPK Modeling Approach to Assess Cytochrome P450 Mediated Drug-Drug Interaction Potential of the Cytotoxic Prodrug Evofosfamide	Yes	Unlikely (access to clinical study data)	No	No	19
2018	Modulation of Cell State to Improve Drug Therapy	Yes	Unlikely (no concentration-time or other PK data used)	No	No	20

## References

1. Dallmann, A., Solodenko, J., Ince, I. & Eissing, T. Applied Concepts in PBPK Modeling: How to Extend an Open Systems Pharmacology Model to the Special Population of Pregnant Women. *CPT Pharmacometrics Syst. Pharmacol.* **7**, 419–431 (2018).
2. Kaddi, C. D. *et al.* Quantitative Systems Pharmacology Modeling of Acid Sphingomyelinase Deficiency and the Enzyme Replacement Therapy Olipudase Alfa Is an Innovative Tool for Linking Pathophysiology and Pharmacology. *CPT Pharmacometrics Syst. Pharmacol.* **7**, 442–452 (2018).
3. Ke, A. B., Greupink, R. & Abduljalil, K. Drug dosing in pregnant women: Challenges and opportunities in using physiologically based pharmacokinetic modeling and simulations. *CPT Pharmacometrics Syst. Pharmacol.* **7**, 103–110 (2018).
4. Adiwidjaja, J., Boddy, A. V. & McLachlan, A. J. A Strategy to Refine the Phenotyping Approach and Its Implementation to Predict Drug Clearance: A Physiologically Based Pharmacokinetic Simulation Study. *CPT Pharmacometrics Syst. Pharmacol.* **7**, 798–808 (2018).
5. Watt, K. M. *et al.* Physiologically Based Pharmacokinetic Approach to Determine Dosing on Extracorporeal Life Support: Fluconazole in Children on ECMO. *CPT Pharmacometrics Syst. Pharmacol.* **7**, 629–637 (2018).
6. Hanke, N. *et al.* PBPK models for CYP3A4 and P-gp DDI prediction: a modeling network of rifampicin, itraconazole, clarithromycin, midazolam, alfentanil and digoxin - Supplementary document. *CPT pharmacometrics Syst. Pharmacol.* (2018).at <<http://www.ncbi.nlm.nih.gov/pubmed/30091221>>
7. Emoto, C., Johnson, T. N., McPhail, B. T., Vinks, A. A. & Fukuda, T. Using a Vancomycin PBPK Model in Special Populations to Elucidate Case-Based Clinical PK Observations. *CPT Pharmacometrics Syst. Pharmacol.* **7**, 237–250 (2018).
8. Boger, E. & Wigström, O. A Partial Differential Equation Approach to Inhalation Physiologically Based Pharmacokinetic Modeling. *CPT Pharmacometrics Syst. Pharmacol.* **7**, 638–646 (2018).
9. Yoshida, K., Guo, C. & Sane, R. Quantitative Prediction of OATP-Mediated Drug-Drug Interactions With Model-Based Analysis of Endogenous Biomarker Kinetics. *CPT Pharmacometrics Syst. Pharmacol.* **7**, 517–524 (2018).
10. Calvier, E. A. M. *et al.* Drugs being eliminated via the same pathway will not always require similar pediatric dose adjustments. *CPT Pharmacometrics Syst. Pharmacol.* **7**, 175–185 (2018).
11. Asaumi, R. *et al.* Comprehensive PBPK model of rifampicin for quantitative prediction of complex drug-drug interactions: CYP3A/2C9 induction and OATP inhibition effects. *CPT Pharmacometrics Syst. Pharmacol.* **7**, 186–196 (2018).
12. Yoshikado, T. *et al.* PBPK Modeling of Coproporphyrin I as an Endogenous Biomarker for Drug Interactions Involving Inhibition of Hepatic OATP1B1 and OATP1B3. *CPT Pharmacometrics Syst. Pharmacol.* **7**, 739–747 (2018).
13. Emoto, C. *et al.* PBPK Model of Morphine Incorporating Developmental Changes in Hepatic OCT1 and UGT2B7 Proteins to Explain the Variability in Clearances in Neonates and Small Infants. *CPT Pharmacometrics Syst. Pharmacol.* **7**, 464–473 (2018).
14. Balazki, P., Schaller, S., Eissing, T. & Lehr, T. A Quantitative Systems Pharmacology Kidney Model of Diabetes Associated Renal Hyperfiltration and the Effects of SGLT Inhibitors. *CPT Pharmacometrics Syst. Pharmacol.* **7**, 788–797 (2018).
15. Nakamura, T. *et al.* Application of PBPK Modeling and Virtual Clinical Study Approaches to Predict the Outcomes of CYP2D6 Genotype-Guided Dosing of Tamoxifen. *CPT Pharmacometrics Syst. Pharmacol.* **7**, 474–482 (2018).

16. Mao, J. *et al.* Prediction of the Pharmacokinetics of Pravastatin as an OATP Substrate Using Plateable Human Hepatocytes With Human Plasma Data and PBPK Modeling. *CPT Pharmacometrics Syst. Pharmacol.* **7**, 251–258 (2018).
17. Reddy, V. P., Walker, M., Sharma, P., Ballard, P. & Vishwanathan, K. Development, verification, and prediction of osimertinib drug-drug interactions using PBPK modeling approach to inform drug label. *CPT Pharmacometrics Syst. Pharmacol.* **7**, 321–330 (2018).
18. Jorga, K., Reigner, B., Chavanne, C., Alvaro, G. & Frey, N. Pediatric Dosing of Ganciclovir and Valganciclovir: How Model-Based Simulations Can Prevent Underexposure and Potential Treatment Failure. *CPT Pharmacometrics Syst. Pharmacol.* **8**, 167–176 (2018).
19. Lüpfer, C. *et al.* A Novel PBPK Modeling Approach to Assess Cytochrome P450 Mediated Drug-Drug Interaction Potential of the Cytotoxic Prodrug Evofosfamide. *CPT Pharmacometrics Syst. Pharmacol.* **7**, 829–837 (2018).
20. Gallo, J. M. Modulation of Cell State to Improve Drug Therapy. *CPT Pharmacometrics Syst. Pharmacol.* **7**, 539–542 (2018).

A.2 SUPPORTING INFORMATION PUBLICATION II - A PHYSIOLOGI-  
CALLY BASED PHARMACOKINETIC (PBPK) PARENT-METABOLITE  
MODEL OF THE CHEMOTHERAPEUTIC ZOPTARELIN DOXORUBICIN  
— INTEGRATION OF IN VITRO RESULTS, PHASE I AND PHASE II  
DATA AND MODEL APPLICATION FOR DRUG-DRUG INTERACTION  
POTENTIAL ANALYSIS

**A physiologically-based pharmacokinetic (PBPK) parent-metabolite model of the chemotherapeutic zoptarelin doxorubicin - integration of in vitro results, Phase I and Phase II data and model application for drug-drug interaction potential analysis**

**Metformin Supplementary**

Nina Hanke <sup>1</sup>, Michael Teifel <sup>2</sup>, Daniel Moj <sup>1</sup>, Jan-Georg Wojtyniak <sup>1</sup>, Hannah Britz <sup>1</sup>, Babette Aicher <sup>2</sup>, Herbert Sindermann <sup>2</sup>, Nicola Ammer <sup>2</sup>, Thorsten Lehr <sup>1</sup>

<sup>1</sup> Clinical Pharmacy, Saarland University, Saarbruecken, Germany

<sup>2</sup> Aeterna Zentaris GmbH, Weismuellerstr. 50, Frankfurt, Germany

Corresponding Author: Thorsten Lehr, Clinical Pharmacy, Saarland University, Campus C2 2, 66123 Saarbruecken, +49 681 302 70255, thorsten.lehr@mx.uni-saarland.de



## PBPK model of metformin

### 1. Introduction

The biguanide metformin is the first-line therapeutic agent for the treatment of type 2 diabetes mellitus. Metformin reduces hepatic gluconeogenesis, reduces intestinal absorption of glucose and increases insulin sensitivity and glucose uptake into peripheral tissues [1].

Because of its hydrophilic structure, metformin shows an exceptionally low lipophilicity ( $\log P = -1.43$ ) and is not bound to plasma proteins [2]. Following oral administration, 50 - 60% of a dose are absorbed and peak plasma concentrations are reached within 2 h. The plasma half-life of metformin is 2.5 - 7 h after intravenous infusion and 4 - 8 h following oral administration [3]. Metformin is not subject to hepatic metabolism and mainly renally excreted. After intravenous administration 80 - 100% of the dose are recovered unchanged in the urine; following oral administration the fraction excreted unchanged alternates between 50 and 75%. The observed renal clearance of metformin is much higher than the glomerular filtration rate (GFR), suggesting active renal secretion [2–4]. Metformin is reported to be a substrate of the organic cation transporter (OCT) 1, the kidney specific OCT2 and of OCT3 [5, 6]. These transporters are localized at the basolateral membranes of renal cells, hepatocytes, enterocytes and cells of many other organs. Metformin is also transported by the  $H^+$  organic cation antiporters "multidrug and toxin extrusion protein" (MATE) 1 and MATE2-K [7]. These efflux transporters are primarily expressed in the liver (MATE1) and in the kidney (MATE1, MATE2-K) at the apical (luminal) membranes. In vivo, OCT and MATE transporters form a functional unit to transport organic cations from the blood through hepatocytes and renal tubule cells into the bile and urine, resulting in effective biliary and renal secretion.

### 2. Materials and Methods

#### Software

PBPK modeling was performed with PK-Sim 7.0.0. Parameter optimization was accomplished using the Monte Carlo algorithm implemented in PK-Sim. Digitization of published plasma concentration-time curves was performed with GetData Graph Digitizer (V 2.26). Graphics and further statistical analyses were generated with R (V 3.3.2) using the graphical interface RStudio (V 1.0.136).

#### Model development

For model development, physicochemical parameters as well as individual and mean plasma concentration-time profiles of metformin after intravenous single dose (250 - 1000 mg), oral single dose (250 - 2550 mg) and oral multiple dose (250 - 1000 mg) administration were obtained from literature. Data was separated into training and test datasets for model development and evaluation, respectively (for a detailed study summary see Suppl. Tab. 1). The training dataset contained a study describing the extent of metformin distribution into erythrocytes [8]. Furthermore, fraction excreted to urine data following intravenous (250 and 500 mg) and oral administration (500 mg) of metformin was used in the training dataset to inform the renal secretion process.

For population simulations, a virtual Caucasian population was generated containing 50 male and 50 female individuals, 20 - 50 years of age, with body weights of 40 - 120 kg. The ICRP (International Commission on Radiological Protection) database in PK-Sim was used for generation of this population [9]. For model evaluation, the medians and 90% prediction intervals of population simulation plasma concentration-time profiles were calculated and used to generate visual predictive checks (predicted versus observed plasma concentrations) for the training and test datasets.

### 3. Results

#### Metformin modeling

To limit the number of parameters to be optimized, only the most important processes were implemented into the final metformin model. These are (1) passive distribution into blood cells and the cells of all organs except renal cells, (2) active uptake from blood into renal cells by OCT2 and (3) renal secretion into urine by MATE2-K. Glomerular filtration and enterohepatic cycling were enabled, as these processes are active under physiological conditions.

#### Drug-dependent parameters

All drug-dependent parameters taken from literature with their references as well as all optimized parameter values are given in Suppl. Tab. 2.

#### System-dependent parameters

Expression of the implemented transporters and the geometric standard deviation of their log-normal distribution in virtual populations are given in Suppl. Tab. 3. No other system-dependent parameters were changed or adjusted.

#### Model performance

**Training dataset:** The training dataset performance of the final metformin model, predicting plasma concentrations following intravenous (250 mg and 500 mg) and oral (500 - 1500 mg) administration of metformin, is presented in Suppl. Fig. 1, 3 and 5 - 8.

Predicted compared to observed fraction excreted to urine following intravenous (250 mg and 500 mg) and oral (500 mg) administration is presented in Suppl. Fig. 2 and 4.

Suppl. Fig. 6 shows predicted and observed plasma and erythrocyte concentrations following oral administration of 850 mg metformin.

**Test dataset:** The test dataset performance of the final metformin model, predicting plasma concentrations following intravenous (1000 mg) and oral (250 - 2550 mg) administration of metformin, is presented in Suppl. Fig. 9 - 20.

### 4. Discussion

#### Model performance

Metformin pharmacokinetics show high inter-individual variability in absorption, apparent volume of distribution (654 +/- 358 L) and renal clearance (335 - 615 mL/min) [1, 10]. The slow absorption of metformin rate-limits its disposition [2, 3] so that variability in absorption causes additional variation during the elimination phase of metformin plasma concentration-time profiles. Evaluation of predicted compared to observed clinical data following intravenous application suggests that the current model overpredicts the velocity of distribution into tissues and underpredicts the rate of excretion of metformin (Suppl. Fig. 1, 2, 9). The model accurately describes the plasma and urine concentrations after single oral administration of 500 mg (Suppl. Fig. 3, 4). The 500 mg multiple dose simulations show a good prediction of the trough concentrations with too rapid absorption and an overprediction of  $C_{max}$  (Suppl. Fig. 5, 12, 13). The same phenomenon can be observed for some of the other studies, especially with administration of higher doses of metformin in the fasted state (Suppl. Fig. 14, 16 - 18), but there are also simulations that underpredict  $C_{max}$  (Suppl. Fig. 8, 10, 15), due to the documented inter-individual variability. The model simulations of metformin administration together with food nicely

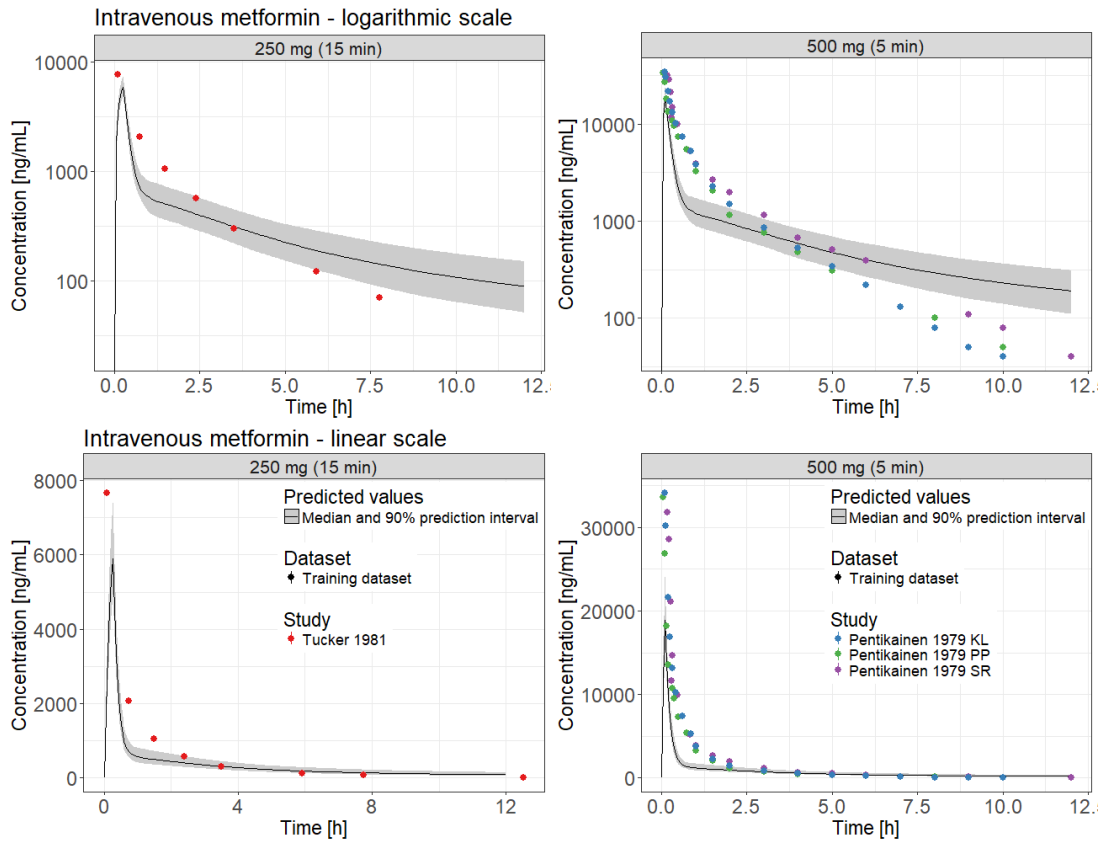
predict the plateau-like shape of the measured plasma concentration-time curves around  $C_{\max}$  (Suppl. Fig. 6, 11). Plasma and erythrocyte concentrations of the study of Robert et al. [8] are also very well described (Suppl. Fig. 6).

#### **Model limitations**

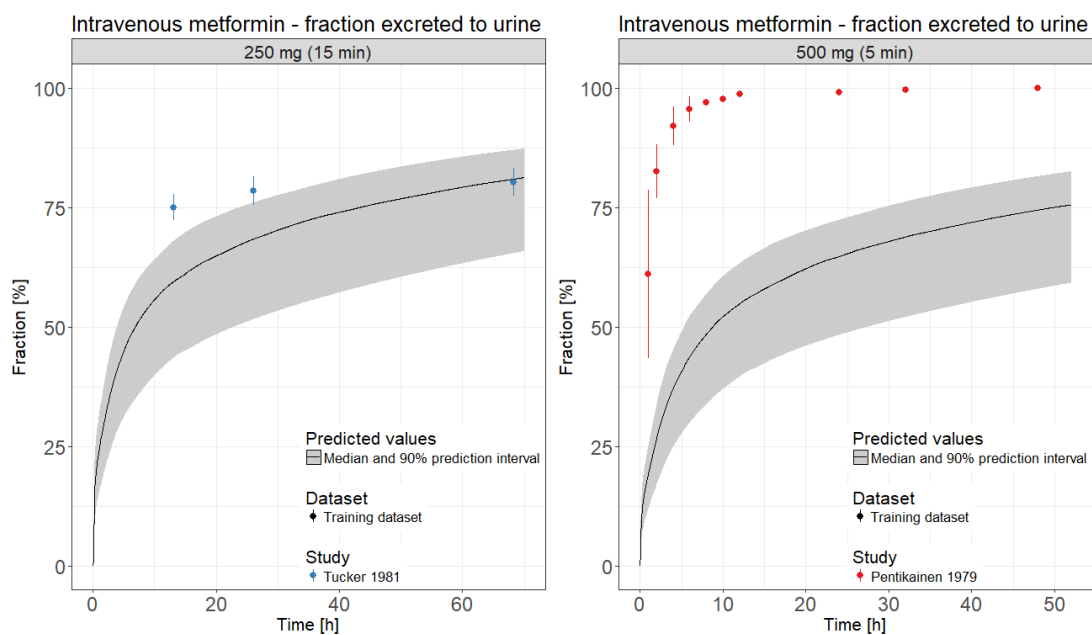
Metformin is recommended by the FDA as OCT2/MATE transport victim drug for the use in clinical DDI studies [11]. The purpose of the presented metformin PBPK model is to accurately incorporate these processes so that this model is fit to be coupled to models of OCT2 and MATE2-K perpetrator drugs and applied for DDI prediction.

Metformin is positively charged at physiological pH ( $pK_a = 11.5$  (base)) and highly hydrophilic ( $\log P = -1.43$ ). Therefore, passive diffusion of metformin through lipid bilayers is very slow. Nevertheless, distribution and accumulation into red blood cells has been described, with a much longer elimination half-life from erythrocytes (23 h), than from plasma (3 h) [8]. Furthermore, the apparent volume of distribution of metformin is high, in spite of its exceptionally low lipophilicity. The mechanism of this partitioning into red blood cells is currently not understood. Transport in combination with target-binding, binding to other intracellular components, some kind of trapping within organelles or sticking to the cellular membranes of red blood cells are possible explanations. As the mechanism of this accumulation is unclear, an asymmetric permeability from plasma into red blood cells was incorporated. The wide distribution into body tissues is most probably mediated by active transport processes and was modeled by an overall asymmetric permeability from the interstitial space into the cells of all organs except kidney, as so far, only the kidney specific isoforms of OCT and MATE transporters have been incorporated into this model.

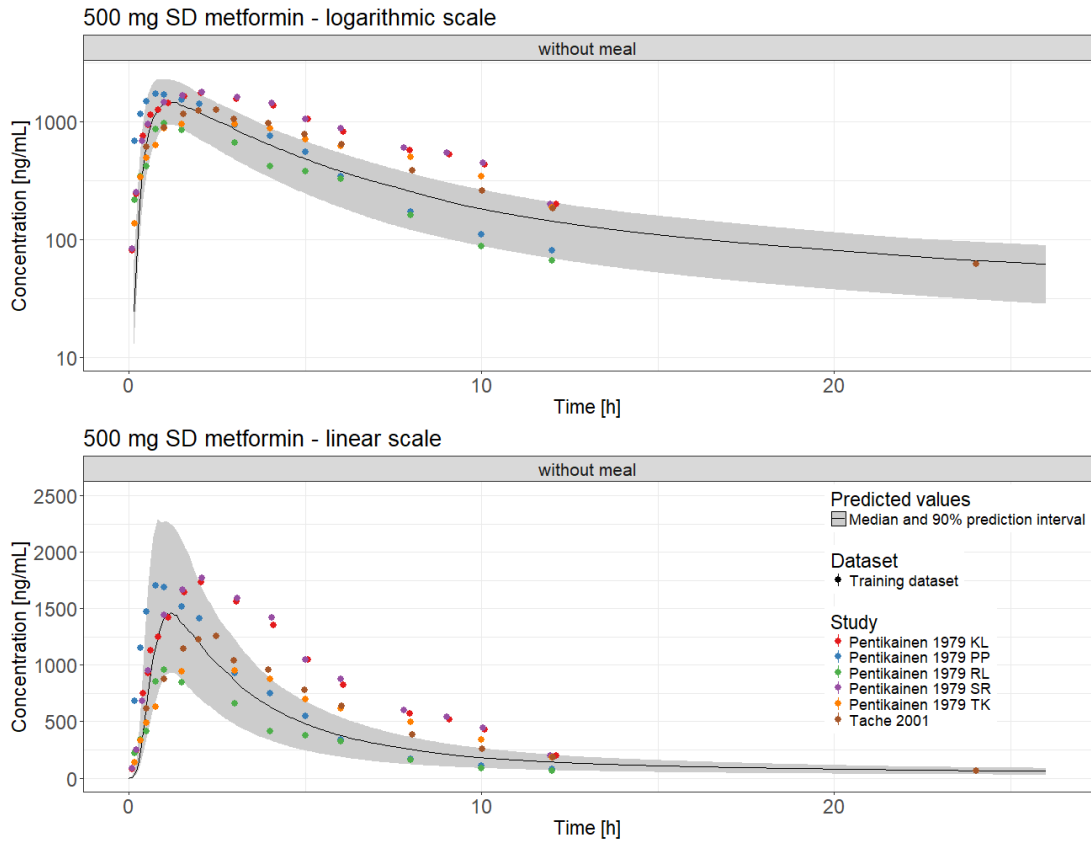
To define the contribution of the two implemented transport processes by OCT2 and MATE2-K, fraction excreted to urine data after intravenous and oral administration of metformin have been included into the training dataset. In addition to an accurate description of unchanged drug recovered in urine, evaluation of this model with measured metformin concentrations in the kidney and by prediction of OCT2 and MATE2-K mediated DDIs is needed.



**Suppl. Fig. 1** Training dataset: Population simulations compared to observed data of metformin plasma concentrations following intravenous administration of 250 mg (left panel) and 500 mg (right panel). Clinical data are shown as dots (Pentikainen KL, PP and SR are individual data) [2, 3]. Population simulation medians are shown as lines; the shaded areas depict the 5<sup>th</sup> - 95<sup>th</sup> percentile population prediction intervals



**Suppl. Fig. 2** Training dataset: Population simulations compared to observed data of metformin fraction excreted to urine following intravenous administration of 250 mg (left panel) and 500 mg (right panel). Clinical data are shown as dots (+/- standard deviation) [2, 3]. Population simulation medians are shown as lines; the shaded areas depict the 5<sup>th</sup> - 95<sup>th</sup> percentile population prediction intervals



**Suppl. Fig. 3** Training dataset: Population simulations compared to observed data of metformin plasma concentrations following single oral administration of 500 mg. Clinical data are shown as dots (Pentikainen KL, PP, RL, SR and TK are individual data) [2, 12]. Population simulation medians are shown as lines; the shaded areas depict the 5<sup>th</sup> - 95<sup>th</sup> percentile population prediction intervals

**A physiologically-based pharmacokinetic (PBPK) parent-metabolite model of the chemotherapeutic zoptarelin doxorubicin - integration of in vitro results, Phase I and Phase II data and model application for drug-drug interaction potential analysis**

**Simvastatin Supplementary**

Nina Hanke <sup>1</sup>, Michael Teifel <sup>2</sup>, Daniel Moj <sup>1</sup>, Jan-Georg Wojtyniak <sup>1</sup>, Hannah Britz <sup>1</sup>, Babette Aicher <sup>2</sup>, Herbert Sindermann <sup>2</sup>, Nicola Ammer <sup>2</sup>, Thorsten Lehr <sup>1</sup>

<sup>1</sup> Clinical Pharmacy, Saarland University, Saarbruecken, Germany

<sup>2</sup> Aeterna Zentaris GmbH, Weismuellerstr. 50, Frankfurt, Germany

Corresponding Author: Thorsten Lehr, Clinical Pharmacy, Saarland University, Campus C2 2, 66123 Saarbruecken, +49 681 302 70255, thorsten.lehr@mx.uni-saarland.de

## PBPK model of simvastatin lactone and simvastatin acid

### 1. Introduction

Simvastatin is a 3-hydroxy-3-methylglutaryl (HMG) coenzyme A reductase inhibitor. It is widely used in the treatment of hypercholesterolemia and belongs to the ten most prescribed drugs in industrial nations [1]. Simvastatin is administered orally as a prodrug in its lactone form (dosing range 5 - 80 mg/day [2]) and is converted to the active acid by a combination of enzyme-mediated hydrolysis and spontaneous chemical conversion [3]. The enzyme predominantly responsible for the hydrolysis of simvastatin lactone to simvastatin acid is paraoxonase 3 (PON3) [4, 5]. Simvastatin lactone is highly lipophilic, resulting in good absorption of approximately 60% of an administered dose, but shows extensive first pass metabolism reducing its oral bioavailability to 5% [3]. Simvastatin lactone is mainly metabolized by CYP3A4 [6], while simvastatin acid is metabolized by CYP3A4 (>80%) and CYP2C8 (<20%) as well as transported by organic anion-transporting polypeptide 1B (OATP1B) [7]. A further process discussed for the pharmacokinetics of simvastatin acid is recyclization to the lactone form, either spontaneously, or via enzymatic formation of an intermediate glucuronide. Suppl. Fig. 1 depicts the metabolization pathways of statins in general.

### Objectives

The purpose of this work was to establish a whole body parent-metabolite PBPK model of simvastatin lactone (prodrug) and acid (pharmacologically active metabolite) as a CYP3A and OATP1B victim drug model for drug-drug interaction studies

- that accurately predicts plasma concentrations of simvastatin lactone and acid over a broad dosing range
- that has been evaluated by showing good prediction of simvastatin lactone and acid plasma concentrations in drug-drug interaction (DDI) studies with rifampicin and clarithromycin as CYP3A4 perpetrator drugs
- that has been evaluated by showing good prediction of simvastatin lactone and acid plasma concentrations in individuals with different OATP1B1 genotypes

### 2. Materials and Methods

#### Software

PBPK modeling was performed with PK-Sim 7.0.0. Parameter optimization was accomplished using the Monte Carlo algorithm implemented in PK-Sim. Digitization of published plasma concentration-time curves was performed with GetData Graph Digitizer (V 2.26). Graphics and further statistical analyses were generated with R (V 3.3.2) and the graphical user interface RStudio (V 1.0.136).

#### Model development

For model development, physicochemical parameters as well as plasma concentration-time profiles of simvastatin lactone and simvastatin acid after oral single dose (SD) and multiple dose (MD) administration (range 20 - 80 mg) were obtained from the literature. Data was separated into training and test datasets for model development and evaluation, respectively (for a detailed study summary see Suppl. Tab. 1). The training dataset contained a study showing the impact of different OATP1B1 genotypes on the plasma concentrations of simvastatin acid [8]. This study was included to define the contribution of this transporter to simvastatin acid pharmacokinetics. For studies that did not specify



the OATP1B1 genotype, the wild type variant was assumed. Due to the lack of clinical trials of direct administration of simvastatin acid, simvastatin lactone and simvastatin acid model development was performed in parallel.

For population simulations, a virtual Caucasian population was generated containing 50 male and 50 female individuals, 20 - 50 years of age, with body weights of 40 - 120 kg. The ICRP (International Commission on Radiological Protection) database in PK-Sim was used for generation of this population [13]. For model evaluation, the arithmetic means and 90% prediction intervals of population simulation plasma concentration-time profiles were calculated and used to generate visual predictive checks (predicted versus observed plasma concentrations) for the training and test datasets.

To test the contribution of the implemented CYP3A4 metabolism, the final simvastatin model was coupled to PBPK models of the CYP3A4 perpetrators rifampicin (CYP3A4 inducer, [9]) and clarithromycin (CYP3A4 inhibitor, [10]). Plasma concentrations of simvastatin lactone and simvastatin acid during co-administration with these perpetrator drugs were predicted and compared to observed data.

### 3. Results

#### Simvastatin modeling

To limit the number of parameters to be optimized, only the most important processes were implemented into the final simvastatin parent-metabolite model. For simvastatin lactone these are (1) PON3 mediated hydrolysis to generate simvastatin acid and (2) CYP3A4 mediated clearance. For simvastatin acid these are (3) hepatic uptake by OATP1B1 and (4) CYP3A4 mediated clearance. The OATP1B1 transport was implemented with two different  $K_M$  values and two different transport rates, to describe the impact of the investigated OATP1B1 polymorphism on simvastatin acid plasma concentrations. For both, parent and metabolite, glomerular filtration and enterohepatic cycling were enabled.

#### Drug-dependent parameters

All drug-dependent parameters taken from the literature with their references as well as all optimized parameter values are given in Suppl. Tab. 2.

#### System-dependent parameters

Expression of the implemented enzymes and transporters as well as the geometric standard deviation of their log-normal distribution in virtual populations are given in Suppl. Tab. 3. No other system-dependent parameters were changed or adjusted.

#### Model performance

**Training dataset:** The training dataset performance of the final model, predicting simvastatin lactone and simvastatin acid plasma concentrations following oral administration of 20, 40, 60 or 80 mg simvastatin lactone, is presented in Suppl. Fig. 2 - 6.

Suppl. Fig. 7 shows the predicted compared to observed plasma concentrations following oral administration of 40 mg simvastatin lactone to individuals with different OATP1B1 genotypes [8]. The transport rates of the two homozygous OATP1B1 isoforms (c.521TT wild type and c.521CC) were optimized, the transport rate of the heterozygous isoform (c.521TC) has been predicted.

**Test dataset:** The test dataset performance of the final model, predicting simvastatin lactone and simvastatin acid plasma concentrations following oral administration of 20, 40 or 80 mg simvastatin lactone, is presented in Suppl. Fig. 8 - 10.

### Model application

As a further means of model evaluation, the final simvastatin model was applied to predict clinical DDI studies. Simvastatin plasma concentrations during two different trials studying co-administration of simvastatin lactone and the CYP3A4 perpetrator drugs rifampicin [11] and clarithromycin [12] were predicted and compared to observed data.

In the rifampicin DDI study, a single dose of 40 mg simvastatin lactone was administered 17 h after the last dose of a 600 mg QD, 5 day rifampicin regimen. Thus, no inhibitory effects of rifampicin on CYP3A4 or OATP1B1 are expected, solely pure CYP3A4 induction. In the clarithromycin DDI study, once daily doses of 40 mg simvastatin lactone were administered together with the morning doses of a 500 mg BID, 7 day clarithromycin regimen. Unfortunately, only simvastatin lactone plasma concentrations have been reported from this study, allowing no interpretation of the effect of clarithromycin on OATP1B1 and simvastatin acid. Predicted and observed plasma concentrations are shown in shown in Suppl. Fig. 11 and 12. Predicted and observed AUC ratios (AUC during perpetrator treatment / AUC without co-administration of DDI perpetrator) of these DDIs are compared in Suppl. Tab. 4 and 5.

## 4. Discussion

### Model performance

The final parent-metabolite PBPK model accurately describes the plasma concentration-time profiles of simvastatin lactone and simvastatin acid after oral administration of 20 - 80 mg simvastatin lactone. There is a slight terminal overprediction of the lactone, but not of the acid concentrations, following single dose administration of 40 mg simvastatin lactone. Nevertheless, the studies of multiple dose administration of 40 mg simvastatin lactone are well predicted. This phenomenon might be caused by variability in body weight or genetic polymorphisms of involved metabolizing enzymes or transporters of these relatively small study populations that have not been taken into account for the model predictions.

To define the contribution of OATP1B1 to the disposition of simvastatin acid, information of a clinical trial studying the impact of the OATP1B1 c.521 polymorphism on simvastatin acid pharmacokinetics has been included into the training dataset. The final simvastatin model accurately predicts the simvastatin acid plasma concentrations of individuals of the three possible OATP1B1 genotypes.

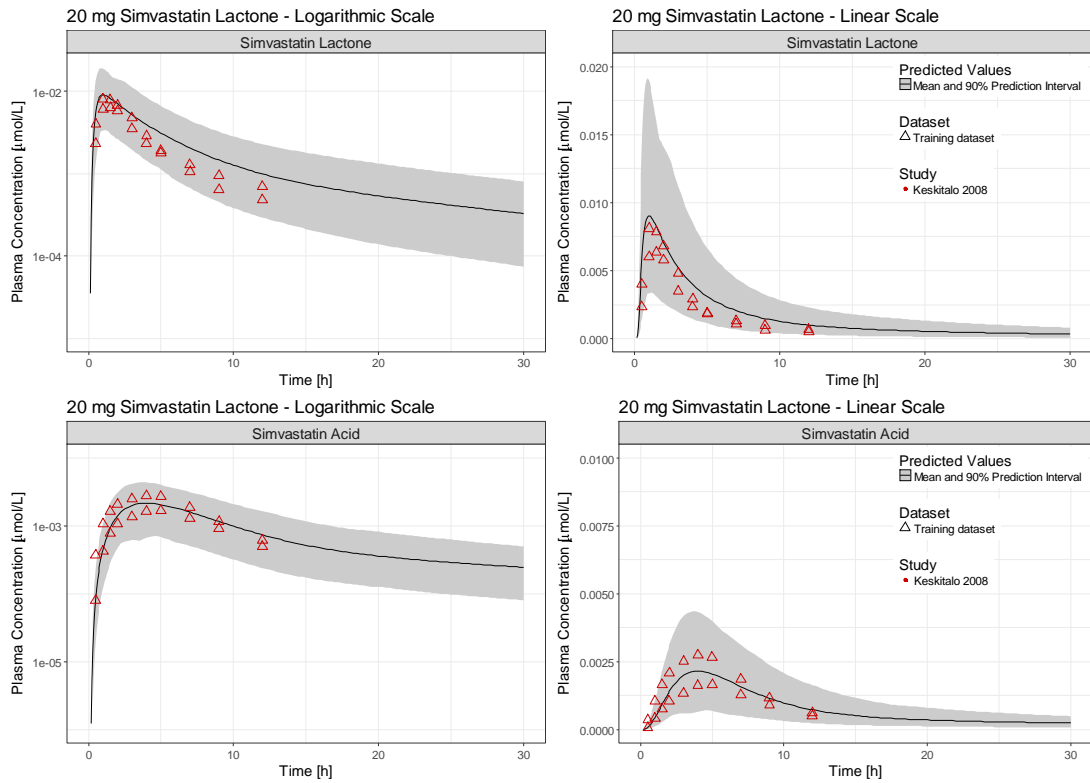
To evaluate the contribution of CYP3A4 to the metabolism of simvastatin lactone and simvastatin acid, clinical DDI studies with the CYP3A4 perpetrators rifampicin and clarithromycin have been predicted and compared to observed data. During the DDI with rifampicin, simvastatin lactone and simvastatin acid plasma concentrations are adequately predicted. In the DDI study with clarithromycin only simvastatin lactone concentrations have been reported and the effect of clarithromycin on simvastatin lactone peak plasma concentrations is underpredicted. Nevertheless, the predicted AUC ratios of simvastatin lactone and simvastatin acid are within twofold of the observed AUC ratios for both of the tested DDIs (see Suppl. Tab. 4 and 5).

### Model limitations

Simvastatin is listed by the FDA as a sensitive CYP3A substrate for the use in clinical DDI studies, and simvastatin acid is an approved OATP1B victim drug [13]. The purpose of the presented simvastatin PBPK model is to accurately incorporate these processes so that this model is fit to be coupled to models of CYP3A and OATP1B perpetrator drugs and applied for DDI prediction.

Mechanisms not implemented into the final simvastatin model include transport by breast cancer resistance protein (BCRP) or p-glycoprotein (P-gp). Genetic polymorphism in the ABCG2 gene encoding for BCRP has been described to influence the plasma concentrations of simvastatin lactone [14], while genetic polymorphisms in ABCB1 (P-gp) have been described to affect the plasma concentrations of simvastatin acid [15]. Implementation of these transport processes would further diminish the contribution of CYP3A4 and was therefore not retained in the final model. Another possible mechanism involved in simvastatin pharmacokinetics is reabsorption (enterohepatic cycling) following BCRP-mediated transport of simvastatin lactone into the bile, or following P-gp-mediated transport of simvastatin acid into bile with subsequent recyclization to the lactone. Information on the pharmacokinetics of simvastatin lactone and acid after intravenous administration, on bioavailability and on enterohepatic cycling would greatly help to improve our current understanding of the mechanisms affecting the plasma concentrations and DDI behaviour of this widely used lipid-lowering drug.





**Suppl. Fig. 2** Training dataset: Population simulations compared to observed data of simvastatin lactone (upper panel) and simvastatin acid (lower panel) plasma concentrations following single oral administration of 20 mg simvastatin lactone. Clinical data [15] are shown as triangles. Population simulation means are shown as lines; the shaded areas depict the 5<sup>th</sup> - 95<sup>th</sup> percentile population prediction intervals

**A physiologically-based pharmacokinetic (PBPK) parent-metabolite model of the chemotherapeutic zoptarelin doxorubicin - integration of in vitro results, Phase I and Phase II data and model application for drug-drug interaction potential analysis**

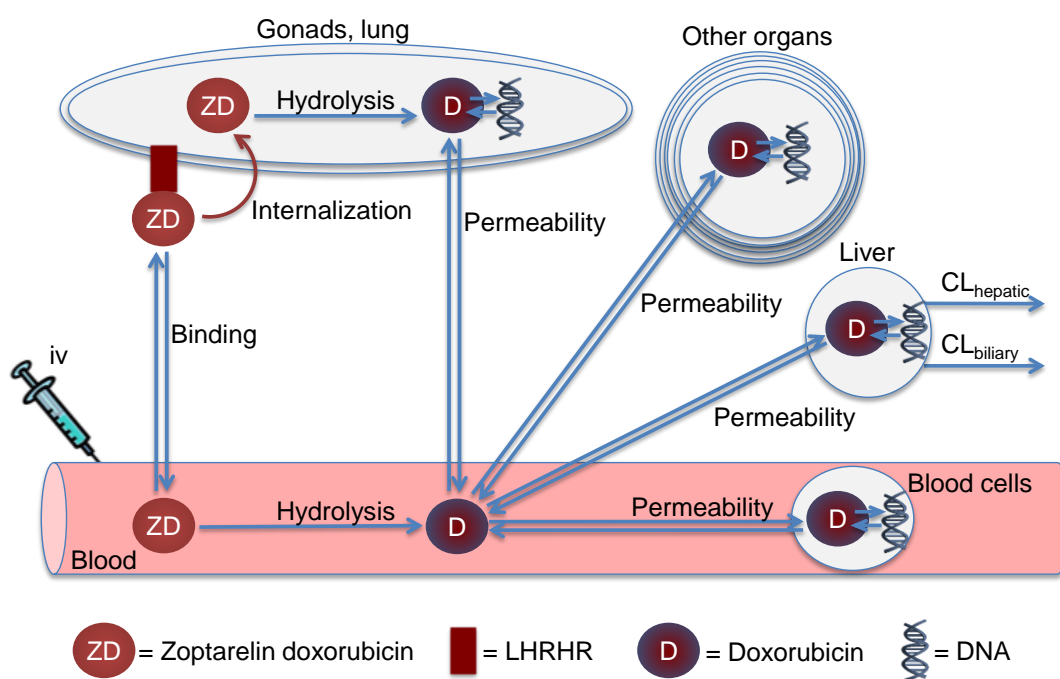
**Zoptarelin Doxorubicin Supplementary**

Nina Hanke <sup>1</sup>, Michael Teifel <sup>2</sup>, Daniel Moj <sup>1</sup>, Jan-Georg Wojtyniak <sup>1</sup>, Hannah Britz <sup>1</sup>, Babette Aicher <sup>2</sup>, Herbert Sindermann <sup>2</sup>, Nicola Ammer <sup>2</sup>, Thorsten Lehr <sup>1</sup>

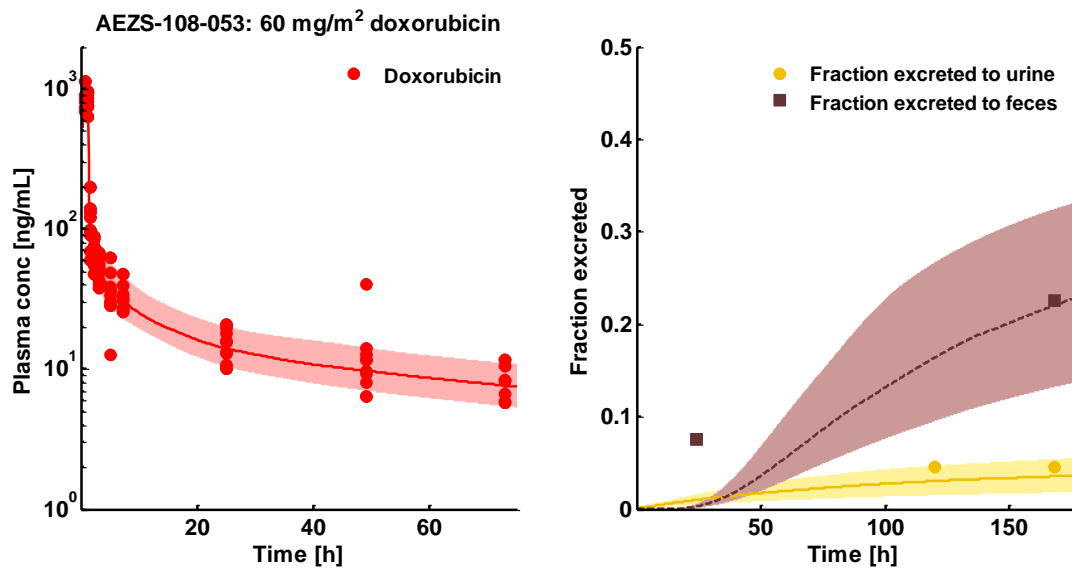
<sup>1</sup> Clinical Pharmacy, Saarland University, Saarbruecken, Germany

<sup>2</sup> Aeterna Zentaris GmbH, Weismuellerstr. 50, Frankfurt, Germany

Corresponding Author: Thorsten Lehr, Clinical Pharmacy, Saarland University, Campus C2 2, 66123 Saarbruecken, +49 681 302 70255, thorsten.lehr@mx.uni-saarland.de

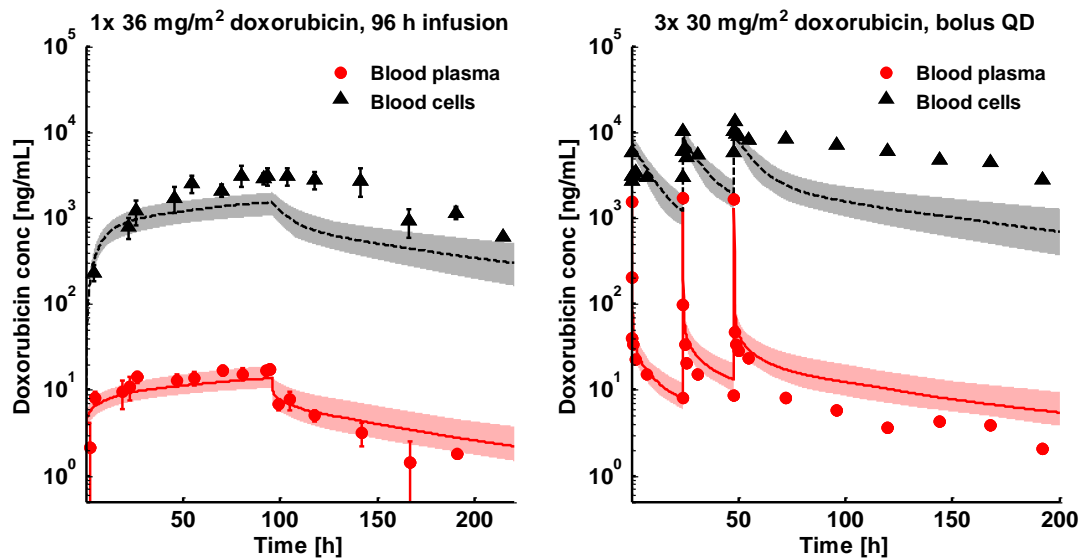


**Suppl. Fig. 1** Zoptarelin doxorubicin parent-metabolite PBPK model structure.  $CL_{biliary}$ : biliary plasma clearance,  $CL_{hepatic}$ : hepatic metabolic plasma clearance, iv: intravenous administration, LHRHR: luteinizing hormone-releasing hormone receptor

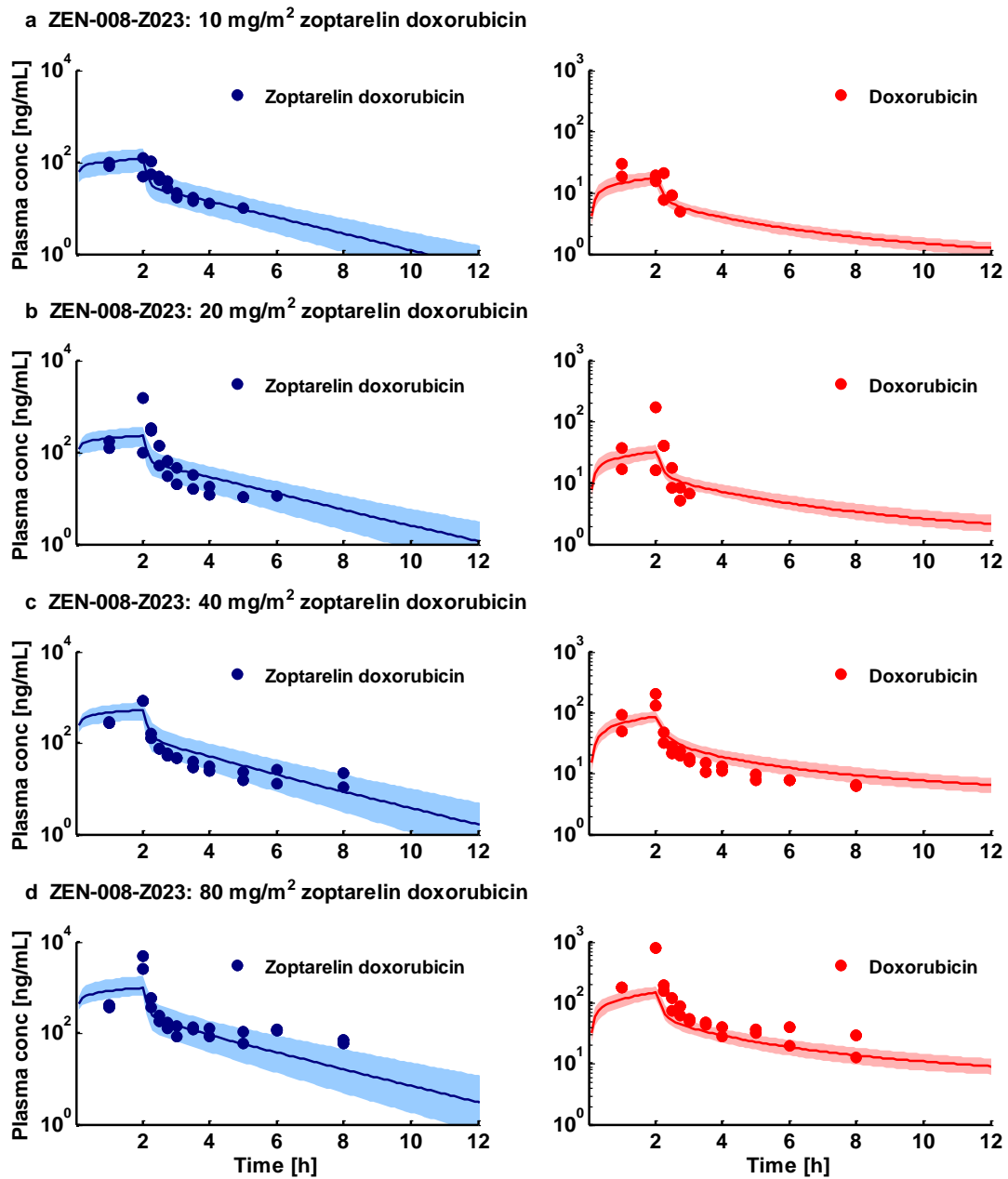


**Suppl. Fig. 2** Training dataset: Population simulations compared to observed data of doxorubicin plasma concentrations (red, semilog scale) and fractions excreted to urine and feces (yellow and brown, linear scale) following intravenous administration of 60 mg/m<sup>2</sup> doxorubicin. Clinical data (Study 3, doxorubicin arm, n = 9 and [1]) are shown as dots and squares. Population simulation medians are shown as lines or dashed lines; the shaded areas depict the 5<sup>th</sup> - 95<sup>th</sup> percentile population prediction intervals

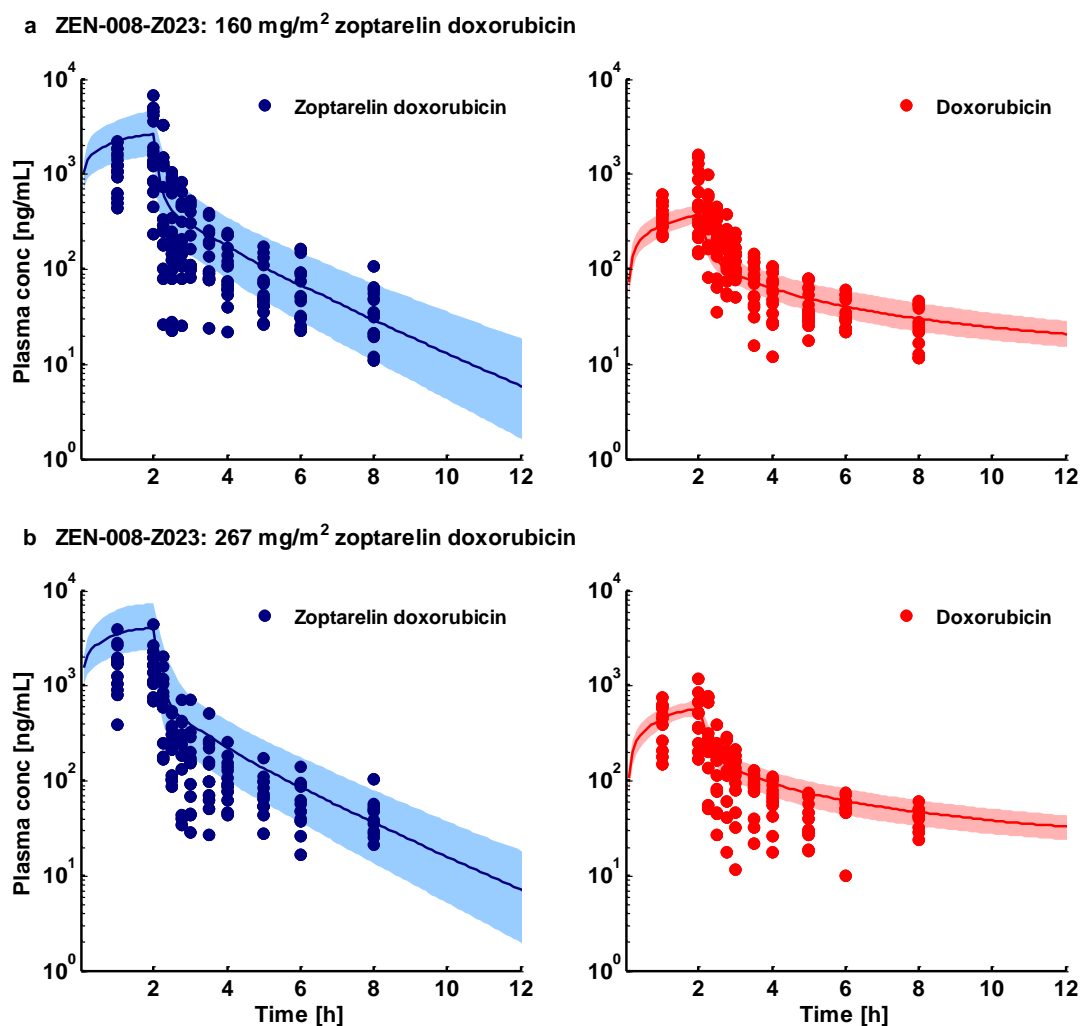




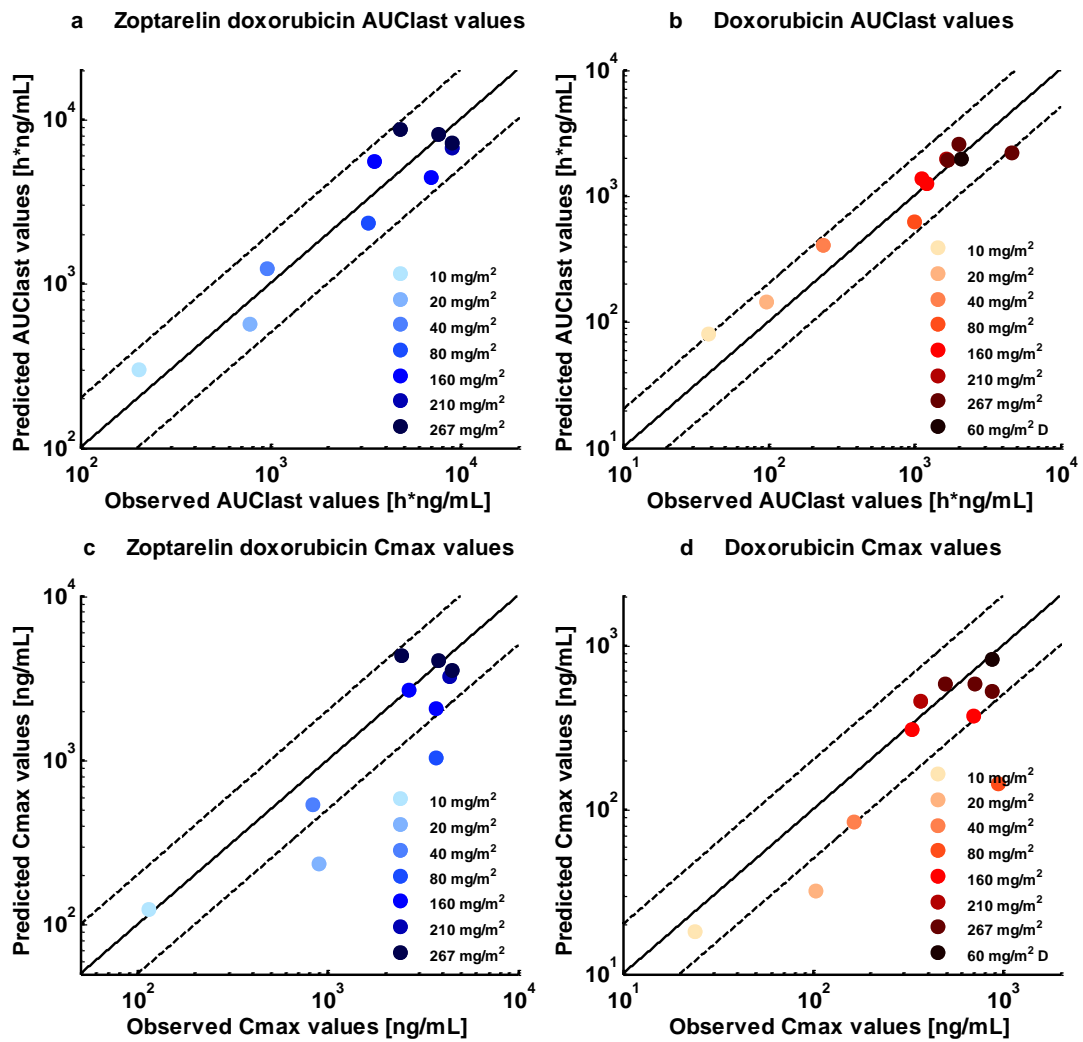
**Suppl. Fig. 3** Training dataset: Population simulations (semilog scale) compared to observed data of doxorubicin concentrations in blood plasma (red) and in nucleated blood cells (black) following intravenous administration of 1x 36 mg/m<sup>2</sup> doxorubicin as 96 h long-term infusion (left) or 3x 30 mg/m<sup>2</sup> doxorubicin as daily bolus infusions (right). Simulated blood cell concentrations represent free plus DNA-bound doxorubicin in the blood cell compartment. Clinical data ([2], n = 7 and [3], n = 7) are shown as dots and triangles ( $\pm$  SD values). Population simulation medians are shown as lines or dashed lines; the shaded areas depict the 5<sup>th</sup> - 95<sup>th</sup> percentile population prediction intervals



**Suppl. Fig. 4** Training dataset: Population simulations (semilog scale) compared to observed data of zoptarelin doxorubicin (blue) and doxorubicin plasma concentrations (red) following intravenous administration of 10, 20, 40 or 80 mg/m<sup>2</sup> (a, b, c, d) zoptarelin doxorubicin. Clinical data (Study 1, n = 1 for each dose, 2 cycles per patient, one dose every 3 weeks) are shown as dots. Population simulation medians are shown as lines; the shaded areas depict the 5<sup>th</sup> - 95<sup>th</sup> percentile population prediction intervals



**Suppl. Fig. 5** Test dataset: Population simulations (semilog scale) compared to observed data of zoptarelin doxorubicin (blue) and doxorubicin plasma concentrations (red) following intravenous administration of 160 or 267 mg/m<sup>2</sup> (a, b) zoptarelin doxorubicin. Clinical data (Study 1, n = 6 and n = 5, multiple cycles per patient, one dose every 3 weeks) are shown as dots. Population simulation medians are shown as lines; the shaded areas depict the 5<sup>th</sup> - 95<sup>th</sup> percentile population prediction intervals



**Suppl. Fig. 6** Model performance: Mean  $AUC_{last}$  (a, b) and  $C_{max}$  (c, d) values of population predictions compared to observed data (log scale) of zoptarelin doxorubicin (blue) and doxorubicin (red) plasma concentrations following intravenous administration of 10 to 267  $mg/m^2$  zoptarelin doxorubicin or of 60  $mg/m^2$  doxorubicin. Each dot represents a dosing group of one clinical study. Number of patients per dosing group and further details are listed in Zoptarelin Doxorubicin Supplementary Tables 1 and 2. The solid line marks the line of identity, the dashed lines show the 0.5 to 2.0-fold prediction success limits.  $AUC_{last}$ : area under the plasma concentration-time curve from time 0 to the last measurement,  $C_{max}$ : peak plasma concentration, D: intravenous administration of doxorubicin

A.3 SUPPORTING INFORMATION PUBLICATION III - PHYSIOLOGICALLY  
BASED PRECISION DOSING APPROACH FOR DRUG-DRUG-GENE  
INTERACTIONS: A SIMVASTATIN NETWORK ANALYSIS

Clinical Pharmacology & Therapeutics

## Physiologically Based Precision Dosing Approach for Drug-Drug-Gene Interactions: A Simvastatin Network Analysis

### Electronic Supplementary Material (ESM)

Jan-Georg Wojtyniak<sup>1,2</sup> (ORCID: 0000-0003-1304-9033), Dominik Selzer<sup>1</sup>, Matthias Schwab<sup>2,3,4</sup>, Thorsten Lehr<sup>1</sup> (ORCID: 0000-0002-8372-1465)

<sup>1</sup>Clinical Pharmacy, Saarland University, Saarbrücken, Germany

<sup>2</sup>Dr. Margarete Fischer-Bosch-Institute of Clinical Pharmacology, Stuttgart, Germany

<sup>3</sup>Departments of Clinical Pharmacology and Pharmacy and Biochemistry, University of Tübingen, Tübingen, Germany

<sup>4</sup>Cluster of Excellence iFIT (EXC2180) "Image-guided and Functionally Instructed Tumor Therapies", University of Tübingen, Tübingen, Germany

#### Corresponding Author:

Thorsten Lehr  
Saarland University  
Campus C2 2  
66123 Saarbrücken  
Germany  
Tel: +49/681/302-70255  
Fax: +49/681/302-70258  
Email: thorsten.lehr@mx.uni-saarland.de

**Conflict of Interest** The authors declare that they have no conflict of interest.

**Funding** This work was funded by the Robert Bosch Stiftung (Stuttgart, Germany), the European Commission Horizon 2020 UPGx grant 668353, a grant from the German Federal Ministry of Education and Research (BMBF 031L0188D), and the Deutsche Forschungsgemeinschaft (DFG, German Research Foundation) under Germany's Excellence Strategy—EXC 2180—390900677.

# Contents

<b>1</b>	<b>General information</b>	<b>1</b>
1.1	Mathematical implementation of DDIs and DGIs . . . . .	1
1.1.1	DDIs . . . . .	1
1.1.2	DGIs . . . . .	1
1.2	Network relevant metabolic enzymes and transporters . . . . .	2
1.3	Model development and system-dependent specifications . . . . .	8
1.3.1	General modeling workflow . . . . .	8
1.3.2	System-dependent parameters . . . . .	8
1.4	Model evaluation . . . . .	11
1.4.1	Statistical model evaluation . . . . .	11
1.4.2	Graphical model evaluation . . . . .	13
1.4.3	Local sensitivity analysis . . . . .	13
1.5	Virtual populations . . . . .	14
<b>2</b>	<b>PBPK modeling of simvastatin</b>	<b>15</b>
2.1	Introduction . . . . .	15
2.1.1	Included processes . . . . .	15
2.1.2	Excluded processes . . . . .	16
2.2	Simvastatin model development . . . . .	17
2.2.1	Clinical studies . . . . .	17
2.2.2	Drug-dependent parameters . . . . .	25
2.3	Simvastatin model evaluation . . . . .	40
2.3.1	Profiles . . . . .	40
2.3.2	Predicted concentrations versus observed concentrations GOF plots . . . . .	64
2.3.3	NCA GOF plots . . . . .	66
2.3.4	MRD and MSA of plasma concentration predictions . . . . .	70
2.3.5	NCA ratios and GMFE of NCA values . . . . .	70
2.3.6	Local sensitivity analysis . . . . .	70
2.4	Simvastatin DGIs . . . . .	71
2.4.1	OATP1B1 (SLCO1B1) . . . . .	71
2.4.2	BCRP (ABCG2) . . . . .	74
2.4.3	P-gp (ABCB1) . . . . .	76
2.4.4	CYP3A5 (CYP3A5 gene) . . . . .	78
2.4.5	MRD and MSA of plasma concentration predictions . . . . .	79
2.4.6	NCA ratios and GMFE of NCA values . . . . .	79

---

 Contents
 

---

<b>3</b>	<b>Simvastatin DDIs</b>	<b>80</b>
3.1	Clinical studies . . . . .	80
3.2	Clarithromycin . . . . .	82
3.2.1	Drug-dependent parameters . . . . .	82
3.2.2	Profiles . . . . .	87
3.3	Rifampicin . . . . .	89
3.3.1	Drug-dependent parameters . . . . .	89
3.3.2	Profiles . . . . .	99
3.4	Itraconazole . . . . .	105
3.4.1	Drug-dependent parameters . . . . .	105
3.5	Gemfibrozil . . . . .	120
3.5.1	Drug-dependent parameters . . . . .	120
3.5.2	Profiles . . . . .	129
3.6	Midazolam . . . . .	133
3.6.1	Drug-dependent parameters . . . . .	133
3.6.2	Profiles . . . . .	136
3.7	DDI evaluation . . . . .	137
3.7.1	Predicted concentrations versus observed concentrations GOF plots .	137
3.7.2	NCA GOF plots . . . . .	138
3.7.3	MRD and MSA of plasma concentration predictions . . . . .	140
3.7.4	NCA ratios and GMFE of NCA values . . . . .	140
<b>4</b>	<b>Drug-drug-gene interaction network</b>	<b>141</b>
4.1	Effect ratios . . . . .	142
	<b>Bibliography</b>	<b>147</b>



# 1 General information

This chapter provides short introduction about all processes and mechanisms relevant for the simvastatin physiologically based pharmacokinetic (PBPK) drug-drug-gene interaction (DDGI) network model. In addition, it provides general information regarding the system-dependent parameters, which were the same for all model simulations to ensure a comparable model environment. Moreover, this chapter describes the methods used for model development as well as for model evaluation.

## 1.1 Mathematical implementation of DDIs and DGIs

### 1.1.1 DDIs

Required equations for the mathematical implementation of drug-drug interactions (DDIs) are predefined in the Open Systems Pharmacology Suite (OSPS) [1]. For a detailed description the reader is kindly referred to the OSP OPS documentation [1].

### 1.1.2 DGIs

Genetic polymorphisms in drug relevant target structures, metabolic enzymes or transporters can affect the pharmacokinetic (PK) or pharmacodynamic (PD) of an active compound [2]. For example, a different genotype might lead to changed metabolic activity of the phenotype and hence, result in poor, intermediate, extensive or ultra rapid metabolic activity states [2]. The main cause for genetic polymorphisms are single nucleotide polymorphisms (SNPs) [3].

For all drug-gene interactions (DGIs) implemented a change in the transporter or enzyme  $k_{\text{cat}}$  was assumed compared to wildtype. Although, also a change in  $K_M$  would be conceivable for the polymorphisms included in this network, no evidence for this mechanism could be found in literature. Besides, DGIs were implemented in a stepwise procedure. First, the homozygous wildtype  $k_{\text{cat}}$  as well as  $k_{\text{cat}}$  for homozygous polymorphic individuals were estimated. Afterwards, the implementation was evaluated using heterozygous individuals. For this purpose the  $k_{\text{cat}}$  for individuals with heterozygous genotypes were estimated according

## 1 General information

to Eq. (S1.1) assuming an additive relationship between the wildtype and the deficient pharmacogene. Besides, for all studies where no information about the genotype was provided, homozygous wildtype genotypes were assumed.

Equation : Drug-gene interaction enzyme / transporter activity for heterozygous individuals

$$k_{cat,heterozygous} = 0.5 * k_{cat,wildtype} + 0.5 * k_{cat,deficient} \quad (S1.1)$$

$k_{cat,heterozygous}$	=	heterozygous catalytic rate constant number
$k_{cat,wildtype}$	=	wildtype catalytic rate constant number
$k_{cat,deficient}$	=	homozygous deficient catalytic rate constant number

## 1.2 Network relevant metabolic enzymes and transporters

This chapter introduces network relevant metabolic enzymes and transporters. Table S1.1 lists the compounds included in the model network and their relationship as substrates, inhibitors or inducers with regard to the metabolic enzymes and transporters. Figures S1.1, S1.2, S1.3 visualize the relationships.

Table S1.1: Substrates, inhibitors and inducers used in the presented model network

	Enzyme	Substrate	Inhibitor	Inducer
<b>Process</b>	Chemical hydrolysis (simvastatin lactone)	Simvastatin Lactone	-	-
	<b>Metabolic enzyme</b>			
	AADAC	Rifampicin	-	Rifampicin
	CYP2C8	Simvastatin Acid	Simvastatin Acid	-
		-	Gemfibrozil	-
		-	Gemfibrozil glucuronide	-
		-	Rifampicin	Rifampicin
	CYP3A4	Simvastatin Lactone	Simvastatin Lactone	-
		Simvastatin Acid	Simvastatin Acid	-
		N-desalkyl-itraconazole	N-desalkyl-itraconazole	-
		Midazolam	-	-
		Keto-itraconazole	Keto-itraconazole	-
		Itraconazole	Itraconazole	-

## 1 General information

Table S1.1: Substrates, inhibitors and inducers used in the presented model network (*continued*)

Type	Enzyme	Substrate	Inhibitor	Inducer
		Hydroxy-itraconazole	Hydroxy-itraconazole	-
		Clarithromycin	Clarithromycin	-
		-	Rifampicin	Rifampicin
	CYP3A5	Simvastatin Lactone	-	-
	PON3	Simvastatin Lactone	-	-
		-	-	Rifampicin
		-	-	Gemfibrozil
		-	-	Gemfibrozil glucuronide
	UGT1A1	Simvastatin Acid	-	-
		-	Gemfibrozil	-
		-	Rifampicin	Rifampicin
		-	Gemfibrozil glucuronide	-
	UGT1A3	Simvastatin Acid	-	-
		-	Gemfibrozil	-
		-	Rifampicin	Rifampicin
	UGT2B7	Gemfibrozil	-	-
	Unspecific liver lactonization (simvastatin acid)	Simvastatin Acid	-	-
	Unspecific plasma hydrolysis (simvastatin lactone)	Simvastatin Lactone	-	-
<b>Influx transporter</b>				
	OATP1B1 (SLCO1B1)	Simvastatin Acid	Simvastatin Acid	-
		-	Clarithromycin	-
		-	Rifampicin	Rifampicin
		-	Gemfibrozil	-
		-	Gemfibrozil glucuronide	-
		-	Hydroxy-itraconazole	-
		-	Keto-itraconazole	-
		-	Simvastatin Lactone	-
	OATP1B3 (SLCO1B3)	-	Clarithromycin	-
		-	Rifampicin	Rifampicin

## 1 General information

Table S1.1: Substrates, inhibitors and inducers used in the presented model network (*continued*)

Type	Enzyme	Substrate	Inhibitor	Inducer
		-	Gemfibrozil	-
		-	Gemfibrozil glucuronide	-
		-	Hydroxy-itraconazole	-
		-	Keto-itraconazole	-
	Unspecific liver influx (gemfibrozil)	Gemfibrozil	-	-
<b>Efflux transporter</b>				
	BCRP (ABCG2)	Simvastatin Lactone	-	-
		-	Rifampicin	Rifampicin
		-	Itraconazole	-
		-	Keto-itraconazole	-
		-	Simvastatin Acid	-
	MRP2 (ABCC2)	Gemfibrozil glucuronide	-	-
		-	Gemfibrozil	-
		-	Rifampicin	-
	P-gp (ABCB1)	Simvastatin Acid	-	-
		-	Clarithromycin	-
		-	Rifampicin	Rifampicin
		-	Itraconazole	-
		-	N-desalkyl- itraconazole	-
		-	Hydroxy-itraconazole	-
		-	Keto-itraconazole	-
		-	Simvastatin Lactone	-

## 1 General information

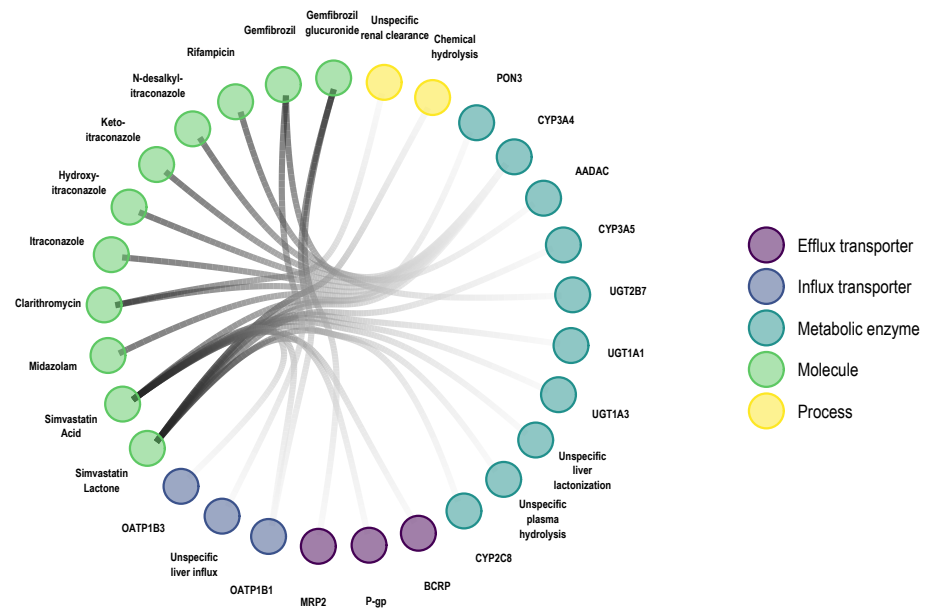


Figure S1.1: Network included compounds and their roles as substrates, inhibitors or inducers: Substrates

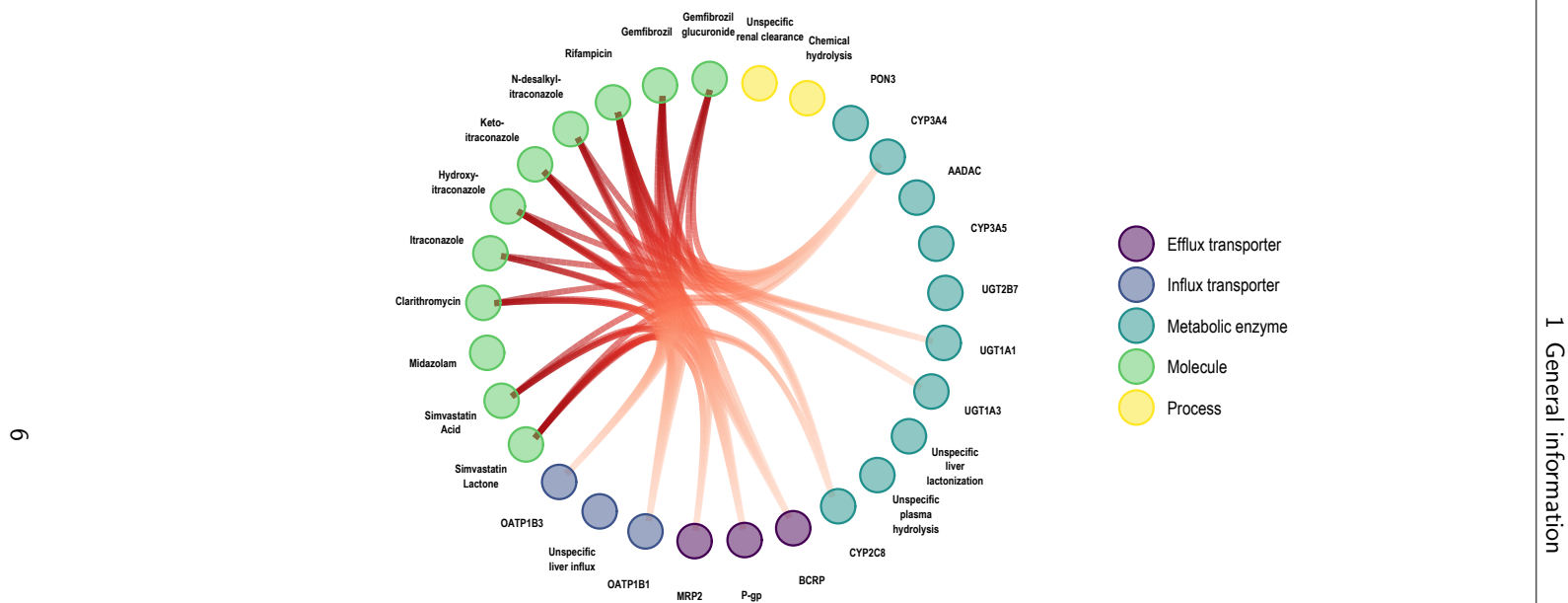


Figure S1.2: Network included compounds and their roles as substrates, inhibitors or inducers: Inhibitors

1 General information

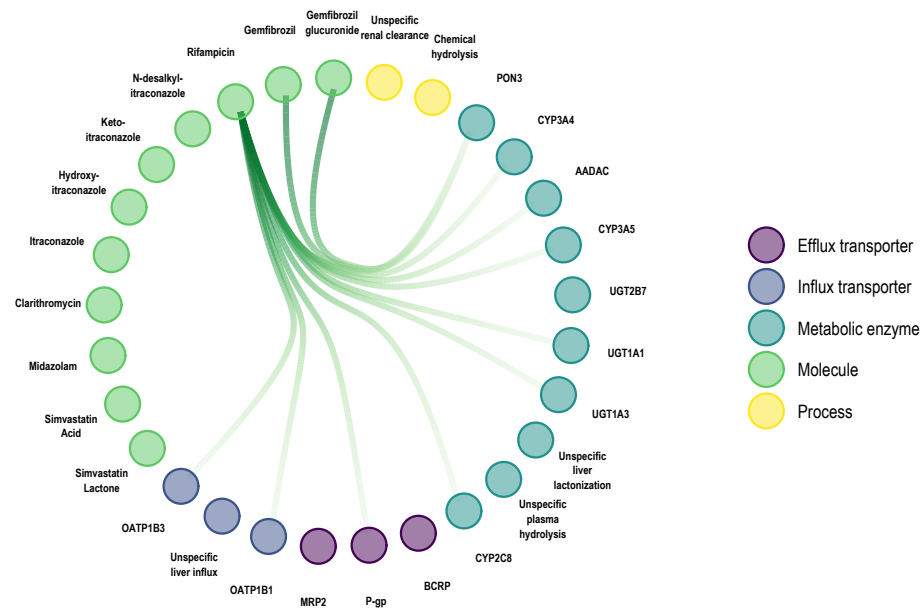


Figure S1.3: Network included compounds and their roles as substrates, inhibitors or inducers: Inducers

## 1.3 Model development and system-dependent specifications

### 1.3.1 General modeling workflow

For model development, concentration-time profiles of published clinical studies covering the full reported dosing range were used. If available this included data of intravenous and oral administration after single or multiple doses. If information about the amount of unchanged drug excreted to urine or feces was available, they were also utilized to inform the model optimization. If parameters had to be identified the Monte-Carlo algorithm implemented in PK-Sim<sup>®</sup> was used, utilizing the root mean square error (RMSE) as described in Eq. (S1.2) for parameter optimization.

Equation : Root-mean-square error

$$RMSE = \sqrt{\sum (c_{obs} - c_{pred})^2} \quad (S1.2)$$

RMSE = root mean square error  
 $C_{obs}$  = observed Concentration  
 $C_{pred}$  = predicted concentration

Parameter identifications were performed if either no literature values were on hand or multiple values with a broad range were available. Besides, model relevant information regarding all clinical studies available are listed in the corresponding Chapters 2.2.1 and 3.1 of the electronic supplementary material (ESM) including information about the assignment of each study to the training (model building) or test data set (model evaluation). For model development a mean prediction was used based on the mean demographic properties (gender, age, weight, height, race) of the respective study for each study in the training dataset. If values were missing, a mean value for age (30 years), weight (73 kg) and height (176 cm) was used. Quality of each parameter optimization was evaluated based on the graphical and statistical evaluation techniques as described in Chapter 1.4 of the ESM. Parameters of the final simvastatin model are given in Tables S2.3 and S2.5. Previously developed PBPK models used for the DDI network development were extended as described in the Chapter 3.1 of the ESM.

### 1.3.2 System-dependent parameters

All system-dependent parameters like reference concentrations, protein half-lives as well as tissue expression profiles of transporters and relevant metabolizing enzymes are listed in Table S1.2.



Table S1.2: System-dependent parameters and expression of relevant enzymes, transporters and other ADME processes

Enzyme / Transporter / Process (Gene)	Mean reference concentration <sup>a</sup>	Geometric standard deviation of the reference concentration <sup>b</sup>	Relative expression in the different organs	Half-life liver [hours]	Half-life intestine [hours]
<b>Enzymes</b>					
AADAC	1 [4]	1.4	RT-PCR [5]	36	23
CYP2C8	2.56 [6]	2.05 [1]	RT-PCR [7]	23	23
CYP3A4	4.32 [6]	1.18 liver [1], 1.46 intestine [1]	RT-PCR [7]	36 [8]	23 [9]
CYP3A5	0.04 [6]	1.4	RT-PCR [7]	36	23
PON3	1	1.4	Array [10]	36	23
UGT1A1	1	1.4	RT-PCR [5]	36	23
UGT1A3	1	1.4	RT-PCR [5]	36	23
UGT2B7	1 [4]	1.6 [1]	EST [1]	36	23
Unspecific liver lactonization (simvastatin acid)	1	1.4	Liver only	36	23
Unspecific plasma hydrolysis (simvastatin lactone)	1	1.4	Plasma only	36	23
<b>Processes</b>					
Chemical hydrolysis (simvastatin lactone)	1	-	Ubiquitous	36	23
<b>Transporters</b>					
BCRP ( <i>ABCG2</i> )	1	1.35 [11]	RT-PCR [12], with relative expression in blood cells set to 0.3046 [13]	36	23
MRP2 ( <i>ABCC2</i> )	1	1.49 [14]	Array [10]	36	23
OATP1B1 ( <i>SLCO1B1</i> )	1 [4]	1.54 (assumed) [15]	RT-PCR [12]	36	23
OATP1B3 ( <i>SLCO1B3</i> )	1 [4]	1.54 [15]	Array [10]	36	23

Table S1.2: System-dependent parameters and expression of relevant enzymes, transporters and other ADME processes (*continued*)

Enzyme / Transporter / Process (Gene)	Mean reference concentration <sup>a</sup>	Geometric standard deviation of the reference concentration <sup>b</sup>	Relative expression in the different organs	Half-life liver [hours]	Half-life intestine [hours]
P-gp ( <i>ABCB1</i> )	1.41 [16]	1.6 [15]	RT-PCR [12], with the relative expression in intestinal mucosa increased by factor 3.57 [16]	36	23
Unspecific liver influx (gemfibrozil)	1	1.4	Liver only	36	23
Unspecific liver influx (simastatin acid)	1	1.4	Liver only	36	23

<sup>a</sup>  $\mu\text{mol protein}^{-1}$  in the tissue of the highest expression. If no information on reference concentration was available it was set to  $1 \mu\text{mol protein}^{-1}$  and the catalytic rate constant ( $k_{cat}$ ) was optimized

<sup>b</sup> PK-Sim expression database profile

1 General information

---

 1 General information
 

---

In all individuals and populations, the enterohepatic circulation (EHC) was enabled (EHC continuous fraction set to one) by assuming a continuous flow from bile to duodenum. Furthermore, if no information about the renal state was specified a glomerular filtration rate of one was assumed which is equivalent to passive filtration without active secretion or reabsorption.

## 1.4 Model evaluation

For all observed concentration-time profiles population simulations using the virtual populations as described in Chapter 1.5 of the ESM for model evaluation were generated. The predicted profiles were subsequently used for the statistical as well as the graphical model evaluation. For this purpose, simulated median and 90 % confidence interval (CI) were calculated. Following, non-compartmental analysis (NCA) parameters like the area under the curve from first to last observation (AUC) and  $C_{\max}$  were calculated and used for further model evaluation.

### 1.4.1 Statistical model evaluation

For statistical model evaluation the following accuracy measures were calculated. For all concentration-time values available the mean relative deviation (MRD) as well as the median symmetric accuracy (MSA) according to Eq. (S1.3) and (S1.4) were calculated.

Equation : Mean relative deviation

$$x = \sqrt{\frac{\sum_{i=1}^N (\log_{10} c_{obs} - \log_{10} c_{pred})^2}{N}}$$

$$MRD = 10^x \quad (S1.3)$$

$C_{obs}$  = observed Concentration  
 $C_{pred}$  = predicted concentration  
 $N$  = number of observations  
 MRD = mean relative deviation

## 1 General information

Equation : Median symmetric accuracy

$$Q_i = \frac{C_{pred}}{C_{obs}}$$

$$\zeta = 100 * (\exp(\text{Mdn}(|\ln(Q_i)|)) - 1) \quad (\text{S1.4})$$

$C_{obs}$  = observed Concentration  
 $C_{pred}$  = predicted concentration  
 $Q_i$  = accuracy ratio  
 $\zeta$  = median symmetric accuracy

Hereby a MRD value  $\leq 2$  characterizes an adequate prediction whereas the MSA gives a easy interpretable impression of the relative deviation of the model predictions compared to the observed values. Additionally, NCA ratios (Eq. (S1.5)) were calculated and compared.

Equation : Non-compartmental analysis ratios

$$NCA_{ratio} = \frac{NCA_{pred}}{NCA_{obs}} \quad (\text{S1.5})$$

$NCA_{ratio}$  = predicted versus observed NCA estimate ratio  
 $NCA_{pred}$  = predicted NCA estimate  
 $NCA_{obs}$  = observed NCA estimate

Values  $\leq 2$  or  $\geq 0.5$  are considered as sufficient. Furthermore, for each DDI and DGI observed and predicted NCA effect ratios were estimated as shown in Eq. (S1.6)).

Equation : Drug-drug interaction and drug-gene interaction effect ratios

$$Effect_{ratio} = \frac{NCA_{pred,DDI/DGI}}{NCA_{pred,placebo}} / \frac{NCA_{obs,DDI/DGI}}{NCA_{obs,placebo}} \quad (\text{S1.6})$$

$Effect_{ratio}$  = predicted versus observed NCA estimate effect ratio  
 $NCA_{pred,DDI/DGI}$  = predicted NCA estimate under DDI and / or DGI conditions  
 $NCA_{pred,placebo}$  = predicted NCA estimate under placebo condition  
 $NCA_{obs,DDI/DGI}$  = observed NCA estimate under DDI and / or DGI conditions  
 $NCA_{obs,placebo}$  = observed NCA Estimate Under Placebo Condition

Finally, as a quantitative measure of the prediction accuracy for each DDI and DGI interaction as well as for all placebo concentration-time profiles the geometric mean fold error (GMFE) was calculated according to Eq. (S1.7):

## 1 General information

Equation : Geometric mean fold error

$$x = \frac{\sum |\log_{10}(\frac{NCA, value_{pred}}{NCA, value_{obs}})|}{N}$$

$$GMFE = 10^x \quad (S1.7)$$

N = number of observations  
 NCA<sub>pred</sub> = predicted NCA estimate  
 NCA<sub>obs</sub> = observed NCA estimate

**1.4.2 Graphical model evaluation**

For graphical model evaluation a set of different figures were generated. For all concentration-time profiles visual predictive checks (VPCs) were created using the virtual populations for model evaluation as described in Chapter 1.5 of the ESM and the subsequently calculated median and 90 % CI profiles. Furthermore, goodness of fit (GOF) plots like observed values versus predicted values were generated. Moreover, predicted versus observed NCA ratios as well as DDI and DGI effect ratios, as calculated in Chapter 1.4.1 of the ESM, were evaluated using the twofold limits, half-fold limits and / or the limits proposed by Guest et al [17].

**1.4.3 Local sensitivity analysis**

NCA parameter sensitivities of the final PBPK models were calculated as relative changes of the AUC of one dosing interval in steady-state conditions for simulations of the highest recommended doses. For this purpose, a mean individual as described in Chapter 1.3 of the ESM was used. Parameters were included into the analysis if they had to be optimized, if they might have a strong influence due to calculation methods used in the model (fraction unbound) or if they had significant impact in former models (solubility).

The sensitivity for the NCA parameter on the input parameter of interest was then calculated as the ratio of the relative change of the NCA parameter and the relative variation of the input parameter (see Eq. (S1.8)). For reasons of numerical stability, sensitivities were calculated as the average of several sensitivities based on different variations (see Eq. (S1.8)). The relative variations are defined by multiplication of the value in the simulation with variation factors (k). For each sensitivity analysis 9 ks were taken. The average of the sensitivities were following visualized as a tornado plot [18].

## 1 General information

Equation : Parameter sensitivity

$$S_{i,j} = \frac{\Delta PK_j}{\Delta p_i} * \frac{p_i}{PK_j} \quad (S1.8)$$

$$S_{i,j} = \frac{\sum_{k=1}^n \frac{\Delta_k PK_j}{\Delta_k p_i} * \frac{p_i}{PK_j}}{n} \quad (S1.8)$$

- PK<sub>j</sub> = pharmacokinetic parameter of a certain output  
 p<sub>i</sub> = input parameter  
 S<sub>i,j</sub> = sensitivity of a pharmacokinetic parameter of a certain output to an input parameter  
 k = variation factors

## 1.5 Virtual populations

For each profile with individual demographics available a virtual population containing 100 individuals with demographic properties (gender, age, weight, height, race) adapted to the mean of each respective study was created based on the International Commission on Radiological Protection (ICRP) database. If data were missing mean values as described in Chapter 1.3 of the ESM were used. Enzyme variability was removed except for protein ontogeny information if available. Subsequently, profiles were simulated and population mean and 90% CI were calculated.

## 2 PBPK modeling of simvastatin

### 2.1 Introduction

Simvastatin is an oral HMG-CoA reductase inhibitor and is among the ten most prescribed drugs in industrial nations [19]. Although statins and especially simvastatin have an excellent cost effectiveness and benefit risk ratio [20, 21] over-dosage can lead to rhabdomyolysis which is a feared and a potentially deadly adverse-drug event [22]. DDIs and DGIs are well known triggers leading to changed simvastatin PK and subsequently raise the risk of over-dosages [23, 24, 25, 26]. This is because simvastatin has a complex PK with high inter-individual variability, which involves many different drug transporters and metabolic enzymes. Hence, if DDIs or DGIs alter transporter or enzyme activity, simvastatin's PK can change dramatically. Simvastatin is given in its oral prodrug form simvastatin lactone (SL). SL is a highly lipophilic class II biopharmaceutical classification system drug with a high permeability but low solubility [27]. After disintegration, it is hydrolyzed partly chemical in a pH dependent manner [28] and mostly enzymatically by paraoxonase 3 (PON3) to its active form simvastatin acid (SA) [29]. Apart from organic anion transporting polypeptide 1B1 (OATP1B1) for all metabolic enzymes and transporters involved in simvastatin's PK polymorphisms with altered activity are reported [26]. Moreover, several inhibitors or inducer, so called perpetrator drugs, for either one or multiple of the above mentioned transporters and enzymes are known [30], changing the PK of simvastatin as a victim drug. Additionally, on top of this SL as well as SA itself show in vitro perpetrator drug effects for a broad range of enzymes and transporters [31, 32, 33, 34, 35, 36, 37, 38].

#### 2.1.1 Included processes

An overview of the processes included in the final whole-body PBPK model is given in Fig. S2.1.

In the final model metabolism of SL (Fig. S2.1 process [1]) and SA (Fig. S2.1 process [2]) by cytochrome P450 3A4 (CYP3A4) as well as SA metabolism by cytochrome P450 2C8 (CYP2C8) (Fig. S2.1 process [14]) and SL metabolism by cytochrome P450 3A5 (CYP3A5) (Fig. S2.1 process [13]) were included. In addition, the transformation of SL to SA was realized by inclusion of SL PON3 metabolism (Fig. S2.1 process [5]) as well as SL chemical hydrolysis (Fig. S2.1 process [3]) and plasma hydrolysis (Fig. S2.1 process [4]). Moreover, the back reaction (SA lactonisation) mediated by acyl glucuronide intermediates (enzymatically

## 2 PBPK modeling of simvastatin

(Fig. S2.1 process [7]) or spontaneously (chemically (Fig. S2.1 process [6])) was included. Furthermore, SL transportation by breast cancer resistance protein (BCRP) (Fig. S2.1 process [12]) was incorporated. For this, the predefined reverse transcription polymerase chain reaction (RT-PCR) BCRP expression profile was adapted to express BCRP also in red blood cells which reduced the blood to plasma ratio SL from values  $>3$  without BCRP expression to values  $<1$  with BCRP expression. Literature values for  $BP_{SL}$  are around 0.57[39]. For description of SA distribution, the relevant transport processes of SA by OATP1B1 (Fig. S2.1 process [8]), organic anion transporting polypeptide 1B3 (OATP1B3) (Fig. S2.1 process [9]) and P-glycoprotein (P-gp) (Fig. S2.1 process [11]) were implemented. To cover the PK for different oral formulations SL dissolution was described using a Weibull function whereas dissolution time of 50% dissolution and dissolution shape were optimized. Genotypes which were included and covered by the model were *solute carrier organic anion transporter family member 1B1 (SLCO1B1)* (rs4149056) c.521T/T, c.521C/C, and c.521T/C *ATP-binding cassette sub-family B member 1 (ABCB1)* (rs1128503, rs2032582 and rs1045642) c.1236T-c.2677T-c.3435T and c.1236C-c.2677G-c.3435C, *ATP-binding cassette sub-family G member 2 (ABCG2)* (rs2231142) c.421C/C, c.421C/A and c.421A/A and *CYP3A5* (rs776746) *CYP3A5\*3/\*3*, *CYP3A5\*3/\*1* and *CYP3A5\*3/\*1*.

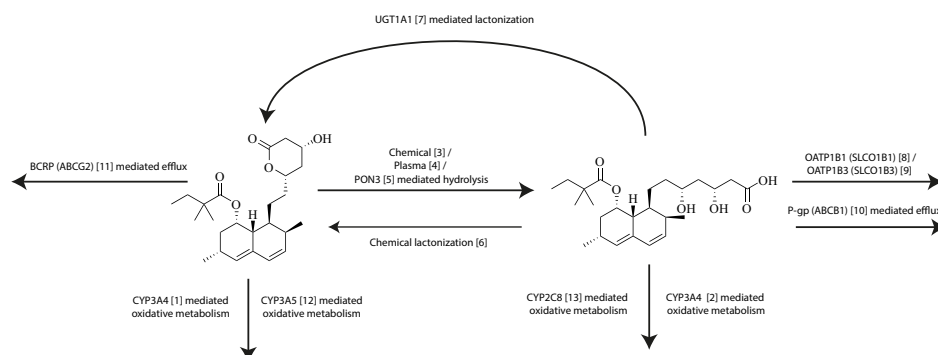


Figure S2.1: Included processes in the final whole-body PBPK model

### 2.1.2 Excluded processes

Few processes were excluded due to either lack of training data or ambiguous literature findings. Namely, no SL or SA multidrug resistance-associated protein 2 (MRP2) transportation was included. Although, there is some evidence that MRP2 and especially polymorphisms in the *ATP-binding cassette sub-family C member 2 (ABCC2)* gene are of relevance for simvastatin information available were too sparse to distinguish between other efflux processes [40, 36]. For the same reason and again because of ambiguous study information no P-gp efflux of SL was included [41, 42, 43]. The same applies to potential relevance of further influx transporters.

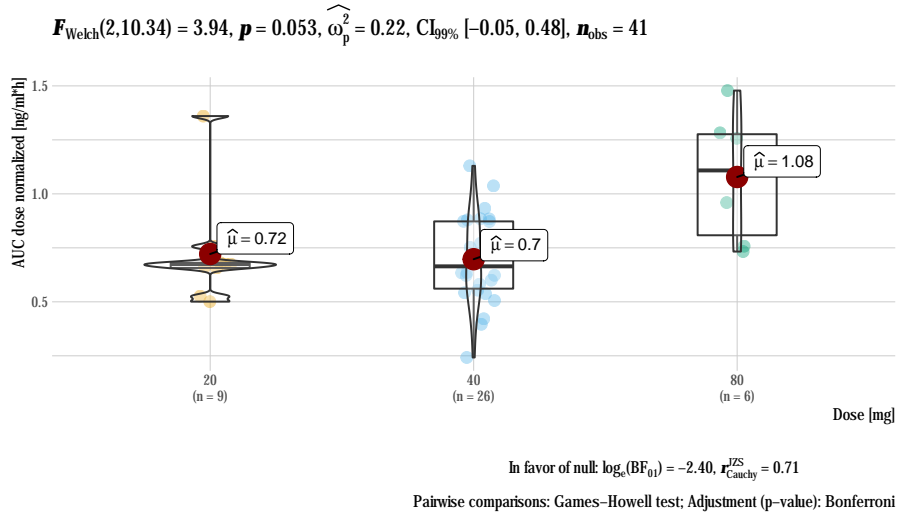


## 2.2 Simvastatin model development

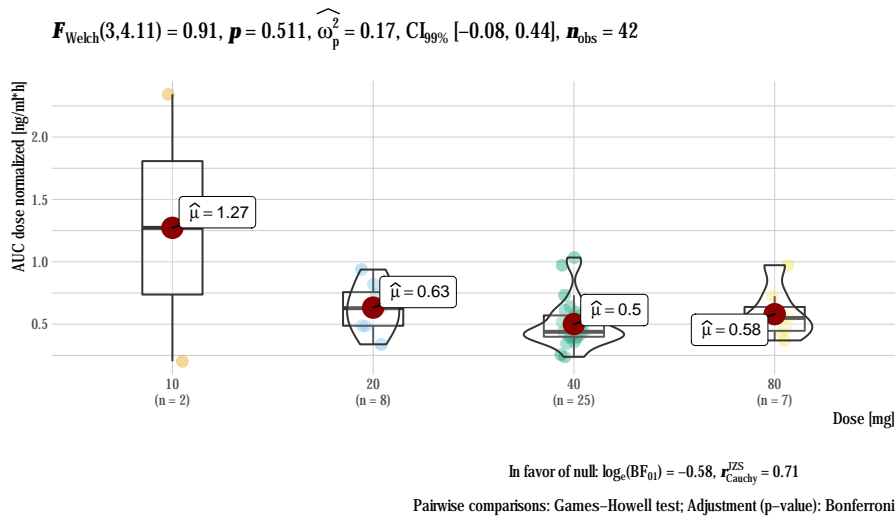
### 2.2.1 Clinical studies

For placebo and DGI model development and evaluation mean profiles from 57 studies were extracted including 59 SL and 57 SA pharmacokinetic profiles which represent information from in total 1271 study participants. An overview of all mean study demographics available can be found in Table S2.1. Doses available ranged from 10 mg to 80 mg after single and multiple doses. Dose linearity was found for SA and likely also for SL as shown in Fig. S2.2, S2.3 based on analysis of variance (ANOVA) analysis and pairwise comparison of dose normalized AUC and  $C_{\max}$  values from placebo single dose profiles.

2 PBPK modeling of simvastatin



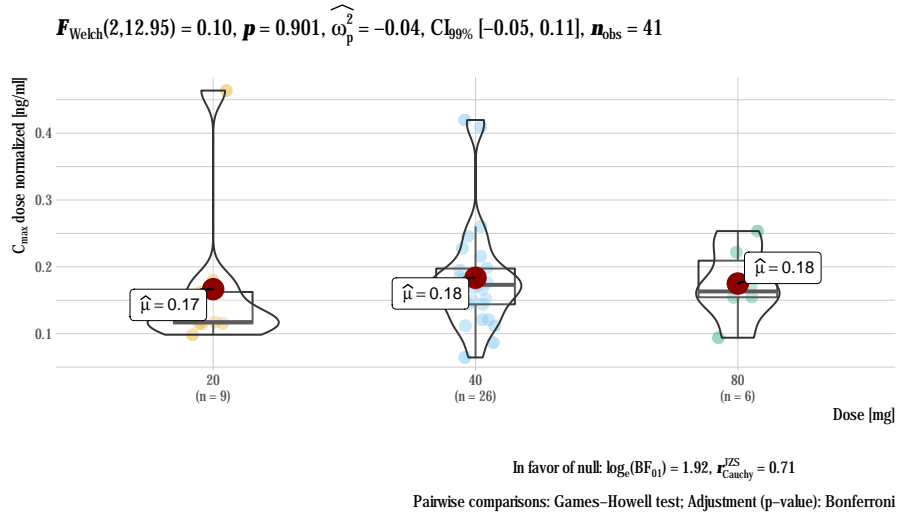
(1) Parameter: AUC Simvastatin Lactone



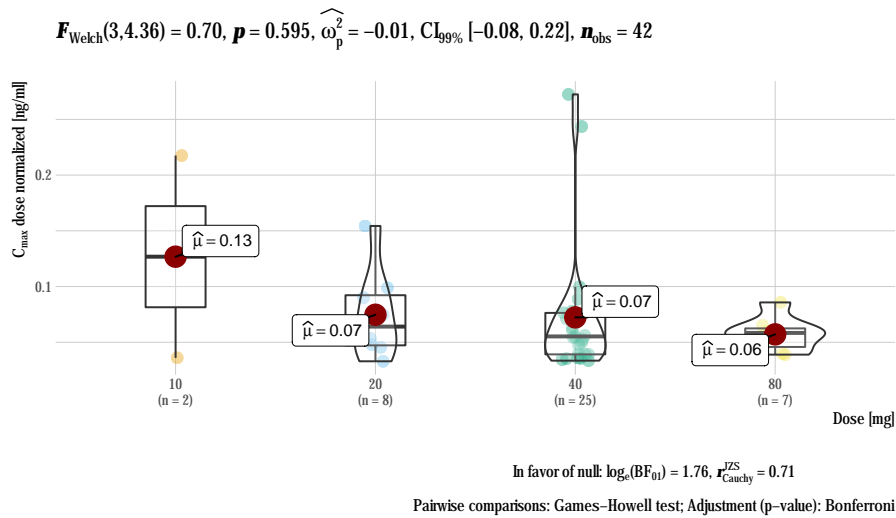
(2) Parameter: AUC Simvastatin Acid

Figure S2.2: Dose normalized AUC and  $C_{max}$  values: AUC Simvastatin Lactone, AUC Simvastatin Acid

2 PBPK modeling of simvastatin



(1) Parameter:  $C_{max}$  Simvastatin Lactone



(2) Parameter:  $C_{max}$  Simvastatin Acid

Figure S2.3: Dose normalized AUC and  $C_{max}$  values:  $C_{max}$  Simvastatin Lactone,  $C_{max}$  Simvastatin Acid

Table S2.1: Mean study data used for simvastatin lactone and simvastatin acid placebo model development

Route	N	Females [%]	Age [years]	Weight [kg]	Height [cm]	Dataset	Profile Ids	References
10 mg SL p.o. (Lipovas, fasted) s.d.	16	0	33 (26–44)	64 (56–75)	-	Test	77, 78	[44]
20 mg SL p.o. (Unknown, fasted) s.d.	12	25	31 (21–40)	-	-	Test	182, 183	[45]
20 mg SL p.o. (Unknown, fasted) s.d.	11	36	33	-	-	Test	196	[46]
20 mg SL p.o. (Unknown, fasted) s.d.	40	0	25	64	-	Training	318, 319	[47]
20 mg SL p.o. (Unknown, fasted) s.d.	40	0	32	66	-	Test	320, 321	[47]
20 mg SL p.o. (Unknown, fasted) s.d.	40	0	24	68	-	Test	322, 323	[47]
20 mg SL p.o. (Unknown, fasted) s.d.	40	0	26	78	-	Training	324, 325	[47]
20 mg SL p.o. (Zocor, fed) daily	31	19	38	72	-	Test	12	[48]
20 mg SL p.o. (Unknown, fasted) s.d.	10	50	-	-	-	Test	234	[49]
20 mg SL p.o. (Zocor, fasted) b.i.d.	11	0	(20–35)	-	-	Test	250, 251	[50]
20 mg SL p.o. (Zocor, fasted) s.d.	7	14	30 (26–42)	77 (70–84)	-	Training	91, 92	[51]
20 mg SL p.o. (Unknown, fasted) s.d.	15	-	-	-	-	Test	139, 144	[52]
40 mg SL p.o. (Unknown, fasted) s.d.	9	0	31 (22–49)	68	168	Test	1	[53]
40 mg SL p.o. (Unknown, fasted) s.d.	25	8	34 (22–45)	74	-	Test	180, 181	[54]
40 mg SL p.o. (Zocor, Unknown) daily	14	0	23	66	172	Test	192, 193	[55]
40 mg SL p.o. (Unknown, Unknown) daily	24	0	42	83	-	Test	190	[56]
40 mg SL p.o. (Zocor, fasted) s.d.	22	23	32	83	-	Training	197, 198	[57]
40 mg SL p.o. (Zocor, fasted) s.d.	5	60	(22–26)	-	-	Test	6, 9	[58]

2 PBPK modeling of simvastatin

Table S2.1: Mean study data used for simvastatin lactone and simvastatin acid placebo model development (*continued*)

Route	N	Females [%]	Age [years]	Weight [kg]	Height [cm]	Dataset	Profile Ids	References
40 mg SL p.o. (Zocor, fasted) s.d.	22	0	35 (21–60)	-	-	Test	223, 224	[59]
40 mg SL p.o. (Zocor, Unknown) s.d.	14	0	36 (23–43)	-	-	Test	209, 210	[60]
40 mg SL p.o. (Zocor, fasted) s.d.	14	0	37 (21–45)	-	-	Test	219, 220	[61]
40 mg SL p.o. (Zocor, fasted) s.d.	12	33	(19–)	-	-	Test	236, 237	[62]
40 mg SL p.o. (Zocor, fasted) s.d.	10	40	24	68	-	Test	30, 31	[63]
40 mg SL p.o. (Unknown, fasted) s.d.	23	4	32 (21–43)	-	-	Test	277, 278	[64]
40 mg SL p.o. (Zocor, fed) daily	12	-	-	-	-	Test	289, 290	[65]
40 mg SL p.o. (Unknown, fasted) s.d.	35	34	(18–55)	-	-	Test	101, 102	[66]
40 mg SL p.o. (Zocor, Unknown) s.d.	10	10	(20–24)	(58–79)	-	Test	53, 52	[67]
40 mg SL p.o. (Zocor, fasted) s.d.	10	0	(20–34)	(63–80)	-	Test	54, 55	[68]
40 mg SL p.o. (Unknown, Unknown) s.d.	21	0	33	81	-	Test	272	[69]
40 mg SL p.o. (Denan, fed) s.d.	20	50	50	(53–111)	(158–192)	Test	135, 137	[70]
40 mg SL p.o. (Unknown, fasted) daily	52	23	38 (19–55)	75 (55–100)	169 (149–190)	Test	316, 317	[71]
40 mg SL p.o. (Zocor, Unknown) daily	24	0	30 (19–44)	84 (59–114)	178 (164–190)	Test	270	[72]
40 mg SL p.o. (Zocor, fasted) s.d.	28	29	39 (21–63)	73 (55–97)	170 (146–184)	Training	76, 75	[73]
40 mg SL p.o. (Zocor, fasted) s.d.	12	67	56 (28–72)	88 (63–111)	-	Test	264, 265	[74]
40 mg SL p.o. (Zocor, fasted) daily	18	28	29 (21–43)	75 (52–93)	175 (152–193)	Training	260, 261	[75]
40 mg SL p.o. (Unknown, Unknown) s.d.	16	19	36	75	-	Test	205, 206	[76]

Table S2.1: Mean study data used for simvastatin lactone and simvastatin acid placebo model development (*continued*)

Route	N	Females [%]	Age [years]	Weight [kg]	Height [cm]	Dataset	Profile Ids	References
40 mg SL p.o. (Unknown, fasted) daily	85	40	39 (21–55)	72 (51–102)	174 (154–196)	Training	174, 177	[77]
40 mg SL p.o. (Unknown, fasted) s.d.	85	40	39 (21–55)	72 (51–102)	174 (154–196)	Training	168, 171	[77]
40 mg SL p.o. (Unknown, fasted) s.d.	20	-	-	-	-	Test	100	[78]
40 mg SL p.o. (Unknown, fasted) s.d.	10	0	39 (18–63)	-	-	Test	246, 247	[79]
40 mg SL p.o. (Unknown, fasted) daily	18	39	29 (19–40)	67 (54–80)	-	Test	281	[80]
60 mg SL p.o. (Zocor, fasted) s.d.	10	50	(18–30)	(55–101)	-	Test	43, 42	[81]
80 mg SL p.o. (Unknown, fasted) daily	24	25	31 (20–45)	74 (49–88)	175 (153–190)	Training	127, 128	[82]
80 mg SL p.o. (Zocor, fed) daily	12	25	-	-	-	Test	186, 187	[83]
80 mg SL p.o. (Zocor, fasted) s.d.	24	67	31 (20–45)	-	170 (152–189)	Training	201, 202	[84]
80 mg SL p.o. (Unknown, fasted) s.d.	30	57	56 (26–74)	86 (56–120)	164 (151–187)	Test	227	[85]
80 mg SL p.o. (Unknown, fasted) daily	24	17	30 (19–47)	68 (49–84)	-	Test	166	[86]
80 mg SL p.o. (Zocor, fasted) s.d.	24	25	32 (18–45)	(50–)	-	Training	131, 132	[87]
80 mg SL p.o. (Zocor, fasted) s.d.	58	7	41 (20–60)	74 (51–92)	173 (156–194)	Training	230, 231	[88]
80 mg SL p.o. (Zocor, fasted) s.d.	12	0	(17–31)	76 (66–93)	-	Training	81, 82	[89]
80 mg SL p.o. (Unknown, fasted) s.d.	36	50	24	69	176	Test	85, 85, 86, 86	[90]
80 mg SL p.o. (Unknown, fed) s.d.	29	52	32 (20–59)	68 (48–101)	170 (153–185)	Test	274, 275	[91]

*Note:*

Values for age, weight and height are given as mean (range); Wild-type genotype was assumed; -, not given; b.i.d., twice daily; n, number of individuals studied; po, oral; s.d., single dose

2 PBPK modeling of simvastatin

Table S2.2: Mean study data used for simvastatin lactone and simvastatin acid DGI model development

Route	Genotype	N	Females [%]	Age [years]	Weight [kg]	Height [cm]	Dataset	Profile Ids	References
10 mg SL p.o. (Unknown, fasted) s.d.	c.521C/C	2	50	14	61	157	Test	338	[92]
10 mg SL p.o. (Unknown, fasted) s.d.	c.521T/C	15	53	14	78	160	Test	337	[92]
10 mg SL p.o. (Unknown, fasted) s.d.	c.521T/T	15	53	14	83	160	Test	336	[92]
20 mg SL p.o. (Zocor, fasted) s.d.	c.1236C- c.2677G- c.3435C	12	42	22	68	178	Training	21, 20	[41]
20 mg SL p.o. (Zocor, fasted) s.d.	c.1236T- c.2677T- c.3435T	12	42	24	66	174	Training	23, 22	[41]
20 mg SL p.o. (Zocor, fasted) s.d.	*3/*1	8	-	25	68	172	Test	98	[93]
20 mg SL p.o. (Zocor, fasted) s.d.	*3/*3	10	-	25	71	173	Test	99	[93]
20 mg SL p.o. (Zocor, fasted) s.d.	*1/*1	4	-	25	69	172	Training	97	[93]
40 mg SL p.o. (Zocor, fasted) s.d.	c.421C/A	4	25	27	73	176	Test	28, 25	[94]
40 mg SL p.o. (Zocor, fasted) s.d.	c.421C/C	23	52	22	68	174	Test	29, 26	[94]
40 mg SL p.o. (Zocor, fasted) s.d.	c.421A/A	5	80	22	56	164	Training	27, 24	[94]
40 mg SL p.o. (Zocor, fasted) s.d.	c.521T/C	12	42	24	69	174	Test	72, 71	[95]
40 mg SL p.o. (Zocor, fasted) s.d.	c.521T/T	16	50	23	68	174	Test	74, 73	[95]
40 mg SL p.o. (Zocor, fasted) s.d.	c.521C/C	4	25	23	84	180	Training	70, 69	[95]
60 mg SL p.o. (Zocor,unknown) s.d.	c.521C/C	1	-	24.9	70.1	174.6	Test	- <sup>a</sup>	[96]
60 mg SL p.o. (Zocor,unknown) s.d.	c.521T/C	42	-	24.9	70.1	174.6	Test	- <sup>a</sup>	[96]
60 mg SL p.o. (Zocor,unknown) s.d.	c.521T/T	88	-	24.9	70.1	174.6	Test	- <sup>a</sup>	[96]

Table S2.2: Mean study data used for simvastatin lactone and simvastatin acid DGI model development (*continued*)

Route	Genotype	N	Females [%]	Age [years]	Weight [kg]	Height [cm]	Dataset	Profile Ids	References
60 mg SL p.o. (Zocor,unknown) s.d.	*3/*1	52	-	24.9	70.1	174.6	Test	-. <sup>a</sup>	[96]
60 mg SL p.o. (Zocor,unknown) s.d.	*3/*3	71	-	24.9	70.1	174.6	Test	-. <sup>a</sup>	[96]
60 mg SL p.o. (Zocor,unknown) s.d.	*1/*1	9	-	24.9	70.1	174.6	Test	-. <sup>a</sup>	[96]
60 mg SL p.o. (Zocor,unknown) s.d.	c.421C/A	56	-	24.9	70.1	174.6	Test	-. <sup>a</sup>	[96]
60 mg SL p.o. (Zocor,unknown) s.d.	c.421C/C	64	-	24.9	70.1	174.6	Test	-. <sup>a</sup>	[96]
60 mg SL p.o. (Zocor,unknown) s.d.	c.421A/A	12	-	24.9	70.1	174.6	Test	-. <sup>a</sup>	[96]

*Note:*

Values for age, weight and height are given as mean; -, not given; n, number of individuals studied; po, oral; s.d., single dose

<sup>a</sup> Only SL / SA AUC and C<sub>max</sub> values were available.



---

## 2 PBPK modeling of simvastatin

---

### 2.2.2 Drug-dependent parameters

Table S2.3 and S2.5 compare the drug-dependent model parameter used in the final model with median literature values and shows the relative deviation from them. Moreover, they mark parameters that were optimized. Table S2.4 and S2.6 lists all parameters that were extracted from literature with the corresponding references.

Table S2.3: Drug-dependent parameters of the final simvastatin lactone model compared to literature values

Parameter	Unit	Model value	Median (range) literature values	Origin	Description
<b>Molecule</b>					
BP	-	0.5445	0.57	Calculated	Blood to plasma ratio after administration of 40 mg simvastatin lactone at steady-state
fu	%	1.34	2.37 (1.09–6)	Literature	Fraction unbound plasma
Lipophilicity	-	4.68	4.595 (2.06–5.19)	Literature	Lipophilicity
MW	-	418.6	418.6	Literature	Molecular weight
Solubility	mg l <sup>-1</sup>	16.4	16.4 (1.4–61.94)	Literature	Solubility in FaSSIF (pH=5)
<b>Enzymes</b>					
CYP3A4 $k_{cat}$	min <sup>-1</sup>	5194	-	Optimized	CYP3A4 catalytic rate constant
CYP3A4 $K_M$	μmol l <sup>-1</sup>	21	2.55 (0.46–30)	Literature	CYP3A4 Michaelis-Menten constant
CYP3A5 $k_{cat}$ *1/*1	min <sup>-1</sup>	162300	-	Optimized	CYP3A5 catalytic rate constant for *1/*1 genotype
CYP3A5 $k_{cat}$ *1/*3	min <sup>-1</sup>	81140	-	Calculated	CYP3A5 catalytic rate constant for *1/*3 genotype
CYP3A5 $k_{cat}$ *3/*3	min <sup>-1</sup>	0	-	Literature	CYP3A5 catalytic rate constant for *3/*3 genotype
CYP3A5 $K_M$	μmol l <sup>-1</sup>	39.08	88 (62–91)	Optimized	CYP3A5 Michaelis-Menten constant
PON3 $K_M$	μmol l <sup>-1</sup>	840	840	Literature	PON3 Michaelis-Menten constant
PON3 $k_{cat}$	min <sup>-1</sup>	4952	-	Optimized	PON3 catalytic rate constant
<b>Transporters</b>					
BCRP ( <i>ABCG2</i> ) $k_{cat}$ c.421AA	min <sup>-1</sup>	7.501	-	Optimized	BCRP catalytic rate constant for c.421AA genotype

Table S2.3: Drug-dependent parameters of the final simvastatin lactone model compared to literature values (*continued*)

Parameter	Unit	Model value	Median (range) literature values	Origin	Description
BCRP ( <i>ABCG2</i> ) $k_{\text{cat}}$ c.421CA	$\text{min}^{-1}$	20.06	-	Calculated	BCRP catalytic rate constant for c.421CA genotype
BCRP ( <i>ABCG2</i> ) $k_{\text{cat}}$ c.421CC	$\text{min}^{-1}$	32.61	-	Optimized	BCRP catalytic rate constant for c.421CC genotype
BCRP ( <i>ABCG2</i> ) $K_M$	$\mu\text{mol l}^{-1}$	5	-	Assumed	BCRP Michaelis-Menten constant (assumed from other statins)
<b>Inhibition</b>					
$K_i$ CYP2C8	$\mu\text{mol l}^{-1}$	1.1	5.7 (1.1–12.3)	Literature	Concentration for half-maximal CYP2C8 competitive inhibition
$K_i$ CYP3A4	$\mu\text{mol l}^{-1}$	0.16	2.1 (0.16–35)	Literature	Concentration for half-maximal CYP3A4 competitive inhibition
$K_i$ MRP2 ( <i>ABCC2</i> )	$\mu\text{mol l}^{-1}$	5	32.1 (5–132)	Literature	Concentration for half-maximal MRP2 competitive inhibition
$K_i$ OATP1B1 ( <i>SLCO1B1</i> )	$\mu\text{mol l}^{-1}$	5	7.85 (5–12.5)	Literature	Concentration for half-maximal OATP1B1 competitive inhibition
$K_i$ P-gp ( <i>ABCB1</i> )	$\mu\text{mol l}^{-1}$	4.6	37.7 (4.6–209)	Literature	Concentration for half-maximal P-gp competitive inhibition
<b>Formulation</b>					
Density	$\text{g cm}^{-3}$	1.2	1.2	Literature	Drug density
Dissolution shape	-	1.297	-	Optimized	Weibull function dissolution shape
Dissolution time (50% dissolved)	min	86.38	-	Optimized	Weibull function dissolution time (50% dissolved)
<b>System</b>					

Table S2.3: Drug-dependent parameters of the final simvastatin lactone model compared to literature values (*continued*)

Parameter	Unit	Model value	Median (range) literature values	Origin	Description
BCRP blood cells	%	30.46	-	Optimized	BCRP relative expression in blood cells (normalized)
Chemical hydrolysis rate	$l \mu\text{mol}^{-1} \text{min}^{-1}$	0.00098	0.0008217 (1.667e-06–0.0196)	Literature	Chemical hydrolysis rate
EHC	-	1	-	Assumed	Fraction of bile continually released from the gallbladder
GFR	-	1	-	Assumed	Fraction of filtered drug reaching the urine
Plasma hydrolysis rate	$l \mu\text{mol}^{-1} \text{min}^{-1}$	0.0603	0.0603	Literature	Plasma hydrolysis rate
Specific intest. perm.	$\text{cm min}^{-1}$	0.001082	0.258	Optimized	Permeation across intestinal mucosa normalized to surface area
Specific organ perm.	$\text{cm min}^{-1}$	0.2561	-	Calculated	Permeation across cell membranes normalized to surface area

*Note:*

Cellular permabilites calculation method: PK-Sim Standard; organ-plasma partition coefficient calculation method: Berezhkovskiy; formulation parameter values were used for solid oral dosage forms only

Table S2.4: Extracted drug-dependent parameter literature values for simvastatin lactone

Parameter	Unit	Literature value	Standard deviation	Note	Reference
BP	-	0.57	-	Blood to plasma ratio	[39]
fu	%	6	-	-	[97]
fu	%	4	-	-	[98]
fu	%	1.09	0.04	Human plasma - ligand concentration: 0.5 µg/ml	[99]
fu	%	1.25	0.07	Human plasma - ligand concentration: 1 µg/ml	[99]
fu	%	1.34	0.03	Human plasma - ligand concentration: 2 µg/ml	[99]
fu	%	1.59	0.15	Human plasma - ligand concentration: 4 µg/ml	[99]
fu	%	1.77	0.16	Human plasma - ligand concentration: 6 µg/ml	[99]
fu	%	2.3	0.28	Dog plasma - ligand concentration: 0.5 µg/ml	[99]
fu	%	2.49	0.34	Dog plasma - ligand concentration: 1 µg/ml	[99]
fu	%	2.44	0.12	Dog plasma - ligand concentration: 2 µg/ml	[99]
fu	%	3.13	0.33	Dog plasma - ligand concentration: 4 µg/ml	[99]
fu	%	3.38	0.51	Dog plasma - ligand concentration: 6 µg/ml	[99]
Lipophilicity	-	4.7	-	log D pH=7.0	[98]
Lipophilicity	-	4.69	-	clogP	[100]
Lipophilicity	-	4.48	-	clogP	[100]
Lipophilicity	-	4.42	-	clogP	[100]
Lipophilicity	-	4.91	-	clogP	[100]
Lipophilicity	-	4.51	-	clogP	[100]
Lipophilicity	-	4.46	-	clogP	[100]
Lipophilicity	-	4.74	-	clogP	[100]
Lipophilicity	-	4.68	-	clogP	[100]
Lipophilicity	-	4.79	-	clogP	[100]
Lipophilicity	-	4.38	-	clogP	[100]
Lipophilicity	-	5.19	-	clogP	[100]

Table S2.4: Extracted drug-dependent parameter literature values for simvastatin lactone (*continued*)

Parameter	Unit	Literature value	Standard deviation	Note	Reference
Lipophilicity	-	2.06	-	logP at pH 7	[100]
Lipophilicity	-	4.47	-	logP at pH 2	[100]
Lipophilicity	-	4.4	-	log D pH=7.0	[101]
Lipophilicity	-	4.68	-	logP	[39]
MW	-	418.6	-	Calculated	[102]
Solubility	mg l <sup>-1</sup>	8.43	-	Intrinsic solubility calculated	[102]
Solubility	mg l <sup>-1</sup>	61.94	-	FaHIF	[58]
Solubility	mg l <sup>-1</sup>	1.4	-	pH=5	[98]
Solubility	mg l <sup>-1</sup>	30	-	Water	[103]
Solubility	mg l <sup>-1</sup>	1.45	-	Distilled water	[27]
Solubility	mg l <sup>-1</sup>	14.5	-	pH=1.2	[27]
Solubility	mg l <sup>-1</sup>	24.4	-	pH=7	[27]
Solubility	mg l <sup>-1</sup>	29.9	-	FeSSIF	[27]
Solubility	mg l <sup>-1</sup>	16.4	-	FaSSIF	[27]
Solubility	mg l <sup>-1</sup>	16.4	-	Intestine	[39]
Solubility	mg l <sup>-1</sup>	14.5	-	Stomach	[39]
CL <sub>int</sub> CYP3A4	μl min <sup>-1</sup> mg <sup>-1</sup> mic.protein	5472	-	-	[104]
CL <sub>int</sub> CYP3A4	μl min <sup>-1</sup> mg <sup>-1</sup> mic.protein	3899	-	L1	[97]
CL <sub>int</sub> CYP3A4	μl min <sup>-1</sup> mg <sup>-1</sup> mic.protein	5141	-	L2	[97]
CL <sub>int</sub> CYP3A4	μl min <sup>-1</sup> mg <sup>-1</sup> mic.protein	5800	-	L3	[97]
CL <sub>int</sub> CYP3A4	μl min <sup>-1</sup> mg <sup>-1</sup> mic.protein	889.9	-	Total clearance males	[105]
CL <sub>int</sub> CYP3A4	μl min <sup>-1</sup> mg <sup>-1</sup> mic.protein	1330	-	Total clearance females	[105]
CL <sub>int</sub> CYP3A4	μl min <sup>-1</sup> mg <sup>-1</sup> mic.protein	2870	-	-	[106]
CL <sub>int</sub> CYP3A4	μl min <sup>-1</sup> mg <sup>-1</sup> mic.protein	1697	-	-	[107]
CYP3A4 K <sub>M</sub>	μmol l <sup>-1</sup>	1.101	-	human liver microsomes corrected for fumic (0.218)	[105]
CYP3A4 K <sub>M</sub>	μmol l <sup>-1</sup>	1.144	-	human liver microsomes corrected for fumic (0.218)	[105]
CYP3A4 K <sub>M</sub>	μmol l <sup>-1</sup>	0.46	-	human liver microsomes corrected for fumic (0.218)	[105]
CYP3A4 K <sub>M</sub>	μmol l <sup>-1</sup>	1.485	-	human liver microsomes corrected for fumic (0.218)	[105]
CYP3A4 K <sub>M</sub>	μmol l <sup>-1</sup>	2.3	-	human liver microsomes corrected for fumic (0.1)	[106]

Table S2.4: Extracted drug-dependent parameter literature values for simvastatin lactone (*continued*)

Parameter	Unit	Literature value	Standard deviation	Note	Reference
CYP3A4 $K_M$	$\mu\text{mol l}^{-1}$	4.27	-	human liver microsomes - 3',5'-dihydrodiol SV corrected for fumic (0.122)	[107]
CYP3A4 $K_M$	$\mu\text{mol l}^{-1}$	2.55	-	human liver microsomes - 3'-hydroxy SV corrected for fumic (0.122)	[107]
CYP3A4 $K_M$	$\mu\text{mol l}^{-1}$	4.416	-	human liver microsomes - 6'-exomethylene SV corrected for fumic (0.122)	[107]
CYP3A4 $K_M$	$\mu\text{mol l}^{-1}$	30	6.4	Recombinant enzyme - 3',5'-dihydrodiol SV	[107]
CYP3A4 $K_M$	$\mu\text{mol l}^{-1}$	7	2.9	Recombinant enzyme - 3'-hydroxy SV	[107]
CYP3A4 $K_M$	$\mu\text{mol l}^{-1}$	25	0.1	Recombinant enzyme - 6'-exomethylene SV	[107]
CYP3A5 $K_M$	$\mu\text{mol l}^{-1}$	91	-	Recombinant enzyme - 3',5'-dihydrodiol SV	[107]
CYP3A5 $K_M$	$\mu\text{mol l}^{-1}$	62	-	Recombinant enzyme - 3'-hydroxy SV	[107]
CYP3A5 $K_M$	$\mu\text{mol l}^{-1}$	88	-	Recombinant enzyme - 6'-exomethylene SV	[107]
PON3 $K_M$	$\mu\text{mol l}^{-1}$	840	-	-	[108]
BCRP ( <i>ABCG2</i> ) $K_M$	$\mu\text{mol l}^{-1}$	2.8	-	Pravastatin (acid)	[109]
BCRP ( <i>ABCG2</i> ) $K_M$	$\mu\text{mol l}^{-1}$	10.1	-	Rosuvastatin (acid)	[110]
BCRP ( <i>ABCG2</i> ) $K_M$	$\mu\text{mol l}^{-1}$	5.73	-	Pitavastatin (acid)	[38]
BCRP ( <i>ABCG2</i> ) $K_M$	$\mu\text{mol l}^{-1}$	10.8	-	Rosuvastatin (acid)	[111]
BCRP ( <i>ABCG2</i> ) $K_M$	$\mu\text{mol l}^{-1}$	2.02	-	Rosuvastatin (acid)	[112]
BCRP ( <i>ABCG2</i> ) $K_M$	$\mu\text{mol l}^{-1}$	1.2	-	Pitavastatin (acid)	[113]
$K_i$ CYP2C8	$\mu\text{mol l}^{-1}$	1.1	-	$K_i$	[114]
$K_i$ CYP2C8	$\mu\text{mol l}^{-1}$	7.5	-	$K_i$	[114]
$K_i$ CYP2C8	$\mu\text{mol l}^{-1}$	5.7	-	$K_i$	[114]
$K_i$ CYP2C8	$\mu\text{mol l}^{-1}$	12.3	-	$K_i$	[114]
$K_i$ CYP2C8	$\mu\text{mol l}^{-1}$	3.3	-	$K_i$	[114]
$K_i$ CYP3A4	$\mu\text{mol l}^{-1}$	6.23	-	$K_i$	[115]
$K_i$ CYP3A4	$\mu\text{mol l}^{-1}$	0.31	-	$K_i$	[116]
$K_i$ CYP3A4	$\mu\text{mol l}^{-1}$	0.54	-	$K_i$	[116]
$K_i$ CYP3A4	$\mu\text{mol l}^{-1}$	16.5	-	$K_i$	[116]
$K_i$ CYP3A4	$\mu\text{mol l}^{-1}$	0.38	-	$K_i$	[116]

Table S2.4: Extracted drug-dependent parameter literature values for simvastatin lactone (*continued*)

Parameter	Unit	Literature value	Standard deviation	Note	Reference
K <sub>i</sub> CYP3A4	μmol <sup>-1</sup>	0.16	-	K <sub>i</sub>	[116]
K <sub>i</sub> CYP3A4	μmol <sup>-1</sup>	0.81	-	K <sub>i</sub>	[116]
K <sub>i</sub> CYP3A4	μmol <sup>-1</sup>	0.37	-	K <sub>i</sub>	[116]
K <sub>i</sub> CYP3A4	μmol <sup>-1</sup>	35	-	K <sub>i</sub>	[116]
K <sub>i</sub> CYP3A4	μmol <sup>-1</sup>	30	-	K <sub>i</sub>	[117]
K <sub>i</sub> CYP3A4	μmol <sup>-1</sup>	2.13	0.14	K <sub>i</sub>	[31]
K <sub>i</sub> CYP3A4	μmol <sup>-1</sup>	2.1	0.56	K <sub>i</sub>	[118]
K <sub>i</sub> CYP3A4	μmol <sup>-1</sup>	10	-	K <sub>i</sub>	[107]
K <sub>i</sub> MRP2 ( <i>ABCC2</i> )	μmol <sup>-1</sup>	56	-	IC50	[119]
K <sub>i</sub> MRP2 ( <i>ABCC2</i> )	μmol <sup>-1</sup>	8.2	-	IC50	[36]
K <sub>i</sub> MRP2 ( <i>ABCC2</i> )	μmol <sup>-1</sup>	5	-	K <sub>i</sub>	[36]
K <sub>i</sub> MRP2 ( <i>ABCC2</i> )	μmol <sup>-1</sup>	132	-	IC50	[120]
K <sub>i</sub> OATP1B1 ( <i>SLCO1B1</i> )	μmol <sup>-1</sup>	9.7	-	IC50	[35]
K <sub>i</sub> OATP1B1 ( <i>SLCO1B1</i> )	μmol <sup>-1</sup>	5	-	IC50	[121]
K <sub>i</sub> OATP1B1 ( <i>SLCO1B1</i> )	μmol <sup>-1</sup>	12.5	-	IC50	[121]
K <sub>i</sub> OATP1B1 ( <i>SLCO1B1</i> )	μmol <sup>-1</sup>	6	-	IC50	[121]
K <sub>i</sub> P-gp ( <i>ABCB1</i> )	μmol <sup>-1</sup>	16.2	-	IC50	[122]
K <sub>i</sub> P-gp ( <i>ABCB1</i> )	μmol <sup>-1</sup>	209	-	IC50	[123]
K <sub>i</sub> P-gp ( <i>ABCB1</i> )	μmol <sup>-1</sup>	59.6	-	IC50	[37]
K <sub>i</sub> P-gp ( <i>ABCB1</i> )	μmol <sup>-1</sup>	4.9	-	IC50	[124]
K <sub>i</sub> P-gp ( <i>ABCB1</i> )	μmol <sup>-1</sup>	59	-	IC50	[43]
K <sub>i</sub> P-gp ( <i>ABCB1</i> )	μmol <sup>-1</sup>	9	-	IC50	[43]
K <sub>i</sub> P-gp ( <i>ABCB1</i> )	μmol <sup>-1</sup>	56	-	IC50	[43]
K <sub>i</sub> P-gp ( <i>ABCB1</i> )	μmol <sup>-1</sup>	8.9	-	IC50	[125]
K <sub>i</sub> P-gp ( <i>ABCB1</i> )	μmol <sup>-1</sup>	26.1	-	IC50	[125]
K <sub>i</sub> P-gp ( <i>ABCB1</i> )	μmol <sup>-1</sup>	56.8	-	IC50	[125]
K <sub>i</sub> P-gp ( <i>ABCB1</i> )	μmol <sup>-1</sup>	4.6	-	IC50	[126]
K <sub>i</sub> P-gp ( <i>ABCB1</i> )	μmol <sup>-1</sup>	49.3	-	IC50	[126]
Density	g cm <sup>-3</sup>	1.2	-	-	[39]
Chemical hydrolysis rate	min <sup>-1</sup>	2.16e-05	-	pH=5; T=60°C phosphate buffer	[127]
Chemical hydrolysis rate	min <sup>-1</sup>	0.000112	-	pH=6; T=60°C phosphate buffer	[127]
Chemical hydrolysis rate	min <sup>-1</sup>	0.00178	-	pH=7; T=60°C phosphate buffer	[127]
Chemical hydrolysis rate	min <sup>-1</sup>	0.0196	-	pH=8; T=60°C phosphate buffer	[127]



Table S2.4: Extracted drug-dependent parameter literature values for simvastatin lactone (*continued*)

Parameter	Unit	Literature value	Standard deviation	Note	Reference
Chemical hydrolysis rate	min <sup>-1</sup>	1.667e-06	-	pH=3; T=40°C phosphate puffer estimated from graph	[127]
Chemical hydrolysis rate	min <sup>-1</sup>	6.667e-06	-	pH=5; T=40°C phosphate puffer estimated from graph	[127]
Chemical hydrolysis rate	min <sup>-1</sup>	2.667e-05	-	pH=6; T=40°C phosphate puffer estimated from graph	[127]
Chemical hydrolysis rate	min <sup>-1</sup>	0.0003433	-	pH=7; T=40°C phosphate puffer estimated from graph	[127]
Chemical hydrolysis rate	min <sup>-1</sup>	0.00159	-	pH=8; T=40°C phosphate puffer estimated from graph	[127]
Chemical hydrolysis rate	min <sup>-1</sup>	0.000433	0.01191	pH=6.8; T=37°C phosphate buffer saline	[28]
Chemical hydrolysis rate	min <sup>-1</sup>	0.0006828	0.01343	pH=7; T=37°C phosphate buffer saline	[28]
Chemical hydrolysis rate	min <sup>-1</sup>	0.0008445	0.01627	pH=7.2; T=37°C phosphate buffer saline	[28]
Chemical hydrolysis rate	min <sup>-1</sup>	0.0008983	0.03727	pH=7.4; T=37°C phosphate buffer saline	[28]
Chemical hydrolysis rate	min <sup>-1</sup>	0.001206	0.006918	pH=7.6; T=37°C phosphate buffer saline	[28]
Chemical hydrolysis rate	min <sup>-1</sup>	0.001129	0.00979	pH=7.8; T=37°C phosphate buffer saline	[28]
Chemical hydrolysis rate	min <sup>-1</sup>	0.0003164	0.002644	pH=6.8; T=37°C Human plasma	[28]
Chemical hydrolysis rate	min <sup>-1</sup>	0.0005424	0.004621	pH=7; T=37°C Human plasma	[28]
Chemical hydrolysis rate	min <sup>-1</sup>	0.0007989	0.003254	pH=7.2; T=37°C Human plasma	[28]
Chemical hydrolysis rate	min <sup>-1</sup>	0.001105	0.0304	pH=7.4; T=37°C Human plasma	[28]
Chemical hydrolysis rate	min <sup>-1</sup>	0.001261	0.006527	pH=7.6; T=37°C Human plasma	[28]
Chemical hydrolysis rate	min <sup>-1</sup>	0.001342	0.003418	pH=7.8; T=37°C Human plasma	[28]
Chemical hydrolysis rate	min <sup>-1</sup>	0.001067	-	pH=7.4	[39]
Plasma hydrolysis rate	l μmol <sup>-1</sup> min <sup>-1</sup>	0.0603	-	-	[128]
Specific intest. perm.	cm min <sup>-1</sup>	0.258	-	Effective permeability calculated from apparent permeability	[39]

*Note:*

If IC50 values could not be used for  $K_i$  value estimation utilizing Cheng Prusoff Equation (e.g. due to missing substrate affinities)  $K_i = IC50$  was assumed

Table S2.5: Drug-dependent parameters of the final simvastatin acid model compared to literature values

Parameter	Unit	Model value	Median (range) literature values	Origin	Description
<b>Molecule</b>					
BP	-	0.56	0.5741 (0.56–0.5882)	Calculated	Blood to plasma ratio after administration of 40 mg simvastatin lactone at steady-state (range 0.54–0.58)
fu	%	5.68	6.255 (5.48–9.61)	Literature	Fraction unbound plasma
Lipophilicity	-	1.45	3.82 (1.45–4.7)	Literature	Lipophilicity
MW	-	436.6	436.6	Literature	Molecular weight
pKa	-	4.2	4.205 (4.18–5.5)	Literature	Acid dissociation constant (acidic)
Solubility	mg l <sup>-1</sup>	13.09	45.1 (0.1263–51.5)	Literature	Solubility at pH=6.84
<b>Enzymes</b>					
CYP2C8 k <sub>cat</sub>	1/min	52.3	-	Literature	CYP2C8 catalytic rate constant (calculated from V <sub>max</sub> )
CYP2C8 K <sub>M</sub>	μmol l <sup>-1</sup>	38.55	38.55 (16–88)	Literature	CYP2C8 Michaelis-Menten constant
CYP3A4 k <sub>cat</sub>	1/min	31	-	Literature	CYP3A4 catalytic rate constant (calculated from V <sub>max</sub> )
CYP3A4 K <sub>M</sub>	μmol l <sup>-1</sup>	26	26 (21–29)	Literature	CYP3A4 Michaelis-Menten constant
UGT1A1 k <sub>cat</sub>	1/min	6.5	-	Literature	UGT1A1 catalytic rate constant (calculated from V <sub>max</sub> )
UGT1A1 K <sub>M</sub>	μmol l <sup>-1</sup>	349	349	Literature	UGT1A1 Michaelis-Menten constant
UGT1A3 k <sub>cat</sub>	1/min	6.5	-	Literature	UGT1A3 catalytic rate constant (calculated from V <sub>max</sub> )

Table S2.5: Drug-dependent parameters of the final simvastatin acid model compared to literature values (*continued*)

Parameter	Unit	Model value	Median (range) literature values	Origin	Description
UGT1A3 $K_M$	$\mu\text{mol l}^{-1}$	349	349	Literature	UGT1A3 Michaelis-Menten constant
<b>Transporters</b>					
OATP1B1 ( <i>SLCO1B1</i> ) $k_{\text{cat}}$ c.521CC	1/min	1.025	-	Optimized	OATP1B1 catalytic rate constant for c.521CC genotype
OATP1B1 ( <i>SLCO1B1</i> ) $k_{\text{cat}}$ c.521TC	1/min	5.637	-	Calculated	OATP1B1 catalytic rate constant for c.521TC genotype
OATP1B1 ( <i>SLCO1B1</i> ) $k_{\text{cat}}$ c.521TT	1/min	10.25	-	Optimized	OATP1B1 catalytic rate constant for c.521TT genotype
OATP1B1 ( <i>SLCO1B1</i> ) $K_M$	$\mu\text{mol l}^{-1}$	2	1.99 (1.17–2.53)	Literature	OATP1B1 Michaelis-Menten constant
OATP1B3 ( <i>SLCO1B3</i> ) $k_{\text{cat}}$	1/min	2.145	-	Optimized	OATP1B3 catalytic rate constant for c.521TT genotype
OATP1B3 ( <i>SLCO1B3</i> ) $K_M$	$\mu\text{mol l}^{-1}$	2	-	Assumed	OATP1B3 Michaelis-Menten constant
P-gp ( <i>ABCB1</i> ) $k_{\text{cat}}$	1/min	50	-	Optimized	P-gp catalytic rate constant for unknown genotype
P-gp ( <i>ABCB1</i> ) $k_{\text{cat}}$ c.1236Cc.- 2677G-c.3435C	1/min	4.64	-	Optimized	P-gp catalytic rate constant for c.1236Cc.-2677G-c.3435C genotype
P-gp ( <i>ABCB1</i> ) $k_{\text{cat}}$ c.1236Tc.- 2677T-c.3435T	1/min	50	-	Optimized	P-gp catalytic rate constant for c.1236Tc.-2677T-c.3435T genotype
P-gp ( <i>ABCB1</i> ) $K_M$	$\mu\text{mol l}^{-1}$	10	-	Assumed	P-gp Michaelis-Menten constant

**Inhibition**

Table S2.5: Drug-dependent parameters of the final simvastatin acid model compared to literature values (*continued*)

Parameter	Unit	Model value	Median (range) literature values	Origin	Description
$K_i$ BCRP ( <i>ABCG2</i> )	$\mu\text{mol l}^{-1}$	18	18	Literature	Concentration for half-maximal BCRP competitive inhibition
$K_i$ CYP2C8	$\mu\text{mol l}^{-1}$	41.1	41.1	Literature	Concentration for half-maximal CYP2C8 competitive inhibition
$K_i$ CYP3A4	$\mu\text{mol l}^{-1}$	69.6	56.1 (42.6–69.6)	Literature	Concentration for half-maximal CYP3A4 competitive inhibition
$K_i$ OATP1B1 ( <i>SLCO1B1</i> )	$\mu\text{mol l}^{-1}$	3.6	3.6	Literature	Concentration for half-maximal OATP1B1 competitive inhibition
<b>System</b>					
EHC	-	1	-	Assumed	Fraction of bile continually released from the gallbladder
GFR	-	1	-	Assumed	Fraction of filtered drug reaching the urine
Liver lactonization rate	$1 \mu\text{mol}^{-1} \text{min}^{-1}$	0.002433	-	Literature	Liver lactonization rate (calculated from liver S9 <a href="#">\cite{Tsamandouras2015}</a> )
Specific intest. perm.	$\text{cm min}^{-1}$	5.925e-07	-	Calculated	Permeation across intestinal mucosa normalized to surface area
Specific organ perm.	$\text{cm min}^{-1}$	0.0001171	-	Calculated	Permeation across cell membranes normalized to surface area

*Note:*

Cellular permeabilities calculation method: Schmitt; organ-plasma partition coefficient calculation method: Charge-dependent Schmitt normalized to PK-Sim

Table S2.6: Extracted drug-dependent parameter literature values for simvastatin acid

Parameter	Unit	Literature value	Standard deviation	Note	Reference
BP	-	0.5882	-	Blood to plasma ratio	[98]
BP	-	0.56	-	Blood to plasma ratio	[39]
fu	%	5.66	0.56	Human plasma - ligand concentration: 0.5 µg/ml	[99]
fu	%	5.92	0.22	Human plasma - ligand concentration: 1 µg/ml	[99]
fu	%	5.48	0.12	Human plasma - ligand concentration: 2 µg/ml	[99]
fu	%	5.68	0.17	Human plasma - ligand concentration: 4 µg/ml	[99]
fu	%	5.79	0.03	Human plasma - ligand concentration: 6 µg/ml	[99]
fu	%	9.61	0.7	Dog plasma - ligand concentration: 0.5 µg/ml	[99]
fu	%	8.35	0.22	Dog plasma - ligand concentration: 1 µg/ml	[99]
fu	%	6.96	0.2	Dog plasma - ligand concentration: 2 µg/ml	[99]
fu	%	6.59	0.1	Dog plasma - ligand concentration: 4 µg/ml	[99]
fu	%	7.32	0.007	Dog plasma - ligand concentration: 6 µg/ml	[99]
Lipophilicity	-	3.85	-	Calculated	[102]
Lipophilicity	-	4.22	-	Calculated	[129]
Lipophilicity	-	3.79	-	Calculated	[129]
Lipophilicity	-	1.8	-	logD pH=7	[130]
Lipophilicity	-	4.7	-	LogP	[98]
Lipophilicity	-	2.1	-	logD pH=7.0	[98]
Lipophilicity	-	1.45	-	logD pH=7.4	[39]
Lipophilicity	-	4.54	-	LogP	[39]
MW	-	436.6	-	Calculated	[129]
pKa	-	4.21	-	-	[129]
pKa	-	4.2	-	-	[130]
pKa	-	5.5	-	-	[98]
pKa	-	4.18	-	-	[131]

Table S2.6: Extracted drug-dependent parameter literature values for simvastatin acid (*continued*)

Parameter	Unit	Literature value	Standard deviation	Note	Reference
Solubility	mg l <sup>-1</sup>	51.5	-	Intrinsic solubility	[102]
Solubility	mg l <sup>-1</sup>	50	-	pH=1.7	[102]
Solubility	mg l <sup>-1</sup>	40.2	-	Calculated	[129]
Solubility	mg l <sup>-1</sup>	0.1263	0.000842	pH=6.84	[58]
CL <sub>int</sub> CYP2C8	μl min <sup>-1</sup> mg <sup>-1</sup> mic.protein	9.4	-	Human liver microsomes	[132]
CL <sub>int</sub> CYP3A4	μl min <sup>-1</sup> mg <sup>-1</sup> mic.protein	57	-	Human liver microsomes	[132]
CL <sub>int</sub>	μl min <sup>-1</sup> mg <sup>-1</sup> mic.protein	55	-	Human liver microsomes	[132]
CYP2C8 K <sub>M</sub>	μmol l <sup>-1</sup>	88	-	CYP2C8 - 3',5'-dihydrodiol SV	[132]
CYP2C8 K <sub>M</sub>	μmol l <sup>-1</sup>	36	-	CYP2C8 - 3'-hydroxy SV	[132]
CYP2C8 K <sub>M</sub>	μmol l <sup>-1</sup>	16	-	CYP2C8 - 6'-exomethylene SV	[132]
CYP3A4 K <sub>M</sub>	μmol l <sup>-1</sup>	21	-	CYP3A4 - 6'-exomethylene SA	[133]
CYP3A4 K <sub>M</sub>	μmol l <sup>-1</sup>	26	-	CYP3A4 - 3',5'-dihydrodiol SA	[132]
CYP3A4 K <sub>M</sub>	μmol l <sup>-1</sup>	29	-	CYP3A4 - 3'-hydroxy SA	[132]
K <sub>i</sub> CYP2C8	pmol mg <sup>-1</sup> mic.protein	41.1	-	K <sub>i</sub>	[32]
K <sub>M</sub>	μmol l <sup>-1</sup>	76	35	human liver microsomes - 3',5'-dihydrodiol SA	[132]
K <sub>M</sub>	μmol l <sup>-1</sup>	47	12	human liver microsomes - 3' - hydroxy SA	[132]
K <sub>M</sub>	μmol l <sup>-1</sup>	47	21	human liver microsomes - 6'-exomethylene SA	[132]
UGT1A1 K <sub>M</sub>	μmol l <sup>-1</sup>	349	-	Human liver microsomes corrected for fumic (0.8341)	[133]
UGT1A1 protein expression	pmol mg <sup>-1</sup> mic.protein	33.2	-	-	[134]
UGT1A1 protein expression	pmol mg <sup>-1</sup> mic.protein	18.3	-	-	[134]
UGT1A1 protein expression	pmol mg <sup>-1</sup> mic.protein	124	-	-	[134]
UGT1A1 protein expression	pmol mg <sup>-1</sup> mic.protein	21.7	-	-	[134]
UGT1A1 protein expression	pmol mg <sup>-1</sup> mic.protein	20.2	-	-	[134]
UGT1A1 protein expression	pmol mg <sup>-1</sup> mic.protein	33.6	-	-	[134]
UGT1A1 protein expression	pmol mg <sup>-1</sup> mic.protein	31.7	-	-	[134]
UGT1A1 protein expression	pmol mg <sup>-1</sup> mic.protein	34.3	-	-	[134]
UGT1A3 K <sub>M</sub>	μmol l <sup>-1</sup>	349	-	Human liver microsomes corrected for fumic (0.8341)	[133]
UGT1A3 protein expression	pmol mg <sup>-1</sup> mic.protein	17.3	-	-	[134]
UGT1A3 protein expression	pmol mg <sup>-1</sup> mic.protein	9.9	-	-	[134]

Table S2.6: Extracted drug-dependent parameter literature values for simvastatin acid (*continued*)

Parameter	Unit	Literature value	Standard deviation	Note	Reference
UGT1A3 protein expression	pmol mg <sup>-1</sup> mic.protein	20.6	-	-	[134]
UGT1A3 protein expression	pmol mg <sup>-1</sup> mic.protein	0.4	-	-	[134]
UGT1A3 protein expression	pmol mg <sup>-1</sup> mic.protein	123.1	-	-	[134]
UGT1A3 protein expression	pmol mg <sup>-1</sup> mic.protein	8.2	-	-	[134]
UGT1A3 protein expression	pmol mg <sup>-1</sup> mic.protein	6.3	-	-	[134]
OATP1B1 ( <i>SLCO1B1</i> ) K <sub>M</sub>	μmol l <sup>-1</sup>	2.09	1	1a	[135]
OATP1B1 ( <i>SLCO1B1</i> ) K <sub>M</sub>	μmol l <sup>-1</sup>	1.99	1.02	2b	[135]
OATP1B1 ( <i>SLCO1B1</i> ) K <sub>M</sub>	μmol l <sup>-1</sup>	1.69	2.58	5	[135]
OATP1B1 ( <i>SLCO1B1</i> ) K <sub>M</sub>	μmol l <sup>-1</sup>	1.17	1.67	15	[135]
OATP1B1 ( <i>SLCO1B1</i> ) K <sub>M</sub>	μmol l <sup>-1</sup>	2.53	1.38	18	[135]
OATP3A1 ( <i>SLCO3A1</i> ) K <sub>M</sub>	μmol l <sup>-1</sup>	0.017	0.002	-	[136]
CYP2C8 K <sub>M</sub>	μmol l <sup>-1</sup>	41.1	-	-	[32]
K <sub>i</sub> BCRP ( <i>ABCG2</i> )	μmol l <sup>-1</sup>	18	-	K <sub>i</sub>	[38]
K <sub>i</sub> CYP3A4	μmol l <sup>-1</sup>	69.6	5.2	K <sub>i</sub>	[31]
K <sub>i</sub> CYP3A4	μmol l <sup>-1</sup>	42.6	4.3	IC50	[137]
K <sub>i</sub> OATP1B1 ( <i>SLCO1B1</i> )	μmol l <sup>-1</sup>	3.6	-	IC50	[35]

*Note:*

If IC50 values could not be used for K<sub>i</sub> value estimation utilizing Cheng Prusoff Equation (e.g. due to missing substrate affinities) K<sub>i</sub> = IC50 was assumed

## 2.3 Simvastatin model evaluation

For simvastatin model evaluation various graphical and statistical evaluation techniques were used. Figures S2.4–S2.26 display the VPCs for the training and test dataset used for model development and evaluation. Figure S2.27 and S2.28 show the predicted versus observed plasma-concentration time values for the training and test dataset, respectively. Figures S2.29–S2.32 compare the calculated predicted versus observed NCA values the training and test data. In addition, Tables S2.7 and S2.8 summarize statistical quality measures like MRD, MSA and GMFE. Finally, Fig. S2.33 shows the results of the performed sensitivity analysis.

### 2.3.1 Profiles



2 PBPK modeling of simvastatin

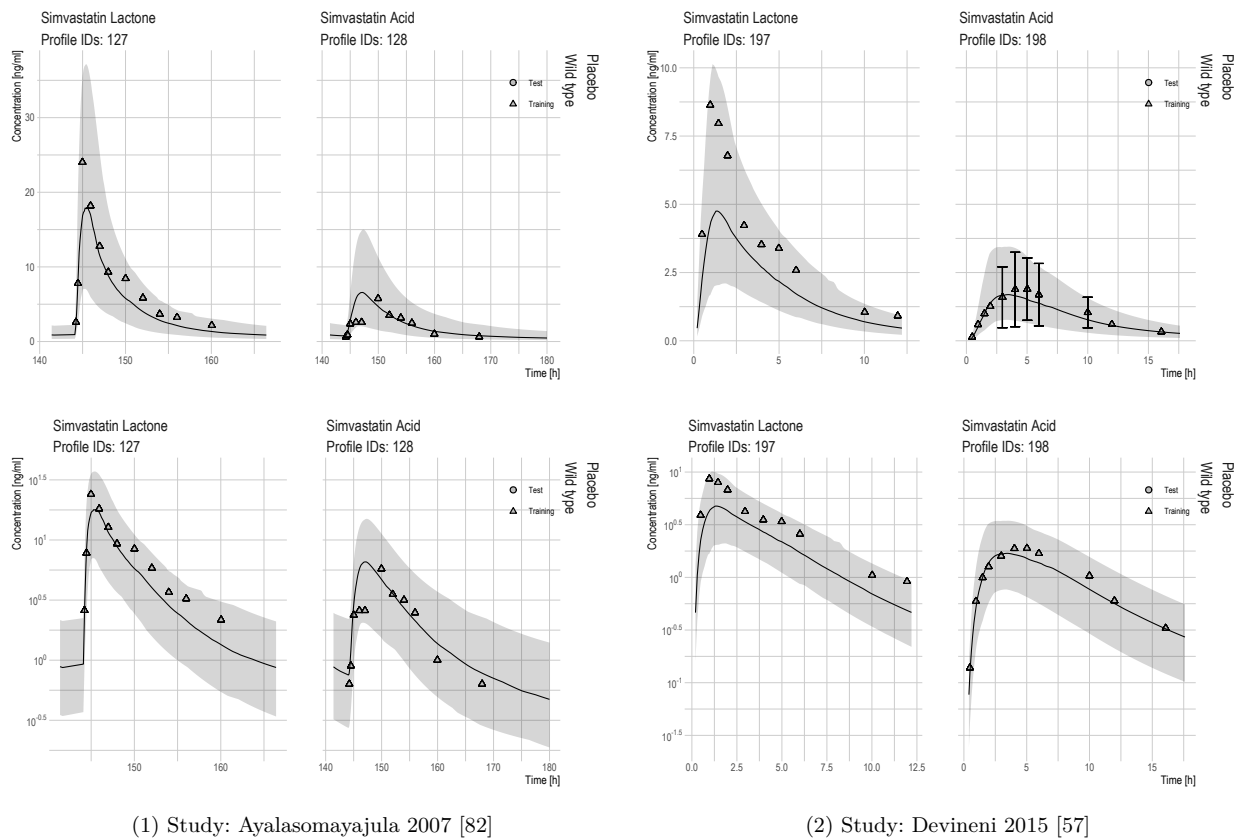


Figure S2.4: Linear and semi-logarithmic VPCs of the plasma concentration-time values in the training dataset. Solid line and shaded area are predicted median and 90 % CI: Ayalasomayajula 2007 [82], Devineni 2015 [57]

2 PBPK modeling of simvastatin

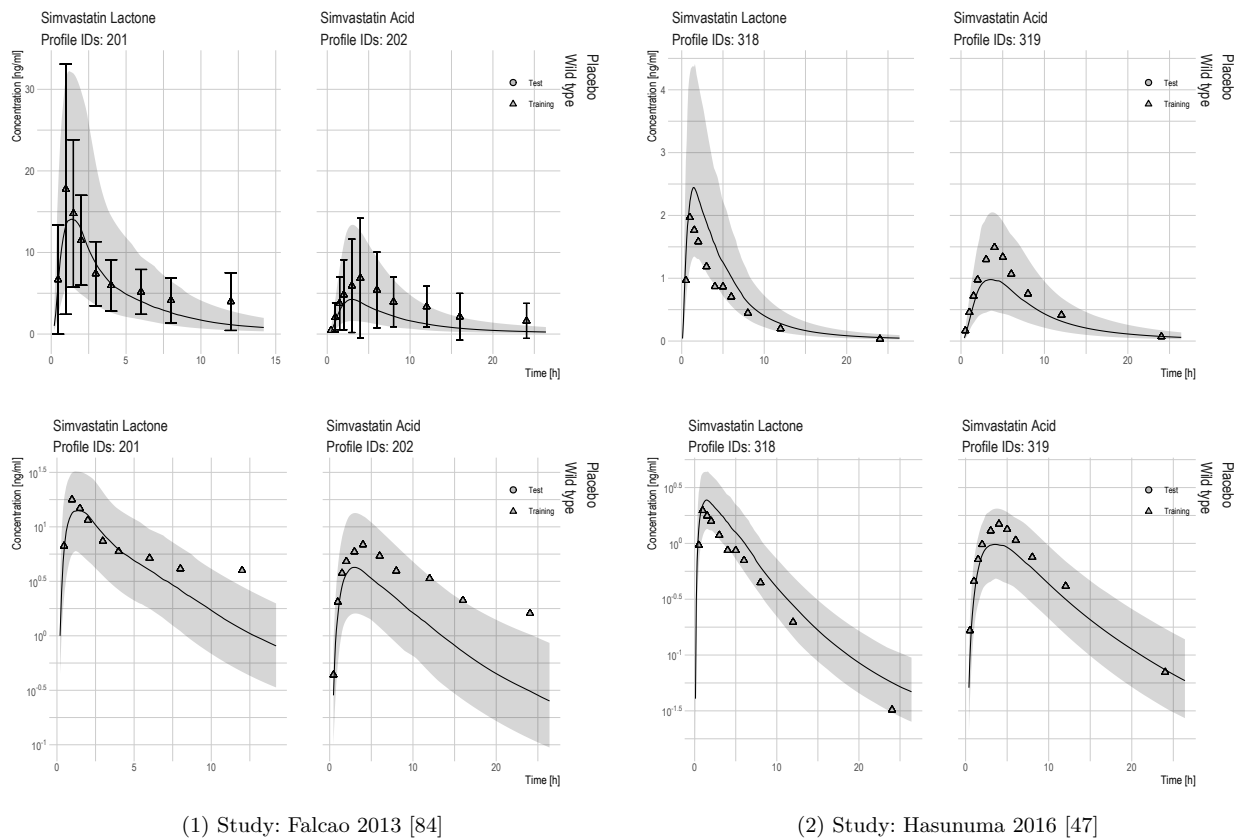


Figure S2.5: Linear and semi-logarithmic VPCs of the plasma concentration-time values in the training dataset. Solid line and shaded area are predicted median and 90 % CI: Falcao 2013 [84], Hasunuma 2016 [47]

2 PBPK modeling of simvastatin

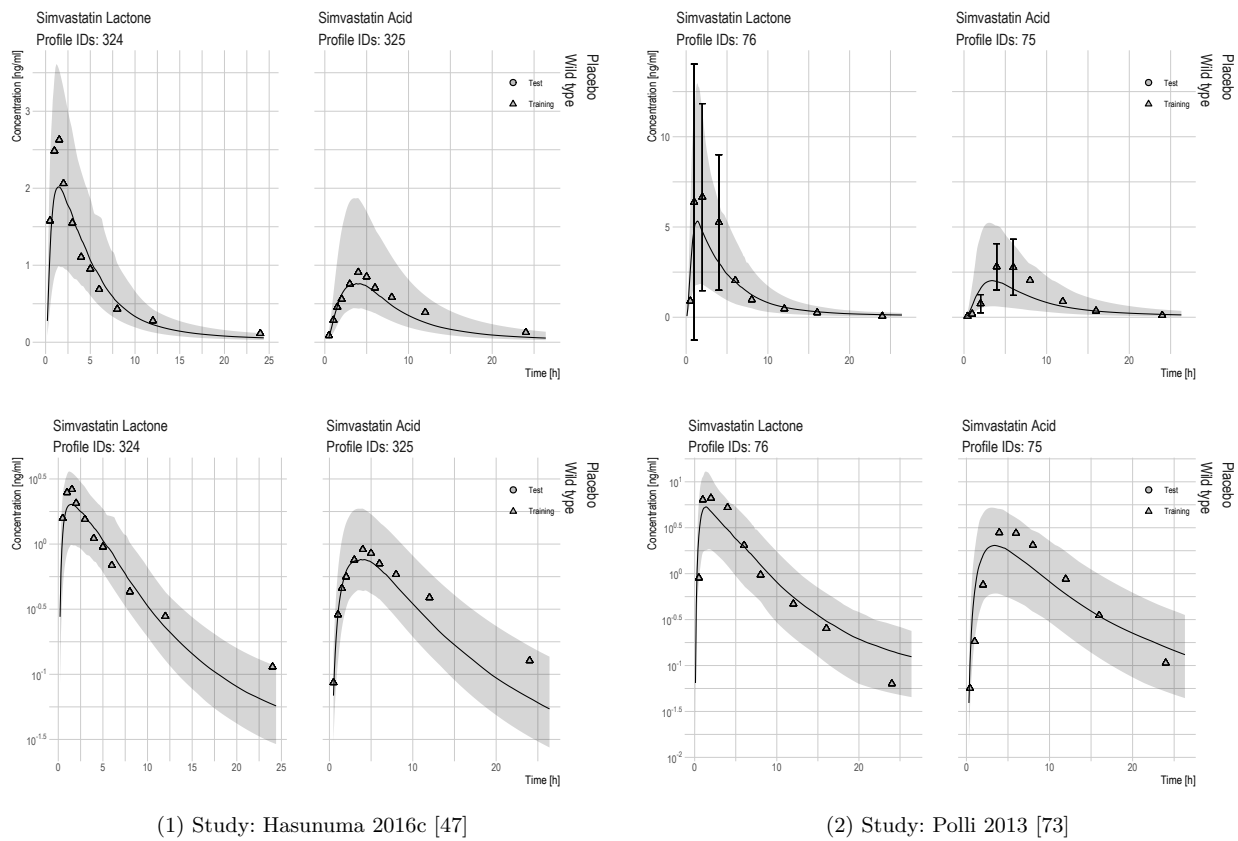


Figure S2.6: Linear and semi-logarithmic VPCs of the plasma concentration-time values in the training dataset. Solid line and shaded area are predicted median and 90 % CI: Hasunuma 2016c [47], Polli 2013 [73]

2 PBPK modeling of simvastatin

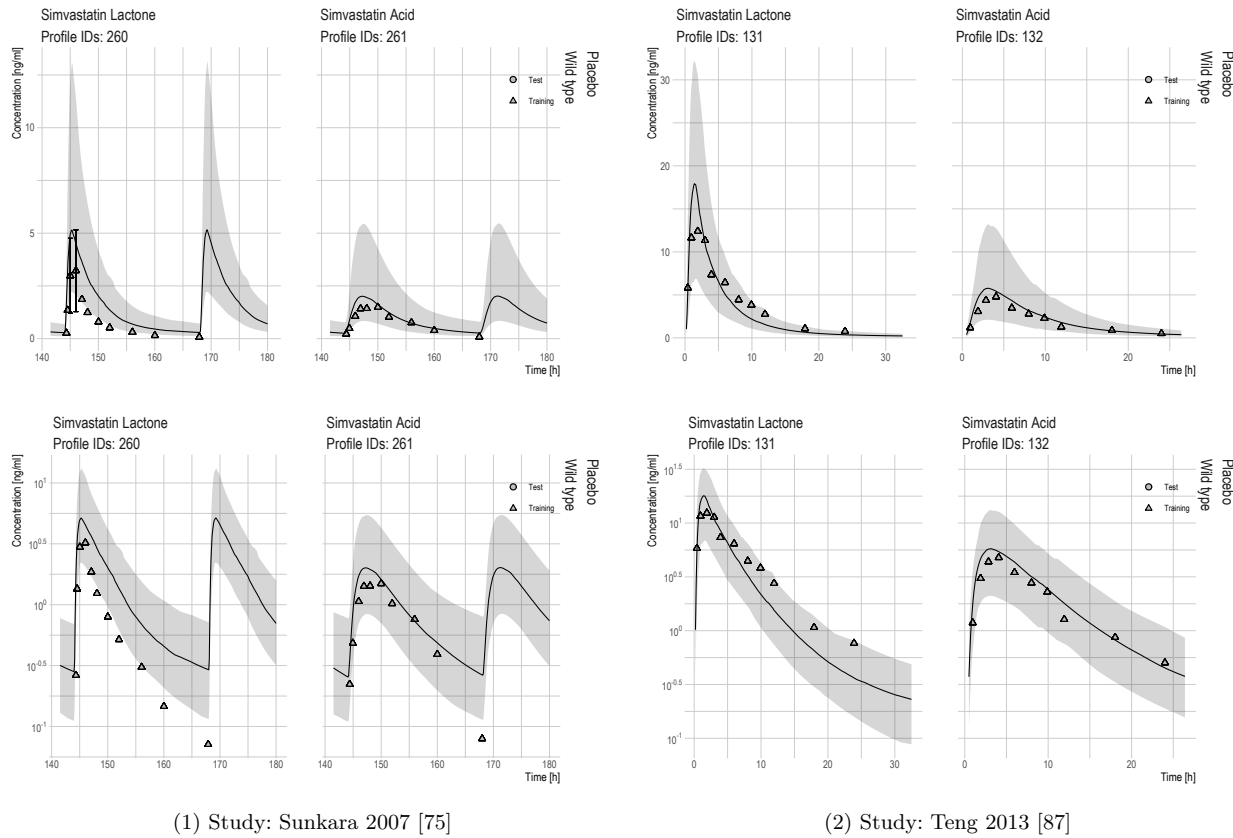


Figure S2.7: Linear and semi-logarithmic VPCs of the plasma concentration-time values in the training dataset. Solid line and shaded area are predicted median and 90 % CI: Sunkara 2007 [75], Teng 2013 [87]

2 PBPK modeling of simvastatin

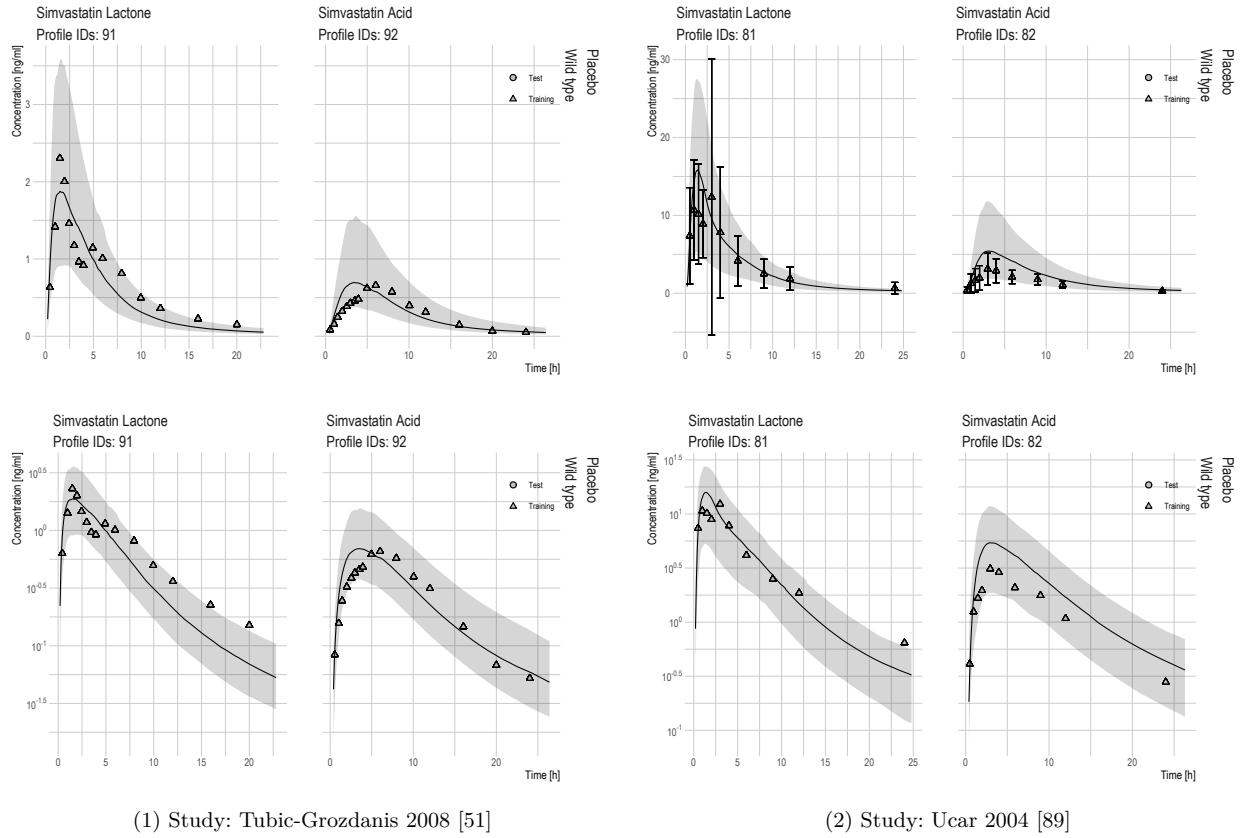


Figure S2.8: Linear and semi-logarithmic VPCs of the plasma concentration-time values in the training dataset. Solid line and shaded area are predicted median and 90 % CI: Tubic-Grozdanic 2008 [51], Ucar 2004 [89]

## 2 PBPK modeling of simvastatin

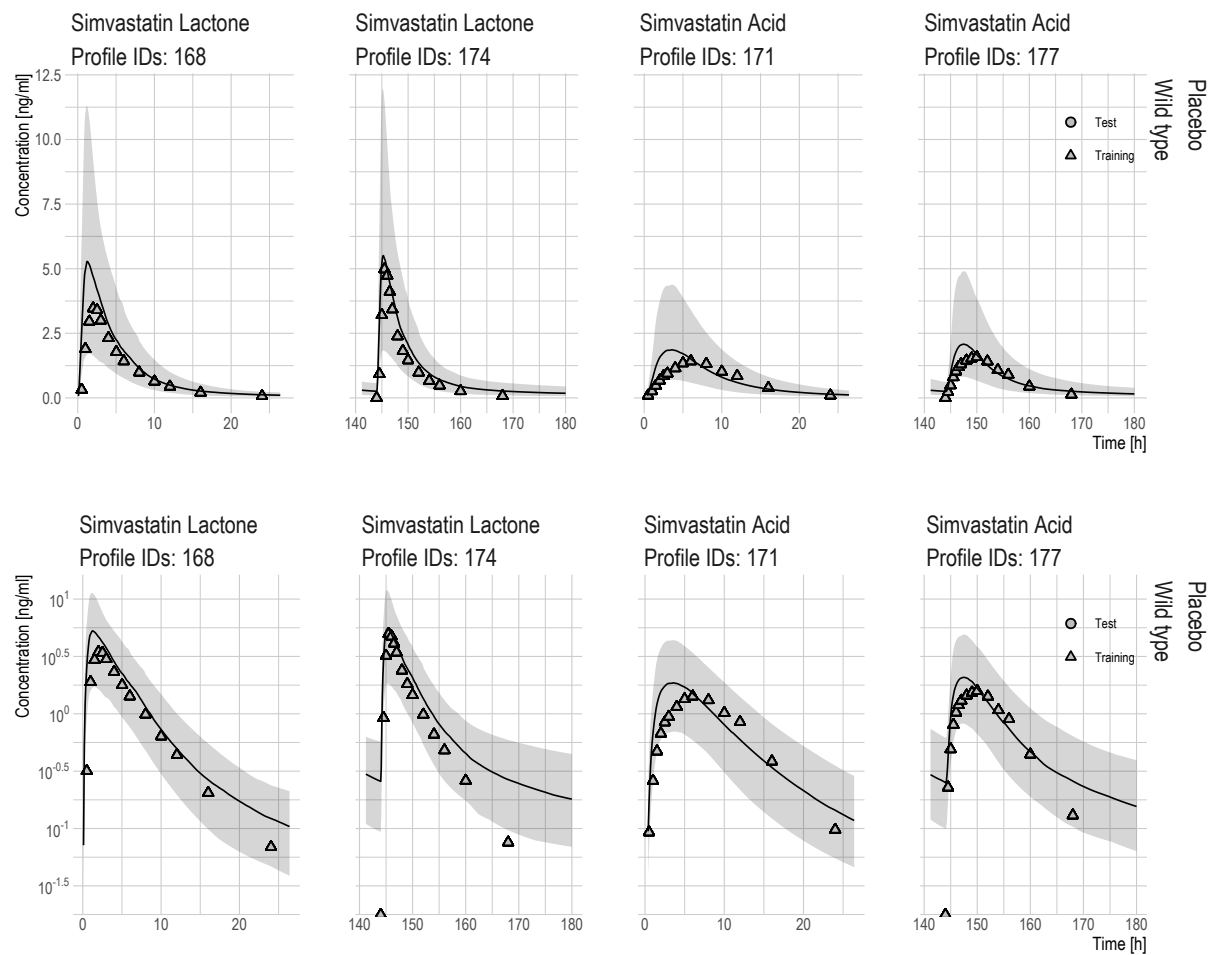


Figure S2.9: Linear and semi-logarithmic VPCs of the plasma concentration-time values in the training dataset. Solid line and shaded area are predicted median and 90% CI: Winsemius 2014 [77]

## 2 PBPK modeling of simvastatin

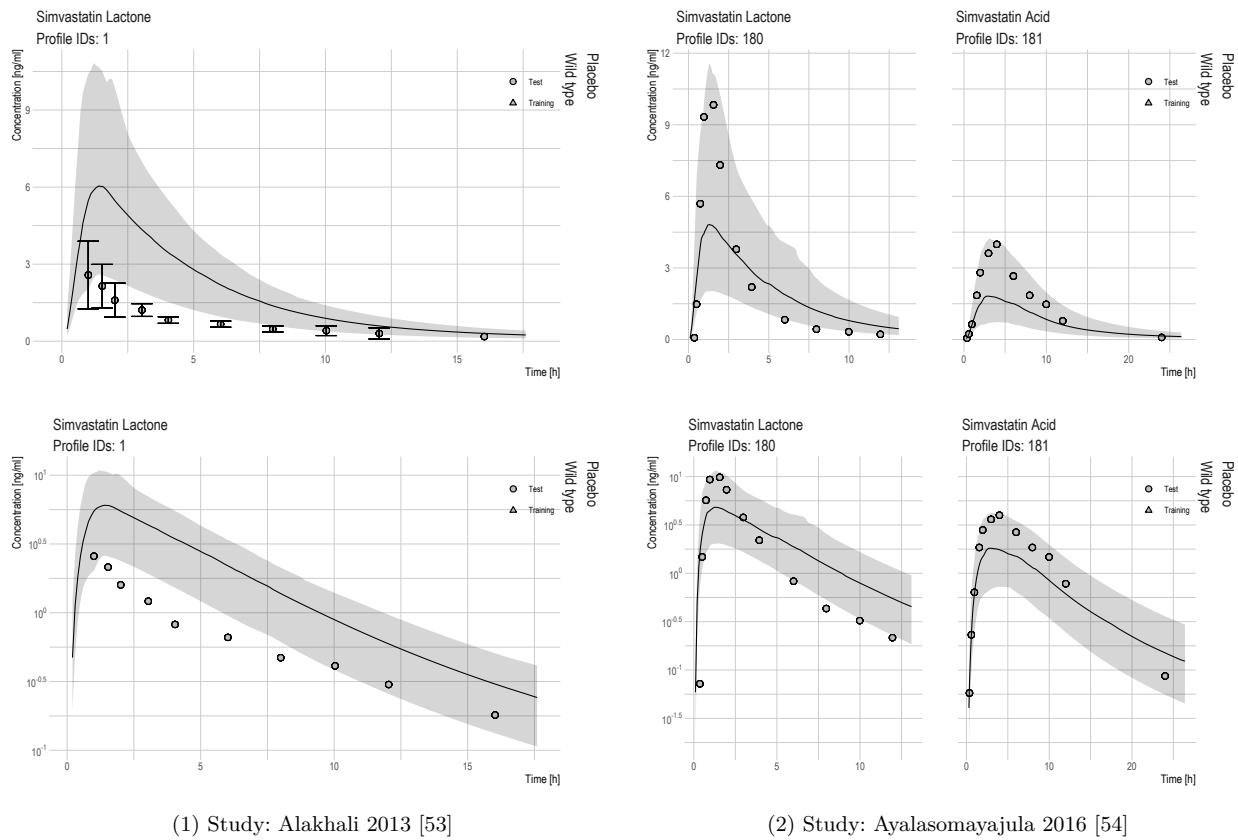


Figure S2.10: Linear and semi-logarithmic VPCs of the plasma concentration-time values in the test dataset. Solid line and shaded area are predicted median and 90 % CI: Alakhali 2013 [53], Ayalasomayajula 2016 [54]

2 PBPK modeling of simvastatin

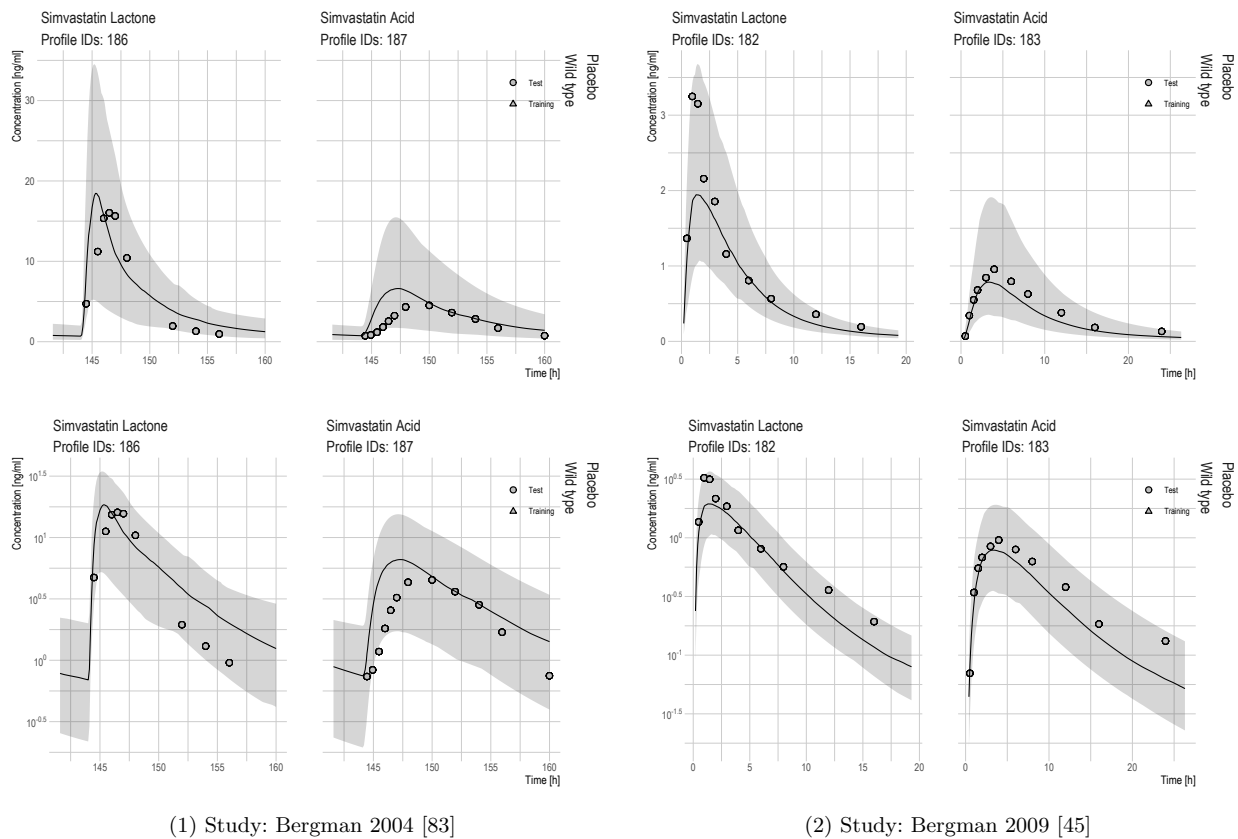


Figure S2.11: Linear and semi-logarithmic VPCs of the plasma concentration-time values in the test dataset. Solid line and shaded area are predicted median and 90 % CI: Bergman 2004 [83], Bergman 2009 [45]



## 2 PBPK modeling of simvastatin

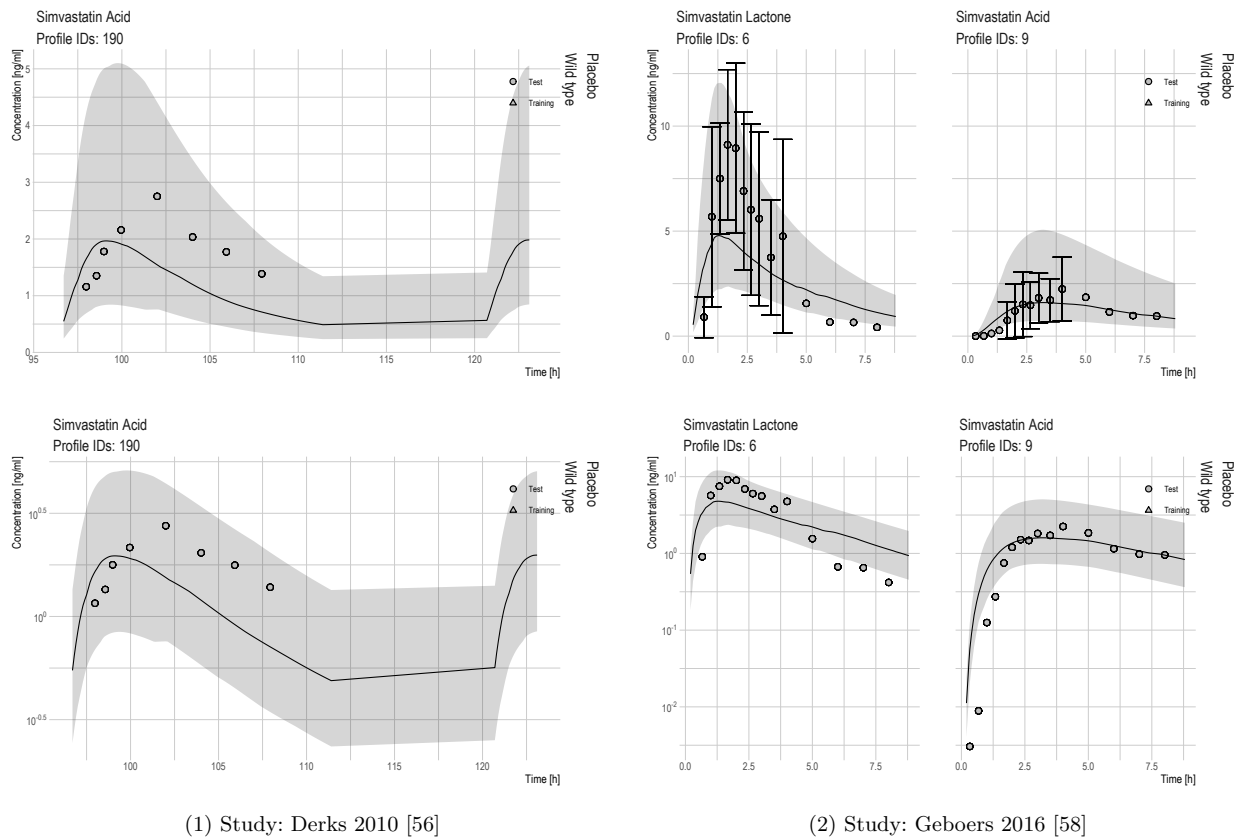


Figure S2.12: Linear and semi-logarithmic VPCs of the plasma concentration-time values in the test dataset. Solid line and shaded area are predicted median and 90 % CI: Derks 2010 [56], Geboers 2016 [58]

2 PBPK modeling of simvastatin

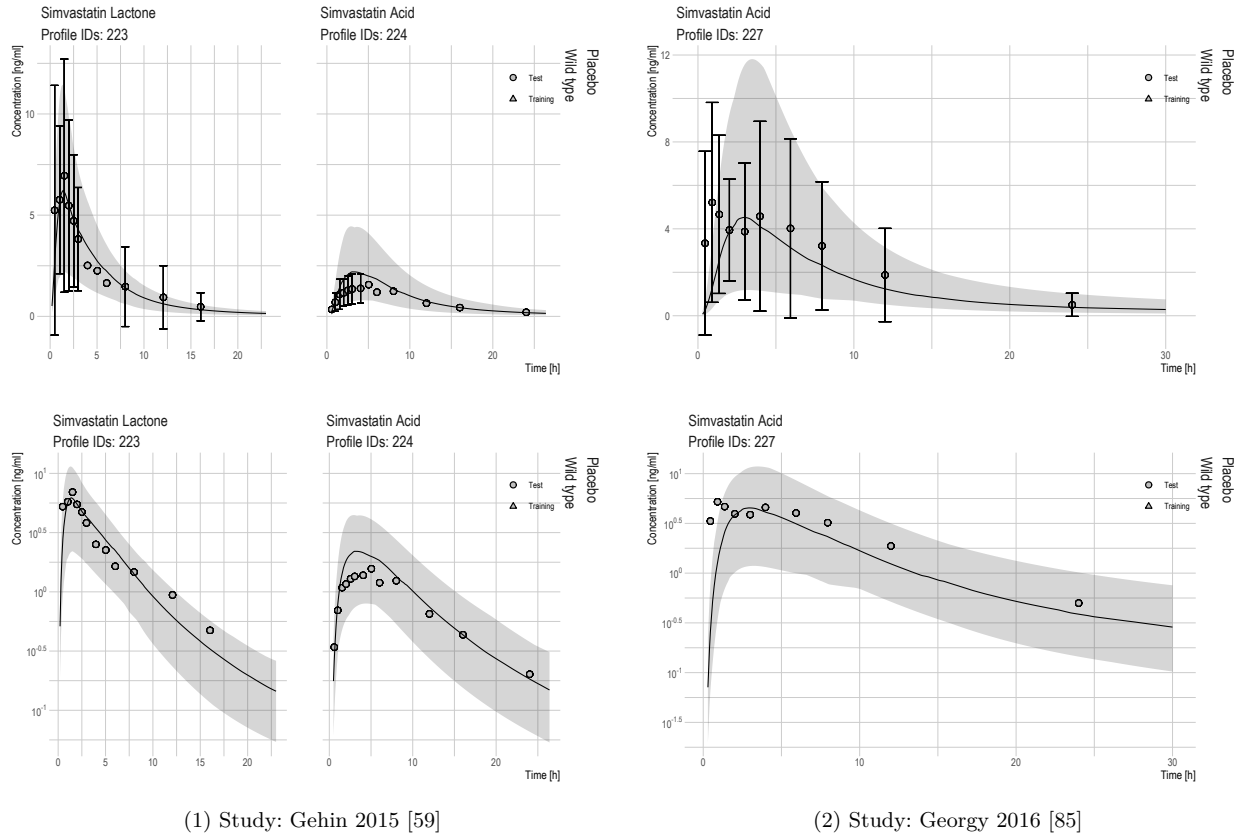


Figure S2.13: Linear and semi-logarithmic VPCs of the plasma concentration-time values in the test dataset. Solid line and shaded area are predicted median and 90 % CI: Gehin 2015 [59], Georgy 2016 [85]

2 PBPK modeling of simvastatin

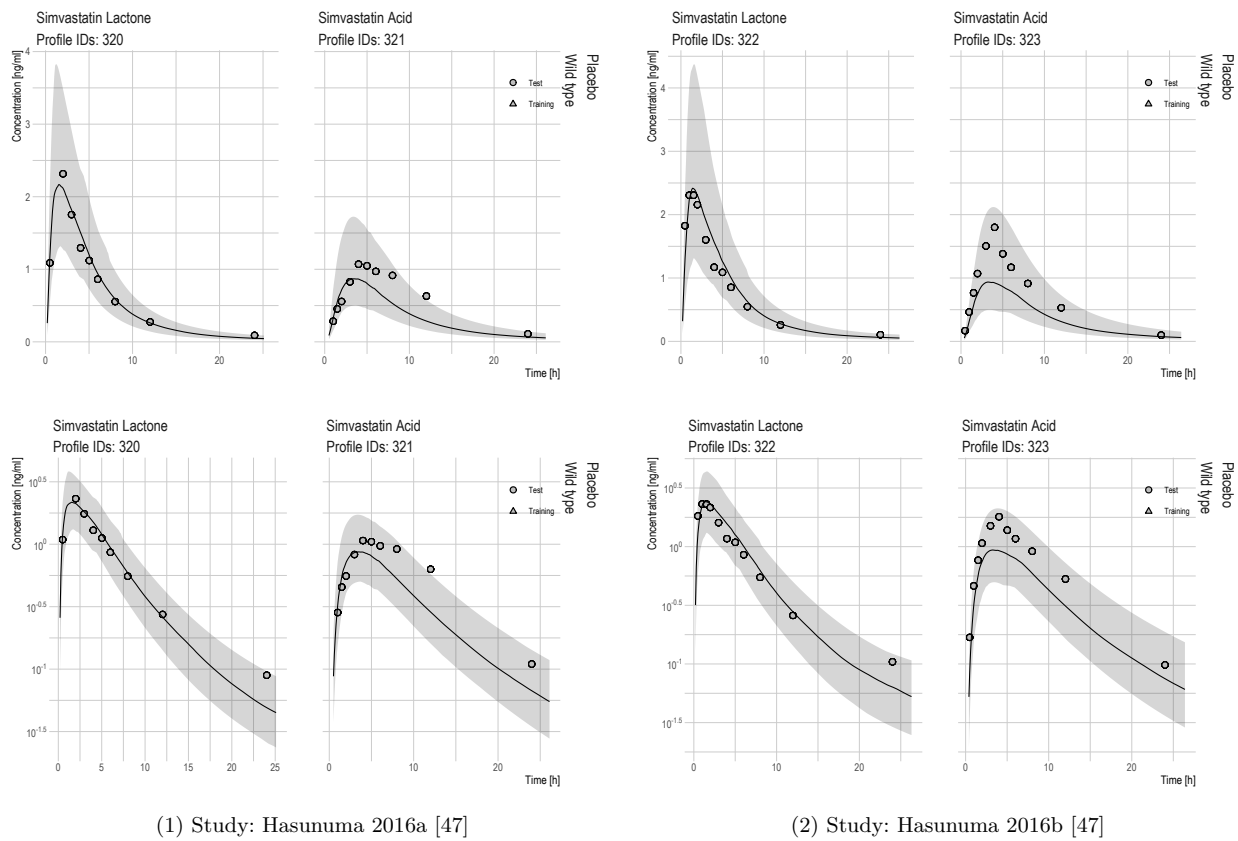


Figure S2.14: Linear and semi-logarithmic VPCs of the plasma concentration-time values in the test dataset. Solid line and shaded area are predicted median and 90 % CI: Hasunuma 2016a [47], Hasunuma 2016b [47]

2 PBPK modeling of simvastatin

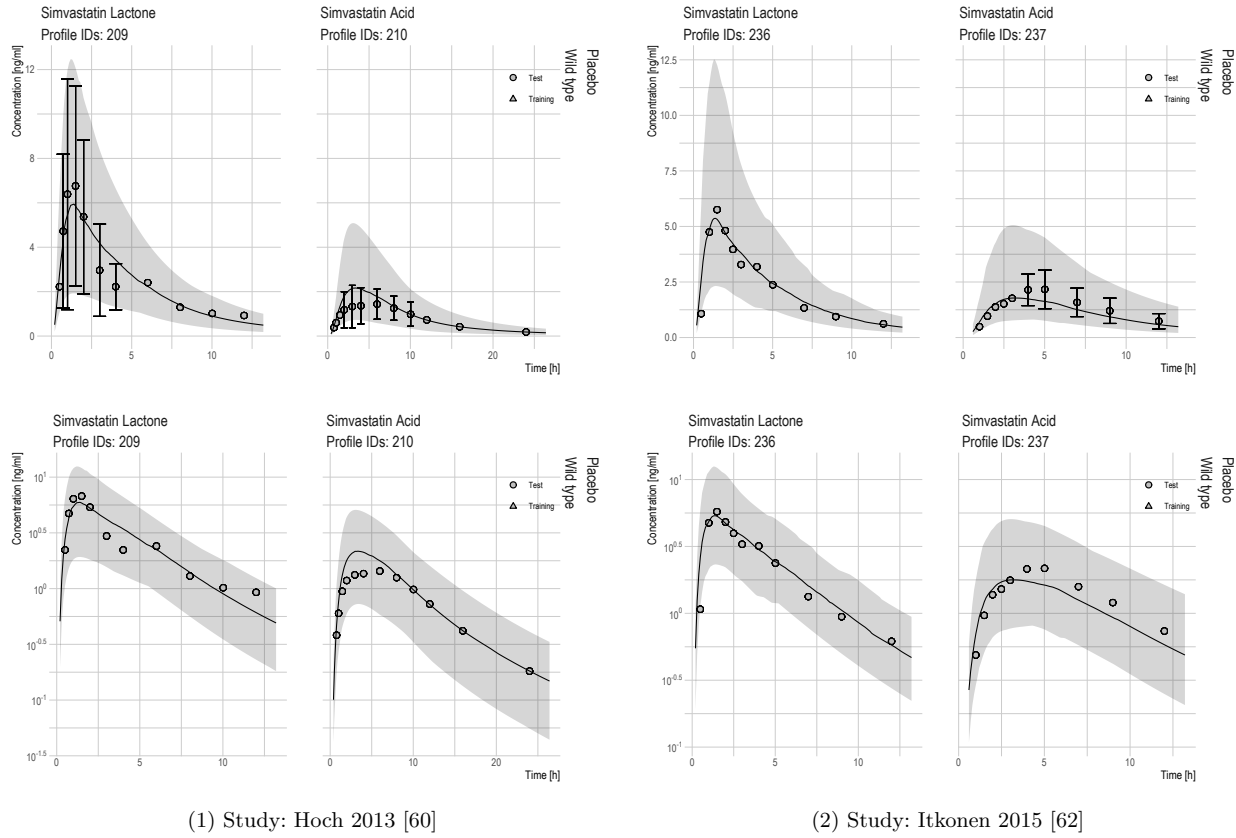


Figure S2.15: Linear and semi-logarithmic VPCs of the plasma concentration-time values in the test dataset. Solid line and shaded area are predicted median and 90 % CI: Hoch 2013 [60], Itkonen 2015 [62]

2 PBPK modeling of simvastatin

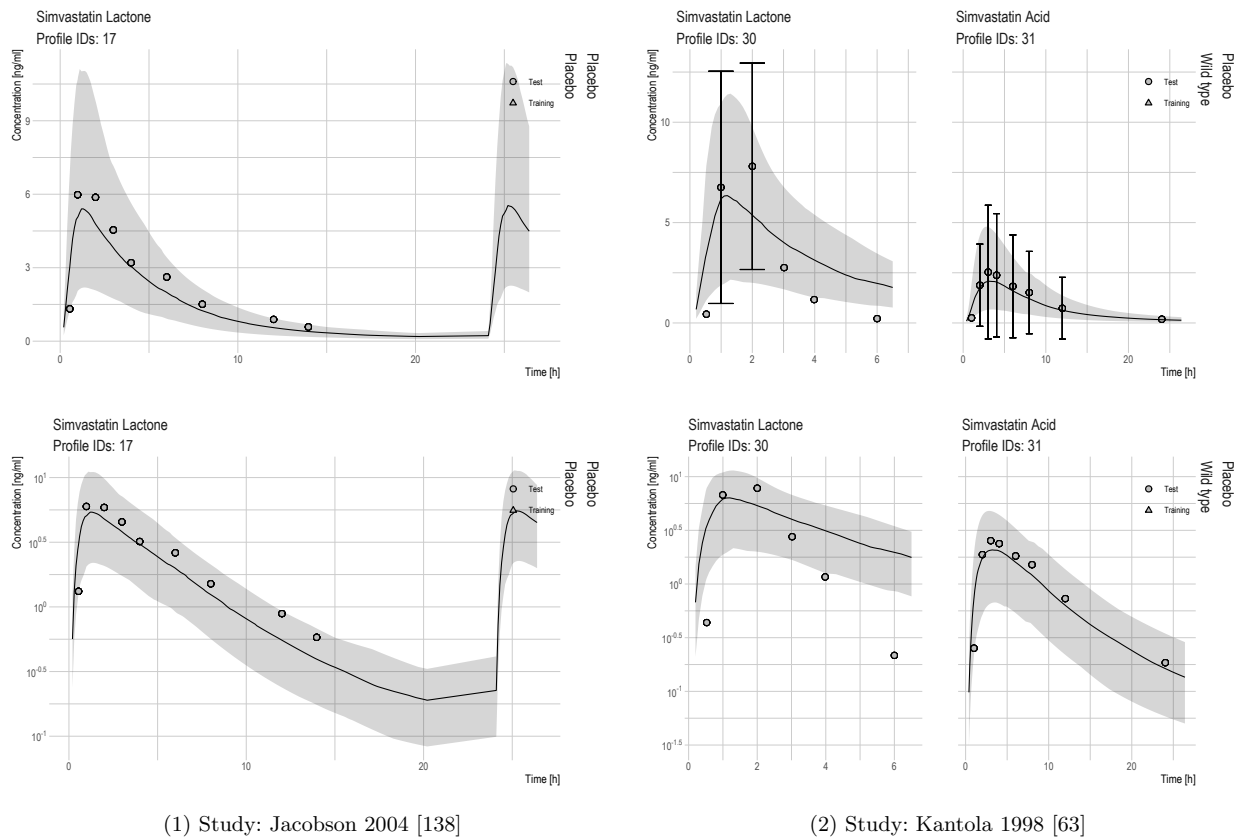


Figure S2.16: Linear and semi-logarithmic VPCs of the plasma concentration-time values in the test dataset. Solid line and shaded area are predicted median and 90 % CI: Jacobson 2004 [138], Kantola 1998 [63]

2 PBPK modeling of simvastatin

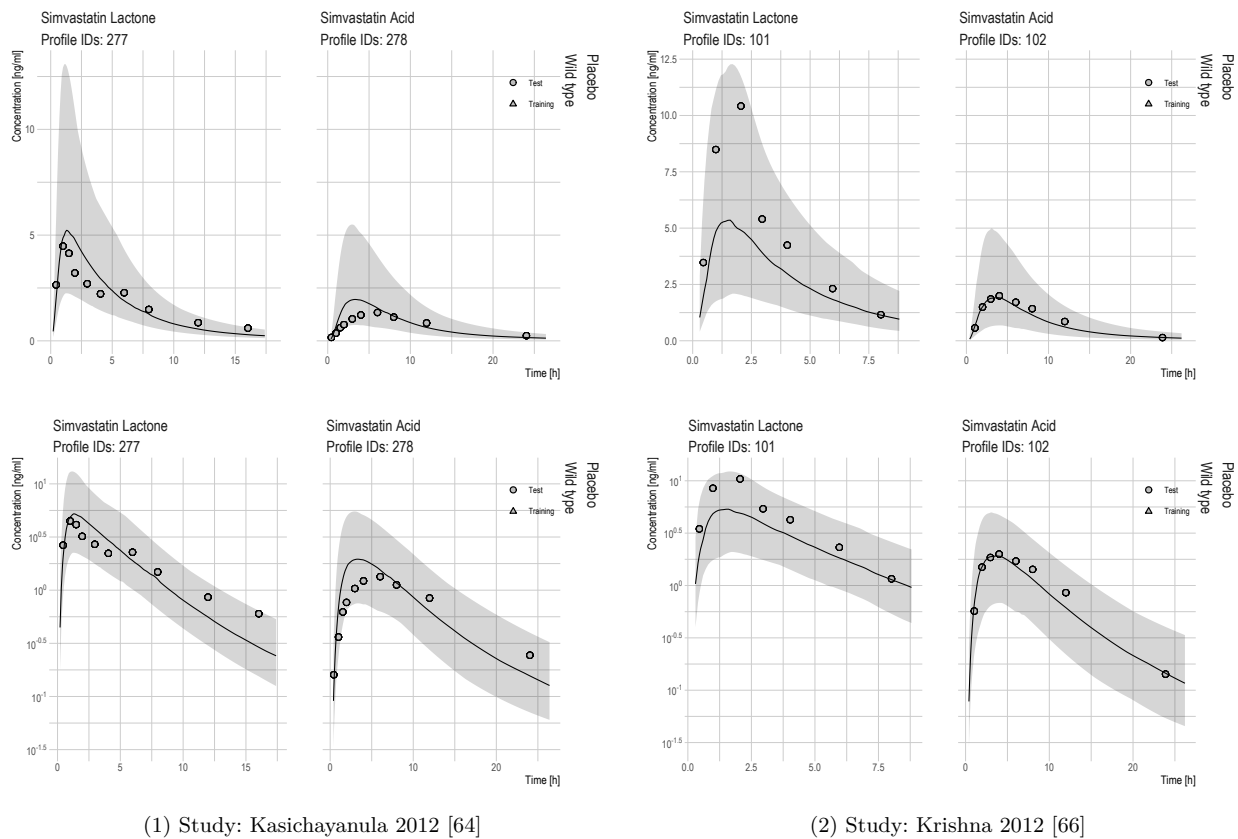


Figure S2.17: Linear and semi-logarithmic VPCs of the plasma concentration-time values in the test dataset. Solid line and shaded area are predicted median and 90 % CI: Kasichayanula 2012 [64], Krishna 2012 [66]

## 2 PBPK modeling of simvastatin

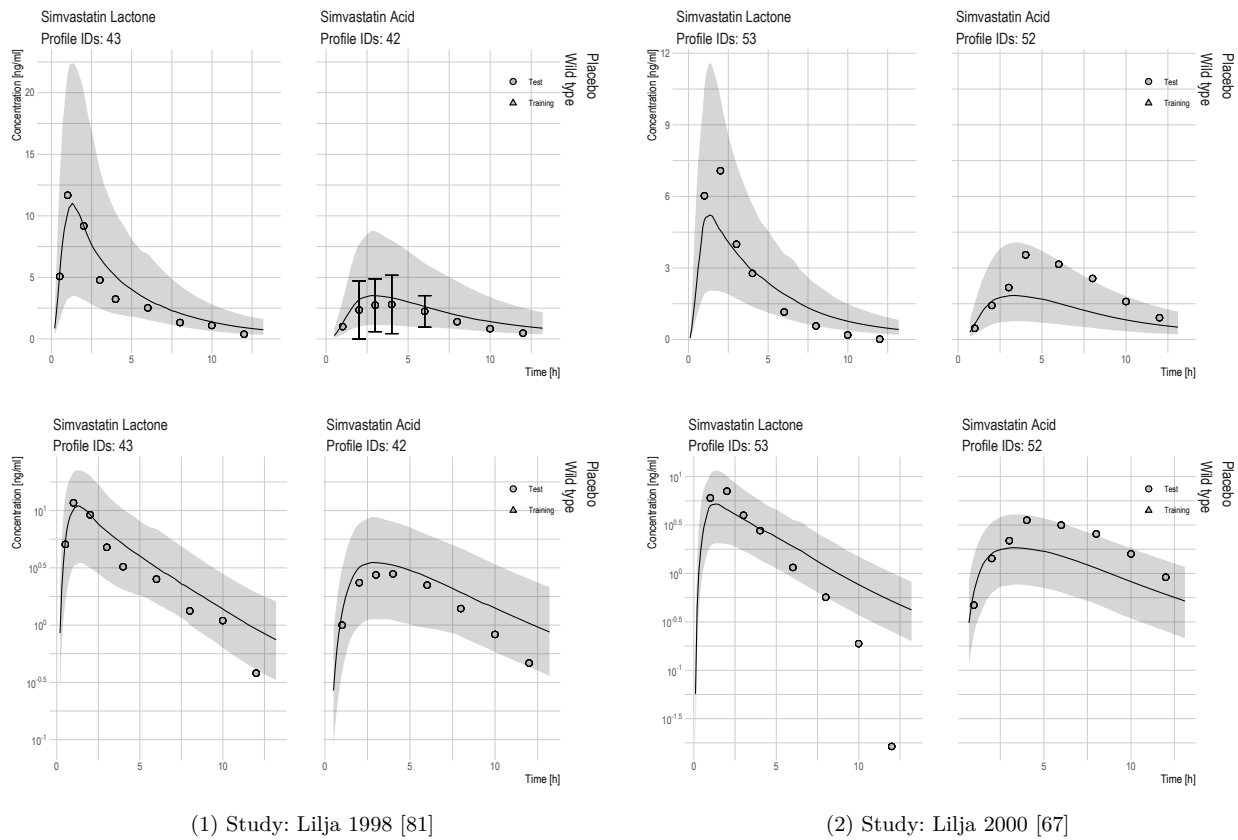


Figure S2.18: Linear and semi-logarithmic VPCs of the plasma concentration-time values in the test dataset. Solid line and shaded area are predicted median and 90 % CI: Lilja 1998 [81], Lilja 2000 [67]

2 PBPK modeling of simvastatin

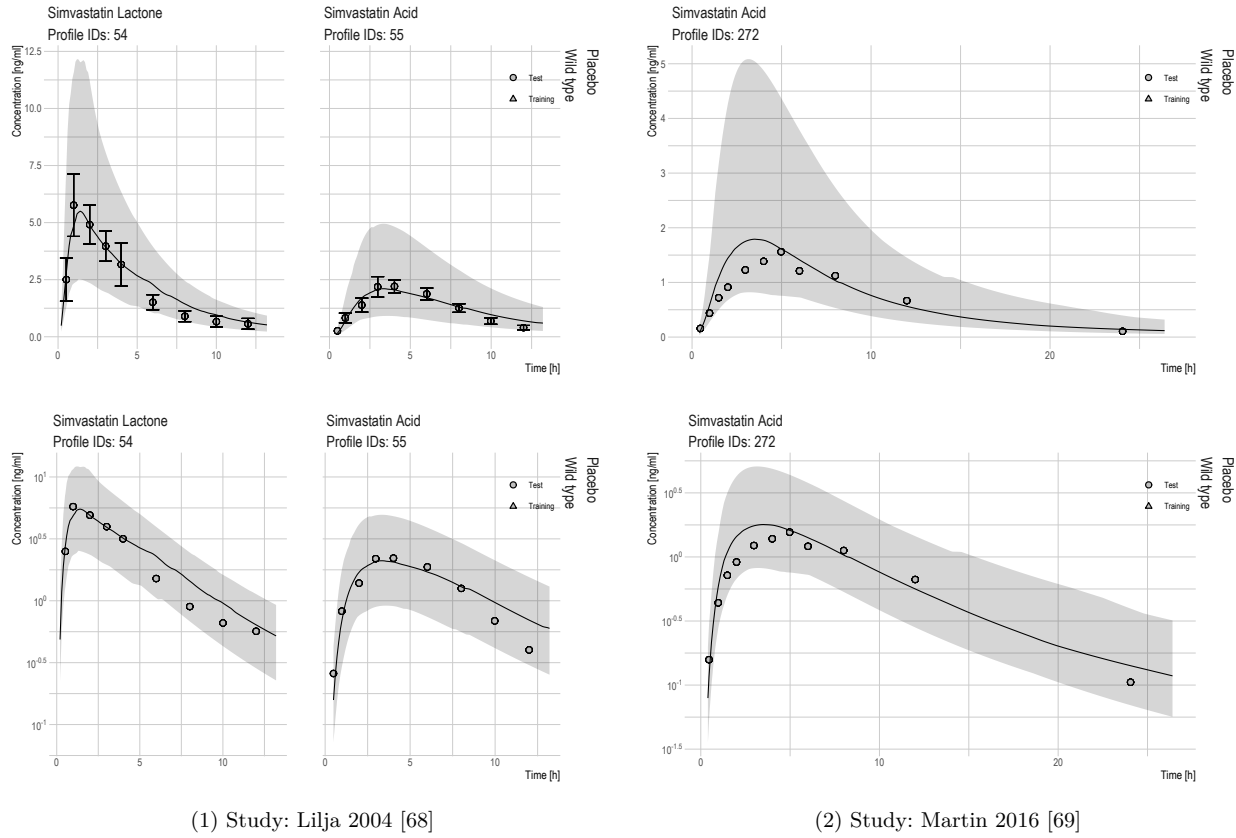


Figure S2.19: Linear and semi-logarithmic VPCs of the plasma concentration-time values in the test dataset. Solid line and shaded area are predicted median and 90 % CI: Lilja 2004 [68], Martin 2016 [69]



2 PBPK modeling of simvastatin

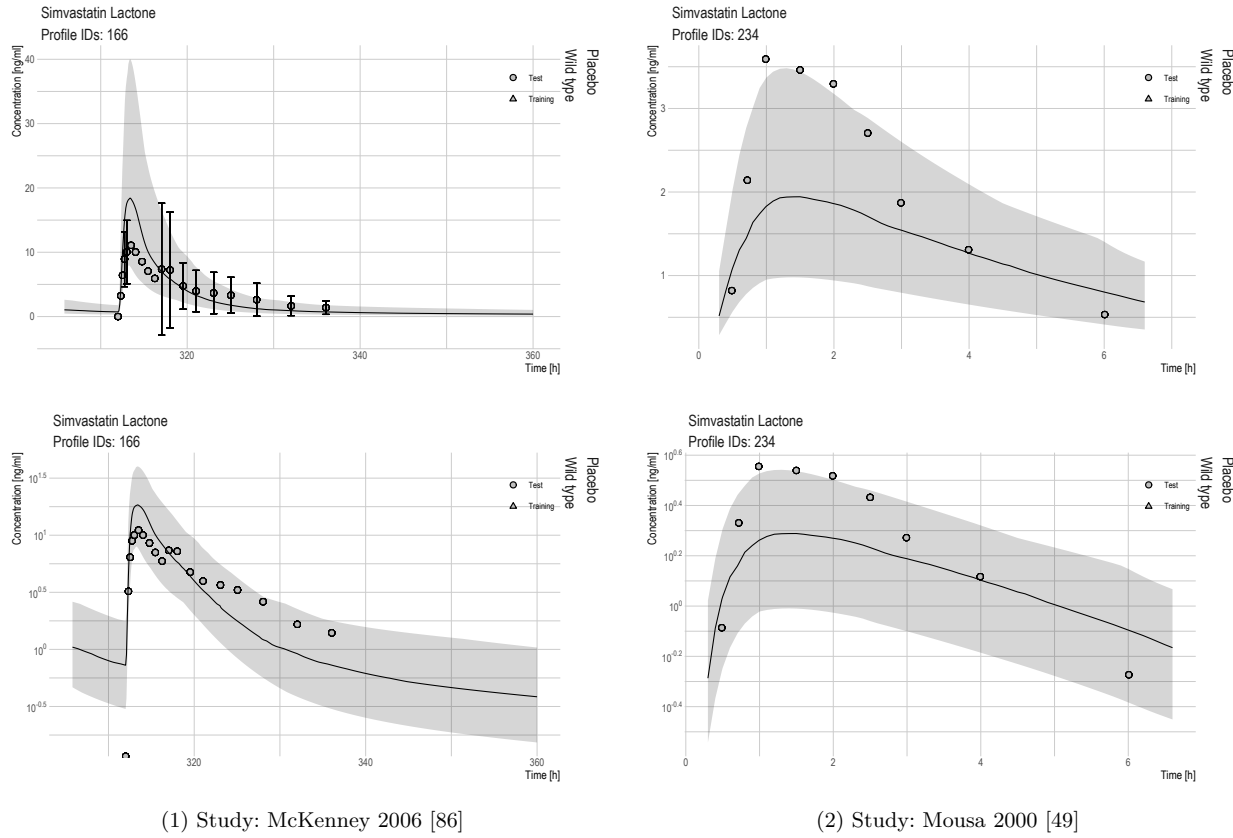


Figure S2.20: Linear and semi-logarithmic VPCs of the plasma concentration-time values in the test dataset. Solid line and shaded area are predicted median and 90 % CI: McKenney 2006 [86], Mousa 2000 [49]

2 PBPK modeling of simvastatin

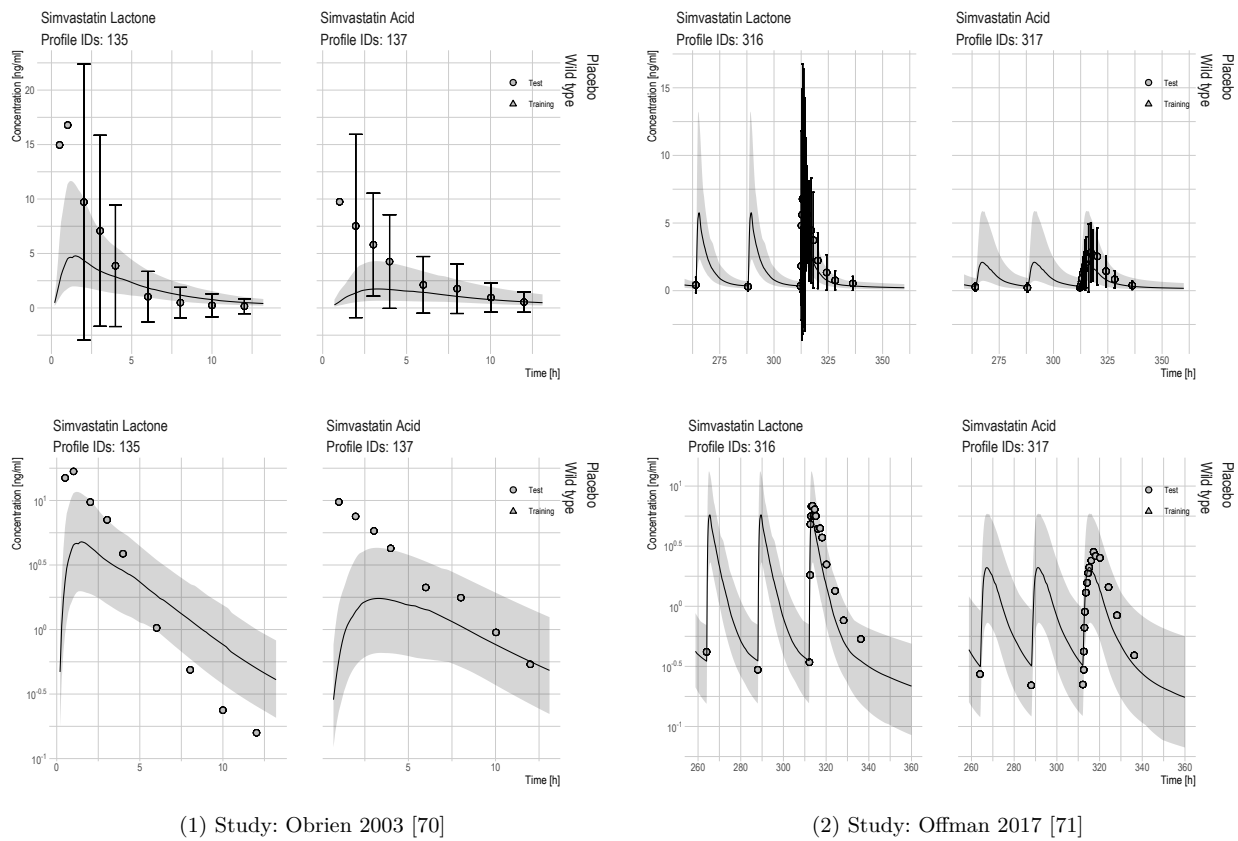


Figure S2.21: Linear and semi-logarithmic VPCs of the plasma concentration-time values in the test dataset. Solid line and shaded area are predicted median and 90 % CI: O'Brien 2003 [70], Offman 2017 [71]

2 PBPK modeling of simvastatin

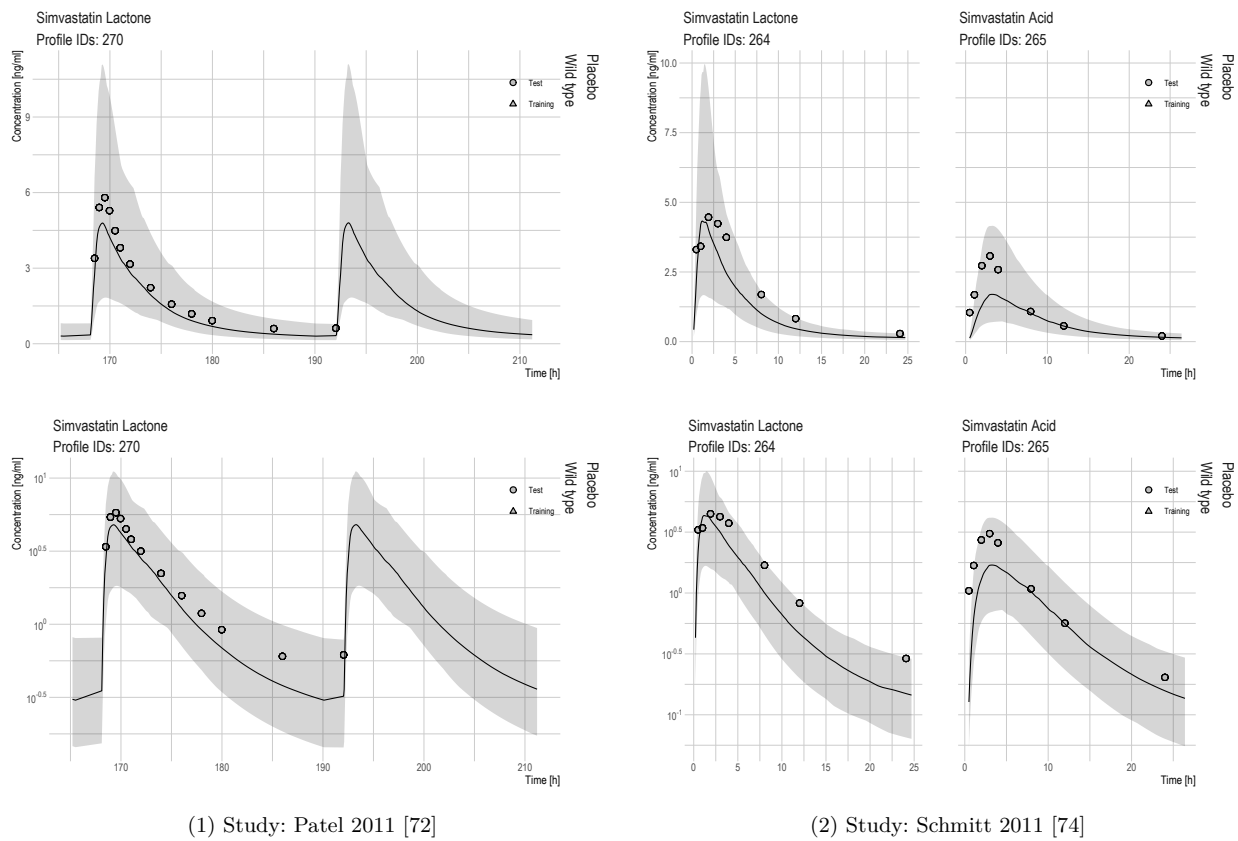
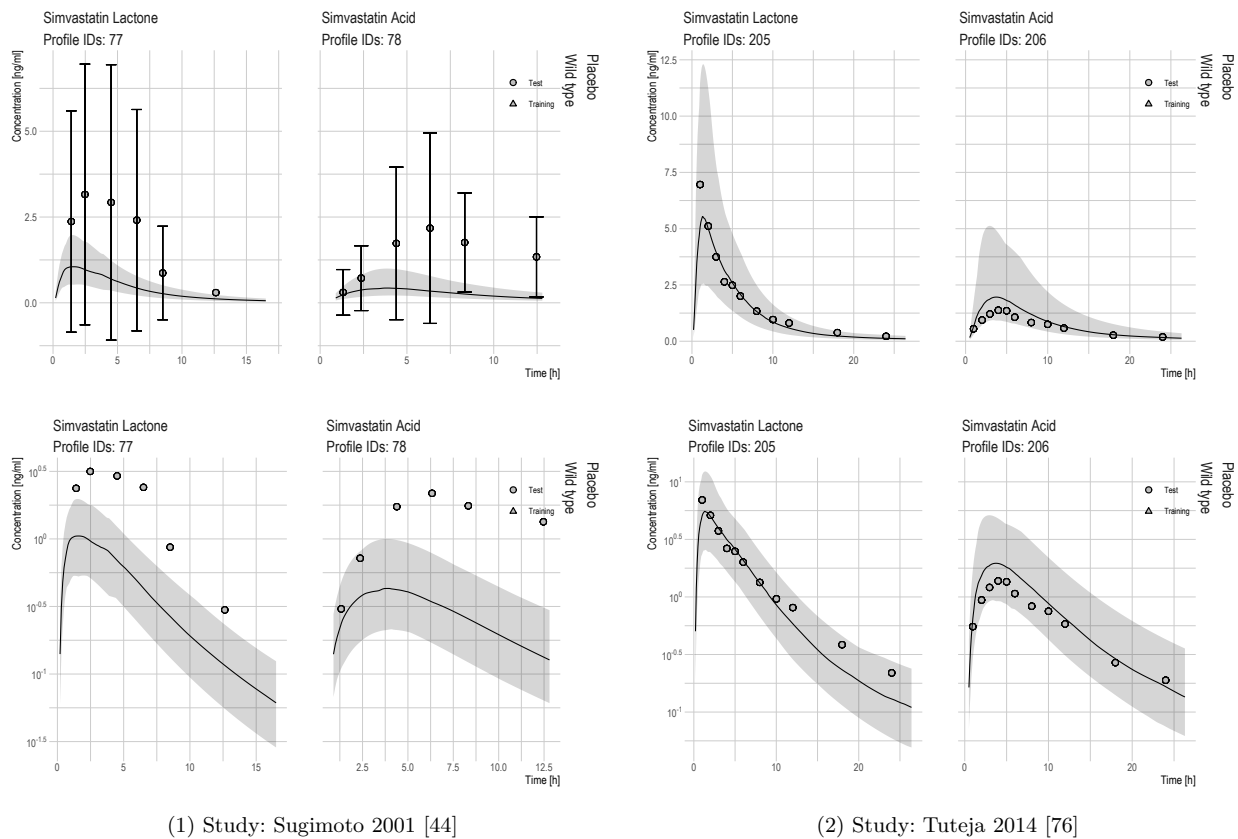


Figure S2.22: Linear and semi-logarithmic VPCs of the plasma concentration-time values in the test dataset. Solid line and shaded area are predicted median and 90 % CI: Patel 2011 [72], Schmitt 2011 [74]

2 PBPK modeling of simvastatin



60

Figure S2.23: Linear and semi-logarithmic VPCs of the plasma concentration-time values in the test dataset. Solid line and shaded area are predicted median and 90 % CI: Sugimoto 2001 [44], Tuteja 2014 [76]

2 PBPK modeling of simvastatin

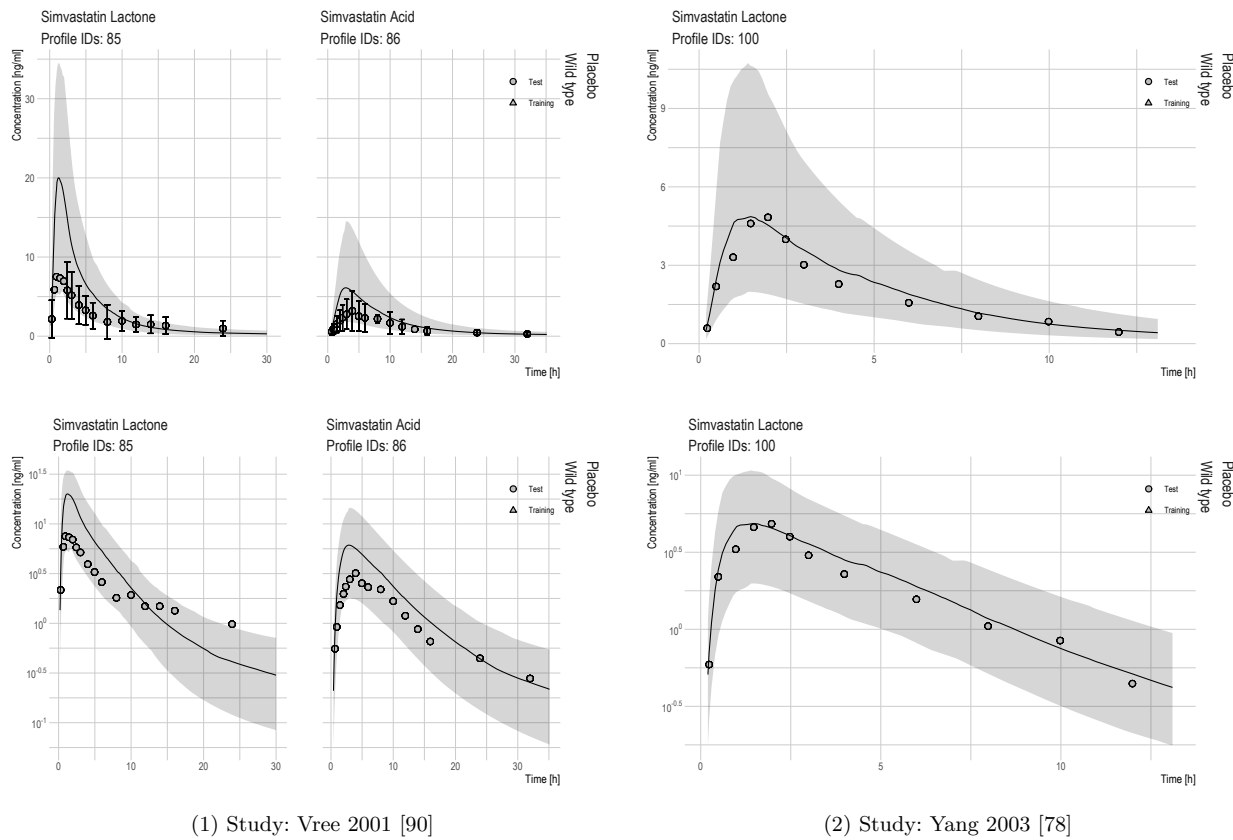
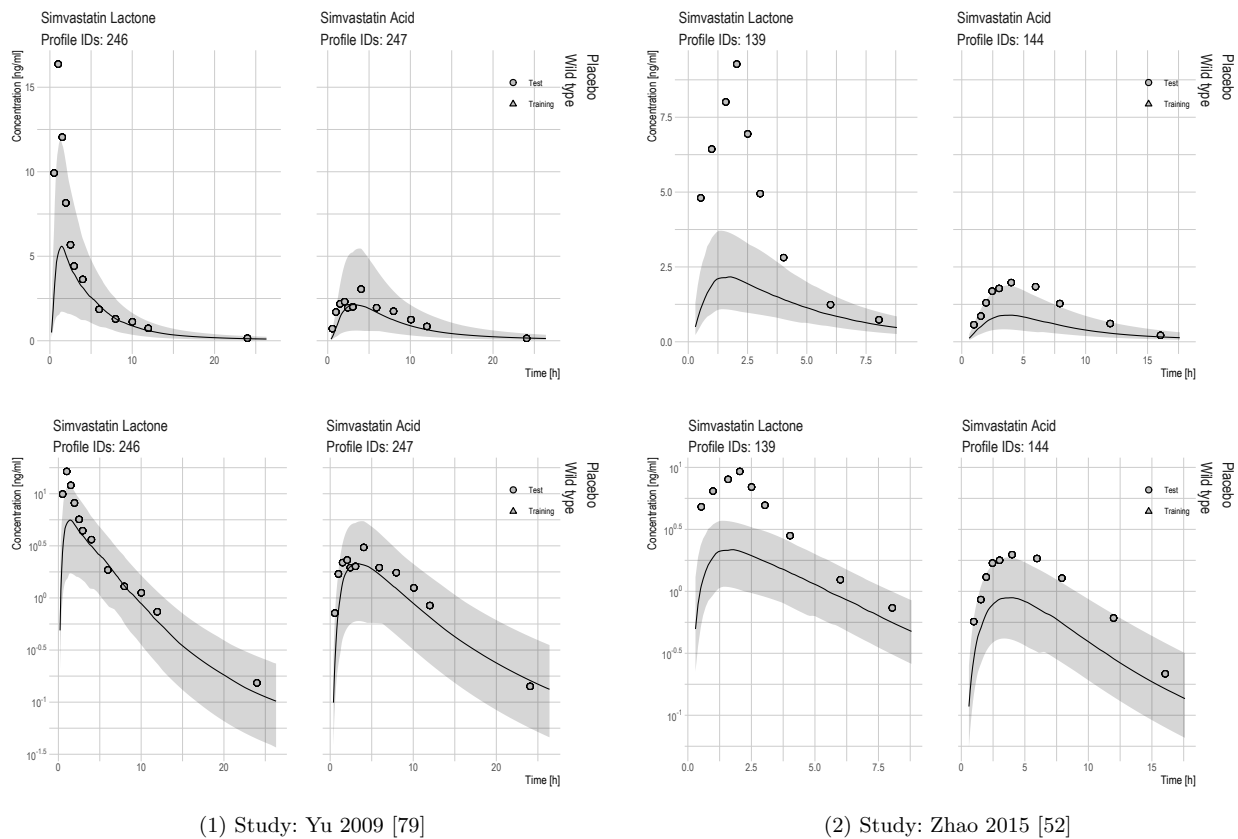


Figure S2.24: Linear and semi-logarithmic VPCs of the plasma concentration-time values in the test dataset. Solid line and shaded area are predicted median and 90 % CI: Vree 2001 [90], Yang 2003 [78]

2 PBPK modeling of simvastatin



62

Figure S2.25: Linear and semi-logarithmic VPCs of the plasma concentration-time values in the test dataset. Solid line and shaded area are predicted median and 90 % CI: Yu 2009 [79], Zhao 2015 [52]

2 PBPK modeling of simvastatin

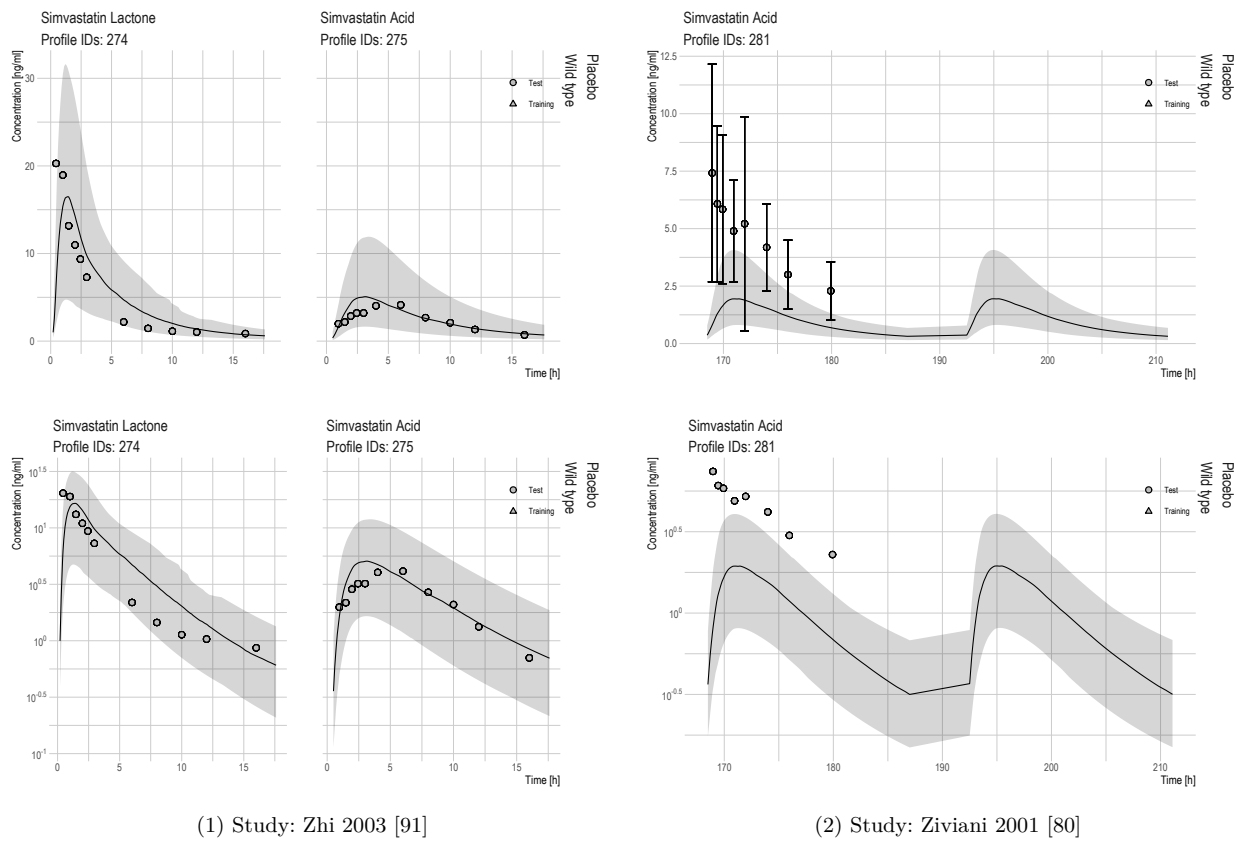


Figure S2.26: Linear and semi-logarithmic VPCs of the plasma concentration-time values in the test dataset. Solid line and shaded area are predicted median and 90 % CI: Zhi 2003 [91], Ziviani 2001 [80]

## 2 PBPK modeling of simvastatin

## 2.3.2 Predicted concentrations versus observed concentrations GOF plots

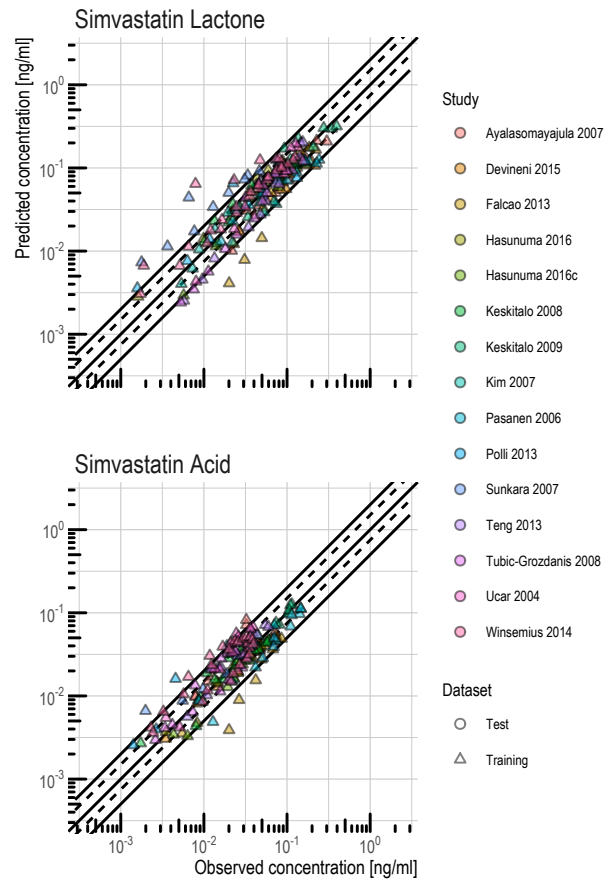


Figure S2.27: Goodness of fit plots - observed versus predicted plasma concentration-time values in the training dataset. The solid lines mark the line of identity as well as the 2-fold deviations. Dashed lines indicate the 1.5-fold deviations



## 2 PBPK modeling of simvastatin

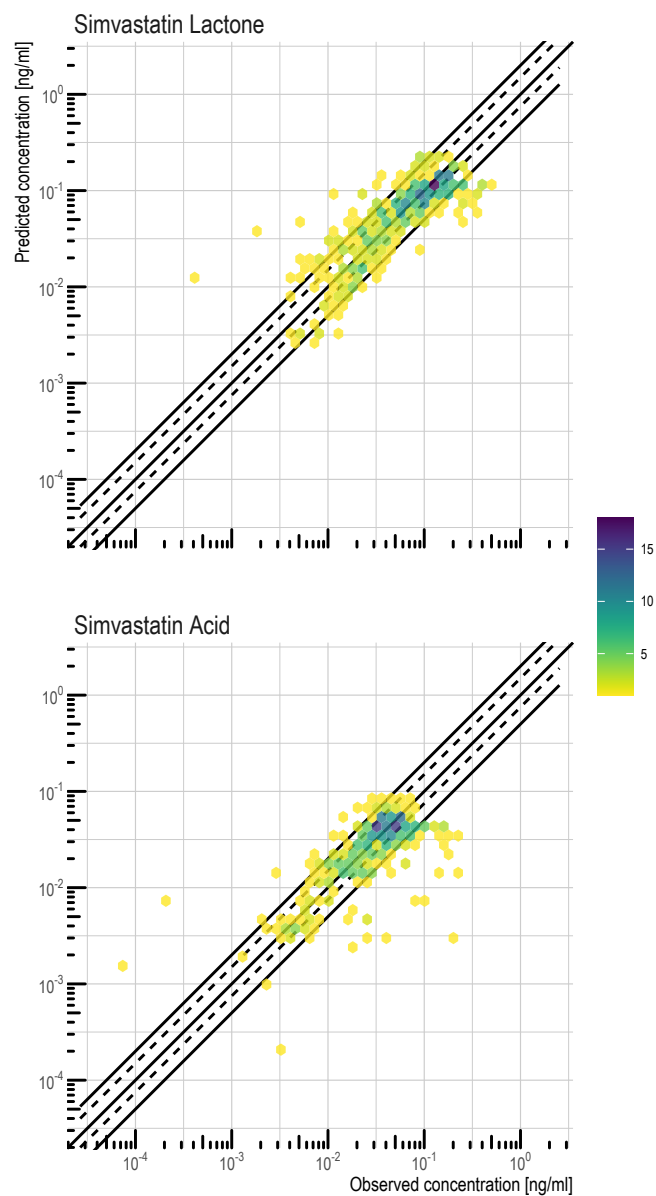


Figure S2.28: Goodness of fit plots - binned observed versus predicted plasma concentration-time values in the test dataset. The solid lines mark the line of identity as well as the 2-fold deviations. Dashed lines indicate the 1.5-fold deviations. The color of a hexagon reflects the binned number of observations in the respective neighborhood

## 2 PBPK modeling of simvastatin

## 2.3.3 NCA GOF plots

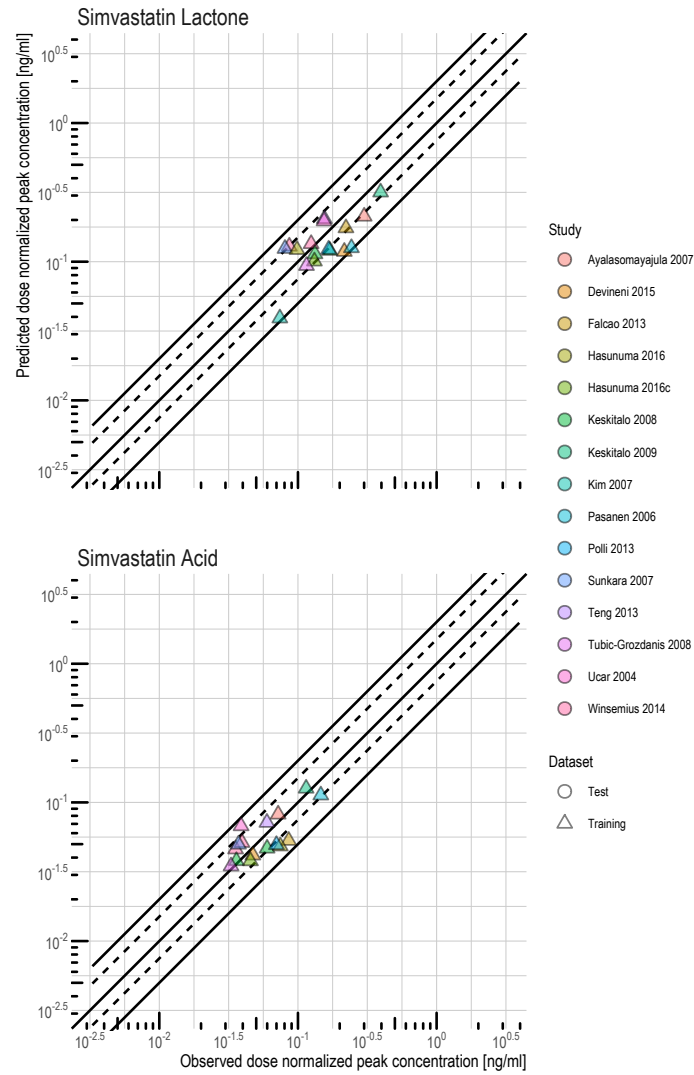


Figure S2.29: NCA ratios of the training dataset. The solid lines mark the line of identity as well as the 2-fold deviations. Dashed lines indicate the 1.5-fold deviations.: Training  $C_{max}$

## 2 PBPK modeling of simvastatin

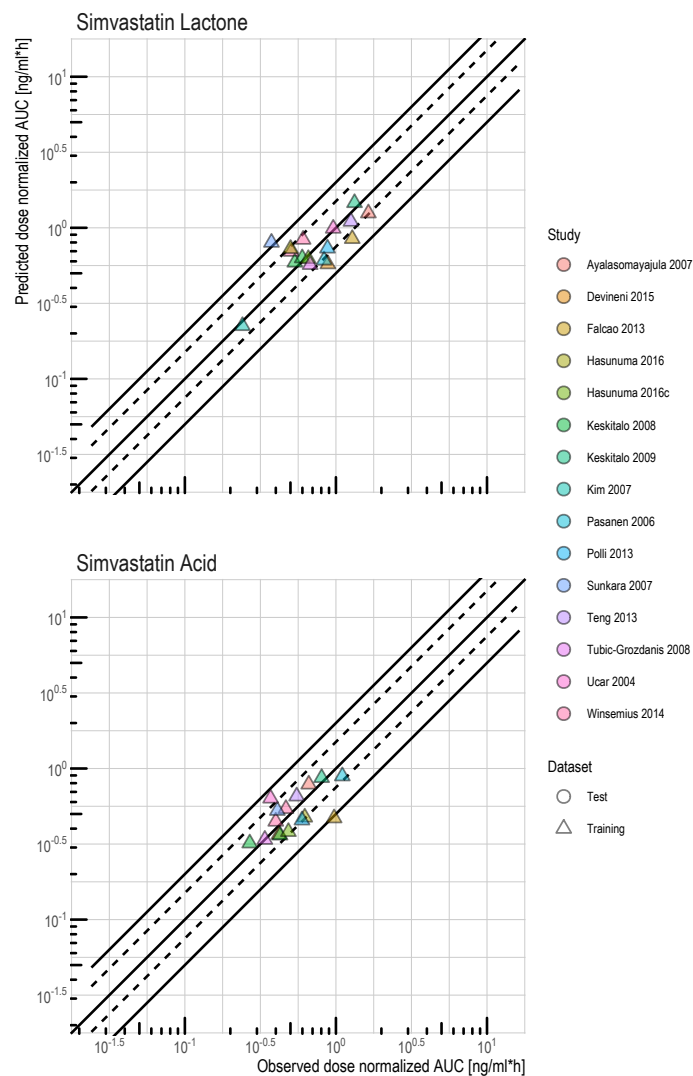


Figure S2.30: NCA ratios of the training dataset. The solid lines mark the line of identity as well as the 2-fold deviations. Dashed lines indicate the 1.5-fold deviations.: Training AUC

## 2 PBPK modeling of simvastatin

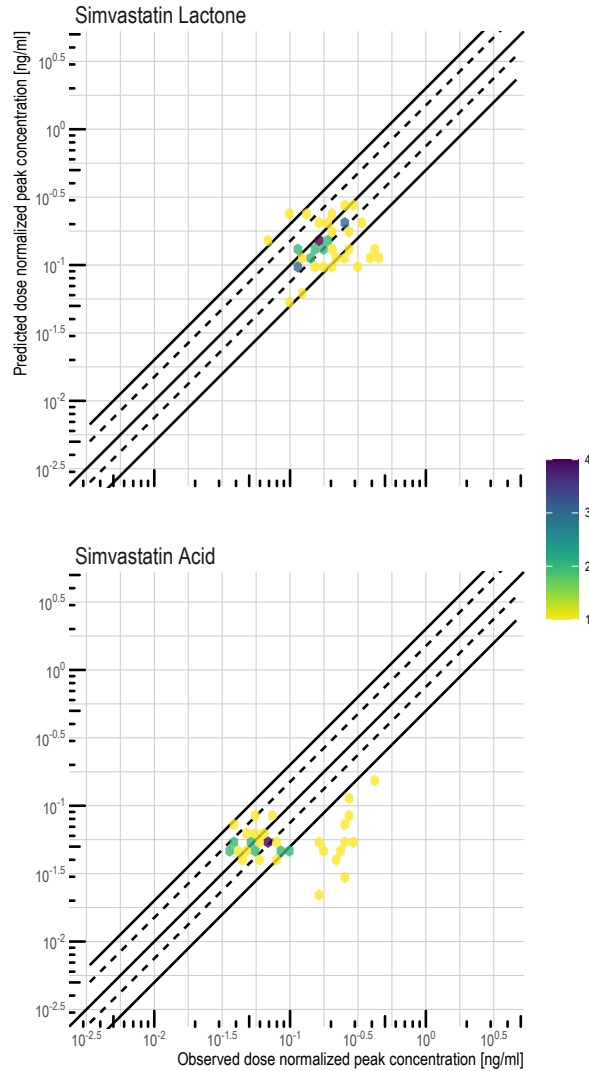


Figure S2.31: NCA ratios of the test dataset. The solid lines mark the line of identity as well as the 2-fold deviations. Dashed lines indicate the 1.5-fold deviations. The color of a hexagon reflects the binned number of observations in the respective neighborhood.: Test  $C_{max}$

## 2 PBPK modeling of simvastatin

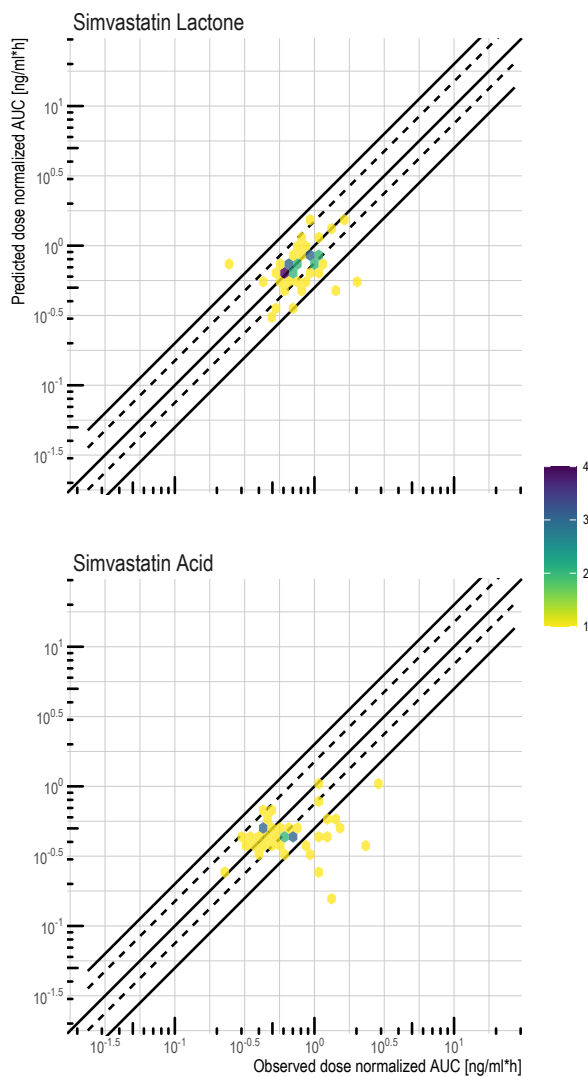


Figure S2.32: NCA ratios of the test dataset. The solid lines mark the line of identity as well as the 2-fold deviations. Dashed lines indicate the 1.5-fold deviations. The color of a hexagon reflects the binned number of observations in the respective neighborhood.: Test AUC

## 2 PBPK modeling of simvastatin

## 2.3.4 MRD and MSA of plasma concentration predictions

Table S2.7: Summary of the statistical placebo model evaluation (MSA and MRD)

Molecule	MRD mean (sd)	MSA mean (sd)
Simvastatin Lactone	1.87 (0.709) N = 42 (N MRD > 2 = 11)	57 (56.3) N = 42 (N MSA > 100 = 7)
Simvastatin Acid	1.98 (1.17) N = 40 (N MRD > 2 = 9)	60.6 (78.5) N = 40 (N MSA > 100 = 4)

## 2.3.5 NCA ratios and GMFE of NCA values

Table S2.8: Summary of the statistical placebo model evaluation (NCA ratio and GMFE)

Parameter	NCA ratio mean (sd)	GMFE
<b>Simvastatin Lactone</b>		
AUC	0.998 (0.401) N = 63 (N ratio > 2   ratio < 0.5 = 5)	1.3
$C_{max}$	0.869 (0.419) N = 63 (N ratio > 2   ratio < 0.5 = 10)	1.47
<b>Simvastatin Acid</b>		
AUC	0.851 (0.362) N = 58 (N ratio > 2   ratio < 0.5 = 12)	1.53
$C_{max}$	0.832 (0.43) N = 58 (N ratio > 2   ratio < 0.5 = 14)	1.71

## 2.3.6 Local sensitivity analysis

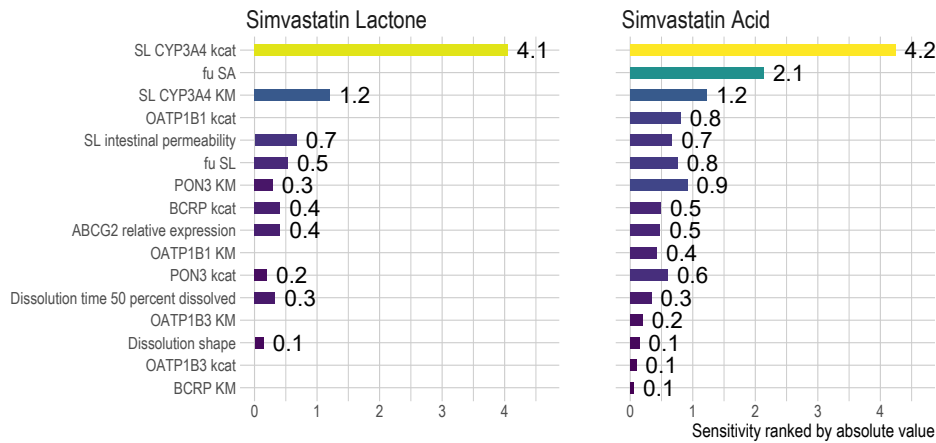


Figure S2.33: Simvastatin PBPK model sensitivity analysis. Sensitivity to single parameter perturbation, measured as change of the simulated AUC in steady-state of a 80 mg oral dose

## 2.4 Simvastatin DGIs

### 2.4.1 OATP1B1 (SLCO1B1)

The *SLCO1B1* polymorphism (rs4149056) is one of the best described and most important SL pharmacogene (PGx) [139]. Available data included one mean study profile from Pasanen et al. [95] for the c.521T/T, c.521T/C and c.521C/C genotypes, respectively. Detailed descriptions are presented in Table S2.2. It has to be noted, that for the c.521C/C genotype from Pasanen et al. [95] an unexpected elevation in the SL plasma concentration-time profile was observed. Interestingly, the elevation was comparable with the study from Keskitalo et al. [94] investigating the influence of rs2231142 in the *ABCG2* gene. In the study by Keskitalo et al. [94], participants hetero- or homozygous for the *ABCG2* c.421A/A genotype (non-functional) were extremely likely also heterozygous for rs4149056 polymorphism (88 % for c.421C/A and c.421A/A compared to 30 % in the c.421C/C group). Unfortunately, in the study from Pasanen et al. [95], participants were not screened for polymorphisms in the *ABCG2* gene. Moreover, a large difference in mean body weight in the c.521C/C and c.421A/A (84 kg versus 56 kg) was observed. As shown by Tsamandouras et al. [26] body weight is a significant covariate on the volume of distribution of simvastatin and thus, this could further obscure the covariate-adjusted difference in both groups.

A comparison of the model predicted an observed plasma concentration-time profile for each profile is shown in Figs. S2.34 and S2.35.

2 PBPK modeling of simvastatin

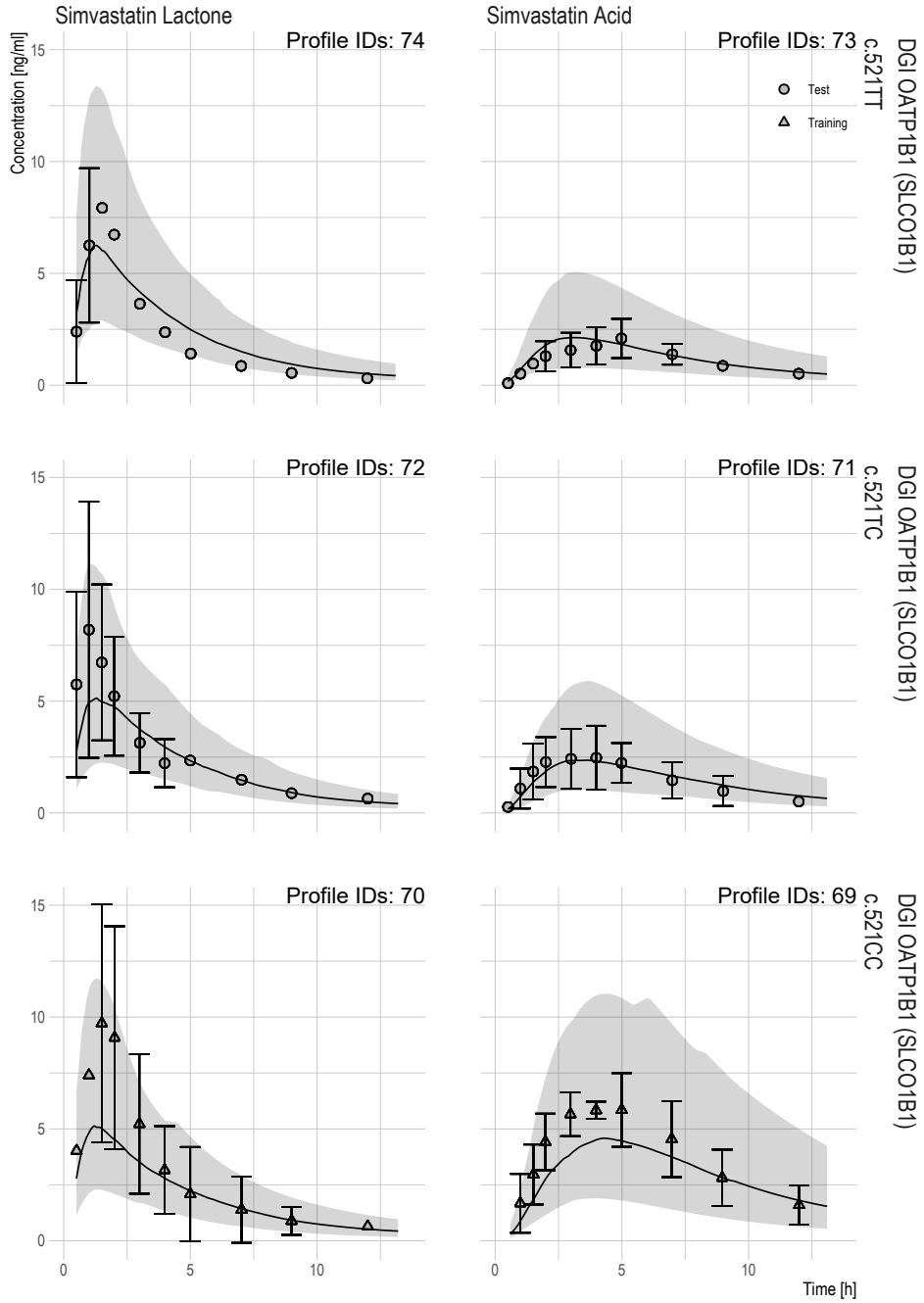


Figure S2.34: Linear VPCs of the plasma concentration-time profiles for investigated DGIs: OATP1B1 *SLCO1B1*. Solid line and shaded area are predicted median and 90% CI



2 PBPK modeling of simvastatin

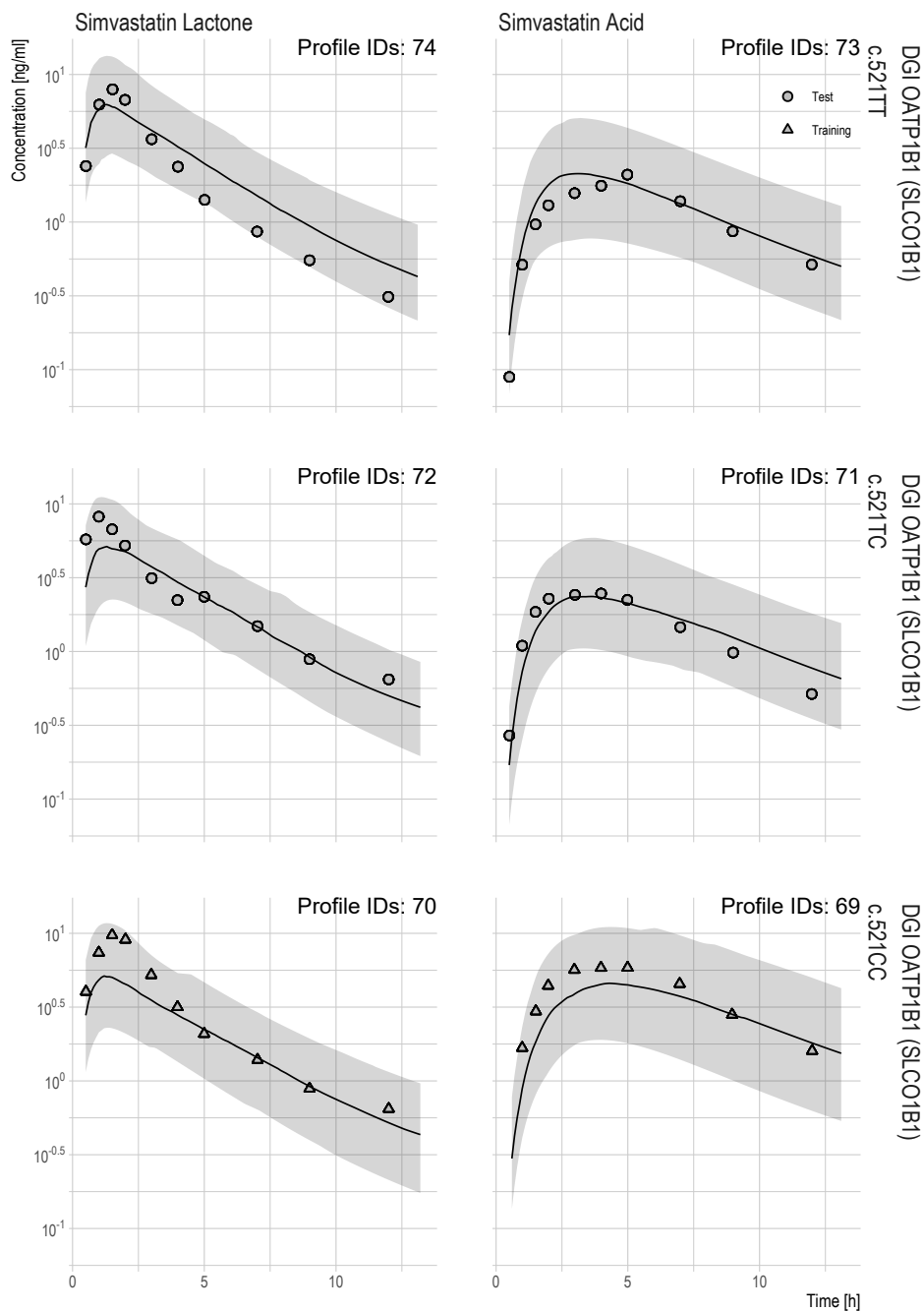


Figure S2.35: Semilogarithmic VPCs of the plasma concentration-time profiles for investigated DGIs: OATP1B1 *SLCO1B1*. Solid line and shaded area are predicted median and 90% CI

## 2 PBPK modeling of simvastatin

## 2.4.2 BCRP (ABCG2)

Although identified as significant covariate in two studies [94, 26] the rs2231142 polymorphism in *ABCG2* ranks only as level 3 clinical annotation on pharmgkb [140]. Nevertheless, it was included in the PBPK model assuming solely an impact on SL PK. Furthermore, for each study arm an individual OATP1B1 activity was calculated based on the observed *SLCO1B1* rs4149056 genotypes assuming an additive relationship. Data available included one SL and SA study mean profile from Keskitalo et al. [94] for the c.421C/C, c.421C/A and c.421A/A genotypes, respectively. Detailed descriptions are presented in Table S2.2. Despite the observed and well predicted effects, further studies should be performed to confirm the relevance and impact of BCRP (*ABCG2*) on SL and SA PK. The model capability to describe and predict the effect is shown in Figs. S2.36 and S2.37.

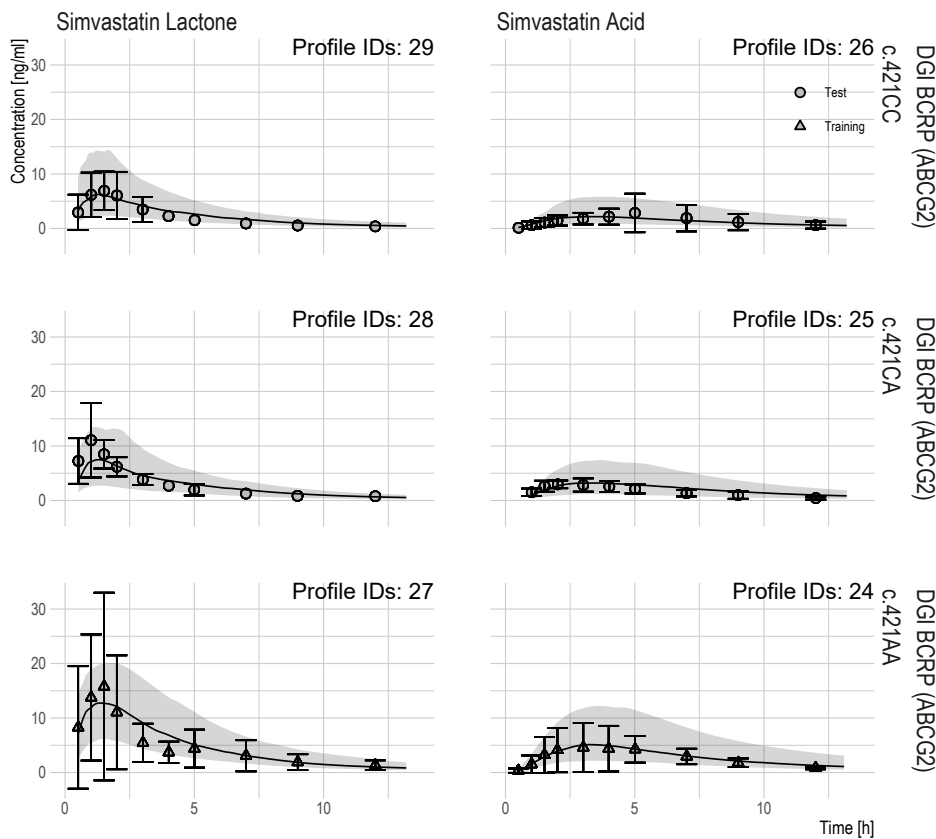


Figure S2.36: Linear VPCs of the plasma concentration-time profiles for investigated DGIs: BCRP *ABCG2*. Solid line and shaded area are predicted median and 90% CI

2 PBPK modeling of simvastatin

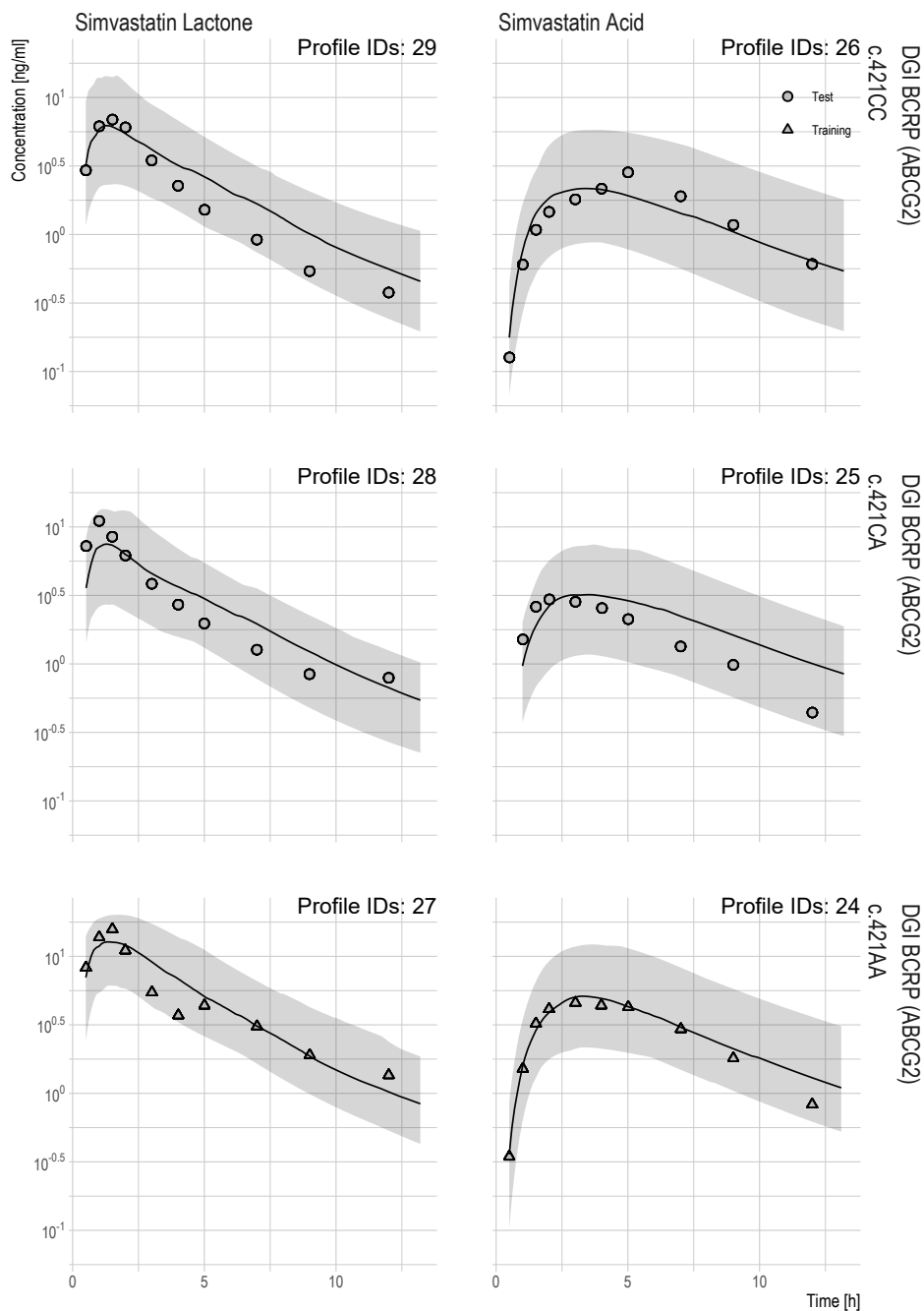


Figure S2.37: Semilogarithmic VPCs of the plasma concentration-time profiles for investigated DGIs: BCRP *ABCG2*. Solid line and shaded area are predicted median and 90 % CI

## 2 PBPK modeling of simvastatin

## 2.4.3 P-gp (ABCB1)

The different P-gp *ABCB1* genotypes were only descriptively included, since no study arm for evaluation was on hand. Hereby, one SL and SA study mean profile from Keskitalo et al. [41] for the *ABCB1* c.1236T-c.2677T-c.3435T and one for the c.1236C-c.2677G-c.3435C were available. Details are shown in Table S2.2. Nevertheless, by solely adapting the P-gp  $k_{cat}$  the different PK profiles of SA could be described accurately as shown in Figs. S2.38 and S2.39.

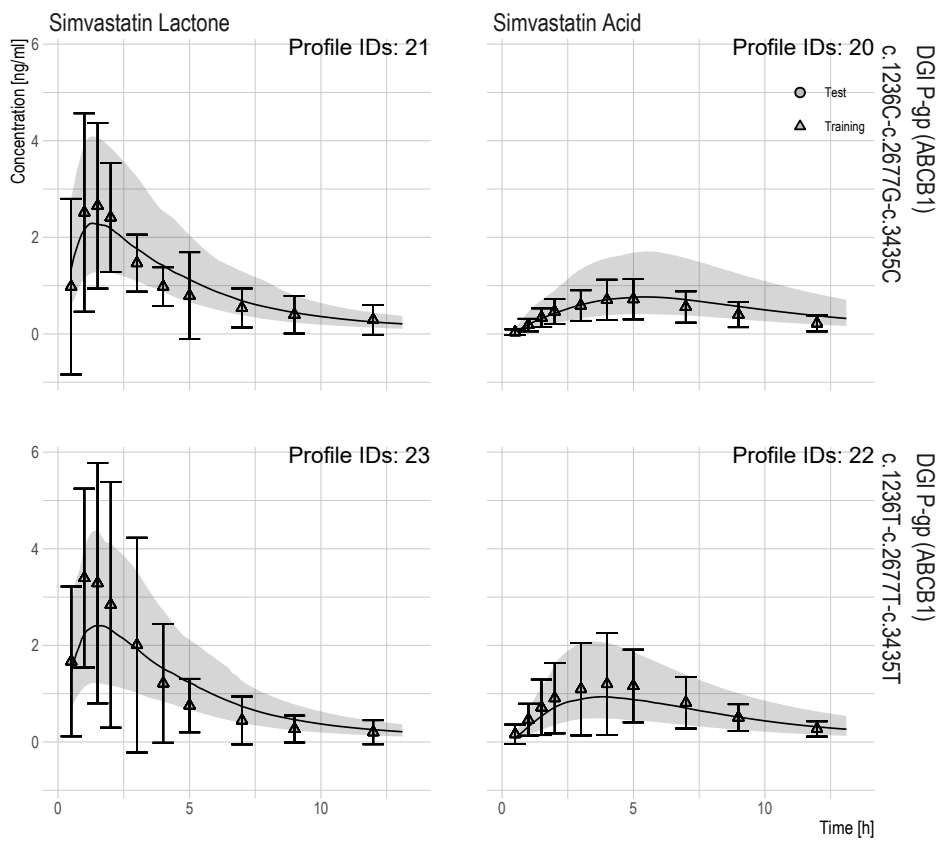


Figure S2.38: Linear VPCs of the plasma concentration-time profiles for investigated DGIs: P-gp *ABCB1*. Solid line and shaded area are predicted median and 90% CI

2 PBPK modeling of simvastatin

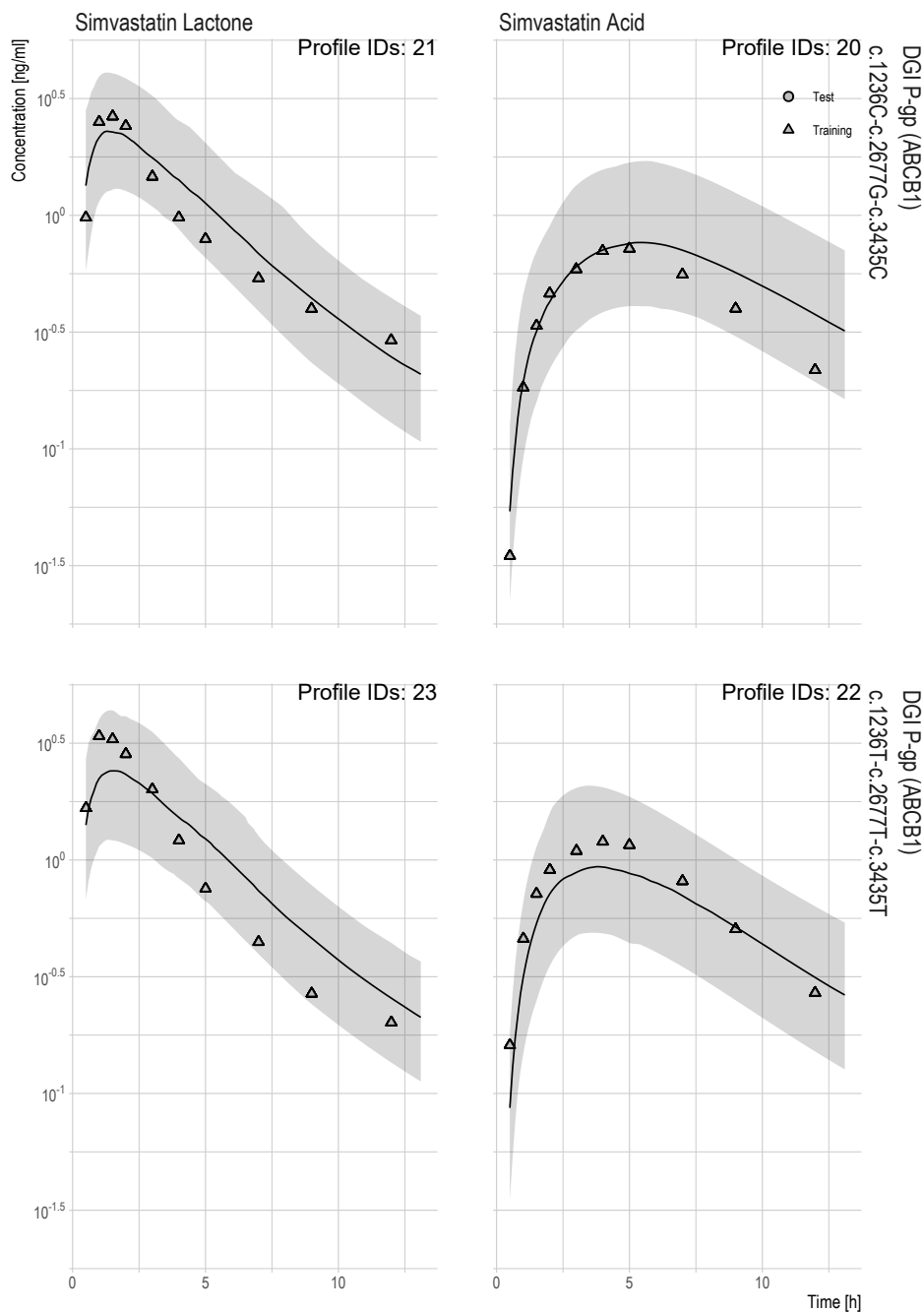


Figure S2.39: Semilogarithmic VPCs of the plasma concentration-time profiles for investigated DGIs: P-gp *ABCB1*. Solid line and shaded area are predicted median and 90% CI

## 2 PBPK modeling of simvastatin

## 2.4.4 CYP3A5 (CYP3A5 gene)

Unfortunately, in the only available study investigating the effects of the *CYP3A5* polymorphism on simvastatin, no SA PK were measured [93]. Following, SA metabolism by CYP3A5 could not be estimated and hence, was not included in the model [132]. Nevertheless, for SL the model showed good accuracy in describing the homozygous *CYP3A5*\*1/\*1 and predicting the heterozygous *CYP3A5*\*1/\*3 genotype as presented in Fig. S2.40.

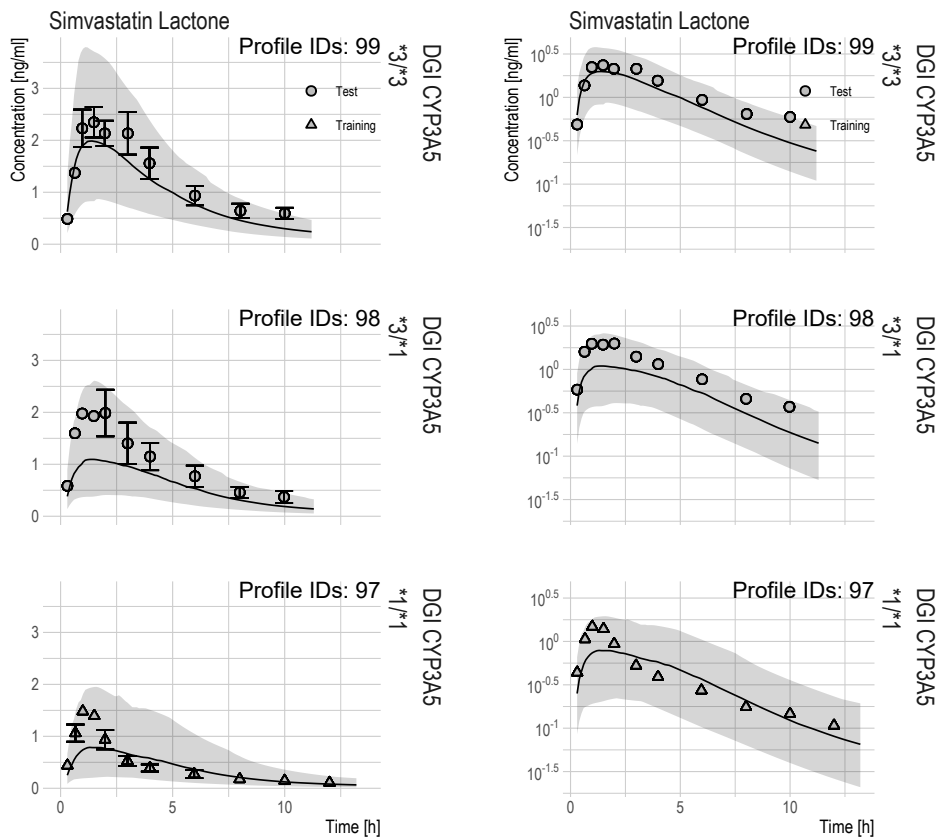


Figure S2.40: Linear (left) and semilogarithmic (right) VPCs of the plasma concentration-time profiles for investigated DGIs: *CYP3A5*. Solid line and shaded area are predicted median and 90% CI

## 2 PBPK modeling of simvastatin

## 2.4.5 MRD and MSA of plasma concentration predictions

Table S2.9 summarizes the statistical quality measures MRD and MSA exclusively for the DGIs data.

Table S2.9: Summary of the statistical DGI model evaluation (MSA and MRD)

Molecule	MRD mean (sd)	MSA mean (sd)
Simvastatin Lactone	1.45 (0.121) N = 11 (N MRD > 2 = 0)	33.3 (16.1) N = 11 (N MSA > 100 = 0)
Simvastatin Acid	1.36 (0.134) N = 8 (N MRD > 2 = 0)	24.3 (11.6) N = 8 (N MSA > 100 = 0)

## 2.4.6 NCA ratios and GMFE of NCA values

Table S2.10 summarizes the NCA ratios and GMFE values exclusively for the DGIs data.

Table S2.10: Summary of the statistical DGI model evaluation (NCA ratio and GMFE)

Parameter	NCA ratio mean (sd)	GMFE
<b>Simvastatin Lactone</b>		
AUC	0.958 (0.265) N = 20 (N ratio > 2   ratio < 0.5 = 1)	1.25
$C_{max}$	0.754 (0.214) N = 20 (N ratio > 2   ratio < 0.5 = 2)	1.43
<b>Simvastatin Acid</b>		
AUC	0.703 (0.363) N = 17 (N ratio > 2   ratio < 0.5 = 7)	1.81
$C_{max}$	0.583 (0.365) N = 17 (N ratio > 2   ratio < 0.5 = 9)	2.23

## 3 Simvastatin DDIs

### 3.1 Clinical studies

For DDI network evaluation mean profiles from 6 studies were extracted including 9 SL and 7 SA pharmacokinetic profiles which represent information from 75 study participants in total. An overview of all mean study demographics available can be found in Table S3.1.



Table S3.1: Mean study simvastatin pharmacokinetic profiles used for drug-drug interaction model evaluation

Route	Route co-medication	N	Females [%]	Age [years]	Weight [kg]	Height [cm]	Dataset	Profile Ids	References
2 mg SL p.o. (Solution, NA) s.d.	Placebo	12	-	-	-	-	Test	306, 307	[141]
40 mg SL p.o. (Zocor, fasted) s.d.	600 mg gemfibrozil p.o. b.i.d.	10	50	22 (20–31)	62 (41–81)	-	Test	4, 5	[142]
40 mg SL p.o. (Zocor, fasted) s.d.	Placebo	10	50	22 (20–31)	62 (41–81)	-	Test	2, 3	[142]
40 mg SL p.o. (Zocor, fasted) s.d.	600 mg rifampicin p.o. daily	18	56	39	73	-	Test	295	[143]
40 mg SL p.o. (Zocor, fasted) s.d.	Placebo	18	56	39	73	-	Test	293	[143]
40 mg SL p.o. (Unknown, Unknown) daily	500 mg clarithromycin p.o. daily	15	300	(18–60)	-	-	Test	15	[138]
40 mg SL p.o. (Unknown, Unknown) daily	Placebo	15	300	(18–60)	-	-	Test	14	[138]
40 mg SL p.o. (Unknown, Unknown) s.d.	Placebo	15	300	(18–60)	-	-	Test	18	[138]
40 mg SL p.o. (Zocor, fasted) s.d.	600 mg rifampicin p.o. daily	10	50	(21–29)	(59–81)	-	Test	38, 39	[144]
40 mg SL p.o. (Zocor, fasted) s.d.	Placebo	10	50	(21–29)	(59–81)	-	Test	36, 37	[144]
40 mg SL p.o. (Zocor, fasted) s.d.	Placebo	10	30	22 (19–29)	69 (52–86)	-	Test	59, 60, 58	[145]

*Note:*

Values for age, weight and height are given as mean (range); -, not given; b.i.d., twice daily; n, number of individuals studied; po, oral; s.d., single dose

## 3.2 Clarithromycin

The antibiotic clarithromycin is a strong inhibitor of CYP3A4 and P-gp as well as an inhibitor of OATP1B1 and OATP1B3 [146]. A previously developed clarithromycin PBPK model was extended by  $K_i$  values to model the competitive inhibition of OATP1B1 and OATP1B3 [16]. The parameters of the extended clarithromycin model are given in the Tables S3.2 and S3.3. For DDI evaluation one SL plasma concentration-time profile and one SA AUC under clarithromycin co-treatment were available [138]. Linear and semilogarithmic VPCs are shown in Figs. S3.1 and S3.2.

### 3.2.1 Drug-dependent parameters

Table S3.2: Drug-dependent parameters of the final clarithromycin model compared to literature values

Parameter	Unit	Model value	Median (range) literature values	Origin	Description
<b>Molecule</b>					
fu	%	29.9	30 (28–40)	Literature	Fraction unbound plasma
Lipophilicity	-	2.3	2.3	Literature	Lipophilicity
MW	-	748	748	Literature	Molecular weight
pKa	-	8.99	6.845 (4.7–8.99)	Literature	Acid dissociation constant (basic)
Solubility	mg l <sup>-1</sup>	12170	12170	Literature	Solubility at pH=2.4
<b>Enzymes</b>					
CYP3A4 k <sub>cat</sub>	min <sup>-1</sup>	76.5	76.5	Literature	CYP3A4 catalytic rate constant
CYP3A4 K <sub>M</sub>	μmol l <sup>-1</sup>	48.7	48.7	Literature	CYP3A4 Michaelis-Menten constant
<b>Inhibition</b>					
K <sub>i</sub> CYP3A4	μmol l <sup>-1</sup>	6.04	5.765 (2.25–39.2)	Literature	Concentration for half-maximal inactivation (MBI)
K <sub>i</sub> OATP1B1 ( <i>SLCO1B1</i> )	μmol l <sup>-1</sup>	10	12.58 (3.44–96)	Literature	Concentration for half-maximal OATP1B1 competitive inhibition
K <sub>i</sub> OATP1B3 ( <i>SLCO1B3</i> )	μmol l <sup>-1</sup>	9.8	9.8	Literature	Concentration for half-maximal OATP1B3 competitive inhibition
K <sub>i</sub> P-gp ( <i>ABCB1</i> )	μmol l <sup>-1</sup>	4.1	31 (3.8–434)	Literature	Concentration for half-maximal P-gp competitive inhibition
K <sub>inact</sub> CYP3A4	min <sup>-1</sup>	0.04	0.06 (0.04–0.23)	Literature	Maximum inactivation rate constant (MBI)
<b>Formulation</b>					
Dissolution shape	-	2.9	2.9	Literature	Weibull function dissolution shape

Table S3.2: Drug-dependent parameters of the final clarithromycin model compared to literature values (*continued*)

Parameter	Unit	Model value	Median (range) literature values	Origin	Description
Dissolution time (50 % dissolved)	min	5	5	Literature	Weibull function dissolution time (50% dissolved)
<b>System</b>					
CL <sub>Ren</sub>	ml/min	100	100	Literature	Renal plasma clearance
EHC	-	1	1	Assumed	Fraction of bile continually released from the gallbladder
GFR	-	1	1	Assumed	Fraction of filtered drug reaching the urine
Perm. Into blood cells	cm min <sup>-1</sup>	0.000362	3.62e-06	Literature	Plasma to blood cells permeability
Perm. Out of blood cells	cm min <sup>-1</sup>	1.04e-05	1.04e-07	Literature	Blood cells to plasma permeability
Specific intest. perm.	cm min <sup>-1</sup>	1.23e-05	1.23e-07	Literature	Permeation across intestinal mucosa normalized to surface area
Specific organ perm.	cm min <sup>-1</sup>	3.28e-05	3.28e-07	Calculated	Permeation across cell membranes normalized to surface area

*Note:*

Cellular permeabilities calculation method: PK-Sim Standard; organ-plasma partition coefficient calculation method: Rodgers and Rowland; formulation parameter values were used for solid oral dosage forms only

Table S3.3: Extracted drug-dependent parameter literature values for clarithromycin

Parameter	Unit	Literature value	Standard deviation	Note	Reference
fu	%	28	-	-	[2]
fu	%	30	-	-	[2]
fu	%	40	-	-	[2]
Lipophilicity	-	2.3	-	-	[2]
MW	-	748	-	-	[2]
Perm. Into blood cells	cm min <sup>-1</sup>	3.62e-06	-	-	[2]
Perm. Out of blood cells	cm min <sup>-1</sup>	1.04e-07	-	-	[2]
pKa	-	4.7	-	-	[2]
pKa	-	8.99	-	-	[2]
Solubility	mg l <sup>-1</sup>	12170	-	-	[2]
CYP3A4 k <sub>cat</sub>	min <sup>-1</sup>	76.5	-	-	[2]
CYP3A4 K <sub>M</sub>	μmol l <sup>-1</sup>	48.7	-	-	[2]
K <sub>i</sub> CYP3A4	μmol l <sup>-1</sup>	2.25	-	-	[2]
K <sub>i</sub> CYP3A4	μmol l <sup>-1</sup>	4.12	-	-	[2]
K <sub>i</sub> CYP3A4	μmol l <sup>-1</sup>	5.49	-	-	[2]
K <sub>i</sub> CYP3A4	μmol l <sup>-1</sup>	6.04	-	-	[2]
K <sub>i</sub> CYP3A4	μmol l <sup>-1</sup>	29.5	-	-	[2]
K <sub>i</sub> CYP3A4	μmol l <sup>-1</sup>	39.2	-	-	[2]
K <sub>i</sub> OATP1B1 ( <i>SLCO1B1</i> )	μmol l <sup>-1</sup>	8.26	-	K <sub>i</sub>	[147]
K <sub>i</sub> OATP1B1 ( <i>SLCO1B1</i> )	μmol l <sup>-1</sup>	3.44	-	K <sub>i</sub>	[148]
K <sub>i</sub> OATP1B1 ( <i>SLCO1B1</i> )	μmol l <sup>-1</sup>	16.9	-	K <sub>i</sub>	[148]
K <sub>i</sub> OATP1B1 ( <i>SLCO1B1</i> )	μmol l <sup>-1</sup>	5.1	-	IC50	[149]
K <sub>i</sub> OATP1B1 ( <i>SLCO1B1</i> )	μmol l <sup>-1</sup>	26.2	-	IC50	[150]
K <sub>i</sub> OATP1B1 ( <i>SLCO1B1</i> )	μmol l <sup>-1</sup>	96	-	IC50	[151]
K <sub>i</sub> OATP1B1 ( <i>SLCO1B1</i> )	μmol l <sup>-1</sup>	5.3	-	IC50	[2]
K <sub>i</sub> OATP1B1 ( <i>SLCO1B1</i> )	μmol l <sup>-1</sup>	75	-	IC50	[152]
K <sub>i</sub> OATP1B3 ( <i>SLCO1B3</i> )	μmol l <sup>-1</sup>	9.8	-	IC50	[151]
K <sub>i</sub> P-gp ( <i>ABCB1</i> )	μmol l <sup>-1</sup>	34	-	IC50	[153]
K <sub>i</sub> P-gp ( <i>ABCB1</i> )	μmol l <sup>-1</sup>	66	-	IC50	[153]
K <sub>i</sub> P-gp ( <i>ABCB1</i> )	μmol l <sup>-1</sup>	7	-	IC50	[154]
K <sub>i</sub> P-gp ( <i>ABCB1</i> )	μmol l <sup>-1</sup>	28	-	IC50	[154]
K <sub>i</sub> P-gp ( <i>ABCB1</i> )	μmol l <sup>-1</sup>	39.7	-	IC50	[123]
K <sub>i</sub> P-gp ( <i>ABCB1</i> )	μmol l <sup>-1</sup>	34	-	IC50	[124]
K <sub>i</sub> P-gp ( <i>ABCB1</i> )	μmol l <sup>-1</sup>	434	-	K <sub>i</sub>	[155]

Table S3.3: Extracted drug-dependent parameter literature values for clarithromycin (*continued*)

Parameter	Unit	Literature value	Standard deviation	Note	Reference
$K_i$ P-gp ( <i>ABCB1</i> )	$\mu\text{mol l}^{-1}$	4.1	-	IC50	[2]
$K_i$ P-gp ( <i>ABCB1</i> )	$\mu\text{mol l}^{-1}$	8.9	-	IC50	[146]
$K_i$ P-gp ( <i>ABCB1</i> )	$\mu\text{mol l}^{-1}$	3.8	-	IC50	[43]
$K_i$ P-gp ( <i>ABCB1</i> )	$\mu\text{mol l}^{-1}$	7.2	-	IC50	[43]
$K_i$ P-gp ( <i>ABCB1</i> )	$\mu\text{mol l}^{-1}$	15.1	-	IC50	[43]
$K_i$ P-gp ( <i>ABCB1</i> )	$\mu\text{mol l}^{-1}$	23.8	-	IC50	[43]
$K_i$ P-gp ( <i>ABCB1</i> )	$\mu\text{mol l}^{-1}$	50.2	-	IC50	[43]
$K_i$ P-gp ( <i>ABCB1</i> )	$\mu\text{mol l}^{-1}$	56.1	-	IC50	[43]
$K_i$ P-gp ( <i>ABCB1</i> )	$\mu\text{mol l}^{-1}$	86.7	-	IC50	[43]
$K_{\text{inact}}$ CYP3A4	$\text{min}^{-1}$	0.04	-	-	[2]
$K_{\text{inact}}$ CYP3A4	$\text{min}^{-1}$	0.05	-	-	[2]
$K_{\text{inact}}$ CYP3A4	$\text{min}^{-1}$	0.07	-	-	[2]
$K_{\text{inact}}$ CYP3A4	$\text{min}^{-1}$	0.23	-	-	[2]
Dissolution shape	-	2.9	-	-	[2]
Dissolution time (50 % dissolved)	min	5	-	-	[2]
$CL_{\text{Ren}}$	m/ min	100	-	-	[2]
EHC	-	1	-	-	[2]
GFR	-	1	-	-	[2]
Specific intest. perm.	$\text{cm min}^{-1}$	1.23e-07	-	-	[2]
Specific organ perm.	$\text{cm min}^{-1}$	3.28e-07	-	-	[2]

*Note:*

If IC50 values could not be used for  $K_i$  value estimation utilizing Cheng Prusoff Equation (e.g. due to missing substrate affinities)  $K_i = IC50$  was assumed

## 3 Simvastatin DDIs

## 3.2.2 Profiles

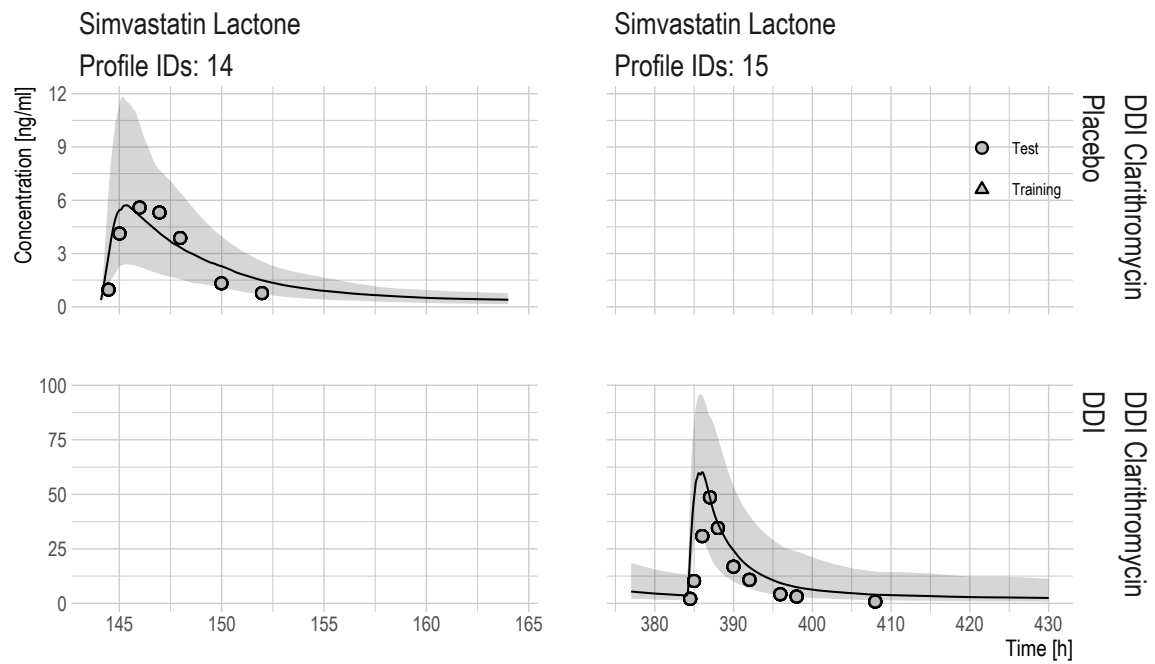


Figure S3.1: Linear VPCs of plasma concentration-time profiles for investigated DDIs: Clarithromycin - Simvastatin Lactone. Solid line and shaded area are predicted median and 90 % CI

3 Simvastatin DDIs

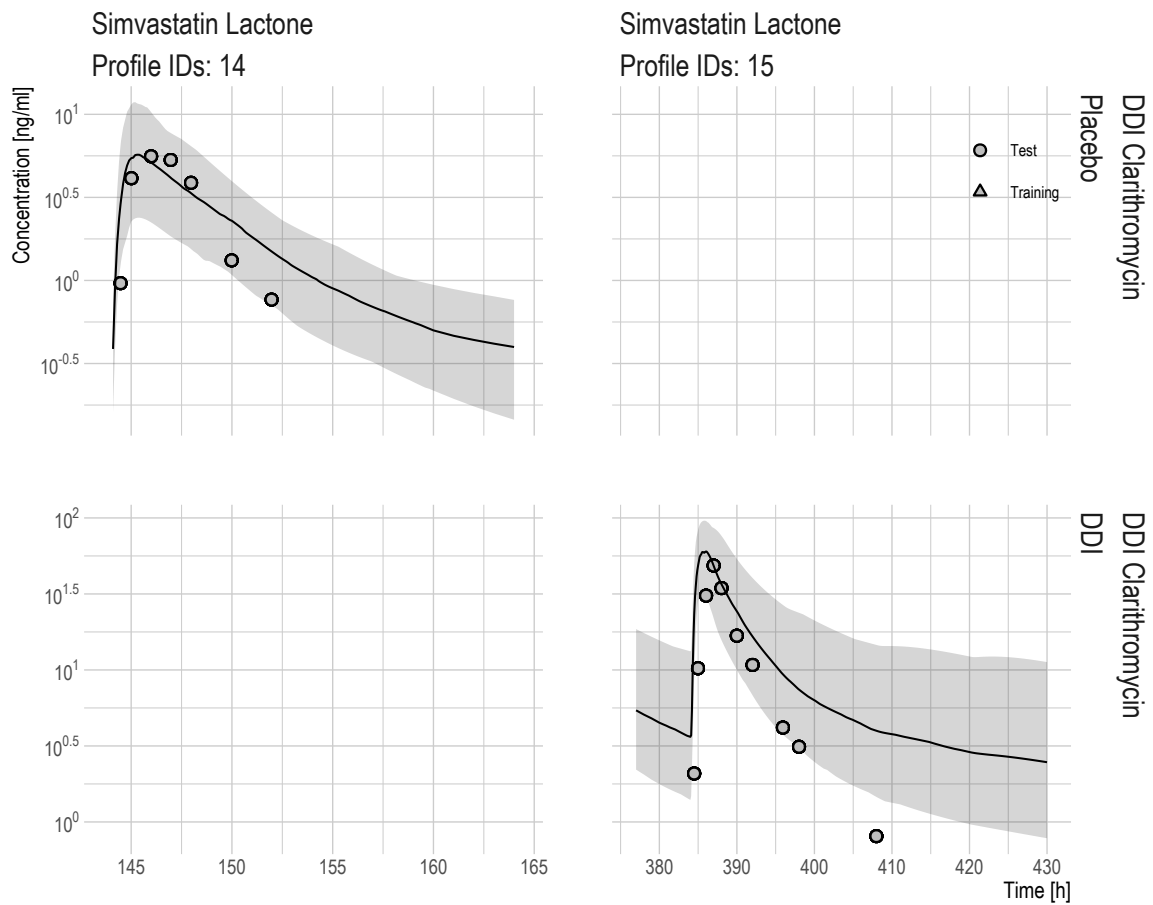


Figure S3.2: Semi-logarithmic VPCs of plasma concentration-time profiles for investigated DDIs: Clarithromycin - Simvastatin Lactone. Solid line and shaded area are predicted median and 90% CI



### 3.3 Rifampicin

The antibiotic rifampicin is a strong inducer and inhibitor of different metabolic enzymes and transporters [156]. A previously developed rifampicin PBPK model was extended by interaction constants [16]. Furthermore, since Hanke et al. [16] found an induction effect on the esterase arylacetamide deacetylase (AADAC) also for the SL relevant esterase PON3 an induction with the same parameter values was assumed. The parameters of the extended rifampicin model are given in Tables S3.4 and S3.5. Results of the simvastatin-rifampicin DDI interaction are shown in Figs. S3.3 - S3.8.

#### 3.3.1 Drug-dependent parameters

Table S3.4: Drug-dependent parameters of the final rifampicin model compared to literature values

Parameter	Unit	Model value	Median (range) literature values	Origin	Description
<b>Molecule</b>					
BP	-	0.89	0.895 (0.89–0.9)	Literature	Blood to plasma ratio
fu	%	17	17 (11–17.5)	Literature	Fraction unbound plasma
Lipophilicity	-	2.5	2.5 (1.3–2.7)	Literature	Lipophilicity
MW	g mol <sup>-1</sup>	822.9	822.9	Literature	Molecular weight
pKa	-	1.7	4.8 (1.7–7.9)	Literature	Acid dissociation constant (acidic)
	-	7.9	4.8 (1.7–7.9)	Literature	Acid dissociation constant (basic)
Solubility	mg l <sup>-1</sup>	2800	2670 (1100–3350)	Literature	Solubility at pH=7.5
<b>Enzymes</b>					
AADAC k <sub>cat</sub>	min <sup>-1</sup>	9.87	9.87	Literature	AADAC catalytic rate constant
AADAC K <sub>M</sub>	μmol l <sup>-1</sup>	195.1	195.1	Literature	AADAC Michaelis-Menten constant
<b>Transporters</b>					
OATP1B1 ( <i>SLCO1B1</i> ) k <sub>cat</sub>	min <sup>-1</sup>	7.8	7.8	Literature	OATP1B1 catalytic rate constant
OATP1B1 ( <i>SLCO1B1</i> ) K <sub>M</sub>	μmol l <sup>-1</sup>	1.5	1.5	Literature	OATP1B1 Michaelis-Menten constant
P-gp ( <i>ABCB1</i> ) k <sub>cat</sub>	min <sup>-1</sup>	0.61	0.61	Literature	P-gp catalytic rate constant
P-gp ( <i>ABCB1</i> ) K <sub>M</sub>	μmol l <sup>-1</sup>	55	55	Literature	P-gp Michaelis-Menten constant
<b>Inhibition</b>					
K <sub>i</sub> BCRP ( <i>ABCG2</i> )	μmol l <sup>-1</sup>	36	36 (14–461)	Literature	Concentration for half-maximal BCRP competitive inhibition

Table S3.4: Drug-dependent parameters of the final rifampicin model compared to literature values (*continued*)

Parameter	Unit	Model value	Median (range) literature values	Origin	Description
K <sub>i</sub> CYP2C8	μmol <sup>-1</sup>	30.2	30.2	Literature	Concentration for half-maximal CYP2C8 competitive inhibition
K <sub>i</sub> CYP3A4	μmol <sup>-1</sup>	18.5	18.5 (-19.7)	Literature	Concentration for half-maximal CYP3A4 competitive inhibition
K <sub>i</sub> MRP2 ( <i>ABCC2</i> )	μmol <sup>-1</sup>	7.9	33.8 (7.9-144)	Literature	Concentration for half-maximal MRP2 competitive inhibition
K <sub>i</sub> OATP1B1 ( <i>SLCO1B1</i> )	μmol <sup>-1</sup>	0.22	1.235 (0.22-3948)	Literature	Concentration for half-maximal OATP1B1 competitive inhibition
K <sub>i</sub> OATP1B3 ( <i>SLCO1B3</i> )	μmol <sup>-1</sup>	0.39	0.39	Literature	Concentration for half-maximal OATP1B3 competitive inhibition
K <sub>i</sub> P-gp ( <i>ABCB1</i> )	μmol <sup>-1</sup>	169	169 (4.3-279)	Literature	Concentration for half-maximal P-gp competitive inhibition
K <sub>i</sub> UGT1A1	μmol <sup>-1</sup>	33	33	Literature	Concentration for half-maximal UGT1A1 competitive inhibition
K <sub>i</sub> UGT1A3	μmol <sup>-1</sup>	600	600	Literature	Concentration for half-maximal UGT1A3 competitive inhibition
<b>Induction</b>					
E <sub>max</sub> AADAC	-	0.99	0.99	Literature	Maximum in vivo induction effect
E <sub>max</sub> CYP2C8	-	5	3.2 (1.3-5)	Literature	Maximum in vivo induction effect
E <sub>max</sub> CYP3A4	-	9	5 (2-30)	Literature	Maximum in vivo induction effect

Table S3.4: Drug-dependent parameters of the final rifampicin model compared to literature values (*continued*)

Parameter	Unit	Model value	Median (range) literature values	Origin	Description
E <sub>max</sub> CYP3A5	-	2	2	Literature	Maximum in vivo induction effect
E <sub>max</sub> OATP1B1 ( <i>SLCO1B1</i> )	-	0.38	0.38	Literature	Maximum in vivo induction effect
E <sub>max</sub> OATP1B3 ( <i>SLCO1B3</i> )	-	0.38	-	Assumed	Maximum in vivo induction effect
E <sub>max</sub> P-gp ( <i>ABCB1</i> )	-	2.5	2.5	Literature	Maximum in vivo induction effect
E <sub>max</sub> PON3	-	0.99	0.99	Assumed	Maximum in vivo induction effect
E <sub>max</sub> UGT1A1	-	1.3	1.3	Literature	Maximum in vivo induction effect
E <sub>max</sub> UGT1A3	-	1.4	1.4	Literature	Maximum in vivo induction effect
Induction EC <sub>50</sub>	μmol <sup>-1</sup>	0.34	-	Literature	Concentration for half-maximal induction
<b>System</b>					
EHC	-	1	-	Assumed	Fraction of bile continually released from the gallbladder
GFR	-	1	-	Assumed	Fraction of filtered drug reaching the urine
Specific intest. perm.	cm min <sup>-1</sup>	1.24e-05	1.24e-05	Literature	Permeation across intestinal mucosa normalized to surface area
Specific organ perm.	cm min <sup>-1</sup>	2.93e-05	2.93e-05	Calculated	Permeation across cell membranes normalized to surface area

*Note:*

Cellular permabilites calculation method: PK-Sim Standard; organ-plasma partition coefficient calculation method: Rodgers and Rowland

Table S3.5: Extracted drug-dependent parameter literature values for rifampicin

Parameter	Unit	Literature value	Standard deviation	Note	Reference
BP	-	0.9	-	-	[2]
BP	-	0.89	-	-	[2]
fu	%	17	-	-	[2]
fu	%	11	-	-	[2]
fu	%	16	-	-	[2]
fu	%	17	-	-	[2]
fu	%	17.5	-	-	[2]
Lipophilicity	-	2.5	-	-	[2]
Lipophilicity	-	1.3	-	-	[2]
Lipophilicity	-	2.7	-	-	[2]
MW	g mol <sup>-1</sup>	822.9	-	-	[2]
pKa	-	1.7	-	acidic	[2]
pKa	-	7.9	-	basic	[2]
Solubility	mg l <sup>-1</sup>	2800	-	pH=7.5	[2]
Solubility	mg l <sup>-1</sup>	1100	-	pH=6.5	[2]
Solubility	mg l <sup>-1</sup>	1400	-	pH=6.8	[2]
Solubility	mg l <sup>-1</sup>	2540	-	pH=6.8	[2]
Solubility	mg l <sup>-1</sup>	2800	-	pH=7.5	[2]
Solubility	mg l <sup>-1</sup>	3350	-	pH=7.4	[2]
AADAC k <sub>cat</sub>	min <sup>-1</sup>	9.87	-	-	[2]
AADAC K <sub>M</sub>	μmol l <sup>-1</sup>	195.1	-	-	[2]
OATP1B1 ( <i>SLCO1B1</i> ) k <sub>cat</sub>	min <sup>-1</sup>	7.8	-	-	[2]
OATP1B1 ( <i>SLCO1B1</i> ) K <sub>M</sub>	μmol l <sup>-1</sup>	1.5	-	-	[2]
P-gp ( <i>ABCB1</i> ) k <sub>cat</sub>	min <sup>-1</sup>	0.61	-	-	[2]
P-gp ( <i>ABCB1</i> ) K <sub>M</sub>	μmol l <sup>-1</sup>	55	-	-	[2]
K <sub>i</sub> BCRP ( <i>ABCG2</i> )	μmol l <sup>-1</sup>	56	-	IC50	[157]
K <sub>i</sub> BCRP ( <i>ABCG2</i> )	μmol l <sup>-1</sup>	461	-	IC50	[158]
K <sub>i</sub> BCRP ( <i>ABCG2</i> )	μmol l <sup>-1</sup>	18.8	-	K <sub>i</sub>	[159]
K <sub>i</sub> BCRP ( <i>ABCG2</i> )	μmol l <sup>-1</sup>	36	-	K <sub>i</sub>	[159]
K <sub>i</sub> BCRP ( <i>ABCG2</i> )	μmol l <sup>-1</sup>	14	-	IC50	[160]
K <sub>i</sub> BCRP ( <i>ABCG2</i> )	μmol l <sup>-1</sup>	14	-	-	[161]
K <sub>i</sub> BCRP ( <i>ABCG2</i> )	μmol l <sup>-1</sup>	36	-	-	[161]
K <sub>i</sub> CYP2C8	-	30.2	-	K <sub>i</sub>	[2]
K <sub>i</sub> CYP3A4	μmol l <sup>-1</sup>	19.7	-	IC50	[162]

Table S3.5: Extracted drug-dependent parameter literature values for rifampicin (*continued*)

Parameter	Unit	Literature value	Standard deviation	Note	Reference
K <sub>i</sub> CYP3A4	μmol <sup>-1</sup>	18.5	-	K <sub>i</sub>	[163]
K <sub>i</sub> CYP3A4	μmol <sup>-1</sup>	18.5	-	-	[2]
K <sub>i</sub> MRP2 ( <i>ABCC2</i> )	μmol <sup>-1</sup>	27	-	IC50	[157]
K <sub>i</sub> MRP2 ( <i>ABCC2</i> )	μmol <sup>-1</sup>	144	-	IC50	[158]
K <sub>i</sub> MRP2 ( <i>ABCC2</i> )	μmol <sup>-1</sup>	83	-	IC50	[120]
K <sub>i</sub> MRP2 ( <i>ABCC2</i> )	μmol <sup>-1</sup>	7.9	-	K <sub>i</sub>	[159]
K <sub>i</sub> MRP2 ( <i>ABCC2</i> )	μmol <sup>-1</sup>	40.6	-	K <sub>i</sub>	[159]
K <sub>i</sub> MRP2 ( <i>ABCC2</i> )	μmol <sup>-1</sup>	14.7	-	IC50	[160]
K <sub>i</sub> OATP1B1 ( <i>SLCO1B1</i> )	μmol <sup>-1</sup>	1.6	-	IC50	[164]
K <sub>i</sub> OATP1B1 ( <i>SLCO1B1</i> )	μmol <sup>-1</sup>	0.99	-	IC50	[165]
K <sub>i</sub> OATP1B1 ( <i>SLCO1B1</i> )	μmol <sup>-1</sup>	3.25	-	IC50	[166]
K <sub>i</sub> OATP1B1 ( <i>SLCO1B1</i> )	μmol <sup>-1</sup>	4.61	-	IC50	[166]
K <sub>i</sub> OATP1B1 ( <i>SLCO1B1</i> )	μmol <sup>-1</sup>	0.29	-	IC50	[167]
K <sub>i</sub> OATP1B1 ( <i>SLCO1B1</i> )	μmol <sup>-1</sup>	0.77	-	IC50	[168]
K <sub>i</sub> OATP1B1 ( <i>SLCO1B1</i> )	μmol <sup>-1</sup>	466.8	-	IC50	[169]
K <sub>i</sub> OATP1B1 ( <i>SLCO1B1</i> )	μmol <sup>-1</sup>	3948	-	IC50	[169]
K <sub>i</sub> OATP1B1 ( <i>SLCO1B1</i> )	μmol <sup>-1</sup>	0.59	-	IC50	[170]
K <sub>i</sub> OATP1B1 ( <i>SLCO1B1</i> )	μmol <sup>-1</sup>	5.16	-	IC50	[171]
K <sub>i</sub> OATP1B1 ( <i>SLCO1B1</i> )	μmol <sup>-1</sup>	4.42	-	K <sub>i</sub>	[171]
K <sub>i</sub> OATP1B1 ( <i>SLCO1B1</i> )	μmol <sup>-1</sup>	3	-	IC50	[172]
K <sub>i</sub> OATP1B1 ( <i>SLCO1B1</i> )	μmol <sup>-1</sup>	1.5	-	IC50	[172]
K <sub>i</sub> OATP1B1 ( <i>SLCO1B1</i> )	μmol <sup>-1</sup>	0.41	-	K <sub>i</sub>	[173]
K <sub>i</sub> OATP1B1 ( <i>SLCO1B1</i> )	μmol <sup>-1</sup>	0.3	-	K <sub>i</sub>	[174]
K <sub>i</sub> OATP1B1 ( <i>SLCO1B1</i> )	μmol <sup>-1</sup>	0.22	-	K <sub>i</sub>	[158]
K <sub>i</sub> OATP1B1 ( <i>SLCO1B1</i> )	μmol <sup>-1</sup>	1.5	-	IC50	[175]
K <sub>i</sub> OATP1B1 ( <i>SLCO1B1</i> )	μmol <sup>-1</sup>	1.3	-	IC50	[176]
K <sub>i</sub> OATP1B1 ( <i>SLCO1B1</i> )	μmol <sup>-1</sup>	0.477	-	K <sub>i</sub>	[147]
K <sub>i</sub> OATP1B1 ( <i>SLCO1B1</i> )	μmol <sup>-1</sup>	2.75	-	IC50	[177]
K <sub>i</sub> OATP1B1 ( <i>SLCO1B1</i> )	μmol <sup>-1</sup>	0.585	-	IC50	[177]
K <sub>i</sub> OATP1B1 ( <i>SLCO1B1</i> )	μmol <sup>-1</sup>	6.96	-	IC50	[177]
K <sub>i</sub> OATP1B1 ( <i>SLCO1B1</i> )	μmol <sup>-1</sup>	0.922	-	K <sub>i</sub>	[178]
K <sub>i</sub> OATP1B1 ( <i>SLCO1B1</i> )	μmol <sup>-1</sup>	0.694	-	K <sub>i</sub>	[178]
K <sub>i</sub> OATP1B1 ( <i>SLCO1B1</i> )	μmol <sup>-1</sup>	0.423	-	K <sub>i</sub>	[178]
K <sub>i</sub> OATP1B1 ( <i>SLCO1B1</i> )	μmol <sup>-1</sup>	1.05	-	K <sub>i</sub>	[178]

Table S3.5: Extracted drug-dependent parameter literature values for rifampicin (*continued*)

Parameter	Unit	Literature value	Standard deviation	Note	Reference
K <sub>i</sub> OATP1B1 ( <i>SLCO1B1</i> )	μmol <sup>-1</sup>	0.442	-	K <sub>i</sub>	[178]
K <sub>i</sub> OATP1B1 ( <i>SLCO1B1</i> )	μmol <sup>-1</sup>	0.358	-	K <sub>i</sub>	[178]
K <sub>i</sub> OATP1B1 ( <i>SLCO1B1</i> )	μmol <sup>-1</sup>	1.07	-	K <sub>i</sub>	[178]
K <sub>i</sub> OATP1B1 ( <i>SLCO1B1</i> )	μmol <sup>-1</sup>	0.653	-	K <sub>i</sub>	[178]
K <sub>i</sub> OATP1B1 ( <i>SLCO1B1</i> )	μmol <sup>-1</sup>	0.598	-	K <sub>i</sub>	[178]
K <sub>i</sub> OATP1B1 ( <i>SLCO1B1</i> )	μmol <sup>-1</sup>	0.952	-	K <sub>i</sub>	[178]
K <sub>i</sub> OATP1B1 ( <i>SLCO1B1</i> )	μmol <sup>-1</sup>	1.23	-	K <sub>i</sub>	[178]
K <sub>i</sub> OATP1B1 ( <i>SLCO1B1</i> )	μmol <sup>-1</sup>	0.377	-	K <sub>i</sub>	[178]
K <sub>i</sub> OATP1B1 ( <i>SLCO1B1</i> )	μmol <sup>-1</sup>	0.355	-	IC50	[179]
K <sub>i</sub> OATP1B1 ( <i>SLCO1B1</i> )	μmol <sup>-1</sup>	3.79	-	IC50	[180]
K <sub>i</sub> OATP1B1 ( <i>SLCO1B1</i> )	μmol <sup>-1</sup>	1.2	-	IC50	[181]
K <sub>i</sub> OATP1B1 ( <i>SLCO1B1</i> )	μmol <sup>-1</sup>	10.46	-	IC50	[182]
K <sub>i</sub> OATP1B1 ( <i>SLCO1B1</i> )	μmol <sup>-1</sup>	2.4	-	IC50	[183]
K <sub>i</sub> OATP1B1 ( <i>SLCO1B1</i> )	μmol <sup>-1</sup>	4.9	-	IC50	[183]
K <sub>i</sub> OATP1B1 ( <i>SLCO1B1</i> )	μmol <sup>-1</sup>	0.56	-	IC50	[183]
K <sub>i</sub> OATP1B1 ( <i>SLCO1B1</i> )	μmol <sup>-1</sup>	4.1	-	IC50	[183]
K <sub>i</sub> OATP1B1 ( <i>SLCO1B1</i> )	μmol <sup>-1</sup>	12.2	-	K <sub>i</sub>	[184]
K <sub>i</sub> OATP1B1 ( <i>SLCO1B1</i> )	μmol <sup>-1</sup>	0.278	-	K <sub>i</sub>	[148]
K <sub>i</sub> OATP1B1 ( <i>SLCO1B1</i> )	μmol <sup>-1</sup>	0.391	-	K <sub>i</sub>	[148]
K <sub>i</sub> OATP1B1 ( <i>SLCO1B1</i> )	μmol <sup>-1</sup>	3.08	-	IC50	[185]
K <sub>i</sub> OATP1B1 ( <i>SLCO1B1</i> )	μmol <sup>-1</sup>	11.9	-	IC50	[186]
K <sub>i</sub> OATP1B1 ( <i>SLCO1B1</i> )	μmol <sup>-1</sup>	120	-	IC50	[187]
K <sub>i</sub> OATP1B1 ( <i>SLCO1B1</i> )	μmol <sup>-1</sup>	32.9	-	IC50	[188]
K <sub>i</sub> OATP1B1 ( <i>SLCO1B1</i> )	μmol <sup>-1</sup>	22.9	-	IC50	[188]
K <sub>i</sub> OATP1B1 ( <i>SLCO1B1</i> )	μmol <sup>-1</sup>	-	-	K <sub>i</sub>	[188]
K <sub>i</sub> OATP1B1 ( <i>SLCO1B1</i> )	μmol <sup>-1</sup>	1.91	-	IC50	[189]
K <sub>i</sub> OATP1B1 ( <i>SLCO1B1</i> )	μmol <sup>-1</sup>	1.3	-	IC50	[149]
K <sub>i</sub> OATP1B1 ( <i>SLCO1B1</i> )	μmol <sup>-1</sup>	0.74	-	IC50	[190]
K <sub>i</sub> OATP1B1 ( <i>SLCO1B1</i> )	μmol <sup>-1</sup>	0.24	-	IC50	[190]
K <sub>i</sub> OATP1B1 ( <i>SLCO1B1</i> )	μmol <sup>-1</sup>	1.9	-	IC50	[191]
K <sub>i</sub> OATP1B1 ( <i>SLCO1B1</i> )	μmol <sup>-1</sup>	-	-	K <sub>i</sub>	[191]
K <sub>i</sub> OATP1B1 ( <i>SLCO1B1</i> )	μmol <sup>-1</sup>	1.6	-	IC50	[160]
K <sub>i</sub> OATP1B1 ( <i>SLCO1B1</i> )	μmol <sup>-1</sup>	1.1	-	IC50	[160]
K <sub>i</sub> OATP1B1 ( <i>SLCO1B1</i> )	μmol <sup>-1</sup>	1.24	-	IC50	[192]

Table S3.5: Extracted drug-dependent parameter literature values for rifampicin (*continued*)

Parameter	Unit	Literature value	Standard deviation	Note	Reference
K <sub>i</sub> OATP1B1 ( <i>SLCO1B1</i> )	μmol <sup>-1</sup>	0.29	-	IC50	[192]
K <sub>i</sub> OATP1B1 ( <i>SLCO1B1</i> )	μmol <sup>-1</sup>	0.55	-	IC50	[193]
K <sub>i</sub> OATP1B1 ( <i>SLCO1B1</i> )	μmol <sup>-1</sup>	1.1	-	IC50	[193]
K <sub>i</sub> OATP1B1 ( <i>SLCO1B1</i> )	μmol <sup>-1</sup>	0.66	-	IC50	[194]
K <sub>i</sub> OATP1B1 ( <i>SLCO1B1</i> )	μmol <sup>-1</sup>	0.79	-	K <sub>i</sub>	[194]
K <sub>i</sub> OATP1B1 ( <i>SLCO1B1</i> )	μmol <sup>-1</sup>	0.6	-	IC50	[121]
K <sub>i</sub> OATP1B1 ( <i>SLCO1B1</i> )	μmol <sup>-1</sup>	2.65	-	IC50	[121]
K <sub>i</sub> OATP1B1 ( <i>SLCO1B1</i> )	μmol <sup>-1</sup>	2.2	-	IC50	[121]
K <sub>i</sub> OATP1B1 ( <i>SLCO1B1</i> )	μmol <sup>-1</sup>	0.62	-	K <sub>i</sub>	[195]
K <sub>i</sub> OATP1B1 ( <i>SLCO1B1</i> )	μmol <sup>-1</sup>	0.39	-	IC50	[196]
K <sub>i</sub> OATP1B1 ( <i>SLCO1B1</i> )	μmol <sup>-1</sup>	5.65	-	IC50	[197]
K <sub>i</sub> OATP1B1 ( <i>SLCO1B1</i> )	μmol <sup>-1</sup>	0.88	-	IC50	[197]
K <sub>i</sub> OATP1B1 ( <i>SLCO1B1</i> )	μmol <sup>-1</sup>	0.818	-	IC50	[198]
K <sub>i</sub> OATP1B1 ( <i>SLCO1B1</i> )	μmol <sup>-1</sup>	1.2	-	IC50	[198]
K <sub>i</sub> OATP1B1 ( <i>SLCO1B1</i> )	μmol <sup>-1</sup>	0.94	-	IC50	[199]
K <sub>i</sub> OATP1B1 ( <i>SLCO1B1</i> )	μmol <sup>-1</sup>	3.2	-	IC50	[200]
K <sub>i</sub> OATP1B1 ( <i>SLCO1B1</i> )	μmol <sup>-1</sup>	50	-	IC50	[200]
K <sub>i</sub> OATP1B1 ( <i>SLCO1B1</i> )	μmol <sup>-1</sup>	0.477	-	-	[2]
K <sub>i</sub> OATP1B1 ( <i>SLCO1B1</i> )	μmol <sup>-1</sup>	3.49	-	IC50	[201]
K <sub>i</sub> OATP1B1 ( <i>SLCO1B1</i> )	μmol <sup>-1</sup>	3.2	-	IC50	[202]
K <sub>i</sub> OATP1B1 ( <i>SLCO1B1</i> )	μmol <sup>-1</sup>	17	-	K <sub>i</sub>	[203]
K <sub>i</sub> OATP1B1 ( <i>SLCO1B1</i> )	μmol <sup>-1</sup>	2.2	-	IC50	[204]
K <sub>i</sub> OATP1B1 ( <i>SLCO1B1</i> )	μmol <sup>-1</sup>	6.75	-	K <sub>i</sub>	[161]
K <sub>i</sub> OATP1B1 ( <i>SLCO1B1</i> )	μmol <sup>-1</sup>	2.4	-	IC50	[205]
K <sub>i</sub> OATP1B1 ( <i>SLCO1B1</i> )	μmol <sup>-1</sup>	8.8	-	IC50	[152]
K <sub>i</sub> OATP1B1 ( <i>SLCO1B1</i> )	μmol <sup>-1</sup>	55.29	-	IC50	[206]
K <sub>i</sub> OATP1B3 ( <i>SLCO1B3</i> )	μmol <sup>-1</sup>	0.39	-	-	[195]
K <sub>i</sub> P-gp ( <i>ABCB1</i> )	μmol <sup>-1</sup>	29	-	IC50	[157]
K <sub>i</sub> P-gp ( <i>ABCB1</i> )	μmol <sup>-1</sup>	279	-	IC50	[158]
K <sub>i</sub> P-gp ( <i>ABCB1</i> )	μmol <sup>-1</sup>	4.3	-	K <sub>i</sub>	[159]
K <sub>i</sub> P-gp ( <i>ABCB1</i> )	μmol <sup>-1</sup>	23	-	K <sub>i</sub>	[159]
K <sub>i</sub> P-gp ( <i>ABCB1</i> )	μmol <sup>-1</sup>	175	-	IC50	[150]
K <sub>i</sub> P-gp ( <i>ABCB1</i> )	μmol <sup>-1</sup>	169	-	IC50	[207]
K <sub>i</sub> P-gp ( <i>ABCB1</i> )	μmol <sup>-1</sup>	169	-	-	[2]



Table S3.5: Extracted drug-dependent parameter literature values for rifampicin (*continued*)

Parameter	Unit	Literature value	Standard deviation	Note	Reference
K <sub>i</sub> UGT1A1	μmol <sup>-1</sup>	33	-	-	[170]
K <sub>i</sub> UGT1A3	μmol <sup>-1</sup>	600	-	-	[208]
E <sub>max</sub> AADAC	-	0.99	-	-	[2]
E <sub>max</sub> CYP2C8	-	4	-	-	[209]
E <sub>max</sub> CYP2C8	-	1.3	-	-	[210]
E <sub>max</sub> CYP2C8	-	3	-	-	[211]
E <sub>max</sub> CYP2C8	-	5	-	-	[128]
E <sub>max</sub> CYP2C8	-	3.2	-	-	[2]
E <sub>max</sub> CYP3A4	-	3.13	-	-	[212]
E <sub>max</sub> CYP3A4	-	10.5	-	-	[213]
E <sub>max</sub> CYP3A4	-	13	-	-	[209]
E <sub>max</sub> CYP3A4	-	6.2	-	-	[214]
E <sub>max</sub> CYP3A4	-	2.8	-	-	[215]
E <sub>max</sub> CYP3A4	-	2	-	-	[216]
E <sub>max</sub> CYP3A4	-	2	-	-	[217]
E <sub>max</sub> CYP3A4	-	18.5	-	-	[218]
E <sub>max</sub> CYP3A4	-	7.5	2.1	-	[219]
E <sub>max</sub> CYP3A4	-	4.3	-	-	[162]
E <sub>max</sub> CYP3A4	-	7.9	2.9	-	[220]
E <sub>max</sub> CYP3A4	-	4.1	-	-	[221]
E <sub>max</sub> CYP3A4	-	9.6	-	-	[222]
E <sub>max</sub> CYP3A4	-	12	4	-	[65]
E <sub>max</sub> CYP3A4	-	5	-	-	[211]
E <sub>max</sub> CYP3A4	-	2.8	0.5	-	[223]
E <sub>max</sub> CYP3A4	-	2.2	0.3	-	[223]
E <sub>max</sub> CYP3A4	-	3.2	0.2	-	[223]
E <sub>max</sub> CYP3A4	-	5.2	3.3	-	[223]
E <sub>max</sub> CYP3A4	-	10	-	-	[224]
E <sub>max</sub> CYP3A4	-	3.2	2.3	-	[225]
E <sub>max</sub> CYP3A4	-	30	-	-	[226]
E <sub>max</sub> CYP3A4	-	4	-	-	[227]
E <sub>max</sub> CYP3A4	-	14.5	-	-	[228]
E <sub>max</sub> CYP3A4	-	14.6	2	-	[229]
E <sub>max</sub> CYP3A4	-	2	-	-	[230]

Table S3.5: Extracted drug-dependent parameter literature values for rifampicin (*continued*)

Parameter	Unit	Literature value	Standard deviation	Note	Reference
$E_{\max}$ CYP3A4	-	2	-	-	[230]
$E_{\max}$ CYP3A4	-	10	-	-	[128]
$E_{\max}$ CYP3A4	-	4.12	0.09	-	[231]
$E_{\max}$ CYP3A4	-	14	-	-	[232]
$E_{\max}$ CYP3A4	-	3.8	-	-	[233]
$E_{\max}$ CYP3A4	-	9	-	-	[2]
$E_{\max}$ CYP3A4	-	4	-	-	[234]
$E_{\max}$ CYP3A4	-	5.9	-	-	[235]
$E_{\max}$ CYP3A4	-	8.9	-	-	[235]
$E_{\max}$ CYP3A4	-	3.2	-	-	[235]
$E_{\max}$ CYP3A4	-	2.1	0.3	-	[236]
$E_{\max}$ CYP3A5	-	2	-	-	[230]
$E_{\max}$ OATP1B1 ( <i>SLCO1B1</i> )	-	0.38	-	-	[2]
$E_{\max}$ P-gp ( <i>ABCB1</i> )	-	2.5	-	-	[2]
$E_{\max}$ PON3	-	0.99	-	-	[2]
$E_{\max}$ UGT1A1	-	1.3	-	-	[233]
$E_{\max}$ UGT1A3	-	1.4	-	-	[237]
Induction $EC_{50}$	$\mu\text{mol l}^{-1}$	0.37	0.1	-	[238]
Induction $EC_{50}$	$\mu\text{mol l}^{-1}$	0.12	0.02	-	[220]
Induction $EC_{50}$	$\mu\text{mol l}^{-1}$	0.6	-	-	[239]
Induction $EC_{50}$	$\mu\text{mol l}^{-1}$	0.14	0.02	-	[231]
Induction $EC_{50}$	$\mu\text{mol l}^{-1}$	3.2	-	-	[240]
Induction $EC_{50}$	$\mu\text{mol l}^{-1}$	0.34	-	-	[2]
Induction $EC_{50}$	$\mu\text{mol l}^{-1}$	0.18	-	-	[241]
Induction $EC_{50}$	$\mu\text{mol l}^{-1}$	0.51	-	-	[241]
Induction $EC_{50}$	$\mu\text{mol l}^{-1}$	0.18	-	-	[235]
Induction $EC_{50}$	$\mu\text{mol l}^{-1}$	1.1	-	-	[235]
Induction $EC_{50}$	$\mu\text{mol l}^{-1}$	0.65	-	-	[235]
Specific intest. perm.	$\text{cm min}^{-1}$	1.24e-05	-	-	[2]
Specific organ perm.	$\text{cm min}^{-1}$	2.93e-05	-	-	[2]

*Note:*

If  $IC_{50}$  values could not be used for  $K_i$  value estimation utilizing Cheng Prusoff Equation (e.g. due to missing substrate affinities)  $K_i = IC_{50}$  was assumed

3 Simvastatin DDIs

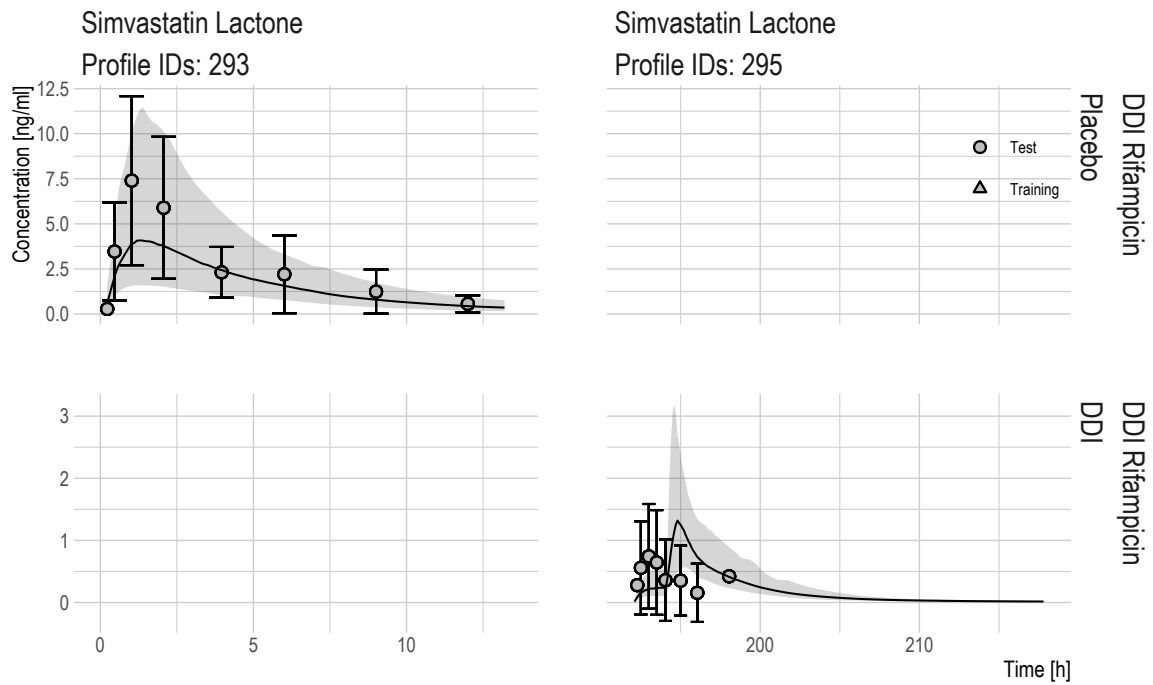


Figure S3.3: Linear VPCs of plasma concentration-time profiles for investigated DDIs: Rifampicin - Simvastatin Lactone. Solid line and shaded area are predicted median and 90% CI

3 Simvastatin DDIs

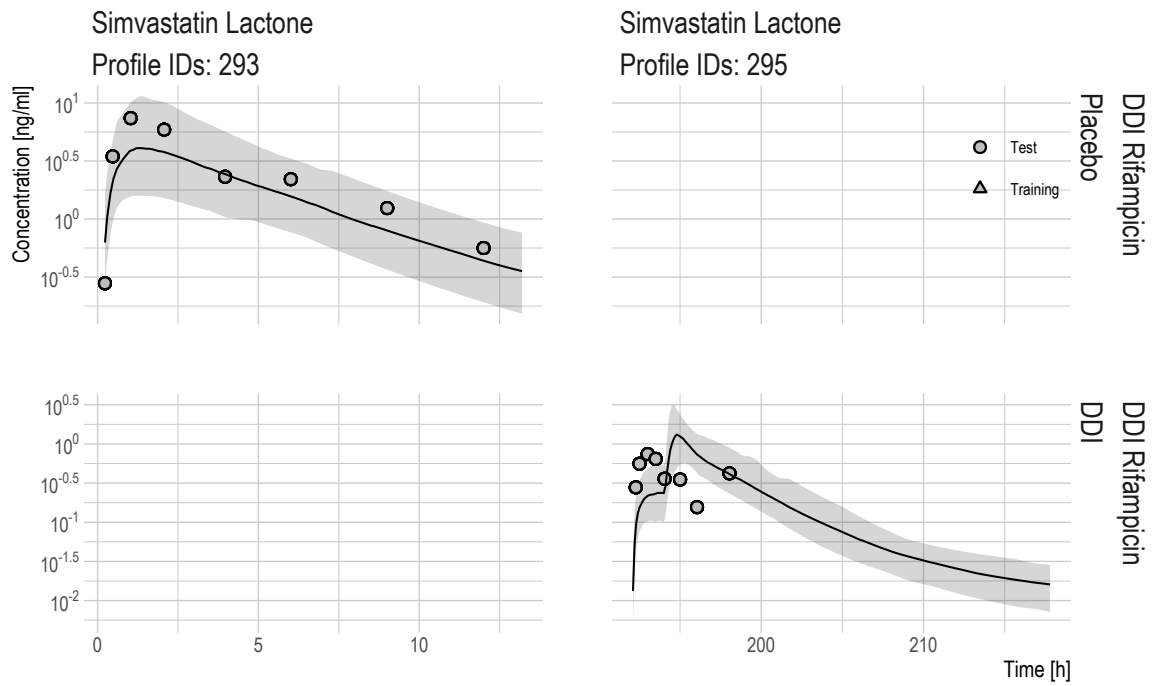


Figure S3.4: Semilogarithmic VPCs of plasma concentration-time profiles for investigated DDIs: Rifampicin - Simvastatin Lactone. Solid line and shaded area are predicted median and 90 % CI

## 3 Simvastatin DDIs

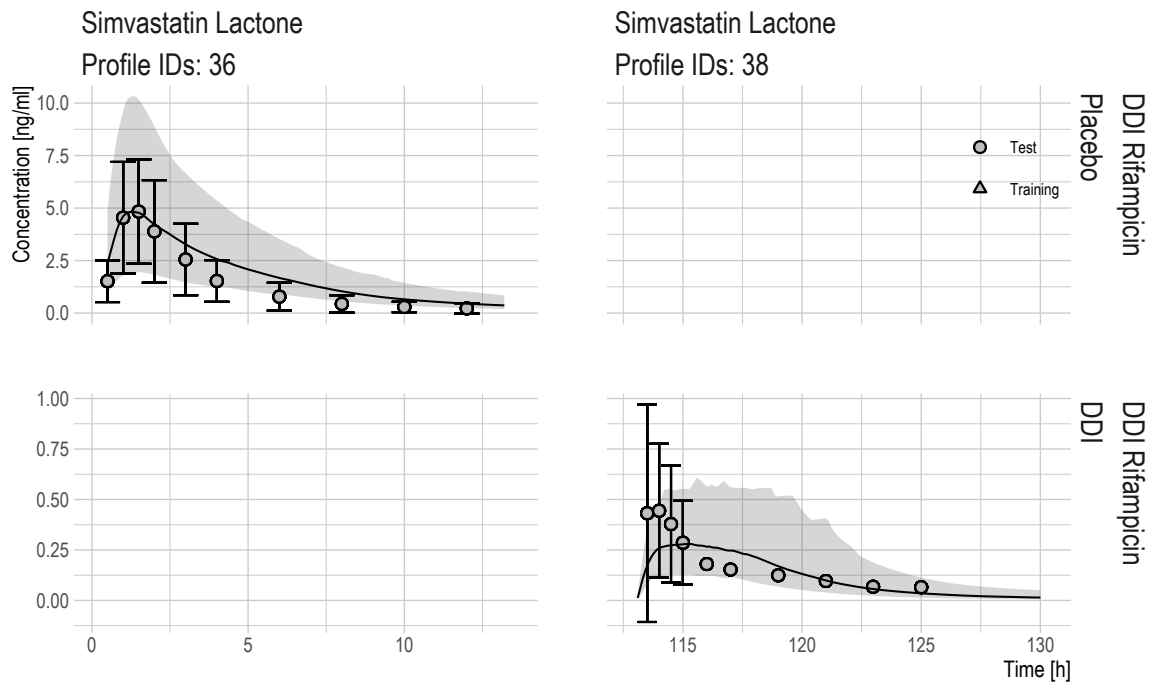


Figure S3.5: Linear VPCs of plasma concentration-time profiles for investigated DDIs: Rifampicin - Simvastatin Lactone. Solid line and shaded area are predicted median and 90% CI

3 Simvastatin DDIs

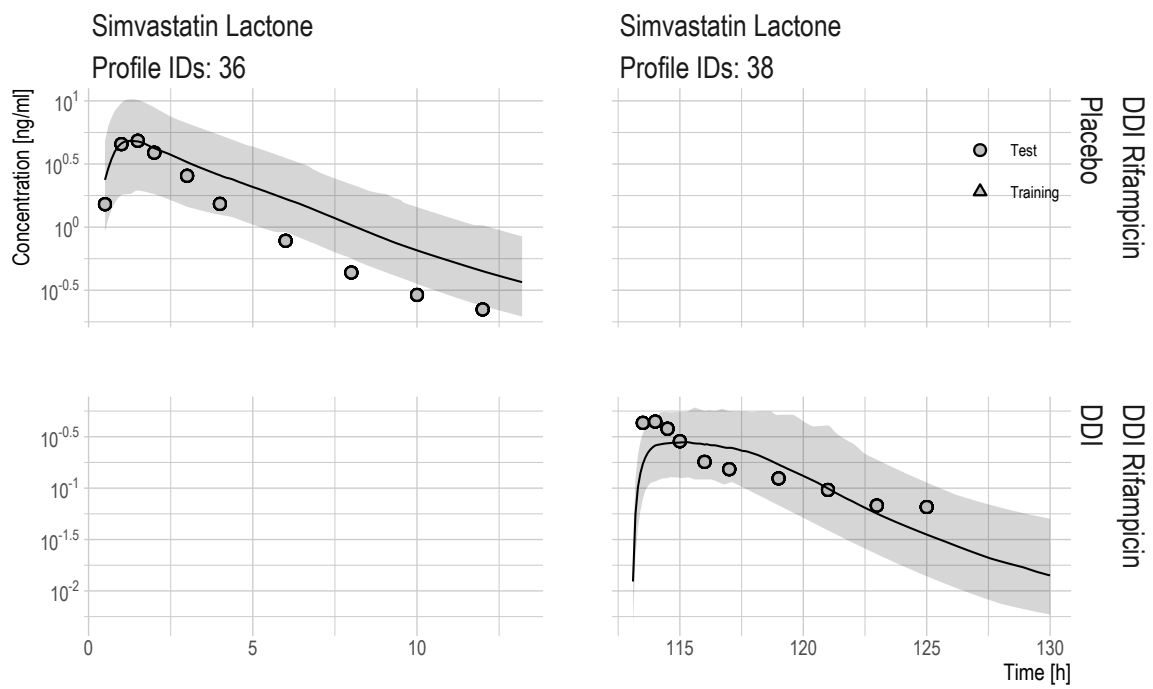


Figure S3.6: Semilogarithmic VPCs of plasma concentration-time profiles for investigated DDIs: Rifampicin - Simvastatin Lactone. Solid line and shaded area are predicted median and 90 % CI

3 Simvastatin DDIs

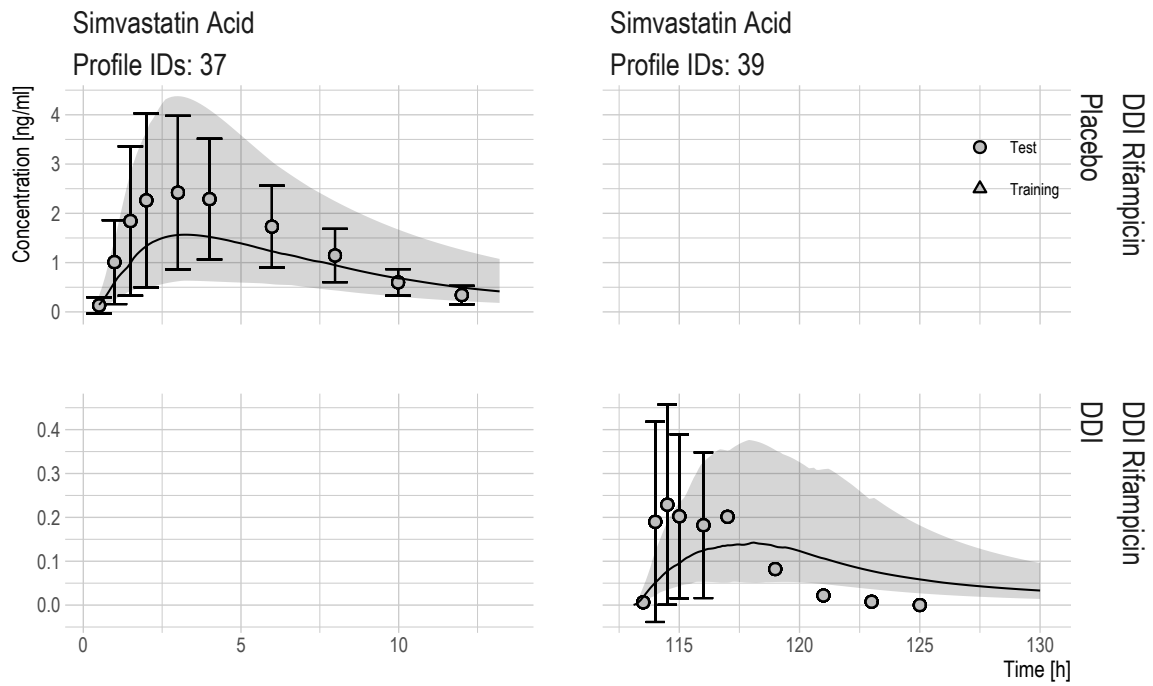


Figure S3.7: Linear VPCs of plasma concentration-time profiles for investigated DDIs: Rifampicin Simvastatin Acid. Solid line and shaded area are predicted median and 90% CI

3 Simvastatin DDIs

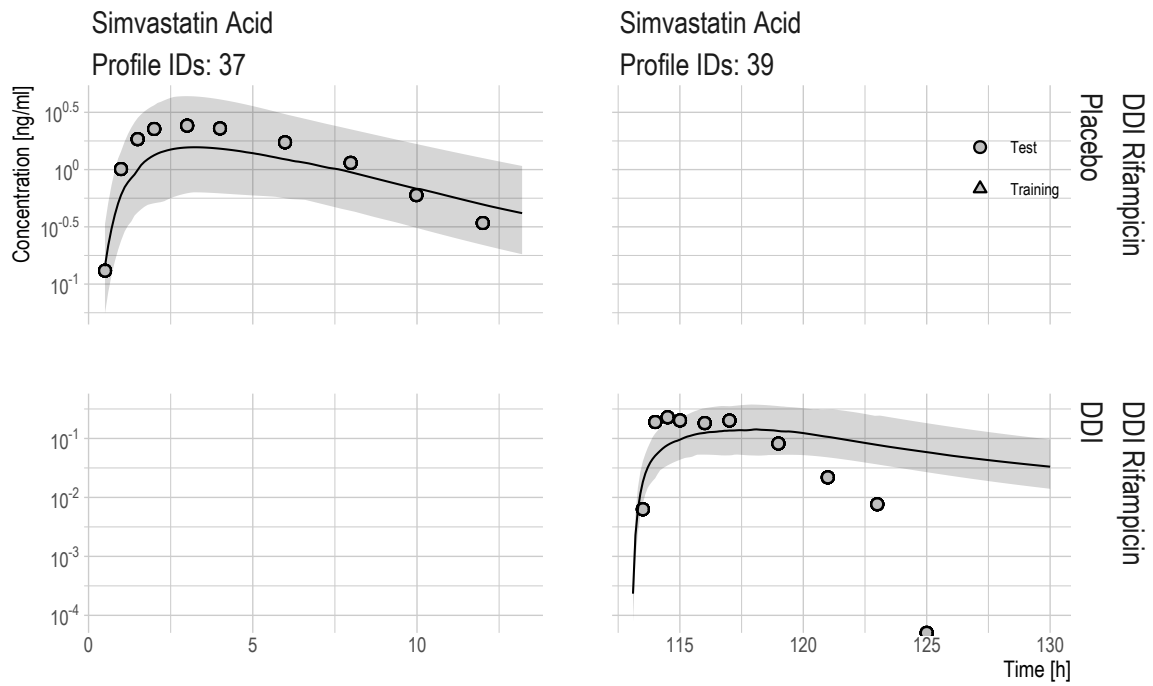


Figure S3.8: Semilogarithmic VPCs of plasma concentration-time profiles for investigated DDIs: Rifampicin Simvastatin Acid. Solid line and shaded area are predicted median and 90 % CI



### 3.4 Itraconazole

The antifungal substance itraconazole and its four metabolites hydroxy-itraconazole, keto-itraconazole and N-desalkyl-itraconazole are inhibitors of CYP3A4, OATP1B1, OATP1B3, P-gp and BCRP [146]. A previously developed itraconazole model was extended and subsequently used to describe the interactions [16]. Unfortunately, as already described by Tsamandouras et al. [39], due to limitation of the assay in the interaction study performed by Neuvonen et al. [145] SL and SA profiles could not be directly compared with model predicted values. However, the authors reportet an at least approximate 10-fold increase in SL AUC and  $C_{\max}$ . Following, this value was used for evaluating the model performance. The parameters of the extended parent-metabolite itraconazole model are given in Tables S3.6 - S3.13.

#### 3.4.1 Drug-dependent parameters

Table S3.6: Drug-dependent parameters in the itraconazole model compared to literature values

Parameter	Unit	Model value	Median (range) literature values	Origin	Description
<b>Molecule</b>					
fu	%	0.6	1.1 (0.2–3.6)	Literature	Fraction unbound plasma
Lipophilicity	-	4.62	5.14 (4.62–5.66)	Literature	Lipophilicity
MW	g mol <sup>-1</sup>	705.6	705.6	Literature	Molecular weight
pKa	-	3.7	3.7	Literature	Acid dissociation constant (basic)
Solubility	mg l <sup>-1</sup>	14.5	1.58 (0.69–14.5)	Literature	Solubility
<b>Enzymes</b>					
CYP3A4 k <sub>cat</sub>	min <sup>-1</sup>	0.04	-	Literature	CYP3A4 catalytic rate constant
CYP3A4 K <sub>m</sub>	μmol l <sup>-1</sup>	0.00207	-	Literature	CYP3A4 Michaelis-Menten constant
<b>Inhibition</b>					
K <sub>i</sub> BCRP ( <i>ABCG2</i> )	μmol l <sup>-1</sup>	10	2 (1.9–10)	Literature	Concentration for half-maximal BCRP competitive inhibition
K <sub>i</sub> CYP3A4	μmol l <sup>-1</sup>	0.0013	0.042 (0.0013–7)	Literature	Concentration for half-maximal CYP3A4 competitive inhibition
K <sub>i</sub> P-gp ( <i>ABCB1</i> )	μmol l <sup>-1</sup>	0.008	1.7 (0.008–9.5)	Literature	Concentration for half-maximal P-gp competitive inhibition
<b>Formulation</b>					
Dissolution shape	-	1.1	0.96 (0.82–1.1)	Optimized	Weibull function dissolution shape
Dissolution time (50% dissolved)	min	407	273 (139–407)	Optimized	Weibull function dissolution time (50% dissolved)
<b>System</b>					

Table S3.6: Drug-dependent parameters in the itraconazole model compared to literature values (*continued*)

Parameter	Unit	Model value	Median (range) literature values	Origin	Description
Specific intest. perm.	cm min <sup>-1</sup>	0.000533	0.000533	Literature	Permeation across intestinal mucosa normalized to surface area
Specific organ perm.	cm min <sup>-1</sup>	0.0144	0.0144	Literature	Permeation across cell membranes normalized to surface area

*Note:*

Cellular permabilites calculation method: PK-Sim Standard; organ-plasma partition coefficient calculation method: Rodgers and Rowland; formulation parameter values were used for solid oral dosage forms only

Table S3.7: Extracted drug-dependent literature values for itraconazole

Parameter	Unit	Literature value	Standard deviation	Note	Reference
fu	%	0.6	-	-	[2]
fu	%	0.2	-	-	[2]
fu	%	1.6	-	-	[2]
fu	%	3.6	-	-	[2]
Lipophilicity	-	4.62	-	-	[2]
Lipophilicity	-	5.66	-	-	[2]
MW	g mol <sup>-1</sup>	705.6	-	-	[2]
pKa	-	3.7	-	-	[2]
Solubility	mg l <sup>-1</sup>	8	-	FaSSIF	[2]
Solubility	mg l <sup>-1</sup>	1.58	-	capsule fasted	[2]
Solubility	mg l <sup>-1</sup>	14.5	-	capsule fasted	[2]
Solubility	mg l <sup>-1</sup>	0.69	-	capsule fed	[2]
Solubility	mg l <sup>-1</sup>	0.78	-	-	[2]
CYP3A4 k <sub>cat</sub>	min <sup>-1</sup>	0.04	-	-	[2]
CYP3A4 K <sub>M</sub>	-	3.09	-	-	[2]
CYP3A4 K <sub>M</sub>	μmol l <sup>-1</sup>	0.00207	-	-	[2]
K <sub>i</sub> BCRP ( <i>ABCG2</i> )	μmol l <sup>-1</sup>	2	-	-	[242]
K <sub>i</sub> BCRP ( <i>ABCG2</i> )	μmol l <sup>-1</sup>	10	-	-	[150]
K <sub>i</sub> BCRP ( <i>ABCG2</i> )	μmol l <sup>-1</sup>	1.9	-	-	[146]
K <sub>i</sub> CYP3A4	μmol l <sup>-1</sup>	0.076	-	-	[243]
K <sub>i</sub> CYP3A4	μmol l <sup>-1</sup>	0.7	0.2	-	[244]
K <sub>i</sub> CYP3A4	μmol l <sup>-1</sup>	0.044	-	-	[116]
K <sub>i</sub> CYP3A4	μmol l <sup>-1</sup>	0.016	-	-	[116]
K <sub>i</sub> CYP3A4	μmol l <sup>-1</sup>	0.045	-	-	[116]
K <sub>i</sub> CYP3A4	μmol l <sup>-1</sup>	0.012	-	-	[116]
K <sub>i</sub> CYP3A4	μmol l <sup>-1</sup>	0.013	-	-	[116]
K <sub>i</sub> CYP3A4	μmol l <sup>-1</sup>	0.016	-	-	[116]
K <sub>i</sub> CYP3A4	μmol l <sup>-1</sup>	0.016	-	-	[116]
K <sub>i</sub> CYP3A4	μmol l <sup>-1</sup>	0.052	-	-	[116]
K <sub>i</sub> CYP3A4	μmol l <sup>-1</sup>	0.013	-	-	[116]
K <sub>i</sub> CYP3A4	μmol l <sup>-1</sup>	0.5	-	-	[245]
K <sub>i</sub> CYP3A4	μmol l <sup>-1</sup>	3.12	-	-	[245]
K <sub>i</sub> CYP3A4	μmol l <sup>-1</sup>	0.32	-	-	[245]
K <sub>i</sub> CYP3A4	μmol l <sup>-1</sup>	0.23	-	-	[245]

Table S3.7: Extracted drug-dependent literature values for itraconazole (*continued*)

Parameter	Unit	Literature value	Standard deviation	Note	Reference
K <sub>i</sub> CYP3A4	μmol <sup>-1</sup>	0.0031	-	-	[105]
K <sub>i</sub> CYP3A4	μmol <sup>-1</sup>	0.0038	-	-	[105]
K <sub>i</sub> CYP3A4	μmol <sup>-1</sup>	0.0014	-	-	[105]
K <sub>i</sub> CYP3A4	μmol <sup>-1</sup>	0.0047	-	-	[105]
K <sub>i</sub> CYP3A4	μmol <sup>-1</sup>	0.0013	-	-	[246]
K <sub>i</sub> CYP3A4	μmol <sup>-1</sup>	0.04	-	-	[247]
K <sub>i</sub> CYP3A4	μmol <sup>-1</sup>	7	-	-	[248]
K <sub>i</sub> CYP3A4	μmol <sup>-1</sup>	2	-	-	[248]
K <sub>i</sub> CYP3A4	μmol <sup>-1</sup>	0.49	-	-	[249]
K <sub>i</sub> CYP3A4	μmol <sup>-1</sup>	1	-	-	[249]
K <sub>i</sub> CYP3A4	μmol <sup>-1</sup>	0.0013	-	-	[2]
K <sub>i</sub> CYP3A4	μmol <sup>-1</sup>	2.3	-	-	[250]
K <sub>i</sub> CYP3A4	μmol <sup>-1</sup>	0.03	-	-	[251]
K <sub>i</sub> P-gp ( <i>ABCB1</i> )	μmol <sup>-1</sup>	6	-	-	[153]
K <sub>i</sub> P-gp ( <i>ABCB1</i> )	μmol <sup>-1</sup>	2	-	-	[153]
K <sub>i</sub> P-gp ( <i>ABCB1</i> )	μmol <sup>-1</sup>	0.16	-	-	[252]
K <sub>i</sub> P-gp ( <i>ABCB1</i> )	μmol <sup>-1</sup>	1.25	-	-	[122]
K <sub>i</sub> P-gp ( <i>ABCB1</i> )	μmol <sup>-1</sup>	0.41	-	-	[154]
K <sub>i</sub> P-gp ( <i>ABCB1</i> )	μmol <sup>-1</sup>	0.46	-	-	[154]
K <sub>i</sub> P-gp ( <i>ABCB1</i> )	μmol <sup>-1</sup>	2	-	-	[242]
K <sub>i</sub> P-gp ( <i>ABCB1</i> )	μmol <sup>-1</sup>	1.8	-	-	[123]
K <sub>i</sub> P-gp ( <i>ABCB1</i> )	μmol <sup>-1</sup>	9.5	-	-	[150]
K <sub>i</sub> P-gp ( <i>ABCB1</i> )	μmol <sup>-1</sup>	6.7	-	-	[150]
K <sub>i</sub> P-gp ( <i>ABCB1</i> )	μmol <sup>-1</sup>	0.45	-	-	[124]
K <sub>i</sub> P-gp ( <i>ABCB1</i> )	μmol <sup>-1</sup>	0.008	-	-	[2]
K <sub>i</sub> P-gp ( <i>ABCB1</i> )	μmol <sup>-1</sup>	0.048	-	-	[146]
K <sub>i</sub> P-gp ( <i>ABCB1</i> )	μmol <sup>-1</sup>	1.7	-	-	[43]
K <sub>i</sub> P-gp ( <i>ABCB1</i> )	μmol <sup>-1</sup>	2.4	-	-	[43]
K <sub>i</sub> P-gp ( <i>ABCB1</i> )	μmol <sup>-1</sup>	1.7	-	-	[253]
Dissolution shape	-	0.82	-	capsule fed	[2]
Dissolution shape	-	1.1	-	capsule fasted	[2]
Dissolution time (50 % dissolved)	min	139	-	capsule fed	[2]

Table S3.7: Extracted drug-dependent literature values for itraconazole (*continued*)

Parameter	Unit	Literature value	Standard deviation	Note	Reference
Dissolution time (50 % dissolved)	min	407	-	capsule fasted	[2]
Specific intest. perm.	cm min <sup>-1</sup>	0.000533	-	-	[2]
Specific organ perm.	cm min <sup>-1</sup>	0.0144	-	-	[2]

*Note:*

If IC50 values could not be used for  $K_i$  value estimation utilizing Cheng Prusoff Equation (e.g. due to missing substrate affinities)  $K_i = IC50$  was assumed

Table S3.8: Drug-dependent parameters in the hydroxy-itraconazole model compared to literature values

Parameter	Unit	Model value	Median (range) literature values	Origin	Description
<b>Molecule</b>					
$f_u$	%	1.7	1.7	Literature	Fraction unbound plasma
Lipophilicity	-	3.72	4.11 (3.72–4.5)	Literature	Lipophilicity
MW	$\text{g mol}^{-1}$	721.6	721.6	Literature	Molecular weight
pKa	-	3.7	3.7	Literature	Acid dissociation constant (basic)
<b>Enzymes</b>					
CYP3A4 $k_{\text{cat}}$	$\text{min}^{-1}$	0.02	0.02	Literature	CYP3A4 catalytic rate constant
CYP3A4 $K_M$	$\mu\text{mol l}^{-1}$	0.00417	0.01558 (0.00417–0.027)	Literature	CYP3A4 Michaelis-Menten constant
<b>Inhibition</b>					
$K_i$ BCRP ( <i>ABCG2</i> )	$\mu\text{mol l}^{-1}$	12	5.7 (0.44–12)	Literature	Concentration for half-maximal BCRP competitive inhibition
$K_i$ CYP3A4	$\mu\text{mol l}^{-1}$	0.0144	0.0378 (0.0144–6.3)	Literature	Concentration for half-maximal CYP3A4 competitive inhibition
$K_i$ OATP1B1 ( <i>SLCO1B1</i> )	$\mu\text{mol l}^{-1}$	0.23	0.23 (0.018–5.9)	Literature	Concentration for half-maximal OATP1B1 competitive inhibition
$K_i$ OATP1B3 ( <i>SLCO1B3</i> )	$\mu\text{mol l}^{-1}$	0.1	0.1	Literature	Concentration for half-maximal OATP1B3 competitive inhibition
$K_i$ P-gp ( <i>ABCB1</i> )	$\mu\text{mol l}^{-1}$	0.49	3.3 (0.49–7)	Literature	Concentration for half-maximal P-gp competitive inhibition
<b>System</b>					
EHC	-	1	-	Assumed	Fraction of bile continually released from the gallbladder

Table S3.8: Drug-dependent parameters in the hydroxy-itraconazole model compared to literature values (*continued*)

Parameter	Unit	Model value	Median (range) literature values	Origin	Description
GFR	-	1	-	Assumed	Fraction of filtered drug reaching the urine
Specific intest. perm.	cm min <sup>-1</sup>	1.52e-05	1.52e-05	Literature	Permeation across intestinal mucosa normalized to surface area
Specific organ perm.	cm min <sup>-1</sup>	0.00155	0.00155	Literature	Permeation across cell membranes normalized to surface area

*Note:*

Cellular permabilites calculation method: PK-Sim standard; organ-plasma partition coefficient calculation method: Rodgers and Rowland



Table S3.9: Extracted drug-dependent literature values for hydroxy-itraconazole

Parameter	Unit	Literature value	Standard deviation	Note	Reference
fu	%	1.7	-	-	[2]
Lipophilicity	-	3.72	-	-	[2]
Lipophilicity	-	4.5	-	-	[2]
MW	g mol <sup>-1</sup>	721.6	-	-	[2]
pKa	-	3.7	-	(basic)	[2]
CYP3A4 k <sub>cat</sub>	min <sup>-1</sup>	0.02	-	-	[2]
CYP3A4 K <sub>M</sub>	μmol l <sup>-1</sup>	0.00417	-	-	[2]
CYP3A4 K <sub>M</sub>	μmol l <sup>-1</sup>	0.027	-	-	[2]
K <sub>i</sub> BCRP ( <i>ABCG2</i> )	μmol l <sup>-1</sup>	12	-	IC50	[242]
K <sub>i</sub> BCRP ( <i>ABCG2</i> )	μmol l <sup>-1</sup>	5.7	-	IC50	[150]
K <sub>i</sub> BCRP ( <i>ABCG2</i> )	μmol l <sup>-1</sup>	0.44	-	IC50	[146]
K <sub>i</sub> CYP3A4	μmol l <sup>-1</sup>	6.3	-	K <sub>i</sub>	[246]
K <sub>i</sub> CYP3A4	μmol l <sup>-1</sup>	0.0144	-	-	[2]
K <sub>i</sub> CYP3A4	μmol l <sup>-1</sup>	0.0378	-	K <sub>i</sub>	[250]
K <sub>i</sub> OATP1B1 ( <i>SLCO1B1</i> )	μmol l <sup>-1</sup>	5.9	-	IC50	[150]
K <sub>i</sub> OATP1B1 ( <i>SLCO1B1</i> )	μmol l <sup>-1</sup>	0.018	-	-	[2]
K <sub>i</sub> OATP1B1 ( <i>SLCO1B1</i> )	μmol l <sup>-1</sup>	0.23	-	IC50	[2]
K <sub>i</sub> OATP1B1 ( <i>SLCO1B1</i> )	μmol l <sup>-1</sup>	0.23	-	IC50	[146]
K <sub>i</sub> OATP1B3 ( <i>SLCO1B3</i> )	μmol l <sup>-1</sup>	0.1	-	-	[146]
K <sub>i</sub> P-gp ( <i>ABCB1</i> )	μmol l <sup>-1</sup>	5	-	IC50	[242]
K <sub>i</sub> P-gp ( <i>ABCB1</i> )	μmol l <sup>-1</sup>	7	-	IC50	[150]
K <sub>i</sub> P-gp ( <i>ABCB1</i> )	μmol l <sup>-1</sup>	1.6	-	IC50	[150]
K <sub>i</sub> P-gp ( <i>ABCB1</i> )	μmol l <sup>-1</sup>	0.49	-	IC50	[146]
Specific intest. perm.	cm min <sup>-1</sup>	1.52e-05	-	-	[2]
Specific organ perm.	cm min <sup>-1</sup>	0.00155	-	-	[2]

*Note:*

If IC50 values could not be used for  $K_i$  value estimation utilizing Cheng Prusoff Equation (e.g. due to missing substrate affinities)  $K_i = IC50$  was assumed

Table S3.10: Drug-dependent parameters in the keto-itraconazole model compared to literature values

Parameter	Unit	Model value	Median (range) literature values	Origin	Description
<b>Molecule</b>					
fu	%	1	1	Literature	Fraction unbound plasma
Lipophilicity	-	4.21	4.355 (4.21–4.5)	Literature	Lipophilicity
MW	g mol <sup>-1</sup>	719.6	719.6	Literature	Molecular weight
pKa	-	3.7	3.7	Literature	Acid dissociation constant (basic)
<b>Enzymes</b>					
CYP3A4 k <sub>cat</sub>	min <sup>-1</sup>	0.393	0.393	Literature	CYP3A4 catalytic rate constant
CYP3A4 K <sub>M</sub>	μmol l <sup>-1</sup>	0.00222	0.00222	Literature	CYP3A4 Michaelis-Menten constant
<b>Inhibition</b>					
K <sub>i</sub> BCRP ( <i>ABCG2</i> )	μmol l <sup>-1</sup>	2.1	1.1 (0.1–2.1)	Literature	Concentration for half-maximal BCRP competitive inhibition
K <sub>i</sub> CYP3A4	μmol l <sup>-1</sup>	0.00512	0.03 (0.00512–0.098)	Literature	Concentration for half-maximal CYP3A4 competitive inhibition
K <sub>i</sub> OATP1B1 ( <i>SLCO1B1</i> )	μmol l <sup>-1</sup>	0.29	5.195 (0.29–10.1)	Literature	Concentration for half-maximal OATP1B1 competitive inhibition
K <sub>i</sub> OATP1B3 ( <i>SLCO1B3</i> )	μmol l <sup>-1</sup>	0.088	0.088	Literature	Concentration for half-maximal OATP1B3 competitive inhibition
K <sub>i</sub> P-gp ( <i>ABCB1</i> )	μmol l <sup>-1</sup>	0.49	2.2 (0.12–2.5)	Literature	Concentration for half-maximal P-gp competitive inhibition
<b>System</b>					
EHC	-	1	-	Assumed	Fraction of bile continually released from the gallbladder

Table S3.10: Drug-dependent parameters in the keto-itraconazole model compared to literature values (*continued*)

Parameter	Unit	Model value	Median (range) literature values	Origin	Description
GFR	-	1	-	Assumed	Fraction of filtered drug reaching the urine
Specific intest. perm.	cm min <sup>-1</sup>	4.79e-05	4.79e-05	Literature	Permeation across intestinal mucosa normalized to surface area
Specific organ perm.	cm min <sup>-1</sup>	0.00492	0.00492	Literature	Permeation across cell membranes normalized to surface area

*Note:*

Cellular permabilites calculation method: PK-Sim standard; organ-plasma partition coefficient calculation method: Rodgers and Rowland

Table S3.11: Extracted drug-dependent literature values for keto-itraconazole

Parameter	Unit	Literature value	Standard deviation	Note	Reference
fu	%	1	-	-	[2]
Lipophilicity	-	4.21	-	-	[2]
Lipophilicity	-	4.5	-	-	[2]
MW	g mol <sup>-1</sup>	719.6	-	-	[2]
pKa	-	3.7	-	(basic)	[2]
CYP3A4 k <sub>cat</sub>	min <sup>-1</sup>	0.393	-	-	[2]
CYP3A4 K <sub>M</sub>	μmol l <sup>-1</sup>	0.00222	-	-	[2]
K <sub>i</sub> BCRP ( <i>ABCG2</i> )	μmol l <sup>-1</sup>	2.1	-	IC50	[150]
K <sub>i</sub> BCRP ( <i>ABCG2</i> )	μmol l <sup>-1</sup>	0.1	-	IC50	[146]
K <sub>i</sub> CYP3A4	μmol l <sup>-1</sup>	0.098	-	IC50	[254]
K <sub>i</sub> CYP3A4	μmol l <sup>-1</sup>	0.053	-	IC50	[246]
K <sub>i</sub> CYP3A4	μmol l <sup>-1</sup>	0.007	-	IC50	[246]
K <sub>i</sub> CYP3A4	μmol l <sup>-1</sup>	0.00512	-	-	[2]
K <sub>i</sub> OATP1B1 ( <i>SLCO1B1</i> )	μmol l <sup>-1</sup>	10.1	-	IC50	[150]
K <sub>i</sub> OATP1B1 ( <i>SLCO1B1</i> )	μmol l <sup>-1</sup>	0.29	-	IC50	[146]
K <sub>i</sub> OATP1B3 ( <i>SLCO1B3</i> )	μmol l <sup>-1</sup>	0.088	-	-	[146]
K <sub>i</sub> P-gp ( <i>ABCB1</i> )	μmol l <sup>-1</sup>	2.5	-	IC50	[150]
K <sub>i</sub> P-gp ( <i>ABCB1</i> )	μmol l <sup>-1</sup>	2.2	-	IC50	[150]
K <sub>i</sub> P-gp ( <i>ABCB1</i> )	μmol l <sup>-1</sup>	0.12	-	IC50	[146]
Specific intest. perm.	cm min <sup>-1</sup>	4.79e-05	-	-	[2]
Specific organ perm.	cm min <sup>-1</sup>	0.00492	-	-	[2]

*Note:*

If IC50 values could not be used for  $K_i$  value estimation utilizing Cheng Prusoff Equation (e.g. due to missing substrate affinities)  $K_i = IC50$  was assumed

Table S3.12: Drug-dependent parameters in the n-desalkyl-itraconazole model compared to literature values

Parameter	Unit	Model value	Median (range) literature values	Origin	Description
<b>Molecule</b>					
fu	%	1.1	1.1	Literature	Fraction unbound plasma
Lipophilicity	-	5.18	4.69 (4.2–5.18)	Literature	Lipophilicity
MW	g mol <sup>-1</sup>	649.5	649.5	Literature	Molecular weight
pKa	-	3.7	3.7	Literature	Acid dissociation constant (basic)
<b>Enzymes</b>					
CYP3A4 k <sub>cat</sub>	min <sup>-1</sup>	0.061	0.061	Literature	CYP3A4 catalytic rate constant
CYP3A4 K <sub>M</sub>	μmol l <sup>-1</sup>	0.00063	0.00063	Literature	CYP3A4 Michaelis-Menten constant
<b>Inhibition</b>					
K <sub>i</sub> CYP3A4	μmol l <sup>-1</sup>	0.00032	0.00032	Literature	Concentration for half-maximal CYP3A4 competitive inhibition
K <sub>i</sub> OATP1B1 ( <i>SLCO1B1</i> )	μmol l <sup>-1</sup>	7.5	7.5	Literature	Concentration for half-maximal OATP1B1 competitive inhibition
K <sub>i</sub> OATP1B3 ( <i>SLCO1B3</i> )	μmol l <sup>-1</sup>	2.1	2.1	Literature	Concentration for half-maximal OATP1B3 competitive inhibition
K <sub>i</sub> P-gp ( <i>ABCB1</i> )	μmol l <sup>-1</sup>	0.26	0.26	Literature	Concentration for half-maximal P-gp competitive inhibition
<b>System</b>					
EHC	-	1	-	Assumed	Fraction of bile continually released from the gallbladder
GFR	-	1	-	Assumed	Fraction of filtered drug reaching the urine

Table S3.12: Drug-dependent parameters in the n-desalkyl-itraconazole model compared to literature values (*continued*)

Parameter	Unit	Model value	Median (range) literature values	Origin	Description
Specific intest. perm.	cm min <sup>-1</sup>	0.000737	0.000737	Literature	Permeation across intestinal mucosa normalized to surface area
Specific organ perm.	cm min <sup>-1</sup>	0.0891	0.0891	Literature	Permeation across cell membranes normalized to surface area

*Note:*

Cellular permeabilities calculation method: PK-Sim standard; organ-plasma partition coefficient calculation method: Rodgers and Rowland

Table S3.13: Extracted drug-dependent literature values for n-desalkyl-itraconazole

Parameter	Unit	Literature value	Standard deviation	Note	Reference
fu	%	1.1	-	-	[2]
Lipophilicity	-	5.18	-	-	[2]
Lipophilicity	-	4.2	-	-	[2]
MW	g mol <sup>-1</sup>	649.5	-	-	[2]
pKa	-	3.7	-	(basic)	[2]
CYP3A4 k <sub>cat</sub>	min <sup>-1</sup>	0.061	-	-	[2]
CYP3A4 K <sub>M</sub>	μmol l <sup>-1</sup>	0.00063	-	-	[2]
K <sub>i</sub> CYP3A4	μmol l <sup>-1</sup>	0.00032	-	-	[2]
K <sub>i</sub> OATP1B1 ( <i>SLCO1B1</i> )	μmol l <sup>-1</sup>	7.5	-	IC50	[150]
K <sub>i</sub> OATP1B3 ( <i>SLCO1B3</i> )	μmol l <sup>-1</sup>	2.1	-	-	[146]
K <sub>i</sub> P-gp ( <i>ABCB1</i> )	μmol l <sup>-1</sup>	0.26	0.05	IC50	[146]
Specific intest. perm.	cm min <sup>-1</sup>	0.000737	-	-	[2]
Specific organ perm.	cm min <sup>-1</sup>	0.0891	-	-	[2]

*Note:*

If IC50 values could not be used for  $K_i$  value estimation utilizing Cheng Prusoff Equation (e.g. due to missing substrate affinities)  $K_i = IC50$  was assumed

### 3.5 Gemfibrozil

Gemfibrozil is an antihyperlipidaemic drug and together with its metabolite gemfibrozil 1-O- $\beta$ -glucuronide they are strong inhibitors of CYP2C8 and OATP1B1 [255, 2]. It has to be noted that at the beginning, the parent-metabolite gemfibrozil model was not capable to describe the observed decrease of SL and increase of SA exposure under gemfibrozil co-treatment. This effect is visible in humans as well as in animals [142, 128, 256]. In a study performed by Prueksaritanont et al. [256] in dogs, SA AUC under gemfibrozil treatment is increased by 160 % accompanied with an SL AUC decrease of 51 %. For this reason, it was assumed that gemfibrozil additionally induces PON3. Although not investigated for PON3, at least this has previously been shown for paraoxonase 1 (PON1) [257]. Following, for the simvastatin co-treatment with gemfibrozil an increase of the PON3 activity by 59 % was assumed which reflects the increase observed for PON1. The parameters of the extended gemfibrozil model are given in Tables S3.14 - S3.17. Results of the simvastatin-gemfibrozil DDI interaction are shown in Figs. S3.9 - S3.12.

#### 3.5.1 Drug-dependent parameters



Table S3.14: Drug-dependent parameters of the final gemfibrozil model compared to literature values

Parameter	Unit	Model value	Median (range) literature values	Origin	Description
<b>Molecule</b>					
fu	%	0.648	2.1 (0.648-3)	Literature	Fraction unbound plasma
Lipophilicity	-	2.8	4.3 (2.8-4.77)	Literature	Lipophilicity
MW	-	250.3	250.3	Literature	Molecular weight
pKa	-	4.7	4.7	Literature	Acid dissociation constant
Solubility	mg l <sup>-1</sup>	170	170	Literature	Solubility at pH=5.9
<b>Enzymes</b>					
UGT2B7 k <sub>cat</sub>	min <sup>-1</sup>	51.98	51.98	Literature	UGT2B7 catalytic rate constant
UGT2B7 K <sub>M</sub>	μmol l <sup>-1</sup>	2.2	2.2	Literature	UGT2B7 Michaelis-Menten constant
<b>Transporters</b>					
Active hepatic uptake k <sub>cat</sub>	min <sup>-1</sup>	59.42	59.42	Literature	Active hepatic uptake catalytic rate constant
Active hepatic uptake K <sub>M</sub>	μmol l <sup>-1</sup>	2.39	2.39	Literature	Active hepatic uptake Michaelis-Menten constant
<b>Inhibition</b>					
K <sub>i</sub> CYP2C8	μmol l <sup>-1</sup>	9.3	19.85 (9.3-30.4)	Literature	Concentration for half-maximal CYP2C8 competitive inhibition
K <sub>i</sub> OATP1B1 ( <i>SLCO1B1</i> )	μmol l <sup>-1</sup>	4	35.8 (4-381)	Literature	Concentration for half-maximal OATP1B1 competitive inhibition
K <sub>i</sub> OATP1B3 ( <i>SLCO1B3</i> )	μmol l <sup>-1</sup>	10	10	Literature	Concentration for half-maximal OATP1B3 competitive inhibition
K <sub>i</sub> UGT1A1	μmol l <sup>-1</sup>	36	36	Literature	Concentration for half-maximal UGT1A1 competitive inhibition

Table S3.14: Drug-dependent parameters of the final gemfibrozil model compared to literature values (*continued*)

Parameter	Unit	Model value	Median (range) literature values	Origin	Description
K <sub>i</sub> UGT1A3	μmol <sup>-1</sup>	37.6	37.6	Literature	Concentration for half-maximal UGT1A3 competitive inhibition
<b>Induction</b>					
PON3 factor	-	1.59	1.59	Literature	Assumed PON3 induction under gemfibrozil co-treatment
<b>Formulation</b>					
Dissolution shape	-	1.56	1.56	Literature	Weibull function dissolution shape
Dissolution time (50 % dissolved)	min	24.45	24.45	Literature	Weibull function dissolution time (50% dissolved)
<b>System</b>					
EHC	-	1	-	Assumed	Fraction of bile continually released from the gallbladder
GFR	-	1	-	Assumed	Fraction of filtered drug reaching the urine
Specific intest. perm.	cm min <sup>-1</sup>	0.00662	0.00662	Literature	Permeation across intestinal mucosa normalized to surface area
Specific organ perm.	cm min <sup>-1</sup>	0.07	0.07	Calculated	Permeation across cell membranes normalized to surface area

*Note:*

Cellular permeabilities calculation method: Charge-dependent Schmitt; organ-plasma partition coefficient calculation method: Berezhkovskiy; formulation parameter values were used for solid oral dosage forms only

Table S3.15: Extracted drug-dependent literature values for gemfibrozil

Parameter	Unit	Literature value	Standard deviation	Note	Reference
fu	%	0.648	-	-	[2]
fu	%	2.1	-	-	[2]
fu	%	3	-	-	[2]
Lipophilicity	-	2.8	-	-	[2]
Lipophilicity	-	4.3	-	-	[2]
Lipophilicity	-	4.77	-	-	[2]
MW	-	250.3	-	-	[2]
pKa	-	4.7	-	-	[2]
Solubility	mg l <sup>-1</sup>	170	-	pH 5.9	[2]
UGT2B7 k <sub>cat</sub>	min <sup>-1</sup>	51.98	-	-	[2]
UGT2B7 K <sub>M</sub>	μmol l <sup>-1</sup>	2.2	-	-	[2]
Active hepatic uptake k <sub>cat</sub>	min <sup>-1</sup>	59.42	-	-	[2]
Active hepatic uptake K <sub>M</sub>	μmol l <sup>-1</sup>	2.39	-	-	[2]
K <sub>i</sub> CYP2C8	μmol l <sup>-1</sup>	30.4	-	K <sub>i</sub>	[2]
K <sub>i</sub> CYP2C8	μmol l <sup>-1</sup>	9.3	-	K <sub>i</sub>	[114]
K <sub>i</sub> OATP1B1 ( <i>SLCO1B1</i> )	μmol l <sup>-1</sup>	7.4	-	IC50	[258]
K <sub>i</sub> OATP1B1 ( <i>SLCO1B1</i> )	μmol l <sup>-1</sup>	25.2	-	K <sub>i</sub>	[147]
K <sub>i</sub> OATP1B1 ( <i>SLCO1B1</i> )	μmol l <sup>-1</sup>	25	-	IC50	[259]
K <sub>i</sub> OATP1B1 ( <i>SLCO1B1</i> )	μmol l <sup>-1</sup>	173	-	IC50	[177]
K <sub>i</sub> OATP1B1 ( <i>SLCO1B1</i> )	μmol l <sup>-1</sup>	26.4	-	IC50	[177]
K <sub>i</sub> OATP1B1 ( <i>SLCO1B1</i> )	μmol l <sup>-1</sup>	381	-	IC50	[177]
K <sub>i</sub> OATP1B1 ( <i>SLCO1B1</i> )	μmol l <sup>-1</sup>	26.4	2.1	K <sub>i</sub>	[178]
K <sub>i</sub> OATP1B1 ( <i>SLCO1B1</i> )	μmol l <sup>-1</sup>	381	60	K <sub>i</sub>	[178]
K <sub>i</sub> OATP1B1 ( <i>SLCO1B1</i> )	μmol l <sup>-1</sup>	173	34	K <sub>i</sub>	[178]
K <sub>i</sub> OATP1B1 ( <i>SLCO1B1</i> )	μmol l <sup>-1</sup>	58.8	10.7	K <sub>i</sub> Pitavastatin	[178]
K <sub>i</sub> OATP1B1 ( <i>SLCO1B1</i> )	μmol l <sup>-1</sup>	46	8.9	K <sub>i</sub> Atorvastatin	[178]
K <sub>i</sub> OATP1B1 ( <i>SLCO1B1</i> )	μmol l <sup>-1</sup>	72.7	8.7	K <sub>i</sub> Fluvastatin	[178]
K <sub>i</sub> OATP1B1 ( <i>SLCO1B1</i> )	μmol l <sup>-1</sup>	63.6	8.4	K <sub>i</sub> Rosuvastatin	[178]
K <sub>i</sub> OATP1B1 ( <i>SLCO1B1</i> )	μmol l <sup>-1</sup>	9.65	2.79	K <sub>i</sub> Pravastatin	[178]
K <sub>i</sub> OATP1B1 ( <i>SLCO1B1</i> )	μmol l <sup>-1</sup>	48.3	18.6	K <sub>i</sub>	[178]
K <sub>i</sub> OATP1B1 ( <i>SLCO1B1</i> )	μmol l <sup>-1</sup>	252	100	K <sub>i</sub>	[178]
K <sub>i</sub> OATP1B1 ( <i>SLCO1B1</i> )	μmol l <sup>-1</sup>	29.6	5.2	K <sub>i</sub>	[178]
K <sub>i</sub> OATP1B1 ( <i>SLCO1B1</i> )	μmol l <sup>-1</sup>	36.6	5.8	K <sub>i</sub>	[178]
K <sub>i</sub> OATP1B1 ( <i>SLCO1B1</i> )	μmol l <sup>-1</sup>	13.4	0.3	K <sub>i</sub>	[178]

Table S3.15: Extracted drug-dependent literature values for gemfibrozil (*continued*)

Parameter	Unit	Literature value	Standard deviation	Note	Reference
K <sub>i</sub> OATP1B1 ( <i>SLCO1B1</i> )	μmol <sup>-1</sup>	49.5	10.8	K <sub>i</sub>	[178]
K <sub>i</sub> OATP1B1 ( <i>SLCO1B1</i> )	μmol <sup>-1</sup>	31.4	4.3	K <sub>i</sub>	[178]
K <sub>i</sub> OATP1B1 ( <i>SLCO1B1</i> )	μmol <sup>-1</sup>	18.1	-	K <sub>i</sub>	[181]
K <sub>i</sub> OATP1B1 ( <i>SLCO1B1</i> )	μmol <sup>-1</sup>	68.05	-	K <sub>i</sub>	[181]
K <sub>i</sub> OATP1B1 ( <i>SLCO1B1</i> )	μmol <sup>-1</sup>	31.5	-	K <sub>i</sub>	[148]
K <sub>i</sub> OATP1B1 ( <i>SLCO1B1</i> )	μmol <sup>-1</sup>	89.5	-	K <sub>i</sub>	[148]
K <sub>i</sub> OATP1B1 ( <i>SLCO1B1</i> )	μmol <sup>-1</sup>	35.8	-	K <sub>i</sub>	[260]
K <sub>i</sub> OATP1B1 ( <i>SLCO1B1</i> )	μmol <sup>-1</sup>	15.5	-	K <sub>i</sub>	[260]
K <sub>i</sub> OATP1B1 ( <i>SLCO1B1</i> )	μmol <sup>-1</sup>	75	-	IC50	[149]
K <sub>i</sub> OATP1B1 ( <i>SLCO1B1</i> )	μmol <sup>-1</sup>	4	-	IC50	[261]
K <sub>i</sub> OATP1B1 ( <i>SLCO1B1</i> )	μmol <sup>-1</sup>	27	-	IC50	[262]
K <sub>i</sub> OATP1B1 ( <i>SLCO1B1</i> )	μmol <sup>-1</sup>	32	-	IC50	[263]
K <sub>i</sub> OATP1B1 ( <i>SLCO1B1</i> )	μmol <sup>-1</sup>	42	-	IC50	[263]
K <sub>i</sub> OATP1B1 ( <i>SLCO1B1</i> )	μmol <sup>-1</sup>	100	-	IC50	[263]
K <sub>i</sub> OATP1B1 ( <i>SLCO1B1</i> )	μmol <sup>-1</sup>	18	-	IC50	[263]
K <sub>i</sub> OATP1B1 ( <i>SLCO1B1</i> )	μmol <sup>-1</sup>	19	-	IC50	[263]
K <sub>i</sub> OATP1B1 ( <i>SLCO1B1</i> )	μmol <sup>-1</sup>	41.4	-	IC50	[193]
K <sub>i</sub> OATP1B1 ( <i>SLCO1B1</i> )	μmol <sup>-1</sup>	72.4	-	IC50	[264]
K <sub>i</sub> OATP1B1 ( <i>SLCO1B1</i> )	μmol <sup>-1</sup>	27.5	-	IC50	[121]
K <sub>i</sub> OATP1B1 ( <i>SLCO1B1</i> )	μmol <sup>-1</sup>	200	-	IC50	[121]
K <sub>i</sub> OATP1B1 ( <i>SLCO1B1</i> )	μmol <sup>-1</sup>	38	-	IC50	[121]
K <sub>i</sub> OATP1B1 ( <i>SLCO1B1</i> )	μmol <sup>-1</sup>	33.7	-	IC50	[198]
K <sub>i</sub> OATP1B1 ( <i>SLCO1B1</i> )	μmol <sup>-1</sup>	32.9	-	IC50	[198]
K <sub>i</sub> OATP1B1 ( <i>SLCO1B1</i> )	μmol <sup>-1</sup>	25.2	-	-	[2]
K <sub>i</sub> OATP1B1 ( <i>SLCO1B1</i> )	μmol <sup>-1</sup>	58	-	K <sub>i</sub>	[204]
K <sub>i</sub> OATP1B1 ( <i>SLCO1B1</i> )	μmol <sup>-1</sup>	12.5	-	K <sub>i</sub>	[265]
K <sub>i</sub> OATP1B3 ( <i>SLCO1B3</i> )	μmol <sup>-1</sup>	10	-	-	[266]
K <sub>i</sub> UGT1A1	μmol <sup>-1</sup>	36	-	-	[267]
K <sub>i</sub> UGT1A3	μmol <sup>-1</sup>	37.6	-	-	[268]
PON3 factor	-	1.59	-	-	[257]
Dissolution shape	-	1.56	-	-	[2]
Dissolution time (50 % dissolved)	min	24.45	-	-	[2]
Specific intest. perm.	cm min <sup>-1</sup>	0.00662	-	-	[2]

## 3 Simvastatin DDIs

Table S3.15: Extracted drug-dependent literature values for gemfibrozil (*continued*)

Parameter	Unit	Literature value	Standard deviation	Note	Reference
Specific organ perm.	cm min <sup>-1</sup>	0.07	-	-	[2]

*Note:*

If IC50 values could not be used for  $K_i$  value estimation utilizing Cheng Prusoff Equation (e.g. due to missing substrate affinities)  $K_i = IC50$  was assumed

Table S3.16: Drug-dependent parameters of the final gemfibrozil glucuronide model compared to literature values

Parameter	Unit	Model value	Median (range) literature values	Origin	Description
<b>Molecule</b>					
fu	%	11.5	14.3 (11.5–17.1)	Literature	Fraction unbound plasma
Lipophilicity	-	1.41	1.83 (1.22–2.44)	Literature	Lipophilicity
MW	-	426.5	426.5	Literature	Molecular weight
pKa	-	2.68	2.68	Literature	Acid dissociation constant
Solubility	mg l <sup>-1</sup>	789	789	Literature	Solubility at pH=7
<b>Transporters</b>					
MRP2 ( <i>ABCC2</i> ) k <sub>cat</sub>	min <sup>-1</sup>	7.13	7.13	Literature	MRP2 ( <i>ABCC2</i> ) catalytic rate constant
MRP2 ( <i>ABCC2</i> ) K <sub>M</sub>	μmol l <sup>-1</sup>	21.49	21.49	Literature	MRP2 ( <i>ABCC2</i> ) Michaelis-Menten constant
OATP1B1 ( <i>SLCO1B1</i> ) k <sub>cat</sub>	min <sup>-1</sup>	15.36	15.36	Literature	OATP1B1 ( <i>SLCO1B1</i> ) catalytic rate constant
OATP1B1 ( <i>SLCO1B1</i> ) K <sub>M</sub>	μmol l <sup>-1</sup>	0.43	0.43	Literature	OATP1B1 ( <i>SLCO1B1</i> ) Michaelis-Menten constant
<b>Inhibition</b>					
K <sub>i</sub> CYP2C8	μmol l <sup>-1</sup>	20	20	Literature	Concentration for half-maximal CYP2C8 inactivation (MBI)
K <sub>i</sub> OATP1B1 ( <i>SLCO1B1</i> )	μmol l <sup>-1</sup>	7.9	22.6 (7.9–24.3)	Literature	Concentration for half-maximal OATP1B1 competitive inhibition
K <sub>i</sub> OATP1B3 ( <i>SLCO1B3</i> )	μmol l <sup>-1</sup>	74	74	Literature	Concentration for half-maximal OATP1B3 competitive inhibition
K <sub>inact</sub> CYP2C8	min <sup>-1</sup>	0.21	0.21	Literature	Maximum inactivation rate constant (MBI)
<b>System</b>					
EHC	-	1	-	Assumed	Fraction of bile continually released from the gallbladder

Table S3.16: Drug-dependent parameters of the final gemfibrozil glucuronide model compared to literature values (*continued*)

Parameter	Unit	Model value	Median (range) literature values	Origin	Description
GFR	-	1	-	Assumed	Fraction of filtered drug reaching the urine
Specific intest. perm.	cm min <sup>-1</sup>	5.98e-07	5.98e-07	Calculated	Permeation across intestinal mucosa normalized to surface area
Specific organ perm.	cm min <sup>-1</sup>	0.000122	0.000122	Calculated	Permeation across cell membranes normalized to surface area

*Note:*

Cellular permabilites calculation method: PK-Sim Standard; organ-plasma partition coefficient calculation method: PK-Sim Standard

Table S3.17: Extracted drug-dependent literature values for gemfibrozil glucuronide

Parameter	Unit	Literature value	Standard deviation	Note	Reference
fu	%	11.5	-	-	[2]
fu	%	17.1	-	-	[2]
Lipophilicity	-	1.22	-	-	[2]
Lipophilicity	-	2.44	-	-	[2]
MW	-	426.5	-	-	[2]
pKa	-	2.68	-	-	[2]
Solubility	mg l <sup>-1</sup>	789	-	pH 7	[2]
MRP2 ( <i>ABCC2</i> ) k <sub>cat</sub>	min <sup>-1</sup>	7.13	-	-	[2]
MRP2 ( <i>ABCC2</i> ) K <sub>M</sub>	μmol l <sup>-1</sup>	21.49	-	-	[2]
OATP1B1 ( <i>SLCO1B1</i> ) k <sub>cat</sub>	min <sup>-1</sup>	15.36	-	-	[2]
OATP1B1 ( <i>SLCO1B1</i> ) K <sub>M</sub>	μmol l <sup>-1</sup>	0.43	-	-	[2]
K <sub>i</sub> CYP2C8	μmol l <sup>-1</sup>	20	-	-	[2]
K <sub>i</sub> OATP1B1 ( <i>SLCO1B1</i> )	μmol l <sup>-1</sup>	22.6	-	K <sub>i</sub>	[147]
K <sub>i</sub> OATP1B1 ( <i>SLCO1B1</i> )	μmol l <sup>-1</sup>	9.3	-	K <sub>i</sub>	[260]
K <sub>i</sub> OATP1B1 ( <i>SLCO1B1</i> )	μmol l <sup>-1</sup>	7.9	2.1	K <sub>i</sub>	[260]
K <sub>i</sub> OATP1B1 ( <i>SLCO1B1</i> )	μmol l <sup>-1</sup>	24.3	-	IC50	[264]
K <sub>i</sub> OATP1B1 ( <i>SLCO1B1</i> )	μmol l <sup>-1</sup>	22.6	-	-	[2]
K <sub>i</sub> OATP1B3 ( <i>SLCO1B3</i> )	μmol l <sup>-1</sup>	74	-	-	[266]
K <sub>i</sub> UGT1A1	μmol l <sup>-1</sup>	69	-	-	[269]
K <sub>inact</sub> CYP2C8	min <sup>-1</sup>	0.21	-	-	[2]
Specific intest. perm.	cm min <sup>-1</sup>	5.98e-07	-	-	[2]
Specific organ perm.	cm min <sup>-1</sup>	0.000122	-	-	[2]

*Note:*

If IC50 values could not be used for  $K_i$  value estimation utilizing Cheng Prusoff Equation (e.g. due to missing substrate affinities)  $K_i = IC50$  was assumed



## 3 Simvastatin DDIs

## 3.5.2 Profiles

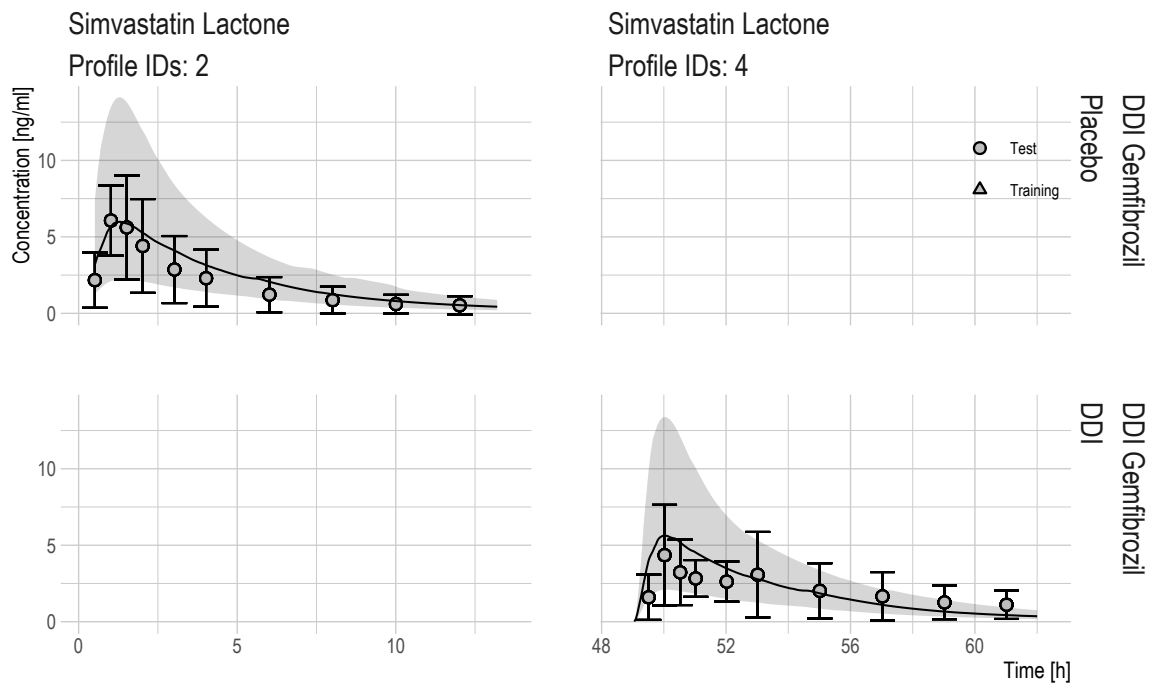


Figure S3.9: Linear VPCs of plasma concentration-time profiles for investigated DDIs: Gemfibrozil - Simvastatin Lactone. Solid line and shaded area are predicted median and 90 % CI

3 Simvastatin DDIs

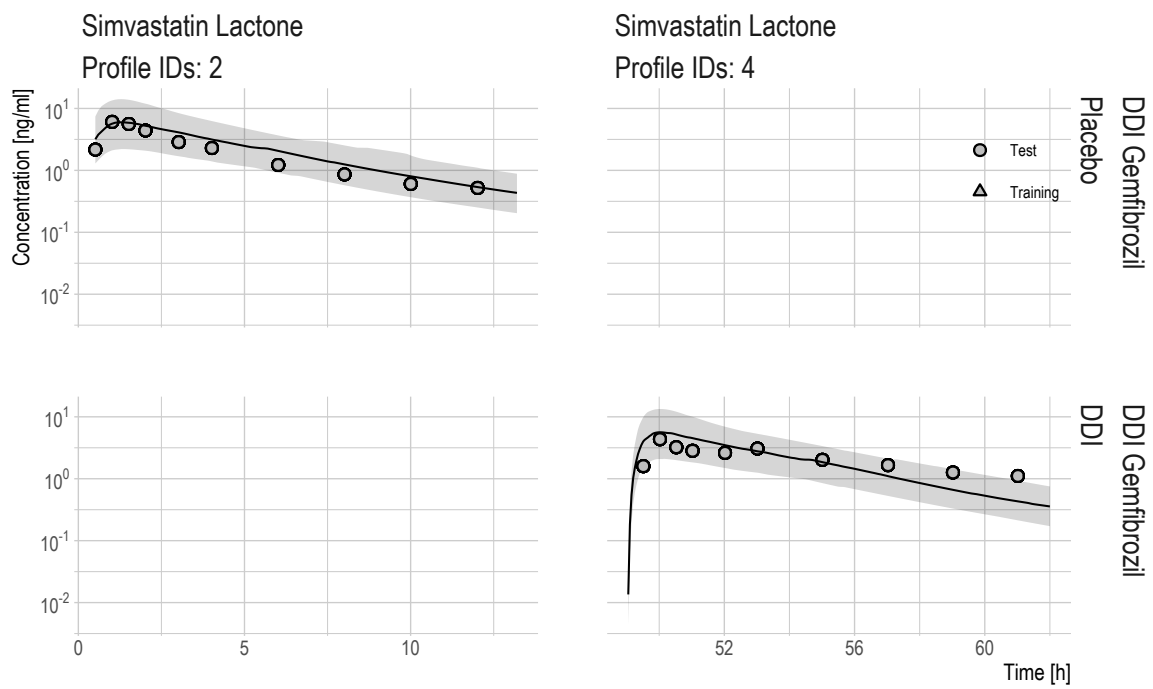


Figure S3.10: Semilogarithmic VPCs of plasma concentration-time profiles for investigated DDIs: Gemfibrozil - Simvastatin Lactone. Solid line and shaded area are predicted median and 90% CI

3 Simvastatin DDIs

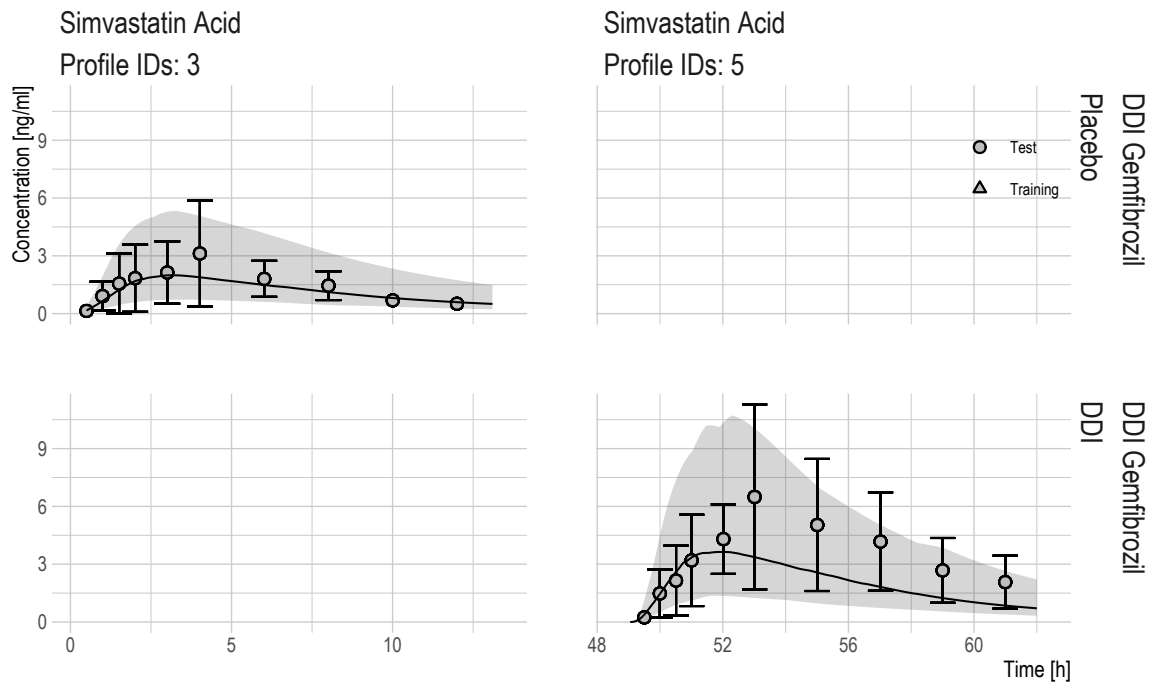


Figure S3.11: Linear VPCs of plasma concentration-time profiles for investigated DDIs: Gemfibrozil - Simvastatin Acid. Solid line and shaded area are predicted median and 90% CI

3 Simvastatin DDIs

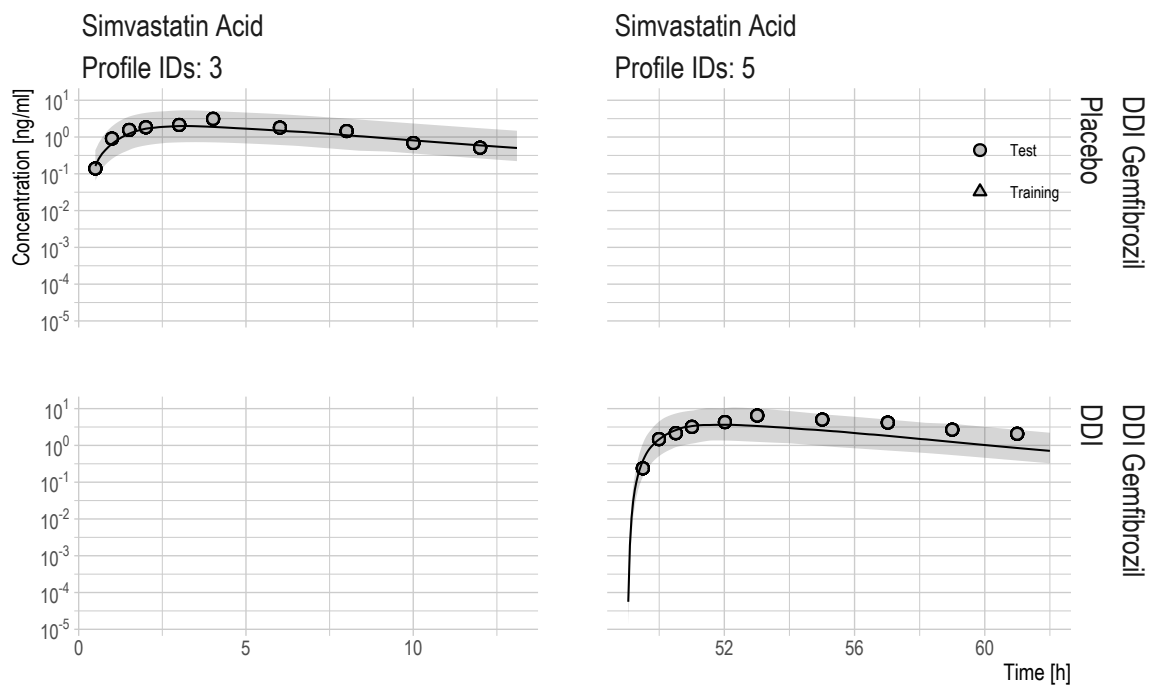


Figure S3.12: Semilogarithmic VPCs of plasma concentration-time profiles for investigated DDIs: Gemfibrozil - Simvastatin Acid. Solid line and shaded area are predicted median and 90 % CI

---

### 3 Simvastatin DDIs

---

## 3.6 Midazolam

Midazolam is a CYP3A4 probe drug. In a study performed by Prueksaritanont et al. [141] it was investigated if simvastatin would affect the PK of midazolam. For this reason a previously established midazolam model was used and coupled with the newly developed simvastatin model. The parameters of the midazolam model are given in Tables S3.18 and S3.19. Results of the midazolam-simvastatin DDI interaction are shown in Fig. S3.13.

### 3.6.1 Drug-dependent parameters

Table S3.18: Drug-dependent parameters in the midazolam model compared to literature values

Parameter	Unit	Model value	Median (range) literature values	Origin	Description
<b>Molecule</b>					
fu	%	1.6	1.6	Literature	Fraction unbound plasma
Lipophilicity	-	3.13	3.13	Literature	Lipophilicity
MW	-	325.8	325.8	Literature	Molecular weight
pKa	-	6.15	6.15	Literature	Acid dissociation constant (basic)
Solubility	mg l <sup>-1</sup>	49	49	Literature	Solubility at pH=6.5
<b>Enzymes</b>					
CYP3A4 k <sub>cat</sub>	min <sup>-1</sup>	13	13	Literature	CYP3A4 catalytic rate constant
CYP3A4 K <sub>M</sub>	μmol l <sup>-1</sup>	2.73	2.73	Literature	CYP3A4 Michaelis-Menten constant
<b>System</b>					
CL <sub>Ren</sub>	ml min <sup>-1</sup>	100	-	Literature	Renal plasma clearance
EHC	-	1	1	Assumed	Fraction of bile continually released from the gallbladder
GFR	-	1	1	Assumed	Fraction of filtered drug reaching the urine
Specific intest. perm.	cm min <sup>-1</sup>	2e-06	2e-06	Literature	Permeation across intestinal mucosa normalized to surface area
Specific organ perm.	cm min <sup>-1</sup>	0.007	0.007	Calculated	Permeation across cell membranes normalized to surface area

*Note:*

Cellular permabilites calculation method: Charge-dependent Schmitt; organ-plasma partition coefficient calculation method: Rodgers and Rowland

Table S3.19: Extracted drug-dependent literature values for midazolam

Parameter	Unit	Literature value	Standard deviation	Note	Reference
fu	%	1.6	-	-	[2]
Lipophilicity	-	3.13	-	-	[2]
MW	-	325.8	-	-	[2]
pKa	-	6.15	-	-	[2]
Solubility	mg l <sup>-1</sup>	49	-	-	[2]
CYP3A4 k <sub>cat</sub>	min <sup>-1</sup>	13	-	-	[2]
CYP3A4 K <sub>M</sub>	μmol l <sup>-1</sup>	2.73	-	-	[2]
EHC	-	1	-	-	[2]
GFR	-	1	-	-	[2]
Specific intest. perm.	cm min <sup>-1</sup>	2e-06	-	-	[2]
Specific organ perm.	cm min <sup>-1</sup>	0.007	-	-	[2]

*Note:*

If IC<sub>50</sub> values could not be used for  $K_i$  value estimation utilizing Cheng Prusoff Equation (e.g. due to missing substrate affinities)  $K_i = IC_{50}$  was assumed

### 3.6.2 Profiles

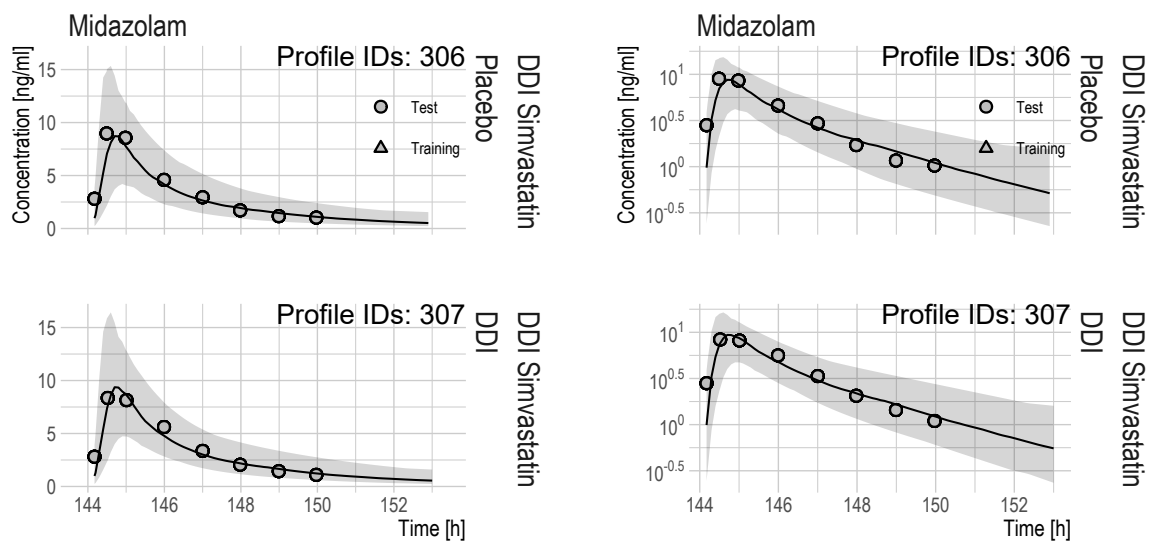


Figure S3.13: Linear VPCs of plasma concentration-time profiles for investigated DDIs: Simvastatin - Midazolam. Solid line and shaded area are predicted median and 90 % CI



## 3 Simvastatin DDIs

## 3.7 DDI evaluation

DDI prediction performance was assessed using the previously described graphical and statistical measures. Figures S3.14–S3.16 show the GOF plots as well as the predicted versus observed NCA ratios for SL and SA, respectively. Tables S3.20 and S3.21 summarise the statistical prediction performance.

## 3.7.1 Predicted concentrations versus observed concentrations GOF plots

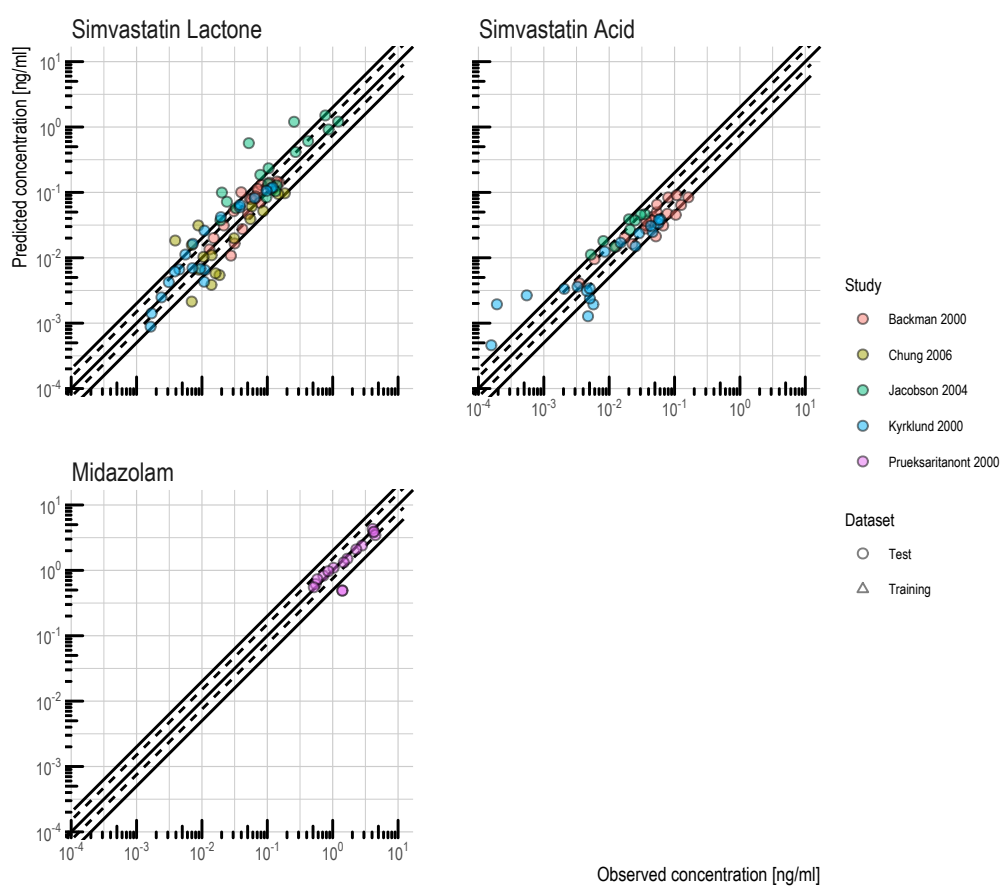


Figure S3.14: Goodness of fit plots - Observed versus predicted plasma concentration-time values of the DDI test dataset. The solid lines mark the line of identity as well as the 2-fold deviations. Dashed lines indicate the 1.5-fold deviations

3 Simvastatin DDIs

3.7.2 NCA GOF plots

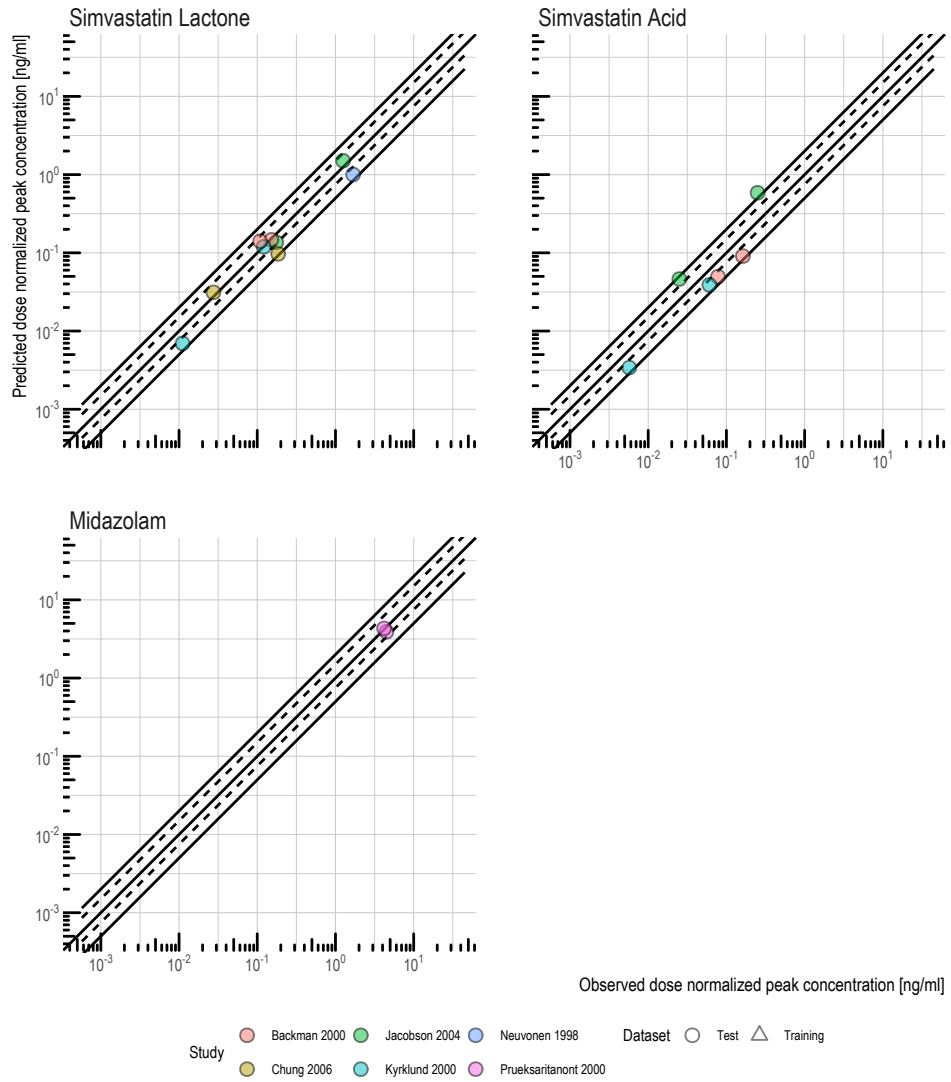


Figure S3.15: NCA ratios of the DDIs. The solid lines mark the line of identity as well as the 2-fold deviations. Dashed lines indicate the 1.5-fold deviations.: Test  $C_{max}$

3 Simvastatin DDIs

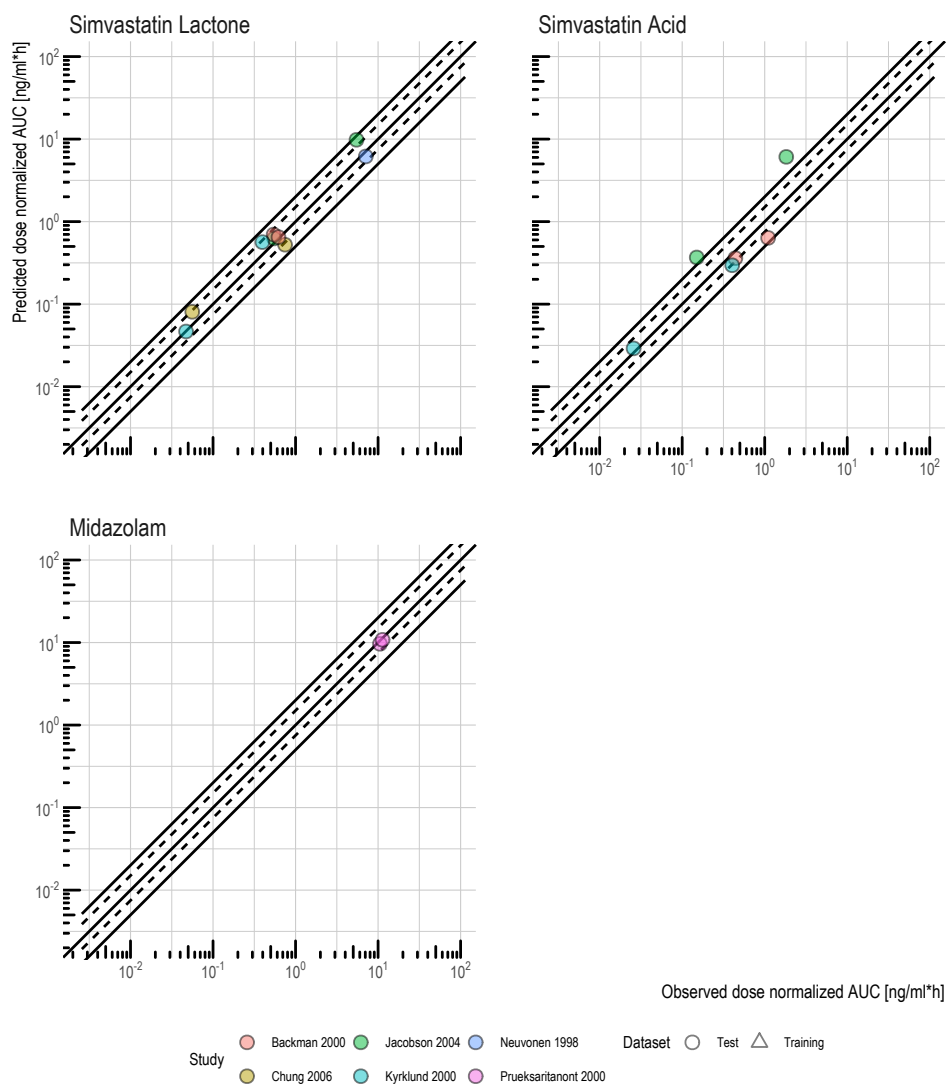


Figure S3.16: NCA ratios of the DDIs. The solid lines mark the line of identity as well as the 2-fold deviations. Dashed lines indicate the 1.5-fold deviations.: Test AUC

## 3 Simvastatin DDIs

## 3.7.3 MRD and MSA of plasma concentration predictions

Table S3.20: Summary of the statistical DDI model evaluation (MSA and MRD)

Molecule	MRD mean (sd)	MSA mean (sd)
Simvastatin Lactone	1.98 (0.674) N = 8 (N MRD > 2 = 2)	78.3 (67.3) N = 8 (N MSA > 100 = 2)
Simvastatin Acid	1.91 (0.815) N = 5 (N MRD > 2 = 1)	77 (67.4) N = 5 (N MSA > 100 = 1)
Midazolam	1.48 (0.019) N = 2 (N MRD > 2 = 0)	12.2 (0.38) N = 2 (N MSA > 100 = 0)

## 3.7.4 NCA ratios and GMFE of NCA values

Table S3.21: Summary of the statistical DDI model evaluation (NCA ratio and GMFE)

Parameter	NCA ratio mean (sd)	GMFE
<b>Simvastatin Lactone</b>		
AUC	1.19 (0.334) N = 9 (N ratio > 2   ratio < 0.5 = 0)	1.28
$C_{max}$	0.902 (0.283) N = 9 (N ratio > 2   ratio < 0.5 = 0)	1.32
<b>Simvastatin Acid</b>		
AUC	1.51 (1.12) N = 6 (N ratio > 2   ratio < 0.5 = 2)	1.73
$C_{max}$	1.1 (0.784) N = 6 (N ratio > 2   ratio < 0.5 = 1)	1.78
<b>Midazolam</b>		
AUC	0.934 (0.0263) N = 2 (N ratio > 2   ratio < 0.5 = 0)	1.07
$C_{max}$	0.951 (0.114) N = 2 (N ratio > 2   ratio < 0.5 = 0)	1.09

## 4 Drug-drug-gene interaction network

For the final DDGI evaluation, effect ratios of all included DDIs and DGIs were calculated and compared. Figures S4.1 and S4.2 display the  $C_{\max}$  and AUC effect ratios. Table S4.1 shows the effect ratio values and Table S4.2 the summary of the effect ratio values.

## 4 Drug-drug-gene interaction network

## 4.1 Effect ratios

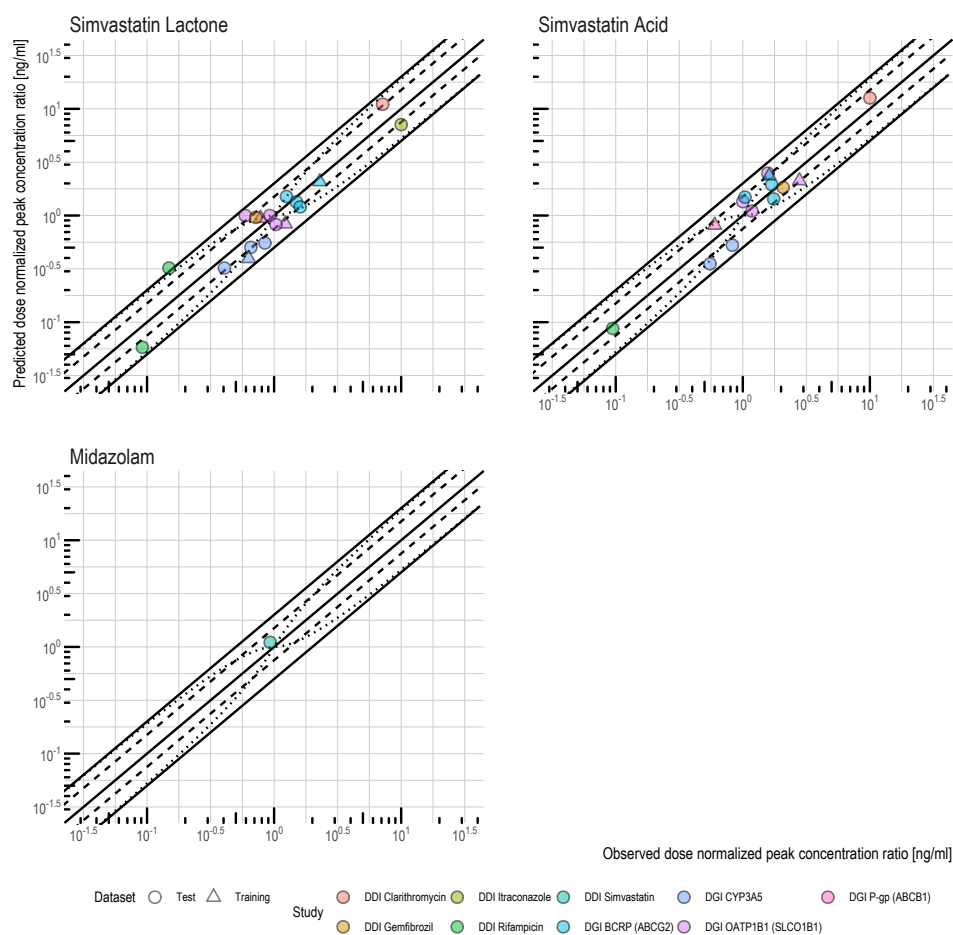


Figure S4.1: NCA effect ratios ( $C_{\max}$ ) of the DDGI network. The solid lines mark the line of identity as well as the 2-fold deviations. Dashed lines indicate the 1.5-fold deviations. Dotted lines show the limits proposed by Guest et al. [17]

## 4 Drug-drug-gene interaction network

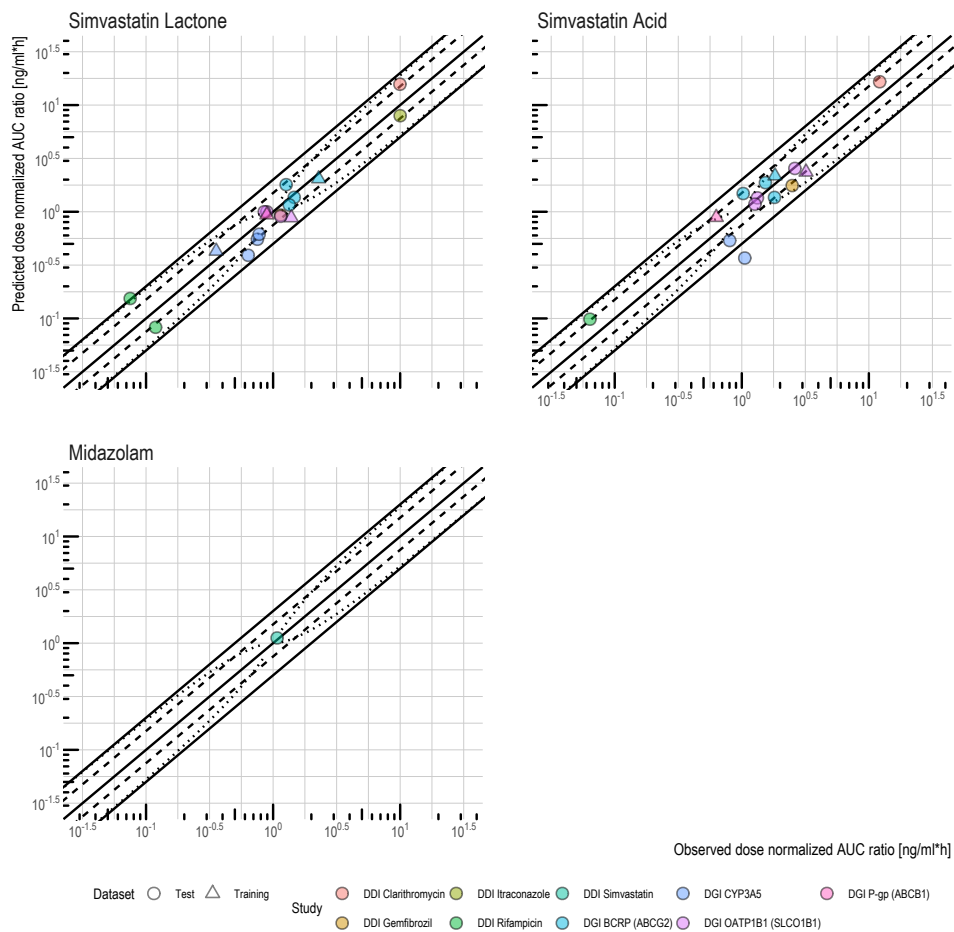


Figure S4.2: NCA effect ratios (AUC) of the DDGI network. The solid lines mark the line of identity as well as the 2-fold deviations. Dashed lines indicate the 1.5-fold deviations. Dotted lines show the limits proposed by Guest et al. [17]

## 4 Drug-drug-gene interaction network

Table S4.1: Predicted and observed DDGI AUC and Cmax effect ratios

Parameter DDI / DGI	Observed effect ratio	Predicted effect ratio	Predicted / Observed	Reference
<b>Simvastatin Lactone</b>				
AUC	DDI Clarithromycin	9.95	15.7	1.58 [138]
	DDI Gemfibrozil	1.15	0.931	0.813 [142]
	DDI Itraconazole	10	7.95	0.795 [145]
	DDI Rifampicin	0.075	0.154	2.05 [143]
	DDI Rifampicin	0.119	0.0826	0.695 [144]
	DGI BCRP (ABCG2) c.421AA	1.27	1.79	1.42 [96]
	DGI BCRP (ABCG2) c.421AA	2.28	2.04	0.894 [94]
	DGI BCRP (ABCG2) c.421CA	1.47	1.37	0.931 [96]
	DGI BCRP (ABCG2) c.421CA	1.34	1.16	0.864 [94]
	DGI CYP3A5 *1/*1	0.637	0.391	0.613 [96]
	DGI CYP3A5 *1/*1	0.357	0.427	1.2 [93]
	DGI CYP3A5 *3/*1	0.752	0.552	0.734 [96]
	DGI CYP3A5 *3/*1	0.777	0.615	0.793 [93]
	DGI OATP1B1 (SLCO1B1) c.521CC	0.853	1	1.17 [96]
	DGI OATP1B1 (SLCO1B1) c.521CC	1.39	0.88	0.633 [95]
	DGI OATP1B1 (SLCO1B1) c.521TC	0.892	1	1.12 [96]
	DGI OATP1B1 (SLCO1B1) c.521TC	1.15	0.906	0.79 [95]
	DGI P-gp (ABCB1) c.1236C-c.2677G-c.3435C	0.893	0.936	1.05 [41]
C <sub>max</sub>	DDI Clarithromycin	7.14	11	1.54 [138]
	DDI Gemfibrozil	0.717	0.96	1.34 [142]
	DDI Itraconazole	10	7.12	0.712 [145]
	DDI Rifampicin	0.149	0.322	2.17 [143]
	DDI Rifampicin	0.0919	0.0582	0.633 [144]
	DGI BCRP (ABCG2) c.421AA	1.25	1.51	1.21 [96]
	DGI BCRP (ABCG2) c.421AA	2.29	2.08	0.908 [94]
	DGI BCRP (ABCG2) c.421CA	1.5	1.34	0.894 [96]
	DGI BCRP (ABCG2) c.421CA	1.6	1.2	0.751 [94]



## 4 Drug-drug-gene interaction network

Table S4.1: Predicted and observed DDGI AUC and Cmax effect ratios (*continued*)

Parameter DDI / DGI	Observed effect ratio	Predicted effect ratio	Predicted / Observed	Reference	
DGI CYP3A5 *1/*1	0.406	0.322	0.792	[96]	
DGI CYP3A5 *1/*1	0.631	0.395	0.627	[93]	
DGI CYP3A5 *3/*1	0.656	0.503	0.767	[96]	
DGI CYP3A5 *3/*1	0.846	0.552	0.653	[93]	
DGI OATP1B1 (SLCO1B1) c.521CC	0.593	1	1.69	[96]	
DGI OATP1B1 (SLCO1B1) c.521CC	1.23	0.835	0.681	[95]	
DGI OATP1B1 (SLCO1B1) c.521TC	0.926	1	1.08	[96]	
DGI OATP1B1 (SLCO1B1) c.521TC	1.03	0.824	0.798	[95]	
DGI P-gp (ABCB1) c.1236C-c.2677G-c.3435C	0.782	0.945	1.21	[41]	
<b>Simvastatin Acid</b>					
AUC	DDI Clarithromycin	12.2	16.5	1.36	[138]
	DDI Gemfibrozil	2.49	1.76	0.706	[142]
	DDI Rifampicin	0.0638	0.0984	1.54	[144]
	DGI BCRP (ABCG2) c.421AA	1.53	1.87	1.22	[96]
	DGI BCRP (ABCG2) c.421AA	1.83	2.17	1.19	[94]
	DGI BCRP (ABCG2) c.421CA	1.81	1.36	0.754	[96]
	DGI BCRP (ABCG2) c.421CA	1.03	1.48	1.45	[94]
	DGI CYP3A5 *1/*1	1.06	0.368	0.349	[96]
	DGI CYP3A5 *3/*1	0.803	0.538	0.669	[96]
	DGI OATP1B1 (SLCO1B1) c.521CC	2.62	2.55	0.974	[96]
	DGI OATP1B1 (SLCO1B1) c.521CC	3.2	2.36	0.736	[95]
	DGI OATP1B1 (SLCO1B1) c.521TC	1.33	1.35	1.02	[96]
	DGI OATP1B1 (SLCO1B1) c.521TC	1.27	1.18	0.928	[95]
	DGI P-gp (ABCB1) c.1236C-c.2677G-c.3435C	0.63	0.886	1.41	[41]
C <sub>max</sub>	DDI Clarithromycin	10	12.7	1.27	[138]
	DDI Gemfibrozil	2.08	1.83	0.88	[142]

## 4 Drug-drug-gene interaction network

Table S4.1: Predicted and observed DDGI AUC and Cmax effect ratios (*continued*)

Parameter DDI / DGI	Observed effect ratio	Predicted effect ratio	Predicted / Observed	Reference
DDI Rifampicin	0.0946	0.0874	0.924	[144]
DGI BCRP (ABCG2) c.421AA	1.69	1.95	1.15	[96]
DGI BCRP (ABCG2) c.421AA	1.61	2.36	1.46	[94]
DGI BCRP (ABCG2) c.421CA	1.75	1.43	0.817	[96]
DGI BCRP (ABCG2) c.421CA	1.04	1.49	1.43	[94]
DGI CYP3A5 *1/*1	0.552	0.353	0.64	[96]
DGI CYP3A5 *3/*1	0.828	0.527	0.637	[96]
DGI OATP1B1 (SLCO1B1) c.521CC	1.58	2.49	1.58	[96]
DGI OATP1B1 (SLCO1B1) c.521CC	2.79	2.12	0.76	[95]
DGI OATP1B1 (SLCO1B1) c.521TC	1	1.35	1.35	[96]
DGI OATP1B1 (SLCO1B1) c.521TC	1.18	1.1	0.934	[95]
DGI P-gp (ABCB1) c.1236C-c.2677G-c.3435C	0.601	0.812	1.35	[41]
<b>Midazolam</b>				
AUC DDI Simvastatin	1.08	1.12	1.04	[141]
C <sub>max</sub> DDI Simvastatin	0.931	1.1	1.18	[141]

Table S4.2: Summary of the predicted and observed DDGI AUC and Cmax effect ratios

Parameter	NCA effect ratio mean (sd)	GMFE
<b>Simvastatin Lactone</b>		
AUC	1.01 (0.372) N = 18 (N ratio > 2   ratio < 0.5 = 1)	1.31
C <sub>max</sub>	1.03 (0.429) N = 18 (N ratio > 2   ratio < 0.5 = 1)	1.38
<b>Simvastatin Acid</b>		
AUC	1.02 (0.354) N = 14 (N ratio > 2   ratio < 0.5 = 1)	1.36
C <sub>max</sub>	1.08 (0.322) N = 14 (N ratio > 2   ratio < 0.5 = 0)	1.31
<b>Midazolam</b>		
AUC	1.04 (NA) N = 1 (N ratio > 2   ratio < 0.5 = 0)	1.04
C <sub>max</sub>	1.18 (NA) N = 1 (N ratio > 2   ratio < 0.5 = 0)	1.18

## Bibliography

- [1] Open Systems Pharmacology Community. Open systems pharmacology suite. [www.open-systems-pharmacology.org](http://www.open-systems-pharmacology.org), 2019. Accessed 01 August 2020.
- [2] Denise Türk, Nina Hanke, Sarah Wolf, Sebastian Frechen, Thomas Eissing, Thomas Wendl, Matthias Schwab, and Thorsten Lehr. Physiologically based pharmacokinetic models for prediction of complex CYP2C8 and OATP1B1 (SLCO1B1) drug–drug–gene interactions: a modeling network of gemfibrozil, repaglinide, pioglitazone, rifampicin, clarithromycin and itraconazole. *Clinical Pharmacokinetics*, 58(12):1595–1607, May 2019. ISSN 0312-5963. doi: 10.1007/s40262-019-00777-x.
- [3] The 1000 Genomes Project Consortium. A global reference for human genetic variation. *Nature*, 526:68–74, October 2015. ISSN 1476-4687. doi: 10.1038/nature15393.
- [4] Michaela Meyer, Sebastian Schneckener, Bernd Ludewig, Lars Kuepfer, and Joerg Lippert. Using expression data for quantification of active processes in physiologically based pharmacokinetic modeling. *Drug metabolism and disposition: the biological fate of chemicals*, 40(5):892–901, May 2012. ISSN 1521-009X. doi: 10.1124/dmd.111.043174. URL <http://www.ncbi.nlm.nih.gov/pubmed/22293118>.
- [5] Masuhiro Nishimura and Shinsaku Naito. Tissue-specific mRNA expression profiles of human phase I metabolizing enzymes except for cytochrome P450 and phase II metabolizing enzymes. *Drug metabolism and pharmacokinetics*, 21(5):357–374, 2006. ISSN 1347-4367. doi: 10.2133/dmpk.21.357.
- [6] A. David Rodrigues. Integrated cytochrome P450 reaction phenotyping: attempting to bridge the gap between cDNA-expressed cytochromes P450 and native human liver microsomes. *Biochemical pharmacology*, 57(5):465–80, March 1999. ISSN 0006-2952. doi: 10.1016/S0006-2952(98)00268-8. URL <http://www.ncbi.nlm.nih.gov/pubmed/9952310>.
- [7] Masuhiro Nishimura, Hiroshi Yaguti, Hiroki Yoshitsugu, Shinsaku Naito, and Tet-suo Satoh. Tissue distribution of mRNA expression of human cytochrome P450 isoforms assessed by high-sensitivity real-time reverse transcription PCR. *Journal of the Pharmaceutical Society of Japan*, 123(5):369–75, May 2003. ISSN 0031-6903. URL <http://www.ncbi.nlm.nih.gov/pubmed/12772594>.

## Bibliography

- 
- [8] K. Rowland Yeo, R. L. Walsky, M. Jamei, A. Rostami-Hodjegan, and G. T. Tucker. Prediction of time-dependent CYP3A4 drug-drug interactions by physiologically based pharmacokinetic modelling: Impact of inactivation parameters and enzyme turnover. *European Journal of Pharmaceutical Sciences*, 43(3):160–73, June 2011. ISSN 0928-0987. doi: 10.1016/j.ejps.2011.04.008.
- [9] David J. Greenblatt, Lisa L. von Moltke, Jerold S. Harmatz, Gengsheng Chen, James L. Weemhoff, Cheng Jen, Charles J. Kelley, Barbara W. LeDuc, and Miguel A. Zinny. Time course of recovery of cytochrome P450 3A function after single doses of grapefruit juice. *Clinical Pharmacology and Therapeutics*, 74(2):121–29, August 2003. ISSN 0009-9236. doi: 10.1016/S0009-9236(03)00118-8.
- [10] Nikolay Kolesnikov, Emma Hastings, Maria Keays, Olga Melnichuk, Y. Amy Tang, Eleanor Williams, Mirosław Dylag, Natalja Kurbatova, Marco Brandizi, Tony Burdett, Karyn Megy, Ekaterina Pilicheva, Gabriella Rustici, Andrew Tikhonov, Helen Parkinson, Robert Petryszak, Ugis Sarkans, and Alvis Brazma. Arrayexpress update-simplifying data submissions. *Nucleic Acids Research*, 43(D1):D1113–D1116, 2015. ISSN 1362-4962. doi: 10.1093/nar/gku1057.
- [11] Bhagwat Prasad, Yurong Lai, Yvonne Lin, and Jashvant D Unadkat. Interindividual variability in the hepatic expression of the human breast cancer resistance protein (BCRP/ABCG2): effect of age, sex, and genotype. *Journal of pharmaceutical sciences*, 102(3):787–93, March 2013. ISSN 1520-6017. doi: 10.1002/jps.23436. URL <http://www.ncbi.nlm.nih.gov/pubmed/23280364>.
- [12] Masuhiro Nishimura and Shinsaku Naito. Tissue-specific mRNA expression profiles of human ATP-binding cassette and solute carrier transporter superfamilies. *Drug metabolism and pharmacokinetics*, 20(6):452–77, 2005.
- [13] Pu Shi, Mingxiang Liao, Bei Ching Chuang, Robert Griffin, Judy Shi, Marc Hyer, John K. Fallon, Philip C. Smith, Chao Li, and Cindy Q. Xia. Efflux transporter breast cancer resistance protein dominantly expresses on the membrane of red blood cells, hinders partitioning of its substrates into the cells, and alters drug–drug interaction profiles. *Xenobiotica*, 48(11):1173–1183, 2018. ISSN 1366-5928. doi: 10.1080/00498254.2017.1397812.
- [14] Anand K Deo, Bhagwat Prasad, Larissa Balogh, Yurong Lai, and Jashvant D Unadkat. Interindividual variability in hepatic expression of the multidrug resistance-associated protein 2 (MRP2/ABCC2): quantification by liquid chromatography/tandem mass spectrometry. *Drug metabolism and disposition: the biological fate of chemicals*, 40(5): 852–5, May 2012. ISSN 1521-009X. doi: 10.1124/dmd.111.043810.
- [15] Bhagwat Prasad, Raymond Evers, Anshul Gupta, Cornelis E C A Hop, Laurent Salphati, Suneet Shukla, Suresh V Ambudkar, and Jashvant D Unadkat. Interindividual variability in hepatic organic anion - transporting polypeptides and P-glycoprotein (ABCB1) protein expression: quantification by liquid chromatography tandem mass

## Bibliography

- spectroscopy and influence of genotype, age, and sex. *Drug metabolism and disposition: the biological fate of chemicals*, 42(1):78–88, 2014. ISSN 1521-009X. doi: 10.1124/dmd.113.053819.
- [16] Nina Hanke, Sebastian Frechen, Daniel Moj, Hannah Britz, Thomas Eissing, Thomas Wendl, and Thorsten Lehr. PBPK models for CYP3A4 and P-gp DDI prediction: A modeling network of rifampicin, itraconazole, clarithromycin, midazolam, alfentanil, and digoxin. *CPT: pharmacometrics & systems pharmacology*, 7(10):647–59, October 2018. ISSN 2163-8306. doi: 10.1002/psp4.12343.
- [17] Eleanor J. Guest, Leon Aarons, J. Brian Houston, Amin Rostami-Hodjegan, and Aleksandra Galetin. Critique of the two-fold measure of prediction success for ratios: application for the assessment of drug-drug interactions. *Drug metabolism and disposition: the biological fate of chemicals*, 39(2):170–3, February 2011. ISSN 1521-009X. doi: 10.1124/dmd.110.036103. URL <http://www.ncbi.nlm.nih.gov/pubmed/21036951>.
- [18] Ted G. Eschenbach. Spiderplots versus tornado diagrams for sensitivity analysis. *Interfaces*, 22(6):40–46, dec 1992. doi: 10.1287/inte.22.6.40.
- [19] IMS Institute for Healthcare Informatics. The use of medicines in the United States: Review of 2011. 2012. URL <http://www.imshealth.com/cds/imshealth/Global/Content/Corporate/IMSHealthInstitute/Reports/Use>.
- [20] Christopher Stomberg, Margaret Albaugh, Saul Shiffman, and Neeraj Sood. A cost-effectiveness analysis of over-the-counter statins. *The American journal of managed care*, 22:e294–e303, May 2016. ISSN 1936-2692.
- [21] Huseyin Naci, Jasper Brugts, and Tony Ades. Comparative tolerability and harms of individual statins: a study-level network meta-analysis of 246 955 participants from 135 randomized, controlled trials. *Circulation. Cardiovascular quality and outcomes*, 6:390–399, July 2013. ISSN 1941-7705. doi: 10.1161/CIRCOUTCOMES.111.000071.
- [22] Polyana Mendes, Priscila Games Robles, and Sunita Mathur. Statin-induced rhabdomyolysis: a comprehensive review of case reports. *Physiotherapy Canada. Physiotherapie Canada*, 66:124–132, 2014. ISSN 0300-0508. doi: 10.3138/ptc.2012-65.
- [23] Kenneth A. Kellick, Michael Bottorff, Peter P. Toth, and Force. A clinician’s guide to statin drug-drug interactions. *Journal of clinical lipidology*, 8:30–46, 2014. ISSN 1933-2874. doi: 10.1016/j.jacl.2014.02.010.
- [24] Stefano Bellosta, Rodolfo Paoletti, and Alberto Corsini. Safety of statins: focus on clinical pharmacokinetics and drug interactions. *Circulation*, 109:III50–III57, June 2004. ISSN 1524-4539. doi: 10.1161/01.CIR.0000131519.15067.1f.
- [25] M. Niemi. Transporter pharmacogenetics and statin toxicity. *Clinical pharmacology and therapeutics*, 87:130–133, January 2010. ISSN 1532-6535. doi: 10.1038/clpt.2009.197.

## Bibliography

- [26] N Tsamandouras, G Dickinson, Y Guo, S Hall, A Rostami-Hodjegan, A Galetin, and L Aarons. Identification of the effect of multiple polymorphisms on the pharmacokinetics of simvastatin and simvastatin acid using a population-modeling approach. *Clinical pharmacology and therapeutics*, 96(1):90–100, July 2014. ISSN 1532-6535. doi: 10.1038/clpt.2014.55. URL <http://www.ncbi.nlm.nih.gov/pubmed/24598718>.
- [27] Monica Rao, Yogesh Mandage, Kaushik Thanki, and Sucheta Bhise. Dissolution improvement of simvastatin by surface solid dispersion technology. *Dissolution Technologies*, 17(2):27–34, 2010. ISSN 1521-298X. doi: 10.14227/DT170210P27.
- [28] Dhiaa A. Taha, Cornelia H. De Moor, David A. Barrett, Jong Bong Lee, Raj D. Gandhi, Chee Wei Hoo, and Pavel Gershkovich. The role of acid-base imbalance in statin-induced myotoxicity. *Translational research : the journal of laboratory and clinical medicine*, 174:140–160.e14, 2016. ISSN 1878-1810. doi: 10.1016/j.trsl.2016.03.015.
- [29] D. I. Draganov and B. N. La Du. Pharmacogenetics of paraoxonases: a brief review. *Naunyn-Schmiedeberg's archives of pharmacology*, 369(1):78–88, January 2004. ISSN 0028-1298. doi: 10.1007/s00210-003-0833-1. URL <http://www.ncbi.nlm.nih.gov/pubmed/14579013>.
- [30] R. Elsby, C. Hilgendorf, and K. Fenner. Understanding the critical disposition pathways of statins to assess drug-drug interaction risk during drug development: it's not just about OATP1B1. *Clinical pharmacology and therapeutics*, 92:584–598, November 2012. ISSN 1532-6535. doi: 10.1038/clpt.2012.163.
- [31] M. Ishigami, T. Honda, W. Takasaki, T. Ikeda, T. Komai, K. Ito, and Y. Sugiyama. A comparison of the effects of 3-hydroxy-3-methylglutaryl-coenzyme a (HMG-CoA) reductase inhibitors on the CYP3A4-dependent oxidation of mexazolam in vitro. *Drug Metabolism and Disposition*, 29(3):282–288, 2001. ISSN 0090-9556.
- [32] Aleksu Tornio, Marja K. Pasanen, Jouko Laitila, Pertti J. Neuvonen, and Janne T. Backman. Comparison of 3-hydroxy-3-methylglutaryl coenzyme A (HMG-CoA) reductase inhibitors (statins) as inhibitors of cytochrome P450 2C8. *Basic and Clinical Pharmacology and Toxicology*, 97(2):104–108, 2005. ISSN 1742-7835. doi: 10.1111/j.1742-7843.2005.pto\_134.x.
- [33] C. Transon, T. Leemann, and P. Dayer. In vitro comparative inhibition profiles of major human drug metabolising cytochrome P450 isozymes (CYP2C9, CYP2D6 and CYP3A4) by HMG-CoA reductase inhibitors. *European journal of clinical pharmacology*, 50:209–215, 1996. ISSN 0031-6970. doi: 10.1007/s002280050094.
- [34] Tatsuki Fukami, Shiori Takahashi, Nao Nakagawa, Taiga Maruichi, Miki Nakajima, and Tsuyoshi Yokoi. In vitro evaluation of inhibitory effects of antidiabetic and antihyperlipidemic drugs on human carboxylesterase activities. *Drug Metabolism and Disposition*, 38(12):2173–2178, 2010. ISSN 0090-9556. doi: 10.1124/dmd.110.034454.

## Bibliography

- [35] Cuiping Chen. Differential interaction of 3-hydroxy-3-methylglutaryl-coa reductase inhibitors with ABCB1, ABCC2, and OATP1B1. *Drug Metabolism and Disposition*, 33(4):537–546, 2005. ISSN 0090-9556. doi: 10.1124/dmd.104.002477.
- [36] Lucy C J Ellis, Gabrielle M. Hawksworth, and Richard J. Weaver. ATP-dependent transport of statins by human and rat MRP2/Mrp2. *Toxicology and applied pharmacology*, 269(2):187–94, June 2013. ISSN 1096-0333. doi: 10.1016/j.taap.2013.03.019.
- [37] Toshiyuki Sakaeda, Hideki Fujino, Chiho Komoto, Mikio Kakumoto, Jiang Shu Jin, Koichi Iwaki, Kohshi Nishiguchi, Tsutomu Nakamura, Noboru Okamura, and Katsuhiko Okumura. Effects of acid and lactone forms of eight HMG-CoA reductase inhibitors on CYP-mediated metabolism and MDR1-mediated transport. *Pharmaceutical Research*, 23(3):506–512, September 2006. ISSN 0724-8741. doi: 10.1007/s11095-005-9371-5. URL <http://www.ncbi.nlm.nih.gov/pubmed/24939652>.
- [38] Masaru Hirano, Kazuya Maeda, Soichiro Matsushima, Yoshitane Nozaki, Hiroyuki Kusuhara, and Yuichi Sugiyama. Involvement of BCRP (ABCG2) in the biliary excretion of pitavastatin. *Molecular pharmacology*, 68(3):800–7, September 2005. ISSN 0026-895X. doi: 10.1124/mol.105.014019.
- [39] Nikolaos Tsamandouras, Gemma Dickinson, Yingying Guo, Stephen Hall, Amin Rostami-Hodjegan, Aleksandra Galetin, and Leon Aarons. Development and application of a mechanistic pharmacokinetic model for simvastatin and its active metabolite simvastatin acid using an integrated population PBPK approach. *Pharmaceutical Research*, 32(6):1864–1883, 2015. ISSN 1573-904X. doi: 10.1007/s11095-014-1581-2.
- [40] M L Becker, L L F S Elens, L E Visser, A Hofman, A G Uitterlinden, R H N van Schaik, and B H Stricker. Genetic variation in the ABCC2 gene is associated with dose decreases or switches to other cholesterol-lowering drugs during simvastatin and atorvastatin therapy. *The Pharmacogenomics Journal*, 13(3):251–6, dec 2011. ISSN 1473-1150. doi: 10.1038/tpj.2011.59. URL <http://www.ncbi.nlm.nih.gov/pubmed/22186618>.
- [41] J E Keskitalo, K J Kurkinen, P J Neuvoneni, and M Niemi. ABCB1 haplotypes differentially affect the pharmacokinetics of the acid and lactone forms of simvastatin and atorvastatin. *Clinical pharmacology and therapeutics*, 84(4):457–61, October 2008. ISSN 0009-9236. doi: 10.1038/clpt.2008.25.
- [42] Jerome H. Hochman, Nicole Pudvah, Julia Qiu, Masayo Yamazaki, Cuyue Tang, Jinn H. Lin, and Thomayant Prueksaritanont. Interactions of human P-glycoprotein with simvastatin, simvastatin acid, and atorvastatin. *Pharmaceutical Research*, 21(9):1686–1691, 2004. ISSN 0724-8741. doi: 10.1023/B:PHAM.0000041466.84653.8c.
- [43] E J Wang, C N Casciano, R P Clement, and W W Johnson. Active transport of fluorescent P-glycoprotein substrates: evaluation as markers and interaction with inhibitors. *Biochemical and biophysical research communications*, 289(2):580–585, 2001. ISSN 0006-291X. doi: 10.1006/bbrc.2001.6000.

## Bibliography

- [44] Koh-ichi Sugimoto, Masami Ohmori, Shuchi Shuichi Tsuruoka, Kenta Nishiki, Atsuhiko Kawaguchi, Ken-ichi Harada, Masashi Arakawa, Koh-ichi Sakamoto, Mikio Masada, Isamu Miyamori, Akio Fujimura, and Akio Fujimara. Different effects of St John's Wort on the pharmacokinetics of simvastatin and pravastatin. *Clinical Pharmacology & Therapeutics*, 70(6):518–524, December 2001. ISSN 0009-9236. doi: 10.1067/mcp.2001.120025.
- [45] Arthur J Bergman, Josee Cote, Andrea Maes, Jamie J Zhao, Brad a Roadcap, Li Sun, Robert J Valesky, Amy Yang, Bart Keymeulen, Zissi Mathijs, Marina De Smet, Tine Laethem, Michael J Davies, John A Wagner, and Gary A Herman. Effect of sitagliptin on the pharmacokinetics of simvastatin. *Journal of clinical pharmacology*, 49(4):483–8, April 2009. ISSN 0091-2700. doi: 10.1177/0091270008330983. URL <http://www.ncbi.nlm.nih.gov/pubmed/19204138>.
- [46] M K DeGorter, B L Urquhart, U Gradhand, R G Tirona, and R B Kim. Disposition of atorvastatin, rosuvastatin, and simvastatin in OATP1B2<sup>-/-</sup> mice and intraindividual variability in human subjects. *Journal of clinical pharmacology*, 52(11):1689–97, November 2012. ISSN 1552-4604. doi: 10.1177/0091270011422815. URL <http://www.ncbi.nlm.nih.gov/pubmed/22167570>.
- [47] Tomoko Hasunuma, Masahiro Tohkin, Nahoko Kaniwa, In Jin Jang, Cui Yimin, Masaru Kaneko, Yoshiro Saito, Masahiro Takeuchi, Hiroshi Watanabe, Yasushi Yamazoe, Yoshiaki Uyama, and Shinichi Kawai. Absence of ethnic differences in the pharmacokinetics of moxifloxacin, simvastatin, and meloxicam among three east asian populations and caucasians. *British Journal of Clinical Pharmacology*, 81(6):1078–1090, 2016. ISSN 1365-2125. doi: 10.1111/bcp.12884.
- [48] P H Hsyu, M D Schultz-Smith, James H. Lillibridge, Ronald H. Lewis, and Bradley M. Kerr. Pharmacokinetic interactions between nelfinavir and 3-hydroxy-3-methylglutaryl coenzyme A reductase inhibitors atorvastatin and simvastatin. *Antimicrobial agents and chemotherapy*, 45(12):3445–50, December 2001. ISSN 0066-4804. doi: 10.1128/AAC.45.12.3445-3450.2001.
- [49] O Mousa, D C Brater, K J Sunblad, and S D Hall. The interaction of diltiazem with simvastatin. *Clinical pharmacology and therapeutics*, 67(3):267–74, March 2000. ISSN 0009-9236. doi: 10.1067/mcp.2000.104609. URL <http://www.ncbi.nlm.nih.gov/pubmed/10741630>.
- [50] Chantale Simard, Gilles E. O'Hara, Jacques Prévost, Rudolf Guilbaud, R Masseur, and Jacques Turgeon. Study of the drug-drug interaction between simvastatin and cisapride in man. *European journal of clinical pharmacology*, 57(3):229–34, June 2001. ISSN 0031-6970. doi: 10.1007/s002280100298. URL <http://www.ncbi.nlm.nih.gov/pubmed/11497338>.
- [51] Marija Tubic-Grozdanic, John M. Hilfinger, Gordon L. Amidon, Jae Seung Kim, Paul Kijek, Petra Staubach, and Peter Langguth. Pharmacokinetics of the CYP 3A



## Bibliography

- substrate simvastatin following administration of delayed versus immediate release oral dosage forms. *Pharmaceutical research*, 25(7):1591–600, July 2008. ISSN 0724-8741. doi: 10.1007/s11095-007-9519-6. URL <http://www.ncbi.nlm.nih.gov/pubmed/18213452>.
- [52] Q Zhao, J Jiang, and P Hu. Effects of four traditional chinese medicines on the pharmacokinetics of simvastatin. *Xenobiotica*, 45(9):803–10, 2015. ISSN 0049-8254. doi: 10.3109/00498254.2015.1019593.
- [53] Khaled Alakhali, Yahaya Hassan, Nornisah Mohamed, and Mohd Nizam Mordi. Pharmacokinetic of simvastatin study in Malaysian. *IOSR Journal of Pharmacy*, 3(1):46–51, 2013.
- [54] S. Ayalalomasajula, Y. Han, T. Langenickel, K. Malcolm, W. Zhou, I. Hanna, N. Alexander, A. Natrillo, B. Goswami, M. Hinder, and G. Sunkara. In vitro and clinical evaluation of OATP-mediated drug interaction potential of sacubitril/valsartan (LCZ696). *Journal of clinical pharmacy and therapeutics*, 41(4):424–31, August 2016. ISSN 1365-2710. doi: 10.1111/jcpt.12408. URL <http://www.ncbi.nlm.nih.gov/pubmed/27321165>.
- [55] Ling-Ling Dai, Lan Fan, Hui-Zi Wu, Zhi-Rong Tan, Yao Chen, Xiang-Dong Peng, Min-Xue Shen, Guo-Ping Yang, and Hong-Hao Zhou. Assessment of a pharmacokinetic and pharmacodynamic interaction between simvastatin and ginkgo biloba extracts in healthy subjects. *Xenobiotica; the fate of foreign compounds in biological systems*, 43(10):862–7, October 2013. ISSN 1366-5928. doi: 10.3109/00498254.2013.773385. URL <http://www.ncbi.nlm.nih.gov/pubmed/23451885>.
- [56] Michael Derks, Markus Abt, Mary Phelan, Lynn Turnbull, Georgina Meneses-Lorente, Nuria Bech, Anne-Marie White, and Graeme Parr. Coadministration of dalcetrapib with pravastatin, rosuvastatin, or simvastatin: no clinically relevant drug-drug interactions. *Journal of clinical pharmacology*, 50(10):1188–201, October 2010. ISSN 1552-4604. doi: 10.1177/0091270009358709.
- [57] Damayanthi Devineni, Prasarn Manitpisitkul, Joseph Murphy, Donna Skee, Ewa Wajs, Rao N V S Mamidi, Hong Tian, An Vandebosch, Shean-Sheng Wang, Tom Verhaeghe, Hans Stieltjes, and Keith Usiskin. Effect of canagliflozin on the pharmacokinetics of glyburide, metformin, and simvastatin in healthy participants. *Clinical pharmacology in drug development*, 4(3):226–36, 2015. ISSN 2160-7648. doi: 10.1002/cpdd.166. URL <http://www.ncbi.nlm.nih.gov/pubmed/27140803>.
- [58] Sophie Geboers, Jef Stappaerts, Jan Tack, Pieter Annaert, and Patrick Augustijns. In vitro and in vivo investigation of the gastrointestinal behavior of simvastatin. *International journal of pharmaceutics*, 510(1):296–303, August 2016. ISSN 1873-3476. doi: 10.1016/j.ijpharm.2016.06.048.

## Bibliography

- [59] Martine Gehin, Patricia N. Sidharta, Carmela Gnerre, Alexander Treiber, Atef Halabi, and Jasper Dingemanse. Pharmacokinetic interactions between simvastatin and setipiprant, a CRTH2 antagonist. *European journal of clinical pharmacology*, 71(1):15–23, January 2015. ISSN 1432-1041. doi: 10.1007/s00228-014-1767-x. URL <http://www.ncbi.nlm.nih.gov/pubmed/25323804>.
- [60] Matthias Hoch, Petra Hoever, Federica Alessi, Rudolf Theodor, and Jasper Dingemanse. Pharmacokinetic interactions of almorexant with midazolam and simvastatin, two CYP3A4 model substrates, in healthy male subjects. *European journal of clinical pharmacology*, 69(3):523–32, March 2013. ISSN 1432-1041. doi: 10.1007/s00228-012-1403-6. URL <http://www.ncbi.nlm.nih.gov/pubmed/22990330>.
- [61] Matthias Hoch, Petra Hoever, Rudolf Theodor, and Jasper Dingemanse. Almorexant effects on CYP3A4 activity studied by its simultaneous and time-separated administration with simvastatin and atorvastatin. *European journal of clinical pharmacology*, 69(6):1235–45, June 2013. ISSN 1432-1041. doi: 10.1007/s00228-012-1470-8. URL <http://www.ncbi.nlm.nih.gov/pubmed/23334403>.
- [62] Matti K Itkonen, Aleksi Tornio, Mikko Neuvonen, Pertti J Neuvonen, Mikko Niemi, and Janne T Backman. Clopidogrel has no clinically meaningful effect on the pharmacokinetics of the organic anion transporting polypeptide 1B1 and cytochrome P450 3A4 substrate simvastatin. *Drug metabolism and disposition: the biological fate of chemicals*, 43(11):1655–60, November 2015. ISSN 1521-009X. doi: 10.1124/dmd.115.065938. URL <http://www.ncbi.nlm.nih.gov/pubmed/26329790>.
- [63] Teemu Kantola, Kari T. Kivistö, and Pertti J. Neuvonen. Erythromycin and verapamil considerably increase serum simvastatin and simvastatin acid concentrations. *Clinical pharmacology and therapeutics*, 64(2):177–82, August 1998. ISSN 0009-9236. doi: 10.1016/S0009-9236(98)90151-5. URL <http://www.ncbi.nlm.nih.gov/pubmed/9728898>.
- [64] Sreeneeranj Kasichayanula, Ming Chang, Xiaoni Liu, Wen-Chyi Shyu, Steven C. Griffen, Frank P. LaCreta, and David W. Boulton. Lack of pharmacokinetic interactions between dapagliflozin and simvastatin, valsartan, warfarin, or digoxin. *Advances in therapy*, 29(2):163–77, February 2012. ISSN 1865-8652. doi: 10.1007/s12325-011-0098-x. URL <http://www.ncbi.nlm.nih.gov/pubmed/22271159>.
- [65] Rajesh Krishna, Amit Garg, Bo Jin, Sara Sadeghi Keshavarz, Frederick A. Bieberdorf, Jeffrey Chodakewitz, and John A. Wagner. Assessment of a pharmacokinetic and pharmacodynamic interaction between simvastatin and anacetrapib, a potent cholesteryl ester transfer protein (CETP) inhibitor, in healthy subjects. *British Journal of Clinical Pharmacology*, 67(5):520–526, 2009. ISSN 0306-5251. doi: 10.1111/j.1365-2125.2009.03385.x.
- [66] Gopal Krishna, Lei Ma, Pratapa Prasad, Allen Moton, Monika Martinho, and Edward O'Mara. Effect of posaconazole on the pharmacokinetics of simvastatin and midazolam in healthy volunteers. *Expert opinion on drug metabolism & toxicology*, 8(1):1–10,

## Bibliography

- January 2012. ISSN 1744-7607. doi: 10.1517/17425255.2012.639360. URL <http://www.ncbi.nlm.nih.gov/pubmed/22176629>.
- [67] Jari J. Lilja, Kari T. Kivistö, and Pertti J. Neuvonen. Duration of effect of grapefruit juice on the pharmacokinetics of the CYP3A4 substrate simvastatin. *Clinical Pharmacology and Therapeutics*, 68(4):384–390, October 2000. ISSN 0009-9236. doi: 10.1067/mcp.2000.110216.
- [68] Jari J. Lilja, Mikko Neuvonen, and Pertti J. Neuvonen. Effects of regular consumption of grapefruit juice on the pharmacokinetics of simvastatin. *British journal of clinical pharmacology*, 58(1):56–60, July 2004. ISSN 0306-5251. doi: 10.1111/j.1365-2125.2004.02095.x.
- [69] P. Martin, M. Gillen, J. Ritter, D. Mathews, C. Brealey, D. Surry, S. Oliver, V. Holmes, P. Severin, and R. Elsby. Effects of fostamatinib on the pharmacokinetics of oral contraceptive, warfarin, and the statins rosuvastatin and simvastatin: Results from phase I clinical studies. *Drugs in R&D*, 16(1):93–107, March 2016. ISSN 1179-6901. doi: 10.1007/s40268-015-0120-x.
- [70] S G O'Brien, P Meinhardt, E Bond, J Beck, B Peng, C Dutreix, G Mehring, S Milosavljević, C Huber, R Capdeville, and T Fischer. Effects of imatinib mesylate (STI571, glivec) on the pharmacokinetics of simvastatin, a cytochrome P450 3A4 substrate, in patients with chronic myeloid leukaemia. *British journal of cancer*, 89(10):1855–9, 2003. ISSN 0007-0920. doi: 10.1038/sj.bjc.6601152.
- [71] Elliot Offman, Michael Davidson, and Catarina Nilsson. Assessment of pharmacokinetic interaction between omega-3 carboxylic acids and the statins rosuvastatin and simvastatin: Results of 2 phase I studies in healthy volunteers. *Journal of Clinical Lipidology*, 11(3):739–748, 2017. ISSN 1876-4789. doi: 10.1016/j.jacl.2017.03.017.
- [72] Chirag G. Patel, Li Li, Suzette Girgis, David M. Kornhauser, Ernest U. Frevert, and David W. Boulton. Two-way pharmacokinetic interaction studies between saxagliptin and cytochrome P450 substrates or inhibitors: simvastatin, diltiazem extended-release, and ketoconazole. *Clinical Pharmacology: Advances and Applications*, 3(1):13–25, jun 2011. ISSN 1179-1438. doi: 10.2147/CPAA.S15227.
- [73] Joseph W Polli, Elizabeth Hussey, Mark Bush, Grant Generaux, Glenn Smith, David Collins, Susan McMullen, Nancy Turner, and Derek J Nunez. Evaluation of drug interactions of GSK1292263 (a GPR119 agonist) with statins: from in vitro data to clinical study design. *Xenobiotica; the fate of foreign compounds in biological systems*, 43(6):498–508, June 2013. ISSN 1366-5928. doi: 10.3109/00498254.2012.739719. URL <http://www.ncbi.nlm.nih.gov/pubmed/23256625>.
- [74] C Schmitt, B Kuhn, X Zhang, A J Kivitz, and S Grange. Disease-drug-drug interaction involving tocilizumab and simvastatin in patients with rheumatoid arthritis. *Clinical pharmacology and therapeutics*, 89(5):735–40, May 2011. ISSN 1532-6535. doi: 10.1038/clpt.2011.35.

## Bibliography

- [75] Gangadhar Sunkara, Christine V Reynolds, Françoise Pommier, Henri Humbert, ChingMing Yeh, and Pratapa Prasad. Evaluation of a pharmacokinetic interaction between valsartan and simvastatin in healthy subjects. *Current medical research and opinion*, 23(3):631–40, March 2007. ISSN 1473-4877. doi: 10.1185/030079906X167471.
- [76] Sony Tuteja, Danielle Duffy, Richard L. Dunbar, Rajesh Movva, Ram Gadi, Leanne T. Bloedon, and Marina Cuchel. Pharmacokinetic interactions of the microsomal triglyceride transfer protein inhibitor, lomitapide, with drugs commonly used in the management of hypercholesterolemia. *Pharmacotherapy*, 34(3):227–39, March 2014. ISSN 1875-9114. doi: 10.1002/phar.1351. URL <http://www.ncbi.nlm.nih.gov/pubmed/24734312>.
- [77] Anneke Winsemius, Jean-Claude Ansquer, Matthias Olbrich, Peter van Amsterdam, Patrick Aubonnet, Katrin Beckmann, Stefan Driessen, Hanneke van Assche, Gabi Piskol, Dirk Lehnick, and Katsuhiko Mihara. Pharmacokinetic interaction between simvastatin and fenofibrate with staggered and simultaneous dosing: Does it matter? *Journal of clinical pharmacology*, 54(9):1038–47, September 2014. ISSN 1552-4604. doi: 10.1002/jcph.291. URL <http://www.ncbi.nlm.nih.gov/pubmed/24691799>.
- [78] Haitao Yang, Yan Feng, and Yiwen Luan. Determination of simvastatin in human plasma by liquid chromatography–mass spectrometry. *Journal of Chromatography B*, 785(2):369–375, 2003. ISSN 1570-0232. doi: 10.1016/S1570-0232(02)00800-0. URL <http://www.sciencedirect.com/science/article/pii/S1570023202008000>.
- [79] Rosie Z. Yu, Richard S. Geary, Joann D. Flaim, Gina C. Riley, Diane L. Tribble, André A VanVliet, and Mark K. Wedel. Lack of pharmacokinetic interaction of mipomersen sodium (ISIS 301012), a 2'-O-methoxyethyl modified antisense oligonucleotide targeting apolipoprotein B-100 messenger RNA, with simvastatin and ezetimibe. *Clinical pharmacokinetics*, 48(1):39–50, 2009. ISSN 0312-5963. doi: 10.2165/0003088-200948010-00003. URL <http://www.ncbi.nlm.nih.gov/pubmed/19071883>.
- [80] Luigi Ziviani, Lucio Da Ros, Lisa Squassante, Stefano Milleri, Mauro Cugola, and Laura E. Iavarone. The effects of lacidipine on the steady/state plasma concentrations of simvastatin in healthy subjects. *British journal of clinical pharmacology*, 51(2):147–52, February 2001. ISSN 0306-5251. doi: 10.1111/j.1365-2125.2001.bcp119.x.
- [81] Jari J. Lilja, Kari T. Kivistö, and Pertti J. Neuvonen. Grapefruit juice-simvastatin interaction: effect on serum concentrations of simvastatin, simvastatin acid, and HMG-CoA reductase inhibitors. *Clinical pharmacology and therapeutics*, 64(5):477–83, November 1998. ISSN 0009-9236. doi: 10.1016/S0009-9236(98)90130-8.
- [82] Surya P Ayalasomayajula, Kiran Dole, Yan-Ling He, Monica Ligueros-Saylan, Yibin Wang, Joelle Campestrini, Henri Humbert, and Gangadhar Sunkara. Evaluation of the potential for steady-state pharmacokinetic interaction between vildagliptin and

## Bibliography

- simvastatin in healthy subjects. *Current medical research and opinion*, 23(12):2913–20, December 2007. ISSN 1473-4877. doi: 10.1185/030079907X233296. URL <http://www.ncbi.nlm.nih.gov/pubmed/17931461>.
- [83] Arthur J Bergman, Gail Murphy, Joanne Burke, Jamie J Zhao, Robert Valesky, Lida Liu, Kenneth C Lasseter, Weili He, Thomayant Prueksaritanont, Yue Qiu, Alan Hartford, Jose M Vega, and John F Paolini. Simvastatin does not have a clinically significant pharmacokinetic interaction with fenofibrate in humans. *Journal of clinical pharmacology*, 44(9):1054–62, September 2004. ISSN 0091-2700. doi: 10.1177/0091270004268044. URL <http://www.ncbi.nlm.nih.gov/pubmed/15317833>.
- [84] Amílcar Falcão, Roberto Pinto, Teresa Nunes, and Patrício Soares-da Silva. Effect of repeated administration of eslicarbazepine acetate on the pharmacokinetics of simvastatin in healthy subjects. *Epilepsy research*, 106(1-2):244–9, September 2013. ISSN 1872-6844. doi: 10.1016/j.eplepsyres.2013.04.009.
- [85] Angela Georgy, Suoping Zhai, Zhenming Liang, Mark Boldrin, and Jianguo Zhi. Lack of potential pharmacokinetic and pharmacodynamic interactions between piragliatin, a glucokinase activator, and simvastatin in patients with type 2 diabetes mellitus. *Journal of clinical pharmacology*, 56(6):675–82, 2016. ISSN 1552-4604. doi: 10.1002/jcph.640. URL <http://www.ncbi.nlm.nih.gov/pubmed/26381165>.
- [86] J M McKenney, D Swearingen, M Di Spirito, R Doyle, C Pantaleon, D Kling, and R A Shalwitz. Study of the pharmacokinetic interaction between simvastatin and prescription omega-3-acid ethyl esters. *Journal of clinical pharmacology*, 46(7):785–91, July 2006. ISSN 0091-2700. doi: 10.1177/0091270006289849. URL <http://www.ncbi.nlm.nih.gov/pubmed/16809804>.
- [87] Shirley Teng, Diane Potvin, Jean-Claude Mamputu, Geneviève Vincent, Monika Zoltowska, Josée Morin, Saida Hatimi, Sophie-Elise Michaud, Kim High, and Murray P. Ducharme. Impact of tesamorelin, a growth hormone-releasing factor (GRF) analogue, on the pharmacokinetics of simvastatin and ritonavir in healthy volunteers. *Clinical Pharmacology in Drug Development*, 2(3):237–245, July 2013. ISSN 2160-763X. doi: 10.1002/cpdd.27.
- [88] Renli Teng, Patrick D. Mitchell, and Kathleen A. Butler. Pharmacokinetic interaction studies of co-administration of ticagrelor and atorvastatin or simvastatin in healthy volunteers. *European journal of clinical pharmacology*, 69(3):477–87, March 2013. ISSN 1432-1041. doi: 10.1007/s00228-012-1369-4. URL <http://www.ncbi.nlm.nih.gov/pubmed/22922682>.
- [89] M. Ucar, M Neuvonen, H. Luurila, R. Dahlqvist, P. J. Neuvonen, and T Mjörndal. Carbamazepine markedly reduces serum concentrations of simvastatin and simvastatin acid. *European journal of clinical pharmacology*, 59(12):879–82, February 2004. ISSN 0031-6970. doi: 10.1007/s00228-003-0700-5.

## Bibliography

- [90] T.B. Vree, E. Dammers, I. Ulc, S. Horkovics-Kovats, M. Ryska, and I. Merckx. Variable plasma/liver and tissue esterase hydrolysis of simvastatin in healthy volunteers after a single oral dose. *Clinical Drug Investigation*, 21(9):643–652, 2001. ISSN 1173-2563. doi: 10.2165/00044011-200121090-00006.
- [91] Jianguo Zhi, Rema Moore, Linda Kanitra, and Thomas E Mulligan. Effects of orlistat, a lipase inhibitor, on the pharmacokinetics of three highly lipophilic drugs (amiodarone, fluoxetine, and simvastatin) in healthy volunteers. *Journal of clinical pharmacology*, 43(4):428–35, April 2003. ISSN 0091-2700. doi: 10.1177/0091270003252236. URL <http://www.ncbi.nlm.nih.gov/pubmed/12723464>.
- [92] Jonathan B. Wagner, Susan Abdel-Rahman, Leon Van Haandel, Andrea Gaedigk, Roger Gaedigk, Geetha Raghuvver, Ralph Kauffman, and J. Steven Leeder. Impact of SLCO1B1 genotype on pediatric simvastatin acid pharmacokinetics. *Journal of clinical pharmacology*, 58:823–833, June 2018. ISSN 1552-4604. doi: 10.1002/jcph.1080.
- [93] Kyoung-Ah Kim, Pil-Whan Park, Ock-Je Lee, Dong-Kyun Kang, and Ji-Young Park. Effect of polymorphic CYP3A5 genotype on the single-dose simvastatin pharmacokinetics in healthy subjects. *Journal of clinical pharmacology*, 47(1):87–93, January 2007. ISSN 0091-2700. doi: 10.1177/0091270006295063.
- [94] Jenni E Keskitalo, Marja K Pasanen, Pertti J Neuvonen, and Mikko Niemi. Different effects of the ABCG2 c.421C>A SNP on the pharmacokinetics of fluvastatin, pravastatin and simvastatin. *Pharmacogenomics*, 10(10):1617–24, October 2009. ISSN 1744-8042. doi: 10.2217/pgs.09.85. URL <http://www.ncbi.nlm.nih.gov/pubmed/19842935>.
- [95] Marja K Pasanen, Mikko Neuvonen, Pertti J Neuvonen, and Mikko Niemi. SLCO1B1 polymorphism markedly affects the pharmacokinetics of simvastatin acid. *Pharmacogenetics and genomics*, 16(12):873–9, December 2006. ISSN 1744-6872. doi: 10.1097/01.fpc.0000230416.82349.90.
- [96] Hee Youn Choi, Kyun-Seop Bae, Sang-Heon Cho, Jong-Lyul Ghim, Sangmin Choe, Jin Ah Jung, Seok-Joon Jin, Hee-Sun Kim, and Hyeong-Seok Lim. Impact of CYP2D6, CYP3A5, CYP2C19, CYP2A6, SLCO1B1, ABCB1, and ABCG2 gene polymorphisms on the pharmacokinetics of simvastatin and simvastatin acid. *Pharmacogenetics and genomics*, 25:595–608, December 2015. ISSN 1744-6880. doi: 10.1097/FPC.000000000000176.
- [97] Michael Gertz, Anthony Harrison, J. Brian Houston, and Aleksandra Galetin. Prediction of human intestinal first-pass metabolism of 25 CYP3A substrates from in vitro clearance and permeability data. *Drug Metabolism and Disposition*, 38(7):1147–1158, 2010. ISSN 1521-009X. doi: 10.1124/dmd.110.032649.
- [98] H Lennernäs and G Fager. Pharmacodynamics and pharmacokinetics of the HMG-CoA reductase inhibitors. similarities and differences. *Clinical Pharmacokinetics*, 32(5):403–425, may 1997. doi: 10.2165/00003088-199732050-00005.

## Bibliography

- 
- [99] S Vickers, C a Duncan, I W Chen, A Rosegay, and D E Duggan. Metabolic disposition studies on simvastatin, a cholesterol-lowering prodrug. *Drug metabolism and disposition: the biological fate of chemicals*, 18(2):138–45, 1990. ISSN 0090-9556.
- [100] Azza H. Rageh, Noha N. Atia, and Hamdy M. Abdel-Rahman. Lipophilicity estimation of statins as a decisive physicochemical parameter for their hepato-selectivity using reversed-phase thin layer chromatography. *Journal of pharmaceutical and biomedical analysis*, 142:7–14, August 2017. ISSN 1873-264X. doi: 10.1016/j.jpba.2017.04.037.
- [101] Yoshihisa Shitara and Yuichi Sugiyama. Pharmacokinetic and pharmacodynamic alterations of 3-hydroxy-3-methylglutaryl coenzyme A (HMG-CoA) reductase inhibitors: Drug-drug interactions and interindividual differences in transporter and metabolic enzyme functions. *Pharmacology and Therapeutics*, 112(1):71–105, 2006. ISSN 0163-7258. doi: 10.1016/j.pharmthera.2006.03.003.
- [102] Chemaxon. Chemicalize - instant cheminformatics solutions. <https://chemicalize.com>, 2020. Accessed 14 October 2019.
- [103] Merck Canada Inc. Product monograph: Zocor, 2006.
- [104] H Fujino, T Saito, Y Tsunenari, J Kojima, and T Sakaeda. Metabolic properties of the acid and lactone forms of HMG-CoA reductase inhibitors. *Xenobiotica; the fate of foreign compounds in biological systems*, 34(11):961–971, 2004. ISSN 0049-8254. doi: 10.1080/00498250400015319.
- [105] Michi Ishigam, Minoru Uchiyama, Tomoko Kondo, Haruo Iwabuchi, Shin Ichi Inoue, Wataru Takasaki, Toshihiko Ikeda, Toru Komai, Kiyomi Ito, and Yuichi Sugiyama. Inhibition of in vitro metabolism of simvastatin by itraconazole in humans and prediction of in vivo drug-drug interactions. *Pharmaceutical Research*, 18(5):622–631, March 2001. ISSN 0724-8741. doi: 10.1023/A:1011077109233. URL <http://www.ncbi.nlm.nih.gov/pubmed/28325716>.
- [106] N. Le Goff, J. C. Koffel, S. Vandenschrieck, L. Jung, and Genevieve Ubeaud. Comparison of in vitro hepatic models for the prediction of metabolic interaction between simvastatin and naringenin. *European Journal of Drug Metabolism and Pharmacokinetics*, 27(4):233–241, 2002. ISSN 0378-7966. doi: 10.1007/BF03192333.
- [107] Thomayant Prueksaritanont, Lynn M Gorham, Bennett Ma, Lida Liu, Xiao Yu, Jianguo J Zhao, D E Slaughter, Byron H Arison, and Kamlesh P Vyas. In vitro metabolism of simvastatin in humans [SBT]identification of metabolizing enzymes and effect of the drug on hepatic P450s. *Drug metabolism and disposition: the biological fate of chemicals*, 25(10):1191–9, October 1997. ISSN 0090-9556. URL <http://www.ncbi.nlm.nih.gov/pubmed/9321523>.
- [108] Haiqin Lu, Jie Zhu, Yuhui Zang, Yuguan Ze, and Junchuan Qin. Cloning, high level expression of human paraoxonase-3 in Sf9 cells and pharmacological characterization

## Bibliography

- of its product. *Biochemical pharmacology*, 70:1019–1025, October 2005. ISSN 0006-2952. doi: 10.1016/j.bcp.2005.07.004.
- [109] Marjan Afrouzian, Rabab Al-Lahham, Svetlana Patrikeeva, Meixiang Xu, Valentina Fokina, Wayne G Fischer, Sherif Z Abdel-Rahman, Maged Costantine, Mahmoud S Ahmed, and Tatiana Nanovskaya. Role of the efflux transporters BCRP and MRP1 in human placental bio-disposition of pravastatin. *Biochemical pharmacology*, 156: 467–478, October 2018. ISSN 1873-2968. doi: 10.1016/j.bcp.2018.09.012.
- [110] Jian Wei Deng, Ji-Hong Shon, Ho-Jung Shin, Soo-Jin Park, Chang-Woo Yeo, Hong-Hao Zhou, Im-Sook Song, and Jae-Gook Shin. Effect of silymarin supplement on the pharmacokinetics of rosuvastatin. *Pharmaceutical research*, 25:1807–1814, August 2008. ISSN 0724-8741. doi: 10.1007/s11095-007-9492-0.
- [111] Liyue Huang, Yi Wang, and Scott Grimm. ATP-dependent transport of rosuvastatin in membrane vesicles expressing breast cancer resistance protein. *Drug metabolism and disposition: the biological fate of chemicals*, 34:738–742, May 2006. ISSN 0090-9556. doi: 10.1124/dmd.105.007534.
- [112] Satoshi Kitamura, Kazuya Maeda, Yi Wang, and Yuichi Sugiyama. Involvement of multiple transporters in the hepatobiliary transport of rosuvastatin. *Drug metabolism and disposition: the biological fate of chemicals*, 36:2014–2023, October 2008. ISSN 1521-009X. doi: 10.1124/dmd.108.021410.
- [113] Anna Vildhede, André Mateus, Elin K Khan, Yurong Lai, Maria Karlgren, Per Artursson, and Maria C Kjellsson. Mechanistic modeling of pitavastatin disposition in sandwich-cultured human hepatocytes: A proteomics-informed bottom-up approach. *Drug metabolism and disposition: the biological fate of chemicals*, 44:505–516, April 2016. ISSN 1521-009X. doi: 10.1124/dmd.115.066746.
- [114] Brooke M. VandenBrink, Robert S. Foti, Dan A. Rock, Larry C. Wienkers, and Jan L. Wahlstrom. Evaluation of CYP2C8 inhibition in vitro: Utility of montelukast as a selective CYP2C8 probe substrate. *Drug Metabolism and Disposition*, 39(9):1546–1554, 2011. ISSN 0090-9556. doi: 10.1124/dmd.111.039065.
- [115] C. S. Cook, L. M. Berry, and E. Burton. Prediction of in vivo drug interactions with eplerenone in man from in vitro metabolic inhibition data. *Xenobiotica*, 34(3):215–228, 2004. ISSN 0049-8254. doi: 10.1080/00498250310001649341.
- [116] Robert S. Foti, Dan A. Rock, Larry C. Wienkers, and Jan L. Wahlstrom. Selection of alternative CYP3A4 probe substrates for clinical drug interaction studies using in vitro data and in vivo simulation. *Drug Metabolism and Disposition*, 38(6):981–987, 2010. ISSN 0090-9556. doi: 10.1124/dmd.110.032094.
- [117] Hideki Fujino, Iwao Yamada, Syunsuke Shimada, Takeshi Nagao, and Michiaki Yoneda. Metabolic fate of pitavastatin (NK-104), a new inhibitor of 3-hydroxy-3-methyl-glutaryl coenzyme A reductase. effects on drug-metabolizing systems in rats



## Bibliography

- and humans. *Arzneimittel-Forschung*, 52(10):745–53, March 2002. ISSN 0004-4172. doi: 10.1055/s-0031-1299961. URL <http://www.ncbi.nlm.nih.gov/pubmed/12442637>.
- [118] Food and Drug Administration (FDA). NDA 21-697: Vaprisol, 2005.
- [119] Federico Colombo, Hugo Poirier, Nathalie Rioux, Maria Arias Montecillo, Jianmin Duan, and Maria D. Ribadeneira. A membrane vesicle-based assay to enable prediction of human biliary excretion. *Xenobiotica; the fate of foreign compounds in biological systems*, 43(10):915–9, October 2013. ISSN 1366-5928. doi: 10.3109/00498254.2013.769649. URL <http://www.ncbi.nlm.nih.gov/pubmed/23402371>.
- [120] Ravindranath Reddy Gilibili, Sagnik Chatterjee, Pravin Bagul, Kathleen W. Mosure, Bokka Venkata Murali, T. Thanga Mariappan, Sandhya Mandlekar, and Yurong Lai. Coproporphyrin-I: A fluorescent, endogenous optimal probe substrate for ABCC2 (MRP2) suitable for vesicle-based MRP2 inhibition assay. *Drug metabolism and disposition: the biological fate of chemicals*, 45(6):604–611, March 2017. ISSN 1521-009X. doi: 10.1124/dmd.116.074740. URL <http://www.ncbi.nlm.nih.gov/pubmed/28325716>.
- [121] Matthew G Soars, Patrick Barton, Manfred Ismair, Rachael Jupp, and Robert J Riley. The development, characterization, and application of an OATP1B1 inhibition assay in drug discovery. *Drug metabolism and disposition: the biological fate of chemicals*, 40(8):1641–8, August 2012. ISSN 1521-009X. doi: 10.1124/dmd.111.042382. URL <http://www.ncbi.nlm.nih.gov/pubmed/22587986>.
- [122] John P. Keogh and Jeevan R. Kunta. Development, validation and utility of an in vitro technique for assessment of potential clinical drug-drug interactions involving P-glycoprotein. *European Journal of Pharmaceutical Sciences*, 27(5):543–54, April 2006. ISSN 0928-0987. doi: 10.1016/j.ejps.2005.11.011. URL <http://www.ncbi.nlm.nih.gov/pubmed/16406207>.
- [123] Agnès Poirier, Anne-Christine Cascais, Urs Bader, Renée Portmann, Marie-Elise Brun, Isabelle Walter, Alexander Hillebrecht, Mohammed Ullah, and Christoph Funk. Calibration of in vitro multidrug resistance protein 1 substrate and inhibition assays as a basis to support the prediction of clinically relevant interactions in vivo. *Drug metabolism and disposition: the biological fate of chemicals*, 42(9):1411–22, September 2014. ISSN 1521-009X. doi: 10.1124/dmd.114.057943. URL <http://www.ncbi.nlm.nih.gov/pubmed/24939652>.
- [124] Hiroshi Sugimoto, Shin-ichi Matsumoto, Miho Tachibana, Shin-ichi Niwa, Hideki Hirabayashi, Nobuyuki Amano, and Toshiya Moriwaki. Establishment of in vitro P-glycoprotein inhibition assay and its exclusion criteria to assess the risk of drug-drug interaction at the drug discovery stage. *Journal of pharmaceutical sciences*, 100(9):4013–23, September 2011. ISSN 1520-6017. doi: 10.1002/jps.22652. URL <http://www.ncbi.nlm.nih.gov/pubmed/22587986>.

## Bibliography

- 
- [125] E. J. Wang, C. N. Casciano, R. P. Clement, and W. W. Johnson. HMG-CoA reductase inhibitors (statins) characterized as direct inhibitors of P-glycoprotein. *Pharmaceutical Research*, 18(6):800–806, 2001. ISSN 0724-8741. doi: 10.1023/A:1011036428972.
- [126] Martin Werner, Bihter Atil, Evelyn Sieczkowski, Peter Chiba, and Martin Hohenegger. Simvastatin-induced compartmentalisation of doxorubicin sharpens up nuclear topoisomerase II inhibition in human rhabdomyosarcoma cells. *Naunyn-Schmiedeberg's archives of pharmacology*, 386(7):605–17, July 2013. ISSN 1432-1912. doi: 10.1007/s00210-013-0859-y.
- [127] Alejandro Álvarez Lueje, Christian Valenzuela, Juan Arturo Squella, and Luis Joaquin Núñez-Vergara. Stability study of simvastatin under hydrolytic conditions assessed by liquid chromatography. *Journal of AOAC International*, 88(6):1631–1636, 2005. ISSN 1060-3271.
- [128] Thomayant Prueksaritanont, Yue Qiu, Lillian Mu, Kimberly Michel, Janice Brunner, Karen M. Richards, and Jiunn H. Lin. Interconversion pharmacokinetics of simvastatin and its hydroxy acid in dogs: Effects of gemfibrozil. *Pharmaceutical Research*, 22(7):1101–1109, 2005. ISSN 0724-8741. doi: 10.1007/s11095-005-6037-2.
- [129] Drugbank. The drugbank database is a unique bioinformatics and cheminformatics resource that combines detailed drug data with comprehensive drug target information. <https://www.drugbank.ca/>, 2020. Accessed 01 August 2020.
- [130] Clifford W Fong. Statins in therapy: Cellular transport, side effects, drug-drug interactions and cytotoxicity -the unrecognized role of lactones. 2016.
- [131] Masao Yoshinari, Kenichi Matsuzaka, Sadamitsu Hashimoto, Kazuyuki Ishihara, Takashi Inoue, Yutaka Oda, Takaharu Ide, and Teruo Tanaka. Controlled release of simvastatin acid using cyclodextrin inclusion system. *Dental materials journal*, 26(3):451–6, 2007. ISSN 0287-4547. doi: 10.4012/dmj.26.451. URL <http://www.ncbi.nlm.nih.gov/pubmed/17694757>.
- [132] Thomayant Prueksaritanont, Bennett Ma, and Nathan Yu. The human hepatic metabolism of simvastatin hydroxy acid is mediated primarily by CYP3A, and not CYP2D6. *British journal of clinical pharmacology*, 56(1):120–4, July 2003. ISSN 0306-5251. doi: 10.1046/j.1365-2125.2003.01833.x.
- [133] Thomayant Prueksaritanont, Raju Subramanian, Xiaojun Fang, Bennett Ma, Yue Qiu, Jiunn H. Lin, Paul G. Pearson, and Thomas A. Baillie. Glucuronidation of statins in animals and humans: a novel mechanism of statin lactonization. *Drug metabolism and disposition: the biological fate of chemicals*, 30(5):505–12, May 2002. ISSN 0090-9556. doi: 10.1124/dmd.30.5.505. URL <http://www.ncbi.nlm.nih.gov/pubmed/11950779>.

## Bibliography

- 
- [134] Guillaume Margaillan, Michèle Rouleau, Kathrin Klein, John K Fallon, Patrick Caron, Lyne Villeneuve, Philip C Smith, Ulrich M Zanger, and Chantal Guillemette. Multiplexed targeted quantitative proteomics predicts hepatic glucuronidation potential. *Drug metabolism and disposition: the biological fate of chemicals*, 43:1331–1335, September 2015. ISSN 1521-009X. doi: 10.1124/dmd.115.065391.
- [135] Hua Huang. *Characterization of in vitro systems for transporter studies*. PhD thesis, Uppsala University, 2010.
- [136] Amandla Atilano-Roque and Melanie S. Joy. Characterization of simvastatin acid uptake by organic anion transporting polypeptide 3A1 (OATP3A1) and influence of drug-drug interaction. *Toxicology in Vitro*, 45:158–165, 2017. ISSN 1879-3177. doi: 10.1016/j.tiv.2017.09.002.
- [137] H Schelleman, X Han, C M Brensinger, S K Quinney, W B Bilker, D A Flockhart, L Li, and Sean Hennessy. Pharmacoeconomic and in vitro evaluation of potential drug-drug interactions of sulfonyleureas with fibrates and statins. *British journal of clinical pharmacology*, 78(3):639–48, September 2014. ISSN 1365-2125. doi: 10.1111/bcp.12353.
- [138] Terry A. Jacobson. Comparative pharmacokinetic interaction profiles of pravastatin, simvastatin, and atorvastatin when coadministered with cytochrome P450 inhibitors. *The American journal of cardiology*, 94(9):1140–6, November 2004. ISSN 0002-9149. doi: 10.1016/j.amjcard.2004.07.080. URL <http://www.ncbi.nlm.nih.gov/pubmed/15518608>.
- [139] A. Kalliokoski and M. Niemi. Impact of OATP transporters on pharmacokinetics. *British Journal of Pharmacology*, 158(3):693–705, 2009. ISSN 0007-1188. doi: 10.1111/j.1476-5381.2009.00430.x.
- [140] PharmGKB. Very important pharmacogene: ABCG2. <https://www.pharmgkb.org/vip/PA166171172>, 2020. Accessed 01 August 2020.
- [141] T. Prueksaritanont, J. M. Vega, J. D. Rogers, K. Gagliano, H. E. Greenberg, L. Gillen, M. J. Brucker, D. McLoughlin, P. H. Wong, and S. A. Waldman. Simvastatin does not affect CYP3A activity, quantified by the erythromycin breath test and oral midazolam pharmacokinetics, in healthy male subjects. *Journal of clinical pharmacology*, 40:1274–1279, November 2000. ISSN 0091-2700.
- [142] Janne T Backman, Carl Kyrklund, Kari T Kivistö, Jun-sheng S Wang, and Pertti J Neuvonen. Plasma concentrations of active simvastatin acid are increased by gemfibrozil. *Clinical pharmacology and therapeutics*, 68(2):122–9, August 2000. ISSN 0009-9236. doi: 10.1067/mcp.2000.108507.
- [143] Ellen Chung, Anne N. Nafziger, David J. Kazierad, and Joseph S. Bertino. Comparison of midazolam and simvastatin as cytochrome P450 3A probes. *Clinical Pharmacology*

## Bibliography

- and Therapeutics*, 79(4):350–361, 2006. ISSN 0009-9236. doi: 10.1016/j.clpt.2005.11.016.
- [144] Carl Kyrklund, Janne T. Backman, Kari T. Kivistö, M Neuvonen, Jouko Laitila, and Pertti J. Neuvonen. Rifampin greatly reduces plasma simvastatin and simvastatin acid concentrations. *Clinical pharmacology and therapeutics*, 68(6):592–7, December 2000. ISSN 0009-9236. doi: 10.1067/mcp.2000.111414.
- [145] Pertti J. Neuvonen, Teemu Kantola, and Kari T. Kivistö. Simvastatin but not pravastatin is very susceptible to interaction with the CYP3A4 inhibitor itraconazole. *Clinical Pharmacology and Therapeutics*, 63(3):332–341, 1998. ISSN 0009-9236. doi: 10.1016/S0009-9236(98)90165-5.
- [146] Lydia M.M. Vermeer, Caleb D. Istringhausen, Brian W. Ogilvie, and David B. Buckley. Evaluation of ketoconazole and its alternative clinical CYP3A4/5 inhibitors as inhibitors of drug transporters: The in vitro effects of ketoconazole, ritonavir, clarithromycin, and itraconazole on 13 clinically-relevant drug transporters. *Drug Metabolism and Disposition*, 44(3):453–459, 2016. ISSN 1521-009X. doi: 10.1124/dmd.115.067744.
- [147] Masaru Hirano, Kazuya Maeda, Yoshihisa Shitara, and Yuichi Sugiyama. Drug-drug interaction between pitavastatin and various drugs via OATP1B1. *Drug metabolism and disposition: the biological fate of chemicals*, 34(7):1229–36, July 2006. ISSN 0090-9556. doi: 10.1124/dmd.106.009290. URL <http://www.ncbi.nlm.nih.gov/pubmed/16595711>.
- [148] Naoki Kotani, Kazuya Maeda, Yasuyuki Debori, Sandrine Camus, Ruoya Li, Christophe Chesne, and Yuichi Sugiyama. Expression and transport function of drug uptake transporters in differentiated HepaRG cells. *Molecular pharmaceutics*, 9(12):3434–41, December 2012. ISSN 1543-8392. doi: 10.1021/mp300171p. URL <http://www.ncbi.nlm.nih.gov/pubmed/22897388>.
- [149] Masanori Nakakariya, Akihiko Goto, and Nobuyuki Amano. Appropriate risk criteria for OATP inhibition at the drug discovery stage based on the clinical relevancy between oatp inhibitors and drug-induced adverse effect. *Drug metabolism and pharmacokinetics*, 31(5):333–339, October 2016. ISSN 1880-0920. doi: 10.1016/j.dmpk.2016.05.003. URL <http://www.ncbi.nlm.nih.gov/pubmed/27567380>.
- [150] T Prueksaritanont, D A Tatosian, X Chu, R Railkar, R Evers, C Chavez-Eng, R Lutz, W Zeng, J Yabut, G H Chan, X Cai, A H Latham, J Hehman, D Stypinski, J Brejda, C Zhou, B Thornton, K P Bateman, I Fraser, and S A Stoch. Validation of a microdose probe drug cocktail for clinical drug interaction assessments for drug transporters and CYP3A. *Clinical pharmacology and therapeutics*, 101(4):519–530, April 2017. ISSN 1532-6535. doi: 10.1002/cpt.525.

## Bibliography

- 
- [151] Annick Seithel, Sonja Eberl, Katrin Singer, Daniel Auge, Georg Heinkele, Nadine B Wolf, Frank Dörje, Martin F Fromm, and Jörg König. The influence of macrolide antibiotics on the uptake of organic anions and drugs mediated by OATP1B1 and OATP1B3. *Drug metabolism and disposition: the biological fate of chemicals*, 35(5): 779–86, May 2007. ISSN 0090-9556. doi: 10.1124/dmd.106.014407.
- [152] Hiroaki Yamaguchi, Toshiko Takeuchi, Masahiro Okada, Minako Kobayashi, Michiaki Unno, Takaaki Abe, Junichi Goto, Takanori Hishinuma, Miki Shimada, and Nariyasu Mano. Screening of antibiotics that interact with organic anion-transporting polypeptides 1B1 and 1B3 using fluorescent probes. *Biological & pharmaceutical bulletin*, 34(3):389–95, March 2011. ISSN 1347-5215. doi: 10.1248/bpb.34.389.
- [153] Jack A Cook, Bo Feng, Katherine S Fenner, Sarah Kempshall, Ray Liu, Charles Roter, Dennis A Smith, Matthew D Troutman, Mohammed Ullah, and Caroline A Lee. Refining the in vitro and in vivo critical parameters for P-glycoprotein, [I]/IC50 and [I2]/IC50, that allow for the exclusion of drug candidates from clinical digoxin interaction studies. *Molecular pharmaceutics*, 7(2):398–411, Apr 2010. ISSN 1543-8392. doi: 10.1021/mp900174z.
- [154] Wataru Kishimoto, Naoki Ishiguro, Eva Ludwig-Schwellinger, Thomas Ebner, and Olaf Schaefer. In vitro predictability of drug-drug interaction likelihood of P-glycoprotein-mediated efflux of dabigatran etexilate based on [I2]/IC50 threshold. *Drug metabolism and disposition: the biological fate of chemicals*, 42(2):257–63, Feb 2014. ISSN 1521-009X. doi: 10.1124/dmd.113.053769.
- [155] Hiroshi Sugimoto, Hideki Hirabayashi, Nobuyuki Amano, and Toshiya Moriwaki. Retrospective analysis of P-glycoprotein-mediated drug-drug interactions at the blood-brain barrier in humans. *Drug metabolism and disposition: the biological fate of chemicals*, 41(4):683–8, Apr 2013. ISSN 1521-009X. doi: 10.1124/dmd.112.049577.
- [156] Jiezhong Chen and Kenneth Raymond. Roles of rifampicin in drug-drug interactions: underlying molecular mechanisms involving the nuclear pregnane X receptor. *Annals of clinical microbiology and antimicrobials*, 5:3, February 2006. ISSN 1476-0711. doi: 10.1186/1476-0711-5-3.
- [157] Lindsey H M Te Brake, Frans G M Russel, Jeroen J M W van den Heuvel, Gerjo J de Knecht, Jurriaan E de Steenwinkel, David M Burger, Rob E Aarnoutse, and Jan B Koenderink. Inhibitory potential of tuberculosis drugs on ATP-binding cassette drug transporters. *Tuberculosis (Edinburgh, Scotland)*, 96:150–7, January 2016. ISSN 1873-281X. doi: 10.1016/j.tube.2015.08.004.
- [158] Jiajia Dong, Olajide E Olaleye, Rongrong Jiang, Jing Li, Chuang Lu, Feifei Du, Fang Xu, Junling Yang, Fengqing Wang, Weiwei Jia, and Chuan Li. Glycyrrhizin has a high likelihood to be a victim of drug-drug interactions mediated by hepatic organic anion-transporting polypeptide 1B1/1B3. *British journal of pharmacology*, 175(17): 3486–3503, September 2018. ISSN 1476-5381. doi: 10.1111/bph.14393.

## Bibliography

- [159] Jenny M Pedersen, Elin K Khan, Christel A S Bergström, Johan Palm, Janet Hoogstraate, and Per Artursson. Substrate and method dependent inhibition of three ABC-transporters (MDR1, BCRP, and MRP2). *European Journal of Pharmaceutical Sciences*, 103:70–76, May 2017. ISSN 1879-0720. doi: 10.1016/j.ejps.2017.03.002.
- [160] Thomayant Prueksaritanont, Xiaoyan Chu, Raymond Evers, Stephanie O Klopfer, Luzelena Caro, Prajakti A Kothare, Cynthia Dempsey, Scott Rasmussen, Robert Houle, Grace Chan, Xiaoxin Cai, Robert Valesky, Iain P Fraser, and S Aubrey Stoch. Pitavastatin is a more sensitive and selective organic anion-transporting polypeptide 1B clinical probe than rosuvastatin. *British journal of clinical pharmacology*, 78(3):587–98, September 2014. ISSN 1365-2125. doi: 10.1111/bcp.12377.
- [161] Chong Wang, Xiaokui Huo, Changyuan Wang, Qiang Meng, Zhihao Liu, Pengyuan Sun, Jian Cang, Huijun Sun, and Kexin Liu. Organic anion-transporting polypeptide and efflux transporter-mediated hepatic uptake and biliary excretion of cilostazol and its metabolites in rats and humans. *Journal of pharmaceutical sciences*, 106(9):2515–2523, September 2017. ISSN 1520-6017. doi: 10.1016/j.xphs.2017.05.011.
- [162] Yasuhiro Horita and Norio Doi. Comparative study of the effects of antituberculosis drugs and antiretroviral drugs on cytochrome P450 3A4 and P-glycoprotein. *Antimicrobial agents and chemotherapy*, 58(6):3168–76, June 2014. ISSN 1098-6596. doi: 10.1128/AAC.02278-13.
- [163] Lauri I Kajosaari, Jouko Laitila, Pertti J Neuvonen, and Janne T Backman. Metabolism of repaglinide by CYP2C8 and CYP3A4 in vitro: effect of fibrates and rifampicin. *Basic & clinical pharmacology & toxicology*, 97(4):249–56, October 2005. ISSN 1742-7835. doi: 10.1111/j.1742-7843.2005.pto\_157.x.
- [164] P Annaert, Z W Ye, B Stieger, and P Augustijns. Interaction of HIV protease inhibitors with OATP1B1, 1B3, and 2B1. *Xenobiotica; the fate of foreign compounds in biological systems*, 40(3):163–76, March 2010. ISSN 1366-5928. doi: 10.3109/00498250903509375.
- [165] Dallas Bednarczyk. Fluorescence-based assays for the assessment of drug interaction with the human transporters OATP1B1 and OATP1B3. *Analytical biochemistry*, 405(1):50–8, October 2010. ISSN 1096-0309. doi: 10.1016/j.ab.2010.06.012.
- [166] Dallas Bednarczyk and Carri Boiselle. Organic anion transporting polypeptide (OATP)-mediated transport of coproporphyrins I and III. *Xenobiotica; the fate of foreign compounds in biological systems*, 46(5):457–66, September 2016. ISSN 1366-5928. doi: 10.3109/00498254.2015.1085111.
- [167] Yi-An Bi, Chester Costales, Sumathy Mathialagan, Mark West, Soraya Eatemadpour, Sarah Lazzaro, Laurie Tylaska, Renato Scialis, Hui Zhang, John Umland, Emi Kimoto, David A Tess, Bo Feng, Larry M Tremaine, Manthena V S Varma, and A David Rodrigues. Quantitative contribution of six major transporters to the hepatic uptake of drugs: "SLC-phenotyping" using primary human hepatocytes. *The Journal of*

## Bibliography

- pharmacology and experimental therapeutics*, 370(1):72–83, July 2019. ISSN 1521-0103. doi: 10.1124/jpet.119.257600.
- [168] S Bins, L van Doorn, M A Phelps, A A Gibson, S Hu, L Li, A Vasilyeva, G Du, P Hamberg, Falm Eskens, P de Bruijn, A Sparreboom, Rhj Mathijssen, and S D Baker. Influence of OATP1B1 function on the disposition of sorafenib- $\beta$ -D-glucuronide. *Clinical and translational science*, 10(4):271–279, July 2017. ISSN 1752-8062. doi: 10.1111/cts.12458.
- [169] Yu Chen, Lin Chen, Hong Zhang, Shibo Huang, Yuqing Xiong, and Chunhua Xia. Interaction of sulfonylureas with liver uptake transporters OATP1B1 and OATP1B3. *Basic & clinical pharmacology & toxicology*, 123(2):147–154, August 2018. ISSN 1742-7843. doi: 10.1111/bcpt.12992.
- [170] William J Chiou, Sonia M de Morais, Ryota Kikuchi, Richard L Voorman, Xiaofeng Li, and Daniel A J Bow. In vitro OATP1B1 and OATP1B3 inhibition is associated with observations of benign clinical unconjugated hyperbilirubinemia. *Xenobiotica; the fate of foreign compounds in biological systems*, 44(3):276–82, March 2014. ISSN 1366-5928. doi: 10.3109/00498254.2013.820006.
- [171] Min-Koo Choi, Qing-Ri Jin, Yeong-Lim Choi, Sung-Hoon Ahn, Myung-Ae Bae, and Im-Sook Song. Inhibitory effects of ketoconazole and rifampin on OAT1 and OATP1B1 transport activities: considerations on drug-drug interactions. *Biopharmaceutics & drug disposition*, 32(3):175–84, April 2011. ISSN 1099-081X. doi: 10.1002/bdd.749.
- [172] Xiaoyan Chu, Xiaoxin Cai, Donghui Cui, Cuyue Tang, Anima Ghosal, Grace Chan, Mitchell D Green, Yuhsin Kuo, Yuexia Liang, Cheri M Maciolek, Jairam Palamanda, Raymond Evers, and Thomayant Prueksaritanont. In vitro assessment of drug-drug interaction potential of boceprevir associated with drug metabolizing enzymes and transporters. *Drug metabolism and disposition: the biological fate of chemicals*, 41(3):668–81, March 2013. ISSN 1521-009X. doi: 10.1124/dmd.112.049668.
- [173] Tom De Bruyn, Sarinj Fattah, Bruno Stieger, Patrick Augustijns, and Pieter Annaert. Sodium fluorescein is a probe substrate for hepatic drug transport mediated by OATP1B1 and OATP1B3. *Journal of pharmaceutical sciences*, 100(11):5018–30, November 2011. ISSN 1520-6017. doi: 10.1002/jps.22694.
- [174] Tom De Bruyn, Gerard J P van Westen, Adriaan P Ijzerman, Bruno Stieger, Peter de Witte, Patrick F Augustijns, and Pieter P Annaert. Structure-based identification of OATP1B1/3 inhibitors. *Molecular pharmacology*, 83(6):1257–67, June 2013. ISSN 1521-0111. doi: 10.1124/mol.112.084152.
- [175] Chunshan Gui, Yi Miao, Lucas Thompson, Bret Wahlgren, Melissa Mock, Bruno Stieger, and Bruno Hagenbuch. Effect of pregnane X receptor ligands on transport mediated by human OATP1B1 and OATP1B3. *European journal of pharmacology*, 584(1):57–65, April 2008. ISSN 0014-2999. doi: 10.1016/j.ejphar.2008.01.042.

## Bibliography

- [176] Chunshan Gui, Amanda Obaidat, Rathnam Chaguturu, and Bruno Hagenbuch. Development of a cell-based high-throughput assay to screen for inhibitors of organic anion transporting polypeptides 1B1 and 1B3. *Current chemical genomics*, 4:1–8, March 2010. ISSN 1875-3973. doi: 10.2174/1875397301004010001.
- [177] Saki Izumi, Yoshitane Nozaki, Takafumi Komori, Kazuya Maeda, Osamu Takenaka, Kazutomi Kusano, Tsutomu Yoshimura, Hiroyuki Kusuhara, and Yuichi Sugiyama. Substrate-dependent inhibition of organic anion transporting polypeptide 1B1: comparative analysis with prototypical probe substrates estradiol-17 $\beta$ -glucuronide, estrone-3-sulfate, and sulfobromophthalein. *Drug metabolism and disposition: the biological fate of chemicals*, 41(10):1859–66, October 2013. ISSN 1521-009X. doi: 10.1124/dmd.113.052290. URL <http://www.ncbi.nlm.nih.gov/pubmed/23920221>.
- [178] Saki Izumi, Yoshitane Nozaki, Kazuya Maeda, Takafumi Komori, Osamu Takenaka, Hiroyuki Kusuhara, and Yuichi Sugiyama. Investigation of the impact of substrate selection on in vitro organic anion transporting polypeptide 1B1 inhibition profiles for the prediction of drug-drug interactions. *Drug metabolism and disposition: the biological fate of chemicals*, 43(2):235–47, February 2015. ISSN 1521-009X. doi: 10.1124/dmd.114.059105. URL <http://www.ncbi.nlm.nih.gov/pubmed/25414411>.
- [179] Saki Izumi, Yoshitane Nozaki, Takafumi Komori, Osamu Takenaka, Kazuya Maeda, Hiroyuki Kusuhara, and Yuichi Sugiyama. Investigation of fluorescein derivatives as substrates of organic anion transporting polypeptide (OATP) 1B1 to develop sensitive fluorescence-based OATP1B1 inhibition assays. *Molecular pharmaceutics*, 13(2):438–48, February 2016. ISSN 1543-8392. doi: 10.1021/acs.molpharmaceut.5b00664.
- [180] Rongrong Jiang, Jiajia Dong, Xiuxue Li, Feifei Du, Weiwei Jia, Fang Xu, Fengqing Wang, Junling Yang, Wei Niu, and Chuan Li. Molecular mechanisms governing different pharmacokinetics of ginsenosides and potential for ginsenoside-perpetrated herb-drug interactions on OATP1B3. *British journal of pharmacology*, 172(4):1059–73, February 2015. ISSN 1476-5381. doi: 10.1111/bph.12971.
- [181] Maria Karlgren, Gustav Ahlin, Christel A S Bergström, Richard Svensson, Johan Palm, and Per Artursson. In vitro and in silico strategies to identify OATP1B1 inhibitors and predict clinical drug-drug interactions. *Pharmaceutical research*, 29(2):411–26, February 2012. ISSN 1573-904X. doi: 10.1007/s11095-011-0564-9.
- [182] Varun Khurana, Mukul Minocha, Dhananjay Pal, and Ashim K Mitra. Inhibition of OATP-1B1 and OATP-1B3 by tyrosine kinase inhibitors. *Drug metabolism and drug interactions*, 29(4):249–59, March 2014. ISSN 2191-0162. doi: 10.1515/dmdi-2014-0014.
- [183] Ryota Kikuchi, Vincent C Peterkin, William J Chiou, Sonia M de Morais, and Daniel A J Bow. Validation of a total IC<sub>50</sub> method which enables in vitro assessment of transporter inhibition under semi-physiological conditions. *Xenobiotica; the fate of*



## Bibliography

- foreign compounds in biological systems*, 47(9):825–832, September 2017. ISSN 1366-5928. doi: 10.1080/00498254.2016.1233372.
- [184] Jung Won Kim, SoJeong Yi, Tae-Eun Kim, Kyoung Soo Lim, Seo Hyun Yoon, Joo-Youn Cho, Min Goo Lee, Im-Sook Song, Sang-Goo Shin, In-Jin Jang, and Kyung-Sang Yu. Increased systemic exposure of fimasartan, an angiotensin II receptor antagonist, by ketoconazole and rifampicin. *Journal of clinical pharmacology*, 53(1):75–81, January 2013. ISSN 1552-4604. doi: 10.1177/0091270011433328.
- [185] Y Y Lau, Y Huang, L Frassetto, and L Z Benet. Effect of OATP1B transporter inhibition on the pharmacokinetics of atorvastatin in healthy volunteers. *Clinical pharmacology and therapeutics*, 81(2):194–204, February 2007. ISSN 0009-9236. doi: 10.1038/sj.clpt.6100038.
- [186] Mirko Leonhardt, Markus Keiser, Stefan Oswald, Jens Kühn, Jia Jia, Markus Grube, Heyo K Kroemer, Werner Siegmund, and Werner Weitschies. Hepatic uptake of the magnetic resonance imaging contrast agent Gd-EOB-DTPA: role of human organic anion transporters. *Drug metabolism and disposition: the biological fate of chemicals*, 38(7):1024–8, July 2010. ISSN 1521-009X. doi: 10.1124/dmd.110.032862.
- [187] Katrin Letschert, Heinz Faulstich, Daniela Keller, and Dietrich Keppler. Molecular characterization and inhibition of amanitin uptake into human hepatocytes. *Toxicological sciences : an official journal of the Society of Toxicology*, 91(1):140–9, May 2006. ISSN 1096-6080. doi: 10.1093/toxsci/kfj141.
- [188] Xiu-li Li, Zi-tao Guo, Ye-dong Wang, Xiao-yan Chen, Jia Liu, and Da-fang Zhong. Potential role of organic anion transporting polypeptide 1B1 (OATP1B1) in the selective hepatic uptake of hematoporphyrin monomethyl ether isomers. *Acta pharmacologica Sinica*, 36(2):268–80, February 2015. ISSN 1745-7254. doi: 10.1038/aps.2014.104.
- [189] Yanli Lu, Qingqing Hu, Lin Chen, Hong Zhang, Shibo Huang, Yuqing Xiong, and Chunhua Xia. Interaction of deoxyschizandrin and schizandrin B with liver uptake transporters OATP1B1 and OATP1B3. *Xenobiotica; the fate of foreign compounds in biological systems*, 49(2):239–246, February 2019. ISSN 1366-5928. doi: 10.1080/00498254.2018.1437647.
- [190] Sonia Pahwa, Khondoker Alam, Alexandra Crowe, Taleah Farasyn, Sibylle Neuhoff, Oliver Hatley, Kai Ding, and Wei Yue. Pretreatment with rifampicin and tyrosine kinase inhibitor dasatinib potentiates the inhibitory effects toward OATP1B1- and OATP1B3-mediated transport. *Journal of pharmaceutical sciences*, 106(8):2123–2135, August 2017. ISSN 1520-6017. doi: 10.1016/j.xphs.2017.03.022.
- [191] M Masud Parvez, Jin Ah Jung, Ho Jung Shin, Dong Hyun Kim, and Jae-Gook Shin. Characterization of 22 antituberculosis drugs for inhibitory interaction potential on organic anionic transporter polypeptide (OATP)-mediated uptake. *Antimicrobial agents and chemotherapy*, 60(5):3096–105, May 2016. ISSN 1098-6596. doi: 10.1128/AAC.02765-15.

## Bibliography

- [192] Juliane Riha, Stefan Brenner, Michaela Böhmendorfer, Benedikt Giessrigl, Marc Pignitter, Katharina Schueller, Theresia Thalhammer, Bruno Stieger, Veronika Somoza, Thomas Szekeres, and Walter Jäger. Resveratrol and its major sulfated conjugates are substrates of organic anion transporting polypeptides (OATPs): impact on growth of ZR-75-1 breast cancer cells. *Molecular nutrition & food research*, 58(9):1830–42, September 2014. ISSN 1613-4133. doi: 10.1002/mnfr.201400095.
- [193] Hong Shen, Zheng Yang, Gabe Mintier, Yong-Hae Han, Cliff Chen, Praveen Balimane, Mohammed Jemal, Weiping Zhao, Renjie Zhang, Sanjith Kallipatti, Sabariya Selvam, Sunil Sukrutharaj, Prasad Krishnamurthy, Punit Marathe, and A David Rodrigues. Cynomolgus monkey as a potential model to assess drug interactions involving hepatic organic anion transporting polypeptides: in vitro, in vivo, and in vitro-to-in vivo extrapolation. *The Journal of pharmacology and experimental therapeutics*, 344(3):673–85, March 2013. ISSN 1521-0103. doi: 10.1124/jpet.112.200691. URL <http://www.ncbi.nlm.nih.gov/pubmed/23297161>.
- [194] Hong Shen, Weiqi Chen, Dieter M Drexler, Sandhya Mandlekar, Vinay K Holenarsipur, Eric E Shields, Robert Langish, Kurex Sidik, Jinping Gan, W Griffith Humphreys, Punit Marathe, and Yurong Lai. Comparative evaluation of plasma bile acids, dehydroepiandrosterone sulfate, hexadecanedioate, and tetradecanedioate with coproporphyrins I and III as markers of OATP inhibition in healthy subjects. *Drug metabolism and disposition: the biological fate of chemicals*, 45(8):908–919, August 2017. ISSN 1521-009X. doi: 10.1124/dmd.117.075531.
- [195] Tadayuki Takashima, Satoshi Kitamura, Yasuhiro Wada, Masaaki Tanaka, Yoshihito Shigihara, Hideki Ishii, Ryosuke Ijuin, Susumu Shiomi, Takahiro Nakae, Yumiko Watanabe, Yilong Cui, Hisashi Doi, Masaaki Suzuki, Kazuya Maeda, Hiroyuki Kusuhara, Yuichi Sugiyama, and Yasuyoshi Watanabe. PET imaging-based evaluation of hepatobiliary transport in humans with (15R)-11C-TIC-Me. *Journal of Nuclear Medicine*, 53(5):741–748, apr 2012. ISSN 1535-5667. doi: 10.2967/jnumed.111.098681.
- [196] Issey Takehara, Hanano Terashima, Takeshi Nakayama, Takashi Yoshikado, Miwa Yoshida, Kenichi Furihata, Nobuaki Watanabe, Kazuya Maeda, Osamu Ando, Yuichi Sugiyama, and Hiroyuki Kusuhara. Investigation of glycochenodeoxycholate sulfate and chenodeoxycholate glucuronide as surrogate endogenous probes for drug interaction studies of OATP1B1 and OATP1B3 in healthy japanese volunteers. *Pharmaceutical research*, 34(8):1601–1614, August 2017. ISSN 1573-904X. doi: 10.1007/s11095-017-2184-5.
- [197] Bani Tamraz, Hisayo Fukushima, Alan R Wolfe, Rüdiger Kaspera, Rheem A Totah, James S Floyd, Benjamin Ma, Catherine Chu, Kristin D Marciante, Susan R Heckbert, Bruce M Psaty, Deanna L Kroetz, and Pui-Yan Kwok. OATP1B1-related drug-drug and drug-gene interactions as potential risk factors for cerivastatin-induced rhabdomyolysis. *Pharmacogenetics and genomics*, 23(7):355–64, July 2013. ISSN 1744-6880. doi: 10.1097/FPC.0b013e3283620c3b.

## Bibliography

- 
- [198] Péter Tátrai, Patrick Schweigler, Birk Poller, Norbert Domange, Roelof de Wilde, Imad Hanna, Zsuzsanna Gáborik, and Felix Huth. A systematic in vitro investigation of the inhibitor preincubation effect on multiple classes of clinically relevant transporters. *Drug metabolism and disposition: the biological fate of chemicals*, 47(7):768–778, July 2019. ISSN 1521-009X. doi: 10.1124/dmd.118.085993. URL <http://www.ncbi.nlm.nih.gov/pubmed/31068368>.
- [199] Rommel G Tirona, Brenda F Leake, Allan W Wolkoff, and Richard B Kim. Human organic anion transporting polypeptide-C (SLC21A6) is a major determinant of rifampin-mediated pregnane X receptor activation. *The Journal of pharmacology and experimental therapeutics*, 304(1):223–8, January 2003. ISSN 0022-3565. doi: 10.1124/jpet.102.043026. URL <http://www.ncbi.nlm.nih.gov/pubmed/12490595>.
- [200] Alexander Treiber, Ralph Schneider, Stephanie Häusler, and Bruno Stieger. Bosentan is a substrate of human OATP1B1 and OATP1B3: inhibition of hepatic uptake as the common mechanism of its interactions with cyclosporin a, rifampicin, and sildenafil. *Drug metabolism and disposition: the biological fate of chemicals*, 35(8):1400–7, August 2007. ISSN 0090-9556. doi: 10.1124/dmd.106.013615.
- [201] E van de Steeg, R Greupink, M Schreurs, I H G Nooijen, K C M Verhoeckx, R Hane-maaijer, D Ripken, M Monshouwer, M L H Vlaming, J DeGroot, M Verwei, F G M Russel, M T Huisman, and H M Wortelboer. Drug-drug interactions between rosuvastatin and oral antidiabetic drugs occurring at the level of OATP1B1. *Drug metabolism and disposition: the biological fate of chemicals*, 41(3):592–601, March 2013. ISSN 1521-009X. doi: 10.1124/dmd.112.049023.
- [202] P L M van Giersbergen, A Treiber, R Schneider, H Dietrich, and J Dingemanse. Inhibitory and inductive effects of rifampin on the pharmacokinetics of bosentan in healthy subjects. *Clinical pharmacology and therapeutics*, 81(3):414–9, March 2007. ISSN 0009-9236. doi: 10.1038/sj.cpt.6100075.
- [203] Stephan R Vavricka, Jessica Van Montfoort, Huy Riem Ha, Peter J Meier, and Karin Fattinger. Interactions of rifamycin SV and rifampicin with organic anion uptake systems of human liver. *Hepatology (Baltimore, Md.)*, 36(1):164–72, July 2002. ISSN 0270-9139. doi: 10.1053/jhep.2002.34133. URL <http://www.ncbi.nlm.nih.gov/pubmed/12085361>.
- [204] Anna Vildhede, Maria Karlgren, Elin K Svedberg, Jacek R Wisniewski, Yurong Lai, Agneta Norén, and Per Artursson. Hepatic uptake of atorvastatin: influence of variability in transporter expression on uptake clearance and drug-drug interactions. *Drug metabolism and disposition: the biological fate of chemicals*, 42(7):1210–8, July 2014. ISSN 1521-009X. doi: 10.1124/dmd.113.056309. URL <http://www.ncbi.nlm.nih.gov/pubmed/24799396>.
- [205] Johanna Weiss, Dirk Theile, Adriana Spalwicz, Jürgen Burhenne, Klaus-Dieter Riedel, and Walter Emil Haefeli. Influence of sildenafil and tadalafil on the enzyme- and

## Bibliography

- transporter-inducing effects of bosentan and ambrisentan in LS180 cells. *Biochemical pharmacology*, 85(2):265–73, January 2013. ISSN 1873-2968. doi: 10.1016/j.bcp.2012.11.020.
- [206] Wen Zhang, Xiaomin Xiong, Lin Chen, Mingyi Liu, Yuqing Xiong, Hong Zhang, Shibo Huang, and Chunhua Xia. Hepatic uptake mechanism of ophiopogonin D mediated by organic anion transporting polypeptides. *European journal of drug metabolism and pharmacokinetics*, 42(4):669–676, August 2017. ISSN 2107-0180. doi: 10.1007/s13318-016-0384-8.
- [207] M L Reitman, X Chu, X Cai, J Yabut, R Venkatasubramanian, S Zajic, J A Stone, Y Ding, R Witter, C Gibson, K Roupe, R Evers, J A Wagner, and A Stoch. Rifampin’s acute inhibitory and chronic inductive drug interactions: experimental and model-based approaches to drug-drug interaction trial design. *Clinical pharmacology and therapeutics*, 89(2):234–42, February 2011. ISSN 1532-6535. doi: 10.1038/clpt.2010.271.
- [208] J. F. Rajaonarison, B. Lacarelle, J. Catalin, M. Placidi, and R. Rahmani. 3'-azido-3'-deoxythymidine drug interactions. screening for inhibitors in human liver microsomes. *Drug metabolism and disposition: the biological fate of chemicals*, 20:578–584, 1992. ISSN 0090-9556.
- [209] Vaishali Dixit, Niresh Hariparsad, Fang Li, Pankaj Desai, Kenneth E Thummel, and Jashvant D Unadkat. Cytochrome P450 enzymes and transporters induced by anti-human immunodeficiency virus protease inhibitors in human hepatocytes: implications for predicting clinical drug interactions. *Drug metabolism and disposition: the biological fate of chemicals*, 35(10):1853–9, October 2007. ISSN 0090-9556. doi: 10.1124/dmd.107.016089.
- [210] S Harmsen, I Meijerman, J H Beijnen, and J H M Schellens. Nuclear receptor mediated induction of cytochrome P450 3A4 by anticancer drugs: a key role for the pregnane X receptor. *Cancer chemotherapy and pharmacology*, 64(1):35–43, June 2009. ISSN 1432-0843. doi: 10.1007/s00280-008-0842-3.
- [211] Li Liu, Ganesh M Mugundu, Brian J Kirby, Divya Samineni, Pankaj B Desai, and Jashvant D Unadkat. Quantification of human hepatocyte cytochrome P450 enzymes and transporters induced by HIV protease inhibitors using newly validated LC-MS/MS cocktail assays and RT-PCR. *Biopharmaceutics & drug disposition*, 33(4):207–17, May 2012. ISSN 1099-081X. doi: 10.1002/bdd.1788.
- [212] Yong Chen, Lisa Liu, Eric Laille, Gondi Kumar, and Sekhar Surapaneni. In vitro assessment of cytochrome P450 inhibition and induction potential of azacitidine. *Cancer chemotherapy and pharmacology*, 65(5):995–1000, April 2010. ISSN 1432-0843. doi: 10.1007/s00280-010-1245-9.

Bibliography

---

- [213] Pankaj B Desai, Srikanth C Nallani, Rucha S Sane, Linda B Moore, Bryan J Goodwin, Donna J Buckley, and Arthur R Buckley. Induction of cytochrome P450 3A4 in primary human hepatocytes and activation of the human pregnane X receptor by tamoxifen and 4-hydroxytamoxifen. *Drug metabolism and disposition: the biological fate of chemicals*, 30(5):608–12, May 2002. ISSN 0090-9556. doi: 10.1124/dmd.30.5.608. URL <http://www.ncbi.nlm.nih.gov/pubmed/11950795>.
- [214] Johannes Doehmer, Bernhard Tewes, Kai-Uwe Klein, Kristin Gritzko, Holger Muschick, and Ulrich Mengs. Assessment of drug-drug interaction for silymarin. *Toxicology in Vitro*, 22(3):610–7, April 2008. ISSN 0887-2333. doi: 10.1016/j.tiv.2007.11.020.
- [215] L Drocourt, J M Pascussi, E Assenat, J M Fabre, P Maurel, and M J Vilarem. Calcium channel modulators of the dihydropyridine family are human pregnane X receptor activators and inducers of CYP3A, CYP2B, and CYP2C in human hepatocytes. *Drug metabolism and disposition: the biological fate of chemicals*, 29(10):1325–31, October 2001. ISSN 0090-9556. URL <http://www.ncbi.nlm.nih.gov/pubmed/11560876>.
- [216] Ana Ferreira, M'arcio Rodrigues, Samuel Silvestre, Am'ílcar Falcão, and Gilberto Alves. HepaRG cell line as an in vitro model for screening drug-drug interactions mediated by metabolic induction: amiodarone used as a model substance. *Toxicology in vitro : an international journal published in association with BIBRA*, 28(8):1531–5, December 2014. ISSN 1879-3177. doi: 10.1016/j.tiv.2014.08.004.
- [217] Anshul Gupta, Ganesh M Mugundu, Pankaj B Desai, Kenneth E Thummel, and Jashvant D Unadkat. Intestinal human colon adenocarcinoma cell line LS180 is an excellent model to study pregnane X receptor, but not constitutive androstane receptor, mediated CYP3A4 and multidrug resistance transporter 1 induction: studies with anti-human immunodeficiency virus protease inhibitors. *Drug metabolism and disposition: the biological fate of chemicals*, 36(6):1172–80, June 2008. ISSN 1521-009X. doi: 10.1124/dmd.107.018689.
- [218] Klarissa D Hardy, Michelle D Wahlin, Ioannis Papageorgiou, Jashvant D Unadkat, Allan E Rettie, and Sidney D Nelson. Studies on the role of metabolic activation in tyrosine kinase inhibitor-dependent hepatotoxicity: induction of CYP3A4 enhances the cytotoxicity of lapatinib in HepaRG cells. *Drug metabolism and disposition: the biological fate of chemicals*, 42(1):162–71, January 2014. ISSN 1521-009X. doi: 10.1124/dmd.113.054817.
- [219] Niresh Hariparsad, Srikanth C Nallani, Rucha S Sane, Donna J Buckley, Arthur R Buckley, and Pankaj B Desai. Induction of CYP3A4 by efavirenz in primary human hepatocytes: comparison with rifampin and phenobarbital. *Journal of clinical pharmacology*, 44(11):1273–81, November 2004. ISSN 0091-2700. doi: 10.1177/0091270004269142.

## Bibliography

- [220] Kajsa P Kanebratt and Tommy B Andersson. HepaRG cells as an in vitro model for evaluation of cytochrome P450 induction in humans. *Drug metabolism and disposition: the biological fate of chemicals*, 36(1):137–45, January 2008. ISSN 1521-009X. doi: 10.1124/dmd.107.017418.
- [221] M Katoh, M Watanabe, T Tabata, Y Sato, M Nakajima, M Nishimura, S Naito, C Tateno, K Iwasaki, K Yoshizato, and T Yokoi. In vivo induction of human cytochrome P450 3A4 by rifabutin in chimeric mice with humanized liver. *Xenobiotica; the fate of foreign compounds in biological systems*, 35(9):863–75, September 2005. ISSN 0049-8254. doi: 10.1080/00498250500296231.
- [222] A Kistler, H Liechti, L Pichard, E Wolz, G Oesterhelt, A Hayes, and P Maurel. Metabolism and CYP-inducer properties of astaxanthin in man and primary human hepatocytes. *Archives of toxicology*, 75:665–75, January 2002. ISSN 0340-5761. doi: 10.1007/s00204-001-0287-5. URL <http://www.ncbi.nlm.nih.gov/pubmed/11876499>.
- [223] Marc Lübberstedt, Ursula Müller-Vieira, Manuela Mayer, Klaus M Biemel, Fanny Knöspel, Daniel Knobloch, Andreas K Nüssler, Jörg C Gerlach, and Katrin Zeilinger. HepaRG human hepatic cell line utility as a surrogate for primary human hepatocytes in drug metabolism assessment in vitro. *Journal of pharmacological and toxicological methods*, 63(1):59–68, May 2010. ISSN 1873-488X. doi: 10.1016/j.vascn.2010.04.013.
- [224] Ajay Madan, Richard A Graham, Kathleen M Carroll, Daniel R Mudra, L Alayne Burton, Linda A Krueger, April D Downey, Maciej Czerwinski, Jameson Forster, Maria D Ribadeneira, Liang-Shang Gan, Edward L LeCluyse, Karl Zech, Philmore Robertson, Patrick Koch, Lida Antonian, Greg Wagner, Li Yu, and Andrew Parkinson. Effects of prototypical microsomal enzyme inducers on cytochrome P450 expression in cultured human hepatocytes. *Drug metabolism and disposition: the biological fate of chemicals*, 31(4):421–31, April 2003. ISSN 0090-9556. doi: 10.1124/dmd.31.4.421. URL <http://www.ncbi.nlm.nih.gov/pubmed/12642468>.
- [225] V Meunier, M Bourrié, B Julian, E Marti, F Guillou, Y Berger, and G Fabre. Expression and induction of CYP1A1/1A2, CYP2A6 and CYP3A4 in primary cultures of human hepatocytes: a 10-year follow-up. *Xenobiotica; the fate of foreign compounds in biological systems*, 30(6):589–607, June 2000. ISSN 0049-8254. doi: 10.1080/004982500406426. URL <http://www.ncbi.nlm.nih.gov/pubmed/10923861>.
- [226] Katalin Monostory, Jean-Marc Pascussi, P’al Szab’o, Manna Temesv’ari, Krisztina Köhalmy, Jure Acimovic, Darko Kocjan, Drago Kuzman, Britta Wilzewski, Rita Bernhardt, L’aszl’o K’obori, and Damjana Rozman. Drug interaction potential of 2-((3,4-dichlorophenethyl)(propyl)amino)-1-(pyridin-3-yl)ethanol (LK-935), the novel nonstatin-type cholesterol-lowering agent. *Drug metabolism and disposition: the biological fate of chemicals*, 37(2):375–85, February 2009. ISSN 1521-009X. doi: 10.1124/dmd.108.023887.

Bibliography

---

- [227] Ganesh M Mugundu, Niresh Hariparsad, and Pankaj B Desai. Impact of ritonavir, atazanavir and their combination on the CYP3A4 induction potential of efavirenz in primary human hepatocytes. *Drug metabolism letters*, 4(1):45–50, January 2010. ISSN 1874-0758. doi: 10.2174/187231210790980453.
- [228] Srikanth C Nallani, Tracy A Glauser, Niresh Hariparsad, Kenneth Setchell, Donna J Buckley, Arthur R Buckley, and Pankaj B Desai. Dose-dependent induction of cytochrome P450 (CYP) 3A4 and activation of pregnane X receptor by topiramate. *Epilepsia*, 44(12):1521–8, December 2003. ISSN 0013-9580. doi: 10.1111/j.0013-9580.2003.06203.x.
- [229] Srikanth C Nallani, Bryan Goodwin, Arthur R Buckley, Donna J Buckley, and Pankaj B Desai. Differences in the induction of cytochrome P450 3A4 by taxane anticancer drugs, docetaxel and paclitaxel, assessed employing primary human hepatocytes. *Cancer chemotherapy and pharmacology*, 54(3):219–29, September 2004. ISSN 0344-5704. doi: 10.1007/s00280-004-0799-9.
- [230] P Olinga, M G L Elferink, A L Draaisma, M T Merema, J V Castell, G P'erez, and G M M Groothuis. Coordinated induction of drug transporters and phase I and II metabolism in human liver slices. *European journal of pharmaceutical sciences : official journal of the European Federation for Pharmaceutical Sciences*, 33(4-5):380–9, April 2008. ISSN 0928-0987. doi: 10.1016/j.ejps.2008.01.008.
- [231] Jasminder Sahi, Stacy S Shord, Celeste Lindley, Stephen Ferguson, and Edward L LeCluyse. Regulation of cytochrome P450 2C9 expression in primary cultures of human hepatocytes. *Journal of biochemical and molecular toxicology*, 23(1):43–58, February 2009. ISSN 1099-0461. doi: 10.1002/jbt.20264.
- [232] Toshiyuki Shimizu, Kei Akimoto, Takuya Yoshimura, Takuro Niwa, Kaoru Kobayashi, Michio Tsunoo, and Kan Chiba. Autoinduction of MKC-963 [(R)-1-(1-cyclohexylethylamino)-4-phenylphthalazine] metabolism in healthy volunteers and its retrospective evaluation using primary human hepatocytes and cDNA-expressed enzymes. *Drug metabolism and disposition: the biological fate of chemicals*, 34(6):950–4, June 2006. ISSN 0090-9556. doi: 10.1124/dmd.105.007997.
- [233] Matthew G Soars, David M Petullo, James A Eckstein, Steve C Kasper, and Steven A Wrighton. An assessment of UDP-glucuronosyltransferase induction using primary human hepatocytes. *Drug metabolism and disposition: the biological fate of chemicals*, 32(1):140–8, January 2004. ISSN 0090-9556. doi: 10.1124/dmd.32.1.140.
- [234] Mei-Fei Yueh, Marleen Kawahara, and Judy Raucy. High volume bioassays to assess CYP3A4-mediated drug interactions: induction and inhibition in a single cell line. *Drug metabolism and disposition: the biological fate of chemicals*, 33(1):38–48, January 2005. ISSN 0090-9556. doi: 10.1124/dmd.104.001594.

## Bibliography

- [235] J George Zhang, Thuy Ho, Alanna L Callendrello, Robert J Clark, Elizabeth A Santone, Sarah Kinsman, Deqing Xiao, Lisa G Fox, Heidi J Einolf, and David M Stresser. Evaluation of calibration curve-based approaches to predict clinical inducers and non-inducers of CYP3A4 with plated human hepatocytes. *Drug metabolism and disposition: the biological fate of chemicals*, 42(9):1379–91, September 2014. ISSN 1521-009X. doi: 10.1124/dmd.114.058602.
- [236] Xi Emily Zheng, Zhican Wang, Michael Z Liao, Yvonne S Lin, Margaret C Shuhart, Erin G Schuetz, and Kenneth E Thummel. Human PXR-mediated induction of intestinal CYP3A4 attenuates  $1\alpha,25$ -dihydroxyvitamin  $d_3$  function in human colon adenocarcinoma LS180 cells. *Biochemical pharmacology*, 84(3):391–401, August 2012. ISSN 1873-2968. doi: 10.1016/j.bcp.2012.04.019.
- [237] Vonda Sheppard, Nicole Poulsen, and Nils Kröger. Characterization of an endoplasmic reticulum-associated silaffin kinase from the diatom thalassiosira pseudonana. *The Journal of biological chemistry*, 285:1166–1176, January 2010. ISSN 1083-351X. doi: 10.1074/jbc.M109.039529.
- [238] Stephanie R Faucette, Hongbing Wang, Geraldine A Hamilton, Summer L Jolley, Darryl Gilbert, Celeste Lindley, Bingfang Yan, Masahiko Negishi, and Edward L LeCluyse. Regulation of CYP2B6 in primary human hepatocytes by prototypical inducers. *Drug metabolism and disposition: the biological fate of chemicals*, 32(3):348–58, March 2004. ISSN 0090-9556. doi: 10.1124/dmd.32.3.348.
- [239] Dermot F McGinnity, George Zhang, Jane R Kenny, Geraldine A Hamilton, Sara Otmani, Karen R Stams, Suzette Haney, Patrick Brassil, David M Stresser, and Robert J Riley. Evaluation of multiple in vitro systems for assessment of CYP3A4 induction in drug discovery: human hepatocytes, pregnane X receptor reporter gene, and Fa2N-4 and HepaRG cells. *Drug metabolism and disposition: the biological fate of chemicals*, 37(6):1259–68, June 2009. ISSN 1521-009X. doi: 10.1124/dmd.109.026526.
- [240] Sunita J Shukla, Srilatha Sakamuru, Ruili Huang, Timothy A Moeller, Paul Shinn, Danielle Vanleer, Douglas S Auld, Christopher P Austin, and Menghang Xia. Identification of clinically used drugs that activate pregnane X receptors. *Drug metabolism and disposition: the biological fate of chemicals*, 39(1):151–9, January 2011. ISSN 1521-009X. doi: 10.1124/dmd.110.035105.
- [241] J G Zhang, Thuy Ho, Alanna L Callendrello, Charles L Crespi, and David M Stresser. A multi-endpoint evaluation of cytochrome P450 1A2, 2B6 and 3A4 induction response in human hepatocyte cultures after treatment with  $\beta$ -naphthoflavone, phenobarbital and rifampicin. *Drug metabolism letters*, 4(4):185–94, December 2010. ISSN 1874-0758. doi: 10.2174/187231210792928224.
- [242] Vincent J C Lempers, Jeroen J M W van den Heuvel, Frans G M Russel, Rob E Aarnoutse, David M Burger, Roger J Brüggemann, and Jan B Koenderink. Inhibitory potential of antifungal drugs on ATP-binding cassette transporters P-Glycoprotein,



## Bibliography

- MRP1 to MRP5, BCRP, and BSEP. *Antimicrobial agents and chemotherapy*, 60(6): 3372–9, 06 2016. ISSN 1098-6596. doi: 10.1128/AAC.02931-15.
- [243] Takeshi Akiyoshi, Takashi Saito, Saori Murase, Mitsue Miyazaki, Norie Murayama, Hiroshi Yamazaki, F Peter Guengerich, Katsunori Nakamura, Koujirou Yamamoto, and Hisakazu Ohtani. Comparison of the inhibitory profiles of itraconazole and cimetidine in cytochrome P450 3A4 genetic variants. *Drug metabolism and disposition: the biological fate of chemicals*, 39(4):724–8, Apr 2011. ISSN 1521-009X. doi: 10.1124/dmd.110.036780.
- [244] D J Back and J F Tjia. Comparative effects of the antimycotic drugs ketoconazole, fluconazole, itraconazole and terbinafine on the metabolism of cyclosporin by human liver microsomes. *British journal of clinical pharmacology*, 32(5):624–6, Nov 1991. ISSN 0306-5251. doi: 10.1111/j.1365-2125.1991.tb03963.x.
- [245] Aleksandra Galetin, Kiyomi Ito, David Hallifax, and J Brian Houston. CYP3A4 substrate selection and substitution in the prediction of potential drug-drug interactions. *The Journal of pharmacology and experimental therapeutics*, 314(1):180–90, Jul 2005. ISSN 0022-3565. doi: 10.1124/jpet.104.082826.
- [246] Nina Isoherranen, Kent L Kunze, Kyle E Allen, Wendel L Nelson, and Kenneth E Thummel. Role of itraconazole metabolites in CYP3A4 inhibition. *Drug metabolism and disposition: the biological fate of chemicals*, 32(10):1121–31, Oct 2004. ISSN 0090-9556. doi: 10.1124/dmd.104.000315.
- [247] Yohei Kosugi, Hideki Hirabayashi, Tomoko Igari, Yasushi Fujioka, Yoko Hara, Teruaki Okuda, and Toshiya Moriwaki. Evaluation of cytochrome P450-mediated drug-drug interactions based on the strategies recommended by regulatory authorities. *Xenobiotica; the fate of foreign compounds in biological systems*, 42(2):127–38, Feb 2012. ISSN 1366-5928. doi: 10.3109/00498254.2011.626087.
- [248] A P Li and M Jurima-Romet. Applications of primary human hepatocytes in the evaluation of pharmacokinetic drug-drug interactions: evaluation of model drugs terfenadine and rifampin. *Cell biology and toxicology*, 13(4-5):365–74, Jul 1997. ISSN 0742-2091. doi: 10.1023/a:1007451911843.
- [249] T L Nielsen, B B Rasmussen, J P Flinois, P Beaune, and K Brosen. In vitro metabolism of quinidine: the (3S)-3-hydroxylation of quinidine is a specific marker reaction for cytochrome P-4503A4 activity in human liver microsomes. *The Journal of pharmacology and experimental therapeutics*, 289(1):31–7, Apr 1999. ISSN 0022-3565.
- [250] J S Wang, X Wen, J T Backman, P Taavitsainen, P J Neuvonen, and K T Kivistö. Midazolam alpha-hydroxylation by human liver microsomes in vitro: inhibition by calcium channel blockers, itraconazole and ketoconazole. *Pharmacology & toxicology*, 85(4):157–61, Oct 1999. ISSN 0901-9928. doi: 10.1111/j.1600-0773.1999.tb00085.x.

## Bibliography

- 
- [251] Hiroshi Yamazaki, Minako Nakamoto, Makiko Shimizu, Norie Murayama, and Toshiro Niwa. Potential impact of cytochrome P450 3A5 in human liver on drug interactions with triazoles. *British journal of clinical pharmacology*, 69(6):593–7, Jun 2010. ISSN 1365-2125. doi: 10.1111/j.1365-2125.2010.03656.x.
- [252] Mark Jean Gnoth, Ulf Buetehorn, Uwe Muenster, Thomas Schwarz, and Steffen Sandmann. In vitro and in vivo P-glycoprotein transport characteristics of rivaroxaban. *The Journal of pharmacology and experimental therapeutics*, 338(1):372–80, Jul 2011. ISSN 1521-0103. doi: 10.1124/jpet.111.180240.
- [253] E Wang, Karen Lew, Christopher N Casciano, Robert P Clement, and William W Johnson. Interaction of common azole antifungals with P glycoprotein. *Antimicrobial agents and chemotherapy*, 46(1):160–5, Jan 2002. ISSN 0066-4804. doi: 10.1128/aac.46.1.160-165.2002.
- [254] Luna Prieto Garcia, David Janzén, Kajsa P Kanebratt, Hans Ericsson, Hans Lennernäs, and Anna Lundahl. Physiologically based pharmacokinetic model of itraconazole and two of its metabolites to improve the predictions and the mechanistic understanding of CYP3A4 drug-drug interactions. *Drug metabolism and disposition: the biological fate of chemicals*, 46(10):1420–1433, 10 2018. ISSN 1521-009X. doi: 10.1124/dmd.118.081364.
- [255] Brian W. Ogilvie, Donglu Zhang, Wenyong Li, A. David Rodrigues, Amy E. Gipson, Jeff Holsapple, Paul Toren, and Andrew Parkinson. Glucuronidation converts gemfibrozil to a potent, metabolism-dependent inhibitor of CYP2C8: implications for drug-drug interactions. *Drug metabolism and disposition: the biological fate of chemicals*, 34:191–197, January 2006. ISSN 0090-9556. doi: 10.1124/dmd.105.007633.
- [256] Thomayant Prueksaritanont, Jamie J. Zhao, Bennett Ma, Brad A. Roadcap, Cuyue Tang, Yue Qiu, Lida Liu, Jiunn H. Lin, Paul G. Pearson, and Thomas A. Baillie. Mechanistic studies on metabolic interactions between gemfibrozil and statins. *The Journal of pharmacology and experimental therapeutics*, 301:1042–1051, June 2002. ISSN 0022-3565. doi: 10.1124/jpet.301.3.1042.
- [257] Lucio G. Costa, Gennaro Giordano, and Clement E. Furlong. Pharmacological and dietary modulators of paraoxonase 1 (PON1) activity and expression: the hunt goes on. *Biochemical pharmacology*, 81:337–344, February 2011. ISSN 1873-2968. doi: 10.1016/j.bcp.2010.11.008.
- [258] Laura K Hinton, Aleksandra Galetin, and J Brian Houston. Multiple inhibition mechanisms and prediction of drug-drug interactions: status of metabolism and transporter models as exemplified by gemfibrozil-drug interactions. *Pharmaceutical research*, 25(5):1063–74, May 2008. ISSN 0724-8741. doi: 10.1007/s11095-007-9446-6. URL <http://www.ncbi.nlm.nih.gov/pubmed/17901929>.

Bibliography

---

- [259] Richard H Ho, Rommel G Tirona, Brenda F Leake, Hartmut Glaeser, Woon Lee, Christopher J Lemke, Yi Wang, and Richard B Kim. Drug and bile acid transporters in rosuvastatin hepatic uptake: function, expression, and pharmacogenetics. *Gastroenterology*, 130(6):1793–806, May 2006. ISSN 0016-5085. doi: 10.1053/j.gastro.2006.02.034. URL <http://www.ncbi.nlm.nih.gov/pubmed/16697742>.
- [260] R Nakagomi-Hagihara, D Nakai, T Tokui, T Abe, and T Ikeda. Gemfibrozil and its glucuronide inhibit the hepatic uptake of pravastatin mediated by OATP1B1. *Xenobiotica; the fate of foreign compounds in biological systems*, 37(5):474–86, May 2007. ISSN 0049-8254. doi: 10.1080/00498250701278442. URL <http://www.ncbi.nlm.nih.gov/pubmed/17523051>.
- [261] Dennis W Schneck, Bruce K Birmingham, Julie A Zalikowski, Patrick D Mitchell, Yi Wang, Paul D Martin, Kenneth C Lasseter, Colin D A Brown, Amy S Windass, and Ali Raza. The effect of gemfibrozil on the pharmacokinetics of rosuvastatin. *Clinical pharmacology and therapeutics*, 75(5):455–63, May 2004. ISSN 0009-9236. doi: 10.1016/j.clpt.2003.12.014. URL <http://www.ncbi.nlm.nih.gov/pubmed/15116058>.
- [262] P Sharma, V E Holmes, R Elsby, C Lambert, and D Surry. Validation of cell-based OATP1B1 assays to assess drug transport and the potential for drug-drug interaction to support regulatory submissions. *Xenobiotica; the fate of foreign compounds in biological systems*, 40(1):24–37, January 2010. ISSN 1366-5928. doi: 10.3109/00498250903351013. URL <http://www.ncbi.nlm.nih.gov/pubmed/19919292>.
- [263] Pradeep Sharma, Caroline J Butters, Veronica Smith, Robert Elsby, and Dominic Surry. Prediction of the in vivo OATP1B1-mediated drug–drug interaction potential of an investigational drug against a range of statins. *European Journal of Pharmaceutical Sciences*, 47(1):244–55, August 2012. ISSN 1879-0720. doi: 10.1016/j.ejps.2012.04.003. URL <http://www.ncbi.nlm.nih.gov/pubmed/22538052>.
- [264] Yoshihisa Shitara, Masaru Hirano, Hitoshi Sato, and Yuichi Sugiyama. Gemfibrozil and its glucuronide inhibit the organic anion transporting polypeptide 2 (OATP2/OATP1B1:SLC21A6)-mediated hepatic uptake and CYP2C8-mediated metabolism of cerivastatin: analysis of the mechanism of the clinically relevant drug-drug interaction. *The Journal of pharmacology and experimental therapeutics*, 311(1):228–36, October 2004. ISSN 0022-3565. doi: 10.1124/jpet.104.068536. URL <http://www.ncbi.nlm.nih.gov/pubmed/15194707>.
- [265] M Yamazaki, B Li, S W Louie, N T Pudvah, R Stocco, W Wong, M Abramovitz, A Demartis, R Laufer, J H Hochman, T Prueksaritanont, and J H Lin. Effects of fibrates on human organic anion-transporting polypeptide 1B1-, multidrug resistance protein 2- and P-glycoprotein-mediated transport. *Xenobiotica; the fate of foreign compounds in biological systems*, 35(7):737–53, July 2005. ISSN 0049-8254. doi: 10.1080/00498250500136676. URL <http://www.ncbi.nlm.nih.gov/pubmed/16316932>.

Bibliography

---

- [266] K. Yoshida, K. Maeda, and Y. Sugiyama. Transporter-mediated drug–drug interactions involving OATP substrates: predictions based on in vitro inhibition studies. *Clinical pharmacology and therapeutics*, 91:1053–1064, June 2012. ISSN 1532-6535. doi: 10.1038/clpt.2011.351.
- [267] Hideki Fujino, Tsuyoshi Saito, Yoshihiko Tsunenari, and Junji Kojima. Effect of gemfibrozil on the metabolism of pitavastatin—determining the best animal model for human CYP and UGT activities. *Drug metabolism and drug interactions*, 20:25–42, 2004. ISSN 0792-5077. doi: 10.1515/dmdi.2004.20.1-2.25.
- [268] Melissa Gabbs, Shan Leng, Jessay G. Devassy, Md Monirujjaman, and Harold M. Aukema. Advances in our understanding of oxylipins derived from dietary PUFAs. *Advances in nutrition (Bethesda, Md.)*, 6:513–540, September 2015. ISSN 2156-5376. doi: 10.3945/an.114.007732.
- [269] Jinping Gan, Weiqi Chen, Hong Shen, Ling Gao, Yang Hong, Yuan Tian, Wenying Li, Yueping Zhang, Yuwei Tang, Hongjian Zhang, William Griffith Humphreys, and A. David Rodrigues. Repaglinide-gemfibrozil drug interaction: inhibition of repaglinide glucuronidation as a potential additional contributing mechanism. *British journal of clinical pharmacology*, 70:870–880, December 2010. ISSN 1365-2125. doi: 10.1111/j.1365-2125.2010.03772.x.

## CREDIT CATEGORIES

---

**CONCEPTUALIZATION:** Ideas; formulation or evolution of overarching research goals and aims

**DATA CURATION:** Management activities to annotate (produce metadata), scrub data and maintain research data (including software code, where it is necessary for interpreting the data itself) for initial use and later reuse

**FORMAL ANALYSIS:** Application of statistical, mathematical, computational, or other formal techniques to analyze or synthesize study data

**FUNDING ACQUISITION:** Acquisition of the financial support for the project leading to this publication

**INVESTIGATION:** Conducting a research and investigation process, specifically performing the experiments, or data/evidence collection

**METHODOLOGY:** Development or design of methodology; creation of models

**PROJECT ADMINISTRATION:** Management and coordination responsibility for the research activity planning and execution

**RESOURCES:** Provision of study materials, reagents, materials, patients, laboratory samples, animals, instrumentation, computing resources, or other analysis tools

**SOFTWARE:** Programming, software development; designing computer programs; implementation of the computer code and supporting algorithms; testing of existing code components

**SUPERVISION:** Oversight and leadership responsibility for the research activity planning and execution, including mentorship external to the core team

**VALIDATION:** Verification, whether as a part of the activity or separate, of the overall replication/reproducibility of results/experiments and other research outputs

**VISUALIZATION:** Preparation, creation and/or presentation of the published work, specifically visualization/data presentation

**WRITING ORIGINAL DRAFT:** Preparation, creation and/or presentation of the published work, specifically writing the initial draft (including substantive translation)

WRITING REVIEW AND EDITING: Preparation, creation and/or presentation of the published work by those from the original research group, specifically critical review, commentary or revision - including pre- or post-publication stages

## PUBLICATIONS

## C.1 ORIGINAL ARTICLES

- 1 Nadine Schaefer, **Jan-Georg Wojtyniak**, Mattias Kettner, Julia Schlote, Matthias W. Laschke, Andreas H. Ewald, Thorsten Lehr, Michael D. Menger, Hans H. Maurer, and Peter H. Schmidt. "Pharmacokinetics of (synthetic) cannabinoids in pigs and their relevance for clinical and forensic toxicology." In: *Toxicology letters* 253 (June 2016), pp. 7–16. ISSN: 1879-3169. DOI: 10.1016/j.toxlet.2016.04.021.
- 2 Nina Hanke, Michael Teifel, Daniel Moj, **Jan-Georg Wojtyniak**, Hannah Britz, Babette Aicher, Herbert Sindermann, Nicola Ammer, and Thorsten Lehr. "A physiologically based pharmacokinetic (PBPK) parent-metabolite model of the chemotherapeutic zoletarelin doxorubicin — integration of in vitro results, Phase I and Phase II data and model application for drug-drug interaction potential analysis." In: *Cancer Chemotherapy and Pharmacology* 81.2 (Feb. 2018), pp. 291–304. DOI: 10.1007/s00280-017-3495-2.
- 3 Robert Miller, **Jan-Georg Wojtyniak**, Lisa J. Weckesser, Nina C. Alexander, Veronika Engert, and Thorsten Lehr. "How to disentangle psychobiological stress reactivity and recovery: a comparison of model-based and non-compartmental analyses of cortisol concentrations." In: *Psychoneuroendocrinology* 90 (Apr. 2018), pp. 194–210. ISSN: 1873-3360. DOI: 10.1016/j.psyneuen.2017.12.019.
- 4 Nadine Schaefer, **Jan-Georg Wojtyniak**, Ann-Katrin Kroell, Christina Koerbel, Matthias W. Laschke, Thorsten Lehr, Michael D. Menger, Hans H. Maurer, Markus R. Meyer, and Peter H. Schmidt. "Can toxicokinetics of (synthetic) cannabinoids in pigs after pulmonary administration be upscaled to humans by allometric techniques?" In: *Biochemical Pharmacology* 155 (Sept. 2018), pp. 403–418. ISSN: 1873-2968. DOI: 10.1016/j.bcp.2018.07.029.
- 5 Maximilian A. Ardelt, Thomas Fröhlich, Emanuele Martini, Martin Müller, Veronika Kanitz, Carina Atzberger, Petra Cantonati, Martina Meßner, Laura Posselt, Thorsten Lehr, **Jan-Georg Wojtyniak**, Melanie Ulrich, Georg J. Arnold, Lars König, Dario Parazzoli, Stefan Zahler, Simon Rothenfuß, Doris Mayr, Alexander Gerbes, Giorgio Scita, Angelika M. Vollmar, and Johanna Pachmayr. "Inhibition of cyclin-dependent kinase 5: a strategy

- to improve sorafenib response in hepatocellular carcinoma therapy." In: *Hepatology* 69.1 (Jan. 2019), pp. 376–393. ISSN: 1527-3350. DOI: 10.1002/hep.30190.
- 6 Michael Ramharter, Matthias Schwab, Ghyslain Mombo-Ngoma, Rella Zoleko Manego, Daisy Akerey-Diop, Arti Basra, Jean-Rodolphe Mackanga, Heike Würbel, **Jan-Georg Wojtyniak**, Raquel Gonzalez, Ute Hofmann, Mirjam Geditz, Pierre-Blaise Matsiegui, Peter G. Kremsner, Clara Menendez, Reinhold Kerb, and Thorsten Lehr. "Population pharmacokinetics of mefloquine intermittent preventive treatment for malaria in pregnancy in gabon." In: *Antimicrobial Agents and Chemotherapy* 63.2 (Nov. 2019), e01113–18. ISSN: 1098-6596. DOI: 10.1128/AAC.01113-18.
  - 7 Simeon Rüdeshheim, **Jan-Georg Wojtyniak**, Dominik Selzer, Nina Hanke, Felix Mahfoud, Matthias Schwab, and Thorsten Lehr. "Physiologically based pharmacokinetic modeling of metoprolol enantiomers and  $\alpha$ -hydroxymetoprolol to describe CYP2D6 drug-gene interactions." In: *Pharmaceutics* 12.12 (Dec. 2020), p. 1200. DOI: 10.3390/pharmaceutics12121200.
  - 8 **Jan-Georg Wojtyniak**, Hannah Britz, Dominik Selzer, Matthias Schwab, and Thorsten Lehr. "Data digitizing: accurate and precise data extraction for quantitative systems pharmacology and physiologically-based pharmacokinetic modeling." In: *CPT: Pharmacometrics & Systems Pharmacology* 9.6 (June 2020), pp. 322–331. DOI: 10.1002/psp4.12511.
  - 9 **Jan-Georg Wojtyniak**, Dominik Selzer, Matthias Schwab, and Thorsten Lehr. "Physiologically based precision dosing approach for drug-drug-gene interactions: a simvastatin network analysis." In: *Clinical Pharmacology & Therapeutics* (Dec. 2020). DOI: 10.1002/cpt.2111.

## C.2 CONFERENCE ABSTRACTS

- 1 **Jan-Georg Wojtyniak**, Johanna Pachmayr, and Thorsten Lehr. "A cancer cell cycle model to predict effects of combination therapy and different dosing schedules on cell cycle, tumor growth and therapy outcome." In: PAGE Meeting (June 7, 2016). Lisboa, June 7, 2016.
- 2 Katharina Martha Götz, **Jan-Georg Wojtyniak**, and Thorsten Lehr. "Package information leaflets (PILs) fail to inform patients – a study on the readability of PILs." In: DPhG Annual Meeting (2017). 2017.
- 3 **Jan-Georg Wojtyniak**, Katharina Martha Götz, and Thorsten Lehr. "The benefits of a one-page summary sheet (OPSS) compared to the patient information leaflet (PIL) to enhance health



- literacy – a randomized crossover trial.” In: DPhG Annual Meeting (2017). 2017.
- 4 **Jan-Georg Wojtyniak**, Roman Tremmel, Elke Schaeffeler, Matthias Schwab, and Thorsten Lehr. “Application of population pharmacokinetic (popPK) modeling to improve physiologically-based pharmacokinetic (PBPK) modeling decision making.” In: Uppsala Pharmacometric Summer School (2017). 2017.
  - 5 **Jan-Georg Wojtyniak**, Nina Hanke, Roman Trellem, Elke Schaeffeler, Matthias Schwab, and Thorsten Lehr. “Physiologically-based pharmacokinetic (PBPK) modeling of simvastatin drug-gene interaction with ABCG2 and drug-drug interactions with rifampicin and clarithromycin.” In: PAGE Meeting (June 6, 2017). Budapest, June 6, 2017.
  - 6 Fatima Zahra Marok, **Jan-Georg Wojtyniak**, Matthias Schwab, and Thorsten Lehr. “Optimizing 5-fluorouracil chemotherapy with regard to DPD drug-gene interactions and circadian effects utilizing a physiologically based pharmacokinetic (PBPK) modeling approach.” In: DPhG annual meeting (2019). 2019.
  - 7 Fatima Zahra Marok, **Jan-Georg Wojtyniak**, Matthias Schwab, and Thorsten Lehr. “Physiologically-based pharmacokinetic modeling of DPYD substrate 5-fluorouracil and its prodrug capecitabine.” In: PAGE (2019). 2019.
  - 8 **Jan-Georg Wojtyniak**, Simeon Rüdeshheim, Roman Tremmel, Matthias Schwab, and Thorsten Lehr. “Physiologically-based pharmacokinetic modelling of metoprolol drug-drug-gene interactions with paroxetine and CYP2D6.” In: PAGE Meeting (June 11, 2019). Stockholm, June 11, 2019.
  - 9 **Jan-Georg Wojtyniak**, Hannah Britz, Fatima Zahra Marok, Denise Türk, Laura Fuhr, Lukas Kovar, Nina Hanke, Matthias Schwab, and Thorsten Lehr. “Physiologically-based pharmacokinetic (PBPK) modelling of a CYP3A4/P-gp ddi network with ketoconazole, midazolam, alfentanil, repaglinide and digoxin.” In: DPhG Doktorandentagung (2019). 2019.

### C.3 ORAL PRESENTATIONS

- 1 **Jan-Georg Wojtyniak**, Thorsten Lehr, Roman Tremmel, and Matthias Schwab. *Physiologically Based Pharmacokinetic (PBPK) Modeling Approaches in WP9 - Systems Pharmacology and Gene-Drug-Drug Interactions*. 3rd U-PGx Consortium Meeting. Liverpool, Sept. 20, 2018.

- 2 **Jan-Georg Wojtyniak.** *Physiologically-Based Pharmacokinetic (PBPK) Modeling Approaches for the Prediction of Drug-Drug and Drug-Gene Interactions.* Boehringer Ingelheim guest lecture. Germany, May 14, 2019.

#### C.4 BOOK CHAPTERS

- 1 **Jan-Georg Wojtyniak,** Christiane Dings, and Thorsten Lehr. "Kardiologie." In: *Pharmakogenetik und Therapeutisches Drug Monitoring.* Ed. by Hanns-Georg Klein. Ed. by Ekkehard Haen. 1st ed. Walter de Gruyter GmbH, Dec. 18, 2017. Chap. Kardiologie. ISBN: 3110352907. URL: [https://www.ebook.de/de/product/31386633/pharmakogenetik\\_und\\_therapeutisches\\_drug\\_monitoring.html](https://www.ebook.de/de/product/31386633/pharmakogenetik_und_therapeutisches_drug_monitoring.html).

#### C.5 OTHERS

- 1 Lukas Kovar, **Jan-Georg Wojtyniak,** Christina Schräpel, and Thorsten Lehr. "Pharmakometrie erklärt - Wie verändert sie die moderne Pharmazie?" In: *PZ PRISMA* 4 (2019). ISSN: 0945-5566.

D

CURRICULUM VITAE

---

# Curriculum Vitae

## Jan-Georg Wojtyniak

### Pharmacist

Focus of research: Physiologically based pharmacokinetic (PBPK) modeling, population pharmacokinetic (popPK) modeling, reproducible analysis and report creation



+49 151 40047794



jan-georg@familie-wojtyniak.de



Königsberger Ring 2C, 65239 Hochheim am Main



www.linkedin.com/in/jan-wojtyniak



### Profile

**Creative, reliable, highly motivated** – these are my value propositions. I am a trained pharmacist with expertise in a broad range of PK/PD related topics working in the field of pharmacometrics

### Skills

#### Modeling and Markup:

R	○○○○○
RMarkdown	○○○○○
PK-Sim/MoBi	○○○○○
NONMEM	○○○○○
R-Shiny	○○○○○
LaTeX	○○○○○
HTML/CSS	○○○○○

#### Languages:

English:	
Reading	C1
Speaking	C1
Writing	C1
French	
Reading	A2
Speaking	A2
Writing	A2
Russian	
Reading	A1
Speaking	A1
Writing	A1

## Work experience

- since 01/2020 **Pharmacometrician**  
Boehringer Ingelheim Pharma GmbH & Co. KG, Ingelheim am Rhein (DE)  
Focus:
- Clinical drug development (oncology)
- 05/2016 – 12/2019 **Doctoral researcher**  
Universität des Saarlandes, Saarbrücken (DE)  
Robert Bosch Gesellschaft für medizinische Forschung mbH, Stuttgart (DE)  
Focus:
- PBPK modeling of pharmacogenetic effects and drug-drug interactions in the context of the European Ubiquitous Pharmacogenomics (U-PGx) projects
- 07/2014 – 12/2019 **Student research assistant**  
Universität des Saarlandes, Saarbrücken (DE)  
Focus:
- Shiny web applications for PK/PD
  - PopPK-analysis and allometric scaling
  - NCA-analysis
  - PBPK video tutorials
  - Method evaluation – data digitization and PBPK-modeling
  - Healthcare research – study design and result evaluation
- 02/2011 – 05/2017 **Freelance first aid trainer**  
Gesellschaft für Notfallmedizin, Saarbrücken (DE)
- 07/2010 – 03/2011 **Civil service as paramedic**  
DRK-LV Saarland e.V., Saarbrücken (DE)

## Education

- since 05/2016 **Ph.D. student**  
Universität des Saarlandes, Saarbrücken (DE)  
Robert Bosch Gesellschaft für medizinische Forschung mbH, Stuttgart (DE)  
Topic:
- Model Informed Drug Development And Precision Dosing for Drug-Drug-Gene-Interactions

# CV – Jan-Georg Wojtyniak

## Education

- 04/2011 – 09/2016 **Approbation as pharmacist**  
Landesamt für Soziales, Saarbrücken (DE)
- 05/2015 – 03/2016 **Diploma pharmacist**  
Universität des Saarlandes, Saarbrücken (DE)  
Topic:
  - A mathematical semi-mechanistic cancer cell cycle model to predict effects of combination therapy and different dosing schedules on cell cycle, tumor growth and therapy outcome
- 02/2011 **First aid trainer**  
Sanitätsschule Nord, Hutzfeld (DE)
- 01/2011 **Paramedic**  
Rettungsdienstschule Saar, St.Ingbert (DE)
- 09/2002 – 06/2010 **Abitur (including Latinum)**  
Gymnasium am Rotenbühl, Saarbrücken (DE)

## Personal information

- Date of birth • 24.02.1992
- Place of birth • Saarbrücken, Saarland (DE)
- Certificates • Leadership  
• Entrepreneurship  
• Uppsala Pharmacometric Summer School
- Organisations • **President** Deutsche Herzwacht e.V. (since 2014)  
• **Vice president** Alumni und Freunde der Fachrichtung Pharmazie an der Universität des Saarlandes e.V. (Universität des Saarlandes, 2014-2017)  
• **Voluntary member** of the Fachschaft Pharmazie (Universität des Saarlandes, 2013-2015)
- Attended conferences • **PK/PD Expert Meeting** (2019 – active participation)  
• **DPhG-Doktorandentagung** (2019 – poster presentation)  
• **Basel M&S Seminar** (2018/2016 – poster presentation)  
• **Uppsala Pharmacometric Summer School** (2017 – poster presentation)  
• **DPhG-Jahrestagung** (2017 – poster presentation)  
• **Population Approach Group Europe (PAGE) meeting** (2019/2017/2016 – poster presentation)
- Hobbies • Go bouldering  
• Learning new technologies  
• Meeting with friend  
• Managing non-profit projects in the health sector

## References

Prof. Dr. Thorsten Lehr  
Klinische Pharmazie  
Universität des Saarlandes

Prof. Dr. Matthias Schwab  
Dr. Margarete Fischer-Bosch-Institut für  
Klinische Pharmakologie

Dr. Nina Hanke  
Klinische Pharmazie  
Universität des Saarlandes

Campus C2 2  
66123 Saarbrücken, Germany  
Phone: +49 681 302 70255  
Mail: thorsten.lehr@mx.uni-saarland.de

Auerbachstraße 112  
70376 Stuttgart, Germany  
Phone: +49 711 8101 3700  
Mail: matthias.schwab@ikp-stuttgart.de

Campus C2 2  
66123 Saarbrücken, Germany  
Phone: +49 681 302 248  
Mail: n.hanke@mx.uni-saarland.de

Hochheim, January 04<sup>th</sup> 2021

